DOCTOR OF PHILOSOPHY

Geophysical properties of surficial sediments : textural and biological controls.

Jones, Sarah Elizabeth

Award date:
1990

GEOPHYSICAL PROPERTIES OF SURFICIAL SEDIMENTS: TEXTURAL AND BIOLOGICAL CONTROLS.

BY

SARAH ELIZABETH JONES M.A.

A thesis submitted to the University of Wales
for the degree of Doctor of Philosphy

October 1990.

School of Ocean Sciences
University College of North Wales
Menai Bridge
Gwynedd.

SUMMARY

Geophysical properties of surficial intertidal sediments: textural and biological controls.

The structural properties of surficial sedimentary deposits strongly influence exchange processes across the benthic boundary layer, and hence are important factors controlling sedimentation and biogeochemical cycling. They are governed by a complex combination of hydrodynamic, chemical and biological controls, and therefore exhibit significant spatial and temporal heterogeneity.

Geophysical techniques have great potential as tools for investigation of these structural properties. Techniques for determining *in situ* Electrical Formation Factor (FF) and acoustic shear-wave velocity (V*s*) in the upper few centimetres of saturated intertidal deposits were developed: FF was measured by a Wenner electrode array at the sediment surface; V*s* was measured by piezoelectric bender transducers inserted to a depth of 40mm.

Geophysical properties, porosity, and textural and biological characteristics were determined *in situ* at a variety of locations, predominantly in sands. The highest variability in all parameters was obtained over large spatial scales, with primary variation in bulk textural composition and benthic infaunal community. Within-location variability was significant over medium spatial scales of tens to hundreds of metres, controlled by local variation in tide-averaged hydrodynamic environment and duration of tidal exposure. In sands, bulk textural variability was of secondary importance over these scales, and was interpreted as due to admixture of relatively small proportions of coarse and fine sub-populations into a uniform sedimentary framework. Localised geophysical variability, while significant, was also of secondary importance, being influenced primarily by properties of this framework.

Seasonal variability was also significant, controlled by temporal variation in hydrodynamic environment and temperature. Structural parameters (porosity, FF, V*s*) were more responsive than textural parameters to temporal variation in hydrodynamic or biological activity.

Porosity was controlled by grain shape and size distribution, and by the depositional environment. It was not apparently directly affected by benthic macrofaunal activity. FF was controlled by porosity, and additionally by factors affecting tortuosity. Tortuosity was increased by increasing both carbonate and mud contents. Burrowing organisms (*Arenicola marina* and *Corophium*) and tube-building organisms (*Lanice conchilega*) reduced FF. V*s* was controlled by porosity, and additionally by factors which control intergranular friction. This was increased by increasing carbonate content, and reduced by increasing mud content. Burrowing organisms (*Arenicola marina* and *Corophium*) reduced V*s*, while tube-building organisms (*Lanice conchilega* and *Pygospio elegans*) increased it.

ACKNOWLEDGEMENTS.

I would like to extend my thanks to all those colleagues who have provided friendship, encouragement and stimulating discussion during my time at the School of Ocean Sciences. In particular, I am grateful to Professor Denzil Taylor Smith, Dr Jim Bennell and Dr Angela Davis for advice, especially during the early stages of the project.

I am also grateful to all members of the technical staff for their skills, dedication, and cheerful optimism in the workshop and in the field. In particular, I thank Mr Dave Boon, Mr Alan Nield, Mr Geraint Williams and Mr Frank Dewes, who contributed several of the diagrams.

This thesis would not, of course, have been possible without the guidance and encouragement of my supervisor, Dr Colin Jago, to whom I am especially indebted for giving me the opportunity and inspiration to progress from a theoretical training and to embrace the fascinating complexity and beauty of the marine environment.

Finally, I would like to thank my mother and father, to whom this thesis is dedicated.

CONTENTS.

Summary
Acknowledgements
Contents.

CHAPTER 1.

Physical properties of surficial sediments: significance, environmental controls and the role of geophysical techniques in their assessment.

1.1. Physical properties of surficial marine sediments. 1

1.1.1. Introduction 1
1.1.2. Characterisation of surficial sediment properties
Textural characteristics 2
Structural characteristics 2
1.1.3. Controls on surficial sediment properties
Controls on sediment texture. 3
Controls on sediment structure 6
Textural controls 8
Hydrodynamic controls 11
Biological controls 12
1.1.4. Variability in surficial sediments: controls and consequences. 14

1.2. Geophysical properties of surficial sediments. 17

1.2.1. Introduction 17
1.2.2. Electrical Formation Factor 19
1.2.3. Geoacoustic properties 20
1.2.4. Bioturbation and geophysical properties. 23

1.3. Scope and objectives of study. 23

CHAPTER 2.

Acoustic and electrical characteristics of unconsolidated sediments: theoretical considerations and controls.

Introduction 25

2.1. Acoustic properties of sediments. 25

2.1.1. Theoretical background. 25
2.1.2. Factors controlling shear wave propagation. 31
2.1.3. Limitations of the theory 36

2.3. Electrical properties of sediments. 37

CHAPTER 3.

An acoustic shear-wave probe: design, testing and preliminary laboratory work.

3.1. Methods of measuring V_s in unconsolidated sediment: background. 44

3.2. Development of the piezo-electric bender element. 46

3.3. A shear-wave probe for small-scale *in-situ* measurement of V_s. 48

3.4. Laboratory investigation of the transducer-sediment system. 52

3.4.1. Experimental objectives. 52

3.4.2. Apparatus and instrumentation.

3.4.2.1. Characterisation of S_H-wave generation and propagation. 54

3.4.2.2. Test sediment. 55

3.4.3. Investigation of the S-wave probes.

3.4.3.1. Electromechanical principles. 57

3.4.3.2. Response to variation in driving signal. 59

3.4.4. Dependence of received signal characteristics on probe separation. 64

3.4.4.1. Propagated pulse characteristics: 65

3.4.4.2. Calculation of true source-receiver separation 70

3.4.4.3. V_s determination using time-separation data. 72

3.4.5. Variation in S-wave velocity with depth. 72

3.4.5.1. Direct measurement of velocity gradients. 73

3.4.5.2. Prediction of time-separation curves in velocity gradients: comparison with measured data. 75

3.4.6. Investigation of the effect of drainage. 78

3.4.7. Velocity-frequency relationships. 83

3.4.7.1. Resonant frequency / velocity dependence 83

3.4.7.2. Investigation of dispersion. 85

3.4.8. The effect of variation in sediment temperature. 87

3.4.9. Artificial burrows: the effect of vertical cylindrical voids. 89

3.5. Summary and conclusions. 93

CHAPTER 4.

An *in situ* electrical resistivity probe: theoretical background, design and application to surficial sediment characterisation.

4.1. Theoretical background 96

4.1.1. Definintions and assumptions. 96

4.1.2. Electric potential due to a point current source:

In an infinite homogeneous medium 98

Effect of a plane boundary between media 99

Effect of two plane boundaries 101

4.2. Measurement of electrical resistivity of sediments.

4.2.1. Background 103

4.2.2. An *in situ* electrical resistivity probe 105

4.2.3. Pore fluid resistivity: importance and controls. 106
4.2.4. Application in surficial sedimentary deposits: complicating factors 107

4.4. Preliminary laboratory investigation. 113

4.4.1. Variation of sediment resistivity with depth 113
4.4.2. Effect of a drainage/saturation cycle 115

4.5. Summary and conclusions. 116

CHAPTER 5.

In-situ measurement of acoustic and electrical properties in surficial intertidal sediments.

5.1. Rationale, experimental procedure and data-analysis techniques.

5.1.1. Introduction : Experimental rationale 118
5.1.1.1 Site selection. 118

5.1.2. Field measurement procedure 120
5.1.2.1. Sampling strategy 121
5.1.2.2. Textural, biological and structural characterisation 122
5.1.2.3. S-wave velocity measurement 124
5.1.2.4. Formation Factor measurement 126
5.1.2.5. Operational details 128

5.1.3. Sample processing and data reduction. 129
5.1.3.1. Sediment porosity 129
5.1.3.2. Textural parameters 131
Grain-size parameters 131
Carbonate Content 137
Organics content. 138
5.1.3.3. Biological parameters 139
5.1.3.4. Box-cores 139
5.1.3.5. S-wave velocity 140
5.1.3.6. Formation Factor 146

5.1.4. Errors: sampling, processing and natural variance 146
5.1.4.1. Sediment porosity 147
5.1.4.2. Textural parameters 148
5.1.4.3. Biological parameters 151
5.1.4.4. S-wave velocity 152
5.1.4.5. Formation Factor 153

5.1.5. Statistical treatment of data 155
5.1.5.1. Single variable statistics 156
5.1.5.2. Analysis of variance 156
5.1.5.3. Bivariate statistics : Correlation 157
5.1.5.4. Multivariate statistics : multiple regression analysis 159

5.2. Local spatial variability and associated textural and biological controls.

5.2.0.1. Introduction 163
5.2.0.2. Relative variability of textural, biological and geophysical parameters. 165
5.2.0.3. Selected benthic macrofauna: salient physiological and behavioural characteristics. 167
Arenicola marina 167
Lanice conchilega 169
Corophium 170

5.2.1. Traeth Llanddwyn: Preliminary measurements on a bioturbated foreshore. 171
5.2.1.1. Site characterisation and within-site variation 171
5.2.1.2. Localised variability. 174
5.2.1.3. Relationships between parameters. 173
5.2.1.4. Summary and interim conclusions. 180

5.2.2. Taf estuary: measurements in clean sand and on a muddy *Corophium* flat. 181
5.2.2.1. Site characterisation 182
5.2.2.2. Localised variability. 185
5.2.2.3. Relationships between parameters 185
5.2.2.4. Comparison of *in-situ* measurements with a laboratory simulation. 188
5.2.2.5. Summary and interim conclusions. 190

5.2.3. Traeth Lligwy: Further measurements on *Arenicola* flats. 191
5.2.3.1. Site characterisation 191
5.2.3.2 Localised variability. 194
5.2.3.3 Relationships between parameters. 195
5.2.3.4. Summary and interim conclusions. 200

5.2.4. Red Wharf Bay: further measurements on a *Lanice* community. 201
5.2.4.1. Site characterisation. 202
5.2.4.2. Localised variability 203
5.2.4.3. Relationships between parameters 204
5.2.4.4. Summary and interim conclusions. 207

5.2.5. Freathy Sands: *in situ* assessment of the drainage effect. 208

5.2.6. Tamar estuary : Measurements in muds. 211
5.2.6.1. Site characteristics. 211
5.2.4.2. Variability of measured properties. 215
5.2.4.3. Relationships between parameters 215
5.2.4.4. Summary and interim conclusions. 217

5.2.7. Summary and conclusions. 218

5.3. Temporal and spatial variability: seasonal controls.

5.3.1. Introduction 223
5.3.2. Site characterisation 224

5.3.3. Temporal and spatial variation of environmental factors. 228
5.3.3.1. Background climatological factors 228
5.3.3.2. Sampling conditions and sediment temperature 229
5.3.3.3. Bed elevation, surficial and subsurface features. 229
5.3.4. Temporal and spatial variation of sediment properties. 234
5.3.4.1. Textural characteristics 236
5.3.4.2. Benthic macrofaunal characteristics 238
5.3.4.3. Porosity and the geophysical properties 245
5.3.5. Relationships between sediment properties 249
5.3.5.1. Interaction between biological and textural characteristics 249
5.3.5.2. Controls on structural and geophysical properties 256
5.3.5.3. Parameters describing small-scale heterogeneity 264
5.3.6. Summary and conclusions. 266
5.4. Larger scale variability: primary controls.
5.4.1. Introduction. 271
5.4.2. Parameter selection. 271
5.4.3. Overall variability: comparison with laboratory data 272
5.4.4. Variability in intertidal sands. 274
5.4.4.1. Relative importance of different scales of spatial and temporal variability. 274
5.4.4.2. Relative variability of textural, biological and geophysical parameters. 278
5.4.4.3. Generalised controls on porosity and the geophysical parameters. 279
CHAPTER 6.
Conclusions. 283
REFERENCES 294
APPENDIX A: Summary tables: procedure and combined data set.
APPENDIX B. Local spatial variability: reference tables and figures.
APPENDIX C: Seasonal variability: reference tables and figures.
APPENDIX D: Plates.

CHAPTER 1.

PHYSICAL PROPERTIES OF SURFICIAL SEDIMENTS: SIGNIFICANCE, CONTROLS AND THE ROLE OF GEOPHYSICAL TECHNIQUES IN THEIR ASSESSMENT.

1.1. Physical properties of surficial sediments.

1.1.1. Introduction.

Physico-chemical properties of unconsolidated marine sediments have long been of interest to oceanographers, geologists and engineers. These three groups have concentrated their attention on the response of sediments to hydrodynamic processes (entrainment, transport and deposition) and to mechanical loading (consolidation and strength failure). Sediment dynamicists have hitherto tended to regard sedimentary deposits as sources or sinks of individual particles: their interest has been confined to the sediment/water interface. In contrast, engineers have studied bulk mechanical properties of deposits averaged over lateral and vertical scales of, at least, decimetres. Between these two extremes of scale and approach lies the growing body of researchers interested in the physical properties of the upper few centimetres of the bed. This region is of paramount importance when considering fluid and particulate exchanges between sea floor and water column, and hence is central to sedimentary processes and biogeochemical cycling in the marine environment.

Physical properties of this region are governed by a complex and interacting combination of controls, which should be assessed *in situ*. Among these controls, both the nature of the sediment supply and the depositional environment are important. In addition, the vast majority of surficial sedimentary deposits are colonised by benthic organisms which affect, and are in turn affected by, sediment properties. It is these small-scale bed properties which form the focus of this thesis.

1.1.2. Characterisation of surficial sediment properties.

Textural characteristics.

Sediment is defined as any particulate material, originating from any part of the earth's surface, which is capable of being deposited from suspension in a fluid [Twenhofel, 1932]. Physical, petrological and chemical properties of individual sedimentary grains constitute sediment *texture*. This includes properties of the primary fabric, characteristics of the grain size distribution, grain shape and roundness, surface texture, chemical adsorption, organic coatings and microbiological colonisation. Investigation of textural properties can generally be performed on disturbed samples, mechanically or chemically separated into components of different size or composition in the laboratory. Sediment texture therefore characterises the basic building blocks from which sedimentary deposits are generated.

Structural characteristics.

A sedimentary deposit is obtained when suspended particulates are deposited under gravity (or via chemical/biological action) at the interface between their transporting fluid and the benthic boundary. Therefore they constitute at least a two-phase medium: a self-supporting connected framework of particles and the fluid-filled pore space, with the two phases forming complex interpenetrating matrices. The 3-dimensional arrangement of the framework is the sediment *structure*. Partial saturation of the pore-fluid matrix introduces a third (gas) phase.

Primary sediment structure is formed at the time of deposition or shortly thereafter and before secondary consolidation [Pettijohn & Potter, 1964]. This includes hydrodynamically, biologically and chemically derived structures, as well as those due to penecontemporaneous deformation under build up of further deposited material.

For a given sediment texture, a range of stable sedimentary structures can be obtained. It is clear that, in contrast to textural properties, structural characteristics of the sediment can only be measured in

undisturbed samples, or on redeposited samples where the depositional environment can be confidently reproduced. It is also clear that, while sediment can usually be considered as a population of individual suspended particles during transport, any study of properties of the sea bed must include an understanding of structural properties of the sediment framework / pore-fluid system. Individual grain characteristics are then considerably less important than their properties *en masse*.

The important physical properties of such a system depend on individual grain characteristics, packing configuration, and nature of intergranular contact forces. From an understanding of these properties it is possible to infer: shape, size, disposition and connectedness of the pore space, and hence pore-fluid transport properties such as diffusivity and permeability; and behaviour of the framework under load, and hence geotechnical properties such as rigidity, compressibility, and shear strength. Geochemical processes within the system, while influenced strongly by sediment structural properties, involve an additional understanding of grain/pore exchange processes.

1.1.3. Controls on surficial sediment properties.

Controls on sediment texture.

The dominant controls over textural properties of a deposit are: nature of the source material, mechanism of particle production, history of hydrodynamic sorting along the transport path and localised depositional environment. Post-depositional sorting by temporal variability in hydrodynamic processes and biological activity can also have a significant effect.

The vast majority of sedimentary particles originate either directly by the weathering of rocks (producing terrigenous sediments) or indirectly by the mediation of organisms that make hard tissues from atmospheric carbon dioxide and/or substances dissolved in natural waters (producing chemical, usually carbonate sediments).

It is generally accepted that processes such as wind, rain, river flow,

tides, waves, frost and glaciation produce sedimentary particles from the parent rock by mechanical means down to around 2μm in diameter [Allen, 1985]. These particles will have identical mineral properties to the parent rock. Chemical weathering breaks down unstable aluminosilicates (feldspars) to produce stable clay minerals. Such particles, although having a chemical content similar to the parent rock, will have a different crystalline structure and are known as clay particles. They form an increasingly important proportion of the particles with decreasing sediment grain size, and are almost exclusive in the sub-2μm fraction. Excess ionic charges on the exposed surfaces of clay minerals interact with ions in the pore-fluid, resulting in mutual attraction which can overcome particle inertia (which is directly proportional to particle size and mass). The degree of attraction is dependent on clay mineralogy, salinity and pH of the pore fluid and temperature. Consequently there is a fundamental difference in sedimentary behaviour between sand and clay fractions. Sand-size sediments are governed by inertia and are cohesionless, whereas clay-size sediments exhibit flocculation in suspension and electrochemical attraction on deposition and are cohesive.

Biological production of hard mineral structures such as shells, which can be transported whole or as abraded fragments, can also contribute significantly to the sediment. In contrast to the generally well-rounded, ellipsoidal clastic sands, biogenic fragments are often highly angular and plate-like. Individual clay particles are also plate-like, although flocs will exhibit variable forms.

Some degree of transport of sediments from source to environment of deposition is involved in the majority of cases. The textural composition of a given deposit will be controlled by the product of the initial composition at the source, the competence of the transporting medium to support individual sediment grains, and the hydrodynamic environment at the deposition site. Sediment is suspended in a fluid against gravity via turbulence (and hence transported along the flow direction), with large, dense particles requiring considerable energy to remain in suspension and settling fast when that energy is removed, small or light particles requiring much less energy and settling more slowly.

The simplest interpretation of this results in 'fining down the transport

path' [Inman, 1949]. However, in many marine environments the end product involves integration over both space and time to allow for spatial and temporal variability in the hydrodynamic regime [Stanley & Swift, 1976]. There can also be modification of sedimentary particles during transport: softer grains such as shell fragments can be abraded or partially dissolved, microbiological coatings or ingestion and defecation by larger organisms can cause aggregation, salinity and temperature changes can result in enhanced flocculation or deflocculation of clay minerals.

Once deposited, further alteration of textural composition can occur through winnowing of fines from a coarser framework, and through temporal variability in the local flow regime (and suspended sediment supply).

Perhaps the most important agent of post-depositional textural change is biological activity. Feeding and burrowing can involve boring into and fragmentation of large grains and breakdown or deformation of aggregates, thus reducing particle size. Conversely all benthic fauna produce mucous exopolymers [Fazio *et al*, 1982] which coat particles and can cause their adhesion into aggregates, thus increasing particle size. Note that intergranular adhesion by external agents, which can act on all particles, is distinguished from electrochemical cohesion of clays [Jumars *et al*, 1982]. Adhesion arises from microbial or diatomic colonisation of mineral grains [Holland *et al*, 1974; Boer, 1981; Grant *et al*, 1982; Paterson *et al*, 1989], production of faecal pellets on passage through the gut [Taghon *et al*, 1984], and burrowing and tracking activity [R.G. Johnson, 1977].

Benthic macrofauna are also capable of sorting deposits by transporting, selecting and rejecting different types of particle at different levels within the substrate [Rhoads and Stanley, 1963; Rhoads, 1967; Tevesz *et al*, 1980]. Criteria for selection may be size, shape or composition: this process results in vertical textural heterogeneity over scales from 10-200mm.

There can also be biological control of sediment supply and stability [Ginsberg and Lowenstam 1958; Yingst and Rhoads, 1978]. By modifying surface roughness the near-bed hydrodynamic regime, and hence the textural properties of subsequently deposited material, can be altered. Bioturbation can both increase and reduce surface roughness, depending on

initial conditions, organism density and nature of surface modification, as reviewed by Jumars and Nowell [1984]. Organisms are capable of trapping suspended material which would not otherwise have been deposited and of exposing sediment to erosion via faecal mounds, ejected pellets and pseudofaeces, as well as altering the erodibility of individual grains through pelletisation or by binding of the surface [Rhoads & Boyer, 1982].

Controls on sediment structure.

The generation of a surficial sedimentary deposit can be conveniently separated into two phases: sedimentation into a stable self-supporting framework in equilibrium with the local flow regime, and post-depositional deformation by subsequent loading, hydrodynamic reworking or biological activity. Structural properties of the sediment/pore-fluid system will be controlled by the nature of the grains constituting the sedimentary framework, by their packing arrangement arising out of initial deposition, and by subsequent rearrangement, reworking or consolidation.

Before discussing the controls on structural properties of the sediment/pore-fluid system, the important features used to characterise it should be defined. It is clear that properties which describe the nature of packing of the sediment framework, such as number and nature of intergranular contacts are important. Equally, the shape, size, disposition and connectedness of the pore space are important factors in determining properties of the fluid phase. The simplest measure which describes the degree of packing is the sediment porosity, which is simply the volume of pore-fluid per unit volume of sediment/pore-fluid system. This is a bulk average property which ignores heterogeneity or anisotropy within the unit volume measured, and also provides no information on shape of the pore space. The following discussion considers first the effect on macroscopic packing density, then on more detailed aspects of the packing configuration.

Given a supply of sedimentary particles, there are a number of ways in which it can be packed to form a stable sedimentary deposit. For simplicity it is assumed for the time being that the deposit is macroscopically homogeneous, i.e. that there is no lateral or vertical

heterogeneity in texture or packing arrangement other than the random microscopic heterogeneity associated with a natural population of particles and the sediment/pore-fluid system itself.

Three categories of packing have been defined [Allen, 1985]: **systematic packing** allows for regular arrangement of particles where the deposit is built up as a series of layers, with the distance between each grain and the number of intergranular contacts per grain precisely defined. Although this is clearly not the case for natural cohesionless deposits, investigation with these packings can provide useful insights into the behaviour of real sediments. Further, this type of structure can be obtained in clays, where electrochemical intergranular adhesion gives rise to a regular arrangement of particles. **Random packing** is, in contrast, totally disordered, where grains are brought together one at a time at random from all directions. Finally, **haphazard packing** is obtained where the grains have been added at random from one direction only: this applies to all naturally occurring cohesionless deposits.

While systematic packings of cohesionless spheres exhibit a theoretically predictable range of discrete porosities depending on coordination number (there being a range of regular packings which yield stable structures), haphazard packings must be investigated empirically. It has been shown from experiments with idealised and natural sedimentary particles that porosity varies according to the nature of deposition.

For cohesionless spheres, porosity has been shown to increase with deposition rate and energy between the two limiting values of 0.44 and 0.36 [Scott, 1960; Haughey and Beveridge, 1969]. These limits are obtained from inversion of a fluid-filled container containing the sediment so that high- concentration, low-energy deposition at the other end of the container is achieved, and subsequent mechanical vibration to a state of minimum porosity. Non-spherical particles exhibit similar limiting behaviour but ranging more widely between dense and loose states [Jackson P D, 1978].

Kolbuszewski (1950) envisaged two effects for cohesionless deposits, one related to the energy of the arriving particles, and the other dependent on their concentration just above the bed. Every falling particle carries

to the bed a certain amount of energy, which can be dissipated only through frictional and other inelastic collisions amongst the particles already emplaced, so causing 'roll' into a closer packing configuration. If near-bed concentration is very high, movement is inhibited, so that not all grains have time to roll into a minimum energy position before being supported by other grains. For cohesive sediments the situation is further complicated by electrochemical attraction and repulsion among deposited particles.

Textural controls on sediment structure.

Natural deposits involve haphazard assemblies of a size distribution of irregularly shaped particles. Such a situation can usually only be handled empirically. Most common cohesionless materials exhibit porosities between 0.3 and 0.5. With non-uniform, angular or cohesive particles, however, almost any degree of porosity can be obtained.

It is clear from the preceding section that a given sediment can be deposited at a range of porosities between limits. To avoid confusion, the remainder of the discussion of textural controls on packing structure has been limited, where relevant, to the minimum porosity obtained for a given sediment texture, and to the effect on shape of the pore-fluid matrix and intergranular contact forces.

The effect of grain size.

Theoretically the actual size of cohesionless grains should have no effect on porosity. However for natural sediments, the porosity tends to increase with decreasing grain size [Hamilton, 1982; Keller, 1970]. Since smaller particles exhibit lower settling velocity and mass-to-surface ratio, they have less energy and are more prone to mutual obstruction on deposition. They are also generally more angular and platy than larger sediments, and therefore are more likely to form bridged structures, as described in the section on grain shape below. Most importantly, fine grained cohesive sediments are subject to complex attractive and repulsive forces which may allow open high-arched arrangements, held together electrochemically

rather than by friction, such as the "honeycomb" or "cardhouse" structures reported by Bennett *et al,* [1981]. Under appropriate conditions the grains may be flocculated, and the flocs may also be loosely aggregated, forming an extremely loose packing structure [Partheniades, 1965].

There is also a granulometric control on intergranular contact forces. For clean sands and gravels, these forces are frictional, and therefore depend on the mineralogical properties of the grains and on their surface roughness, rather than on size. However, the number of intergranular contacts per unit volume varies according to size. For silts and clays friction is less important than electrochemical cohesion. In the absence of biological effects (which will be dealt with later) intergranular forces depend on distance between grains, mineralogy, salinity and temperature [Young and Southard, 1978]. For aggregates a range of intergranular forces will be present, between mineral grains, between flocs and between aggregates, with those between aggregates the weakest.

The effect of grain shape and orientation.

From investigation of systematic packings, it has been suggested that the porosity of cohesionless haphazard deposits should vary with degree of elongation of the particles, and with strength of preferred orientation [Allen, 1985]. An important property of elongated, angular or platy grains is that they are capable of 'bridging' across voids, thus preventing the close packing of smaller or otherwise oriented particles. There is some experimental evidence to confirm this, from experiments with natural biogenic fragments and chopped spaghetti [Allen, 1985]. Since naturally deposited platy or elongated particles tend to be aligned horizontally and into the flow direction [Dyer, 1986], the bridging effect is of enhanced importance.

The configuration of the pore space will also be affected by shape and orientation of non-spherical particles. It is clear that, for a given packing density, angular particles will result in a much more convoluted pore space than smooth, round ones. Equally, the number of intergranular contacts would be expected to be higher.

The effect of a distribution of sizes.

Non-uniformity of grain size will have a significant effect on packing density and porosity. This is because small particles within the distribution can occupy the pore-spaces between the larger grains. Sohn & Moreland [1968] found that porosity was a function only of the dimensionless standard deviation of the size distribution in sands. For a given porosity, the configuration of the pore space should also be more tortuous for a spread of sizes, and the number of intergranular contacts should increase.

Many natural sediment populations contain a mixture of cohesive and cohesionless particles: this results in a combination of frictional and cohesive intergranular forces. A deposit is generally considered to exhibit significant cohesion if it contains greater than around 10% clay [Dyer, 1986].

The effect of mixing widely different sizes.

When smaller particles are mixed into a bed of larger cohesionless particles, opposing effects are found that jointly determine the combination yielding minimum porosity. Smaller particles, on the one hand, tend to force larger particles apart, but on the other hand, can fall into voids between larger particles, the latter predominating for a size ratio greater than about 3:1. In this case, porosity depends not only on particle shape and size ratio but also on the proportion of each size class present. Generally a minimum in porosity is obtained at a certain proportion which is lower than the porosity obtained for either pure component. This has been shown for binary mixtures of cohesionless spheres [Yerazumis *et al*, 1962; Wakeman, 1975] and for mixtures of log-normal and Gaussian populations of natural sands [Rogers & Head, 1961; Sohn & Moreland, 1968]. Minimum porosity varies with diameter ratio more than with relative composition. Ternary sand mixtures also yield minima at a specific combination of the three components [Dexter and Tanner (1971), Statham (1974)]

For mixtures of sands and clays, porosity also depends on the relative

proportions of coarse and fine particles. For predominantly sandy deposits, small quantities of fines are distributed within interstices formed by the sand framework, and should behave as cohesionless deposits. For predominantly clay deposits, coarse particles are 'suspended' within a cohesive sediment matrix, and may have little effect on porosity.

The effect of surface properties of the grains:

There are incidental experimental data to suggest that rough-surfaced particles pack a little less densely than smooth ones of a similar shape and size, but the question has yet to be investigated systematically [Allen, 1985]. Intergranular friction will certainly be increased for rough particles. Attached microorganisms and biological secretions cause adhesive forces between grains, and may lubricate frictional intergranular contacts.

Hydrodynamic controls on sediment structure.

The dependence of packing on deposition rate, which is governed by the hydrodynamic environment, has already been discussed. Further hydrodynamic controls on sediment structure include post-depositional liquefaction and consolidation by wave action and storm-induced slumps and slides [Reineck and Singh, 1975].

More significantly, sediments are seldom deposited in a manner that results in homogeneous sediment. Furthermore, the surface layers represent a time-integration of temporally varying processes of deposition and erosion. There is a vast literature on primary hydrodynamic structures [Allen, 1982]. A layer or lamina arising from settlement of a distribution of sizes results in grading from coarser material at its base to finer material at its top. Bedload transport of sands can generate current ripples, dunes, anti-dunes and plane beds. Bedforms may be two- or three-dimensional, depending on water-depth and flow regime. They can also migrate, resulting, in the case of ripples and dunes, in inclined laminations formed by repeated avalanching from the crests. These internal structures can then be preserved whole or in truncated form, if the bed is

accreting. Non-spherical grains are generally preferentially aligned into the flow direction, causing anisotropy and affecting porosity. Cohesive deposits are affected by the degree of flocculation, which in turn is partially controlled by turbulent energy.

Biological controls on sediment structure.

The effects of benthic organisms on the physical properties of sediments are well documented and have been extensively reviewed [Dapples, 1942; Schafer, 1972; Rhoads 1974; Rowe, 1974; Richards & Parks, 1976; Lee & Swartz 1980; Carney 1981; Rhoads & Boyer, 1982; Jumars & Nowell, 1984; Krantzberg 1985]. Depending on available technology, and experimental objective, a variety of techniques has been utilised to measure biological modification of different aspects of the sediment/pore-fluid system. These include porosity, water content, compaction, stability, erodibility, shear strength, cone penetration and geoacoustic properties. Since for the purpose of this discussion the technique is not important, results have been interpreted in more general terms of packing configuration and intergranular contact forces.

The autoecological parameters that appear to be most directly related to physical modification of sediments include: organism size and population density, degree of mobility and depth range of influence, method and level of feeding, mode of construction of burrows or tubes.

The size class of the organism is important: meiofauna (50 - 500 μm in size) occupy the interstices between sedimentary grains: only fine grained deposits are physically bioturbated by their activity [Cullen, 1973]. The influence of microfauna (less than 50μm in size), whilst it can be highly significant, is confined to the modification of physical properties of individual grains already discussed and to chemical exchange processes between sediment, pore fluid and the water column. In contrast, macrofauna (greater than 500 μm in size) cause direct disturbance of the packing arrangement in most natural sedimentary deposits.

A classification of meio- and macrofaunal biogenic structures based on ethology includes resting traces, crawling traces, feeding structures,

grazing traces and dwellings [Sielacher, 1953]. Crawling can involve movement by anchoring an extended foot to the substrate and pulling the rest of the organism up to the point of attachment [Trueman, 1968], by whip-like side to side action or by peristaltic movement along the organism [Wells, 1969]. Frey [1973] reports that crawling is 'transient' and results in considerable homogenisation of any sedimentary or relict biogenic structure. Dwellings can be broadly divided into burrow systems and tubes. Burrows are excavated by displacement or swallowing of sediment, and are generally lined with mucilaginous secretions. Active maintenance of the burrow is required or they collapse within several days [Rice and Chapman, 1971]. Tubes are more elaborate structures constructed from naturally occurring components of the sediment such as shell fragments, from mucilaginous or chitinous secretions, or a combination of both. They often protrude above the sediment water interface.

There are three broad categories of feeding activity: carnivorous, deposit feeding and suspension feeding. Deposit feeders either selectively or indiscriminately ingest particles from the sediment/water interface or from within the sediment bulk, digest attached organic material, and excrete the remainder as faecal pellets or casts. These can be bound with mucus, and are generally deposited at the sediment surface. Within the sediment, the process generally involves local disturbance as grains are selected and swallowed, and further disturbance as they are excreted. Sessile organisms actively liquefy and pump fresh supplies of sediment into an accessible region near the mouth [Rhoads 1974]. Considerable volumes of sediment can be processed in this way, sorting sediment from the substrate and depositing it at the surface.

Suspension feeders trap organic-rich detritus from the water column, either by pumping and filtering water through their tube or burrow, or by constructing elaborate structures protruding from the bed for direct entrapment. Both suspension and deposit feeders can also be categorised as grazers. Grazers also select particles, but rather than ingest them whole they utilise the organic films and microorganisms coating their surfaces. There is evidence to suggest that bioturbation by macrofauna actively encourages microbial regeneration by maintaining favourable environments within the sediment, described as 'gardening' [Yingst and Rhoads, 1980].

Now that important biogenic structures have been described, the effects of this activity on structural properties of sediments can be discussed. Bioturbation can clearly have a profound effect on packing configuration, and on intergranular contact forces. It is also clear that these effects can be extremely complex and can act to oppose each other. Therefore prediction of the overall effect of any one species can be problematic, even if the effects of individual aspects of its behaviour are understood.

Thus burrows will cause localised increases in porosity, although depending on whether grains are excavated or merely pushed apart the sedimentary framework may be compacted in the vicinity of the burrow [Aller & Yingst, 1980]. High densities of rigid-walled tubes result in a compacted, cohesive and tight fabric [Rhoads, 1974]. Movement through the sediment may either cause compaction (through liquefaction or breakdown of aggregates) or dilation, depending on the initial state of packing and on grain size. In contrast to muds, mixing of sands tends to cause dilation rather than compaction [Webb, 1969, Myers, 1977]. Pelletisation generally increases porosity, forming loosely compacted surficial 'fluff' layers up to 90mm in depth [Rhoads, 1974; Rhoads & Boyer, 1982; Richardson *et al*, 1983] with very low intergranular attractive forces, although organic adhesion can bind these pellets to the sediment surface [Yingst & Rhoads, 1980]. Microorganisms and mucopolysaccharide secretions result in increased intergranular adhesion: for sands, however, they can also lubricate rough intergranular contacts, thus reducing friction.

The problem is further complicated by the fact that it is extremely rare to find a deposit containing just one species of organism. Interaction and competition between species in a benthic community will cause interaction between their different effects on the sediment. Feedback is also possible: the activity of one organism may inhibit successful colonisation by another. Even in a monospecific macrofaunal community, there will be complex interaction with meiofauna and microorganisms.

1.1.4. Variability in surficial sediments: controls and consequences.

The problem of assessing structural properties in surficial sediments is further exacerbated by marked spatial and temporal variability. From a

consideration of the controls discussed in the preceding sections, it is clear that spatial variability can occur over a range of scales from microns through to kilometres, with the controls ranging from meiofaunal disturbance within the pore space to large scale differences in hydrodynamic regime. Temporal variability is also clearly important, again on a range of scales from turbulence and individual actions of organisms, through waves and tides to seasonal hydrodynamic and biological cycles. The ecologically realistic concept of benthic communities proposed by R.G. Johnson (1971, 1972), can be extended to include hydrodynamic factors, so that bottom sediments can be viewed as a temporal and spatial mosaic, each part having a different history of disturbance, deposition, benthic colonisation and ecological succession, with shorter term variability in activity and environment superimposed.

Spatial variability in sediment structural properties can be separated into lateral and vertical heterogeneity. As has been discussed in the previous sections, overburden, gradients in textural properties and biological activity can cause significant vertical variability in surficial sediment properties, and this has been demonstrated by a number of workers [Keller, 1974; Silva, 1974; Richardson, 1983, Briggs *et al* 1985; Richardson, 1985].

Lateral variability has also been shown to be significant on a variety of scales [Bader, 1953; Richards, 1962, 1964; Bennett et al, 1970; Faas (1973)]. Marked heterogeneity of sites only a few metres apart has been reported by Young and Southard [1978]. Richardson [1985] found significant variability in textural and physical properties on scales of a kilometre or less, and compared the relative importance of biological, hydrodynamic and sedimentological processes in determining spatial distributions of surficial sediment properties. Large scale variability was controlled by hydrodynamic processes acting on local relict features. Medium scale variability (10 to 100m) was controlled by patchiness in organism density, which is extremely common and can arise from restricted substrate selection stimuli or differential mortality [Webb *et al*, 1976]. In fine grained sediments, bioturbation tends to reduce small scale lateral variability, although high densities of tube dwelling species stabilise the sediment surface, thus preserving heterogeneity. In sandy substrates, surface deposit feeders reduce lateral heterogeneity. In deposits where

the dominance of hydrodynamic and biological processes alternate a high degree of both lateral and vertical variability is obtained. Lateral variability is much less than vertical variability in deep sea environments [Briggs *et al*, 1985, Lambert *et al*, 1985].

Temporal variability exists on a variety of scales. Tidal and lunar variation can affect depositional texture and structure, and some organisms exhibit rhythmic activity patterns over these periods. In cohesive sediments, consolidation under gravity, dewatering and geochemical action is time dependent [Sills and Thomas, 1984]. 'Events' such as storms, large scale disturbance such as dredging or dumping, and pollution disasters, can also have a profound effect on sediment physical properties. Rhoads and Boyer [1982] have found that, in a post disturbance succession from opportunistic colonisers to equilibrium community, the physical properties of fine-grained surficial sediments are modified in different ways. Thus pioneering species tend to stabilise the sediment, while equilibrium species destabilise it.

Seasonal variability can affect hydrodynamic, textural and biological controls of surficial sediments. Shallow water environments experience a greater frequency of storms during the winter, which can cause freak disturbance and erosion of the bed. Seasonal water-column stratification can influence the supply of sediment. Many benthic organisms exhibit seasonal behaviour in activity, reproduction, dispersal and recruitment, either in direct response to temperature (with metabolic rates increasing by up to a factor of two per 10°C [Rhoads & Boyer, 1982]) or in response to seasonal sedimentation of detrital products from pelagic primary production [Honjo, 1976, Hargrave, 1980]. Benthic microorganisms also exhibit seasonality, and there is a temperature dependence on the rate of mucopolysaccharide production and degradation, which can affect adhesion [Yingst and Rhoads, 1980; Aspiras *et al*, 1971].

Investigation of the seasonal variability of sediment physical properties requires intensive sampling and has not yet been comprehensively addressed. Studies of sediment erodibility have shown that springtime benthic recruitment causes reduced sediment stability [Rhoads *et al*, 1978], while Grant *et al* [1982] suggests that seasonal changes in benthic primary productivity may be important in determining temporal patterns in

the erodibility of intertidal sediments. Myers [1977] reports strong seasonal variability in biological activity in a shallow subtidal pond, with sediment structure controlled by hydrodynamic processes in winter, macrofaunal activity in summer. Amos [1988] reported seasonal changes in the physical properties of intertidal mudflats, with a reduction in density during the summer combined with an increase in shear strength, due to the combined 'hardening' effects of sub-aerial exposure and high temperature.

In the longer term still, climatic and sea level change represent further scales of temporal variability. Although beyond the immediate scope of this study, current recognition of the urgency of prediction of the effects of long term change provides further impetus to the need for understanding controls on the history and fate of surficial sediments.

It is clear that any programme of sampling of the physical properties of surficial sediments must allow for, and preferably incorporate, assessment of spatial and temporal variability.

1.2. Geophysical properties of surficial sediments.

1.2.1. Introduction.

There are many problems associated with quantitative assessment of physical properties of unconsolidated sediments. The most important requirement of a technique is that it should provide accurate, repeatable measurements of an appropriate structural aspect of the sediment/pore-fluid system. In order to assess the complex structures reviewed in the previous sections, it must be possible to perform measurements *in situ*, or failing that on undisturbed cores. The actual measurement should involve a minimal degree of sediment disturbance. A further requirement is that the technique should measure over small length and depth scales, so that the near surface layers can be adequately characterised. It should also be possible to perform replicate measurements to enable appropriate resolution of variability: thus the technique should be as rapid and straightforward as possible.

To date, most investigations have utilised standard geotechnical techniques, modified to the particular requirements of marine sampling. Many conventional laboratory procedures cannot be adapted, because they involve introduction of a sample into a test cell. Those that have been more successfully applied *in situ* include: measurement of porosity from the dry weight of cores of known volume (or of water content from the ratio of wet to dry weight) to establish degree of packing; cone penetration to establish compaction or hardness; shear vane techniques to establish shear strength [Valent, 1974]. These techniques all involve extremely labour intensive coring and sub-sampling exercises, which explains the paucity of *in situ* data. Also, instruments such as the cone penetrometer and shear vane are strongly dependent on the particular device and procedure employed, which can lead to problems for intercomparison and conversion of measured properties to other properties of interest [Silva, 1974].

Recent developments in geophysical techniques and advances in modelling have led to increased interest in their application to remote sensing of physical properties of sediments. Geophysical properties, in their broadest sense, are macroscopic physical properties of the earth, its oceans and its surrounding atmosphere [Telford *et al*, 1976]. Albeit on a slightly less grand scale, geophysical properties of sedimentary deposits are also macroscopic physical properties, which govern the propagation of energy through, and distribution of potentials in, the sediment/pore-fluid system. They are therefore more fundamental (which does not necessarily imply more useful) than geotechnical engineering parameters, which in contrast generally relate to specific standardised tests. Also, in theory if not yet in routine practice, geophysical techniques for measuring propagation characteristics or potential distributions can be applied over a range of length and depth scales, enabling rapid and detailed data acquisition.

Geophysical techniques have been developed for exploration purposes based on gravity, electrical resistivity, magnetism, and mechanical stress-wave propagation. Over the past few decades there has been a considerable amount of work relating geophysical properties of sediments to properties of interest to construction engineers, to the oil industry, to naval operations and to marine and environmental scientists [Jackson *et al*,

1978; Stoll, 1980; Urish, 1981; Hamilton, 1982; Schultheiss, 1980, 1983; Taylor-Smith, 1983, 1985; Davis and Bennell, 1985; Lovell, 1985].

Of particular relevance to the study of surficial sediments are electrical properties and acoustic wave propagation characteristics.

1.2.2. Electrical Formation Factor.

The electrical resistivity of a saturated sediment (ρ_s) is a function of the electrical resistivity of the saturating fluid (ρ_w), the resistivity of sediment grains (ρ_g), the surface conductance of the grains or matrix conduction ($1/\rho_m$), and the relative volume and tortuosity of the pore-fluid matrix [Urish, 1981]. Pore-fluid resistivity is inversely related to temperature, salinity and pressure [Bradshaw and Sclacher, 1978]. For reasons which will become apparent, it is common to convert measured values of ρ_s to Formation Factor (FF), defined by:

$$FF = \frac{\rho_s}{\rho_w} \qquad (1.1)$$

Sand grains have a very high resistivity, so for pore-fluids of high salinity (low electrical resistivity) and clay-free sediment or sediment of low clay content, it is typically assumed that all of the electricity is conducted by the fluid through the pore space. In this case FF remains constant, and is known as the **Intrinsic Formation Factor.** It can be shown both theoretically [Sen *et al*, 1981] and empirically [e,g. Jackson *et al*, 1978] that FF is dependent only on porosity and tortuosity in these sediments. In other words, resistivity is controlled by the relative volume of fluid available for electrical conduction, the conducting path length and the degree of constriction of the pores. Thus it is a property which is controlled only by structural properties of the pore fluid matrix. For clay-rich sediments or low-salinity pore-fluid, FF varies as a function of pore-fluid resistivity and is known as the **Apparent Formation Factor.** For a spatially uniform ρ_w, however, which is common in many marine environments, variation in Apparent Formation Factor will also be controlled only by structural properties of the pore-fluid matrix.

A variety of techniques has been successfully developed for *in situ* measurement of ρ_s and ρ_w in surficial marine sedimentary deposits. Discussion of these techniques has been reserved until Chapter 4.

1.2.3. Geoacoustic properties.

Acoustic waves are small-strain mechanical disturbances which propagate through the sediment without disrupting the fabric. They can be considered as a limiting case in the more general category of mechanical waves which incorporate a wide range of strain amplitude and frequency [Stoll, 1980]. They are of key importance in marine environmental research, and have application in the fields of underwater acoustics, seismic profiling, engineering site exploration, and surface and near-surface imaging (e.g. sidescan sonar and high frequency backscatter systems).

Over the past thirty years, models describing acoustic propagation in porous media have been under development, with most being based on the seminal work of Maurice Biot [1956, 1962a, 1962b] and subsequent adaptation for practical predictive purposes by Stoll [1974, 1977, 1980], although a more empirical viscoelastic approach has been favoured by Hamilton [1974, 1980]. Fortunately, acoustic propagation is at low enough strains to enable mathematical handling using linear or quasilinear equations, based on elastic or "nearly elastic" operators. These models, which have been discussed in greater detail in the next chapter, predict that three kinds of stress waves can propagate in a fluid-saturated, porous medium: two compressional waves, where strain is in the direction of propagation, and a rotational or shear wave, where strain is perpendicular to the direction of propagation.

The theory allows viscous coupling between the fluid and solid components of the system which is dependent on the frequency of vibration and on the shape and relative volume of the pore-fluid matrix. The two kinds of compressional wave arise from two possible relative modes of vibration of pore-fluid and sediment framework. However, the second or 'slow' wave, which is a form of diffusion wave, is highly attenuated and has yet to be identified in saturated unconsolidated sediments [Stoll, 1980]. Compressional waves are strongly influenced by both pore-fluid and

sediment framework components. In contrast, since fluids have no shear strength there are no shear waves in fluids, and the rotational wave is least influenced by sediment/pore-fluid coupling [Nacci *et al*, 1974].

The two propagation characteristics most commonly measured are the velocity and attenuation, which are measures of the speed of energy transfer and the rate of dissipation of that energy respectively. For approximately linear response, and assuming perfect coupling between fluid and sediment motion, these can be related to bulk properties of the sediment/pore-fluid system. Shear wave velocity (V_s) is related to the dynamic rigidity modulus, μ and the bulk density (ρ_{bulk}) of the system:

$$V_s = \left(\frac{\mu}{\rho_{bulk}} \right)^{1/2} \qquad (1.2)$$

Compressional wave velocity (V_p) is related to the dynamic rigidity modulus and the bulk modulus or incompressibility, K:

$$V_p = \left(\frac{K + \frac{4}{3}\mu}{\rho_{bulk}} \right)^{1/2} \qquad (1.3)$$

Bulk sediment density is related to the density of separate fluid and solid components and to the porosity n by:

$$\rho_{bulk} = n\rho_{fluid} + (1-n)\rho_{grains} \qquad (1.4)$$

Since most sediment grains have very similar densities [5.1], ρ_{bulk} is most strongly controlled by porosity.

In unconsolidated sediments, the shear or dynamic rigidity modulus is primarily dependent on the number of grain contacts (and hence on porosity and grain size) and the strength of intergranular contact forces under shear stress, since the propagating shear disturbance must pass across these 'weak points' in the sediment framework. Thus V_s is strongly controlled by these intergranular contact forces and porosity. It is clearly related to the same factors which control shear strength and sediment erodibility.

In contrast, the bulk modulus (K) depends on three separate moduli: the bulk modulus of the pore fluid (K_w), the bulk modulus of the sediment grains (K_s) and the bulk modulus of the sediment framework (K_f) [Hamilton, 1971]. Their relative contributions to the overall bulk modulus are governed by porosity. K_w and K_s are virtually constant in many marine environments, so bulk modulus will vary with porosity and K_f. The framework modulus is controlled by number of grain contacts (and hence on porosity and grain size) and magnitude of intergranular contact forces under compressional stress. Since the rigidity of most unconsolidated sediments is much lower than their incompressibility, from (eqn 1.3) compressional wave velocity is most strongly controlled by K and porosity [Richardson and Young, 1980].

Attenuation of both shear and compressional waves is caused by dissipation of propagating energy through frictional or anelastic losses at the intergranular contacts, and through viscous losses if there is significant relative motion between pore-fluid and sediment framework [Stoll, 1980]. It is therefore controlled by number of grain contacts, nature of intergranular contact forces, and frequency of the propagated wave.

The velocity and attenuation of acoustic propagation are therefore related to structural properties of the sediment/pore-fluid system, and have great potential in assessment of surficial sedimentary deposits. To date, most progress has been made in characterising and interpreting compressional wave propagation. However, V_p is partially controlled by rigidity, and partial conversion of P-waves into S-waves occurs at interfaces, so there has been increasing attention paid to shear waves. Further, V_s is controlled primarily by properties of the sediment framework. It therefore complements the electrical Formation Factor, which is controlled primarily by properties of the pore-fluid matrix, and provides important additional information about intergranular contact forces.

Over the past few decades, there has been considerable interest in the development and application of geophysical techniques for various aspects of sea floor investigation. While the preceding justification for their use in assessment of surficial sediments is convincing, suitable *in situ* techniques have unfortunately lagged behind theoretical advances and laboratory investigations. Further development of geophysical techniques

to their full potential requires detailed and intensive acquisition of 'ground-truth' data, and *in situ* investigation of controls on the geophysical properties of sediments.

1.2.4. Bioturbation and geophysical properties.

There have been remarkably few specific studies of the effect of bioturbation on geophysical properties of sediments. Richardson and Young [1980] hypothesised that bioturbation by benthic organisms affects the geoacoustic properties of unconsolidated marine sediments. Subsequently Richardson confirmed this hypothesis by showing that highly bioturbated muds had lower compressional velocity and higher attenuation than moderately bioturbated muds, and that surface deposit feeders reduce compressional velocity and increase attenuation in sands [Richardson, 1983, Richardson *et al*, 1985]. The interpretation of these results has been incorporated into the more general discussion of bioturbation in Section 1.

At the time of this study, no *in situ* investigation of the effect of bioturbation on S-wave velocity or electrical Formation Factor had been reported. There was clearly considerable scope for further investigation.

1.3. Scope and objectives of study.

The primary concern of this study was to further the investigation of *in situ* variability in the physical properties of surficial sediments over a range of spatial and temporal scales, encompassing differences in sediment texture, hydrodynamic environment and biological activity. To this end, a novel approach based on the application of geophysical techniques was adopted. Two geophysical properties were selected, which can be directly related to complementary structural properties of the sediment: the Electrical Formation Factor (FF), which is primarily controlled by relative volume and shape of the pore-fluid matrix, and Acoustic S-wave velocity (V_s), which is primarily controlled by the nature of the grains and intergranular contacts within the sedimentary framework.

First, instruments for measuring *in situ* FF and V_s in surficial sediments were to be developed and tested, based on recently developed or acquired techniques and equipment.

Then, appropriate sampling was to be performed to examine the degree of variability in geophysical properties in surficial sediments. Spatial variability over scales ranging from centimetres to hundreds of metres, and temporal variability over a seasonal cycle were to be assessed. By simultaneous sampling of a range of standard sediment parameters the textural, biological and hydrodynamic controls on geophysical (and, by inference, structural) properties of the sediment could be investigated. In particular, the effect of spatial and seasonal variation in population density of benthic macrofaunal organisms was to be examined. Three autoecological categories, based on burrowing and feeding behaviour, were identified for their expected contrasting effects on sediment properties, namely:

(1) A sedentary burrowing deposit feeder (e.g. *Arenicola marina*)
(2) A mobile burrowing suspension feeder (e.g. *Corophium volutator*)
(3) A sessile tube building suspension feeder (e.g. *Lanice conchilega*)

By restricting sampling to exposed but saturated intertidal deposits the technological difficulties associated with developing techniques for undisturbed subtidal sampling were avoided. Further, two requirements justified limitation of the bulk of the sampling programme to sandy (cohesionless) sediments, as opposed to muds. First, the relatively hostile environments offered by intertidal sandflats restricted species diversity at any one location, thereby the problems of interpreting interaction in multispecific communities could be avoided. Second, characterisation of sedimentary deposits in terms of composition and granulometric parameters, and subsequent interpretation in terms of packing structure and intergranular contact forces, is less complex for sandy sediments than for cohesive deposits. This limitation, which was deemed unavoidable for this preliminary study, must nevertheless be removed for future experiments, to widen the scope of the investigation.

CHAPTER 2.

ACOUSTIC AND ELECTRICAL CHARACTERISTICS OF UNCONSOLIDATED SEDIMENTS: THEORETICAL CONSIDERATIONS AND CONTROLS.

The significance of acoustic and electrical properties of sediments has been outlined in Chapter 1, along with a brief introduction to their relationships with structural properties of the sediment/pore-fluid system. This chapter presents a brief review of theoretical and empirical investigation of these geophysical properties, with special emphasis on electrical Formation Factor (FF) and acoustic shear wave velocity (V_s), under conditions expected in surficial marine sedimentary deposits. Discussion of techniques for measurement of these properties has been reserved until Chapters 3 and 4.

2.1. Acoustic properties of sediments.

2.1.1. Theoretical background.

The mechanics of deformation and acoustic propagation in fluid-saturated porous media has received considerable attention over the past few decades Early advances include those made by Wood [1930] and Gassmann [1953]. The semi-phenomenological model developed by Maurice Biot in a series of classic papers [1956a,b; 1962a,b] has since been applied extensively in the interpretation of experimental data and is now generally accepted as an appropriate basic framework for the analysis of systems as diverse as porous rocks, unconsolidated sediments, snow and polymer gels [Attenborough, 1982; Johnson and Plona, 1984].

These two-component systems are characterised first by the fact that one component is a fluid and the other a solid, and second by the topological requirement that each forms its own infinite percolating cluster. The system can then be treated as two distinct interpenetrating 'effective

media' in which the average motions of fluid and solid constituents are followed separately.

The real power of this theory arises from the fact that it is based on semi-phenomenological operators which can be related to independently measured or calculated bulk parameters of the sediment/pore-fluid system [Hardin and Richart, 1963; Stoll and Bryan, 1974; Stoll, 1977, 1980; Domenico; 1977; Hovem and Ingram, 1979; Berryman, 1980a; Ogushwitz, 1984a,b,c]. This means that the need to formulate microscopic physical theories for prediction of these operators has been effectively bypassed, although some progress is now also being made in this area [Berryman, 1980b,c; Johnson and Plona, 1984; Bedford *et al*, 1984; Ogushwitz, 1984a].

The key underlying assumptions of the theory are as follows:

(1) The system is adequately described by two different displacement fields (commonly solid and relative fluid displacement)
(2) There is no force due to the relative displacement of the centres of mass of the two components (i.e, the fluid is interconnected throughout the sample)
(3) The fluid neither creates nor reacts to a shear force
(4) The system can be divided into volume elements which are large compared to the size of the pores (so that macroscopically averaged parameters such as porosity can be defined for the volume element) but small compared to the wavelength of the disturbance (to avoid scattering phenomena)
(5) The equations of motion are linear.

Within the context of this thesis, detailed theoretical consideration was not considered to be appropriate. The most general formulation requires fourth-rank tensors in the constitutive stress-strain equations governing deformation of the sediment framework and relative motion of fluid within the pores [Biot, 1962b]. A brief summary of the set of equations describing the simplest case of a macroscopically homogeneous, isotropic medium (in which the tensors can be replaced by constants from symmetry considerations) has been presented, taken from Stoll's formulation of Biot theory [1977]. The origin of relevant parameters is discussed and placed in context with properties of natural intertidal sandy deposits.

It is necessary to define four parameters: $\tilde{\mu}$ is the shear modulus of the sediment framework, $\tilde{K}_f$ is the bulk modulus of the sediment framework, K_s is the bulk modulus of the individual sediment grains and K_w is the bulk modulus of the pore water. Strictly, the mathematical formulations are only valid for materials where the sediment frame moduli are isotropic, homogeneous and linear (K_s and K_w are always assumed homogeneous and linear). However, Stoll [1977, 1980] decided that it was reasonable to allow for 'slight non-linearity' or heterogeneity provided that the frame undergoes the same volumetric strain as the pores (i.e. has only very limited internal degrees of freedom). Despite some criticism of this approach [Johnson and Plona, 1984; McCann and McCann, 1985] it remains necessary to include slight non-linearity in the frame moduli to account for the attenuation observed in dry sediments.

Consideration of energy and momentum conservation (based on linear Lagrangian dynamics) and the constitutive stress-strain relationships, combined with a frequency-dependent dissipation term to account for viscous attenuation created by relative fluid-solid motion, yields a set of equations of motion which have three non-trivial solutions, corresponding to three normal modes of vibration. They are the two compressional modes, which correspond to dilatational in-phase and out-of-phase relative motions of fluid and sediment frame, and the shear mode, corresponding to rotational motion of the sediment frame.

The two dilatational modes result in compressional waves of the first kind [FAST: fluid motion in phase with frame] and second kind [SLOW: fluid motion out of phase with frame]. The fast wave is always propagatory in character: the slow wave may be propagatory or diffusive, depending on frequency, frame stiffness, and properties of the pore fluid matrix [Johnson and Plona, 1984]. Since measurements of compressional wave propagation were not envisaged, a more detailed review was not considered appropriate. The literature offers substantial and detailed accounts of theoretical development and experimental verification, using laboratory and *in situ* data [Bell, 1979; Hamilton, 1980; Shirley, 1981; Berryman, 1981; Bedford *et al*, 1982; Schultheiss, 1983; Ogushwitz, 1984a; McCann and McCann, 1969, 1985]. A brief summary of the important controls has already been included in 1.2.

For the rotational mode, the equations of motion are:

$$\tilde{\mu}\nabla^2\psi = \frac{\partial^2}{\partial t^2}(\rho_{bulk}\psi - \rho_{fluid}\vartheta)$$

$$F(\kappa)\frac{\eta}{k}\frac{\partial\vartheta}{\partial t} = \frac{\partial^2}{\partial t^2}(\rho_{fluid}\psi - m\vartheta) \qquad (2.1)$$

Where: $\psi = \underset{\sim}{\nabla}\wedge\underset{\sim}{u}$

$$\vartheta = \phi\ \underset{\sim}{\nabla}\wedge(\underset{\sim}{u}-\underset{\sim}{U}) \qquad (2.2)$$

In the above equations $\underset{\sim}{u}$ is the frame displacement, $\underset{\sim}{U}$ is the fluid displacement, ρ_{bulk} and ρ_{fluid} are the total mass and fluid density respectively, η is the fluid viscosity and k is the coefficient of permeability of the porous frame. This will depend on porosity (ϕ) and on shape, disposition and tortuosity of the pore-fluid matrix, and it must be measured directly for natural deposits. Generally it is assumed to be proportional to the square of the pore size: for parallel uniform cylindrical tubes of radius r, then $k = \phi r^2/8$. For packings of uniform spheres and well-sorted sands of grain diameter d_g, permeability has been shown to obey the Kozeny Carman equation:

$$k = \frac{d_g^2}{36k_0}\frac{\phi^3}{(1-\phi)^2} \qquad (2.3)$$

The empirical constant $36k_0$ is necessary to adapt equations found for flow in parallel cylindrical tubes to the irregular pore shapes found in a loose aggregate [Carman, 1956]. k_0 has been found to lie between 4.0 (glass beads) and 5.6 (well-sorted sands) [Bell, 1979, Nolle *et al* 1963].

The parameter m in eqns. 2.1, is given by:

$$m = \alpha\rho_{fluid}/\phi \qquad (2.4)$$

This accounts for the fact that not all of the fluid moves in the direction of the macroscopic pressure gradient because of the shape and orientation of interstitial cavities. The parameter α is the 'inertial coupling factor' or 'structure constant', and is related to the tortuosity

of the pore-fluid matrix. It must be greater than 1, which is obtained when all pores are uniform and aligned along the pressure gradient. Several approaches have been suggested for determining the value of α [Johnson and Plona, 1984]. Berryman [1980] concludes that α may be derived from a microscopic model of relative fluid/sediment motion as:

$$\alpha = 1 - r_0(1 - 1/\phi) \tag{2.5}$$

with r_0 lying between 0 and 1, and with a value of 0.5 for spheres. It has also been shown that, for sands, α is simply related to the electrical Formation Factor by $\alpha = \phi FF$ [Johnson and Sen, 1981; Brown, 1980], since both are determined by solution of Poisson's equation with identical boundary conditions. This can be further simplified for well-sorted, well-rounded sands, since FF is known to be simply related to sediment porosity:

$$\alpha = \phi FF = \phi^{(1-m)} \tag{2.6}$$

As will be seen in the following section on Formation Factor, the coefficient m is approximately 1.5 for sands. Note that Berryman's result for spheres is only equivalent to this for $\phi = 1$.

The frequency correction factor $F(\kappa)$ accounts for the fact that the effective fluid-solid coupling changes when the viscous skin depth becomes smaller than the pore size as frequency increases. Provided that there is only a narrow distribution of pore sizes, it is given by:

$$F(\kappa) = \frac{1}{4} \frac{\kappa T(\kappa)}{1-2T(\kappa)/i\kappa} \tag{2.7}$$

where $T(\kappa)$ is obtained from derivatives of the Kelvin function and:

$$\kappa = \Lambda(\omega\rho_{fluid}/\eta)^{1/2} \tag{2.8}$$

Λ is a parameter with the dimension of length that depends on both the size and shape of the pores. For uniform cylindrical pores aligned along the pressure gradient, Λ is the pore radius: for well-sorted sands it has been found to correspond to between 1/6 and 1/7 of the mean grain diameter d [Stoll, 1974]. A theoretical estimate based on the Kozeny Carman

equation for the permeability of uniform spheres [Carman, 1956] yields:

$$A = \frac{d_g}{3} \left(\frac{\phi}{(1-\phi)} \right) \tag{2.9}$$

which compares favourably with Stoll's value [Hovem and Ingram, 1979].

For one-dimensional propagation in the x-direction, equations admit harmonic solutions of the form:

$$(\psi, \vartheta) \propto e^{i(\omega t - \tilde{\ell} x)} \tag{2.10}$$

where ω is the angular frequency and $\tilde{\ell}$ is a complex function of frequency from which, for each mode of vibration a phase velocity (ω/ℓ_r) and attenuation (ℓ_i) can be calculated.

Substituting harmonic ψ, ϑ into eqns. 2.1 yields the dispersion relation for shear waves. There is only one solution to this equation, yielding a complex-valued, frequency dependent root $\tilde{\ell}$ of attenuation a = ℓ_i and phase velocity $V_s = \omega/\ell_r$:

$$\tilde{\ell}^{\,2} = \omega^2 \left\{ \frac{\rho_{bulk} - (\phi \rho_{fluid} / \tilde{\alpha})}{\tilde{\mu}} \right\} \tag{2.11}$$

$$\text{where } \tilde{\alpha}(\omega) = \alpha - \frac{i \eta F(\kappa) \phi}{\omega k \rho_{fluid}} \tag{2.12}$$

Therefore it is possible to predict frequency-dependent velocity and attenuation for shear (and compressional) waves provided that the assumptions underlying the hteory are valid and that the following parameters are known:

(1) Bulk moduli of the sediment grains (K_s) and the pore fluid (K_w).
(2) Sedimentary framework moduli $\tilde{\mu}$ and $\tilde{K}_f$. Note that in the absence of an electrochemical interfacial effect these are independent of the pore-fluid, including a vacuum.
(3) Porosity, permeability and tortuosity of the pore-fluid matrix.
(4) A pore size parameter related to a characteristic radius of the pores.
(5) Sediment and pore-fluid density, and pore-fluid viscosity.

2.1.2. Factors controlling shear-wave propagation.

The theory outlined above can be used to investigate controls on shear wave propagation, although since it remains semi-phenomenological there are aspects which cannot be calculated theoretically as yet.

Frequency.

Both V_s and attenuation (a_s) can be modelled as functions of frequency, provided that the required input parameters can be estimated or measured. The important controls over the nature of frequency dependence are the structure constant α, the pore size parameter Λ, porosity and permeability, and fluid density and viscosity.

The function $(1/\tilde{\alpha}(\omega))$ (eqn. 2.12) is well-behaved at both low and high frequency limits. When the frequency is low enough that viscous effects in the fluid dominate inertial effects (when the viscous skin depth is large compared to any characteristic pore dimension Λ), $F(\omega) \Rightarrow 1$. Thus $\tilde{\alpha}(w) \Rightarrow \alpha + i\eta\phi/\omega k\rho_{fluid}$. This leads to a shear wave velocity which is more or less constant, and a viscous attenuation (a_v) which is proportional to the square of the frequency (neglecting sediment framework attenuation for the time being).

In the extreme low frequency limit, $(1/\tilde{\alpha}) \Rightarrow 0$ as $\omega \Rightarrow 0$. Viscosity causes the fluid motion to 'lock on' to that of the solid at low frequencies, for both fast longitudinal and shear modes [Gassman, 1951]. Assuming a 'nearly elastic' (small-damping) framework, i.e. a complex shear modulus ($\mu_r + i\mu_i$) which is independent of frequency, the phase velocity (V_s) and sediment framework attenuation (a_f) are given by:

$$\lim_{\omega \Rightarrow 0}(V_s^2) = \frac{\mu_r}{\rho_{bulk}} \tag{2.13}$$

$$a = \frac{\omega\delta}{2\pi V_s} \tag{2.14}$$

where δ is the constant log-decrement, $\mu_i = \delta\mu_r/\pi$. This is the viscoelastic model favoured by Hamilton [1976b].

If frequency is increased to the point where the viscous skin depth is much less than the pore size, then $F(\kappa) \propto \omega^{1/2}$ [Biot, 1956]. This leads to an approximately constant V_s and a viscous attenuation (a_v) which is proportional to the square root of the frequency. In the extreme high frequency limit, as $\omega \Rightarrow \infty$, $\tilde{\alpha}(\omega) \Rightarrow \alpha$, a real constant, so:

$$\lim_{\omega \Rightarrow 0}(V_s^2) = \frac{\mu_r}{\rho_{bulk} \cdot (\phi \rho_{fluid}/\alpha)} \qquad (2.15)$$

Thus at low frequencies, flow in the pores is laminar, speed is constant, and viscous attenuation varies as the square of frequency. At high frequencies the flow pattern is complex, speed is again approximately constant although higher than the low frequency case (comparing eqns. 2.13 and 2.15), and viscous attenuation varies as the square root of frequency. At intermediate frequencies, a transition zone exists. Experiment has shown that total attenuation must include frame losses in addition to viscous losses due to fluid/sediment coupling, since attenuation is still finite in the absence of pore fluid. Most models incorporate a constant log-decrement to account for frame loss, which results in a component of the total attenuation which is directly proportional to frequency [Stoll and Bryan, 1970; Bell, 1979; Stoll, 1980].

Fig. 2.1 illustrates V_s as a function of frequency for the input parameters corresponding to a well-sorted, medium-fine sand [Table 2.1]. The absolute magnitude of the low-frequency limit is arbitrary, being based on a typical value for sand. Assuming that the pore fluid is water, the transition zone between low and high frequency limits, and the difference between high- and low-frequency V_s, are controlled by α, Λ, k, and ϕ. These are all structural properties of the pore-fluid matrix which show marked sensitivity to textural, hydrodynamic and biological controls. Higher porosity, higher permeability (and hence larger Λ) result in a lower frequency transition zone, while the constant α controls the relative range in V_s (eqn. 2.15). Allowing for a natural distribution in Λ, and hence $F(\kappa)$, will have the effect of extending or 'smearing out' the transition zone.

There has been little progress in measuring the variation in V_s with

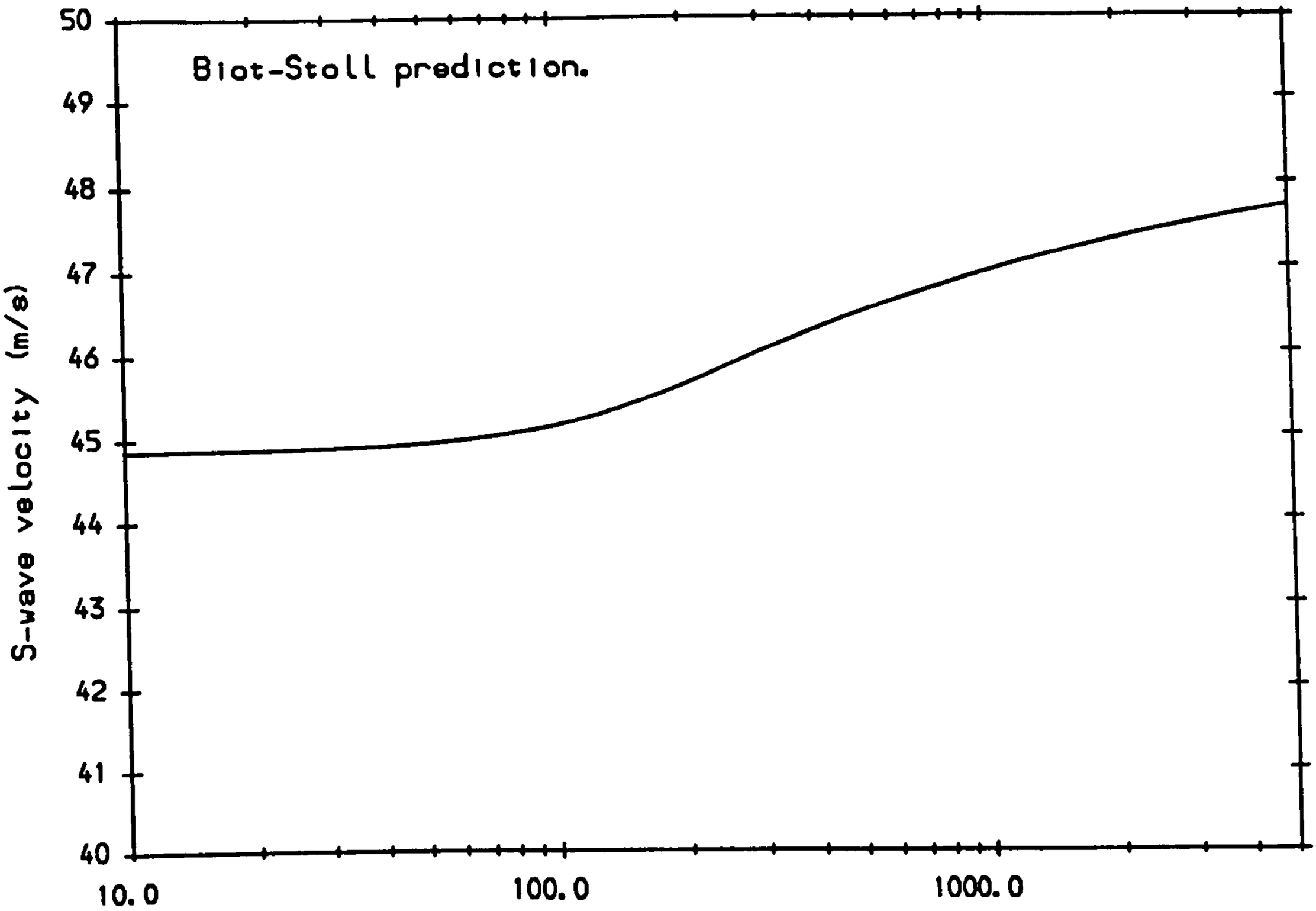

Figure 2.1. Predicted dispersion due to fluid/solid coupling.

Parameter	Symbol	Source	Value	Units
Fluid density	ρ_w	–	1.00	gcm^{-3}
Fluid viscosity	η	–	0.01	$dynsec/cm^2$
Grain density	ρ_g	–	2.65	gcm^{-3}
Grain diameter	d_g	(typical)	0.03	cm
Porosity	ϕ	(typical)	0.425	-
Bulk density	ρ_{bulk}	(1.4)	1.949	gcm^{-3}
Dry V_S	V_S	(arbitrary)	50.0	m/s
Dry log decrement	δ_S	(typical)	0.2	-
Permeability	k	(2.13)	0.1×10^{-5}	cm^2
Pore size parameter	Λ	(2.20)	0.0074	cm
Structure constant	α	(2.16)	1.53	-

Table 2.1. Parameters used for velocity dispersion prediction (Fig. 2.1).

frequency in sediments at low confining pressures, largely because appropriate techniques have been unavailable. Significant but relatively unimportant positive dispersion has generally been measured [Bell, 1979; Hurley, 1989]. There is also some evidence to support the predicted non-linear frequency variation in attenuation due to viscous interaction [Bell, 1979, Brunson, 1987].

The structural parameters of the pore-fluid matrix control relative variation in V_s and attenuation with frequency above given low frequency limits. Absolute values of V_s and attenuation in the low-frequency limit are controlled by the complex shear modulus $\tilde{\mu}$ and sediment density (which, for water-saturated natural sediments, is related directly to porosity). In fact these controls are much more important than dispersive effects. This can be seen from eqn. 2.11, where appropriate variations in α, A, and $F(\kappa)$ are of secondary importance to variation in $\tilde{\mu}$, and from Fig. 2.1, which illustrates a typical change in V_s of only a few percent over the full frequency range for a given frame modulus and porosity. This is true both for V_s and attenuation, with frame rigidity and intergranular contact losses tending to dominate over viscous and inertial coupling between sediment and fluid [Hamilton, 1976, Bell, 1979]. Thus V_s is most strongly controlled by μ_r and porosity (eqn. 2.13), while attenuation is controlled by V_s, frequency and the constant log-decrement (eqn. 2.14).

Frame shear modulus (μ_r).

As yet, no theory has been formulated to predict frame rigidity from microscopic considerations of the packing configuration and intergranular contact forces. Hardin and Richart [1963] proposed the following empirical formulation:

$$\mu_r = \frac{c(d - e_v)^2}{(1 + e_v)} p_a \left(\frac{\bar{\sigma}_0}{p_a} \right)^{2n} \qquad (2.17)$$

where e_v is the voids ratio, $\phi/(1-\phi)$, p_a is atmospheric pressure and $\bar{\sigma}_0$ is the effective stress. The constants n, *c*, *d* are generally adjusted to fit the experimental data. Alternatively, μ can be obtained directly from measurements of V_s in the dry sediment, or from measurements in the

extreme low-frequency limit of saturated sediment. This arises from the fact that μ is assumed independent of pore-fluid (and frequency), and therefore can be obtained from V_s measured at low frequencies (eqn. 2.13) or from V_s in dry sediment (eqn. 2.15, $\rho_{fluid} \approx 0$).

Controls on frame rigidity include any property which affects number of grain contacts or intergranular contact forces (Chapter 1). Thus porosity, grain roughness and angularity, and cohesion or adhesion will all affect μ_r, and hence V_s [Hamilton, 1971]. Several workers report relationships between V_s (and hence μ_r) and porosity, although data for fully saturated unconsolidated sediments at low confining pressures remain sparse. Hardin and Richart [1963] observed an inverse relationship between porosity and V_s for a given sediment. Hamilton [1976a] presented data from a range of depositional environments indicating a complex and highly scattered relationship between V_s and porosity, with maximum V_s at porosities obtained in fine sands: this is attributed to variation in frictional or cohesive effects, number of intergranular contacts and degree of interlocking. Schultheiss [1983] identified individual inverse V_s:ϕ relationships for a range of natural and artificial sands using a laboratory compaction cell, and isolates three broad categories based on grain size, shape and sorting. Pilbeam and Vaisnys [1973], Bell [1979] and Schultheiss [1983] report marked sensitivity of V_s to grain shape, with deposits of highly angular grains having higher velocity than those of similar porosity but well-rounded grains.

The frame modulus is also strongly dependent on effective stress, due to increased interparticle forces, and also in some cases to compaction of the sediment framework in response to stress. This is important in surficial sediments because effective stress is related to the self-weight of overlying sediment, leading to marked gradients in V_s [Hardin and Richart, 1963; Domenico, 1977; Bell, 1979; Hamilton, 1976a, Stoll, 1980; Davis, 1982; Lovell, 1983; Ogushwitz, 1984].

Frame log decrement (δ)

The frame logarithmic decrement is also an important contributor to the complex relationship in eqn. 2.11. Provided that it can be assumed to be

small and frequency-independent, it can be calculated from attenuation measurements under dry conditions, or in the saturated extreme low-frequency limit where viscous losses can be neglected [Hamilton, 1976b]. It arises from frictional or anelastic losses at the intergranular contacts, and will therefore depend on the number and nature of these contacts. Stoll [1980] discusses the additional possibility of viscous losses associated with the frame due to local 'squeezing' of fluid during deformation at the grain contact points. For small strains, the framework can be modelled as an assemblage of particles separated by slightly nonlinear 'springs'.

Shear-wave attenuation data are even more sparse than V_s. Hamilton [1976b] reviews available low-strain, low confining pressure measurements and concludes that attenuation is approximately linear in frequency, with values of δ lying between 0.1 and 0.6; and most likely to fall between 0.2 and 0.4 for saturated sands, 0.1 and 0.3 for silts and clays. In laboratory deposits under no confining pressure, Bell [1979] found generally higher values and a much wider range between 0.34 and 2.0, with a slight decrease with increasing grain size or angularity. There were also marked decreases associated with increases in effective stress due to overburden pressure.

Properties of the Pore fluid.

Pore fluid density and viscosity will affect both absolute values and frequency-dependence of V_s and a_s. As an extreme comparison, V_s measured in dry sand will always be higher than the low-frequency limiting value in saturated sand. This is supported by experimental observation [Hardin and Richart, 1963; Bell, 1979; Domenico, 1977]. Pore-fluid characteristics (such as salinity or temperature) will additionally influence cohesion and hence packing configuration in clays.

There is also marked dependence on degree of saturation. Conditions of partial saturation represent a more complex three-phase system, in contrast to the two-phase sediment/pore-fluid system which the theory describes. The presence of air within the pore-fluid matrix affects viscous fluid-solid coupling and density, and can also disrupt the

connectivity of the pore space, leading to isolated pockets of water or gas which will affect α.

Three basic sediment-water-gas systems may exist in a partially saturated sediment: 'Closed water', 'Closed gas' and 'Bi-opened' [Wu *et al*, 1984]. These describe whether fluid, gas, or neither phases are fully interconnected throughout the sample. In closed gas systems, small isolated gas bubbles in the pore-fluid matrix affect compressibility, density and viscosity of the pore fluid, and tend to be compressed, thus reducing effective stress (and hence μ_r, δ). In closed water systems, capillary forces around the grain contacts create negative effective pressures within the air spaces, thus increasing effective stress (and hence μ_r, δ). These effects have been observed using a resonant column apparatus (Wu *et al*, 1984] and geotechnical measurements of shear strength [Hryciw and Dowding, 1987; Wheeler, 1986].

2.1.4. Limitations of the theory.

Although recent developments in experimental techniques have enabled some encouraging comparisons between the Biot theory and experiment in simple sedimentary deposits, there are a number of limitations which must be borne in mind.

An important limitation of the theory is that it applies only to small-strain disturbances [e.g Stoll, 1980]. This leads to difficulties in the development and application of appropriate measurement techniques. It is well known that dynamic rigidity and shear attenuation are functions of strain amplitude [e.g. Seed and Idriss, 1970; Iwasaki *et al*, 1977; Davis and Bennell, 1985]. In order to incorporate variation in propagation characteristics with strain amplitude, the equations of motion must be non-linear, which leads to considerable mathematical complexity, although earthquake modellers have been making progress in this area. Fortunately, in all problems involving acoustic waves the amplitudes are small enough that the problem of non-linearity may be avoided. Dynamic rigidity is at a maximum limiting constant at strains less than 10^{-5}, and its subsequent reduction at increasing strain levels has been modelled as hyperbolic. Acoustic measurements correspond to the maximum value.

Perhaps the most important limitation from the point of view of this study is the requirement of macroscopic homogeneity. Unless an appropriately small volume element can be defined with a mean porosity, permeability and pore size; and unless a fairly narrow distribution of pore sizes is present, the underlying assumptions governing inertial and viscous coupling are invalid. Clearly this is the case for many natural sedimentary deposits which may contain a wide range of particle types and sizes, and which may have been subjected to hydrodynamic or biological re-working into strongly heterogeneous structures.

The theory is better able to cope with *anisotropy*: that is, where the sediment is macroscopically homogeneous but where the strain varies according to the direction of stress. By substituting 'quasi-elastic' tensors into the constitutive equations, a rather more complex set of dispersion equations is obtained with more roots corresponding to displacement in different planes within the sediment. For example, the commonly occurring case of transverse isotropy yields differences between vertically and horizontally propagating pairs of compressional waves, and differences between vertically and horizontally polarised shear waves.

In conclusion, considerable progress has been made in relating acoustic propagation characteristics to the microscopic textural and structural properties of a macroscopically homogeneous sedimentary deposit, and to other physical parameters. More generally, shear-wave velocity has been shown to be highly sensitive to structural properties of the sediment framework, and therefore to have great potential for assessment of sediment physical properties.

2.2. Electrical properties of sediments.

Electrical sounding has immense potential for non-destructive subsurface remote sensing of properties of sediments and sedimentary rocks. As will be seen in Chapter 4, all electrical sources employed during this study can be considered as direct current. Therefore the following discussion ignores skin-depth effects and other problems specific to alternating current.

The electrical resistance (R) of a volume of conducting material is related to the bulk resistivity (ρ) by a geometric factor (F) which accounts for the area available for conduction normal to the direction of current flow and for the current path length. As a simple example, for a cylindrical uniform conducting wire of radius *r* and length *L*:

$$R = \frac{\rho L}{\pi r^2}, \quad = F\rho, \quad F = L/\pi r^2 \qquad (2.17)$$

As a basic rule, resistivity is reduced on increasing cross-sectional area and increased on increasing path-length.

As has been seen for the theoretical treatment of acoustic propagation the macroscopic properties of a composite material, containing phases with very different physical properties, depend not only on the volume fractions of constituents, but involve interaction between them and are extremely sensitive to the geometry and topology of the boundary surfaces between phases. The physical difference between fluid and solid phases for acoustic properties is the absence of shear strength within the pore-fluid matrix. For electrical properties, the difference lies in the mechanism of conduction: via free ions in the saline pore fluid, free electrons in the solid (and hence not at all for most common sedimentary particles).

The electrical resistivity of a fluid-saturated sediment is a function of resistivity of the saturating fluid, shape and relative volume of the pore fluid matrix, resistivity of the sediment grains (and shape and relative volume of the sediment frame), and finally surface conductance along the sediment/pore fluid interfaces within the system [Patnode and Wyllie, 1950]. The basis for this surface conduction is the electrical double layer which forms at the solid/fluid interface: sediment grains have exposed unsaturated ions at their surfaces, so electrostatic attraction causes counterions in the pore fluid to migrate towards the interface, resulting in a conducting layer of increased ion density. As the ionic concentration of the pore fluid increases, this double layer is effectively compressed, so the conductivity is inversely related to salinity (although a maximum must occur at very low salinities, below which there are insufficient ions in solution to form the double layer). There is also a temperature dependence related to the kinetic energy of

the ions: they are less strongly influenced by electrostatic fields at high temperatures. For sands the phenomenon is only significant at very low salinities. It is much more significant for clay minerals, which have more excess charges on their surfaces due to their more open crystalline structure [e.g. Dyer, 1986]. .

Empirical 'parallel resistor' models of these controls have been used to examine the effects of grain conductivity and surface conduction [Patnode and Wyllie, 1950]. The measured resistance of a given macroscopically defined volume is viewed as a set of interconnected contributory resistors wired in parallel:

$$\frac{1}{R_{app}} = \frac{1}{R_w} + \frac{1}{R_g} + \frac{1}{R_m} \qquad (2.18)$$

where R_w, R_g are the resistances of the pore-fluid matrix and sediment frame respectively, and R_m is due to surface (matrix) conduction via the electrical double layer. As in eqn. 2.17, R_w can be written as:

$$R_w = F_0.FF.\rho_w \qquad (2.19)$$

where FF, the **Intrinsic Formation Factor**, is a geometric factor describing the relative volume and shape of the pore fluid matrix within the bulk volume considered, ρ_w is the pore fluid resistivity and F_0 is an arbitrary factor to account for geometry of the bulk sample. If the medium is macroscopically homogeneous and isotropic, then an arbitrary cross-sectional area will contain a fractional area of pore-fluid corresponding to the porosity (ϕ) of the sample [e.g. Biot, 1956]. The conduction path through the pore-fluid matrix will be a function of the tortuosity (T) of the pore space. Therefore, by simple arguments it is clear that FF should depend on ϕ and T. ρ_w is inversely related to both temperature and salinity, since it will be reduced if the free ions in solution are either at higher concentration or have higher thermal energy, as has been illustrated in Chapter 4 (Fig. 4.6).

Similarly, R_g is a function of the grain resistivity (ρ_g), F_0 and a complementary geometric factor to account for the relative size and shape of the sediment frame. Perhaps fortunately, the resistivity of most common sedimentary particles is very much higher than that of the pore-fluid or

the matrix conduction effect, so in general its reciprocal in eqn. 2.18 can be disregarded.

A 'matrix resistivity' ρ_m is also defined such that $R_m = F_0 S_g \rho_m / d_L$. d_L is the thickness of the electrical double layer while ρ_m is a function of the concentration and mobility of excess ions within it. (ρ_m/d_L) will depend on grain mineralogy (and hence surface electrostatic charges) and pore-fluid salinity, pH and temperature. S_g is a geometric factor with units of length related to total available grain surface area and conduction path length. It will therefore depend on grain size (since there is much greater surface area in a given volume of finer sediment), porosity (which determines the number of grains in a given volume) and tortuosity (which determines the current path along the grain surfaces).

Eqn. 2.18 can therefore be rewritten as:

$$\frac{1}{\rho_{app}} = \frac{1}{FF\rho_w} + \frac{d_L}{S_g \rho_m} \qquad (2.20)$$

As indicated in 1.2, it is common to define an Apparent Electrical Formation Factor ($FF_{app} = \rho_{app}/\rho_w$) which on substitution yields:

$$FF_{app} = \frac{FF}{[1 + FF(d_L/S_g)(\rho_w/\rho_m)]} \qquad (2.21)$$

For sands and most clays at low pore fluid resistivities (which is the case for sea water), the ratio $(d_L\rho_w/\rho_m)$ is negligibly small, so the apparent Formation Factor is equivalent to the intrinsic Formation Factor [Hill and Milburn, 1956]. However, for fine sands saturated with very high resistivity pore fluid (greater than 2000 ohm-cms [Urish, 1981]), or for sediments with significant clay content, the dependence of FF_{app} on fluid resistivity may have to be considered.

For a given grain texture, most sediments have been shown empirically to obey Archie's Law [Archie 1942; Winsauer, 1952; Wyllie and Gregory, 1953; Atkins and Smith, 1961; Boyce, 1968; Taylor Smith, 1971, 1975, 1985; Erchul and Nacci, 1972; Barnes *et al*, 1972; Windle and Wroth, 1975; Jackson, 1975, 1978; Lovell, 1984]. This relates bulk mean sediment

resistivity to mean porosity, along with an empirical exponent (m) which is related to the tortuosity of the pore-fluid matrix:

$$FF_{app} = \frac{\rho_{app}}{\rho_w} = a_F \phi^{-m} \qquad (2.22)$$

Generally, a_F is approximately 1 for clean marine sands. This is fortunate, because in the limit as $\phi \Rightarrow 1$, both FF_{app} and FF must also tend to 1 (no sediment phase). A non-unit value of a_F is often found for clay-rich sediments [Boyce, 1968; Lovell, 1984]: FF_{app} should still tend to 1 in the high porosity limit, but the denominator in eqn. 2.21 will also change with increasing porosity (i.e. $d_L/S_g\rho_m$ will become negligibly small as sediment framework connectivity is destroyed in the high porosity limit). If the intrinsic Formation Factor is assumed to obey Archie's Law (by analogy with the clean sand case) then

$$FF_{app} = \phi^{-m}\left(1 + \frac{\phi^{-m}\rho_w d_L}{S_g\rho_m}\right)^{-1} \qquad (2.23)$$

Note that, while S_g should be related to porosity, unless it exactly cancels the porosity term in this equation, a_F cannot be a constant. However, for the relatively low porosity ranges usually encountered for a given sediment, it may be approximately so, especially since $(d_L/S_g\rho_m)$ is generally small [Bikerman, 1970].

Although models of the double layer effect have been formulated: [e.g. Pfannkuch, 1969] there are as yet no detailed microscopic models for the prediction of matrix conduction as a function of porosity, grain size and mineralogy, pore fluid salinity, and packing configuration. Therefore work in muddy sediments remains largely empirical. There has been rather more success with models of sand-sized sediments and sedimentary rocks, which have been critically reviewed in Sen *et al* [1981]. They include capillary tube/network models; percolation theories; and effective medium theories. Matrix conduction, and conduction by the sediment grains, can be effectively ignored in these sediments.

Modelling the conducting properties of fluid-saturated sediments involves solution of Maxwell's equations, in which an effective dielectric response

appears which includes a frequency dependent dielectric term and the (frequency-independent) sediment resistivity. [Landau and Lifshitz, 1960]. Only the theoretical considerations which affect sediment resistivity are discussed here.

Sen *et al* have developed a theory of the complex dielectric response of a clay-free sedimentary deposit based on a simple, realistic geometric model which guarantees continuity of the fluid-filled pore space. Since clay-free sediment grains are effectively insulators, this requirement of continuity is essential for finite direct-current ρ_s.

The model utilises multiple scattering techniques in which physical behaviour of a random system is divided into two parts: an average property and second-order fluctuations or perturbations around that average. The sediment as an assemblage of a large number of arbitrarily sized cells, each consisting of a spherical insulating particle coated with a film of fluid. Sen *et al* concluded that a single site self-consistent effective medium approximation (which considers each cell to be subjected to a local electric field which has been averaged over all other cells) was too simplistic, and found that the local environment around each sediment grain must also be considered. This was achieved by considering gradually increasing clusters of cells, where the grains are surrounded not only by fluid but by other grains as well. This results in numerically complex solutions which have only been solved for some simple cases. For example, for uniformly coated spheres at porosity less than 0.5 they compute an effective dielectric constant from which FF can be obtained:

$$FF = \phi^{-3/2} \tag{2.29}$$

This agrees extremely well with empirical observations for well-sorted, well-rounded sands [Taylor Smith, 1971; Barnes *et al*, 1972; Windle and Wroth, 1975; Jackson, 1978], and more detailed predictions of the theory were verified using controlled experiments with glass beads. Subsequent extensions of the model have included the effects of ellipsoidal particles [Mendelsohn and Cohen, 1982; Sen, 1984]. The model allows for oblate (disc-shaped) and prolate (needle shaped) ellipsoids.For randomly distributed ellipsoidal grains, Archie's Law is also obtained but with a value of m higher than 3/2, and highest for highly oblate grains. This

also agrees with empirical observations for oblate (plate-like) particles. For example, both Atkins and Smith [1961] and Jackson, [1978] showed that m increased as the constituent grains became more plate-like, with values of 1.8-2.0 for kaolinite and illite, 1.9 for shell fragments, and 3.0 for montmorillonite. The Sen model is formulated for cells (and hence coated particles) of arbitrary size: this suggests that FF is not strongly dependent on grain size or size distribution, but on porosity and grain shape. This is supported by Jackson's experiments on artificial sand mixtures [1978], where no consistent dependence of m on either size or spread of sizes was identified (although the maximum and minimum porosities obtained, and hence ranges in FF, were affected (Chapter 1).

Limitations of the theory.

The major limitation to the theoretical explanation of Archie's empirical Law is its restriction to relatively clay-free sands, or to sediments saturated by highly saline pore fluids, since matrix conduction has not been accounted for in the formulation. It also applies only to two-phase media: the partially saturated case involves further complexity.

There are further limitations to the application of Archie's Law itself. It is obvious that this simple relationship, while apparently highly successful for macroscopically homogeneous haphazard packings, will be less applicable in heterogeneous sediments, for example those containing hydrodynamic or biogenic structures. Even macroscopically homogeneous deposits may be anisotropic, resulting in different fractional areas (and hence conductivity) of pore fluid along different planes within the sediment. It is this fractional area along the direction of current, rather than volume porosity, which controls FF.

In conclusion, there has been some success in theoretical modelling and identification of empirical controls on electrical Formation Factor in unconsolidated sediments. FF has been shown to be primarily dependent on structural properties of the pore-fluid matrix: namely, its relative volume and tortuosity. These are governed by porosity and grain shape in macroscopically homogeneous and isotropic sediments: additional controls would be anticipated in sediments exhibiting structural heterogeneity.

CHAPTER 3.

AN ACOUSTIC SHEAR-WAVE PROBE: DESIGN, TESTING AND PRELIMINARY LABORATORY WORK.

3.1 Methods of measuring V_s in unconsolidated sediments: background

The official ASTM recognised method of measuring V_s in the laboratory uses the resonant column [Hardin and Richart, 1963]. A cylindrical soil (sediment) specimen is placed in this apparatus and forced to vibrate in torsional mode. The angular frequency is varied until a resonant peak is obtained which is a function of V_s, sample length and shear strain [Bennell *et al*, 1984]. Apart from being an excellent laboratory technique for the determination of V_s of both cohesive and non-cohesive samples, it has several additional advantages. In particular, V_s can be investigated over a range of shear strain amplitudes, which is of fundamental importance in earthquake modelling and in the design of structures subjected to dynamic loading [Hardin & Drnevich, 1972]. A further advantage is that the system can be used as a triaxial cell so that the effect of varying confining pressure and axial load can be measured, which allows simulation of *in situ* conditions such as depth of burial.

There are also, however, some disadvantages. The resonant column system is difficult to incorporate into other laboratory tests which could benefit from simultaneous measurement of V_s. A more fundamental problem is that some degree of sample disturbance is involved during coring, transportation, preparation and mounting in the cell, so that *in situ* conditions cannot be reliably reproduced. Finally, the technique is completely unsuitable for *in situ* deployment.

Appropriate alternative geophysical techniques are without exception based on generation of a transient or continuous shear-wave disturbance, propagation through the medium of interest, and sensing and characterising the propagated energy as a function of distance from the source. This has

the advantage of being a direct, non-destructive technique which can be performed *in situ* in undisturbed deposits, provided that efficient generation and detection of a relatively pure, appropriately polarised shear displacement can be achieved.

The specific requirements for this project were:

(1) Generation and detection of a shear-wave in saturated, unconsolidated sediment under atmospheric conditions (i.e. at low confining pressure) over length and depth scales of centimetres.
(2) Minimal sediment disturbance on deployment.
(3) Robust, weatherproof, battery-powered and portable equipment.

Until comparatively recently, achievement of these requirements has proved problematic. Unconsolidated sediment has a high compliance, especially at low confining pressure, and for efficient transfer of energy the source compliance should correspond as closely as possible to that of the sediment. Further, shear waves are highly attenuated, this attenuation increasing rapidly with increasing frequency. Therefore the operating frequency band-width of the source should extend as low as possible to minimise signal degradation over reasonable path lengths. Finally compressional waves travel faster than shear waves and are less highly attenuated. Therefore, if they form a significant component of the transmitted disturbance they may interfere with the shear wave arrival at the receiver.

These problems are primarily associated with the physical properties, geometry and positioning of both source and receiver, although signal processing techniques can also be used to improve a shear wave data acquisition system. A variety of solutions have been successfully developed for a range of length and depth scales of measurement for both land-based and offshore applications over the past two decades. [Viskne, 1976; Stoll, 1980; Davis & Schultheiss, 1980; Bennell *et al*, 1982; Whitmarsh & Lilwall, 1982; Gehrman *et al*, 1985; Hepton, 1988; Davis *et al*, 1989]. For small-scale and laboratory cell measurements, development work has concentrated on piezo-electric transducers, which deform when a potential difference is applied across them, and conversely produce an

electrical signal on deformation. Therefore they can be used both as electronically driven sources and as receivers. Both polarisation of the transducer relative to the applied potential and its mechanical properties must be selected to generate, and respond to, shear deformation in the medium of interest.

Early laboratory applications met with only partial success. Laughton [1957] used specially cut quartz crystals to measure shear waves in ocean bottom sediments, but only at very high compaction pressures. Celikkol and Vogel [1973] used transducers mounted on aluminium probes, but were unable to measure V_s in sediments with water content greater than 35%, despite a transmitter-receiver separation of only 7mm. Stephenson [1978] has described V_s measurements using piezo-electric radial expanders with a resonant frequency of 90kHz, but Schultheiss [1983] suggests that his anomalously high V_s values were due to incorrect interpretation of received signals as shear wave arrivals. More recently James [1987] has reported using transducers in a commercially available 'Pulse Shearometer' for laboratory-based rheometric studies of high porosity clays.

3.2. Development of the piezo-electric bender element.

The most significant developments in small-scale shear wave transduction were made by Shirley and associates at the Applied Research Laboratories, Austin, Texas. Shirley (1975) first recognised the potential of piezo-electric ceramic bender elements as shear wave transducers, with the primary aim of designing an *in situ* V_s measurement system for use in conjunction with compressional transducers attached to the cutter of modified sea floor coring equipment [Shirley & Anderson, 1975].

A bender element consists of two piezo-electric transverse expander plates, commonly manufactured from lead zirconate and lead titanate, which are bonded together along one of their electrode surfaces (Fig. 3.1). They can be in two configurations depending on whether the plates are to be connected in series or in parallel [Scultheiss, 1983]: for simplicity only the series connected version is described here. The plates are oppositely polarised so that, on application of a potential difference across the

plates, one plate expands whilst the other contracts. This results in bending of the transducer (analogous to a bimetallic strip thermostat), which when appropriately coupled to the surrounding medium will cause shear wave propagation parallel with, and polarised perpendicular to, the plane of the plates. Their overriding advantage is that their thin (0.5mm) plate geometry exhibits higher compliance and lower resonant frequencies than other types of transducer, resulting in better mechanical coupling with the sediment and less attenuated signals.

Much of the design effort at ARL was expended on composite transducers comprising several stacked bender elements which were designed for robustness so that only the end of each element was in contact with the sediment [Shirley & Bell, 1978]. Almost as an offshoot from the main programme, single bender elements were recognised as eminently suitable for laboratory monitoring of shear wave propagation characteristics of unconsolidated sediments [Shirley *et al* 1979]. Single bender elements are positioned so that they are completely surrounded by the sediment, so that maximum coupling, and hence energy transfer, is possible. A further advantage is that they can be vertically inserted into a sedimentary deposit with very little disturbance, which makes them ideally suited to *in situ* work.

Schultheiss spent some time working at ARL, then transferred to UCNW and continued his work with bender elements. Versions were mounted in three laboratory cells to further basic research into shear waves in saturated sediment [Schultheiss, 1981]. An *in situ* probe for sea-floor measurement was also developed and used with reasonable success [Bennell *et al*, 1982]. Measurements were made over probe separations of 80mm in the top 100mm of the sea bed, using robust transducer housings mounted on an adapted seafloor sledge. A sensible range of *in situ* V_s values was obtained, albeit with a considerable degree of sediment disturbance within the zone of measurement. Nevertheless the technique was shown to be feasible, and remains ripe for further development.

Since 1983 work at UCNW has concentrated on improvement of transducer design and signal processing techniques, and collection of much-needed data for model testing and empirical comparison with standard geotechnical

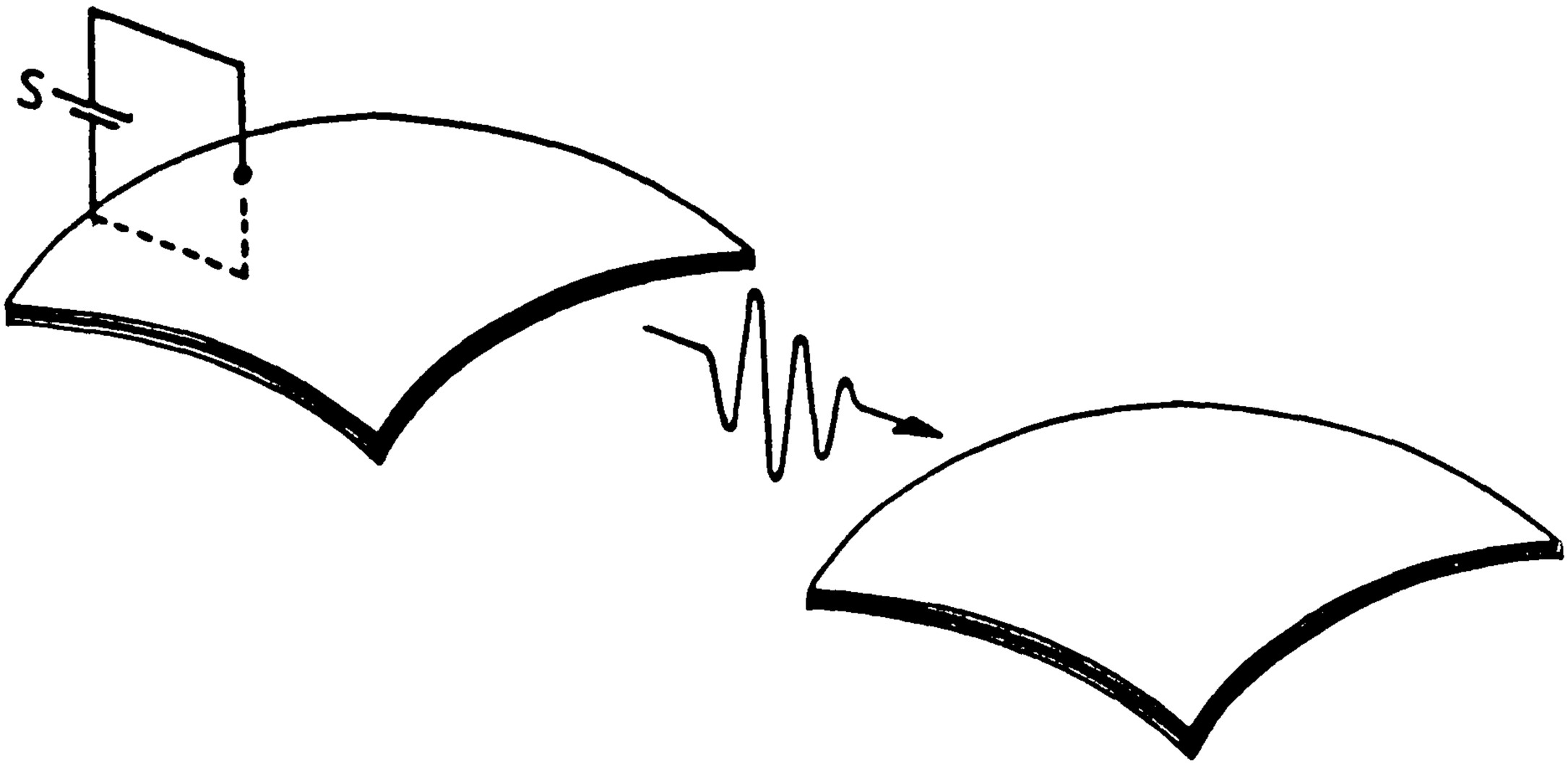

Fig. 3.1. The piezoelectric bender element

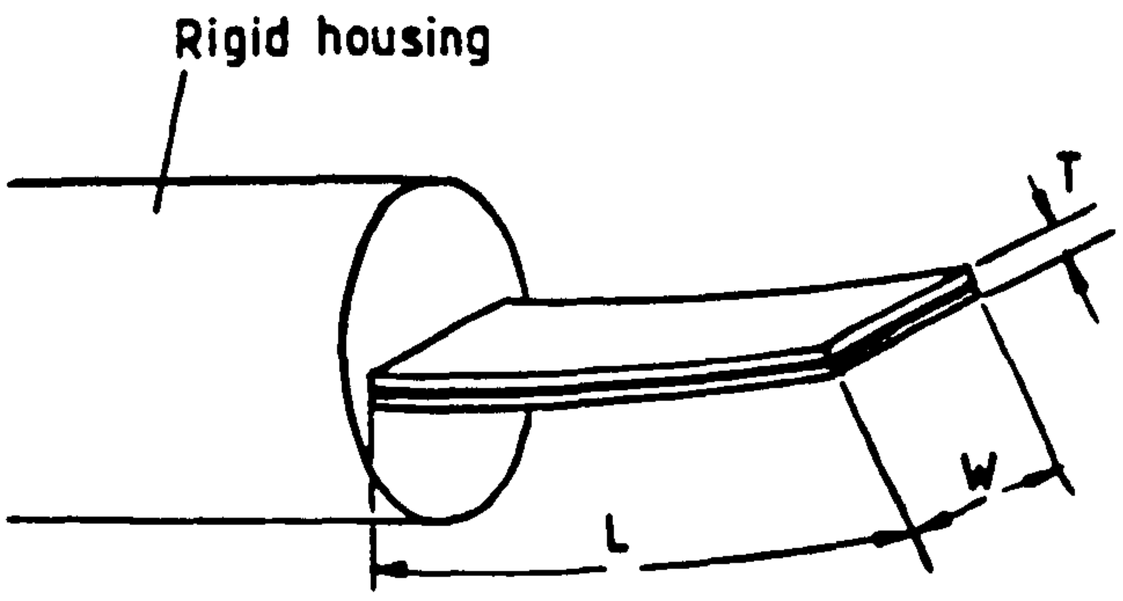

Fig. 3.2. Cantilever mounted bender element.
(before resin encapsulation).

parameters. Perhaps most importantly, bender elements have been mounted in a triaxial resonant column [Bennell *et al*, 1984] which has provided an opportunity for intercalibration of the two techniques. To date, excellent agreement has been obtained between V_s measured using bender elements and V_s(max) measured using the resonant column, for a variety of sediment types and over the full operating range of the column [Davis & Bennell 1986, Hurley 1989, Hepton, 1989]. In addition, this work has been independently confirmed in a different resonant column using transducers donated by UCNW [Dyvik & Madshus, 1986]. Note that bender elements operate in the low shear-strain regime, so that V_s measurements yield the maximum limiting value of the rigidity modulus.

3.3. A shear wave probe for small-scale *in situ* measurement of V_s.

Background.

The proven design advantages of the single bender element for generation and detection of shear waves in unconsolidated sediment made it the obvious choice for this study. The major disadvantage which had led to its rejection for *in situ* application at ARL was its lack of robustness. Fortunately, this was not a problem for the proposed deployment in intertidal deposits.

Although the bender element is a standard commercial product, there is considerable scope for selection of transducer properties by varying the bimorph geometry, mode of mounting and housing design. All probes must consist of a support, an electrical connection to the exposed transducer electrode surfaces, and a means of insulation of these electrodes from the surrounding (and conducting) saturated sediment. The last usually involves encapsulating the transducer in epoxy resin.

Naturally the shape and size of the transducer, the physical properties of the encapsulant and the mode of fixing of the plate to its support will all affect the response of the probe: in particular, its resonant frequency and maximum generated displacement. The design used most extensively at UCNW consists of a cantilever-mounted series-connected

VERNITRON PZT5BN bimorph element encapsulated in 0.5mm thick Araldite (Fig. 3.2). The semi-rigid resin acts as a support for the element, thus removing the requirement of a frame. This has the advantages of compact size, ease of incorporation into laboratory test cells and relatively straightforward and documented electromechanical properties.

Although, as will be shown, this particular design was not in the event adopted for *in situ* V_S measurement, its well-understood properties can be used to illustrate the effect of variation in basic design on the performance of a transducer. Fig. 3.2 defines appropriate symbols. The following definitions have been taken from VERNITRON product specification literature [Bulletin no. 66012/D]. Listed constants have been replaced for generality by constants of the form α_i, each representing a constant depending on the manufacture of the bimorph, the mode of mounting of the plate, and the units of length used.

The resonant frequency of the element when operating in air is given by:

$$f_R = \alpha_f \frac{T}{L^2} \tag{3.1}$$

while the maximum free end displacement in air is given by:

$$D_{max} = \alpha_d \frac{L^2}{T^2} \tag{3.2}$$

Note that the width W does not affect either resonance or displacement, because in the configurations considered the element is rigidly constrained along this dimension. These formulae do not apply to transducers which are free to bend in both length and width modes.

Using the above equations, it is possible to explore the effect of varying basic properties of the transducer plate on its performance. It is clear that increasing the length of the element causes a reduction in resonant frequency and increase in displacement. Both of these effects are desirable, provided that the increased displacement is still within the small-strain regime, and that the plate remains coupled to the sediment, so that the increased displacement is translated into increased propagating shear wave amplitude.

The effect of encapsulation in a semi-rigid potting compound can be simply related to an increase in T, typically by at least an order of magnitude. This will result in increased resonant frequency and reduced free-end displacement. The situation is complicated because behaviour will be additionally affected by the elastic moduli of the encapsulant, which may be different from the transducer, and which should change the values of the constants α_i. Recent work using 15mm cantilever-mounted transducers encapsulated in 0.5mm thick Araldite showed an increase in air resonance from 500 - 900Hz and a reduction in free-end displacement from 380 to 24 μm for 33V (r.m.s) excitation [I. McDermott, *pers. comm.*].

The effect of inserting the bimorph plates into sediment will clearly have an even more drastic effect on transducer response. Full discussion of this has been reserved until Section 3.4.3.2. In general, resonant frequency should be increased, and displacement should be reduced still further, because the sediment will act to confine the transducer. However, this ignores the response of the sediment itself. It has been suggested that a bender element will be most sensitive when the wavelength of the propagating disturbance corresponds to a multiple of the vibrating length of the probe [Shirley, 1978], provided that the transducer is mechanically capable of responding at the appropriate frequency, and is perfectly coupled to the medium.

The cantilever mounted bimorph has proved highly successful at UCNW, is now reasonably well understood, and has been calibrated in a resonant column. There have been some problems, which were highlighted by Hurley [1989]. Most of these relate to the detection of compressional components in the received pulse, which interfere with shear wave onsets, especially at high confining pressures. The rigid mounting of the probes can also result in energy transmission through the cell walls which affects signal interpretation. Considerable progress has now been made in interpreting received signals and in digitally filtering out these unwanted components. However, an additional drawback is that their necessarily small size and rigid encapsulant results in an operating frequency in saturated sediment of 2-5kHz, which typically exhibits attenuation of *c.* 100dB/m [Shirley *et al*, 1979]. This can be dramatically reduced to *c.* 25dB/m by reducing the operating frequency to 1kHz.

For this reason, and because for this application the probes were not restricted by laboratory test-cell dimensions, a different probe design was selected for *in situ* measurements. Design and construction was undertaken by Dr. J. Bennell, with the specific requirements of the project in mind.

Schultheiss [1983] conducted experiments to establish the best configuration of two rectangular bender elements for transmitting and receiving shear wave signals in dry sand. He found that by far the best signal was obtained when the plates were positioned unclamped and with their longer edges parallel. Note that these transducers are free to bend in both length and width modes, therefore are not directly comparable to the cantilever-mounted case. Also, the optimisation procedure was performed using a transmitter/receiver system in sediment, so that arguments used to explain unloaded transducer behaviour can no longer be applied.

The probes were therefore constructed so that the transducer plate was suspended without rigid fixing in a protective stainless steel housing, held in position by epoxy resin encapsulant [Fig.3.3]. Naturally this does not completely satisfy the requirement of lack of constraint, since the potting compound possesses some rigidity and bonds the transducer to the housing. However, by selecting a highly flexible encapsulant it was expected that the transducer plate would be effectively decoupled from the rest of the probe.

The probe is designed to generate horizontally polarised shear waves, by vertical insertion into the sediment. Since natural deposits should display shear wave anisotropy, it would have been desirable to monitor vertically polarised propagation in addition. Unfortunately the bender element is unsuitable for use in this mode without unacceptable levels of sediment disturbance. The problem of *in situ* generation and detection of S_v waves over small spatial scales remains unresolved.

The transducer size selected represents a trade-off between the requirement for a high amplitude/low frequency signal and the need to minimise sediment disturbance and accurately monitor vertically

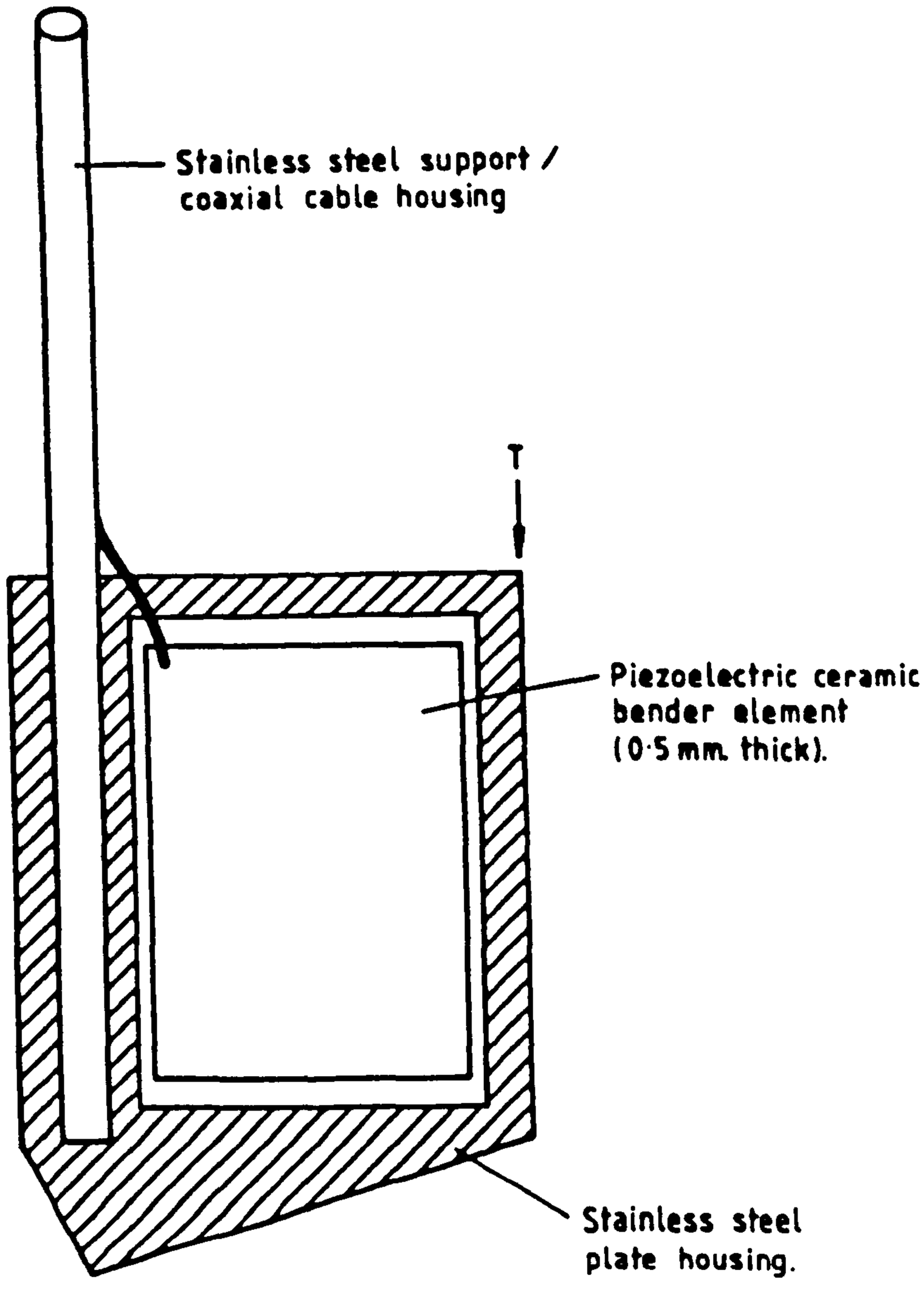

To scale

Fig. 3.3. Probe for in-situ shear wave characterisation.

heterogeneous deposits. This involved erring on the side of good signal quality, and therefore, as will be seen, sacrifice of resolution of near-surface velocity gradients.

The probes were not mounted on a supporting frame-work for two reasons. First, the intended mode of deployment required a variable probe separation (and a facility for removal and reinsertion of the receiver), which would have involved considerable mechanical design complications. Second, one of the major problems of interpretation of S-wave signals is caused by transmission of signals through rigid connections instead of through the sediment. The reduction in accuracy of separation measurement incurred by avoiding a rigid frame was felt to be justified in the light of this.

A set of much smaller probes was also constructed, for monitoring over smaller sediment volumes (Fig. 3.4). They were produced from bimorph off-cuts, and represent the best that could be achieved at the time. However, this design could be improved considerably, probably using a longer cantilever-mounted bender and more flexible encapsulant.

Transducer development is still under way at UCNW. McDermott [1991] has mounted a series of 0.9kHz (15mm) bender elements in a consolidation column, for monitoring the change in V_s with depth and time in cohesive sediment deposits. Current projects include a system for monitoring V_s profiles in the near-surface of cohesive deposits, both *in situ* and in a laboratory flume, and relating them to erodibility of the bed. Future development of *in situ* probe design will focus on providing better resolution of depth gradients in the near surface layers, and wider operating frequency ranges.

3.4. Laboratory investigation of the transducer-sediment system.

3.4.1. Experimental objectives.

The basic design of the ceramic bimorph transducer has undergone extensive development and testing under a variety of conditions and configurations,

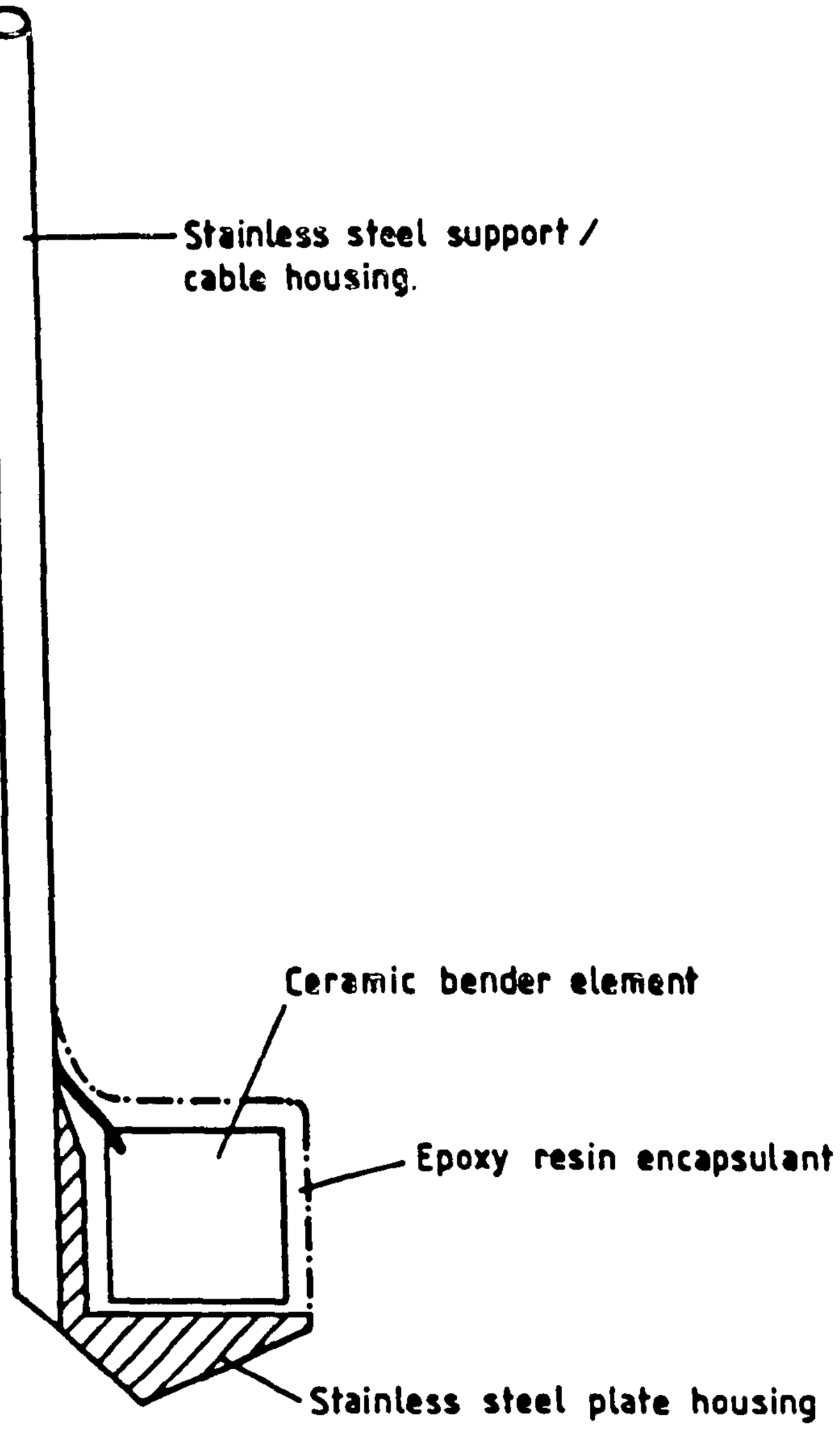

To scale

Fig. 3.4. Small laboratory shear wave probe.

and has been adapted for a number of field and laboratory applications. The S-wave probes constructed for this particular study, although in principle identical to other probes developed at ARL and UCNW, represented a further advance in design based on previous experience as well as a specific adaptation for the project requirements. Hence some laboratory based investigation of the new probes, and of the proposed deployment configuration, was justified.

First, a preliminary investigation of the properties of the transducer/sediment system was performed. Potential problems specific to the proposed mode of deployment in surficial intertidal sedients were then investigated, in particular the effect of near-surface vertical gradients and the degree of saturation. An experimental strategy for subsequent field measurements could then be designed based on measured transducer and sediment characteristics. Finally the effect of artificial macrofaunal burrows was investigated under laboratory conditions, in order to isolate one important biogenic sedimentary structure from the expected complex biological and textural interactions *in situ*.

The order in which the experimental results have been described and discussed does not in fact represent a chronological sequence. The laboratory assessment facility was set up as a permanent back-up to ongoing field-work, as well as a means of testing equipment before deployment. As questions arose, especially during the early stages of the study, laboratory experiments were conducted to aid interpretation of *in situ* observations. Also, delays in supply of the bimorph transducer plates meant that six months had elapsed before the custom-built S-wave probes could be deployed. During this time the bulk of the work with artificial burrows, and some preliminary investigation of surficial propagation under varying sediment conditions, were carried out using probes designed and constructed by P.J. Schultheiss for a rather different application [Schultheiss, 1983]. Their robust but cumbersome mounting restricted their use to fixed-separation experiments only, to avoid sediment disturbance.

In order to avoid confusion, the new S-wave probes will be referred to henceforth as the FIELD PROBES, those used during the first six months as the SCHULTHEISS PROBES (Schultheiss termed these the Mark II probes). The

SMALL PROBES described in 3.3 were also deployed under laboratory conditions, both for testing purposes and for some laboratory measurements which benefitted from their smaller size, and hence minimal associated sediment disturbance.

3.4.2. Apparatus and instrumentation.

3.4.2.1. Characterisation of S_H wave generation and propagation.

The specific combination of components adopted varied according to the requirements of any particular experiment: however, the basic system for S-wave generation, detection and characterisation remained the same. Fig. 3.5. is a schematic representation of the equipment used. One transducer is excited by a signal generator, with this signal also triggering the sweep of a digital oscilloscope. The resulting displacement pulse is transmitted through the surrounding medium and converted back to an electrical signal by another identical transducer, this signal being displayed on the oscilloscope. The time delay between triggering and received pulse onset corresponds to the travel time of the pulse through the medium, assuming that electronic delays through cabling and instrumentation are negligible. S-wave signal arrival-times were of the order of milliseconds, which justifies this assertion for short cable lengths [Scultheiss, 1983]. Towards the end of the study, possibly because of degeneration of transducer insulation, it was found that 'pick-up' of the excitation spike by the receiving equipment adversely affected signal quality. Earthing the equipment to the sediment was found to reduce this.

In order to maintain consistency, wherever possible the equipment intended for field deployment was used. This consisted of the field probes and an OYO Sonic Viewer Model 5217A, which combined signal generation and triggering with a digital oscilloscope for received signal display and arrival time measurement. Plate 1 illustrates the instrument in use in the laboratory, in this case in conjunction with an external attenuator and amplifier for testing purposes.

Transmitted pulse rate, oscilloscope time-base and gain, and received

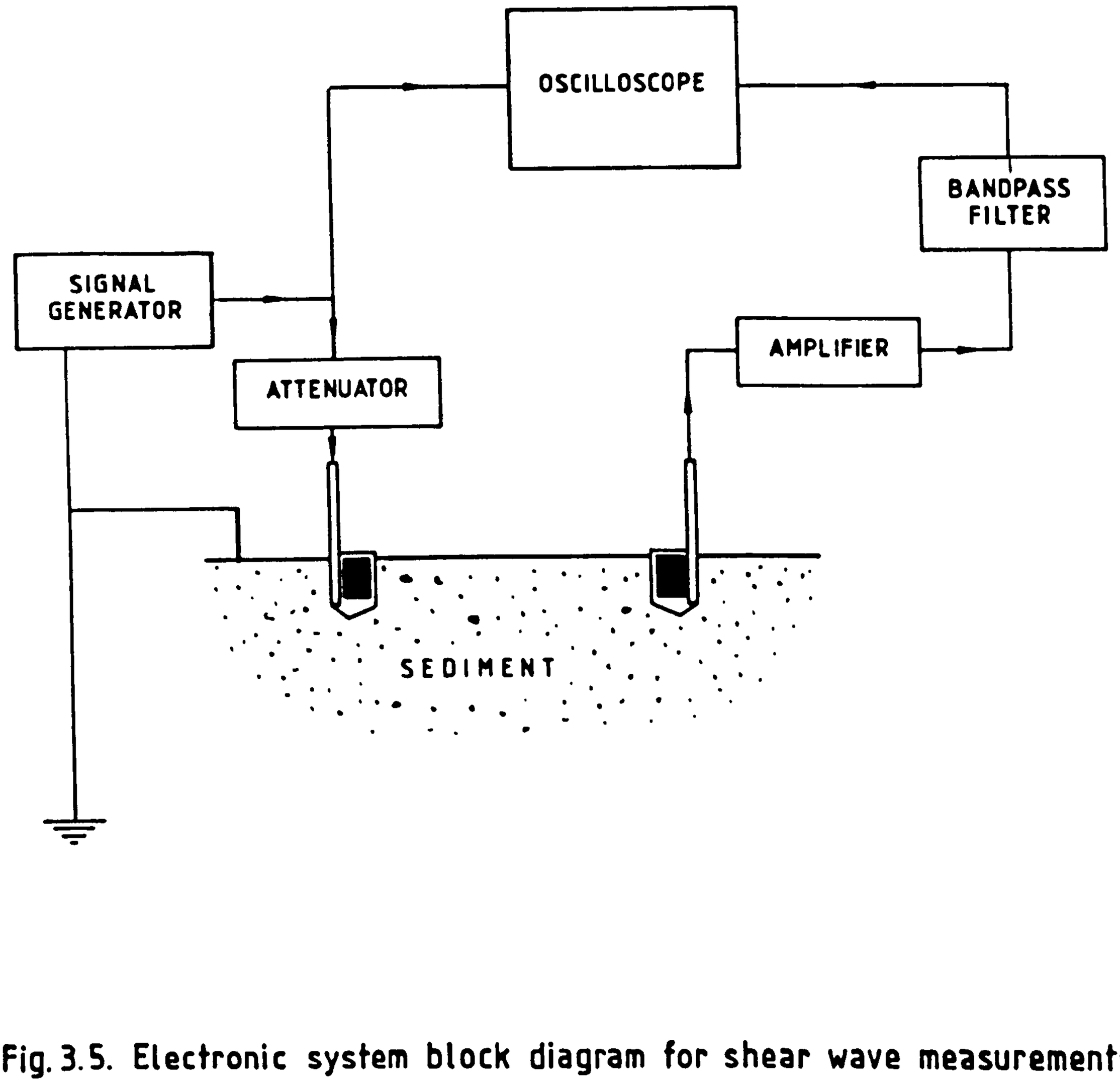

Fig. 3.5. Electronic system block diagram for shear wave measurements.

signal amplitude could be varied using in-built controls. The best feature was a signal averaging facility which allowed rapid 'stacking' of low-amplitude signals, thus providing much better signal to noise ratios than could be obtained by direct amplification [Telford *et al*, 1976]. An optional high frequency filter (30kHz) further reduced noise without significantly affecting the transmitted pulse. Additional features included: a paper printout of the oscilloscope display, concurrent display of up to two signals for direct comparison of different received traces, and a relatively robust and portable design, powered by a separate 12V car battery.

There were two major disadvantages in using the Sonic Viewer, which limited the scope of *in situ* S-wave characterisation. First, transmitter excitation consists of a single, sharp negative 'spike', which can generate a wide range of frequency components in the transmitter response. Other than amplitude, the characteristics of this pulse cannot be varied. Second, received signal amplitude could not be measured because there is no digital vertical axis facility on the Sonic Viewer, and because signal stacking was used in varying amounts under different conditions.

Where either the transmitted signal characteristics were required to be varied, or received signal amplitude measurement was to be investigated, a FARNELL FG1 function generator was used in conjunction with a NICOLET 3091 digital oscilloscope. No signal filtering or amplification was performed in this case, to eliminate additional electronic pulse modification.

3.4.2.2. Test sediment.

All of the objectives listed in the introduction required provision of a test material which at least approximated to a natural sedimentary deposit. Fig.3.6 illustrates the design and dimensions of the specially constructed system, which was used for all laboratory work except, as will be described, for some preliminary experiments in air and for the investigation of the effect of temperature. Sand was evenly deposited underwater to simulate natural conditions, at initially high porosities which could then be reduced by vibration of the tank.

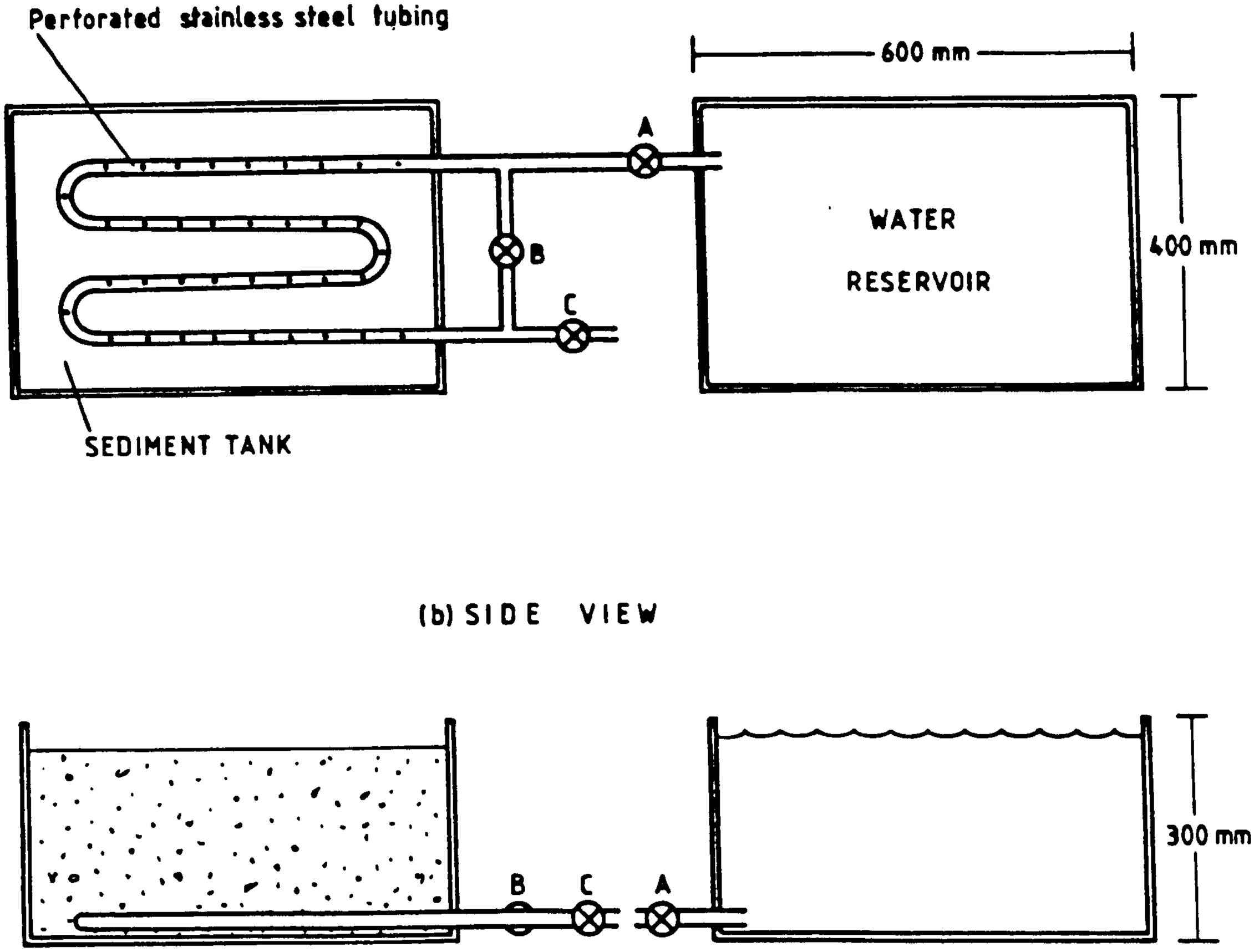

Fig. 3.6. The laboratory test tank.

Since much of the proposed field-work was to be in intertidal deposits, a mechanism for repeated saturation and drainage of the test material was required in order to simulate the effects of tidal inundation and exposure. Even saturation was achieved from a header tank of water through perforated stainless steel tubing at the base of the sediment tank. Plate 1 shows the main tank containing sediment in a drained state, with simulated worm burrows, photographed during the experiments described in Section 3.4.9.

A batch of well sorted medium-fine sand from the dunes at Newborough, Anglesey was washed, dried and deposited into the tank underwater. Bleach was added to the tap-water saturant to prevent microbial growth. The packing structure of the sand in the tank could be crudely controlled by repeated hammering of the sides with a rubber hammer. This caused liquefaction and compaction of the high porosity, freshly deposited material. However, uniformity of packing across the tank could not be guaranteed. Other workers have identified the extreme sensitivity of S-wave characteristics to minor variation in packing [e.g. Shirley & Hampton, 1978, Hurley, 1989]. At ARL, probes were placed in much smaller tanks which were then mounted onto vibrating tables and compacted until a given porosity (usually the minimum) was achieved. An equilibriation period of up to 24 hours under constant conditions was then required before consistent reproducibility could be ensured.

This time-consuming procedure was necessary for measurement of absolute values of S-wave propagation characteristics, which could then be compared quantitatively with those of samples with, for example, different textural parameters or different porosity. This was not one of the aims of this set of experiments. It was observed that, although measurements in the tank on different days could not be relied upon to be consistent, over the shorter periods associated with any experimental run a high degree of repeatability could be obtained, provided that a consistent procedure was adopted between measurements. Therefore less time-consuming consolidation and equilibriation procedures were required for general investigation of transducer-sediment behaviour, than for precise measurement of the characteristics of particular sedimentary deposits.

An important consequence of this approach is that, in general, comparisons cannot usefully be made between absolute values measured at different times during the laboratory work. This is not only due to the lack of precise control over sediment packing: different batches of test sand and deliberate qualitative control of the degree of consolidation (to monitor a wider range of sediment properties) introduced additional variation. Neglecting absolute differences, the nature of the results obtained was consistent in all cases where repeat runs were performed.

3.4.3. Investigation of the S-wave probes.

3.4.3.1. Electromechanical principles of the transducer-sediment system.

Before presenting and discussing the results of this set of experiments the basic principles underlying the behaviour of the S-wave transducer-sediment system will be summarised:

(1) The transmitter is excited by a voltage signal.

(2) This signal induces distortion of the transducer plate, which in turn imparts a shearing displacement to the surrounding sediment, aligned along the plane of the plate and polarised horizontally. (Other components will clearly also be generated, but the receiver is positioned so as to be affected primarily by this one). The amplitude and frequency of this displacement depend on the physical and geometrical characteristics of the probe, the nature of the excitation signal, and also on the physical properties of the sediment in contact with the transducer plate.

(3) The resultant displacement is transmitted through the sediment at the S_H velocity (for simplicity, assumed here to be homogeneous). Depending on its initial amplitude/frequency spectrum, on the propagation characteristics of the sediment, and on the length of the travel path, its form may be modified by frequency-dependent attenuation and dispersion.

(4) The modified signal arrives at the receiver, which responds in a manner again determined by sediment and probe characteristics.

It is clear that the system is highly sensitive to the properties of the sediment in which the probes are placed, since these affect transducer response to excitation (and therefore source frequency and amplitude) as well as pulse propagation characteristics (velocity and attenuation). Ideally the transducer response should be known, so that differences in received signal can be related directly to propagation characteristics of the sediment. Unfortunately, it is impossible to separate the two effects on the excitation signal under normal circumstances. This problem is largely due to the lack of a suitable calibration material of known shear wave propagation characetristics, such as distilled water in the case of compressional wave characterisation.

In the absence of a calibration procedure, investigation of the response of the transducer or transducer-sediment system must be indirect. It involves characterising a signal which will have been attenuated and filtered by the medium through which it has passed. Incidentally, not only amplitude and frequency of the transmitter excitation are unknown. The exact position of the source is also uncertain due to the finite size of the transducer plate.

Fortunately the main purpose for which these transducers were intended does not require accurate characterisation of the transducer response. Measurement of velocity and attenuation of different sediments is possible by using the receiver at more than one distance from the transmitter. The relative change in received-signal arrival time or amplitude, as a function of the relative change in probe separation, can be converted into velocity or attenuation without requiring source position, amplitude or frequency. This also provides some scope for calibration of the transducers by extrapolation back to source, provided that the measurement can be transformed into a linear relationship with separation. This will be developed further in 3.4.4.

Returning to the problem of transducer-sediment response, some useful experiments were still possible in spite of the unfeasibility of direct measurement. In particular, by maintaining a fixed probe separation within a uniform sediment, the effect of variation of excitation characteristics on the received signal can be investigated. The result obtained is

specific to the sediment and probe separation used, but the form of the amplitude/frequency response should give an insight into transducer behaviour.

3.4.3.2. Response to variation in transmitter driving signal.

An excitation or driving signal voltage is usually in the form of a pulse ('tone burst') of known frequency, duration and maximum amplitude, repeated at intervals, although single pulses and continuous sine wave or square wave signals can also be used. The advantage of a series of repeated pulses is that signal stacking (averaging) is enabled, which increases the received signal-noise ratio. Its disadvantage, especially under confined laboratory conditions, is that 'wrap-around' of the tail-end of the signal can occur if the received pulse envelope lasts longer than the transmitted pulse repeat time. Reflections from the tank boundaries cause broadening of the pulse envelope and exacerbate this problem: provided that sensible pulse rates were chosen, *in situ* signals were not found to be affected.

Continuous excitation, most usefully as a pure sine wave, can be used where only the received signal amplitude is of interest: clearly if the signal travel time is to be measured this is unsuitable. Its advantage is that much purer driving frequencies can be measured: a pulse, even of a single frequency, generates other frequency components as it is switched on and off. Its disadvantage is that reflections from tank walls in confined experiments will form part of the received signal.

This part of the investigation was concerned with the characterisation of transmitter response, rather than with measurement of sediment properties. In order to remove the problem of variation in sediment properties and separation-dependent effects such as attenuation or dispersion, each experiment was performed under uniform conditions over a fixed probe separation. The received amplitude:frequency response was determined using sine wave tone bursts of fixed duration over a range of frequencies from 10Hz-100kHz.

The other point of interest was the response to the Sonic Viewer output ('spike' or delta-function) or square-wave ('step') excitation. Both of these result in generation of a range of frequency components associated with an impulsive 'kick' of the transducer, followed by a decaying reverberation at its resonant frequency. The form of the received signal was compared with that received from monochromatic sine wave excitation to aid interpretation of later field results.

Unloaded transmitter response: behaviour of S-wave transducer in air.

Air is a fluid, hence does not support a shear wave. However, unloaded transducer behaviour could be monitored by clamping the transducers in air with their plates parallel to each other, at fixed separation. In this configuration, vibration of the transmitter sends a compressional pulse towards the receiver. Transmitter displacement is the same as that excited in the more conventional S-wave configuration: it is simply being measured from a different direction. Rubber tubing around the shafts prevented travel through the probe supports, and minimised the risk of forcing vibration of the whole apparatus rather than just the transmitter.

There were two objectives: first, investigation of the amplitude response of the transducers in free space and secondly characterisation of their response to the Sonic Viewer transmitter 'spike'.

Fig. 3.7. illustrates the amplitude response obtained from continuous sine wave excitation. Except at extreme ends of the range received frequency was identical to the driving signal. This represents high transducer band-width, with a measurable signal being obtained over a range from 55 to 4,000Hz. Received amplitude was at most only 2% of the signal voltage, which indicates considerable energy loss within the system. This will be mainly accounted for by spreading and vibration polarised along different directions in this configuration. A sharp resonance is shown between 600 and 700 Hz, corresponding to maximum transducer energy transmission at this driving frequency. The other, lesser peaks correspond approximately to multiples of this resonant frequency, although they could also be additional modes of vibration introduced by the complex probe geometry.

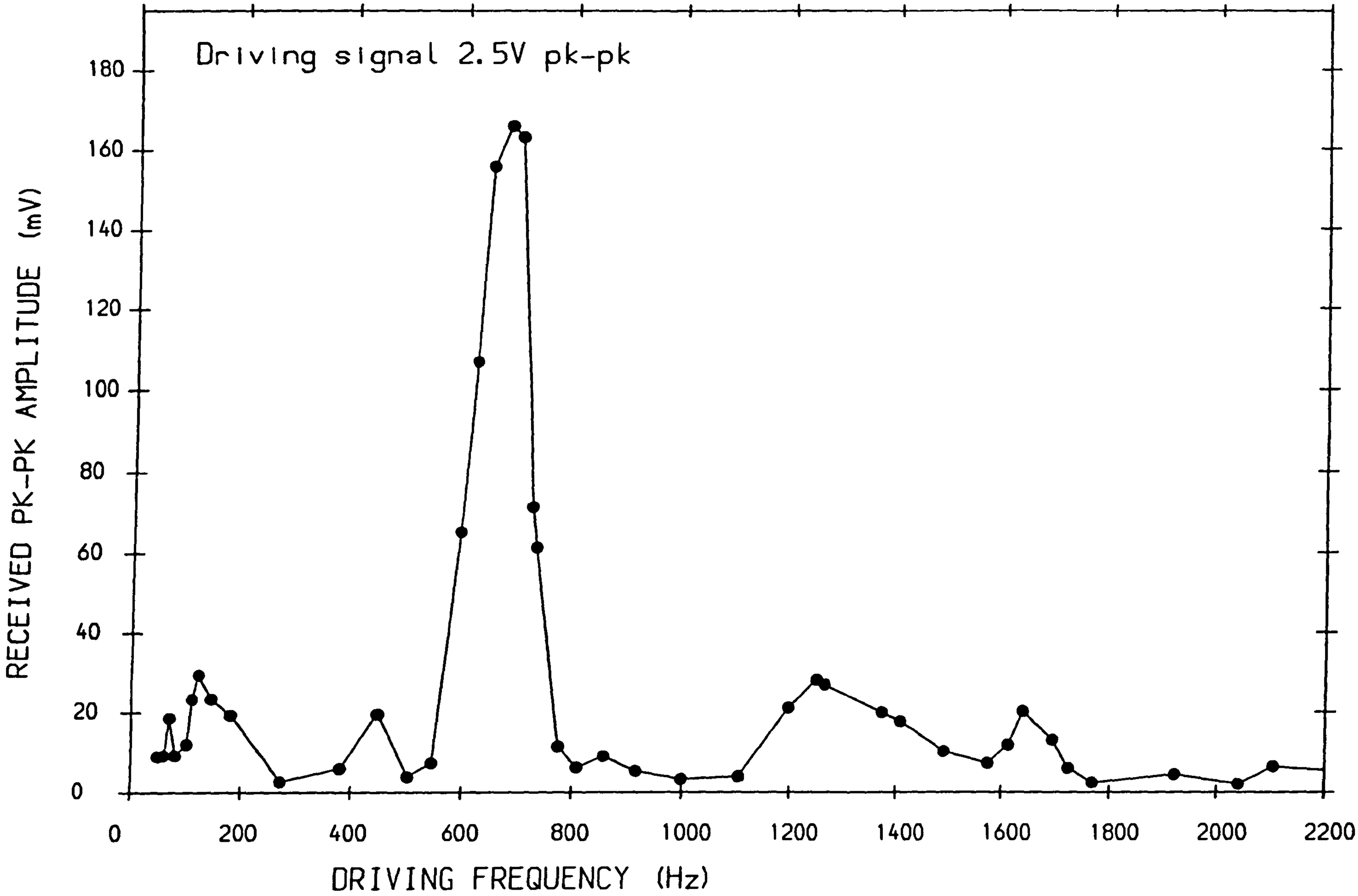

Fig. 3.7. Unloaded response of field probe transmitter/receiver system.

Note that this experiment represents a study of the response of the transmitter-receiver system, rather than a single transducer. The probes were manufactured in a batch using identical procedures, but some degree of variation was unavoidable.

Since the Sonic Viewer was intended to be used for field work, unloaded transmitter-receiver response to its driving voltage 'spike' was also examined. Figs.3.8(a) & (b) show the excitation spike and received signal respectively (note the difference in time bases). Excitation of the transmitter by a delta-function would be expected to generate a range of frequency components due to the initial impulse, dominated by a decaying signal at the resonant frequency. The maximum amplitude signal in Fig.3.8(b) was estimated at 685-715Hz, reducing to a minimum of around 615Hz in the decay envelope. The highest frequency measured was 2360Hz, with the high frequency components decaying much more rapidly. Spectral analysis of this received signal was not performed, but the estimated results show good agreement with the resonant peaks obtained from Fig.3.7.

Loaded transmitter response: the transducer/sediment system.

When surrounded by sediment, two independent effects must be considered: the transducer frequency response will be altered, and the signal will be modified by propagation through the sediment. From simple mechanical arguments, and provided that the sediment is properly coupled to the transducer, resonance would be expected when the bending length of the transducer corresponds to some multiple of the wavelength of the S-wave disturbance in the sediment. The multiple depends upon the mode of fixing of the transducer: if it is free to vibrate around its centre of gravity, this should form the node of vibration, and resonance should occur at a disturbance corresponding to twice the length of the plate (Fig.3.9). If it is fixed at one edge, this forms the node, and resonance will occur at a wavelength corresponding to four times the length of the plate.

The important proviso of perfect coupling of vibration of transducer and sediment has been developed further in sections 3.4.7. It should be a primary consideration when designing appropriate S-wave probes for

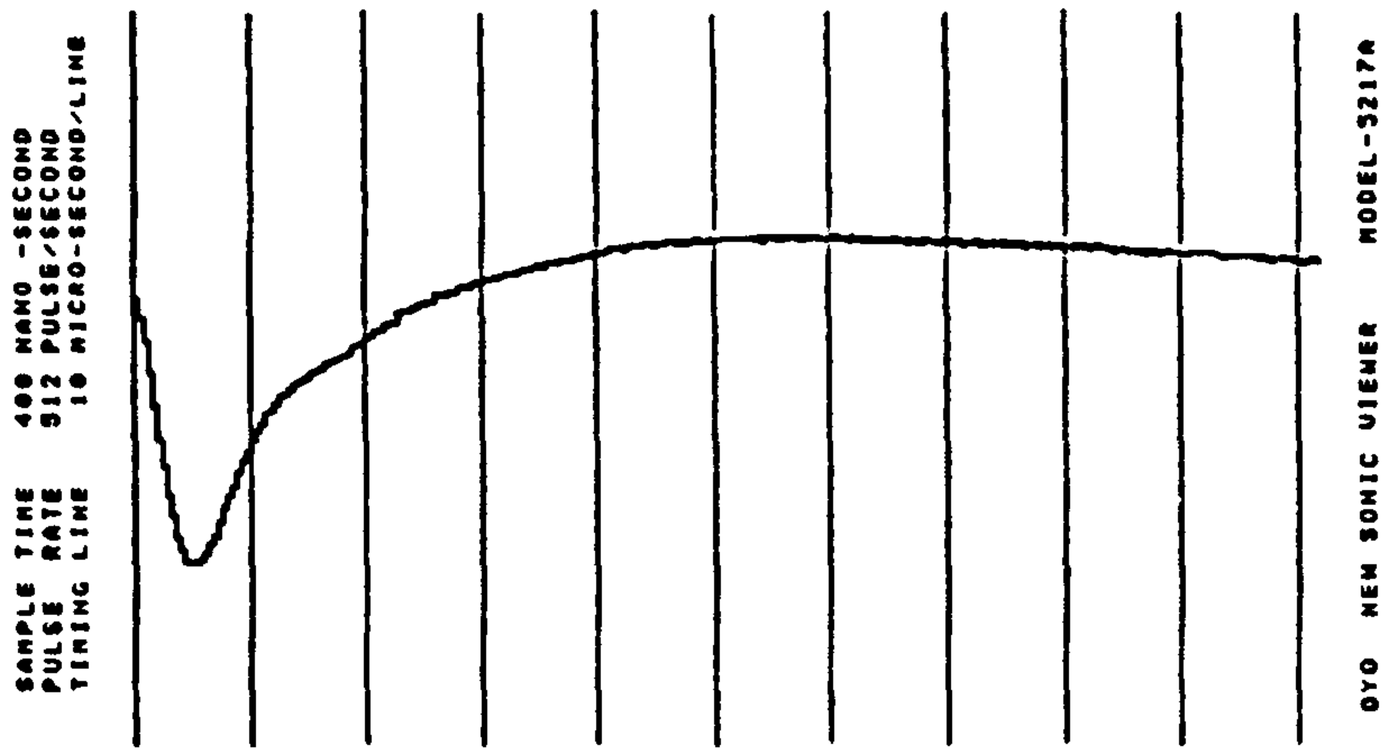

Fig. 3.8(a) SonicViewer Excitation spike.

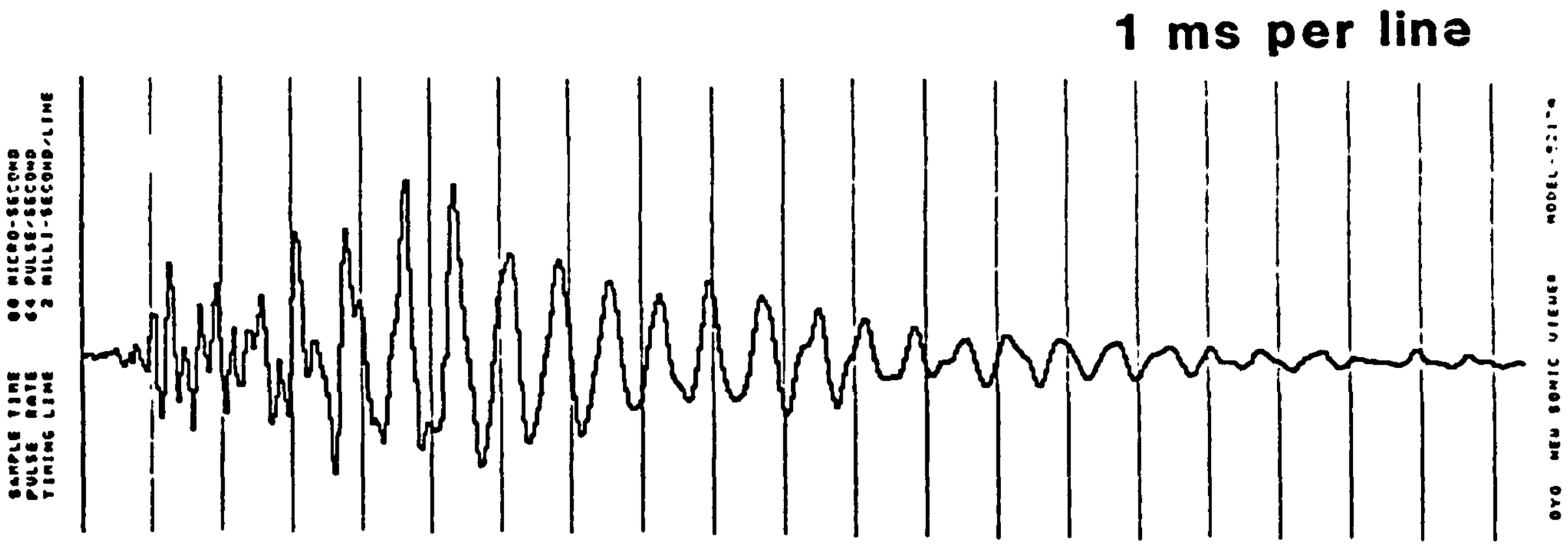

Fig. 3.8(b) Unloaded transducer response.

(SonicViewer).

(a) Cantilever mounting

'Quater-wavelength resonator'

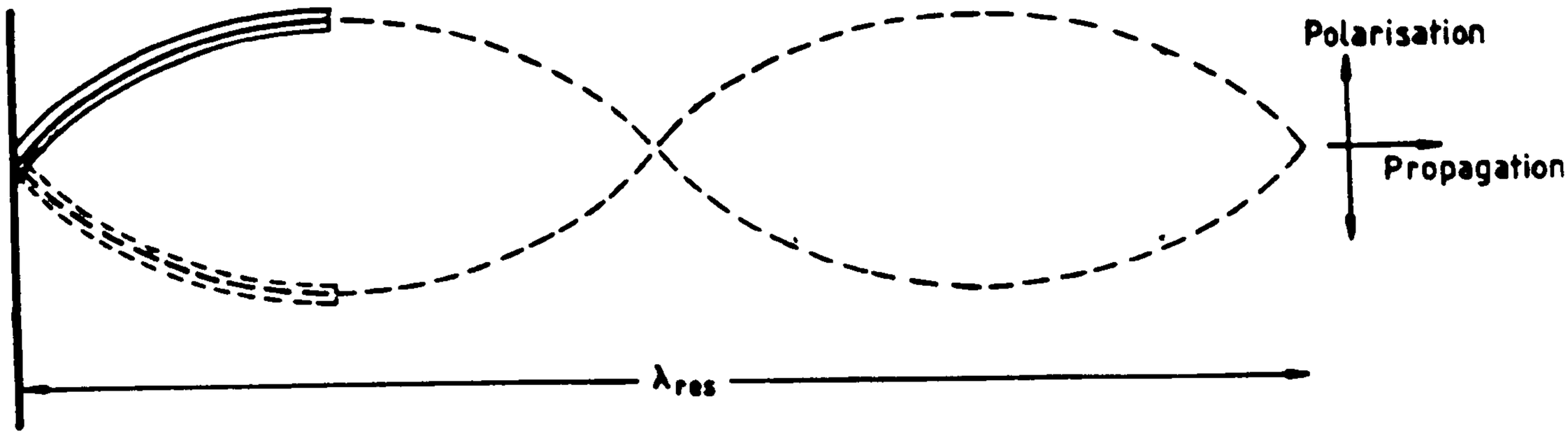

(b) Unconstrained

'Half-wavelength resonator'

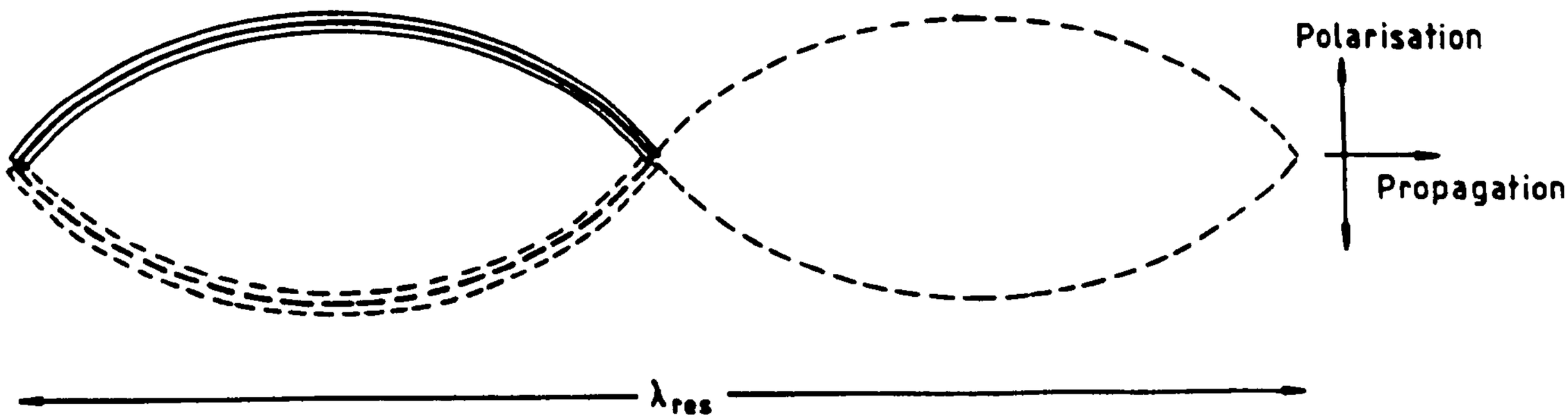

$f_{RES} = \frac{V_S}{\lambda_{res}}$ λ_{res} = Resonant wavelength of SH disturbance.

Fig. 3.9. Resonant behaviour of bender elements in an elastic medium.

different media, since their unloaded operating band-width should encompass typical loaded resonances in natural sedimentary deposits. This range is determined by the physical and piezoelectric characteristics of the transducer, its mode of fixing, and the compliance of the potting compound. For maximum response, the unloaded resonant frequency should correspond to the calculated resonance of the transducer-sediment system. If this calculated resonance is too low, the transducer will decouple from the sediment and vibrate at a higher, more natural frequency closer to its unloaded value. If it is too high, the transducer will again decouple, this time vibrating at a lower frequency.

As a first stage in gaining an understanding of the transducer-sediment system, a pair of field probes was placed in saturated sediment in the test tank to a fixed depth and at fixed probe separation. These conditions were then maintained throughout the experiment, so that only the excitation voltage characteristics were varied.

Fig.3.10 illustrates the variation in received amplitude with frequency for two different probe separations in the same saturated deposit, using sine-wave tone-burst excitation. Both show a broad resonance peak, with the high frequency tail at lower amplitude than the low frequency one. This is caused by higher attenuation of the higher frequency components over the travel path, and illustrates the problems in measuring the transmitter response directly. The frequency range was limited at both ends by breakdown of the transmitted signal into more complicated superpositions of higher or lower frequency components: over the rest of the range, however, a faithful reproduction of the driving frequency was obtained at the receiver.

The marked difference in amplitude of the two curves is easily explained by the difference in probe separation: at higher separations the signal is more attenuated. The slight difference in frequency is predicted because increased attenuation of the higher frequency components will cause a shift in resonance measured at the receiver, which will increase with increasing probe separation. A rather more extreme, higher frequency example of this has already been documented and interpreted by Shirley [1978]. The finding will be discussed more fully in 3.4.4.1.

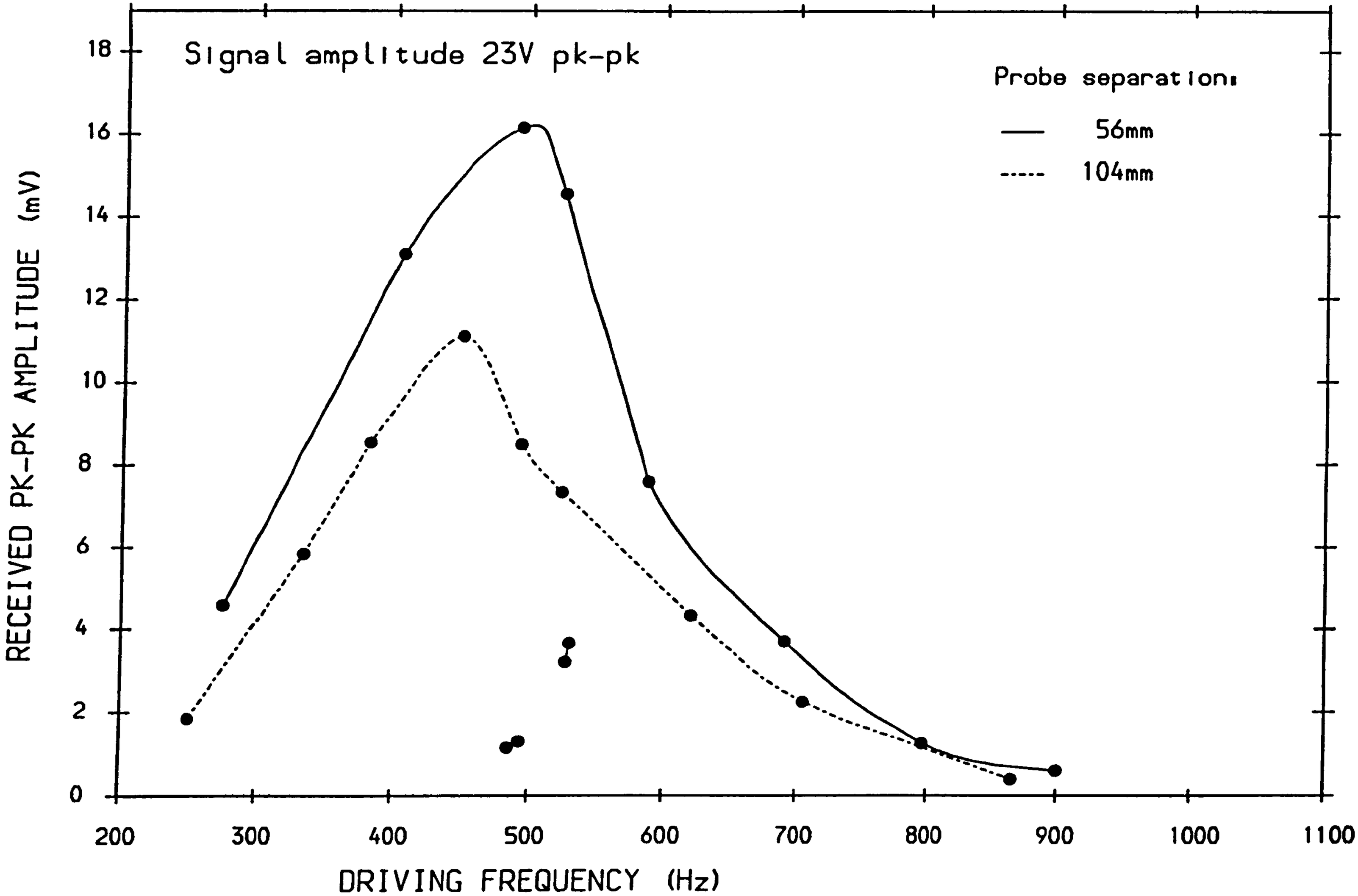

Fig. 3.10. Typical response of field probes in saturated sediment.

Also superimposed onto Fig.3.10 are the response to a step-function driving signal, measured at the beginning and end of each experiment, to check for any drift in physical properties. A 'typical' received signal is illustrated in Fig.3.11. This is, in fact, a signal obtained from Sonic Viewer excitation: however, it was invariably found to be identical in form to that obtained using the step-function. A high quality, predominantly monochromatic signal was obtained in nearly all cases. Received pulse amplitude, period and arrival time have been defined using this figure: all subsequent measurements can be referred to these definitions.

As can be seen from Fig.3.10, the signals received from a step-function excitation have frequencies corresponding well to the resonant peaks, but with much lower amplitudes. This would be expected because much of the square wave energy will be lost as higher frequency components, which are very rapidly attenuated. Sonic Viewer excitation also resulted in signals of frequency corresponding to resonance of the transducer-sediment system.

The broad single-peaked form of these amplitude responses typifies a series of laboratory experiments in saturated sediment. Resonance was observed at a range of frequencies from 400-1000Hz: this indicates the effect of different sediment properties on transducer response, which will be discussed further in Section 3.4.7.1. Response to step- or spike-excitation was also found in all cases to be dominated by a decaying signal at the resonant frequency for a given sediment and probe separation. Thus the step or spike excitation technique effectively 'tunes' the measurement system to its natural resonance, without external adjustment. A considerable energy loss is clearly incurred in the process, which must be counteracted by signal stacking.

The proximity of resonance of the transducer-sediment system to unloaded resonance (Fig. 5.3.7) suggests that transducer compliance was well-matched to saturated sediment, with the probes operating at or near their ideal frequency in saturated sands. Frequencies recorded *in situ* yielded a total range of 300-1300Hz, with most values falling between 500 and 1000Hz. More complicated results were obtained in drained deposits and muds, as will be discussed in the relevant sections 3.4.6 and in 5.2.6.

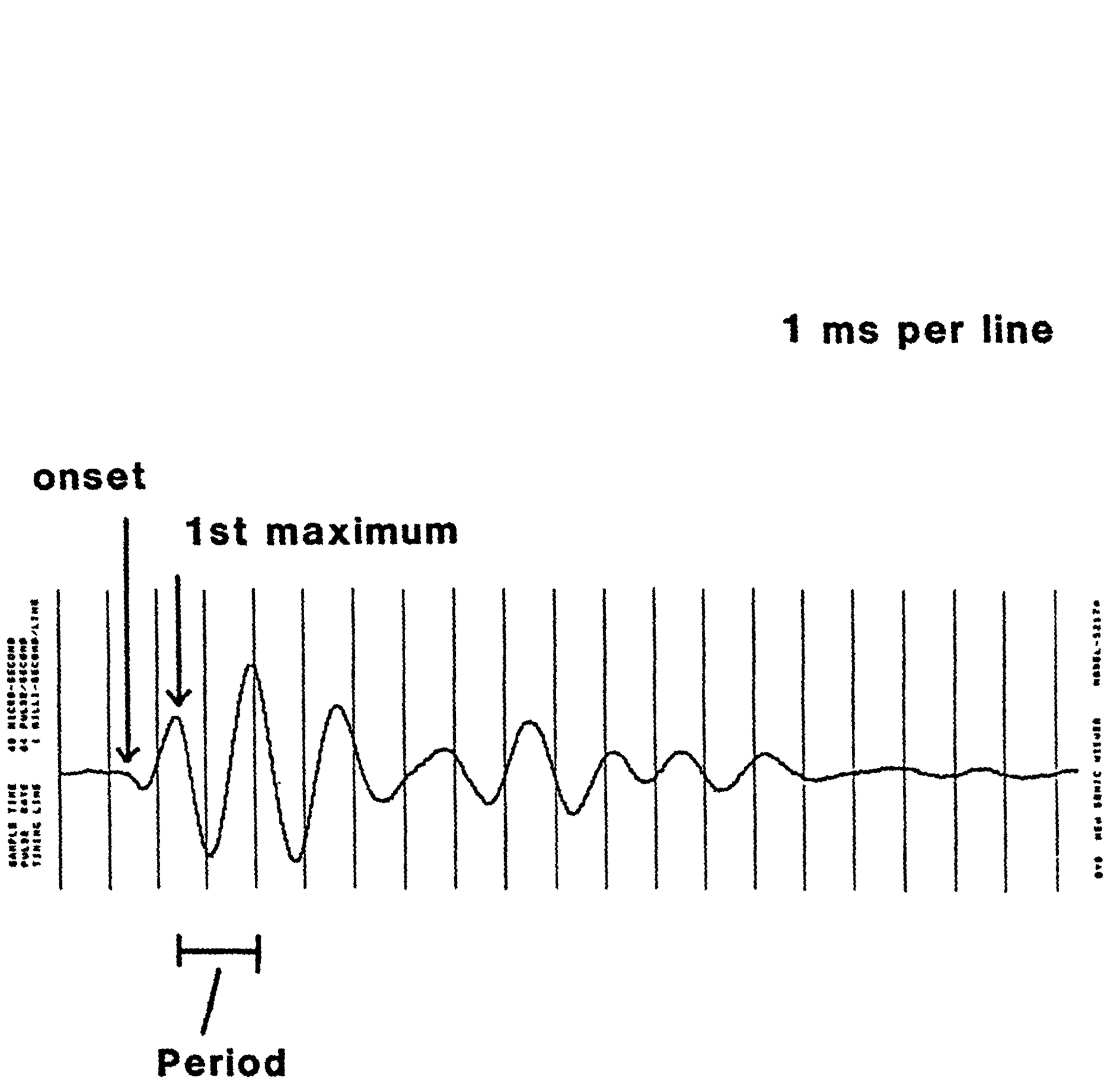

Fig.3.11 Typical received signal in saturated sand.

3.4.4 Dependence of received signal characteristics on probe separation.

The acoustic properties of the sediment, as distinct from the sediment-transducer system, can be best studied by comparison of received waveforms at different transmitter/receiver separations. The difference in received pulse characteristics and arrival times, expressed as a function of the difference in transmitter-receiver separation, is then determined by the physical properties of the sediment alone. This avoids the problems associated with characterising transducer behaviour in different sediments, by using identical transmitter-receiver pairs so that the transducer response effectively cancels out in the difference calculation, and carries two further advantages:

(1) The 'true' transmitter-receiver separation is not required, provided that all separation measurements are made relative to fixed positions on the probes.
(2) The 'true' pulse arrival time is also not strictly required. Later trace features, which may be more easily identifiable than signal onsets, can be used provided that pulse frequency does not change significantly with separation.

This technique of differential measurement of pulse characteristics has been investigated and applied in laboratory deposits of natural and artificial sands by Shirley et al [1979] and Schultheiss [1983], using bimorph transducers. It has also, of course, been widely applied in compressional wave measurements, in larger scale studies using mechanical sources and geophone arrays, and in earthquake seismology. Measurements of V_s and attenuation, from differences in received signal arrival-times and amplitudes respectively, have proved highly successful.

However, since different probes and procedure were involved in this study, some further investigation of the technique was performed. The main differences between the proposed procedure and that employed at ARL were:

(1) The Sonic Viewer generates a delta-function excitation rather than a single frequency tone burst.
(2) The transducers were to be deployed at the sediment surface, rather

than buried within the sediment bulk.

(3) The large size of the transducers suggested their use over longer separations and raised the possibility of near-field effects over small separations.

(4) The proposed deployment *in situ* required that, for each separation change, the receiver be removed from the sediment and replaced. This contrasts with horizontal racking of the receiver at ARL while liquefying the sediment by vibration to facilitate its passage and maintain minimum porosity.

A series of separate experiments were performed at different times during the study period, using the same basic procedure. Probes were placed in saturated sediment, to a fixed depth (40mm). Probe separation, defined as the distance between plate edges (point T, Fig. 3.3) was measured using a steel rule to within +/-1mm. The receiver was removed and reinserted to the same depth at successively shorter separations. At each position, arrival times of several received trace features were recorded, including wherever possible the signal onset. An estimate of the frequency was also obtained, by direct measurement of the first wave period of the pulse train (Fig. 3.11).

Each of the experiments corresponds to a different period of use of the laboratory tank (and therefore different packing configuration and/or test sediment structure). Quantitative comparison is not useful because sediment properties such as texture or porosity were not measured.

3.4.4.1. Propagated pulse characteristics

Fig.3.12 shows a set of paper records from one of the experiments. Probe separation varied from 240-15mm, with eleven positions monitored in all. Only six of these records have been shown for clarity. It is clear that a high-quality, clean signal could be obtained throughout the separation range, with onsets becoming less well defined after 180mm. Pulse 'form', especially for the first few cycles, is relatively uniform over the range, although the pulse train lengthens with increasing separation, presumably due to container-wall reflections merging with the primary signal.

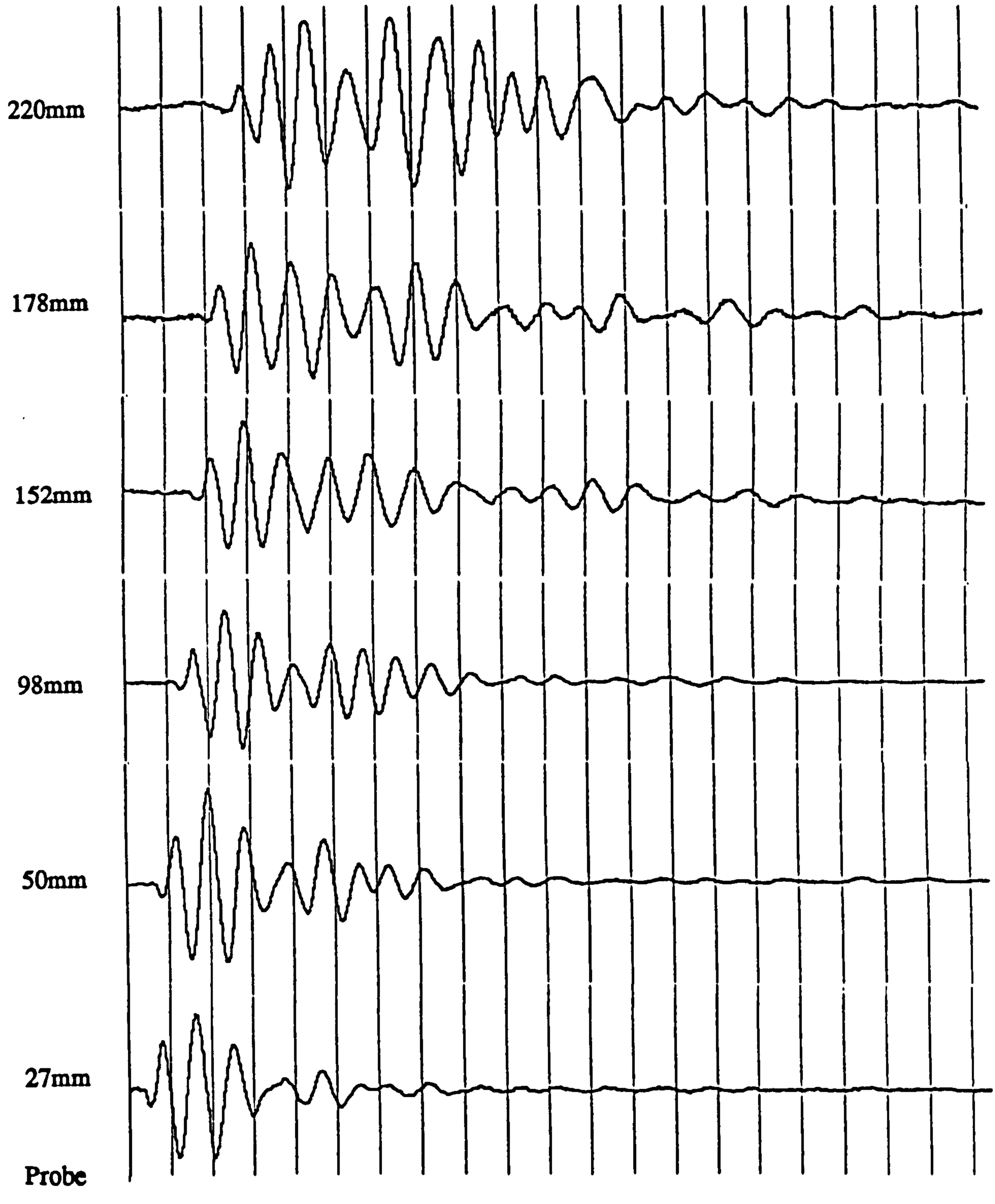

Fig. 3.12. Variation in received signals with probe separation.

Increased signal attenuation with increasing probe separation was also observed (although not quantified), since higher input gain and multiple stacking were required to improve signals at higher separations. It is clear from the figure that the stacking process does not seriously distort the received signal.

The maximum probe separation is controlled by this attenuation and also by the dimensions of the test tank. If the probes are placed too far apart, multiple reflections act to increase the stacked pulse length to longer than the interval between transmission pulses, causing 'wrap-around' and hence masking the signal onset. The minimum separation is controlled by the observed extent of localised sediment disturbance on insertion, and by the fact that as separation decreases the proportional errors in its measurement increase. In addition, measurements made at separations less than the transducer width have been treated with caution, because in these instances less than a wavelength separates transmitter and receiver. Shirley *et al* [1979] identified 'near-field' effects at this range due to the breakdown of pulse interpretation based on spherical spreading, and sensitivity to localised sediment disturbance around the probes would also have been increased.

Variation of received signal frequency with separation.

The maximum-amplitude frequency component received from a spike or step-function excitation has already been shown to be lower at higher separations, due to the strong frequency dependence of attenuation. In other words, the response of the transmitter-sediment system at source is modified during its passage through the sediment by selective attenuation of higher frequency components. The effect would be expected to be stronger for broad transmitter-sediment resonance peaks, and for higher frequency resonances.

Fig.3.13 shows the variation observed for three separate experiments. The superimposed lines are based on a least squares regression, amd indicate a linear downward trend. It is interesting that the gradient appears to increase with increasing mean frequency, although more work would be

required to confirm this as a general case. The observed increases are considerably less marked than those observed at ARL [Shirley et al, 1978], which may be due to the much lower frequencies involved.

A simple model for the behaviour can be proposed along the following lines. The received signal amplitude (U_r) is given by:

$$U_r = U(f)e^{-a(f)x} \tag{3.3}$$

Where U(f) is the amplitude resonse of the transmitter and a(f) is the attenuation. The amplitude response is not known, but examination of the curves in Fig. 3.10 suggests a Gaussian distribution of standard deviation σ around the resonant frequency f^c as a simple approximation. This yields:

$$U_r = U_0\, e^{-\left\{\frac{(f^c - f)^2}{2\sigma^2}\right\}} e^{-a(f)x} \tag{3.4}$$

Differentiation yields a maximum received amplitude at:

$$f(x) = f^c - \sigma^2\left(\frac{da}{df}\right)x \tag{3.5}$$

This frequency should therefore correspond to that received at x.

The form of the attenuation coefficient has been discussed in Chapter 2. In generalised empirical studies, an approximately linear dependence on frequency has been proposed, leading to a constant log decrement for the material. More rigorously, it has been related to a constant log decrement contribution from the sediment frame combined with a contribution due to viscous loss from relative frame/pore fluid motion, which is not linearly frequency dependent.

Using the constant log-decrement approximation, which seems reasonable over these short frequency ranges (since deviation from linearity is generally only discernible over longer ranges), a linear relationship between frequency and probe separation should be obtained, with slope given by $-\sigma^2 a_0$, ($a=a_0 f$). However, the most important conclusion from this section is that variation in received signal frequency with probe separation is, while measurable and roughly what should be expected, not

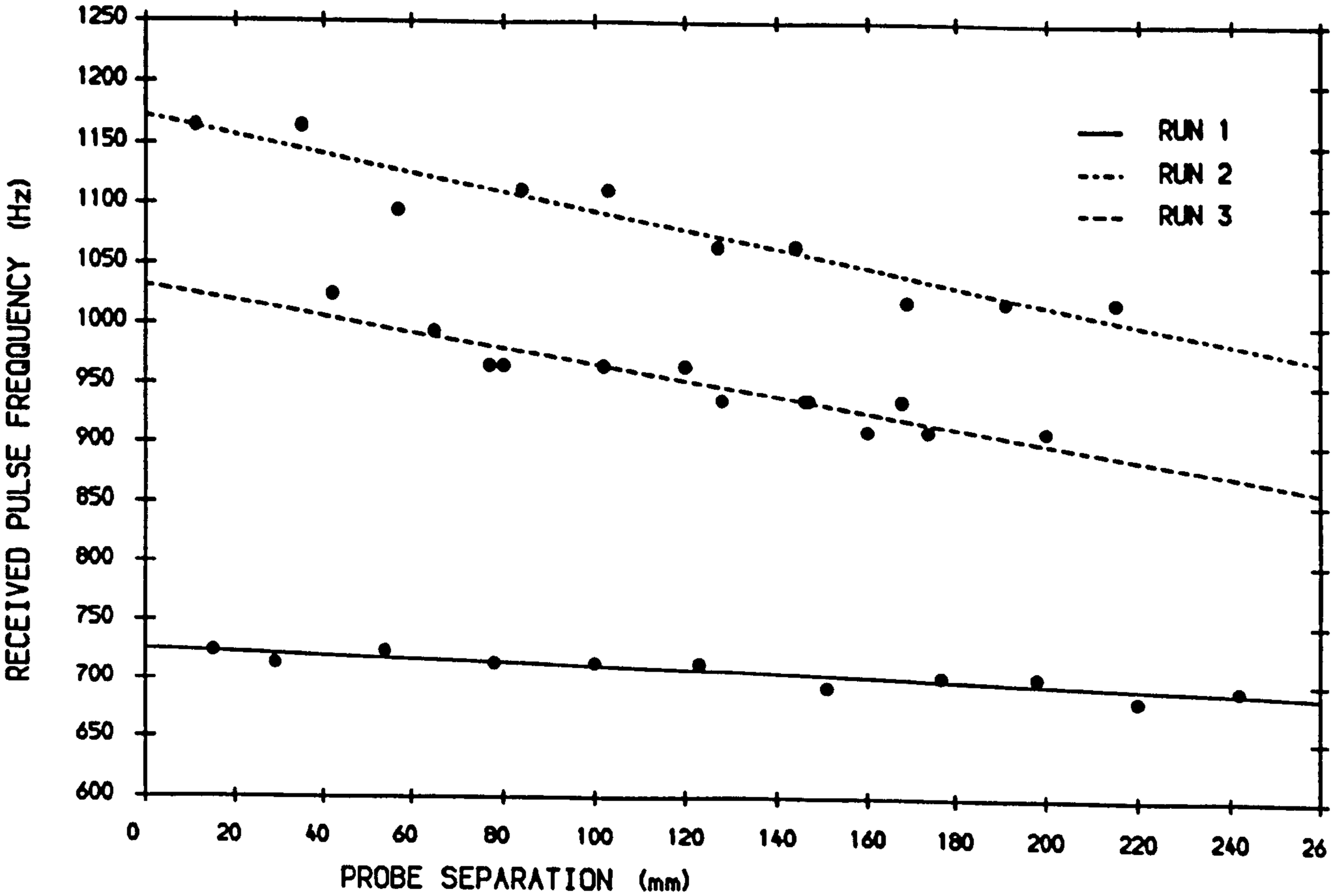

Fig. 3.13. Variation in received frequency with probe separation.

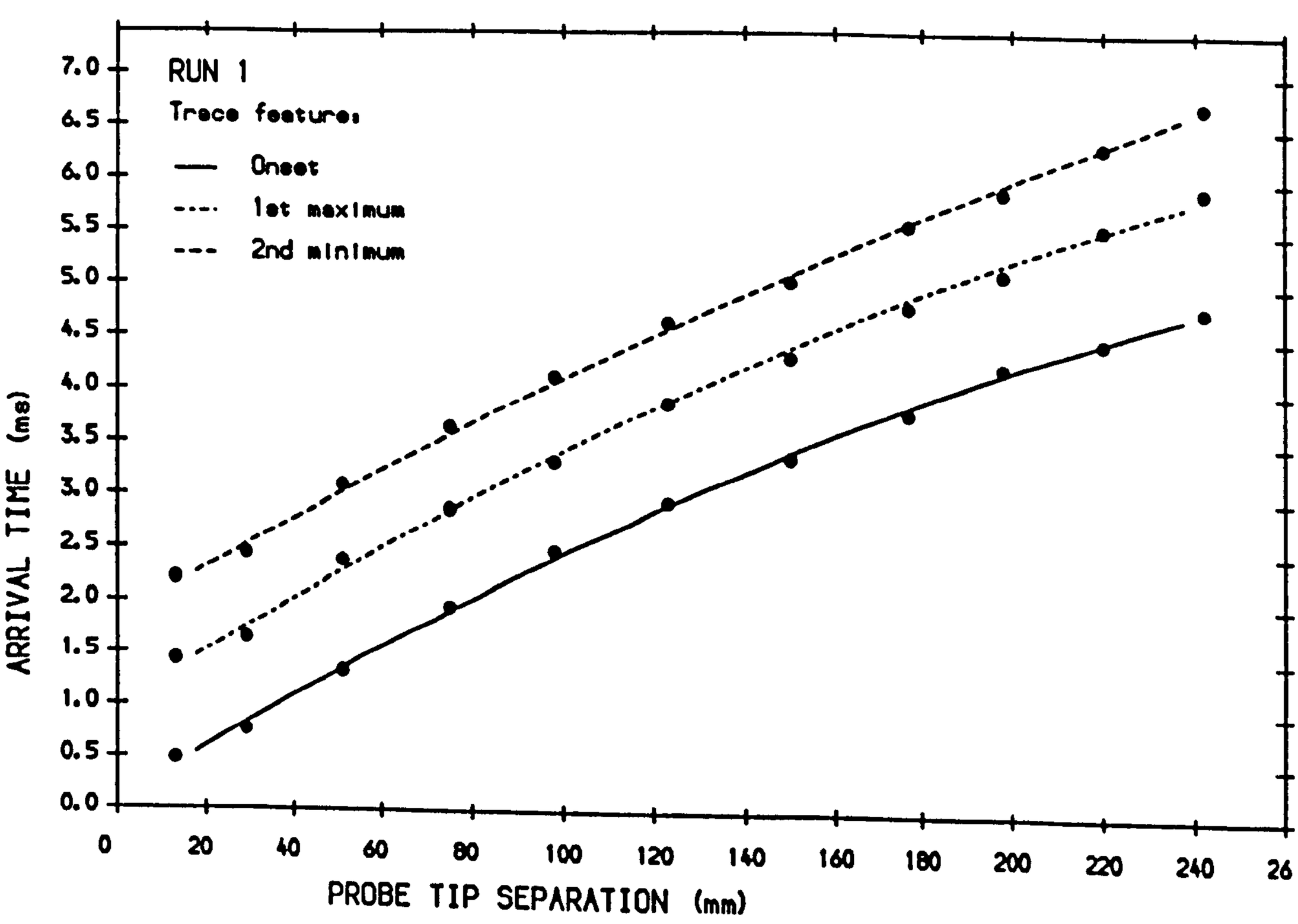

Fig. 3.14. Variation in signal arrival time with probe separation.

very important. The maximum change observed was 10%.

Variation in pulse travel time with separation: velocity calculations.

Fig. 3.14 illustrates a typical example of arrival time versus probe separation for three trace features. Because separation represents the controlled variable, linear regression of arrival time on separation is performed to calculate V_s. A least-squares fit of the form $t_i = b_i s + a_i$ is calculated, along with associated standard errors for both intercept and gradient. 95% confidence limits for each can then be computed [Sokal and Rohlf, 1977]. Table 3.1 lists velocities and confidence limits obtained from the regression coefficient of the *i*th trace-feature arrival-time against probe separation:

$$V_i = \frac{1}{b_i} \tag{3.6}$$

Several coefficients have been calculated from different separation ranges, in an attempt to identify any non-linear effects. In general, slight curvature is observed at high and low separations, especially for the onset measurement, as illustrated in Fig. 3.14.

TABLE 3.1. Calculations of V_s from arrival-time/separation measurements in Fig. 3.14 [as V_s +/- ℓ, where ℓ is the 95% confidence limit].

Separation range (mm)	V_s(ONSET) m/s	ℓ	V_s(P1) m/s	ℓ	V_s(P2) m/s	ℓ
(all)	52.7	4.1	51.2	3.0	50.9	2.6
0:200	49.4	3.9	49.5	3.9	49.5	3.5
0:100	41.7	3.7	43.3	9.0	43.3	5.7
0:75	41.4	8.8	40.9	17.0	42.2	12.3
50:180	52.1	7.4	52.2	3.2	51.5	4.3
150:300	64.4	10.6	57.3	3.6	55.0	3.8

The differences between V_s calculated from the full data-set and that from the intermediate more linear range are generally well within 95% limits: sharper differences are obtained if sub-sets from opposite ends of the

separation range are compared. V_s is also independent of which trace feature is used in the calculation, although deviations from linearity are slightly more marked for onset arrival times.

There are three possible causes of this slight non-linearity, which is effectively a shorter than expected arrival time as separation increases. First, the increased effect encountered for onset arrivals could be due to 'onset broadening' caused by multiple signal stacking at large separations. This should have no effect on the other trace features. A completely opposite interpretation could be that the onset curve is the 'true' relationship, while the slight reduction in received frequency at higher separations effectively increases the arrival time of later trace features, thus straightening out the curve. Both effects might be expected to be more important for low velocities, since the associated higher attenuation leads to more marked frequency reduction with separation and more signal stacking. Finally, however, all trace features exhibit, to variable extent, a curve typical of those found in media containing positive velocity gradients. This suggests that V_s increases with depth in the near-surface, which has been investigated further in Section 3.4.5.

The small probes were also deployed in the test tank over a range of separations. Because the smaller size of the probes resulted in much less sediment disturbance, they were used to check the consistency and repeatability of the procedure. Two experiments were performed successively on adjacent lines in the test tank, without altering conditions in the tank. Fig.3.15 illustrates the combined arrival-time/probe separation data. Note that probe shaft separation was measured in this case because the probe tips were beneath the sediment surface. 44mm must be subtracted from this measurement to obtain the probe-tip separation (Fig.3.4). A reasonable degree of consistency was obtained, with no significant differences being identified between velocities calculated from individual lines. Table 3.2 lists velocities calculated from the combined data set.

In contrast to the field probe data, there is no evidence of curvature, at least within the observed scatter. An important additional point to note is the difference between V_s measured using onsets and that measured using

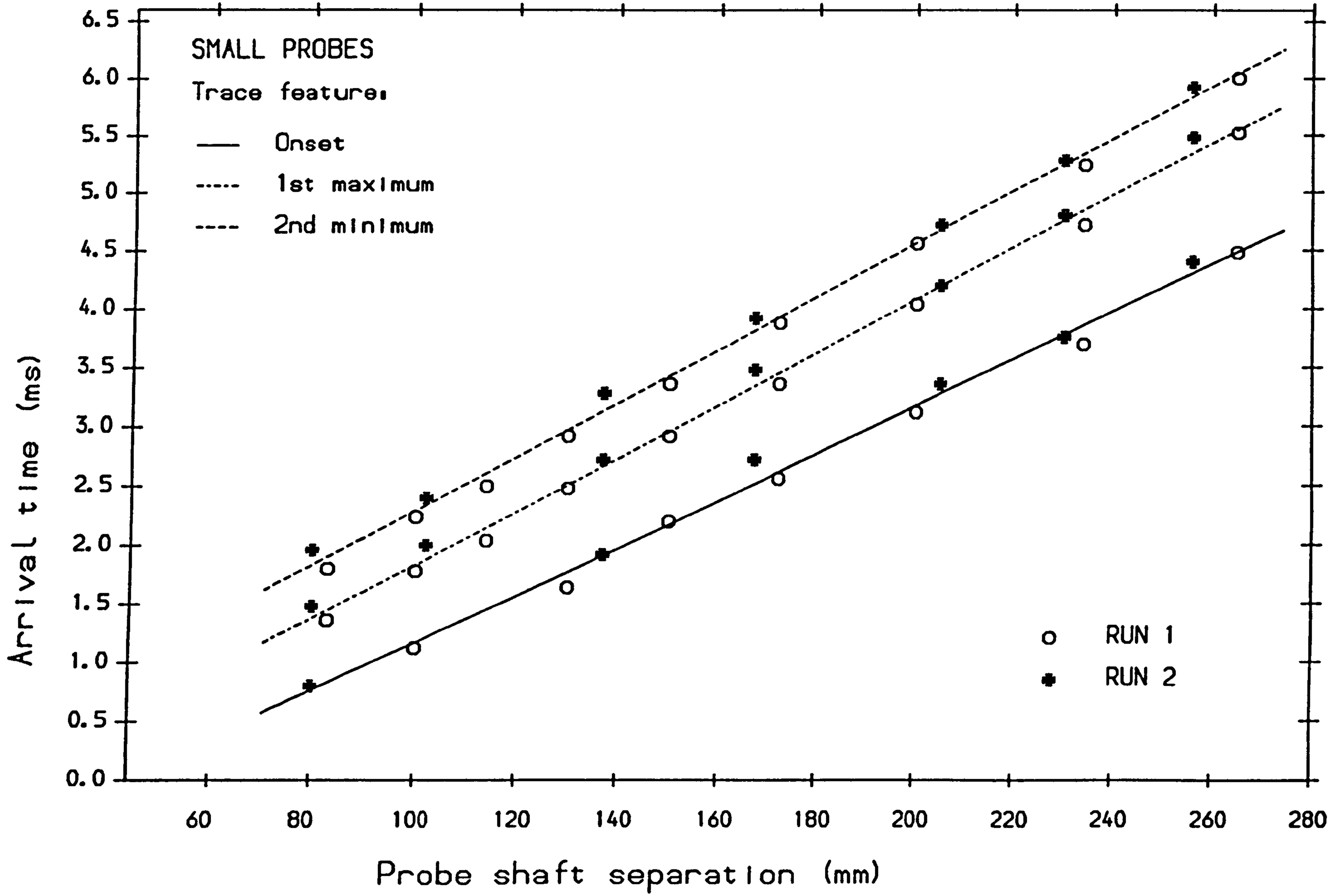

Fig. 3.15. Variation in signal arrival time with probe separation: SMALL PROBES.

Table 3.2. Regression calculations for small probes.

Separation range (mm)	V_s(ONSET) m/s	ℓ	V_s(P1) m/s	ℓ	V_s(P2) m/s	ℓ
(all)	49.7	2.7	44.4	1.6	43.9	1.5
0:200	49.3	6.2	44.8	3.5	43.8	3.5
50:180	47.9	7.9	44.4	4.6	43.6	4.6
150:300	51.3	6.0	44.0	3.9	43.8	2.9

later arrivals. This is not statistically significant for probe separations up to 160mm, but becomes much more important at higher separations. The fact that the onset measurement yields higher velocities is further evidence of separation-dependent signal distortion, which is more apparent for the small probes because propagating signals are at lower amplitudes and higher frequencies. Although this effect was not observed in the laboratory with the field probes, *in situ* velocities calculated from onsets were generally slightly higher than those from later trace features, especially over high separation ranges. Fortunately by restricting the separation range monitored the difference could be contained to well within experimental error.

3.4.4.2. Calculation of offset for 'true' source-receiver separation.

Although the 'true' probe separation is not required for measurements of V_s or attenuation using multiple receiver positions, it is needed where only one probe separation is used in the calculation. This was necessary during laboratory experiments where the effect of variation in parameters other than separation were under investigation, for example transmitter excitation frequency, probe depth, or artificial burrow density. Perhaps more importantly, it was found to be necessary for full characterisation of the S-wave propagation characteristics under certain *in situ* conditions. In situations where a thin surface layer of considerably reduced rigidity is present, the characteristics of this layer will only be measured by considering the propagation path between the transmitter and nearest receiver position. To illustrate this point, consider the two hypothetical arrival-time separation curves in Fig.3.16(b). Both yield a V_s of $50ms^{-1}$ on regression of measured arrival-time against separation.

(a)

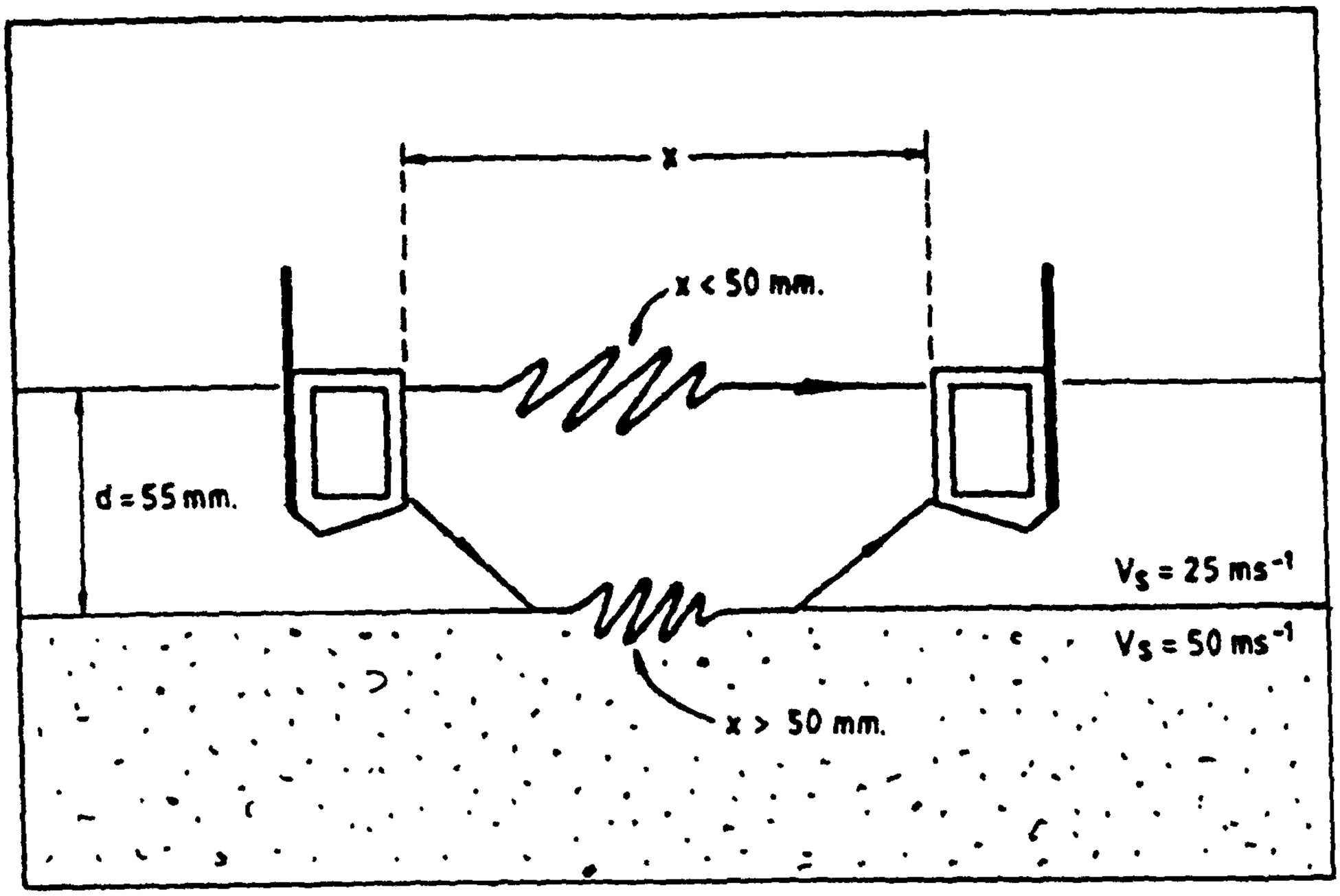

(b)

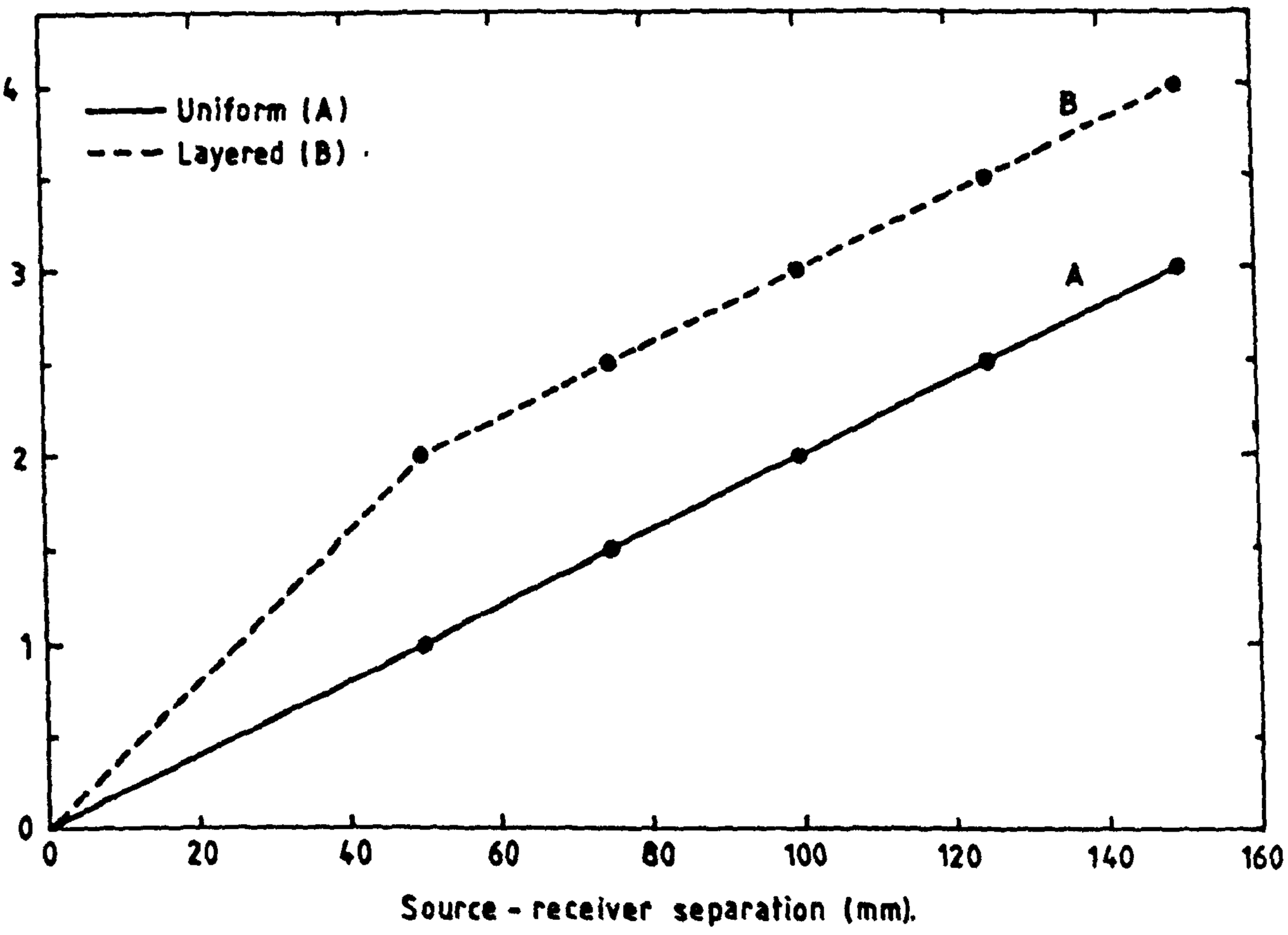

Fig. 3.16. (a) **Refraction in layered sediment.**
(b) **Comparison of time-separation data.**

However, while curve A would be obtained in a homogeneous deposit, curve B would be obtained in a deposit with a 55mm thick surface layer at $25ms^{-1}$ (from simple refraction theory, Telford et al, 1976) [Fig.3.16(a)]. This can only be calculated from the onset arrival time and the true source receiver separation, and is defined here as Surface V_s.

This parameter still, of course, represents only an apparent value, since any number of additional layers might exist within this one, which could only be measured by further reducing the probe separation, and the interval between measurements. Ultimately the physical dimensions of the probes limit the resolution of surficial velocity gradients. This will be discussed further in 3.4.5.

The true source of vibration can be obtained by extrapolation of regression equations calculated for onset arrival times only, from the separation offset (Δs) at which arrival time is zero. From this the 'true' source-receiver separation can be calculated as:

$$s_{true} = s - \Delta s \qquad (3.7)$$

Estimation of Δs was complicated by the slight non-linearity of the time-separation plots. Strictly, perhaps, best fit curves as in Fig. 3.14 should have been extrapolated to obtain the true source in each case. However, this would assume first that the data is reliable enough to precisely define a curve, and second that the curvature is genuine and not wholly or partly due to separation-dependent signal distortion. Since neither of these could confidently be assumed, a linear extrapolation, restricted to small separation measurements to reduce the effect of any genuine velocity gradient, was chosen as the most reliable procedure. The choice of separation range was made by examination of confidence limits for the intercept calculated from increasing separation ranges. For small numbers of measurements, there is a high degree of uncertainty. As the range increases, a minimum error is generally obtained before curvature adds further uncertainty. It was found that 10+/-5mm represents the best possible estimate over all experiments. Dividing this by two (to allow for both transmitter and receiver) yields a true vibration source at 5+/-2.5mm behind the probe tips, i.e. somewhere between the edge of the bimorph plate and the metal housing of the probe. This implies that the potting

compound distorts beyond the element, but is not rigid enough to transmit significant vibration to the housing.

For the small probes, the offset for conversion of probe-shaft separation to true source-receiver separation was found to be - 44 +/- 10mm, suggesting that the true source is at the probe tip. This contrasts with the field probes in that the entire probe contributes to S-wave excitation (rather than just the transducer element), probably because of the much stiffer resin used. This is supported by other similar calibrations performed on bender elements at UCNW.

3.4.4.3. V_s determination using time-separation data.

In the light of the preceding investigation, an experimental strategy could be devised for deployment of the field probes *in situ* in surface deposits. The conclusions were specific to the particular probes under consideration: it would be advisable to conduct a similar investigation for all new probes at the development stage. They can be summarised as:

(1) Arrival time *vs.* probe separation is approximately linear in surficial homogeneous sediment over a probe-tip separation range of 50-180mm, for probes pushed 30-50mm into the sediment.
(2) Using this separation range, V_s can be determined to within 5-7ms^{-1} in homogeneous laboratory deposits. Time and separation errors generally exceed any curvature due to velocity gradients or signal distortion.
(3) Since frequency is approximately constant over this range, velocity can be calculated from trace features other than the onset.
(4) The effective S-wave source lies between the leading edge of the bimorph and its metal housing. Thus to obtain true source-receiver separation 10+/-5mm must be added to probe tip separation.

3.4.5. Variation in V_s with depth.

Experiments discussed in the preceding sections indicated that positive gradients in V_s may be present within the surface layers of homogeneous

sands. Such gradients have been theoretically predicted and experimentally verified over depth ranges of 1 - 1000m [Hamilton 1976, Stoll 1980]. The exact form and parameters of any velocity:depth relationship will be dependent on textural parameters, post-depositional history and biological or geochemical factors. In general, empirical relationships of the form:

$$V_s(z) = A_z z^r \qquad (3.14)$$

have been favoured with the parameters A and r falling within reasonable ranges, and in general agreement with theoretical predictions. Obviously, very much shallower depths are of interest when considering the proposed *in situ* deployment. The empirical fits quoted by other workers cannot therefore be relied upon as predictors in this case. For this reason it was necessary to measure the variation in V_s with depth in the top 100mm of the laboratory test tank.

3.4.5.1. Direct measurement of velocity gradients.

The field probes were partially inserted to a depth of 10mm in saturated sediment. Pulse onset arrival time and frequency were measured, then both probes were pushed 10mm further into the sediment maintaining a constant separation. The process was repeated until a maximum depth of 50mm, or full insertion of the transducer plates was achieved. Further penetration of the sediment would have caused too much sediment disturbance from the bulky connections on the probe shaft. V_s was calculated at each depth from arrival time and true source-receiver separation using the offset defined in the previous section. The small probes described in 3.3 were also used: these could be inserted to a maximum depth of 90mm.

Before discussing the results obtained, two points about the experimental procedure should be made. First, varying probe depth involves a change in transducer response and hence propagation frequency. In particular, with the larger field probes a varying proportion of the transducer plate was in contact with the sediment at different depths. Second, if the medium has a velocity gradient, each V_s measurement may be an overestimation of the 'true' velocity at that depth, since the fastest arrival could be refracted through deeper sediment layers. Relatively short probe

separations (less than 120mm) were used to minimise this effect.

Measured V_s has been plotted as a function of depth in Fig.3.17. It is clear that relatively sharp gradients in V_s can be measured within 10cm of the sediment surface. It is important to appreciate that this does not necessarily imply a reduction in porosity with depth, since overburden pressure is not thought to be capable of causing significant compaction in the upper 2m of sands [Hamilton, 1979]. Instead, the weight of the overlying sediment acts to force grain contacts together, thus increasing intergranular friction. For this reason, V_s would be expected to be extremely low at the surface, increasing rapidly in the bulk sediment matrix. Measurements have been placed in context with other observations and theoretical predictions in Fig.3.18.

The middle curve in Fig.3.18 illustrates Hamilton's empirical fit [1976]. A similar equation has been fitted to the 5 data sets in Fig.3.18: parameters are listed in Table 3.3. The outer limits are from Stoll's theoretically predicted limits for a range of sand properties based on Biot theory [Stoll, 1980]. The spread in measured absolute values and relative increases with depth is probably due to differences in packing conditions at the time of measurement, over which no control was exercised. Further, more controlled work in this area would be useful, investigating near surface gradients in deposits of differing textural and structural properties.

The fact that sharp gradients have been observed in the surface layers leads to some problems in interpreting measured values of V_s. An increase in V_s from zero to around $45ms^{-1}$ is indicated in the upper 40mm, even in homogeneous sediment. The problem is complicated by the finite size of the field probes. The transducer element will generate a series of horizontally polarised shear displacements along its length, each at different amplitude and phase, which propagate at different speeds through the surface layer. The simplest interpretation is that the measured pulse onset should represent the fastest transmitted disturbance, which corresponds to that emanating from the lowest part of the plate at 40mm. However, slower and possibly larger amplitude disturbances travelling through the upper layers will also affect the received signal, probably

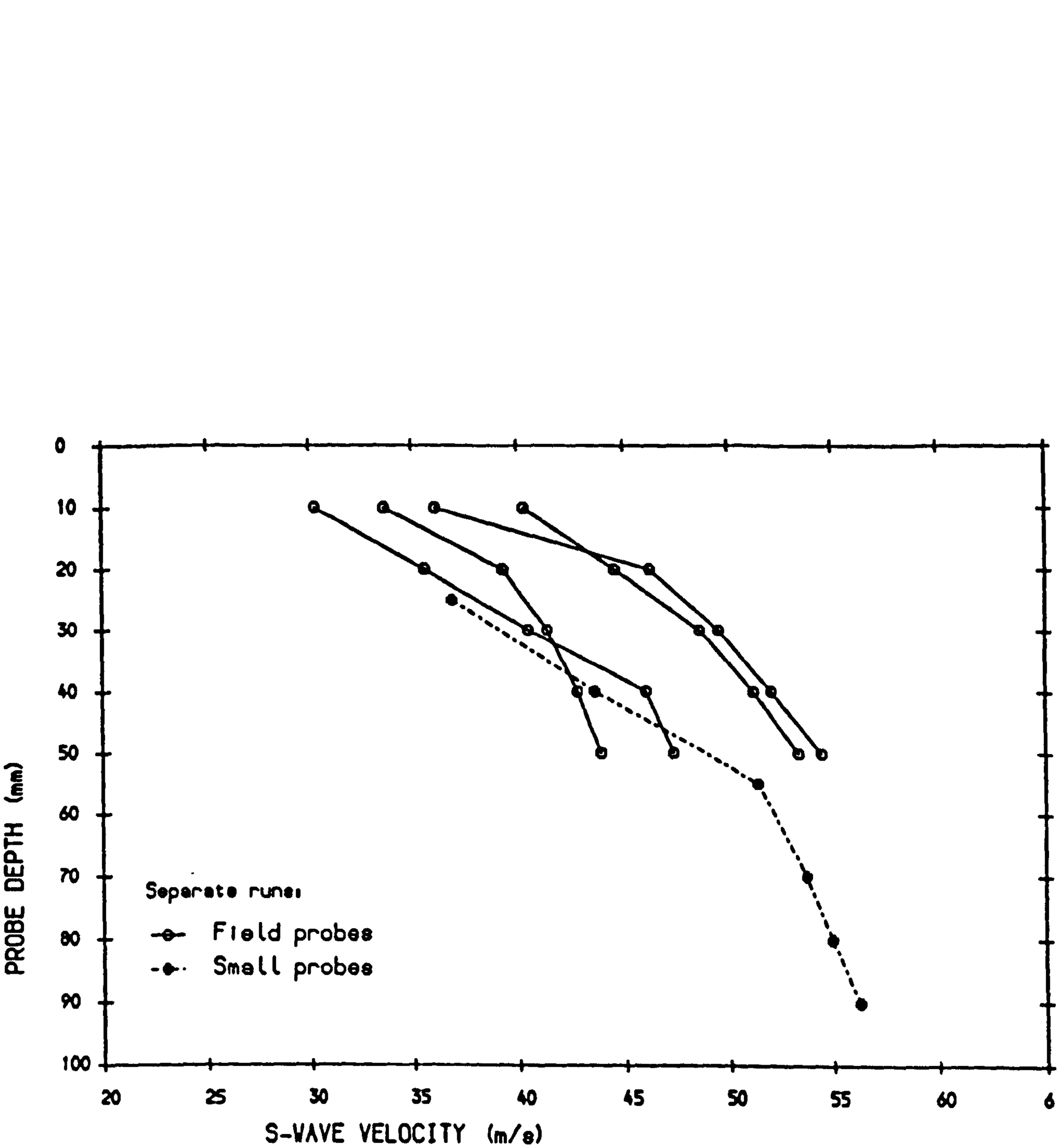

Fig. 3.17. Variation of V_s with depth.

'smearing out' the pulse train, and possibly interfering with components of opposite phase.

It is evident that complete characterisation of surficial deposits requires detailed measurements at a series of depths. In theory, the transducers could operate to within 10mm of the surface, and were capable of 10mm resolution. However, this form of intensive measurement at individual sites would have drastically limited the number of different sites which could be monitored in any sampling period, and was unnecessary considering that *in situ* measurements were to be compared with vertically averaged bulk textural and biological properties within the upper 50mm.

It was, however, essential to standardise the depth of insertion and the minimum probe separation used, since comparisons could only be usefully made between values measured over identical sediment volumes. The companion problem of interpreting multiple time-separation measurements in depth-varying media is dealt with in the following section.

Table 3.3. Empirical coefficients for measured V_s gradients: $V_s = A_z z^r$. [V_s in m/s, z in m]

Source	A_z	r
Field probes: 1	113	0.29
" " 2	72	0.16
" " 3	90	0.18
" " 4	118	0.25
Small probes: 1	130	0.34
Hamilton (1976)	128	0.28
Stoll (1980)	95/155	0.26/0.19

3.4.5.2. Prediction of time-separation curves in velocity gradients: comparison with measured data.

The velocity:depth relationships indicated in Table 3.3 can now be used to predict the form of the arrival-time separation curves for transducers

deployed at the surface, which can be compared with those directly measured (Section 3.4.4). Unfortunately, no concurrently measured sets of velocity:depth and time:separation data were obtained, so comparisons can only be general.

Empirical velocity / depth relationships imply a continuous variation with depth. The simplest method of modelling pulse arrival time as a function of probe separation involves splitting the sediment into discrete layers of small thickness and constant velocity. The problem then reduces to one of multi-layer refraction, assuming that the principles of ray theory can be applied. Note that, because of the size of the transducers, resolution of surface layers down to 40mm is lost.

The arrival time (t) of an S_H wave pulse propagating through *n* discrete layers of increasing velocity is given by:

$$t = \frac{s_{true}}{V_n} + \sum 2(z_i/V_i)\cos\vartheta_i \qquad (3.15)$$

where s_{true} is the true probe separation, V_i is the velocity of the *i*th layer (of thickness z_i) and $\sin\vartheta_i = (V_i/V_n)$. If the sediment is split into layers of constant thickness d, then $z_i = d$, and if the probes are inserted to a depth $z_0 = m_0 d$, then the velocity of the i^{th} layer beneath this is given by:

$$V_i = A((m_0 + i)d)^r \qquad (3.16)$$

d was taken as 0.01m, m_0 as 4, and the values of A and r were taken from Table 3.3. The number of layers traversed by the pulse depends on the rate of velocity increase and on the probe separation. Measured signal arrival time will correspond to the fastest travel path, which is through the surface at small probe separations but curves into the sediment as separation (or relative velocity of sub-layers) increases.

Measured onset-time / probe-separation data from two of the experiments described in 3.4.4 have been corrected to 'true' probe separation and plotted in Fig.3.19 along with predicted values from the five velocity-depth relationships from Table 3.3. The main point is that very little

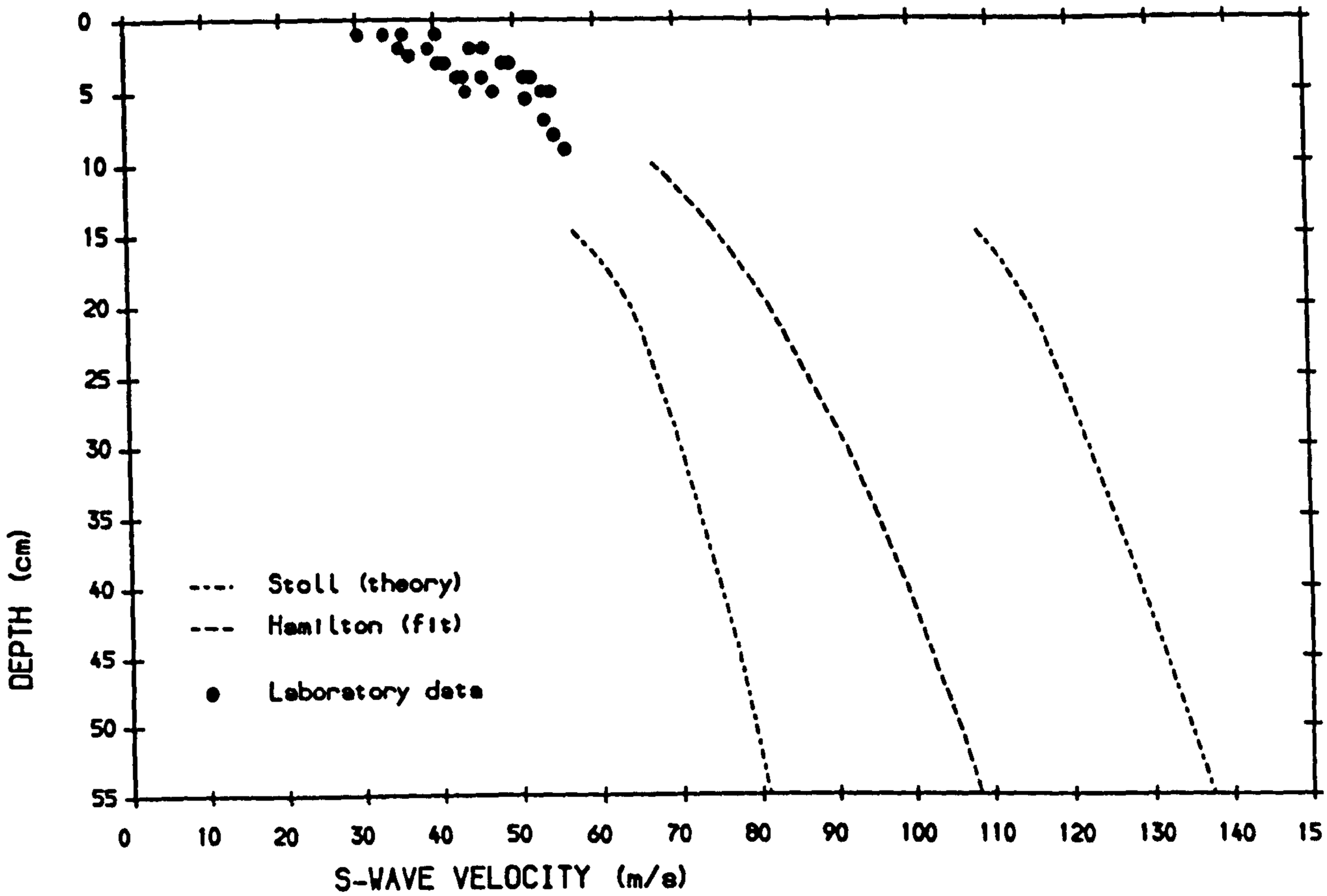

Fig. 3.18. Comparison of measured V_s:depth variation with published relationships.

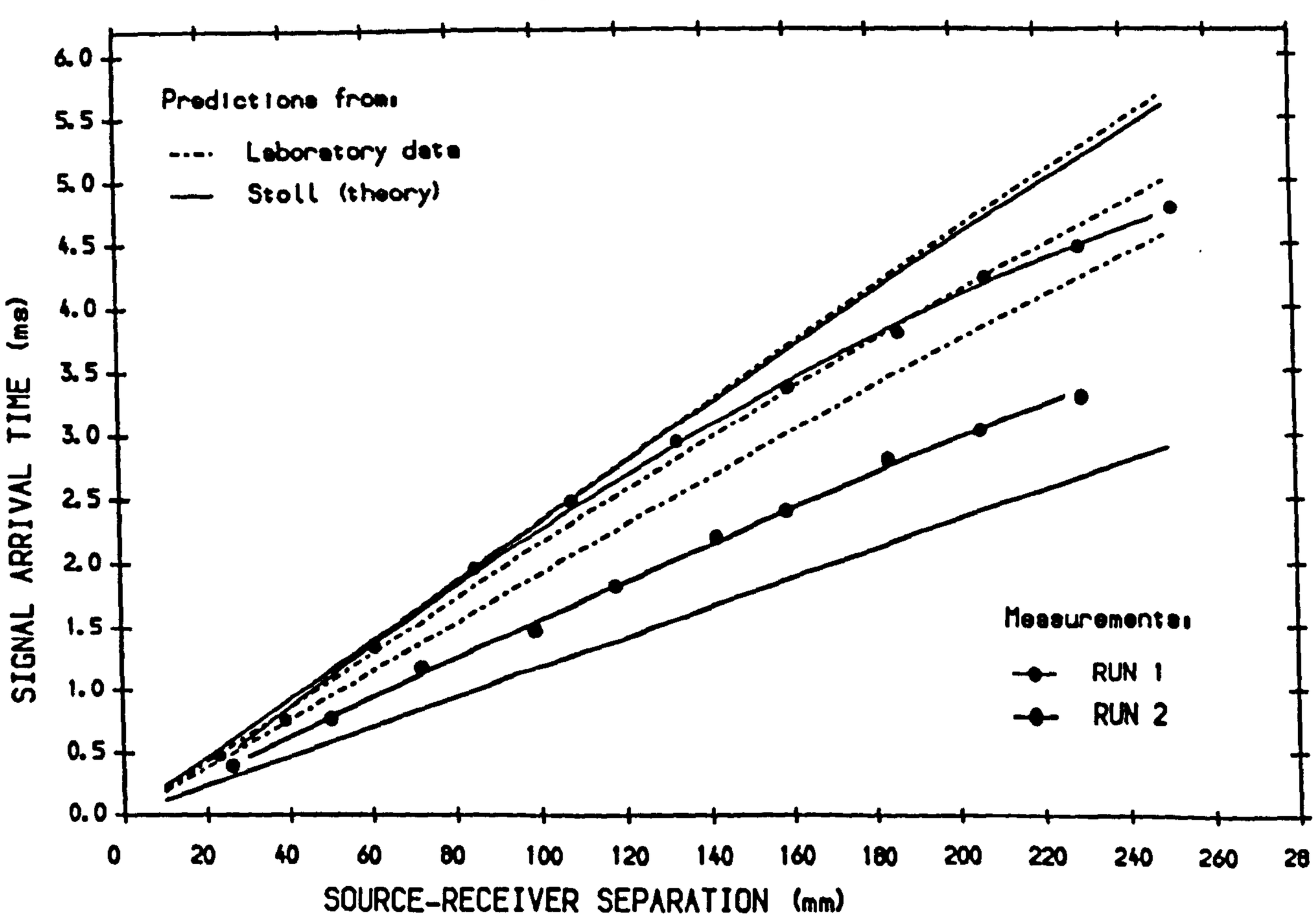

Fig. 3.19. Effect of velocity gradients:
measured and predicted time/separation curves.

curvature is predicted over these relatively small separations, with the maximum depth of penetration of the pulse at around 80mm. It is interesting that the measured data indicate a rather stronger velocity-depth relationship if the full separation range is considered.

There are two possible explanations for this apparent disagreement. The first is that in this case S-wave propagation is unlikely to be completely described by a far-field refracted plane wave-front model. The second and perhaps most important explanation is that two effects combine to distort the 'true' pulse arrival times at near- and far- field separations, especially for the signal onsets under consideration here. The implication is that the primary cause of curvature in arrival time/separation plots is not an increase in velocity with depth, at least in homogeneous deposits. Signal distortion is proposed to be the major cause. Fortunately, provided that the separation range is restricted to 50-180mm, the degree of curvature is in any case sufficiently small to be ignored.

A final consideration is the actual velocity being measured by this technique. Table 3.4 lists values of V_s calculated for different separation ranges in gradients selected from Table 3.3. It was found that over the ranges which yield high quality signals the multiple probe-separation method of measuring V_s is relatively insensitive to measured velocity gradients in texturally homogeneous deposits. Taking a typical example, where V_s varies from 46 to 58 ms^{-1} between 40 and 80mm depth, linear regression of time separation data over probe separations from 50 - 200mm yields a value of 48 ms^{-1}. Regression of time-separation data results in an apparent single velocity for the sediment which has been defined here as **BULK V_s**. This represents a value of V_s which can be assigned to a homogeneous deposit of given textural properties and porosity (which are not themselves normally subject to gradients), but which is clearly not unique, and which is dependent on the size of the S-wave probes, on their depth of insertion, and to a lesser extent on the separation ranges used.

It is important to note from Table 3.4 that for homogeneous sands SURFACE V_s, calculated from the shortest transmitter/receiver arrival time and the true probe separation, is not measurably different from Bulk V_s, so that a

Table 3.4. V_s (m/s) calculated from linear regression of time-separation curves predicted from measured velocity gradients.

Source		Separation range (mm) 0:200	0:50	50:150
Field probes:	1	47.4	44.8	45.8
" "	4	54.6	52.4	53.2
Hamilton (1976)		57.3	55.3	55.8
Stoll (1980)	min:	44.6	43.3	43.6
	max:	86.2	84.9	85.1

single velocity parameter can be used. This parameter should then represent the bulk textural properties, and the porosity, of the top 80mm of the deposit. Only in sediments exhibiting marked textural or structural heterogeneity (e.g. Fig. 3.15) will these two measurements be different.

It should be remembered, therefore, that all measured velocities must be considered as functions of the depth of measurement, and care should be exercised when making comparisons between other data sets. This is a general point which applies over all separation scales from cm to hundreds of metres.

3.4.6. Investigation of the effect of drainage of a surficial deposit.

The S-wave characteristics of surficial intertidal deposits should be highly sensitive to the degree of saturation, as discussed in Chapter 2. Both 'gas-closed' and 'fluid-closed' systems might be expected in intertidal deposits at different stages of the tidal cycle: in flats exposed on the ebb, drainage results in voids sealed at the grain contacts by surface tension resulting in negative pore pressures which act to pull grains together, thus increasing intergranular contact forces and hence sediment rigidity.

Partially saturated sediments constitute a three-phase system, and therefore require special theoretical consideration. In particular,

experimental and theoretical predictions of properties such as dispersion or attenuation, based on two-phase gas or fluid saturated media should be extended to the partially saturated case with caution. For this reason, S-wave propagation in drained sediment has been considered separately.

This part of the laboratory work was concerned with identifying changes in S-wave characteristics of the sediment as it changes from a fully saturated to a fully drained state. No means of quantifying the degree of saturation was available so the results had to be rather qualitative: however, the two end-points could be reasonably well defined. The investigation was divided into three sections: assessment of transducer/sediment frequency response under drained conditions; comparison between saturated and drained V_s; and measurement of V_s during the drainage process.

Amplitude/frequency response.

The response of the field probes in drained sand was found to be more complicated than that obtained for saturated sediment. A series of experiments was performed in which the field probes were placed in saturated sediment and their amplitude response was measured following the procedure outlined in Section 3.4.3.2. The tank was then drained and the experiment repeated without moving the probes.

Two examples have been selected to illustrate the results. In Fig.3.20 a broad single-peaked curve, with lower amplitude at the higher frequency tail is obtained under both saturated and drained conditions. The drained measurements fall within a much higher frequency bracket, over a larger measurable range, and the maximum amplitude is more than twice that under saturated conditions. This is interpreted as lower attenuation for the drained sand, and greater rigidity (and hence S-wave velocity), so that the sediment-transducer system resonates at a higher frequency. The step-excitation response corresponds reasonably well with the resonant peak, and again shows higher amplitude and frequency for the drained case. Measured V_s is indeed higher than for the saturated case, this being discussed in more detail in section 3.4.6.2.

Fig. 3.21 illustrates a different example, this time with a double-peaked response under drained conditions. The main difference between this experiment and the one illustrated in Fig.3.20 is that the sand was left in the drained state overnight before measuring, so that a high degree of rigidity (and V_s) was obtained. Maximum amplitude and resonant frequency are again much higher than the saturated case. The drained step-excitation response was also observed to have at least two frequency components: these could not be quantified without digitising and transforming the signal. Where measurable, received pulse frequency was generally found to correspond to the highest frequency mode, rather than the maximum-amplitude mode. This can be explained by the fact that lower frequency components in the received pulse train will necessarily appear later, and will interfere with the higher frequency signal, although they are usually at higher amplitudes. Clearly the definition of received pulse frequency used in saturated sediment breaks down when the pulse is multichromatic.

The most likely explanation for these bimodal amplitude responses is supported by comparing with the unloaded response curve in Fig.3.7. The high-amplitude low-frequency peak in Fig.3.21 corresponds reasonably well with the unloaded transducer resonance, while the higher frequency mode corresponds to a low amplitude part of the unloaded response. This suggests that the sediment is less well-matched to the field probes when drained, causing partial breakdown of the pulse into a component near the transducer resonance, and one corresponding to the appropriate wavelength of vibration in the sediment. In other words, in this case the transducer must be partially decoupling from the sediment. A similar phenomenon has been observed in a laboratory cell on increasing the effective stress [Bennell, *pers. comm.*].

The response of the small probes was also characterised under saturated and drained conditions. Fig.3.22 illustrates one comparison. Much higher frequency brackets are involved, as expected since the probes are both smaller and stiffer than the field probes. The small probes were not found to break down into multiple frequency components in response to a step excitation in drained sand, because they are clearly better matched to the higher velocities involved. Note, however that received amplitudes are

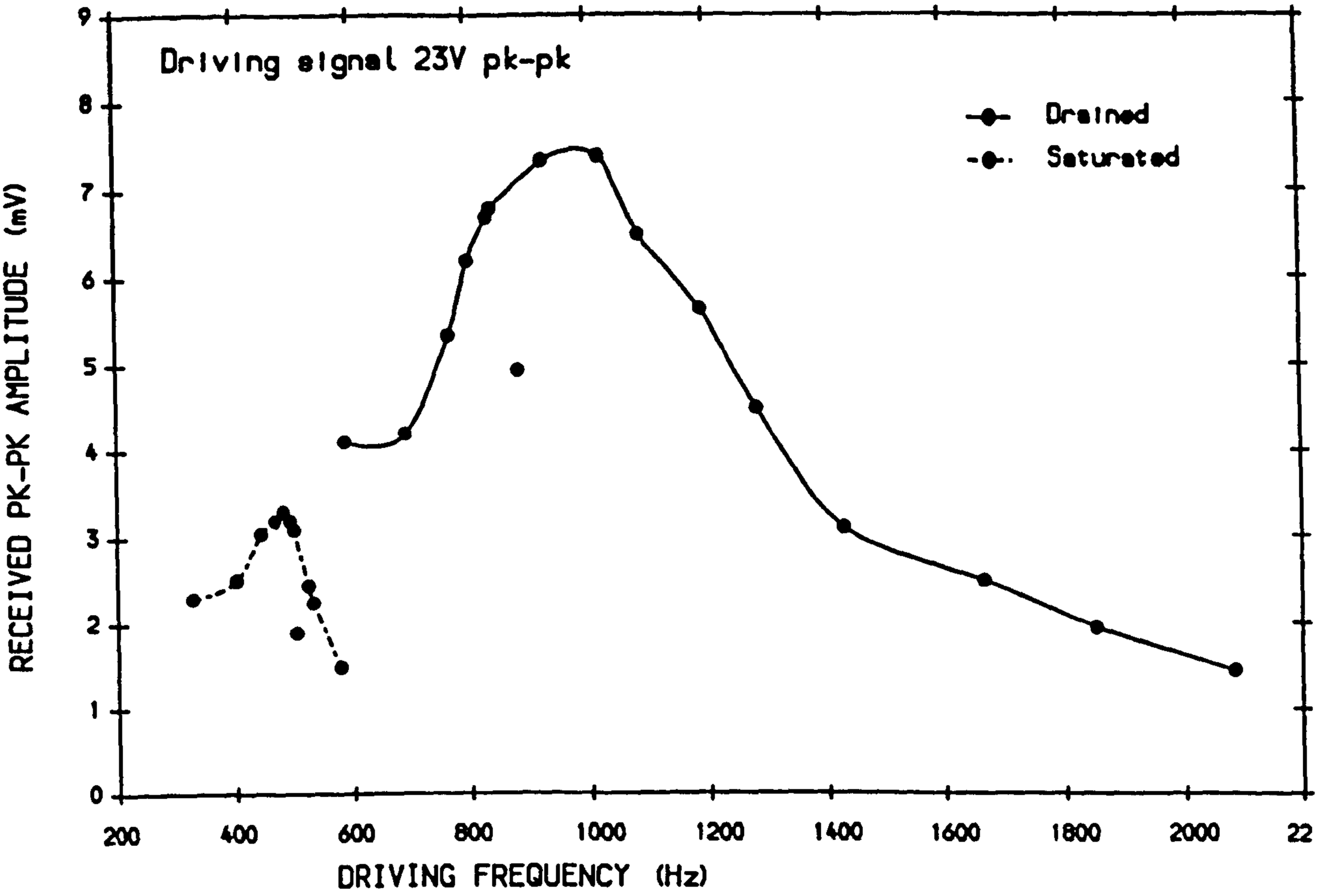

Fig. 3.20. Effect of drainage on sediment/field probe response (RUN A).

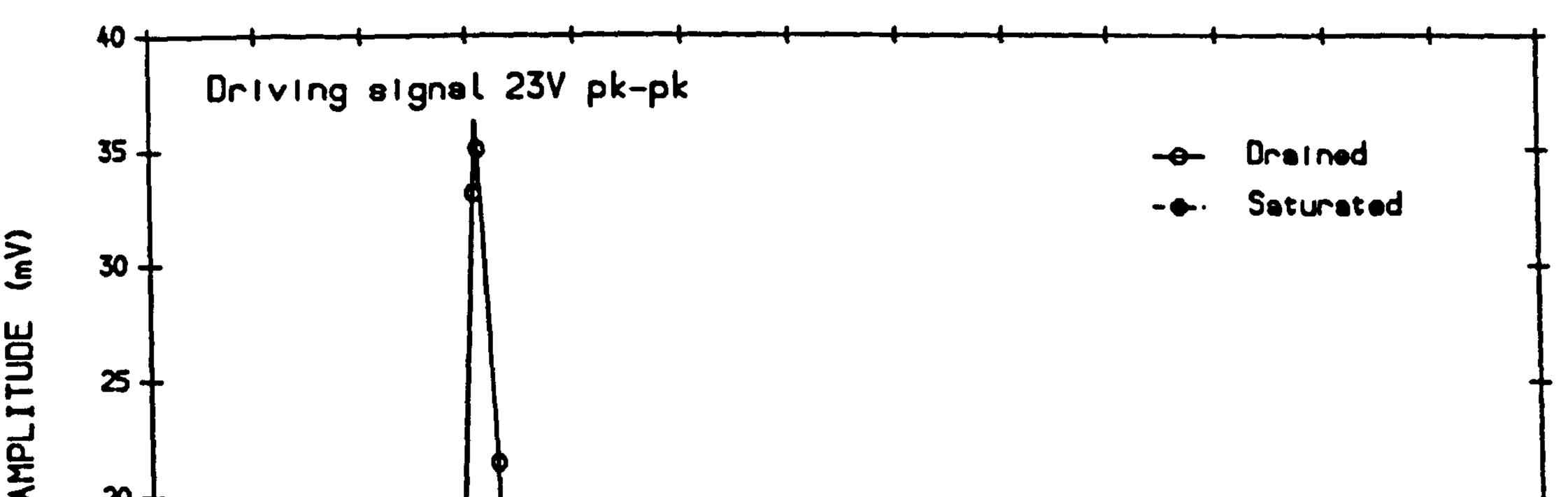

Fig. 3.21. Effect of drainage on sediment/field probe response (RUN B).

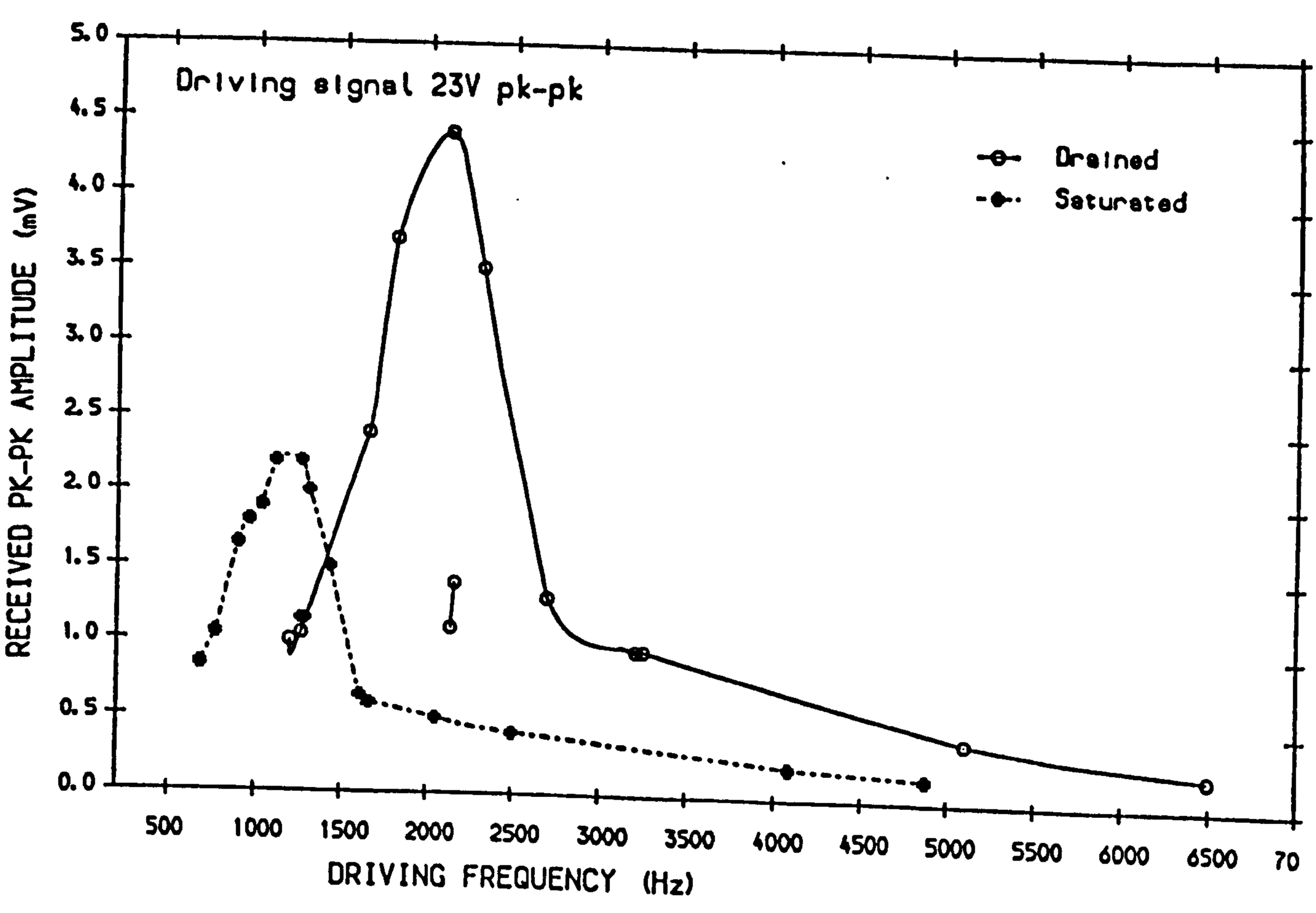

Fig. 3.22. Effect of drainage on sediment/small probe response.

much lower, even allowing for signal breakdown, presumably due to their smaller size.

The behaviour of the S-H probe/sediment system under partially saturated conditions clearly requires further experimental investigation beyond the scope of this study, in particular performing proper frequency analysis of received signals. Fortunately, the problem of interpretation of the amplitude frequency response curves is not required to be solved before measuring V_s under drained conditions. The response to step-excitation remains a clearly defined pulse envelope with sharp onset.

Comparison of V_s under saturated and drained conditions.

Saturated and drained V_s were determined in a series of experiments using the field probes (at fixed separation and depth) and the Sonic Viewer. The two end-points of the process are defined as follows:

Fully drained: the tank was drained from full saturation until the tap ran dry, and measurements were performed within the following 15 minutes. Immediately after drainage, the degree of saturation will be a function of the textural properties and porosity of the sediment. This drained state will contain water, concentrated around the grain contact points, which in exposed intertidal flats may eventually evaporate until a virtually dry state is obtained. Time dependent '*consolidation*' under negative pore pressures within the voids may also occur.

Fully saturated: water was added slowly and evenly to the sand from beneath while the tank was thumped with a rubber hammer. This process was intended to minimise the amount of entrapped air within the pore-space, but complete removal of air could not be ensured. Shirley et al [1978] found that only vibration under vacuum could guarantee complete saturation in the laboratory. The same group later reported [1979] adding the sand to boiling water to ensure complete expulsion of air. However, under field conditions there may also be incomplete pore-fluid saturation as the tide covers the sediment (as, for example, in the extreme case of cavity sand formation).

More important than the precise nature of the end-points was the necessity of being able to repeat the saturation-drainage cycle, and obtain consistent results. It was found that once established, there was good repeatability of measurements in repeated cycles of fully-saturated to fully-drained conditions. Nevertheless, several drainage-saturation repeats were sometimes necessary before the measurements 'settled down' to a consistent value. This was particularly noticeable in sand which had been left in the drained state for a long period. Once drained, further time-dependence was also observed, presumably due to consolidation under negative pore pressures, and evaporation from or diffusion of air into the surface layers.

Fig.3.23 illustrates drained V_s plotted against saturated V_s. A reasonably consistent relationship is apparent which has been approximated using a quadratic polynomial. Naturally a much wider range of sediment texture and porosity should be considered before generalising this simple relationship. Note that the increase was, as expected, greater than that found elsewhere between saturated and dry sand [Shirley et al, 1979], which was of the order of 20%. The increased values for dry sand are caused by the absence of viscous coupling between sediment and pore-fluid, and by the increase in intergranular friction caused by the removal of Archimedean upthrust. The drained state represents a special case because of the presence of sealed voids at negative effective pore pressures.

Observation of the drainage process.

Although it was not possible to quantify intermediate stages in the change in sediment state from fully saturated to fully drained, several sets of measurements were made which enabled interpolation between the end-points. The relevant tap was simply closed on several occasions during drainage, and the received pulse characteristics monitored.

Measurements from three separate experiments have been presented in Fig.3.24. Intermediate measurements between defined end-points have been arbitrarily positioned for clarity of presentation: a rapid increase in V_s is obtained from the point where water has just left the sediment surface

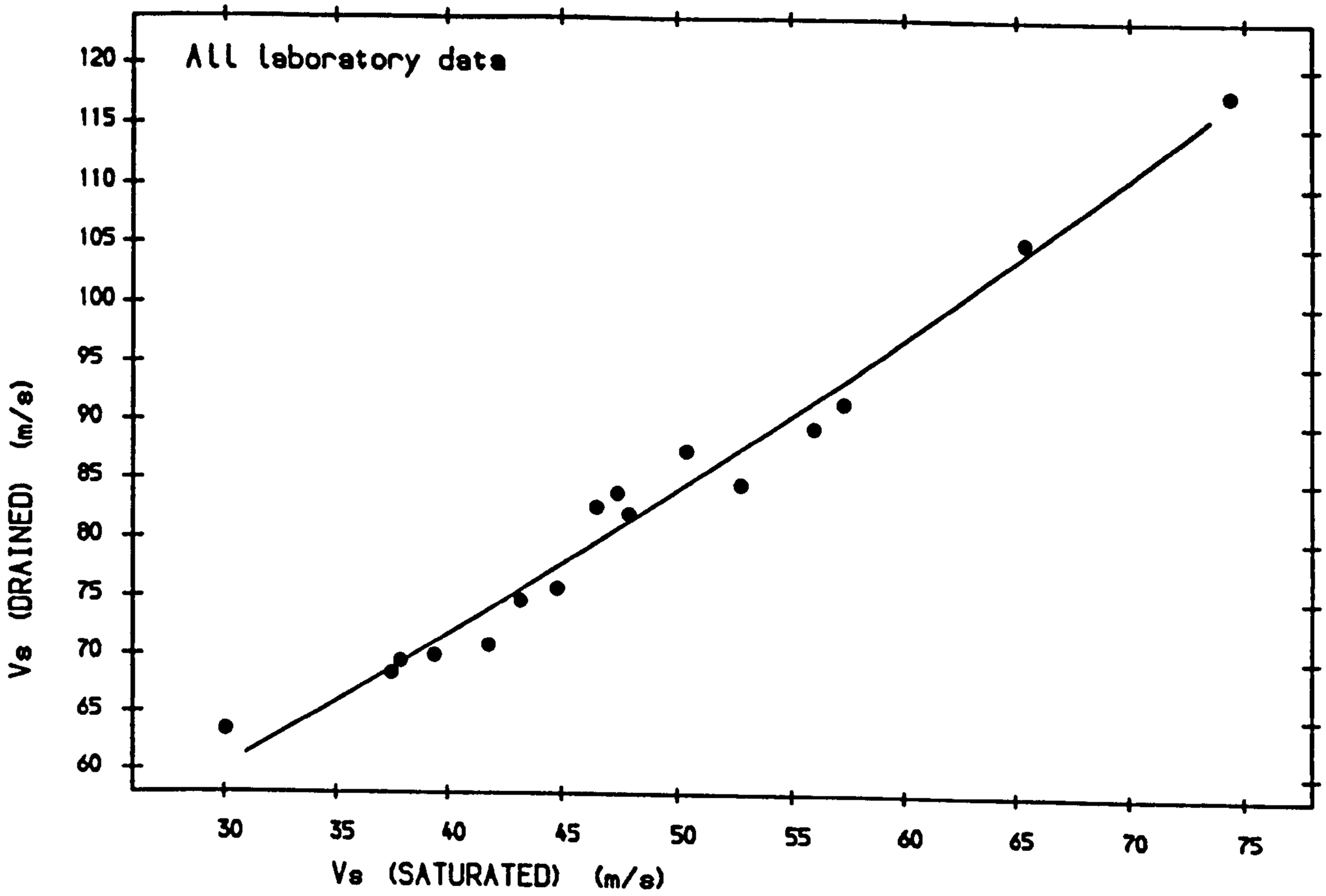

Fig. 3.23. Comparison between fully drained and fully saturated V_s.

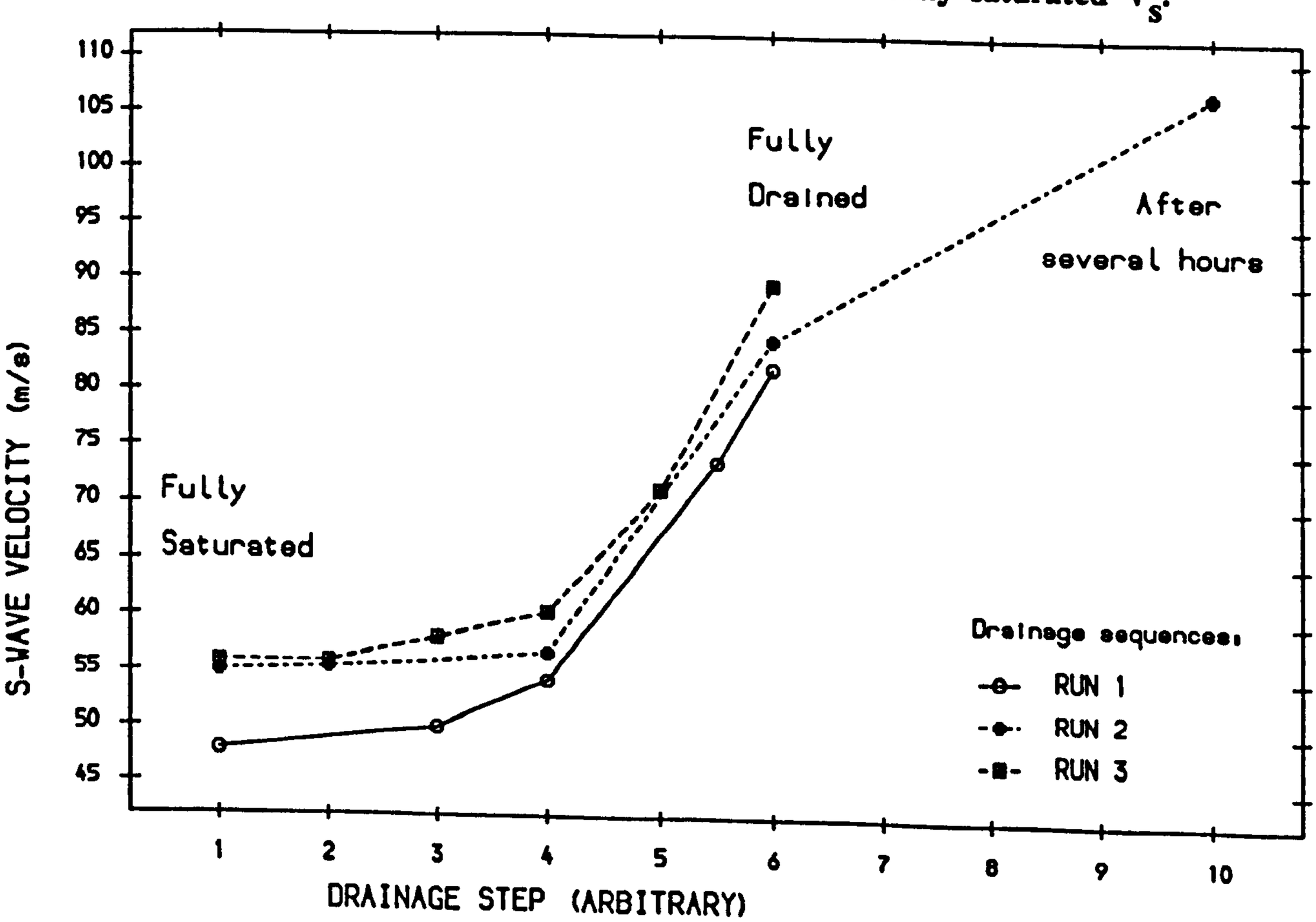

Fig. 3.24. Variation of V_s during drainage.

to the fully drained state. A further increase in V_s is observed on leaving the sediment drained for several hours. This was thought to be caused by a gradual 'tightening up' of the sediment fabric under negative pore pressures (or under its own unsaturated weight), or possibly by increased numbers of voids forming due to evaporation at the surface. Another possibility is that cementation occurred at the grain contacts due to organic matter and salt left by the tap-water on evaporation. The assumption that diffusion and evaporation would eventually remove the excess pressures and therefore cause a reduction in V_s until its dry state was reached was not verified experimentally.

3.4.7. Investigation of velocity-frequency relationships.

Two important questions about velocities and frequencies associated with the field-probe/sediment system remained outstanding:

(1) Investigation of the relationship between the frequency received from a step or spike excitation, which has already been shown to correspond to a resonant frequency of the transducer-sediment system, and the S-wave velocity of the sediment.
(2) Investigation of the relationship between the driving frequency of a forced sine wave excitation, and its velocity within the sediment.

It is important to distinguish between these two relationships, since the first should depend on transducer dimensions and compliance, and the degree of coupling with the sediment, while the second is a fundamental property of the sediment which is independent of the measuring system.

3.4.7.1. Resonant frequency - velocity relationships.

In many of the experiments using impulsive transmitter excitation, received frequency was measured in addition to V_s. It has already been stated that, assuming proper coupling with the sediment, a maximum in vibration amplitude of the transducer-sediment system would be expected when its wavelength in the sediment, λ, corresponds to a multiple of the

transducer length, L_{TD}, along the S-wave propagation direction:

$$\lambda_{res} = k\, L_{TD} \tag{3.18}$$

Substituting ($\lambda_{res} = V_S/f_{res}$) yields:

$$f_{res} = \left(\frac{1}{k\, L_{TD}} \right) V_S \tag{3.19}$$

It has been shown that the dominant received component of an impulsive excitation corresponds well with this resonant frequency. Therefore a plot of received frequency against measured V_s from the pulse arrival time should yield a straight line passing through the origin, of gradient given by the above equation. This, incidentally, should hold whether or not the medium is dispersive, provided that the measured received frequency and velocity correspond to the same component of the pulse. It should also apply equally to both saturated and drained sediment, provided that proper coupling can be achieved across the frequency range involved.

Arrival times, received pulse periods and true probe separations for all laboratory measurements involving spike or step excitations of the field probes have been collected together, converted into V_s and frequency, and plotted in Fig.3.25. Considerable scatter is obtained from: measurement error; pulse modification by dependence of received frequency on probe separation or dispersion; velocity gradients and multiple frequency components in drained sediment.

The data have been analysed using least-squares regression. The gradient yields a value for (kL_{TD}) of 79mm+/- 3.5 mm. The true-source offset calculation (3.4.4.2) suggests that the vibrating length (L_{TD}) of the transducer corresponds to fractionally more than the actual bimorph plate width, which was 37.5mm. Considering the scatter involved, the value of k calculated from this is surprisingly close to the expected value of 2 for a freely vibrating plate.

Thus the transducer-sediment response has been shown to correspond to a perfectly coupled system over the frequency range encountered in the laboratory. Note, however, that for measurements in drained sand, additional lower frequency components are also often observed in the

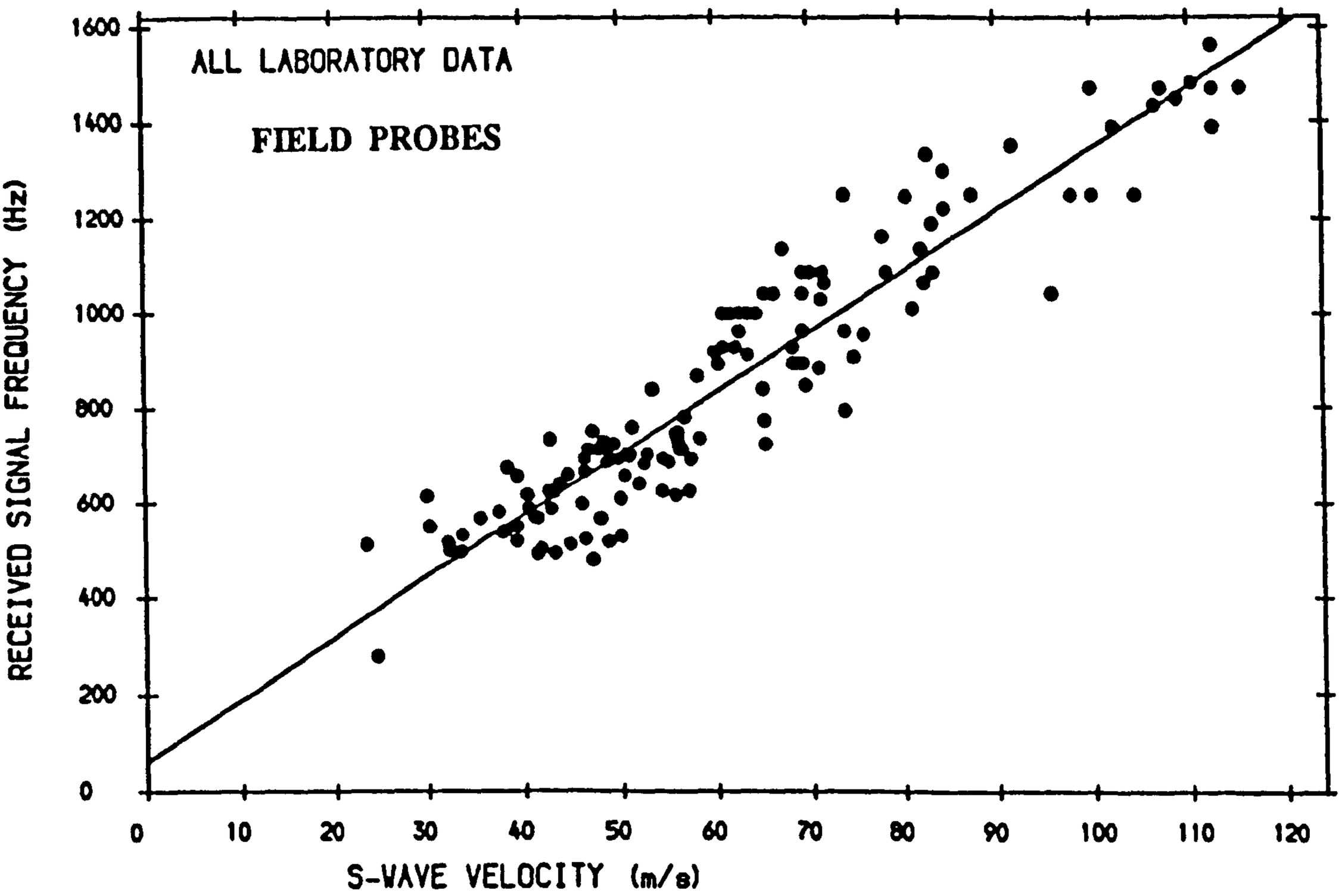

Fig. 3.25. Relationship between received (resonant) frequency and V_s:

received pulse train, sometimes at higher amplitudes than that of the measured frequency component, which implies a partial decoupling of the system at frequencies closer to the unloaded transducer resonance (Section 3.4.6.1).

For the small probes, a less extensive data set yielded a slope of 22.7 ± 3. Bimorph width in this case was 18.5 mm, indicating a k-value of 2.1-2.7: however, the source offset calculation suggested that the true vibrating length of the probe was 22mm, indicating a k-value of 1.7-2.3. The small probes therefore produce well-coupled signals at much higher frequencies than the field probes, due to their smaller size. This was exploited in order to increase the frequency range monitored in the investigation of dispersion in the next section.

This section has provided further evidence that the primary frequency component of an S-wave pulse transmitted by an impulsive excitation is at the resonant frequency of the transducer-sediment system, at least within the range of frequencies monitored in the laboratory. It also contributes to the indirect assessment of transducer-sediment response, indicating the mode of vibration of the probes. However, it does not provide any insight into the S-wave properties of the sediment itself. The investigation of dispersion presents a much more fundamental problem, which will be dealt with next.

3.4.7.2. Investigation of velocity dispersion.

Confirmation of the existence of V_s dispersion in unconsolidated sediment has been hampered by two main problems: experimental error in V_s measurement generally exceeds the predicted increase in velocity with frequency; and the band-width over which accurate measurements can be made may not coincide with the expected range of transition between low and high frequency regimes (Section 2.1).

Comparison of the frequency range in Fig.3.25 with the predicted velocity-frequency curve for sands (Fig.2.1) shows that the field probes should encompass part of the transition range for saturated sand.

Therefore an investigation of the variation of V_s with driving signal frequency, under uniform conditions to minimise experimental error, was undertaken. The probes were placed at a fixed separation and depth in the test tank, and remained in this position throughout the experiment.

The transmitter was driven using a single sine-wave tone burst, triggered by a square wave which also triggered a digital storage oscilloscope. Frequency was varied between limits where decoupling of the received signal from the driving signal was observed. A multi-cycle tone burst was used to limit the problems of additional frequency components being introduced via pulse 'gating', but no filtering was performed.

Several separate experiments were performed in saturated sand: results have been illustrated in Fig. 3.26. In one case an experiment with the field probes was immediately repeated with the small probes, at identical probe separation and insertion depth. This served to extend the frequency range of measurement, although it introduced systematic errors which may have affected the relative positions of the two curves.

In all cases a slight increase in V_s was measured with increasing frequency. At first sight this agrees well with the predicted dispersion curve in Fig.2.1, with an overall increase of less than 10% across the frequency range. However, the measured change occurs over a much smaller frequency range than the predicted transition period, resulting in a sharper gradient. The predicted transition is itself probably sharper than would be expected in natural sands, because it is based on a single grain size (and hence pore-space parameter). A spread of sizes should 'smear out' this transition even further.

The best agreement obtained was for the combined probe data set, which has been superimposed onto the curve predicted for medium fine sand at porosity 0.45 in Fig.3.27. The absolute agreement of the data is meaningless, because the equation solved to generate the curve uses estimates of dry V_s values, obtained by equating dry bulk modulus with the low frequency saturated case. Without a much broader frequency range, and more information about physical and textural properties of the deposit, the comparison remains inconclusive.

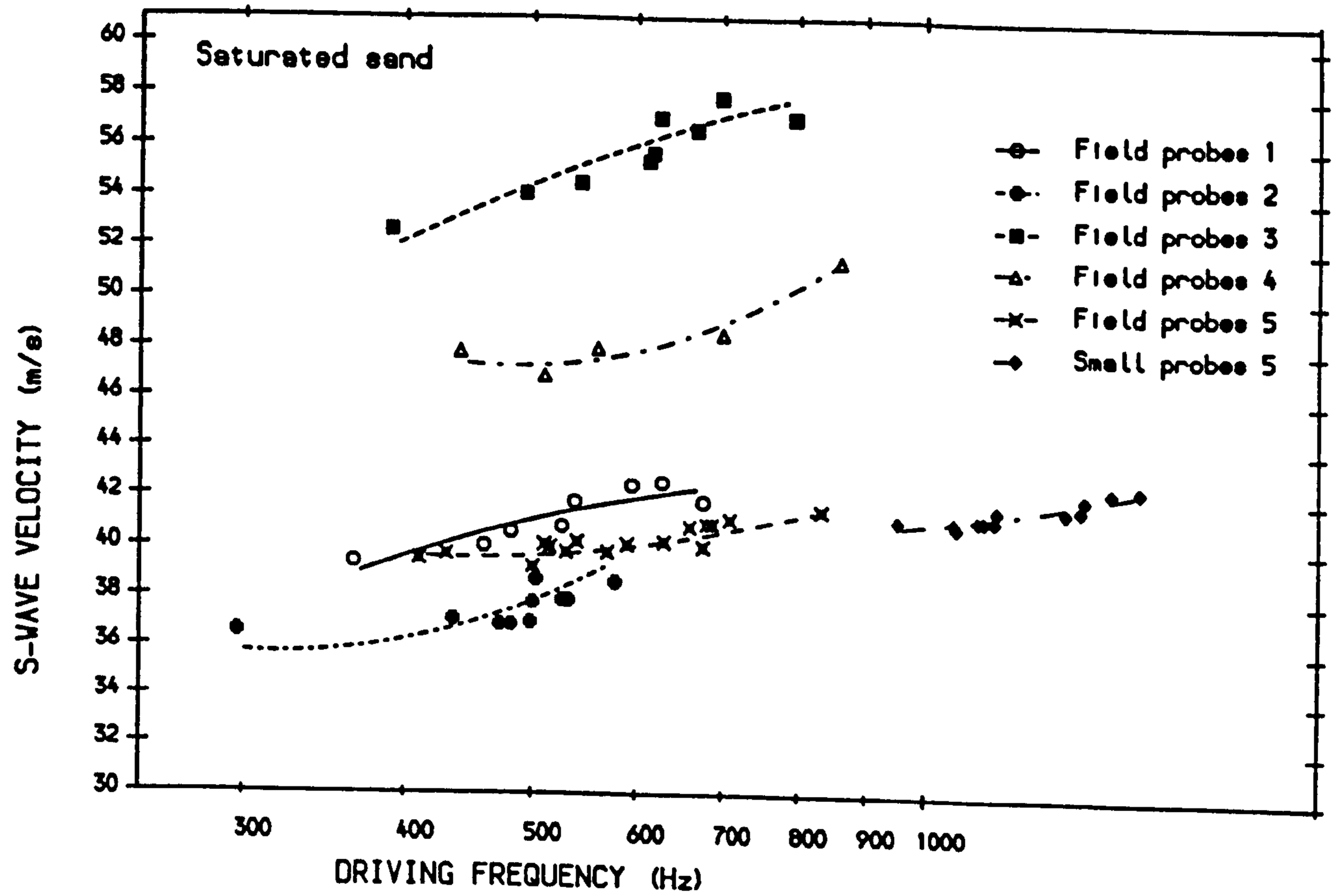

Fig. 3.26. Dispersion of V_s in saturated sand.

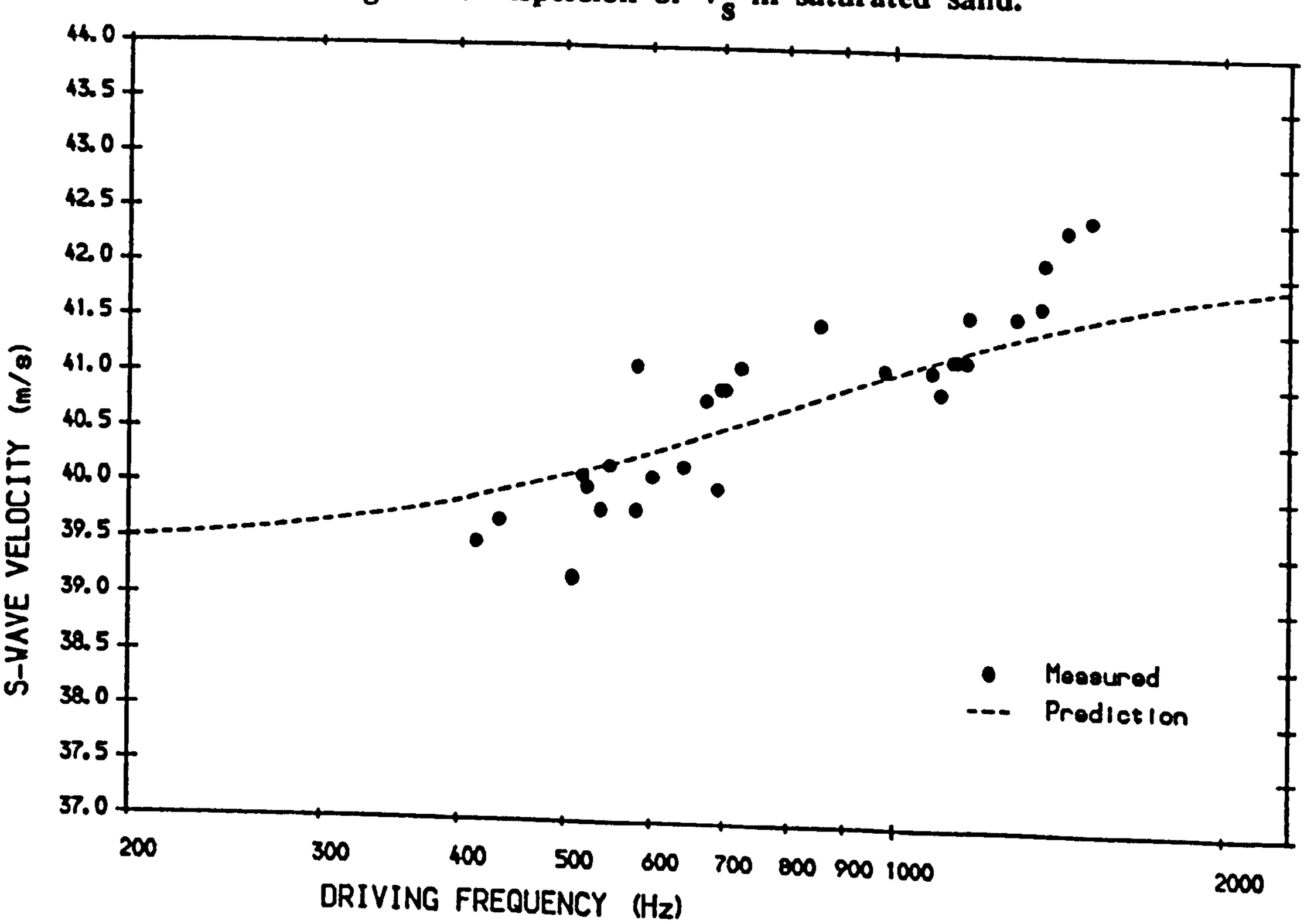

Fig. 3.27. Comparison between measured and predicted S-H dispersion.

In conclusion, rather stronger dispersion was measured than is predicted by viscous interaction of the pore fluid with the sediment matrix: however, the measured change is still considerably less than estimated absolute *in situ* experimental error (5.1.4). For the purposes of this study, therefore, where *in situ* measurement of V_s at the resonant frequency was proposed, the effect of dispersion can be safely ignored.

3.4.8. The effect of variation in sediment temperature.

There are three aspects of the response of the sediment-transducer system to variation in sediment temperature which merit attention:

(1) The compliance of the transducer, or of the potting compound, will be temperature dependent [Shirley *et al*, 1980]. This should affect unloaded frequency response, but not V_s.
(2) V_s may be temperature dependent. This could be introduced via three of the parameters in eqn.2.11, namely fluid viscosity and density and to a lesser extent grain density. Intergranular contact forces, which affect the frame shear modulus term, may also be temperature dependent, especially in cohesive sediment.
(3) Rapid heating or cooling of the deposit may result in variation of internal stresses (due to differential expansion or contraction along temperature gradients) which will in turn affect intergranular forces and hence sediment rigidity. Where the sediment is in a loose packing configuration the porosity may also change during this process.

Shirley *et al* [1980] undertook an experiment which investigated the effect of temperature on V_s in a saturated sand, a dry sand and a saturated kaolinite clay. They found that, provided a foam liner was incorporated into the sediment chamber to act as a 'pressure release', no significant change in V_s with temperature could be measured. If, however, the liner was not present a sharp decrease in V_s with increasing temperature was observed. This was interpreted as being caused by expansion of the aluminium container walls, which effectively reduced confining pressure on the fully compacted sediment.

It was not possible to set up elaborate equipment for strictly controlled equilibrium temperature variation for this study, nor, in the light of the ARL work, was it deemed necessary. Any fundamental temperature dependence of V_s has been shown to be within experimental error for both sands and clays. [Biologically modified sediment, of course, may prove an important exception]. However, it was considered useful to examine the effects of cooling or heating a sedimentary deposit, since these processes might be expected to occur in intertidal sands during sampling.

A cylindrical plastic container, 350mm in diameter, with flexible 1.5mm thick walls, which was filled with saturated sand from the laboratory test tank. The field probes were inserted at a separation of 75mm, depth 40mm, and a thermometer was inserted to 40mm depth at the same distance from the container walls. The sample was then vibrated on a sieve shaker until V_s measurement stabilised, presumably at minimum porosity. This was done to avoid changes in porosity caused by accidental disturbance of the container, or by electrical vibration of the cooling equipment used. The container was not foam-lined, because it was thought that its thin-walled, flexible construction would avoid the problems obtained with a rigid aluminium container at ARL. In retrospect this decision was mistaken, because it meant that effects caused by the container cannot be ruled out when interpreting the results.

The compacted sample was placed in an open refrigerator and allowed to stabilise at room temperature. It was then subjected to two complete cycles of cooling to near freezing, then re-equilibriating to room conditions (around 12 ^{0}C). After the first cycle the door was left open and the interior was heated to 30 ^{0}C using an electric heater, followed by re-equilibriation before the second cycle. A time series of measured sediment temperature is presented in Fig. 3.28. It is important to emphasise that this was not an equilibrium property, except at room temperature, neither does it necessarily represent the temperature of the sediment throughout the sample.

The corresponding S-wave velocities have also been presented in Fig. 3.28. It is clear that sharp increases in V_s occur whenever cooling takes place, with equally sharp reversions to a lower velocity as soon as refrigeration

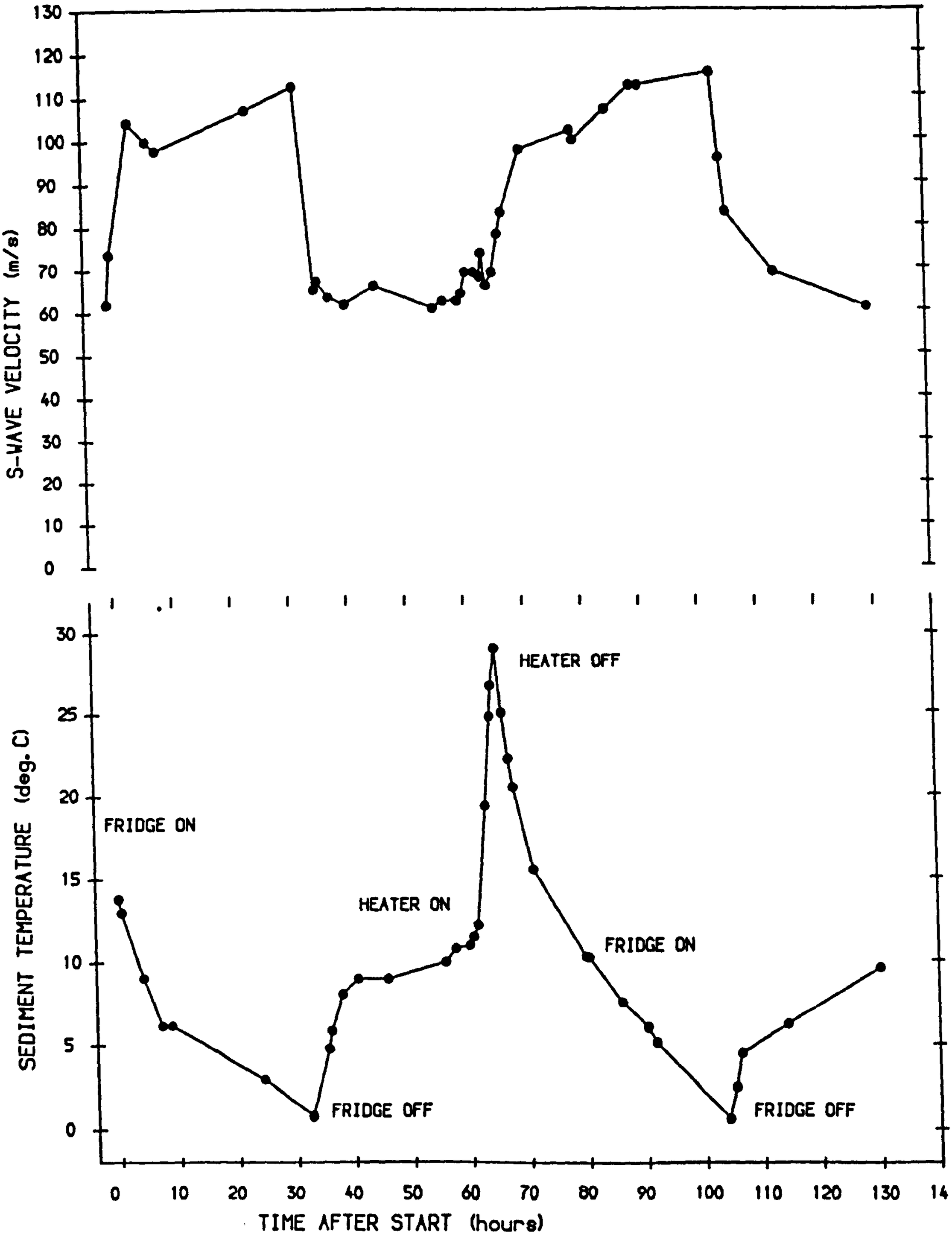

Fig. 3.28. Effect of change in temperature: time-series of V_s and sediment temperature.

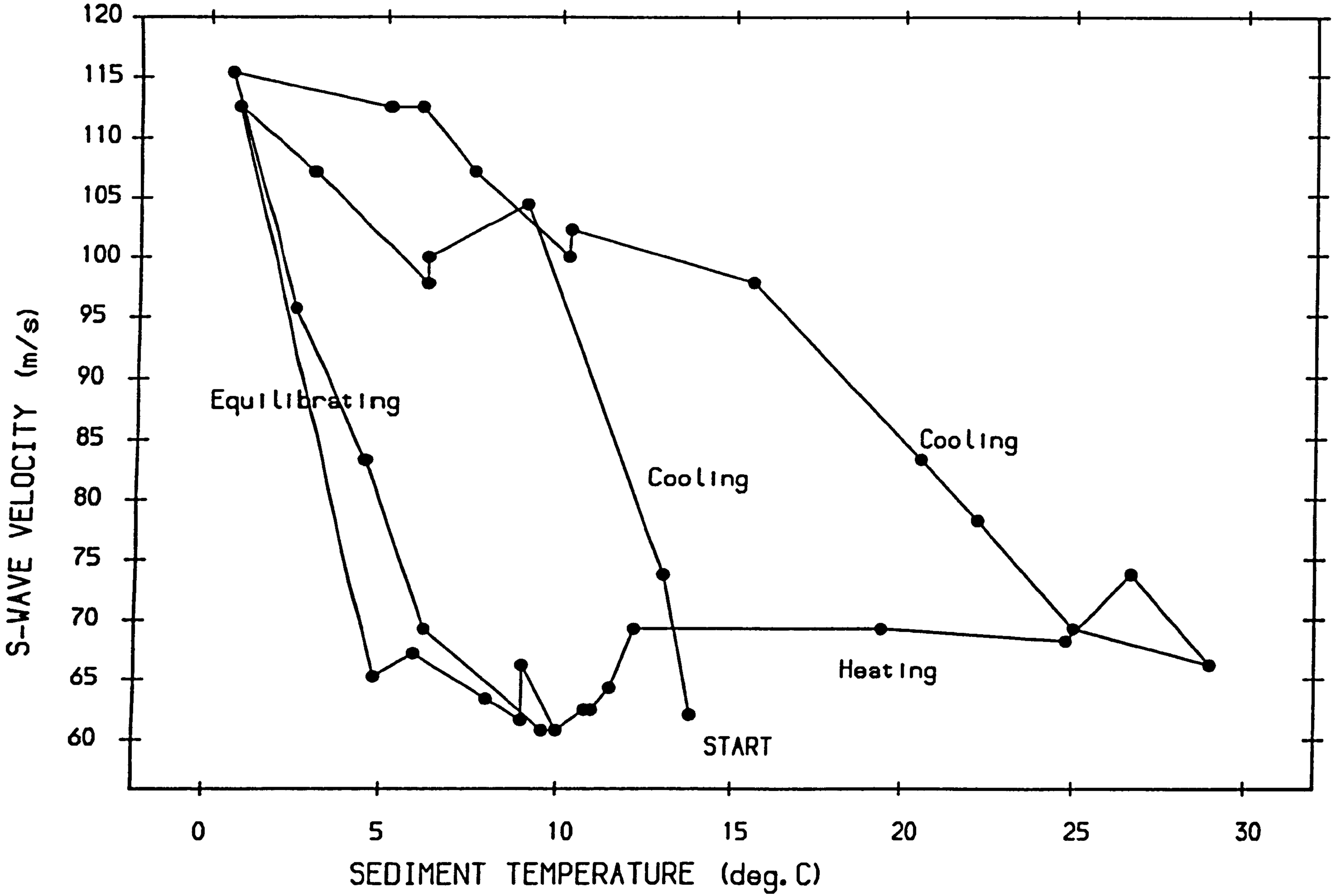

Fig. 3.29. Cooling/equilibration hysteresis.

is stopped. Rapid heating to 30 ^{0}C apparently has no effect. When V_s is plotted against temperature (Fig. 3.29), with a smooth curve joining the points in the order that they were measured, a marked hysteresis is observed. The curve follows two complete cooling/ equilibration cycles and one period of heating. The equilibrations after refrigeration correspond closely, indicating a relaxation to a lower velocity over a time period of 3-4 hours. The two parts of the curve representing cooling, however, do not correspond although they both attain a similar velocity.

The results indicate that V_s is increased during cooling, by an overall amount which is independent of the starting temperature. This increase is reversed when cooling stops, with V_s returning to its original value. Once this has been reached, further increases in temperature have no apparent effect. The best explanation for this phenomenon is that temperature gradients within the sample set up stresses which affect intergranular contact forces. V_s will then be a function of the temperature gradient rather than absolute temperature. It is obviously a negative temperature gradient, and therefore some form of sample contraction, which affects V_s, since equally sharp positive gradients had no effect.

Two questions remain to be answered: first, whether these changes were caused by the sample container, or the finite size of the sample, and secondly, if not, whether they could occur in exposed intertidal deposits in the field. For example, in sub-zero air conditions negative temperature gradients might be set up between subsurface layers and the exposed surface which might increase measured V_s, provided that the stresses generated cannot be released.

3.4.9. Artificial burrows: the effect of vertical cylindrical voids.

A typical sedentary benthic macrofaunal burrow consists of a hollow, vertical tube, with its walls coated by a mucous secretion in order to maintain the feature in unconsolidated, saturated sediment. Another typical form is the U-shaped burrow, which can be viewed simply as two, interconnected vertical tubes. Tube diameters depend on textural characteristics and environment: in intertidal sandy deposits the range is

from 2-8mm, with typical lengths of 20-150mm [Eltringham, 1971].

These burrows clearly represent significant internal sedimentary structures which should affect bulk sediment properties such as porosity, permeability and, by inference, S-wave velocity and rigidity. The investigation of their effect *in situ* was one of the key aims of this study. However, *in situ* assessment of the effects of these burrows is complicated by additional and potentially complex biological, biochemical, textural and hydrodynamic interactions. For this reason, a series of experiments was devised with the aim of isolating the physical presence of such burrows from other effects of bioturbationary activity.

The major experimental difficulty was in creating suitable artificial burrows. Benthic macrofauna exhibit highly specialised burrow construction and maintenance activity: excavating sediment, lining burrow walls and pumping through a steady supply of oxygenated water. Preliminary experiments established that it was impossible to maintain an open tube in saturated, unconsolidated sand without the aid of some sort of cementation of the tube walls.

The problem was solved by resorting to a natural 'cementation' process which had already been identified. Cylindrical rods were inserted into saturated sediment and left there while the tank was drained. On their removal, the increased 'adhesion' caused by drainage maintained impressions of the rods. This process, which is illustrated in Plate 1, also ensured no distortion of sediment packing structure around the tubes.

The intended procedure involves two assumptions: the first experimental, the second more fundamental. Since sediment had to be re-saturated, re-compacted and drained for each alteration of tube density, procedure was required to be standardised and repeatable. Furthermore, drained sand represents at best a special case, at worst a fundamentally different system from the saturated state, and therefore reults cannot be simply extrapolated to include *in situ* saturated burrows. At best, drained sand can be considered as air-saturated with increased intergranular adhesion.

As indicated in 3.4.1, much of this part of the work was carried out

before the field probes were produced. Therefore the Schultheiss probes were used, placed at a fixed separation in the test tank, to a depth of 50mm. Saturated sand in the laboratory tank was fully compacted by hammering until V_s stabilised. Drainage and resaturation was then repeated until V_s once again stabilised. V_s was then determined at zero tube density. A number of point-ended, coated alloy rods were inserted to a depth of 150mm. The sediment was drained, the rods carefully removed and V_s was measured. The rods were then replaced, sediment resaturated and the whole procedure repeated with an increased number of rods. The exeriment was repeated with different rod diameters ranging between 2 and 8mm (in accordance with expected *in situ* burrow diameters).

Tube numbers were converted into density per square metre by considering the area covered by the tubes and multiplying accordingly. This involved estimation of the width of the deposit monitored by the measurement technique. It was found that additional tubes outside a swathe of about 60mm across had no appreciable effect on S-wave arrival time: this was taken as the 'beam width'. For example, 4 tubes placed along the probe axis over a separation of 100mm leads to an effective density of $168m^{-2}$. This represents the approximate density measured in the field which would result in 4 burrows lying between the transducers on deployment.

Several sets of measurements were performed, with different diameters of tubes, using the Schultheiss probes. In addition, the field probes were deployed for two sets of measurements, including one involving a slightly different procedure. In this instance three probes were placed in the test tank in triangular formation, with the transmitter at one apex. Tubes were formed between the transmitter and one receiver, whilst the path between transmitter and the other receiver was kept clear.

Results from this experiment are presented first. Fig.3.30 shows the calculated V_s for each of the two source-receiver travel paths, and number of tubes formed along one of them, in the order in which measurements were taken. While V_s remained fairly constant in undisturbed sediment, it decreased sharply along the travel path where tubes were formed. The initial rise illustrates the 'settling down' period which was generally required at the start of each experiment.

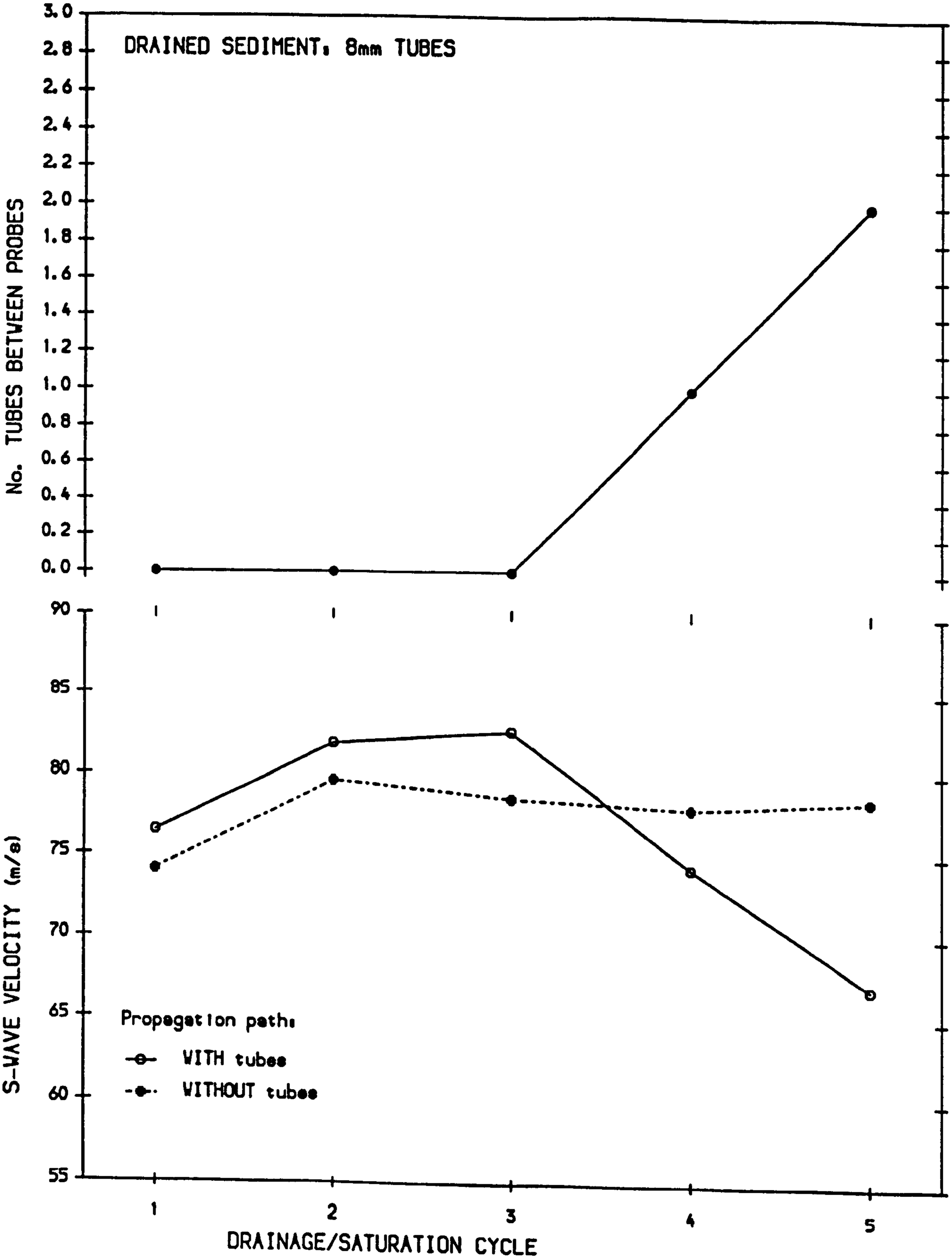

Fig. 3.30. Effect of vertical cylindrical voids on V_s: time series.

The technique was also checked for reversibility, by increasing tube density then reducing it. If rods were removed and the saturated sand re-compacted, V_s only rarely returned exactly to its starting point (although it did always increase to some extent). This was probably because conditions of uniform packing could not be reintroduced after tubes had been formed. For this reason the data presented here has been restricted to that obtained where tube density was gradually increased, with the rods replaced before resaturation. Repeated experimental runs using the same tube diameters have also been kept separate.

The results from all these runs has been combined in Fig.3.31. This illustrates the range of 'starting' velocities obtained, under different packing conditions. It is clear that, in all cases, V_s is reduced by the presence of increasing numbers of cylindrical voids. The results can be clarified by plotting the ratio of measured V_s to its value at zero tube density (Fig.3.32). Apart from better indicating the overall effect, it is also now apparent that 2mm diameter tubes had less effect on S-wave properties than the other diameters: however, no systematic increase in effect with increasing diameter could be identified.

The reduction in V_s caused by cylindrical voids is intuitively reasonable. A shear disturbance must travel through the sediment frame: when it encounters a void which is large relative to the pore-size (and to the amplitude of the disturbance) it will clearly be obstructed and hence 'slowed down'. Another argument can be inferred by considering that it should be easier to shear sediment containing vertically oriented voids because the number of grain contacts providing rigidity in the S-H plane will be reduced. This effect cannot, incidentally, be attributed solely (and therefore quantitatively) to the increase in bulk sediment porosity caused by the tubes. This is because the porosity parameter used in the Biot model can only be applied to macroscopically homogeneous media: moreover, a wide distribution of pore-sizes (which arises when the pore-space and the artificial tubes are considered) is unacceptable. The underlying principles of the Biot model remain fundamental, but the assumptions on which existing practical formulations are based do not hold in this case.

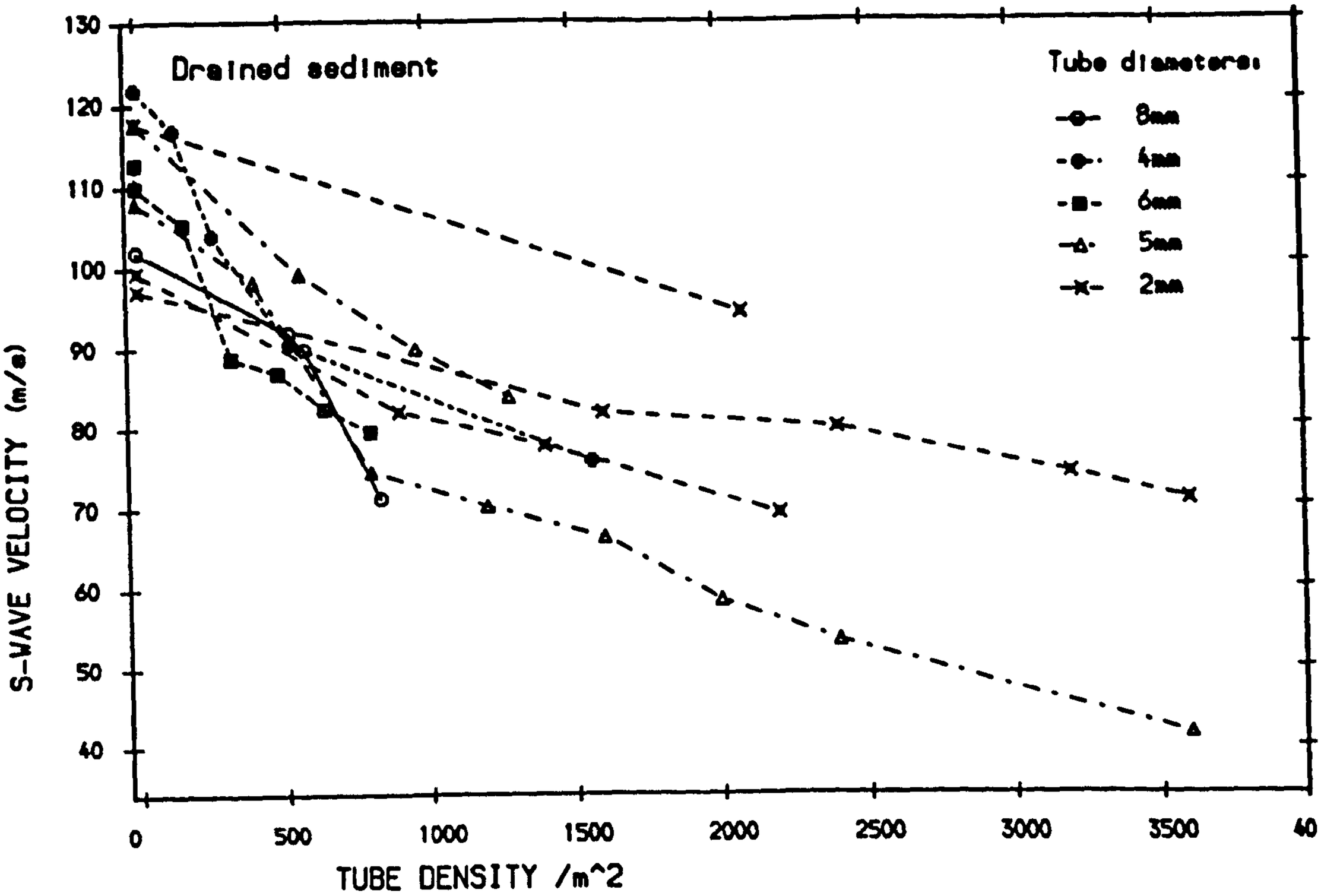

Fig. 3.31. Effect of vertical cylindrical voids on V_s: all data.

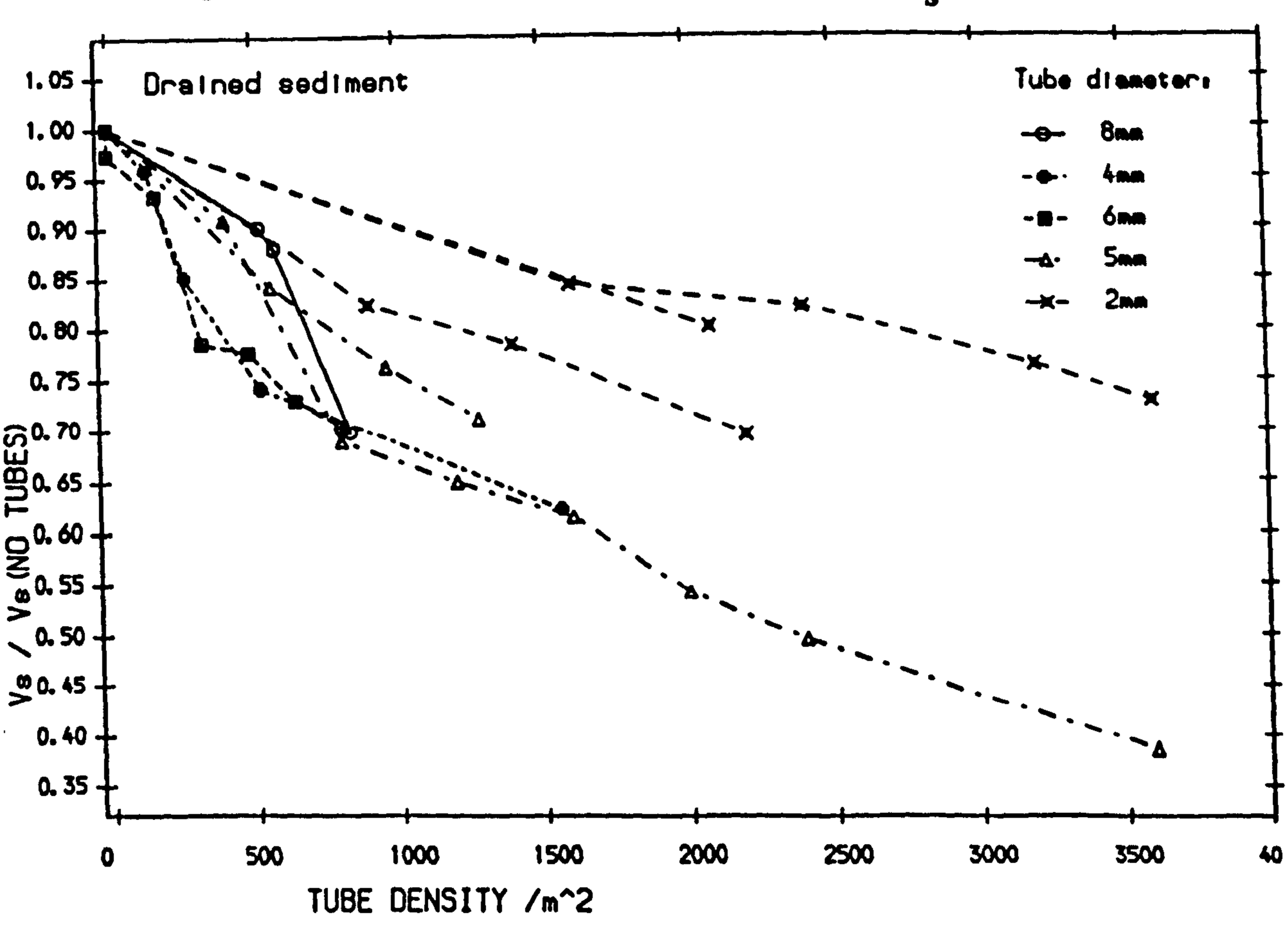

Fig. 3.32. Relative effect of vertical cylindrical voids.

3.5. Summary and Conclusions.

A system for measuring *in situ* S-H velocity in surficial deposits has been developed and tested in the laboratory. The system consists of two Vernitron piezoelectric bimorph transducers encapsulated unclamped in epoxy resin, protected by stainless steel plate housings, acting as transmitter and receiver. A portable, battery operated Sonic Viewer is used to generate the driving signal and display, stack and characterise the received S-wave pulse train, using a pulsed negative delta-function as the transmitter excitation.

The probes have a compliance which is well-matched to that of saturated sand: thus their vibration is perfectly coupled to the propagating S-wave disturbance. A broad resonant peak is therefore obtained at a disturbance wavelength corresponding to approximately twice the width of the bimorph plate. This resonance of the probe-sediment system is reduced by a maximum of 10% over a probe separation range of 200 - 50mm, due to frequency dependent attenuation along the pulse travel-path. For delta-function excitation, the resonant frequency is the dominant component of the received signal in saturated sands.

The system was intended for measurement of V_s using multiple receiver separations, to avoid the uncertainty in precise location of the vibration source and identification of signal onsets. A virtually linear, constant frequency signal arrival-time/probe-separation relationship is obtained in homogeneous saturated sand over a separation range of 50-180mm. Deviations from linearity observed at lower and higher separations were only partly explained by measured velocity gradients in the surface layers: separation-dependent distortion is thought to be primarily responsible. This also explains the fact that V_s calculated from signal onsets tends to be slightly higher than that calculated using other trace features. The true vibration source (and point at which the receiver picks up the disturbance) was estimated at between the leading edge of the bimorph plate and the metal housing. This indicates that the transducer plate is effectively decoupled from the rest of the probe, and allows calculation of V_s from a single transmitter-receiver separation.

Measured V_s was found to be sensitive to depth of insertion of the probes because of velocity gradients in the surface layers. Measured gradients tied in with other work based on increased overburden pressure, indicating that values obtained at greater depths can be extrapolated back to the extreme near-surface.

This led to the problem of defining a representative value of V_s in a depth-varying medium. It is essential to standardise probe separation and depth of insertion (in this case to 40mm). This immediately limits resolution of the upper 40mm, in which velocity should increase most sharply. This 'layer' was characterised using an effective surface V_s, defined as the velocity calculated from the shortest pulse onset arrival time and true source-receiver separation. Bulk V_s, defined as the velocity calculated from the linear portion of measured time-separation curves, represents an average for the sediment lying between 40 and 80mm, assuming multi-layer refraction through a (typical) velocity range of $10ms^{-1}$. In fact, in homogeneous sediment, even allowing for the measured depth gradients, bulk V_s should not be measurably different from surface V_s. In this case a single V_s calculation adequately characterises the sediment. However, in strongly texturally or biologically layered media, significant differences may be obtained between the two calculations, so that both parameters are necessary for complete characterisation.

A high degree of sensitivity to degree of saturation was measured by simulating tidal inundation and exposure of the deposit in a purpose built laboratory test tank. V_s increases by *c.* 60% on full drainage of the sediment, and further over a period of hours if the deposit is left in the drained state. This was interpreted as being caused by negative effective pore-pressures being built up in capillary-sealed voids left in the pore fluid matrix, which act to increase intergranular friction. The transducers are less well matched in drained sand, which results in decoupling and breakdown of the transmitted pulse into multiple frequency components. The most important conclusion from this part of the study is that *in situ* measurements can only be compared with those under identical conditions of pore-fluid saturation, which in this case was selected as the fully saturated state.

Apparent velocity dispersion was measured in saturated sand, with V_s increasing by a maximum of 10% over the full frequency range achievable. Thus increase is steeper than that predicted by theory: however, it is still less than absolute sampling error estimated for *in situ* measurements, so that error introduced via dispersion can be safely ignored.

Another source of variability identified was rapid cooling of the deposit, which set up differential contraction rates and hence internal stresses which acted to increase measured V_s. However, whether the confined laboratory experiment effectively simulated conditions on intertidal flats is questionable. *In situ* intertidal measurements during sharp winter frosts are required in order to confirm this.

Finally, the effect on V_s of macrofaunal burrows was simulated by forming vertical cylindrical voids of varying number density and diameter. Measurements were limited to drained sand only by practical constraints. In all cases, V_s was found to be reduced by increasing number density, with the smallest diameter 'burrow' having less effect than the others. The result is intuitively reasonable, but should be extended to include *in situ* measurements with caution, because macrofaunal burrows are constructed, coated in biological secretions and actively maintained by much more complex processes than the laboratory procedure used.

CHAPTER 4.

AN *IN SITU* ELECTRICAL RESISTIVITY PROBE: THEORETICAL BACKGROUND, DESIGN AND APPLICATION TO SURFICIAL SEDIMENT CHARACTERISATION.

The electrical resistivity (ρ_s) of a fluid saturated sediment has been defined and theoretically explored in Chapter 2. This chapter addresses itself to the *in situ* measurement of ρ_s, specifically in surficial sediments. For this purpose the sediment can be considered as any macroscopically defined conducting medium, and conventional electromagnetic theory applies. The theoretical background to resistivity measurement is briefly discussed, and surficial measurement techniques are reviewed in the light of this. The resistivity probe used throughout the study is described along with its associated instrumentation. The effects of some expected *in situ* conditions on measured resistivity are investigated and discussed, and finally preliminary laboratory work to assess some of these effects is described.

4.1. Theoretical background.

4.1.1. Definitions and assumptions.

For the purposes of this investigation, the effect of point (infinitesimally small) sources in a macroscopically defined medium will be considered. The first assumption simplifies the theoretical treatment, and forms an important design criterion for electrical sounding equipment. In other words, the physical size of the electrode providing the current is considered to be negligible compared to other length scales involved. The second assumption is rather more fundamental and can be interpreted as follows: any spatial heterogeneity on a microscopic scale must be amenable to statistical averaging, again over the length scales under investigation. This, incidentally, is not an assumption which has to be made exclusively for the treatment of porous media: all other media contain highly variable electrical properties on atomic scales, and many

crystalline solids exhibit variability on scales corresponding to a sedimentary deposit [J.D. Jackson, 1975].

The equations governing the distribution of non time-varying fields in a linear, isotropic, macroscopic medium are expressed as:

$$\underset{\sim}{E}(\underset{\sim}{r}) = - \underset{\sim}{\nabla}\ V(\underset{\sim}{r}) \tag{4.1}$$

$$\underset{\sim}{J}(\underset{\sim}{r}) = \sigma(\underset{\sim}{r})\ \underset{\sim}{E}(\underset{\sim}{r}) \qquad \text{[Ohm's Law]} \tag{4.2}$$

Where $\underset{\sim}{E}$ is the electric field strength, V is a scalar potential, $\underset{\sim}{J}$ is the current density and σ is the electrical conductivity. In addition, conservation of charge requires that for an arbitrary surface *S* enclosing a volume *V* containing charge density $\rho_q(\underset{\sim}{r})$, the net current flowing out through that surface is matched by the rate of change in total charge within the volume, (assuming no current sources or sinks). Thus:

$$\oint_S \underset{\sim}{J}.d\underset{\sim}{S} = -\frac{\partial}{\partial t}\int_V \rho_q(\underset{\sim}{r})\ d\tau \tag{4.3}$$

From the divergence theorem:

$$\oint_S \underset{\sim}{J}.\underset{\sim}{dS} = \int_v \underset{\sim}{\nabla}.\underset{\sim}{J}\ d\tau \tag{4.4}$$

So, from 4.3, for any volume and therefore for any point in space:

$$\nabla.J = -\frac{\partial \rho}{\partial t}_q \tag{4.5}$$

For the applications under consideration, time variation in charge density is everywhere zero (steady state). Substitution of 4.1 into 4.2, then of 4.2 into 4.5 leads to :

$$\underset{\sim}{\nabla}\sigma.\underset{\sim}{\nabla}V + \sigma\nabla V^2 = 0 \tag{4.6}$$

For the simplest case of a homogeneous medium the conductivity is constant throughout. Eqn. 4.6 then reduces to Laplace's equation:

$$\sigma\ \nabla^2 V = 0 \tag{4.7}$$

For practical reasons electrical properties of linear isotropic media are usually characterised in terms of their resistivity ρ, which is related to the conductivity by:

$$\rho = \frac{1}{\sigma} \tag{4.8}$$

Because of its widespread application in the solution of potential distribution problems, Laplace's equation has been explored in exhaustive detail. Two important properties of solutions to this equation are relevant:

Uniqueness theorem: given a homogeneous region enclosed within a boundary along which the distribution of V is known, any solution $V(\underset{\sim}{r})$ which satisfies these boundary conditions is the only solution.

Superposition theorem: the potential at any point can be considered as the linear sum of separate contributions from individual point sources.

4.1.2. Electric potential due to a point current source:

Infinite homogeneous medium.

Consider a source I at $\underset{\sim}{r} = 0$ within an infinite homogeneous medium. Consideration of any volume element except the one enclosing the current source confirms the validity of Laplace's equation for all space except at $\underset{\sim}{r} = 0$. The axial and azimuthal symmetry of the problem suggests adoption of spherical polar coordinates $V(r,\vartheta,\phi)$, such that:

$$\nabla^2 V = \frac{1}{r^2}\frac{d^2 V}{dr^2} + \frac{2}{r}\frac{d V}{d r} = 0. \tag{4.9}$$

Multiplication by r^2 and double integration yields the solution:

$$V(r) = -\frac{A}{r} + B \tag{4.10}$$

In this case the boundary conditions are taken at infinity, i.e in the limit as $r \Rightarrow \infty$, V must tend to 0, thus $B = 0$. A is then found by

considering a spherical surface S of arbitrary radius r enclosing the current source. From continuity, the total current flow normal to this surface must be the same as the current source I:

$$\oint_S \underset{\sim}{J}.d\underset{\sim}{S} = I \qquad (4.11)$$

From Eqns. 4.1 and 4.2 and the spherical polar representation of a surface element dS:

$$\oint_S \underset{\sim}{J}.d\underset{\sim}{S} = -\frac{1}{\rho}\oint_S \underset{\sim}{\nabla}V .d\underset{\sim}{S}$$

$$= -\frac{4\pi A}{\rho} = I . \qquad (4.12)$$

Thus: $A = \frac{-I\rho}{4\pi}$, and $V = \frac{I\rho}{4\pi r}$, $r \neq 0$. (4.13)

Effect of a plane boundary between two macroscopic media.

The presence of a boundary between two media of different electrical characteristics cannot be ignored when investigating surficial sediment properties. The boundary between sediment and the overlying water or air divides media of widely different electrical properties, and subsurface layers of different textural characteristics may also be present.

The general problem of a plane boundary dividing two conducting media is illustrated in Fig. 4.1. The problem is now two-dimensional, in contrast to the spherically symmetrical (and hence one-dimensional) case for an unbounded medium. Laplace's equation still applies, with additional boundary conditions based on continuity of current flow and potential at the interface:

$$J_{\perp}(1) = J_{\perp}(2) \qquad (4.14)$$

$$E_{\parallel}(1) = E_{\parallel}(2) \qquad (4.15)$$

$$V(1) = V(2) \qquad (4.16)$$

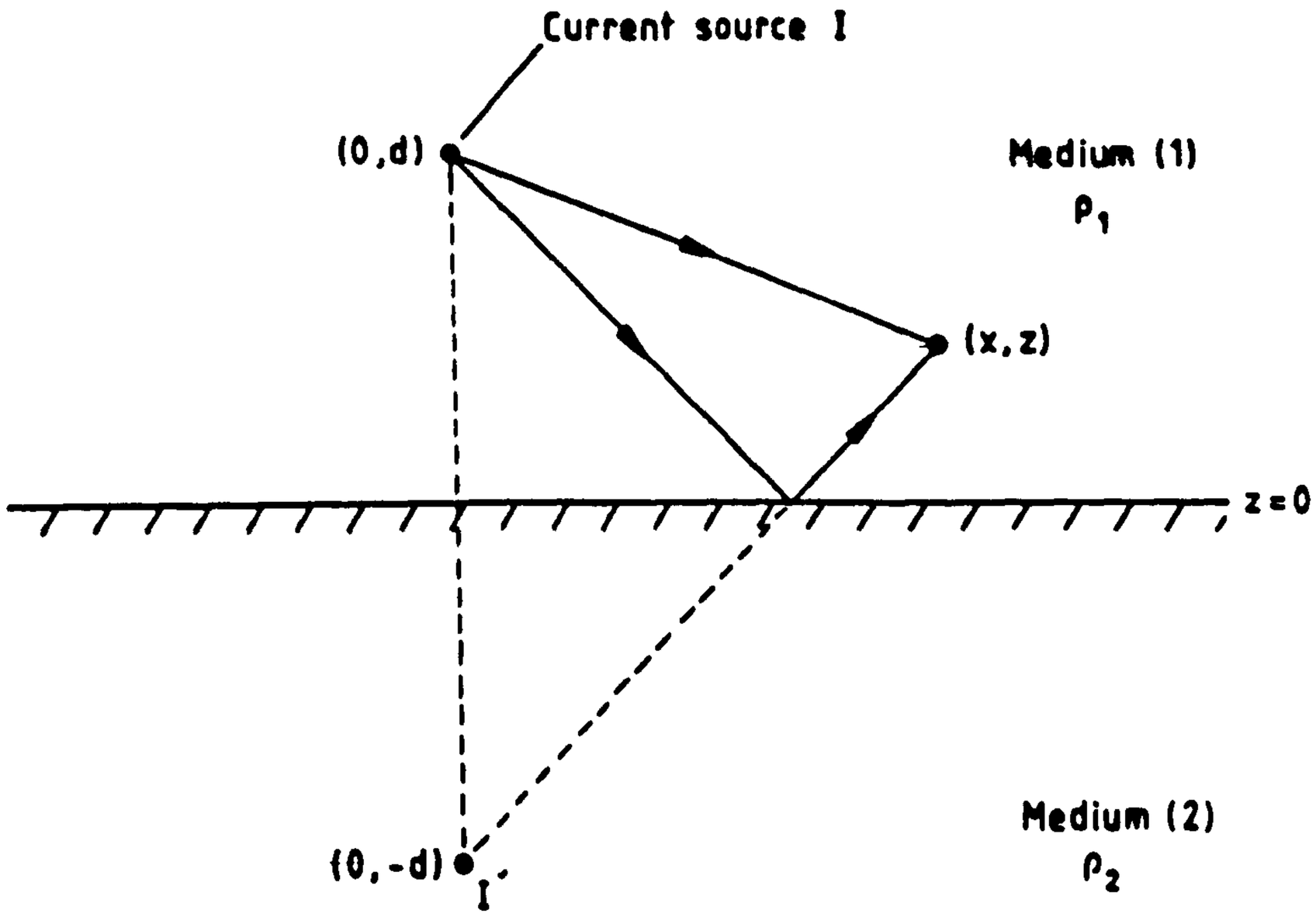

Fig. 4.1. Effect of a plane boundary on a point current source.

where ($\perp$) and ($\parallel$) denote components normal and tangential to the surface. Instead of analytical solution of Laplace's equation and application of these boundary conditions, a far simpler technique can be employed which is a direct consequence of the Uniqueness Theorem. Under favourable conditions it can be inferred (from geometrical considerations) that a small number of suitably placed sources of appropriate magnitudes, external to the region of interest, can simulate required boundary conditions. Superposition of the potential (eqn. 4.13) due to each of these imaginary sources on that due to the real source then yields the true potential at any point within the region of interest. This technique is known as the 'Method of Images', from analogy with ray optics. The analogy is valid because current density, like light ray intensity, decreases with the inverse square of the distance from a point source:

$$|\underset{\sim}{J}| = \frac{1}{\rho}|\underset{\sim}{E}| = -\frac{1}{\rho}|\underset{\sim}{\nabla}V| = \frac{I}{4\pi r^2} \qquad (4.17)$$

It can be easily shown that for medium (1) the required boundary conditions at the interface (4.14-4.16) can be simulated by placing an 'image' source on its opposite side, its magnitude (I', Fig. 4.1) appropriately adjusted to account for the difference in conductivity. For medium (2) the source magnitude (but not position) must also be adjusted to satisfy boundary conditions at the interface (I''). The magnitudes of I',I'' can be obtained from (4.13-4.16). The analogous optical case for this problem would be a point source of light in region (1) separated from (2) by a semi-transparent mirror, having reflection and transmission coefficients k_{21} and $(1-k_{21})$ respectively.

Thus for $z \geq 0$:
$$V_1 = \frac{\rho_1}{4\pi}\left\{ \frac{I}{(x^2+(d-z)^2)^{1/2}} + \frac{Ik_{21}}{(x^2+(d+z)^2)^{1/2}} \right\} \qquad (4.18)$$

Whilst for $z \leq 0$:
$$V_2 = \frac{\rho_2}{4\pi}\left\{ \frac{I(1-k_{21})}{(x^2+(d-z)^2)^{1/2}} \right\} \qquad (4.19)$$

Since $V_1(z=0) = V_2(z=0)$ (from eqn. 4.16), k_{21} can be calculated as:

$$k_{21} = \left(\frac{\rho_2 - \rho_1}{\rho_2 + \rho_1} \right) \qquad (4.20)$$

Special cases of interest.

(1) ρ_2 is an insulator (e.g. air):
From (4.19), as $\rho_2 \Rightarrow \infty$, $k_{12} \Rightarrow 1$. Thus V = 0 for z < 0, and is a maximum for z > 0.

(2) Source is at the boundary (d=0):
By considering the limit as d $\Rightarrow$ 0, the common case where the current source is applied at the boundary between two media can be simulated. Taking z = 0 (since potential is also commonly measured along the boundary),

$$V(x) = \frac{I\rho_1}{4\pi x}(1 + k_{21}) \equiv \frac{I\rho_2}{4\pi x}(1 - k_{21}) \qquad (4.21)$$

Effect of two boundaries.

Where more than one boundary are involved, the theory becomes rather more complicated. It is a commonly occurring case, however, for example in surficial electrical sounding over a layered medium or for surveys where the electrodes are at the sea surface. Fortunately the problem is still amenable to the Method of Images technique, and is solved as follows.

Consider the problem illustrated in Fig. 4.2. The analogous optical case causes multiple reflections of a partially transmitted ray between two semi-transparent mirrors, with each multiple being partially transmitted back into the medium of interest, in addition to the direct affect of the source and the first reflection. This first contribution to the total potential is, from (4.18):

$$V_0 = \frac{I\rho_1}{4\pi}\left\{ \frac{1}{(x^2+(d-z)^2)^{1/2}} + \frac{k_{21}}{(x^2+(d+z)^2)^{1/2}} \right\} \qquad (4.22)$$

whilst the *n*th multiple reflection will have traversed a path length of $(a^2 + (d+z+2nw)^2)^{1/2}$, and will have been transmitted through interface {12}, reflected off interface {23} n times, reflected off interface {21}

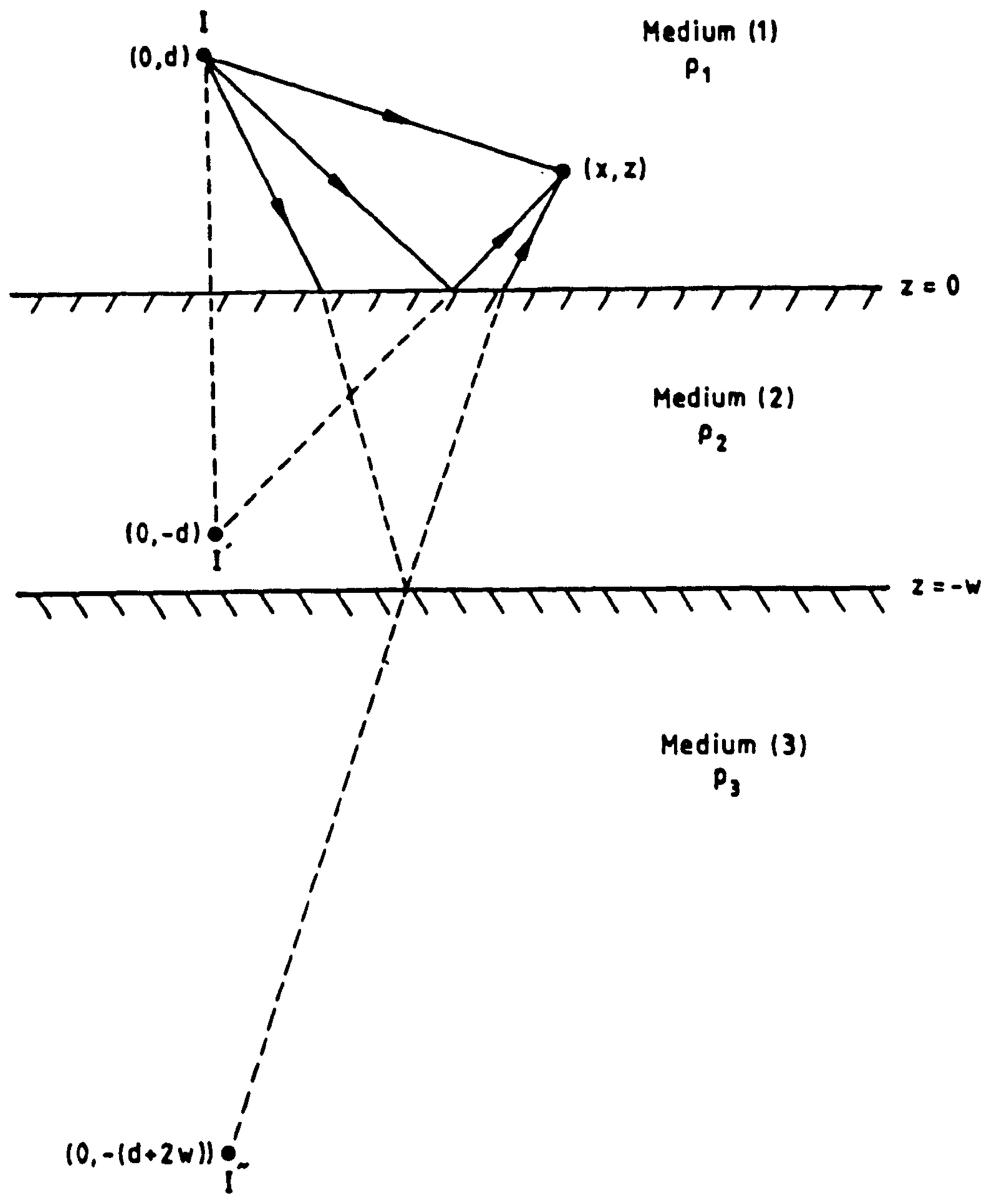

Fig. 4.2. Effect of two plane boundaries on a point current source.

n-1 times, and transmitted back through interface {12}. Thus its contribution to the potential will be:

$$V_n = \frac{I\rho_1}{4\pi}\left\{\frac{(1-k_{21})k_{32}^{n}\,k_{12}^{n-1}(1-k_{12})}{(x^2+(d+z+2nw)^2)^{1/2}}\right\} \qquad (4.23)$$

Fig. 4.2 illustrates the image and ray-path for n=1. The potential at any point (x,z) within medium (1) will be given by:

$$V(x,z) = V_0 + \sum_{n=1}^{\infty} V_n \qquad (4.24)$$

with V_0 and V_n defined in 4.22, 4.23.

Special cases of interest.

Two special cases have been singled out for consideration. The first describes the common case of a source placed at the interface between a layered medium and the overlying air. Thus d=0, $\rho_1 \Rightarrow \infty$, $\rho_2=\rho_{s1}$, $\rho_3=\rho_{s2}$, and z is also taken as 0. Thus $k_{21}\Rightarrow$ -1. Using the identities $\rho_1(1+k_{21}) \equiv \rho_2(1-k_{21})$ and $k_{12} \equiv -k_{21}$ yields:

$$V_0 = \frac{I\ \rho_2}{4\pi x}(1 - k_{21}) \Rightarrow \frac{I\ \rho_{s1}}{2\pi x} \qquad (4.25)$$

$$V_n = \frac{I\ \rho_2}{4\pi}\left\{\frac{(1-k_{21})^2\ k_{32}^{n}k_{12}^{n-1}}{(x^2 + (2nw)^2)^{1/2}}\right\} \Rightarrow \frac{I\ \rho_{s1}}{2\pi x}\left\{\frac{2k_{s1s2}^{n}}{(1 + \left(\frac{2nw}{x}\right)^2)^{1/2}}\right\} \qquad (4.26)$$

The second describes electrodes placed at the interface between sediment and a finite overlying water layer, with an air layer over that. This represents a possible situation encountered during sampling of intertidal sediments, where surface water is still present. In this case $\rho_1 = \rho_s$, $\rho_2 = \rho_w$, and $\rho_3 \Rightarrow \infty$, with d,z = 0.

$$V_0 = \frac{I\ \rho_s}{4\pi x}(1 + k_{ws}) \qquad (4.27)$$

$$V_n = \frac{I\,\rho_s}{4\pi x}\left\{\frac{(1-k_{ws}^2)(-k_{ws})^{n-1}}{(1+\left(\frac{2nw}{x}\right)^2)^{1/2}}\right\} \qquad (4.28)$$

Both of these cases have been discussed further in relation to electrical resistivity measurements in Section 4.2.4.

It can be seen that in simple cases analytical solutions to Laplace's equation yield the spatial distribution of potential in terms of magnitude of a current source, resistivity of the surrounding medium, and appropriate boundary conditions. Thus if potential due to a known current is measured within a conducting medium at a given position away from the source, and if the effects of boundaries are understood, the resistivity of the medium can be calculated.

4.2. Measurement of the electrical resistivity of sediments.

4.2.1. Background.

Most of the techniques developed for measuring the electrical resistivity of marine sediments are based on standard techniques for ground prospecting [Kunetz, 1966, Keller and Frischknecht 1966, Telford *et al*, (1974)]. They all employ one or more electrodes providing a known current (I), which can be considered effectively as either point sources or infinitely long line sources. The potential field around these sources is obtained, usually by measuring the voltage drop (ΔV) between two electrodes. Conversion of this to an **Apparent Electrical Resistance** ($R_{app} = \Delta V/I$) removes the current dependence.

The theoretically predicted relationship between this measured resistance, electrode spacings, and ρ_s can then be used to determine an effective or **Apparent Resistivity** (ρ_{app}) for the volume of sediment monitored. Note that this represents a bulk average over localised lateral or vertical heterogeneity, since the theory assumes a macroscopically homogeneous isotropic medium. Thus, as for the V_s measurements, the volumes and depths

of sediment effectively sampled constitute an important consideration.

For practical reasons, a 4-electrode array is usually adopted. Two electrodes provide a current loop within the medium under investigation, with the remaining two being used to measure potential drop between two appropriate points within this medium. The use of separate potential electrodes is generally preferred because it avoids the problems of contact impedance at the current electrodes, thus ensuring that potential difference variations are as representative of the ground resistivity variations as possible [P.D. Jackson, 1975]. However, this does lead to uncertainty about the volume of sediment being assessed, which has led to the adoption of 2 electrode arrays in laboratory work [McCarter, 1984]. Time-dependent build-up of unwanted contact potentials due to polarisation of the current electrodes, especially in saline pore fluids which are capable of electrolysis, is minimised by using radio frequency alternating current. The frequency chosen is a trade-off between this low-frequency polarisation and high frequency skin-depth effects, where current is inversely proportional to frequency and the conductivity of the medium [Sachs & Spiegler, 1964]. At 4Hz, theoretical treatment assuming direct current is valid in the upper few decimetres of marine sediments.

For land-based (and many sea-bed) applications, the electrodes are placed in line on the surface of the medium under investigation, with the current electrodes as the outer pair [Schlumberger *et al*, 1934, Bogolovsky & Ogilvy, 1974]. This enables rapid and straightforward positioning of field equipment, minimises disturbance of the medium and simplifies (to 1 dimension) the theoretical relationships between measured potential difference and sediment resistivity. Good electrical contact with the medium is required, however, which can lead to problems for towed sea floor arrays or over rock.

Figure 4.3 illustrates this 4 electrode system in its most general form. Using Eqn. 4.21 and the Principle of Superposition, the potentials at P1 and P2 are as follows:

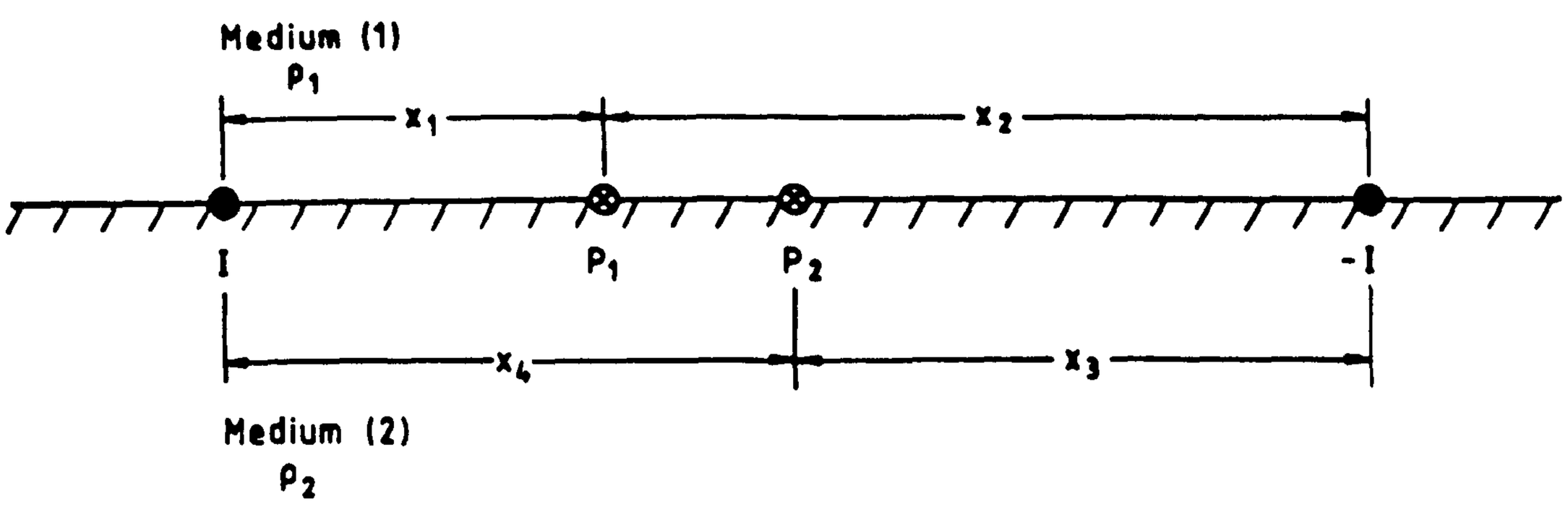

Fig. 4.3. Four electrode system at sediment surface.

$$V(P_1) = \frac{I\rho_2(1+k_{12})}{4\pi x_1} - \frac{I\rho_2(1+k_{12})}{4\pi x_2}$$

$$V(P_2) = \frac{I\rho_2(1+k_{12})}{4\pi x_4} - \frac{I\rho_2(1+k_{12})}{4\pi x_3}$$

So the resistance between P1 and P2 is:

$$R = \frac{\Delta V}{I} = \frac{\rho_2}{4\pi}(1+k_{12})\left\{\left(\frac{1}{x_1} - \frac{1}{x_4}\right) - \left(\frac{1}{x_2} - \frac{1}{x_3}\right)\right\} \qquad (4.29)$$

The Wenner configuration is one of the most popular. This consists of four equally spaced electrodes, so that $x_1 = x_3 = a$, $x_2 = x_4 = 2a$. Thus:

$$\frac{\Delta V}{I} = \frac{\rho_s}{4\pi a}(1+k_{is}) \qquad (4.30)$$

For measurements between the sediment-air interface, $k_{is} \Rightarrow 1$, while for those between the sediment-water interface, $k_{is}=(\rho_w-\rho_s)/(\rho_w+\rho_s)$. Then:

$$\frac{\Delta V}{I} = \frac{1}{4\pi a}\left\{\frac{2\rho_w\rho_s}{(\rho_w+\rho_s)}\right\} = \frac{1}{2\pi a}\left\{\frac{\rho_w}{1+\rho_w/\rho_s}\right\} \qquad (4.31)$$

Note that for the usual case $\rho_s >> \rho_w$, measured resistance will not be very sensitive to changes in ρ_s. Thus surficial Wenner or similar line arrays are not particularly suitable for subtidal investigations. More complex arrays which incorporate an insulating mat to isolate the sediment from the water column, and which 'focus' the current into the sediment have been developed to overcome this problem [Jackson, 1975, Bennell *et al*, 1982].

4.2.2. An *in situ* electrical resistivity probe.

The field-work programme undertaken involved monitoring of exposed intertidal deposits over short length and depth scales. For this reason a simple Wenner array was ideal, with electrode spacing suitably chosen to ensure sensitivity to near-surface variability. Fig. 4.4 illustrates the

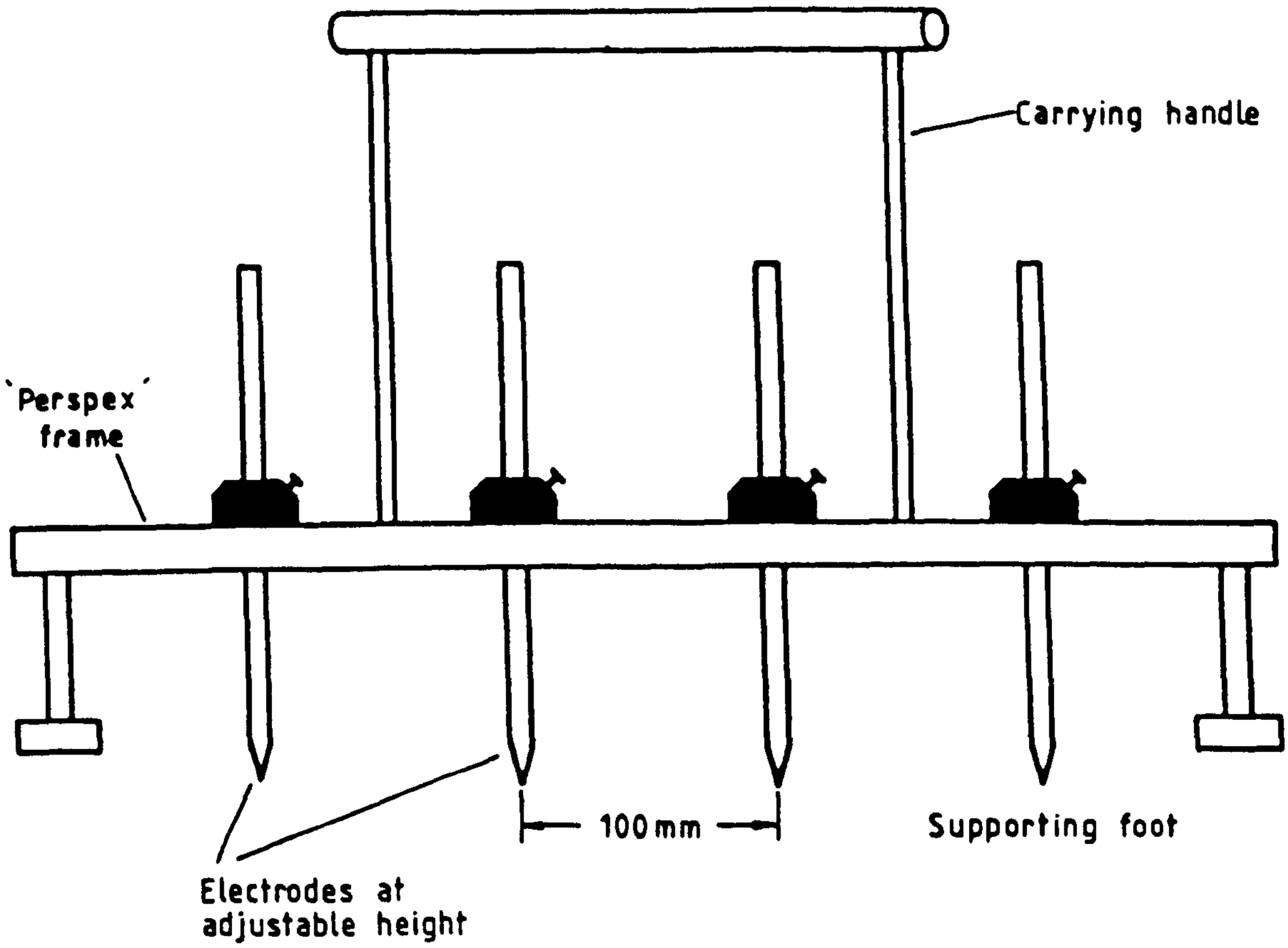

Fig. 4.4. In-situ resistivity probe ; side view.

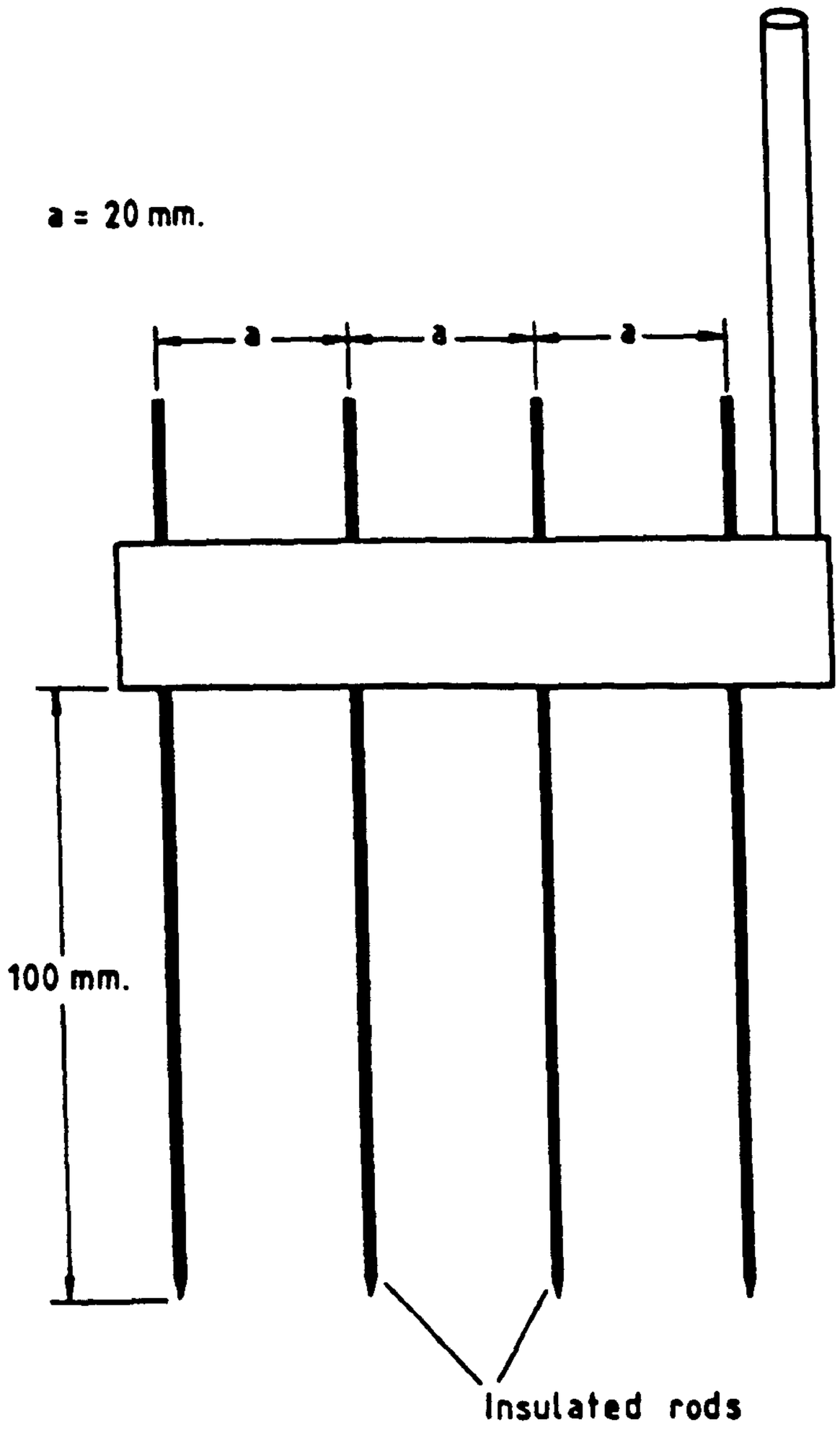

Fig. 4.5. Small resistivity probe.

probe which was used for *in situ* work throughout the study. The supporting framework was constructed of perspex, with adjustable electrode heights so that point contact with the sediment surface could be achieved irrespective of degree of penetration into the sediment surface by the feet of the probe. The probe tips were sharpened into points with diameters of less than 1% of the electrode spacing, which justified the assumption of point sources for theoretical interpretation.

A much smaller probe was also constructed, which was more suited to work in the laboratory test tank described in Chapter 3. This is illustrated in Fig. 4.5. Other than at their finely sharpened tips, the electrodes were encapsulated in heat-shrinking insulating tubing, so that they could be inserted into the sediment for investigation of the depth dependence of sediment resistance. This will be described further in 4.4.

The current source and resistance measurement were supplied by an ABEM TERRAMETER SAS 300. This uses a 4Hz square wave alternating current to avoid polarisation. Discrimination circuitry and programming separates DC voltages, self potentials and noise from the incoming signal. The measurement circuitry has a virtually infinite input impedance, so results are unaffected by electrode contact resistances (Hoyer & Rumble, 1976). Automatic continuous averaging over several cycles is performed, resistance being calculated and displayed as a digital readout. The instrument is battery powered, robust and portable, and thus is eminently suitable for field work.

4.2.3. Pore fluid resistivity: controls and effect on ρ_s.

Since ρ_s effectively measures resistivity of the pore fluid matrix, controls on pore-fluid resistivity (ρ_w) are clearly important. Seawater conductivity has widespread application for high resolution assessment of salinity structure in the ocean. It depends on pressure, salinity and temperature, and accurate empirical relationships between conductivity and these properties have been calculated and standardised as the Practical Salinity Scale [Bradshaw & Schlacher, 1980]. Fig. 4.6 illustrates the dependence of ρ_w on salinity and temperature at 1 atmosphere, which simulates the conditions encountered during intertidal work.

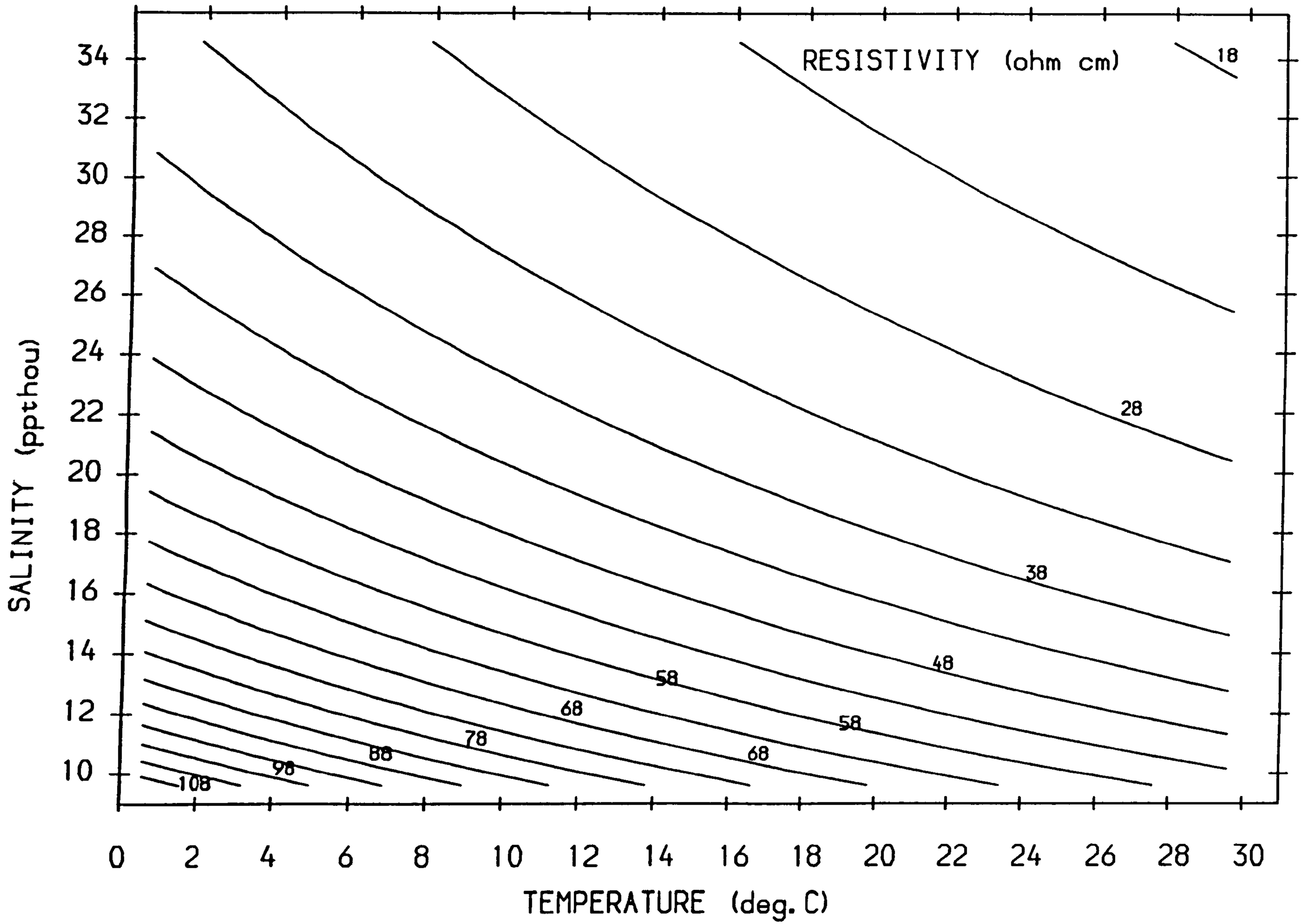

Figure 4.6. Variation of resistivity of water with salinity and temperature.

In order to remove the implicit dependence of ρ_s on ρ_w, which is desirable if structural characteristics of the pore-fluid matrix are to be investigated or compared with measurements from different sites, the Electrical Formation Factor (FF) defined in 1.2 must be calculated. This means that measurement of ρ_w, either directly or indirectly through salinity and temperature, is required in addition to ρ_{app}. The selection of suitable *in situ* measurement techniques, especially under conditions of time-varying salinity and temperature, proved problematic, and has been discussed in some detail in 5.1.

4.2.4. Application in surficial sedimentary deposits: complicating factors.

Calculation of sediment resistivity from measured resistance will yield an 'apparent' estimate (ρ_{app}) for an isotropic, homogeneous medium, bounded by plane interfaces, based on the theoretical relationships presented above. This apparent value should be distinguished from the Apparent Formation Factor defined in 2.2, since it depends on the measurement technique rather than on any fundamental properties of the sediment/pore-fluid system. It is clear that in many natural sedimentary deposits these assumptions are either invalid or only approximately valid, so that ρ_{app} provides only a partial description of the electrical properties of the medium. Before deployment of the resistivity probe in the field, the effects of some expected *in-situ* conditions on this Apparent Resistivity were investigated. The key problems anticipated were:

(1) Spatial heterogeneity over horizontal and vertical scales.
(2) Anisotropy of the electrical properties of the sediment.
(3) Irregular or non-planar surface.
(4) Water lying on the sediment surface.
(5) Partial saturation of the sediment.

The effect of spatial heterogeneity.

Two manifestations of spatial heterogeneity will be discussed. The first involves discontinuities in electrical properties, and therefore

boundaries between homogeneous, isotropic media. These affect the boundary conditions, rather than the underlying theory, and simple one and two-layer cases for plane boundaries have already been discussed. The second involves continuous variation of electrical properties over appropriate length and depth scales, which for example might be obtained in a deposit containing a porosity gradient with depth. Since conductivity varies in space, eqn. 4.6 cannot be reduced to Laplace's equation [i.e. $\underset{\sim}{\nabla}\sigma(\underset{\sim}{r}) \neq 0$]. Each case must therefore be considered from first principles and analytical solutions will rarely be found.

ρ_{app} will be dependent on electrode spacing both for the extent of influence of lateral heterogeneity and for the maximum depth of penetration. This is identical to the situation for V_s measurement described in the previous chapter. Replicate measurements within a localised area should yield information on lateral heterogeneity: unfortunately no information about vertical heterogeneity can be obtained from a fixed separation surficial Wenner array.

It is therefore important to know what sample volumes are involved in the resistivity determination. The depth of penetration of the measurement can be approximated by considering the depth at which a layer of different resistivity fails to affect the measured resistance, and therefore does not contribute to the measurement. This corresponds to the layered medium described by 4.24, 4.27 & 4.28. Thus for a Wenner array:

$$R_{app} = \frac{\Delta V}{I} = 2(V(a)-V(2a)) \tag{4.32}$$

$$= \frac{I\rho_{s1}}{2\pi a}\left[1 + \sum_{n=1}^{\infty} 2k_{s1s2}^{n} \left\{ \frac{2}{(1+(2nw/a)^2)^{1/2}} - \frac{1}{(1+(nw/a)^2)^{1/2}} \right\} \right] \tag{4.33}$$

Taking an increasing sub-layer depth w as a factor of a, R_{app} was computed until the summation term in 4.33 constituted less than 0.01, i.e. less than 1% of the unperturbed value. The depth at which this occurs, which represents the maximum depth of sublayer which can influence the surface measurement, has been calculated as a function of the ratio ρ_{s1}/ρ_{s2} (from which k_{s1s2} is calculated [eqn. 4.20]) and plotted in Fig. 4.7. Assuming

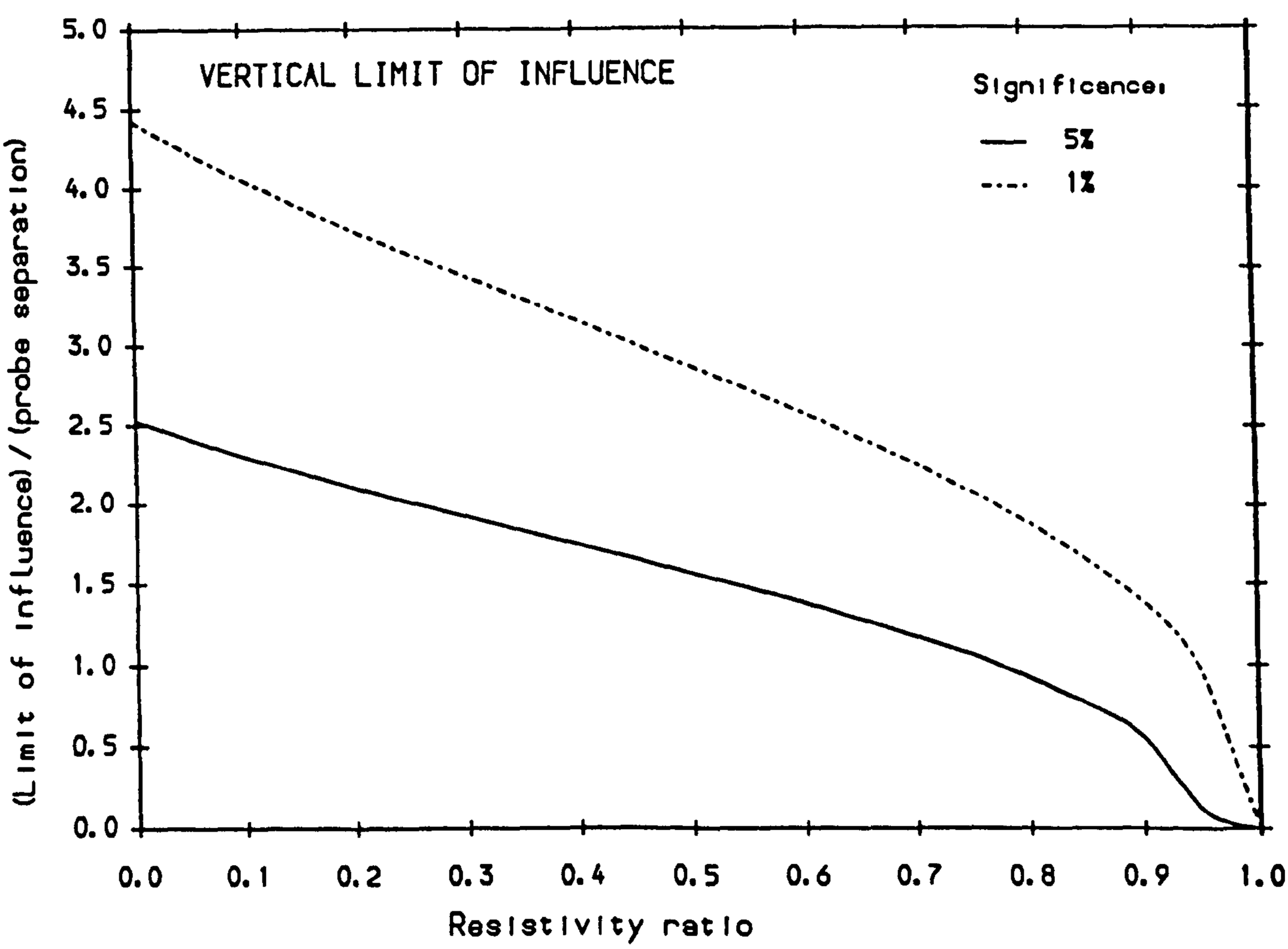

Figure 4.7. Limit of influence of subsurface boundary.

that the sublayer has higher resistivity than the surface, (ρ_{s1}/ρ_{s2}) can vary from 1 (as $\rho_{s2} \Rightarrow \rho_{s1}$) to 0 (as $\rho_{s2} \Rightarrow \infty$). However, natural sediments have values of FF ranging from 1.5 - 8.0 [Lovell, 1984], with the ratio within a given deposit unlikely to exceed 0.5. For a sublayer of very similar resistivity to the surface, a greater than 1% change in R_{app} is obtained when the interface is at a depth corresponding to less than the probe separation (100mm in this case). This can therefore be interpreted as the effective depth of penetration of the current in approximately homogeneous sediment.

For a sublayer of sharply contrasting resistivity ((ρ_{s1}/ρ_{s2}) $\Rightarrow$ 0.5), greater than 1% change in R_{app} is obtained at depths up to three times the probe separation, or 300mm in this case. Fig. 4.7 also illustrates the depth at which a sublayer alters the unperturbed value by 5%, since differences less than 5% would normally be masked by experimental error [Section 5.1]. It is clear that, whilst in most *in situ* conditions of relatively uniform electrical properties the measured resistance will reflect the properties of the top 50-100mm to within experimental error, the presence of marked heterogeneities within the top 250mm may significantly affect results.

The depths of sediment monitored using the field resistivity probe are therefore, under most conditions, slightly greater than the bulk V_s measurement defined in Chapter 3. However, it should be borne in mind that under certain circumstances they may be sensitive to sedimentary structures situated well beneath this near surface layer.

The limits of lateral influence are less straightforward to determine. Fig. 4.8 illustrates the two problems, the first (4.8(a)) concerns breadth of influence, the second length (4.8(b)). These illustrations are plan-views from above the air-sediment interface. Therefore an additional boundary is present which can be allowed for by considering the unperturbed potential within the medium of interest as a semi-infinite half-space. From analogy with eqn. 4.18, the potential at (x,z) due to a point source at (0,d) within this air-sediment interface will therefore be:

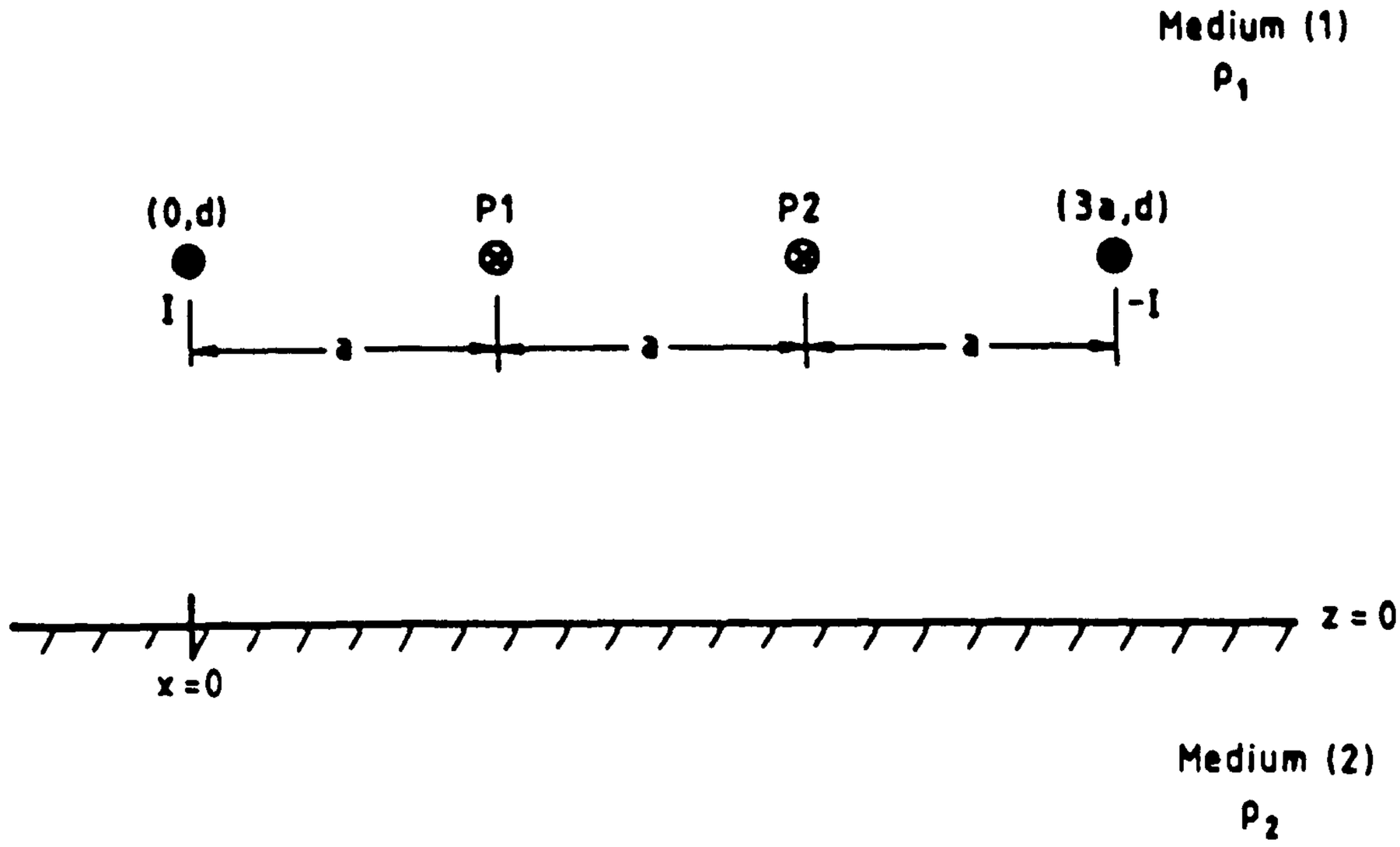

Fig. 4.8 (a). Plan view of surficial Wenner array near parallel vertical plane boundary.

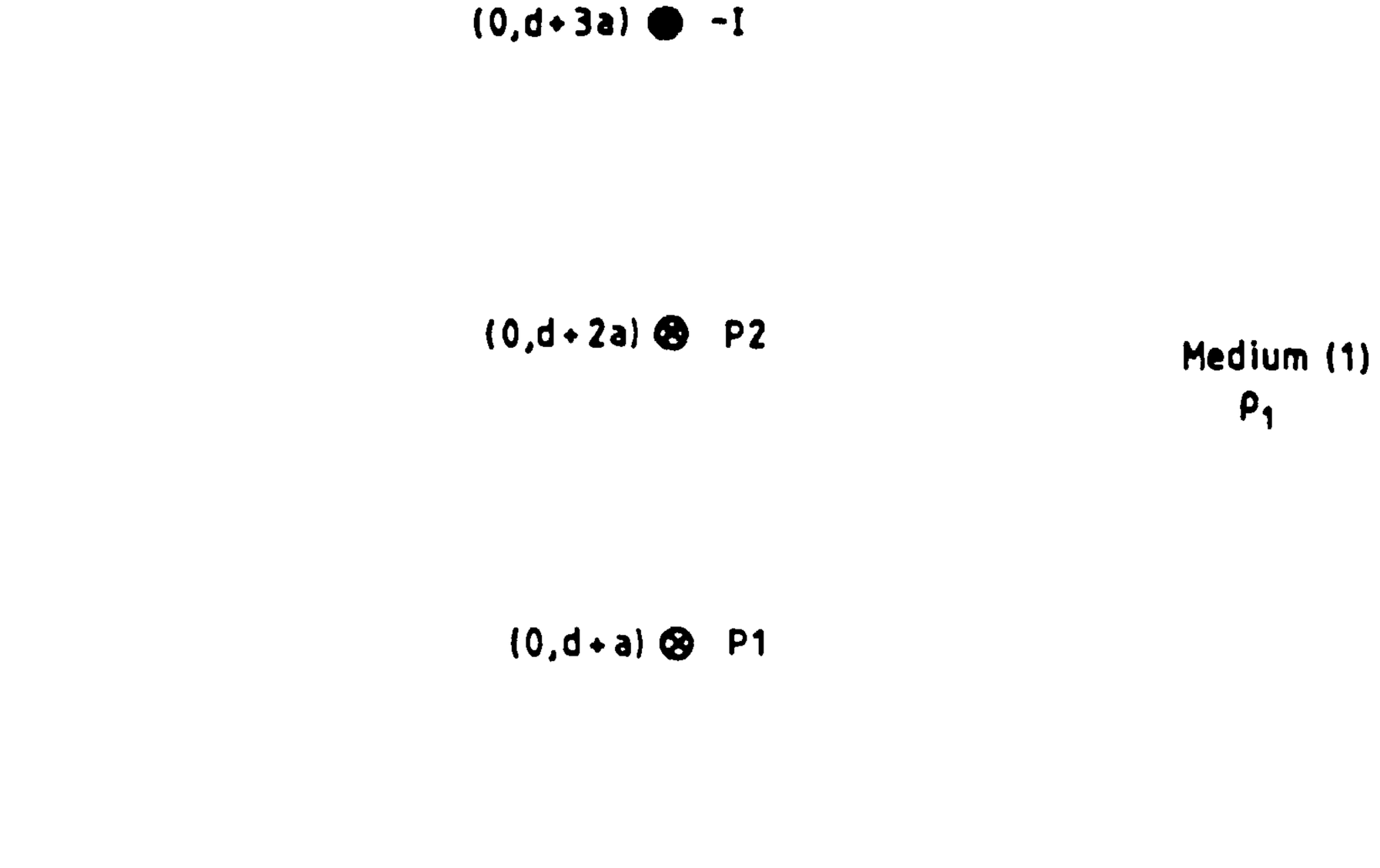

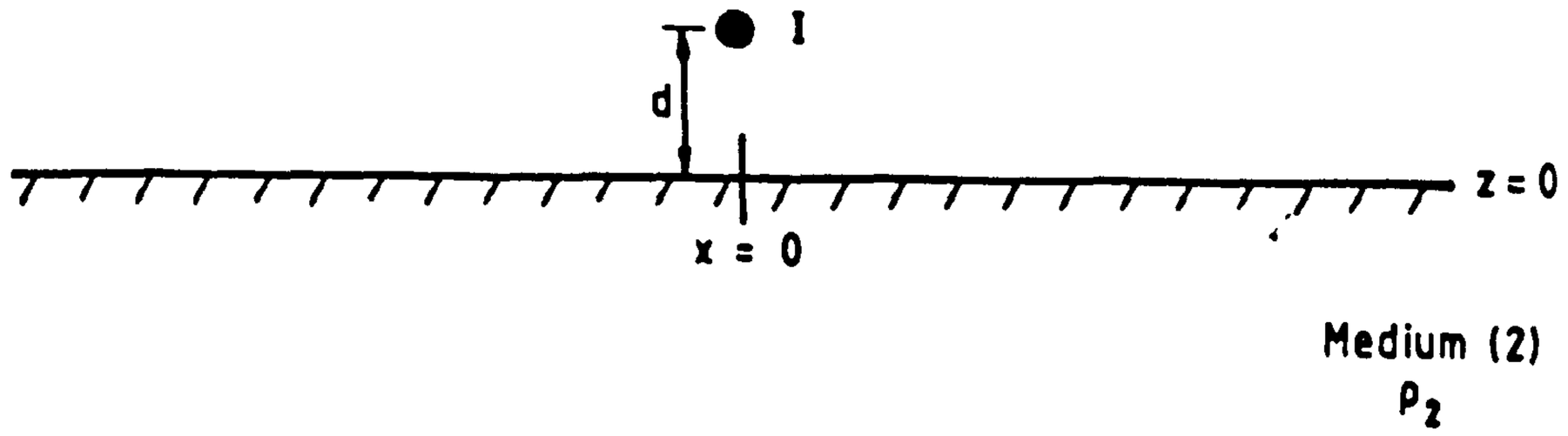

Fig. 4.8 (b). Plan view of surficial Wenner array near perpendicular plane boundary.

$$V(x,z) = \frac{I\rho_1}{2\pi}\left\{ \frac{1}{(x^2+(d-z)^2)^{1/2}} + \frac{k_{21}}{(x^2+(d+z)^2)^{1/2}} \right\} \qquad (4.34)$$

For the case illustrated in Fig. 4.8(a), potential electrodes are at (a,d) and (2a,d), and current electrodes are at (0,d) and (3a,d):

$$R_{app}(d) = \frac{\rho_a}{2\pi a}\left\{ 1 + k_{12}\left[\frac{2}{(1+(2d/a)^2)^{1/2}} - \frac{1}{(1+(d/a)^2)^{1/2}} \right] \right\} \qquad (4.35)$$

For the case illustrated in Fig. 4.8(b), current electrodes are at (0,d) and $(0,d_2)$ where $d_2 = d + 3a$, whilst potential electrodes are at (0,d+a) and (0,d+2a). Thus:

$$V(0,z) = \frac{I\rho_1}{2\pi}\left[\left\{ \frac{1}{|(d-z)|} + \frac{k_{21}}{(d+z)} \right\} - \left\{ \frac{1}{|(d_2-z)|} + \frac{k_{21}}{(d_2+z)} \right\} \right] \qquad (4.36)$$

$$R_{app} = \frac{I}{2\pi a}\left[1 + k_{21}\left\{ \frac{1}{(2d/a+1)} + \frac{1}{(2d/a+5)} - \frac{1}{(2d/a+4)} - \frac{1}{(2d/a+2)} \right\} \right] \qquad (4.37)$$

Fig. 4.9 illustrates the boundary distances at which R_{app} is changed by greater than 1% and 5% for a range of values of (ρ_1/ρ_2). From this figure it can be seen that the effective breadth of sediment monitored is normally 100 mm to either side of the array, whilst the length extends approximately 50 mm beyond the current electrodes. Thus the volume of sediment which could affect R_{app} is considerably more than that part between the potential electrodes, and is rather more than the volume expected to influence the V_s measurements [Chapter 3]. The two measurements correspond to comparable volumes only in sediments exhibiting a low degree of heterogeneity.

The effect of macroscopic anisotropy.

In contrast to spatial heterogeneity, which reflects variation of

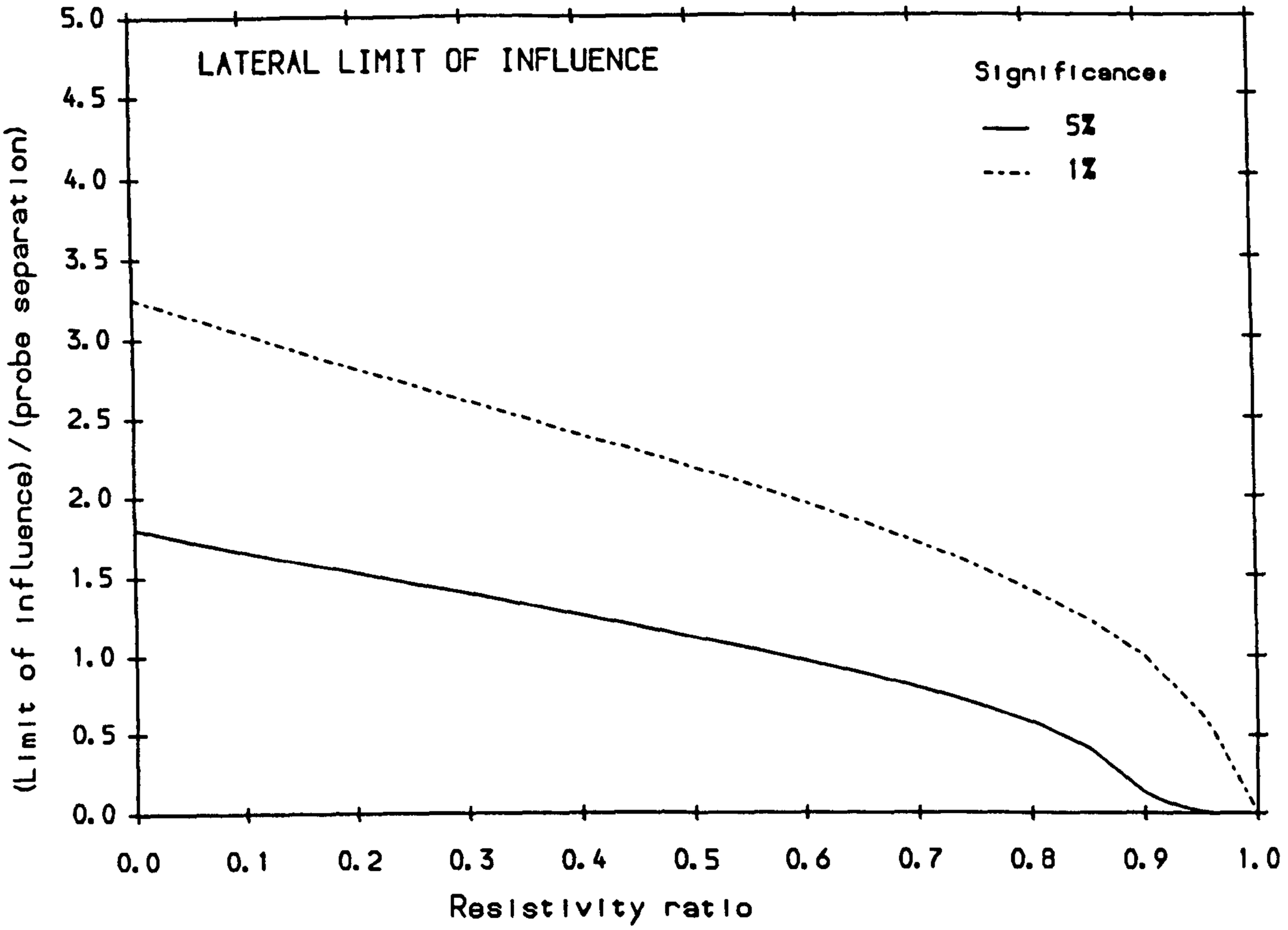

Figure 4.9(a). Limit of influence of parallel boundary.

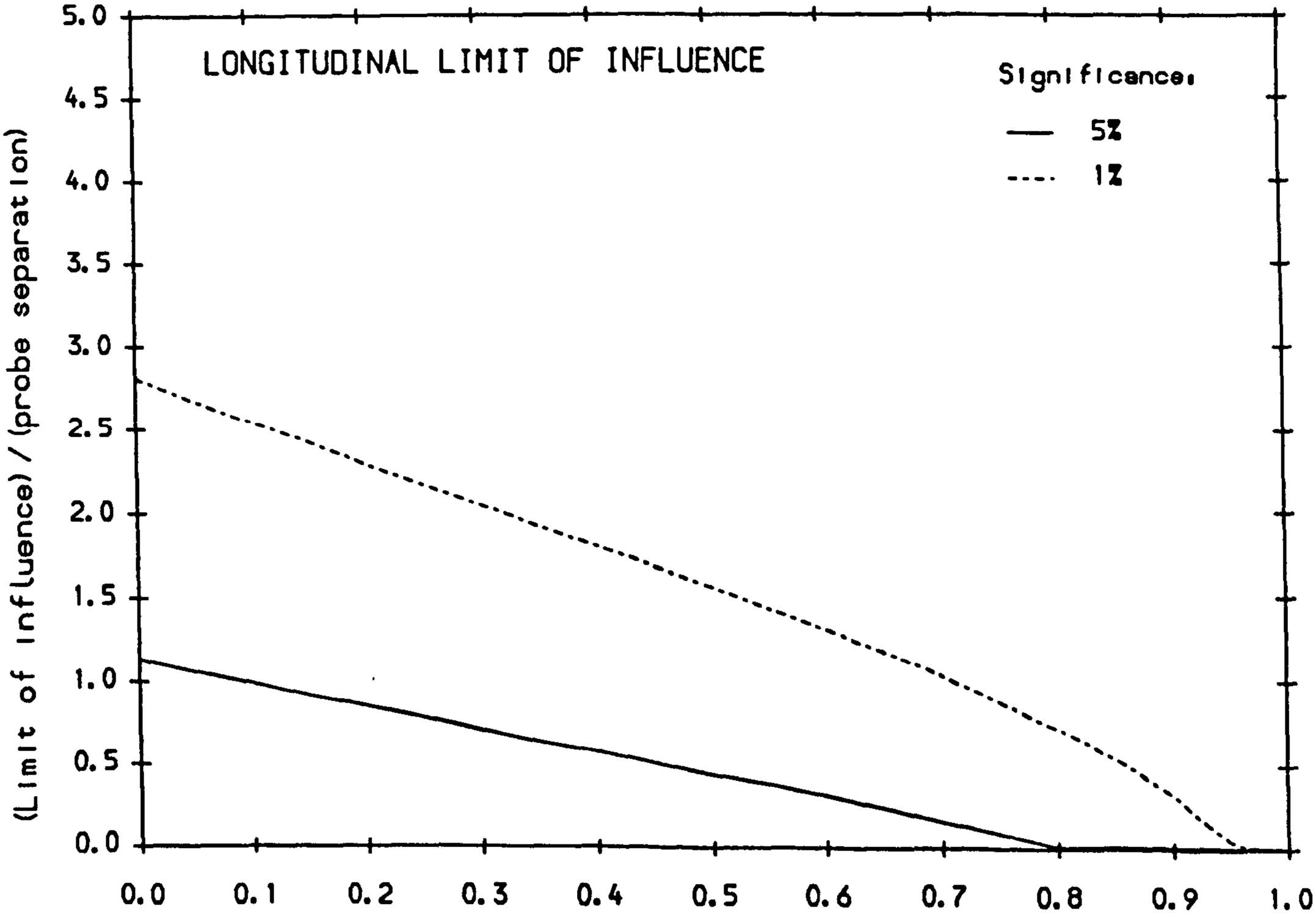

Figure 4.9(b). Limit of influence of normal boundary.

electrical properties on macroscopic scales, anisotropy reflects microscopic structural asymmetry, so that current can pass more easily in one direction than another. For the homogeneous but anisotropic case, Ohm's Law [eqn. 4.2] must be generalised as:

$$J_i = \sigma_{ij} E_j \tag{4.34}$$

where J_i is the *i*th component of $\underset{\sim}{J}$, σ_{ij} is a symmetric conductivity tensor and summation over *j* is implicit [Landau and Lifshitz, 1960]. Analysis can no longer be reduced to 1 dimension, so solutions to eqn. 4.5, though still valid, will be much more complicated. For example a commonly occurring case in layered media is of transverse isotropy, where $\rho_x = \rho_y = \rho_t$, $\rho_z = \rho_v$. It can be shown [Telford *et al*, 1976] that the potential due to a source placed at the sediment-air interface is:

$$V(x,z=0) \approx \frac{-I\sqrt{\rho_t \rho_v}}{2\pi x} \tag{4.35}$$

That is, sediment resistivity calculated from such a measurement of V will be an average of both transverse and vertical values. It is not possible to detect this type of anisotropy from surface measurements.

Irregular or non-planar surface boundary.

The theoretical relationships discussed have all involved plane boundaries between media. Many natural sedimentary deposits involve irregular air-sediment and sub-layer interfaces over appropriate length scales, caused by both biogenic and hydrodynamic topographical features such as feed pits and ripplemarks. Theoretical treatment of these cases is beyond the scope of this study, since handling of boundary conditions is extremely complicated. Small scale irregularity will 'perturb' the field calculated for a plane interface, as when a plane sublayer adds a series of extra terms (Eqn. 4.26) to that for a homogeneous half-space (Eqn. 4.25). For the purposes of this study, the apparent resistivity measured must incorporate this perturbation, in addition to that due to subsurface heterogeneity or anisotropy. Once again, replicates measured within a localised area help to average over surface irregularities.

The effect of an overlying water layer.

Since the resistivity of saline water is considerably less than that of sediment, a surface water layer was expected to have a strong effect on measured R_{app}. From eqns. 4.24, 4.27 and 4.28, resistance can be calculated for a Wenner array (4.32):

$$R_{app} = \frac{I\,\rho_s}{4\pi a}\left[(1 - k_{sw}) \quad + \quad \ldots \right.$$

$$\left. \ldots \sum (1-k_{sw}^2)(k_{sw})^{n-1}\left\{ \frac{2}{(1 + \left(\frac{2nw}{a}\right)^2)^{1/2}} - \frac{1}{(1 + \left(\frac{nw}{a}\right)^2)^{1/2}} \right\} \right] \qquad (4.36)$$

Fig. 4.10 illustrates the ratio $(R_{app}(w)/R_{app}(w=0))$ as a function of layer depth w for typical values of ρ_s and ρ_w. Note that as $w \Rightarrow 0$, $R_{app} \Rightarrow I\rho_s/2\pi a$. As w increases, R_{app} decreases sharply, with a 5% reduction occurring at 5mm layer depth for $\rho_w/\rho_s = 4$, 10mm for $\rho_w/\rho_s = 2$. Thus even a thin continuous surficial water layer can significantly affect results.

The effect of partial fluid saturation.

Sediment resistivity has already been shown to depend on the relative size and shape of the pore-space, with current carried by ions within the saline pore fluid. Where the pore space is only partially saturated, measured resistivity would be expected to be increased, since current cannot pass through voids. This has been shown experimentally for artificially compacted clays and soils in the laboratory (M^{c}Carter, 1984). The resistivity corresponds to that part of the pore space which is continuous, interconnected and fluid saturated. No model of this effect has been constructed, since as yet there is no model to predict the effect of the drainage process on pore-fluid distribution within the sediment. Some laboratory investigation was performed, as will be described in 4.4.2. To avoid any problems, care was taken to ensure that all *in situ* sampling was carried out only in fully saturated deposits.

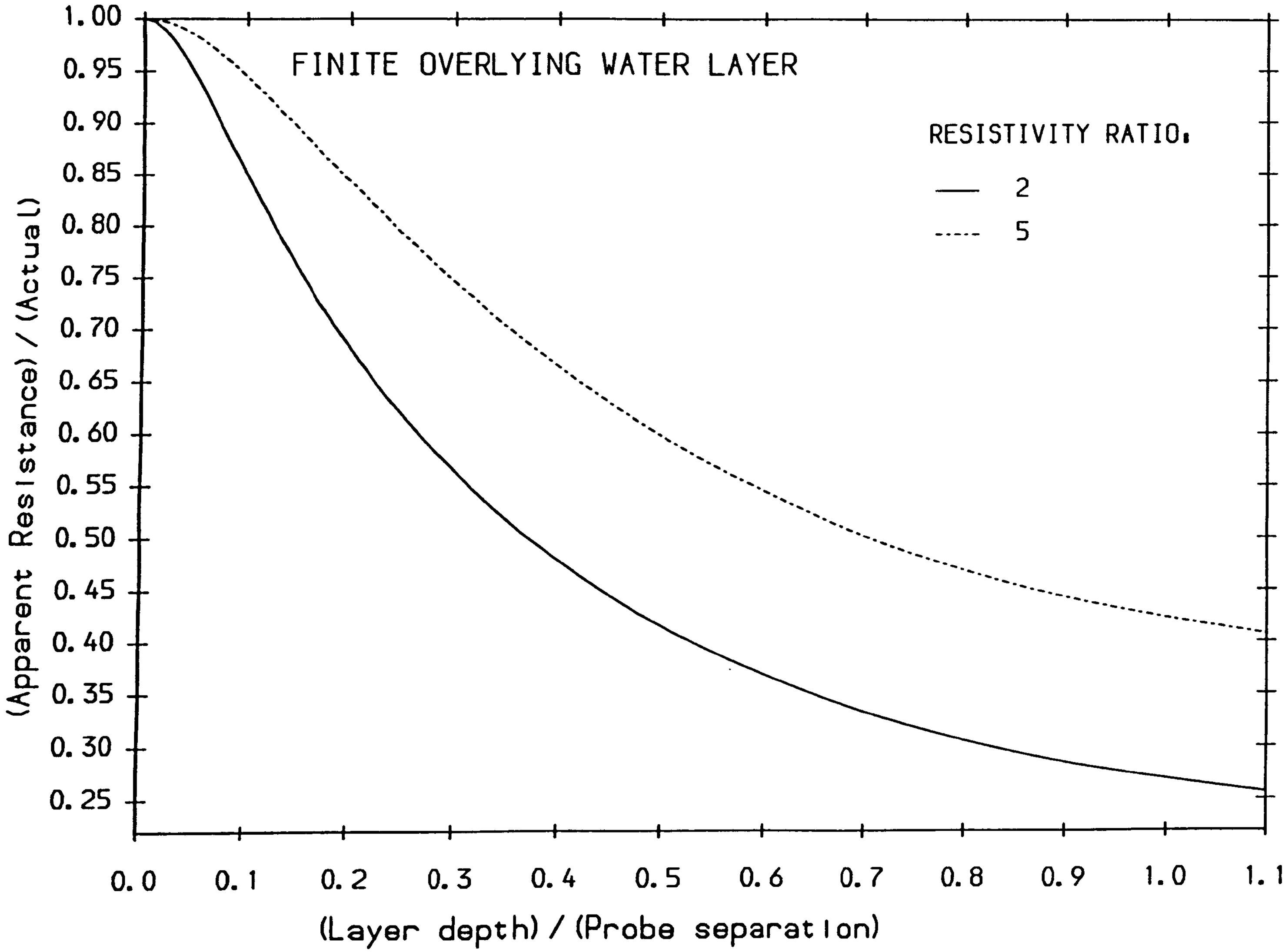

Figure 4.10. Effect on Apparent sediment resistance of an overlying water layer.

4.3. Preliminary laboratory investigation.

Because the field resistivity probe was too large for use in laboratory work, the smaller probes (Fig. 4.5) were constructed. The test tank and sediment described in Chapter 3 were used, following the same procedures for deposition, compaction, saturation and stabilisation as those used for the investigation of V_s. To avoid problems of variable salinity of ρ_w due to evaporation, and of corrosion of the apparatus, tap water was used as the saturant. This has a high but measurable resistivity. In addition, the marked dependence of ρ_w on temperature required that the temperature of both sediment and pore water should be monitored regularly throughout each experiment. Long equilibration times after initial deposition were allowed to ensure that sediment and saturant were at the same temperature. Measurements were also conducted over short time periods (generally 15-30 mins) to avoid problems with diurnal temperature variation. All measurements were performed at least four times the probe separation (i.e 80mm) away from the tank walls and base, to avoid the effects of an insulating boundary.

4.3.1. Variation of electrical properties with depth.

In Chapter 3 a marked dependence of V_s on depth was measured, and interpreted in terms of increasing overburden pressure on the intergranular contacts. It was not anticipated that ρ_s should be as strongly dependent on depth, since increasing pressure does not necessarily affect the properties of the pore-space. Only if compaction or grain orientation (and hence tortuosity) increase significantly within the surface layers would an increase in ρ_s be expected.

Direct measurement of ρ_s as a function of depth was not as straightforward as that of V_s. As for V_s, two approaches were possible: direct measurement by varying the depth of insertion of the electrodes; and variation of separation of electrodes, and hence depth of penetration of the current. It was decided that the simplest approach involved gradual insertion of a constant separation Wenner array, because this avoided problems of lateral heterogeneity and tank wall boundary effects. The most important complication is that as the electrodes are pushed into the sediment, their

changing position relative to the sediment-air interface must be taken into account. Thus, from Eqns. 4.18 (k_{21}=1, z=d) and (4.32), measured resistance corresponds to:

$$R_{app}(d) \approx \frac{\rho_s}{2\pi a}\left\{1+\left[\frac{2}{(1+(2d/a)^2)^{1/2}}-\frac{1}{(1+(d/a)^2)^{1/2}}\right]\right\} \qquad (4.37)$$

This does represent an approximation, because the insulating vertical supports of the electrodes have been ignored. Fig. 4.11 illustrates measured values of R_{app} for three sets of experiments during which electrode depth was varied from zero to 90mm, at approximately 10mm intervals. The three sets correspond to measurements made in different parts of the laboratory test tank. Comparison with the predicted values for $R_{app}(d)$, calculated from the measured $R_{app}(d=0)$ and Eqn. 4.37, indicates that, whilst the first 10-20mm show good agreement with expected values based on a homogeneous ρ_s in the surface layers, there is significant and reasonably consistent divergence above these values with increasing depth. This suggests that ρ_s is in fact increasing with depth, which in turn suggests that porosity or tortuosity are changing with increasing overburden pressure, even over relatively shallow depths. This result would be expected for fine cohesive deposits, but was rather surprising for sands.

Inversion of Eqn. 4.37, using measured $R_{app}(d)$, yields estimates of Apparent $\rho_s(d)$ at each depth, although it should be remembered that the underlying theory is based on homogeneous media and that measurement of continuously varying resistivity involves much more complex theoretical treatment. Fig. 4.12 illustrates these estimates, indicating an increase in resistivity of 40-50% in 10cm. This compares with 80-100% for $V_{s'}$ indicating that V_s is additionally sensitive to increasing intergranular friction with increasing overburden.

Unfortunately, time constraints prevented more thorough investigation of the variation in electrical properties with depth in the near surface. Several shortcomings may have affected the reliability and scope of this particular experiment: in particular, it was difficult to ensure a spatially homogeneous deposit in the test tank, and there was poor control

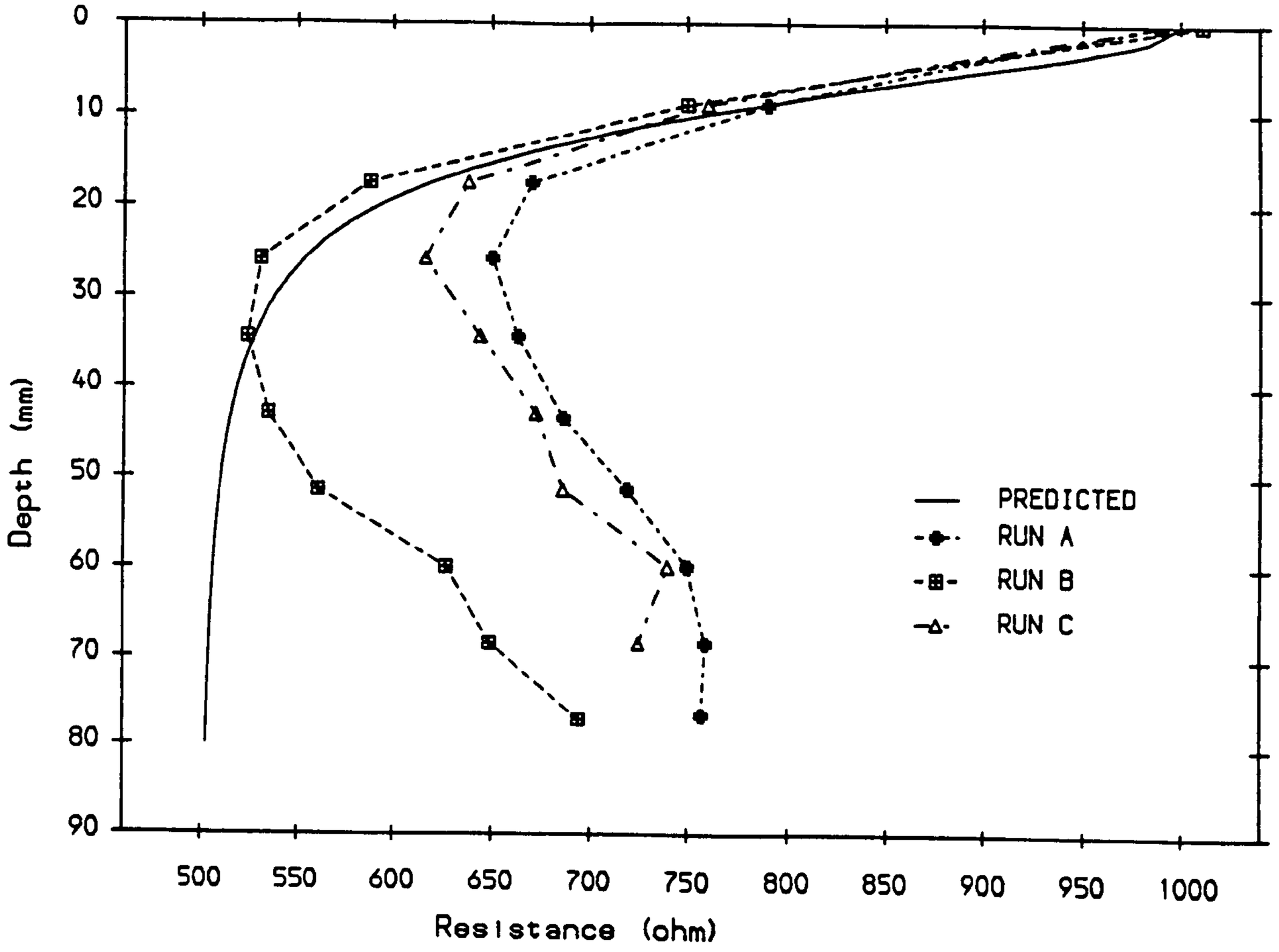

Figure 4.11. Variation in apparent sediment resistance with depth.

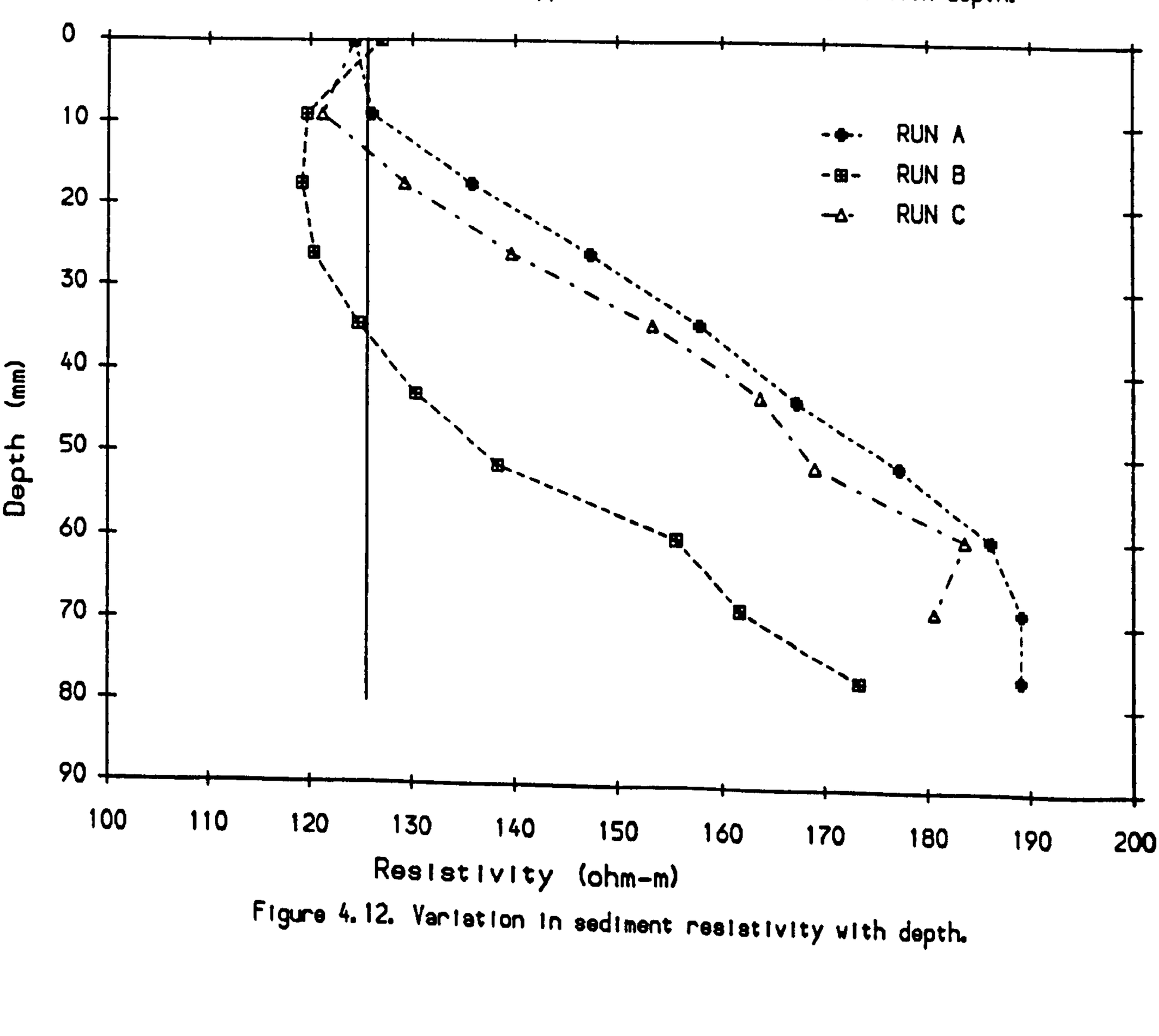

Figure 4.12. Variation in sediment resistivity with depth.

over post-depositional consolidation and disturbance. More controlled measurements, covering a wide range of sediment textures, both in the laboratory and *in situ*, are clearly required.

4.3.2. Effect of drainage.

A significant increase in V_s was observed when saturated sand in the laboratory test tank was drained (Chapter 3). This is thought to be caused by the formation of sealed voids which exert negative effective pressures, thereby increasing intergranular friction. As indicated in 4.2.4, the electrical resistivity would also be expected to increase significantly, since drainage will cause a reduction in relative volume of the interconnected conducting pore-fluid matrix, and an increase in tortuosity.

Fig. 4.13 illustrates values of R_{app} for two separate experiments, during each of which the test tank was successively saturated, drained and resaturated. The difference between the two runs is probably due to differences in compaction of the test deposit. Temperature of both saturant and sediment had been allowed to reach equilibrium with the surroundings, to ensure that temperature did not vary significantly during the saturation/drainage cycle. As expected, drained sediment showed an increase in R_{app}, but the magnitude of the increase was surprisingly small. Fig. 4.14 indicates the relationship observed between successive saturated/drained measurements: the superimposed line represents a 1:1 relationship between drained and saturated sediment resistance. For the test sand used, the increase measured on drainage corresponds to around 3%, which contrasts with 60% for V_s.

In the absence of information on pore-fluid distribution within the pore space, it is difficult to postulate reasons for this unexpectedly low increase. There are many aspects of the drained sediment system which are poorly understood. The system represents a three-phase system, which may exhibit complex electrical properties, with conduction along both sediment-water and air-water interfaces within the sediment, and with probable vertical heterogeneity in degree of saturation. A major shortcoming of the experiment was that the actual volume of water removed

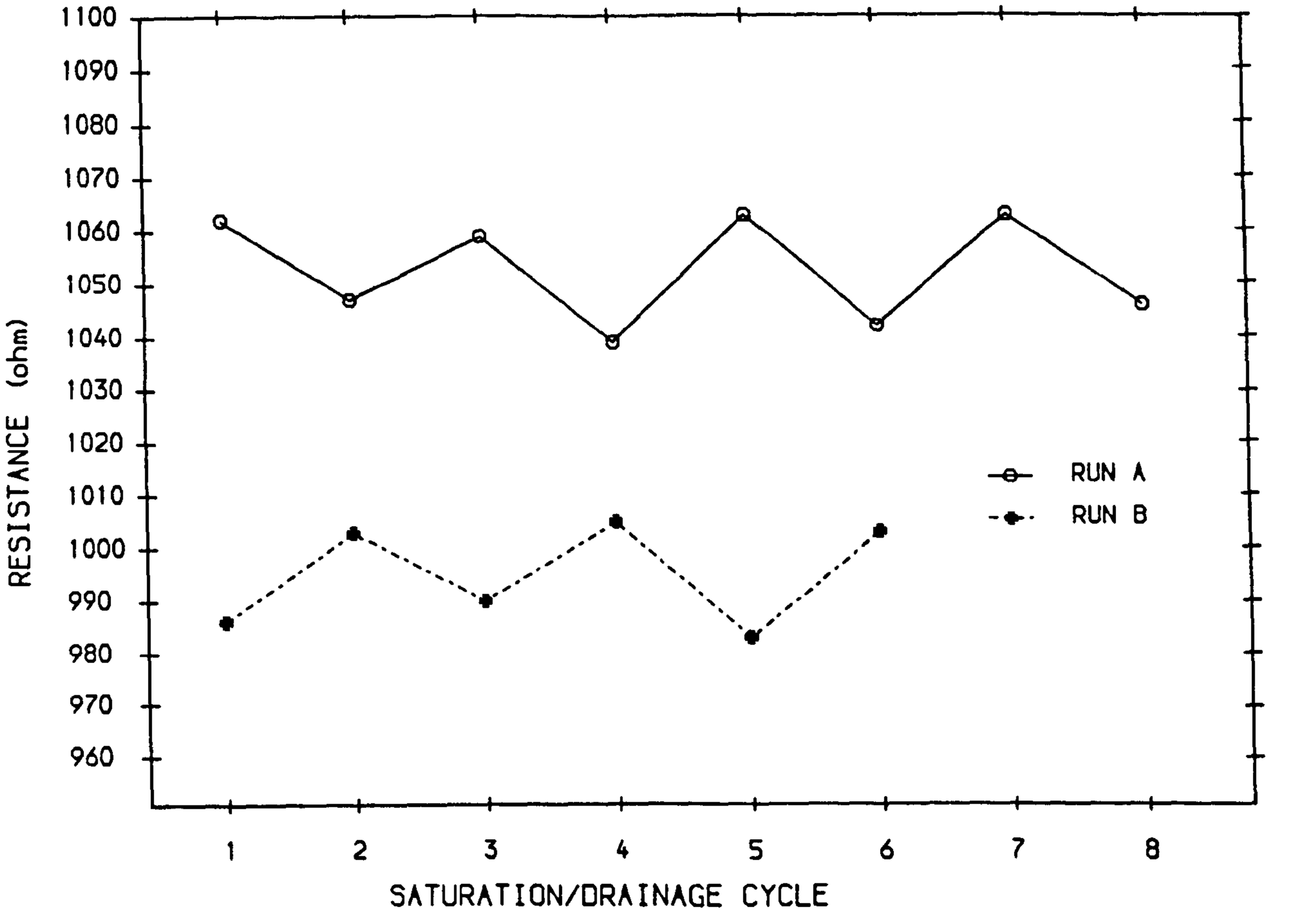

Figure 4.13. Effect of repeated drainage and resaturation.

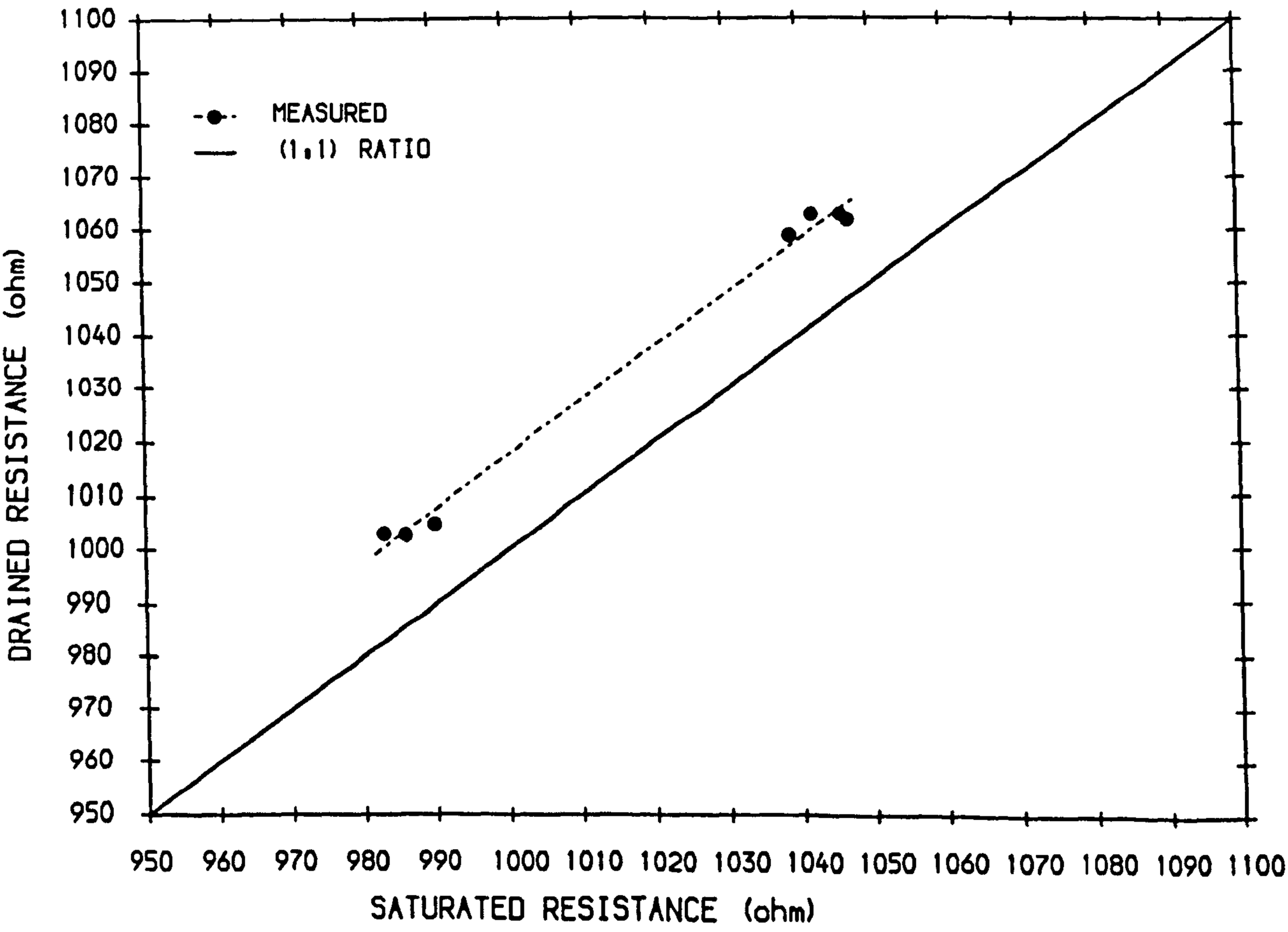

Figure 4.14. Comparison between drained and saturated resistance.

by the drainage process was not quantified. Thus the relative change in pore-fluid volume, which would have been expected to significantly increase electrical resistance, could not be calculated. It would also have been better to have repeated the experiment with a range of pore-fluid salinities, since at higher salinity conduction by the sediment frame work may have played a less significant role [Urish, 1981]. However, as has been described in 5.2, a surprisingly low increase was also recorded *in situ* in beach sands.

4.5. Summary and conclusions.

Many sedimentary deposits can be treated as macroscopic conducting media, and their electrical properties are therefore amenable to theoretical analysis based on solutions to Laplace's equation. Given appropriate boundary conditions, sediments near the air-sediment or water-sediment interface can be modelled, although the simplest treatment assumes plane interfaces and lateral and vertical homogeneity, which may not be strictly true for many natural deposits.

Using this theory, electrode arrays can be designed which yield simple relationships between measured potential distribution due to a current source and sediment resistivity, although the resistivity calculated from these relationships represents an 'apparent' value for a homogeneous, isotropic half-space. A simple Wenner line array, consisting of two current electrodes outside two potential electrodes with constant spacing between adjacent electrodes, has been constructed for intertidal sampling of exposed surficial sediments. A commercially available ABEM TERRAMETER SAS 300 is used both to provide a radio frequency current source and to perform measurement of sediment resistance R_{app}, which is converted to apparent sediment resistivity ρ_{app} by the relationship:

$$\rho_{app} = 2\pi a\, R_{app} \qquad (4.38)$$

In order to remove the implicit dependence of sediment resistivity on that of the pore-fluid, this is converted to Formation Factor (FF) by dividing by ρ_w, which can be obtained empirically from salinity, temperature and pressure of the saturant, or measured directly.

Some theoretical and experimental investigation of the effect on R_{app} of conditions expected in intertidal sediments was performed. It was predicted that marked heterogeneity within a volume of sediment approximately 400 x 200 x 250 mm was capable of significantly influencing measurement, which represents a rather larger zone of influence than was found for the V_s measurement system described in Chapter 3. In reasonably homogeneous sediment the effective volume sampled is approximately 300 x 150 x 125 mm. Laboratory measurements with a smaller version of the field electrode array indicated the existence of significant gradients in sediment resistivity within the upper few centimetres of sand, which was surprising considering that overburden pressure was not expected to cause compaction of the sediment over such shallow depths. The measured increase was considerably less than that observed for V_s.

Measurement was also found to be highly sensitive to surface water, so that measurements made under a continuous overlying water layer of only 5mm in depth would lead to significant underestimation of sediment resistivity. In contrast, although sediment resistivity was expected to be sensitive to the degree of saturation, measurements performed during repeated saturation and drainage of the sediment yielded only a 3% increase in sediment resistance between fully saturated and fully drained states. This contrasts with the marked increase observed for V_s.

The electrical resistivity probe described in this Chapter is clearly capable of producing rapid, accurate and repeatable measurements of R_{app}, with virtually no sediment disturbance. However, interpretation of these measurements in terms of sediment resistivity and ultimately Formation Factor involves some assumptions which result in potential but unavoidable error. Thus lateral and vertical heterogeneity on scales of centimetres, patches of overlying water and non-planar surface topography will all contribute variability to measured values, while laterally uniform media exhibiting anisotropy or vertical gradients will introduce systematic bias.

CHAPTER 5.

IN SITU MEASUREMENTS OF ACOUSTIC AND ELECTRICAL PROPERTIES IN SURFICIAL INTERTIDAL SEDIMENTS.

5.1. RATIONALE, EXPERIMENTAL PROCEDURE AND DATA ANALYSIS TECHNIQUES.

5.1.1. Introduction : experimental rationale

The acoustic S-wave and electrical resistivity probes were designed primarily for *in-situ* measurements of the top 10cm of unconsolidated sedimentary deposits. The objectives behind the proposed field measurements were :

(1) To develop and test an experimental strategy for *in-situ* determination of V_s and FF over short length and depth scales, initially in intertidal sediments.
(2) To perform measurements in a range of sediments and assess the extent of variability in the geophysical (and, by inference, structural) properties of natural deposits.
(3) To investigate, by simultaneous measurement of a range of standard sediment parameters, the effect of localised (and larger-scale) variation in biological, physical and textural characteristics on the geophysical properties of surficial sediments.

5.1.1.1 Site selection.

Two practical constraints influenced site selection. First, the marked sensitivity of V_s to drainage led to the requirement that the sampled sediment be fully saturated, as far as it was possible to determine. This

was ensured by timing measurements to coincide with exposure of intertidal flats on the ebb, when they had been submerged for a maximum period. Thus any air entrapped on inundation would have had ample opportunity to diffuse into the water column. This requirement limited both the number of sites sampled and their spatial separation, especially on sharply sloping banks and foreshores. Second, sites had to be accessible to within half a mile by road or small boat, because field equipment was both too heavy and too delicate for manhandling over long distances.

Given these practical constraints, scientific criteria for site-selection could then be addressed. First, a wide range of hydrodynamic, textural and geomorphological environments should be sampled, to enable investigation of large-scale variation in sediment properties. Second, within this overall framework, the effects of variation in specific sediment characteristics should be monitored. Natural sedimentary deposits can have complex physical structures which are controlled by interaction between depositional environment; composition, shape and size of sedimentary particles; and biological activity. It is extremely unlikely that simple universal multivariate relationships exist between measurable textural and biological parameters and geophysical properties. Even if they did, the large number of variables would require a huge data set before multivariate analysis could be reliably performed. For this reason, the 'ideal' study site consists of a deposit which is uniformly identical in all respects except one. By performing a set of measurements within a localised area, the effect of varying this one parameter can then be investigated. Any relationship identified should also, of course, be verified elsewhere before concluding that it is universal.

In practice this ideal is impossible to achieve. One reason is that other variables may be independently sensitive to the spatial variability in environmental controls necessary to induce change in one property. Another complicating factor is the interrelationships between many sediment properties, either through direct interaction or indirectly through a common cause. Minimisation of these problems can be achieved by selecting sites where most sediment properties were either uniform or nearly uniform. Two examples were considered practically realisable: first, sediment from the same source and with the same modal population, but with a varying proportion of admixed shell-fragments or mud; and second,

sediment containing varying densities of a single species of macrofaunal benthic organism.

The task of suitable site selection was still not simple, not least because it was not always easy to tell in advance which properties comprised the dominant variables. It was necessary to identify an area where a few sediment properties were more sensitive to localised environmental control than the rest. A further constraint was that variation had to be highly localised to enable sampling during one ebb-tide.

The most obvious environmental control which causes spatial variation in the properties of intertidal sediments is the interaction between tide and bed morphology. Significant factors are: tidal current velocities on inundation and exposure of the sediment, local hydrodynamic regime, and duration of immersion over a tidal cycle. These factors can affect both sediment texture and packing configuration, especially if wave-action is also present [Reineck & Singh, 1975]. In addition, benthic macrofauna are highly sensitive to duration of exposure, with the result that both community structure and number densities of organisms grade sharply between low and high-water marks [Eltringham, 1971]. This phenomenon can be further enhanced in estuaries by salinity and temperature variation over tidal cycles.

It was therefore possible to select environments which displayed variability in a relatively small number of properties within a localised area, controlled primarily by position between high and low water-marks. Since one of the key aims of the study was to investigate the effect of benthic macrofaunal activity on geophysical properties of the sediment, many locations were selected because they exhibited a wide range in density of a single benthic macrofaunal species. There is still scope for data collection in a far wider range of sedimentary deposits.

5.1.2. Field measurement procedure.

All field-work was carried out over the 2.5-year period from June 1985 to January 1988. A series of experiments was performed, each in different

localities or at different times over this period, which were designed both to be complete in themselves and to be incorporated into the overall data collection exercise. Fig.5.1.1 illustrates the geographical distribution of the study areas. Results from individual experiments have been described and discussed in Sections 5.2-5.3, and then compared, combined and placed in a wider context in Section 5.4.

Experimental procedure was subject to an evolutionary process during this time, both as experience led to improvements in measurement and analysis techniques, and as experimental objectives changed. However, the basic components remained essentially the same. In order to avoid excessive repetition, and to present an overview of the development of each component of data collection and analysis, procedural details have been collected together and discussed before presentation of experimental results. An extensive set of sediment properties was characterised during the study. The following sections describe, for each measured property: data collection, laboratory processing and data-reduction where relevant, errors, and finally statistical analysis.

5.1.2.1. Sampling strategy.

For each experiment an appropriate sampling strategy was adopted, using the following terminology:

Sample: taken here to represent either a sediment sample or a physical or geophysical measurement of the sediment.

Location: area (typically 200 - 1000 m^2) within which all sampling is performed.

Site: A sub-area of the location (typically 0.25-1 m^2) within which a range of sediment properties is characterised by taking sets of replicate samples. A number of these sites was marked out and characterised at each location.

Strategy varied during the course of the study. Initial experiments were performed in rather haphazard fashion, selecting sites for their abundance or scarcity of a particular organism without measuring the relative positions of the sites. Later experiments made use of a measuring tape,

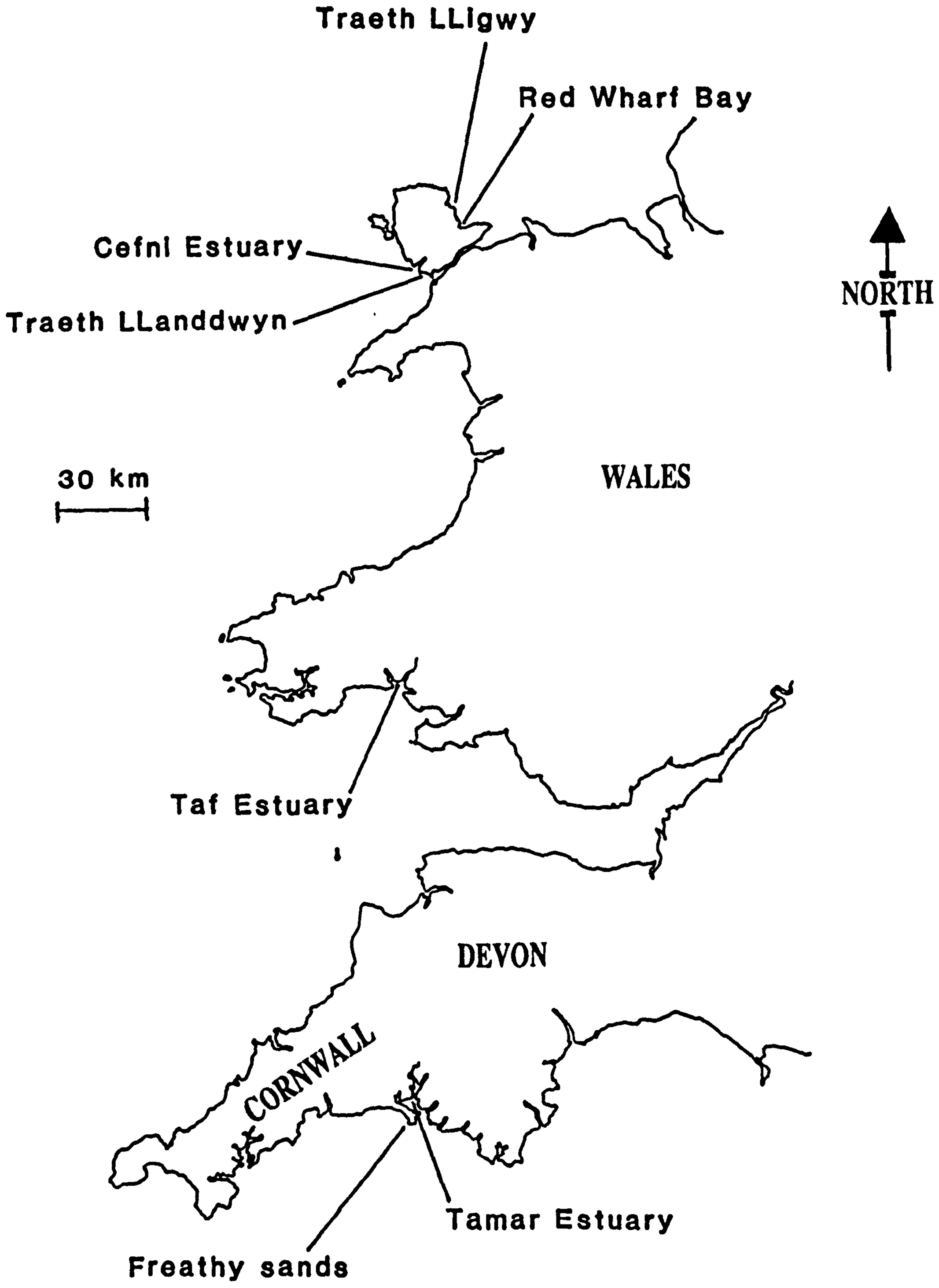

UNITED KINGDOM (SOUTH & WEST)

Fig. 5.1.1. Map showing sampled locations.

usually set up at right-angles to low-water mark, with sites marked out at regular intervals along the tape. This had the advantage of quantifying length scales of variation, and also of enabling identification of trends in biological, textural or geophysical characteristics. Finally, the investigation of seasonal variation involved setting up five sites which were fixed by measuring relative to a concreted-in post, and re-sampled at monthly intervals over a period of 13 months.

It should be emphasised that much more intensive sampling in the form of a grid-survey would have been required to obtain statistically rigorous estimates of spatial variability (Joliffe, 1986). This was not feasible in the time available at any location. It was also, fortunately, not one of the primary aims of the study, which instead was attempting to investigate relative spatial variability of, and identify any covariation between, measured properties of the sediment. However, a measure of the degree of spatial variation could be defined, and used, within the context of these experiments.

5.1.2.2. Textural, biological and structural site characterisation.

Each site was characterised by a set of physical, textural and biological parameters in addition to the geophysical measurements. Where relevant, bed height was levelled in relative to a suitable temporary bench-mark, and any surface features were also noted.

Textural characteristics.

Several site-replicate samples of the upper 5cm of sediment were collected and removed to the laboratory for processing. Sample size was approximately 150g. Standard laboratory techniques were then applied to determine the following properties, where relevant:

- Grain-size distribution
- Percentage by weight of silt and clay.
- Percentage by weight of carbonate.
- Percentage by weight of organic material.

Structural characteristics.

At all sites after the initial trial experiment, replicate samples of a known volume of sediment were taken for determination of sediment porosity. A standard soil sampler was used, which consisted of an accurately machined cylindrical stainless steel core 5cm in height, with a calibrated volume of $100cm^3$. The cutting edge was bevelled to minimise distortion of the sample on penetration. Once cored, the sample was dug out with a trowel, trimmed, and extruded into a plastic bag. Extremely soft or cohesive muds and sands with close-packed sub-surface shell or pebble layers were the only types of sediment which proved difficult to sample in this way.

An additional, qualitative approach to characterisation of sediment structure was adopted on a number of occasions. Standard Senckenberg-type box-cores of dimensions 400mm × 250mm × 50mm were taken and removed to the laboratory for resin impregnation [Reineck, 1961]. Transportation problems, given the already heavy equipment load, limited the numbers of box-cores taken. There were also problems with cores containing living organisms which tended to disturb the sediment before it could be impregnated. The simpler and much quicker method of structural characterisation usually adopted involved digging up a portion of sediment with a trowel, allowing it to fracture along weak vertical planes, and observing exposed burrows and structures.

Biological characteristics.

The method chosen to characterise benthic macrofaunal activity depended on species. Three species were under special consideration during the study:

- *Arenicola marina*
- *Lanice conchilega*
- *Corophium sp.*

In addition, *Pygospio elegans* and *Hydrobia ulva* were found in significant abundance in the Cefni Estuary.

Brief summaries of feeding and burrowing activity of these organisms have been presented in the appropriate sections of 5.2 and 5.3. *Arenicola marina* activity was quantified by simply counting the characteristic coiled faecal casts which were usually clearly visible on the sediment surface as the ebb tide receded [Plate 2]. Sometimes, especially on exposed sand-flats after high winds, the funnel-like head-shafts were more distinctive, in which case they were counted instead.

Lanice conchilega was also quantified by counting surface features, this time the protruding fringed tube [Plate 3]. For high densities, the sites were marked into quadrants before counting.

Corophium species were initially quantified by 'fracturing' the sediment with a trowel and counting the U-shaped burrows along exposed fracture planes [Plate 4]. This rough and ready technique was later replaced by removal of cores of a fixed volume of sediment to the laboratory. These were then washed through a set of sieves, the organisms separated out, identified and counted.

Pygospio elegans and *Hydrobia ulva* were also quantified by counting after separation from the sediment by sieving. The volume chosen in all cases was $300cm^3$, made up from three randomly sampled $100cm^3$ cores. This limitation on sample size was imposed because, for this particular experiment, the sampling sites were returned to once every month. Thus sediment disturbance was required to be a minimum. Naturally, these small volumes could not be expected to provide representative counts of organisms present at low population densities. However, *Corophium*, *Pygospio*, and *Hydrobia* were identified in numbers of up to 130 per sample. Further discussion of the accuracy of biological characterisation will be presented in Section 5.1.3.3.

5.1.2.3. S-wave Velocity Measurement.

The equipment selected for *in situ* measurement of V_s has been described in detail in Chapter 3. Two field probes were pushed into the sediment to a constant depth of 40mm. The same transmitter and receiver were used throughout to avoid the problems of unknown tolerance in transducer

response. An Oyo Sonic Viewer was used to transmit, receive, stack and display the signal.

Trace feature arrival-times were then determined directly from the digitised display. Arrival-times of the pulse onset were recorded wherever possible, with further measurements of the first signal maximum and minimum. These could be used to calculate velocity from multiple receiver positions, and had the advantage of being generally more accurate than the onset measurements (Section 5.1.4.4). In addition to the direct arrival-time measurement, a paper record of the received signal was usually obtained for more leisurely examination in the laboratory.

The fundamental elements of this technique proved extremely successful throughout the study, and were not therefore subjected to change. The only aspects of S-wave velocity measurement which underwent development were the combination of probe separations used, and the method of fixing them.

Experimental procedure had to allow variable probe separation and complete decoupling from any rigid frame during measurement. The first approach utilised a perspex template, with three accurately cut slots. With the template placed on the sediment surface, the transmitter was pushed through one of these until the 'plate' of the transducer passcd beneath the template. The receiver was then pushed in at each of the other slots in turn, resulting in transmitter-receiver separations of 150mm and 80mm. This method had the advantage of ensuring fixed probe separations and vertical insertion of the probes. However, after deployment in the preliminary field trials at Llanddwyn this method was abandoned, for two reasons. First, it was difficult to push the probes into the sand by simply applying a direct vertical force. Slight vibration along the plane of insertion was found to alleviate this problem, but this was impossible using the tight-fitting template. Second, it was decided that increasing the number of probe separations monitored would allow for calculation of velocity by linear regression in uniform deposits, and facilitate interpretation of anomalous measurements.

A solution to these problems was found by reverting to the tried and tested laboratory procedure, with the receiver positioned at a total of four separations. Care was taken to ensure vertical insertion, and the

separation between the probe tips was measured using a ruler or Vernier calipers. Probe separations were constrained near four selected constants, to aid interpretation of results. In fact it was usually possible, by slightly vibrating the transducer, to adjust its position to a separation within 1-2mm of the pre-determined value. Sediment liquefaction occurring during this procedure was observed to be highly localised around the transducer plate, and hence should not have affected the bulk of sediment through which the disturbance was passing.

This four-separation technique, adopted very early on, was successful enough to be retained throughout the study, which enabled consistency of experimental data and intercomparison of results. The increased experimental error incurred by independently positioning the transducers was considered unavoidable given the need to characterise multiple probe separations with the same transducer pair. The probe separations used were initially fixed at 200mm - 50mm, in 50mm intervals. This range was found to be suitable for beach sands but was too large for the generally more highly attenuated estuarine deposits. In addition, separations of greater than 150mm had been shown to result in non-linear effects (Chapter 3). The separations eventually selected as standard were between 125mm and 50mm, in 25mm increments.

5.1.2.4. Formation Factor measurement.

Measurement of sediment electrical resistance was performed throughout the study using the beach probe described in Chapter 4 in conjunction with an ABEM Terrameter model SAS 300B. A current-setting of 20μA was found to produce consistent results, with the instrument performing internal averaging over a period of 4 seconds before displaying the resistance, in ohms, to 2 or 3 decimal places depending on the pore-fluid salinity.

Sediment Resistance (R_s) could readily be converted to electrical resistivity (ρ_s) using the probe separation (a):

$$\rho_s = \frac{2\pi R_s}{a} \qquad (5.1.1)$$

Conversion to FF requires the electrical resistivity of the pore-fluid

(ρ_w) which is a function of salinity and temperature, as has been shown in Chapter 4. This proved rather problematic, with a succession of only partially successful procedures being adopted.

For the preliminary work at Llanddwyn, pore-fluid salinity and temperature were assumed constant, and equivalent to that of the surface water of the ebbing tide, throughout the sampling period. This seemed reasonable since measurements were taken virtually at the water's edge on a receding tide over a period of two to three hours. The pore-fluid should have equilibrated with the overlying water-column during immersion, and would not have had time to adjust to exposed conditions through evaporation or insolation. Seawater resistance (R_w) was measured by wading out to sea and deploying the beach probe at the sea surface. Then:

$$FF = \frac{2\pi a R_s}{2\pi a R_w} = \frac{R_s}{R_w} \qquad (5.1.2)$$

This simple technique proved difficult to perform when waves were present, and impossible to implement under estuarine conditions of time-varying salinity.

The next attempt to characterise pore-fluid resistivity was to dig a shallow (10-15cm) hole in the surrounding sediment, allow it to fill with water, then use the beach probe to measure the resistance of this water. This could be repeated at each sampling site, or at slightly larger intervals along an intensively sampled transect. This method has been used successfully on beaches in the past (J. Bennell, *pers. comm.*). However, when it was attempted in the Taf estuary it was found to produce consistent overestimates of pore-fluid resistance, yielding FF values which were much lower than expected for natural sedimentary deposits.

This overestimation was probably caused by interference from the bottom of the hole, as discussed in Section 4.2.3. It was impossible to dig and maintain a hole of sufficient depth (more than *c.* 1.5a) to remove this effect in poorly consolidated estuarine sediments.

Since the above method of obtaining a representative pore-fluid sample

could not be improved, the method of measuring its resistivity had to be modified. The obvious solution was to use a resistance probe which measured over much smaller volumes, thus reducing the influence of the surrounding sediment. One such instrument which was readily available was an N.I.O. Type M.C.5. S-T bridge, which measures the conductivity of fluid within a cylindrical coil and is therefore unaffected by the surrounding sediment. This instrument had been calibrated to measure temperature and salinity, which had then to be converted back to pore-fluid resistivity using the empirical equations described in 4.2.3.

A final refinement, which saved carrying this extra piece of equipment around, involved collecting a pore-water sample from the filled hole and removing it to the laboratory for salinity measurement. *In situ* temperature was recorded using a thermometer. 1 litre samples were taken to provide a bulk estimate, ignoring small-scale heterogeneity and averaging over similar volumes to those measured by the resistance probe. Temperature was thought to be most sensitive to environmental variation during sampling, and could be sampled more frequently using this technique.

The problems of accurate pore-fluid resistivity measurement were not completely overcome during this investigation, with several potential sources of error (Section 5.1.4.5). However, some useful results were obtained using these relatively simple and extremely quick methods.

5.1.2.5. Operational details.

The equipment described in the preceding sections was fitted into two plastic ball-barrows which enabled relatively straightforward transport to the location and around the sampling sites. When adverse weather conditions prevailed, the instrumentation had to be protected by plastic sheeting, taped to the barrows, with access points for the operator. Two personnel were required for efficient field operation, effectively separating out 'wet' and 'dry' operations and minimising the time spent at each site.

The number of replicate samples taken at each site varied depending on

number of sites sampled, time available and also as results from earlier experiments suggested more intensive data collection. For reference, procedural details for each location have been summarised in Table A1.1.

5.1.3. Sample processing and data reduction.

The samples collected and measurements made required a considerable amount of laboratory-based processing and data manipulation before yielding the desired set of sediment characteristics. The requirement in most cases was to produce the best estimate possible of the mean value of a parameter for each site, so that comparisons between properties at different sites could be made. An estimate of the degree of within-site variability due either to sampling error or natural small-scale spatial heterogeneity was also attempted for some parameters.

In the following discussion, all statistical definitions are standard and can be found in Sokal and Rohlf [1980]. In cases where replicate measurements were made the standard deviation was calculated. This provides a good parametric estimate of within-site variability for large numbers of replicates, in which case it can be converted into a standard error for the site-mean. However, for small numbers of replicates all that can be achieved is an improved estimate of the site mean, and a general idea of variability. By dividing the standard deviation by the mean, the coefficient of variation can be obtained for comparing degrees of variability among different properties.

5.1.3.1 Sediment porosity.

With the exception of the preliminary survey at Llanddwyn all sediment samples were collected using the $100cm^3$ porosity corer. Thus, whatever other procedure it was subjected to, care was taken to ensure that the total dried weight of the complete sample was also obtained. It was washed in several changes of tap-water followed by distilled water, then placed in a pre-weighed evaporating basin. After drying at 105^0C for 24 hours and cooling in a desiccator the basin was reweighed. Three methods of washing were adopted depending on the sample and its intended subsequent analysis.

The simplest involved centrifugation and decantation of the entire sample. Where size analysis was to be performed, the sample was washed through a 63μm wet-sieve for separation of fines, the washings then being centrifuged. Finally, where organic fraction was to be determined the sample was vacuum-filtered using a Buchner funnel, to ensure preservation of all light organic matter.

Porosity (ϕ) was then calculated from dry sediment weight (m_{sed}) using:

$$\phi = 1 - \frac{m_{sed}}{100\rho_{grains}} \qquad (5.1.7)$$

Sediment grain density (ρ_{grains}) was not directly measured. Most samples were composed of quartz sands with relatively small admixed proportions of shell-fragments and clay minerals. As indicated in Table 5.1.1, a relatively small range in density is involved. For clean quartz sands, and sands containing less than 5% mud, density was calculated using:

$$\rho_{sed} = 1 - m_{sed}\left\{\frac{(1-f_c-f_m)}{\rho_q} + \frac{f_c}{\rho_c} + \frac{f_m}{\rho_m}\right\} \qquad (5.1.8)$$

where f_c , f_m are measured shell and clay fractions. Two or three replicate samples of porosity were obtained per site.

Constituent		Density
Quartz	(ρ_q)	2.65
Carbonate:		
Calcite	(ρ_c)	2.72
Aragonite		2.95
Feldspars		2.58
Micas		2.90
Clay minerals:	(ρ_m)	
Kaolinite		2.60
Illite		
Montmorillonite		

Table 5.1.1.

Specific gravity (density, in gcm^{-3}) of commonly occurring marine and estuarine sedimentary constituents. From: [Bolton, 1979: Bell, 1983].

5.1.3.2 Textural parameters.

Characterisation of sediment textural parameters was performed on separate porosity samples, or on sub-splits of these samples. The techniques employed were standard laboratory procedures at UCNW. The main source of reference for this part of the analysis, other than advice and comment from colleagues, was Carver [1971].

Grain-size parameters.

The grain-size distribution was thought to be important because of its effect on stable packing configurations of a sedimentary deposit. There is some debate over the correct mathematical form of natural grain-size distributions. In the past they have been considered as generally approximately either Gaussian or log-normal [Herdan *et al*, 1960]. Since a log-normal distribution can be considered as arising from the action of a random multiplicative combination of processes, which best describes the majority of natural environments, it would appear to be a logical basic 'unit' of a sedimentary deposit. This argument has led to the widespread technique of 'splitting' grain-size distributions into a series of overlapping or truncated log-normal sub-populations, and attributing the separate components to different natural sorting processes [e.g. Visher, 1969; Moss, 1972]. More recently, it has been argued that grain-size distributions are more naturally described by a log-hyperbolic representation [Bagnold and Barndorff- Nielsen, 1980].

In terms of the effect on packing structure of the sediment, which is of primary interest in this study, the precise mathematical formulation of the grain size distribution is of little importance. A log-hyperbolic distribution can also be expressed in terms of superimposed log-normal sub-populations, which reduces the problem to one of mathematical semantics. For the purposes of this study, the more conventional approach was preferred. This views a sedimentary deposit as a stable, randomly-packed log-normal 'framework', comprising a dominant modal population, combined with one or more coarse and fine sub-populations [Moss,1972]. The fine sub-population forms the 'interstitial' component, residing in the pore space between the framework grains, while the coarse

sub-population is randomly distributed within the framework, causing localised packing distortion or 'bridging'. These definitions apply for relatively small proportions of coarse and fine sub-populations: if the fine fraction increases beyond a certain critical amount, the interstices will become clogged and excess grains will begin to affect the framework. Similarly, if the coarse fraction is increased until coarse particles are in contact with each other over significant volumes of sediment, a secondary 'framework' may be formed which can also be stable.

These considerations have influenced the method of analysis of the grain-size distribution, especially in the choice of parameters used to characterise the sediment. In all cases grain diameters were transformed into phi-units [Krumbein, 1938]. The parameters which describe important features of the distribution are listed below. Note that with the possible exception of the grain-size mode, these parameters can in practice be defined uniquely for perfect log-normal distributions only, using parametric population statistics. Otherwise the parameters computed will vary according to the range and resolution of the analysis technique, and the method of computation.

Mode grain diameter: the diameter at which the grain size distribution curve forms a maximum. Some distributions also exhibit several lesser maxima or modes.

Mean grain diameter: a standard and widely used textural parameter which is not, in fact, particularly useful for assessing packing characteristics of a sediment. For log-normal distributions mean and mode grain diameters are identical. However, natural grain size distributions are generally only approximately log-normal.

Sorting: the standard deviation of the grain-size distribution, which is measures the spread of sizes around the mean. It can be related to packing characteristics of the sediment: for example, poorly sorted sands tend to exhibit lower porosities [Sohn and Morland, 1968].

Skewness: a measure of symmetry of the distribution around the mean which therefore indicates whether the bulk of the contribution to grain sorting is caused by finer or coarser sub-populations.

Fines content: defined as the weight-percentage of material finer than 63μm, which incorporates both silt and clay fractions. Silts and especially clays differ markedly from sands in their physical properties, due to electrochemically-derived cohesion between particles. Since it was thought that these properties might have an important effect on structural (and hence geophysical) characteristics of a sediment, the total proportion of fines was considered an important variable, irrespective of the size distribution. There were other powerful arguments for its treatment as a separate parameter: first its size distribution, where determined, was obtained by a radically different technique from that employed for the sand fraction which may have introduced systematic bias into the overall results; and second, because of the different mechanisms governing both source-weathering, transport and deposition processes, the fines population may be logically viewed as a separate entity.

Analysis techniques.

The procedure used to characterise the grain-size distribution depended on the sediment. Samples were first separated into sand-sized and silt- and clay- sized fractions, by wet-sieving through a 63μm screen. The sand fraction was dried at 105^0C before cooling under room conditions and weighing. If the fine fraction was less than 5% of the total sample, it was dried, cooled in a dessiccator and re-weighed. 5% was chosen as the threshold beyond which some information about the distribution of the fines fraction was required. The choice was not arbitrary: the 5% and 95% percentiles are required for computation of grain-size parameters by the Folk graphical method.

For samples containing more than 5% fines, standard pipette analysis was performed. The sample was diluted with 0.1% Calgon solution as a dispersant, placed in a 1000ml measuring cylinder in a water-bath at constant temperature, and thoroughly stirred. 20ml pipette withdrawals were then made at set time intervals, placed in accurately pre-weighed crucibles, then dried and re-weighed to four decimal places to obtain, on correction for the dispersant, a set of cumulative percentages finer than equivalent spherical diameters between 4 and 10 phi.

The sand-fraction was analysed using one of two available techniques:

(1) Dry-sieving to intervals of 0.25phi
(2) Analysis of grain settling velocity distribution using a Fall Tower.

Both techniques yield a curve representing the cumulative weight-percentage coarser than grain diameter in phi units. The basis of measurement in each case, however, is different: sieving involves separation on purely geometrical grounds while the Fall-tower method separates on the basis of settling velocity in a quiescent fluid. This is then related to an effective grain diameter of natural sands using an empirical relationship [Hallermaier, 1981]. The techniques are therefore identical (within experimental error) for sands in categories incorporated in the empirical curve-fitting, but may diverge for more complicated grain geometries such as shell-fragments. The empirical calibration is also limited to a size range between -1 and 3.75phi.

Dry-sieving was adopted for most of the sandy samples analysed. The reasoning behind this decision was threefold: first, the grain-size distribution was being investigated for its effect on the packing configuration of an *in situ* deposit, and therefore grain geometry was considered more important than hydrodynamic behaviour. Sieving analysis lent itself more naturally to this viewpoint, although volume geometries for complex grains cannot be completely characterised even by this method. Second, sediment could be assessed across the full range of grain-sizes from coarse gravels to the silt fraction. Third, the sample-sizes were larger for sieving analysis, resulting in a better bulk average. These arguments are specific to this study: more general criticism of the fall-tower technique is not implied.

The third point leads to the sand-fractions which could not be analysed by sieving because they were too small (less than 15g [Carver,1971]). In this case 5g sub-splits were processed using the 1.8m Fall-tower at UCNW. Since this applied to very few samples, the procedure will not be described further. A detailed account can be found in Larcombe [1991].

Sieving analysis was performed on 20 - 50g subsplits of the sand-fraction, separated using a motorised rotary splitter. Sample size was based on the

amount available, combined with two counterbalancing requirements: that the sample be as large as possible to provide a good bulk estimate and reduce the problem of splitting errors, but that it should not be so large that individual screens become clogged with sediment, obstructing the passage of finer grains [Rogers, 1959]. Dry-sieving was then performed using one or two stacks of ten to twelve screens selected to cover the full range of sizes present [Carver, 1971]. Care was taken to standardise the procedure by using the same operator, and the same screens and shaker settings. A final consideration was that wherever possible samples from individual experiments should be batch-processed to minimise within-location errors.

Preliminary Data Analysis.

A comprehensive FORTRAN grain-size analysis package was developed which combined raw sieve, pipette or fall-tower data and generated and analysed combined cumulative percentage - grain diameter curves. This package, in conjunction with a program for preliminary analysis of fall-tower data contributed by Larcombe [1990], has now been adopted as a standard for research and contract work in the sedimentology group. It has been revised recently to incorporate fine-particle analysis by Micromeritics Sedigraph, through an IBM-PC interface.

The combined and converted data-sets were processed according to the following procedure:

(1) A smooth curve was fitted through all the data points.
(2) For incompletely determined distributions, if required, this curve was extrapolated to 0% and/or 100%, assuming normally distributed tails, following the method suggested by Folk [1966].
(3) A weight-percentage frequency distribution was calculated by interpolation and differentiation at user-specified intervals along the cumulative curve.
(4) Two sets of grain-size parameters were then calculated based on the Folk graphical method (by interpolation of percentiles from the cumulative frequency curve), and the method of Moments Analysis from the frequency distribution. Grain-size mode was also calculated.

The choice of grain-size parameters was provided to satisfy preferences within the research group. Moments analysis [Dyer, 1986] represents the most sensitive and mathematically rigorous approximation to the grain size distribution statistics, but only within the limits of the analysis technique. Parameters are computed as summations using the mid-points of size-classes, rather than as integrals over a continuous distribution. For techniques such as the Fall-tower or Sedigraph these size-classes can be very small, providing good resolution of the grain-size curve. However, sieve and pipette data are determined at much more discrete intervals. A further limitation is that the interval of summation may not correspond to the full range of the distribution, which can severely affect the statistics, especially for higher order parameters.

Folk grain size parameters [Folk & Ward, 1957] were derived before the use of computers became widespread, and represent a graphical approximation based on the cumulative percentage curve. Five percentiles are interpolated from this curve, and used to compute population statistics. This results in some loss in sensitivity to small-scale variation between percentiles. However its major advantage is that the most extreme percentiles are 5% and 95%. Thus details of the distribution of coarse and fine tails are not required beyond these limits. This enables direct comparison of parameters obtained from a much wider range of textural characteristics than would be possible by applying moment statistics.

Folk parameters were selected for this study, mainly because of the last point. A range of sediments could be completely described without having to analyse small proportions of tail populations, or rely on extrapolation. This was considered to be more important than sensitivity to minor variations, which might only serve to enhance processing errors. In fact, more emphasis was generally placed on examination of the grain-size distribution than on computed statistical parameters.

Population Splitting.

Population splitting was performed on selected samples to provide insight into sedimentary packing configuration. As earlier indicated, structural variation was interpreted using a model based on the classification of

sub-populations defined by Moss [1972], although no physical basis for separating the populations is assumed. An interactive computer package enables selection of the log-normal 'framework' population (uniquely defined by its mode and standard deviation), then computes the remaining coarse and fine sub-populations. Clearly an infinite number of log-normal populations can be identified, with a range in standard deviations from zero up to a maximum depending on the distribution: this maximum was used as the selection criterion. Fig. 5.1.2. illustrates a typical three-component population split. This technique results in two truncated tail populations which are generally only very approximately log-normal.

In practice the technique, while extremely useful for exploring the grain-size distribution of a 'typical' distribution, was subject to a degree of uncertainty which made it less useful for comparison between sites. An apparently equally good fit to the data was possible using a small but relatively significant range of proportions of coarse and fine sub-populations, which introduced potential subjectivism into estimates of these proportions. This is a general criticism of the technique whether it is performed manually or by computer, and is unavoidable given the slight scatter inherent in all cumulative frequency curves.

For the vast majority of cases, where samples sediment consisted primarily of a uniform modal population, it was considered physically justifiable to characterise sub-populations by selecting appropriate 'cut-off' sizes, and dividing the grain size distribution between them. The percentage finer or coarser than a selected cut-off will incorporate some of the modal population for overlapping distributions, but will also be directly related to the sub-population fraction. This time-saving and arguably more objective approach has been illustrated and justified in the relevant parts of Sections 5.2 and 5.3.

Carbonate content [Black *et al*, 1965].

The weight-percentage of carbonate present in the grain-matrix was thought to be an important indicator of grain packing. In the deposits studied carbonate was primarily present in the form of shells or shell fragments of various sizes, which tend to be highly angular and platy in shape, and

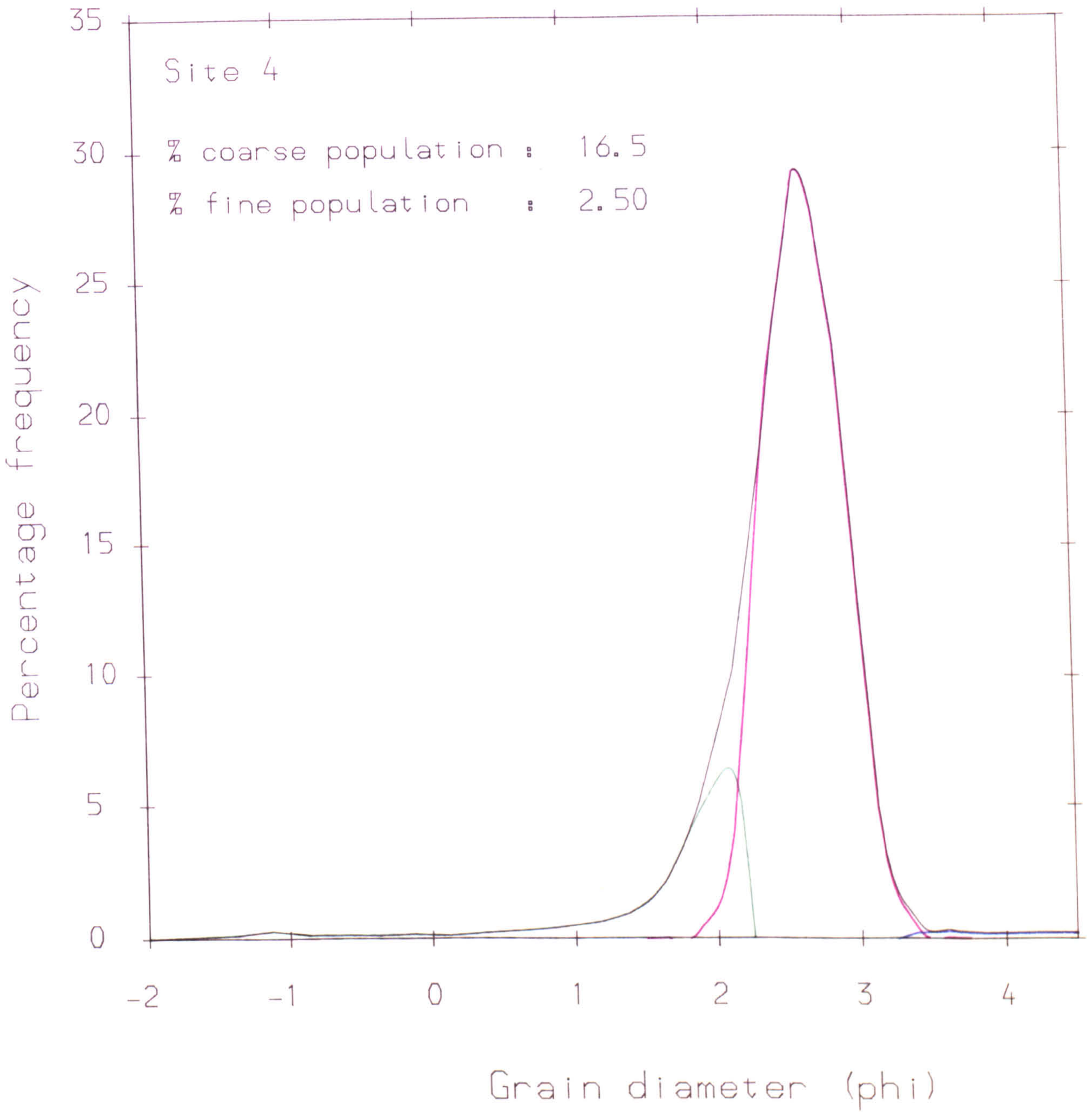

Fig. 5.1.2. 3-way population split into a lognormal framework population and truncated coarse and fine subpopulations.

therefore would be expected to affect the nature of packing of the framework grains.

Carbonate content was obtained by weighing a washed, dried sub-split of between 20 and 50g, then adding excess 10% HCl solution. The reaction was monitored over a period of 2-3 hours, adding more HCl as necessary, until it was observed to have stopped. The sample was then re-washed thoroughly before drying at 105^0C for 24hrs, cooling and re-weighing. Relatively large samples (compared to standard procedure) were used in an attempt to average over occasional whole shells or larger fragments.

Organic Content.

Samples for organics determination were always either washed and dried within 6 hrs of sampling or refrigerated to minimise any deterioration of organic material. Two approaches were adopted for analysis of the organics fraction, both involving the determination by oxidation of total organic matter.

Initially sediments which had been washed, dried and cooled in a desiccator were powdered in a pestle and mortar, then split into weighed subsamples of 10 - 20g. These were then treated with excess 30% Hydrogen Peroxide solution, warmed to 60^0C, and left for up to 24 hours until the reaction was seen to have stopped. The sample was then washed, dried, desiccator-cooled and weighed [Jackson, 1958]. This proved reasonably accurate for organic-rich muds, but was unsuccessful for sands, where weighing errors were of similar order to the organic content.

The second approach attempted to circumvent this problem by weighing much smaller samples to greater accuracy, this time based on a loss-on-ignition technique [e.g. Carver, 1971]. The washed, dried and powdered sample was split into 1-2g sub-samples. These were placed in pre-weighed crucibles, dried at 105^0C for 1 hour, desiccator-cooled and weighed. They were then heated in a muffle furnace at 480^0C for two hours, cooled in a desiccator and re-weighed to yield the total organic fraction. Four replicate sub-samples were processed per site.

5.1.3.3 Biological parameters.

As indicated in Section 5.1.2.3, most biological parameters were obtained from straightforward counts of surface features or burrows *in situ*. These counts were converted into number densities per m^2 using site area or length of exposed sediment along which burrows were counted.

The exception occurred during the study of seasonal variation in the Cefni estuary, where 3×100cm^3cores of sediment were removed to the laboratory for sieving and counting. The three organisms identified in sufficiently high quantities to be included in further analysis were *Corophium*, *Pygospio* and *Hydrobia*. Samples were washed through a set of 3 sieves, chosen rather arbitrarily at 710μm, 1400μm, and 2.36mm mesh size. Different mesh sizes were used because it was thought that the size of the organisms might be an important additional parameter to a simple head-count. However, this was subsequently realised to have been too ambitious given the small volumes of sediment characterised.

The numbers of organisms counted on the sieves could be readily converted into density per square metre by appropriate multiplication. It should be emphasised that, since the porosity sampler was 5cm in height these densities refer to a 1m^2, 5 cm thick surface layer. The number per unit area of surface was considered to be the most useful count, rather than the number per unit volume of sediment. Other parameters were also restricted to surface or near-surface layers, so vertical distribution of organisms within the surface layers was not investigated. Note that *Arenicola*, which resides at 15-20cm depth, is nevertheless able to affect the surface layer through its feeding and excretionary activity.

5.1.3.4 Box cores.

Box-cores were removed to the laboratory and prepared by one of two impregnation techniques:

(1) *Resin impregnation.* A 0.5cm deep layer was removed from the exposed sediment surface leaving a 1cm border all around the core. The core was then dried for several days at room temperature, then in an oven for 24hrs

at 100°C, and cooled. Approximately 300mls of a 10 to 1 mixture of resin and hardener [Ciba-Geigy Araldite MY753, hardener HY951] was then poured into the prepared core. After leaving for at least two days to cure, the hardened part was marked, removed from the box and inverted. Loose sand was then brushed off to expose the sedimentary structures delineated by differential rate of resin penetration.

(2) *Lacquer impregnation*. Much finer structures could generally be preserved using a thinned lacquer, although the underlying principle of differential penetration remains the same. The final core is also much more fragile. The opened box-core was dried gradually as before, then gauze was placed as a backing onto the exposed surface and fixed by spraying with a very dilute mixture of lacquer and thinner [Sigma Profielvernis CL33, thinner CL105]. Around 300mls of a (2:1) mixture was then prepared and gradually and evenly painted onto the wetted gauze. Once application had been completed, the core was left for a fortnight before careful loosening, inversion and brushing.

5.1.3.5. S-wave velocity.

Conversion of raw signals to representative values of V_s presented some interpretation difficulties. Ideally, the application of digital signal processing techniques (such as cross-correlation) would have enabled accurate, fast and automatic data analysis. Unfortunately the Sonic Viewer, which was the only available instrument suitable for field use, does not have a digital storage facility. Processing therefore relied on individual 'picking' of appropriate trace features on records.

Preliminary data preparation.

Preliminary data preparation involved obtaining a set of (usually three) trace-feature arrival times for each probe separation. As already indicated in Section 5.1.2.3, these were generally measured directly on site. However, where paper records were taken another opportunity to measure arrival-times arose, as well as to assess the form of the pulse envelope and signal quality.

In order to present some of the raw data obtained during the study, and to illustrate the procedural steps involved in processing it, a selection of paper records has been presented in Fig. 5.1.3. These represent the full range of propagation characteristics obtained. To improve accuracy, measurement of arrival times was made on enlarged photocopies of the original records. Distortion by the photocopier was found to be negligible within an A4 window with enlargement of 140%.

Velocity calculation: single transmitter emplacement.

For the purposes of illustration, the records presented in Fig 5.1.3 (b) & (c) have been worked through. Table 5.1.2 lists arrival times for onset, first maximum and first minimum for each of the two cases, and the measured probe-tip separations. It is clear that a series of velocity calculations is possible:

(1) A set of four velocities calculated from <u>true</u> probe separation and onset arrival times only. These represent direct measurement from source to receiver, and are calculated from:

$$V_0^0 = \frac{s_i + s_{off}}{t_i^0} \qquad (5.1.14)$$

This method has the advantage of monitoring the full volume of sediment traversed by the S-wave disturbance, which is important in media containing vertical heterogeneity (see Chapter 3). However, as will be discussed in more detail in Section 5.1.4.4, it can incur higher errors, due to the difficulty in accurately locating the pulse onset (especially over higher separations) and to uncertainty in the offset separation.

(2) A set of velocities calculated from the difference between two arrival times of identical trace features, at different probe separations:

$$V_{ij}^k = \frac{(s_i - s_j)(1 - \delta_{ij})}{t_i^k - t_j^k} \qquad (5.1.15)$$

where k indicates trace feature; i,j indicate receiver position; s is the

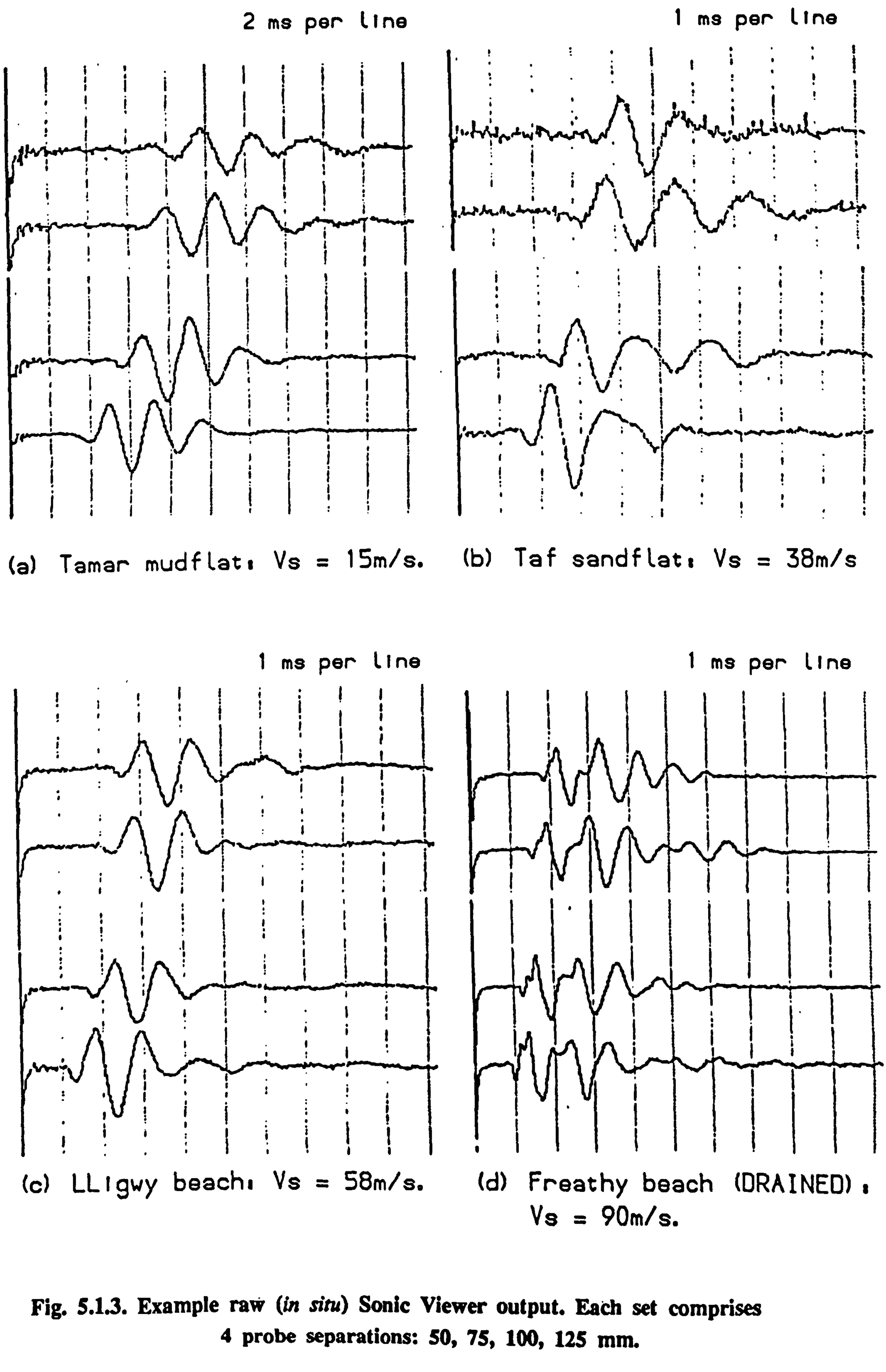

Fig. 5.1.3. Example raw (*in situ*) Sonic Viewer output. Each set comprises 4 probe separations: 50, 75, 100, 125 mm.

Table 5.1.2. Measured arrival times for records illustrated in Fig. 5.13.

TAF ESTUARY (T/11):S1 [Fig. 5.1.3(b)]				
i	s_i(mm)	t_i^k (ms) k: (0)	(1)	(2)
1	50	1.52	2.26	2.78
2	75	2.17	2.96	3.57
3	100	2.87	3.83	4.52
4	125	3.35	4.22	4.87

TRAETH LLIGWY(A) S3 [Fig. 5.1.3(c)]				
i	s_i(mm)	t_i^k (ms) k: (0)	(1)	(2)
1	50	1.09	1.70	2.17
2	75	1.52	2.13	2.61
3	100	1.91	2.61	3.13
4	125	2.44	3.13	3.61

Table 5.1.3. Velocity calculations: single transmitter emplacement.

TAF ESTUARY (T/11):S1 [Fig. 5.1.4(a)]							
Trace feature	k	V_{ij}^k (i:j) (ms^{-1}) (1:4)	(1:2)	(2:3)	(3:4)	(1:3)	(2:4)
Onset	0	41.1	38.3	35.9	52.3	37.1	42.6
1st Max	1	38.3	35.9	28.9	63.9	31.9	39.7
1st Min	2	35.9	31.9	26.1	71.9	28.8	38.3
		V_{0j}^0 (0:j) (ms^{-1}) (0:1)	(0:2)	(0:3)	(0:4)		
		39.4	39.1	38.3	40.3		

TRAETH LLIGWY (A):S3 [Fig. 5.1.4(b)]							
Trace feature	k	V_{ij}^k (i:j) (ms^{-1}) (1:4)	(1:2)	(2:3)	(3:4)	(1:3)	(2:4)
Onset	0	55.9	57.8	64.2	48.1	60.8	55.0
1st Max	1	52.5	57.8	52.5	48.1	55.0	50.2
1st Min	2	52.5	57.8	48.1	52.5	52.5	50.2
		V_{0j}^0 (0:j) (ms^{-1}) (0:1)	(0:2)	(0:3)	(0:4)		
		55.4	56.1	57.8	55.7		

separation (mm); t is the arrival time (ms); V is the velocity (m/s). The subtractions involved effectively remove systematic error in the offset determination and enable arrival times for trace-features other than the signal onset to be used. They do, however, limit the range of sediment monitored to that between the two receiver positions, which can also increase the importance of separation error. This will be discussed more fully in Section 5.1.4.

(3) A set of three velocities calculated from simple linear regression of measured arrival times against probe separation for each trace feature. Regression was performed using a standard NAG-library FORTRAN subroutine [NAG, 1985], which also generates standard errors. The significance of the regression coefficient (b_r^k) was tested: where the result is significant at the 99% level a set of 95% confidence limits was generated. If these confidence limits represented a range of less than +/- 15% of b_r^k, the regression velocity was calculated, along with the separation intercept.

The reason for this final condition is that if velocity could only be determined to within more than 15%, the arrival-time/probe separation relationship was assumed to be non-linear, and the sediment heterogeneous. One of the problems incurred in regression calculations was the small number of probe separations used. Whereas up to 12 receiver positions were monitored in the laboratory, a maximum of four was thought to be feasible *in situ* given the need to characterise as many sites as possible. At these low degrees of freedom, even highly significant regression coefficients may still incur large confidence limits.

In order to illustrate these velocity calculations, data from Table 5.1.2have been processed. Results have been tabulated in Table 5.1.3 and graphically presented in Fig. 5.1.4.

The original objective was to use the regression velocity, since it averages over all probe separations measured. However, two problems limited its effectiveness. First, its calculation ignores sediment traversed by the pulse before arriving at the nearest receiver position, which is important in layered deposits. Second, small-scale heterogeneity leads to high 95% confidence limits. Perhaps understandably, a high proportion of the data did not yield a useful regression velocity.

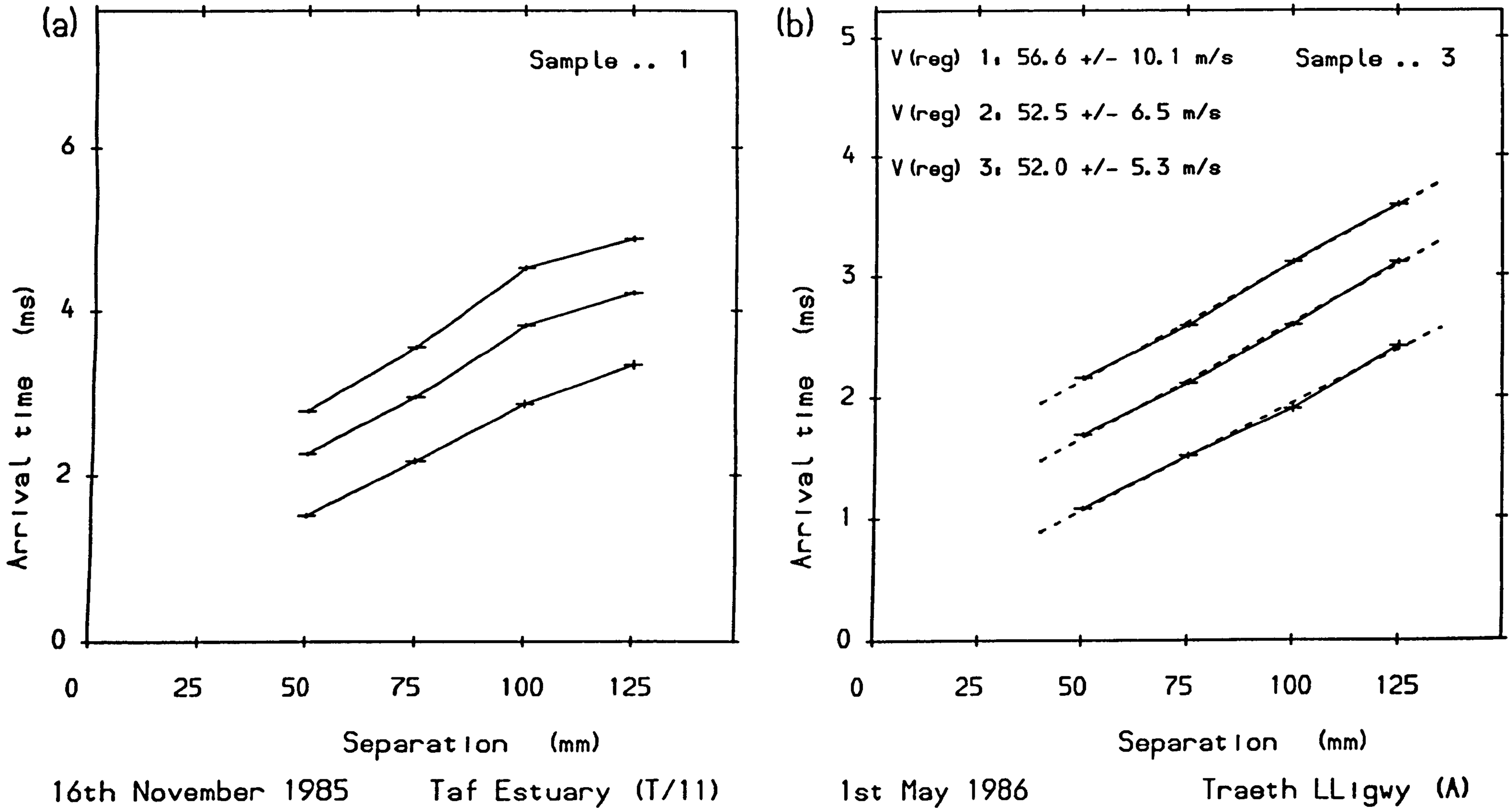

Fig. 5.1.4. Example arrival-time/probe separation plots (Table 5.1.2).

The first problem can only be solved by using a velocity calculated from the onset and true probe separation. The shortest probe separation was selected, first because errors were found to be least in this case, and second because this represents the velocity of the shallowest 'effective surface layer' that can be characterised using this data. This velocity was defined as Surface V_s (V^0_{01}). It represents the 'effective' velocity of a surficial layer approximately 40mm in depth (Chapter 3). The main drawbacks to this parameter are its reliance on an empirically determined true probe separation, and on pulse onset measurements which were not always easy to determine.

It was decided that the rather high errors associated with small differences in probe separation limited the effectiveness of most of the remaining set of velocity calculations. In other words, the technique was not accurate enough to resolve genuine heterogeneity over scales monitored by less than 50mm separation increments. For this reason, only velocities calculated from the two probe separations which were furthest apart (V^k_{14}) were selected, since errors were lowest for this measurement. This was defined as bulk V_s, which corresponds to an effective velocity of a sub-surface layer between 40 and 80mm.

Fortunately, a further simplification was possible in cases where bulk and surface parameters were not found to be significantly different, indicating that the upper layers were reasonably homogeneous. In these cases the better reliability of the 'bulk' velocity dictated its selection in preference to the 'surface' calculation.

As with the grain-size analysis, inclusion of the computer-generated output for all the sites monitored was not felt to be appropriate. All raw and processed data has been stored at UCNW for future reference. In the meantime, further analysis and discussion has concentrated on the two S-wave parameters defined above as Surface V_s and Bulk V_s.

Calculation of site-mean velocities.

At least two sets of measurements were made at each site throughout the study. The simple averaging employed for all other parameters is not

applicable in this case because velocity is calculated from a number of different measurements, each of which is subject to error. A set of measurements from the Cefni estuary has been worked through and presented as an illustration. Fig. 5.1.5 illustrates the raw signals. At each site, the full set of arrival-times can be averaged in two ways:

Method I: As replicate sets of arrival times, each set encompassing all four receiver positions for one transmitter emplacement.

Method II: As sets of replicate arrival times, each set corresponding to a different transmitter-receiver separation.

The difference between the two approaches becomes clear when averaging is performed. In the first case, velocities calculated independently from the replicate sets of arrival-time/separation data are averaged. In the second case, the arrival times are averaged first, then the velocity is obtained from these averages.

Therefore before calculating site-mean values for V_s, it had to be decided which method to adopt. For surface V_s (and all V^{o}_{oi}), a similar argument to that used for the regression calculation (Chapter 3) can be employed, since arrival time is the 'dependent' variable, with the separation fixed (within experimental error). Therefore averaging over arrival-time, rather than velocity, is more appropriate (Method II). Site-mean regression velocity is also calculated by combining all arrival times.

For bulk V_s (and all V^{k}_{ij}), the situation is rather more complicated. Method I provides, in theory, a clearer picture of genuine variability between the independent sets of measurements, and is perhaps therefore a better measure of spatial variability between separate 125mm sections of the site. However, if measured variability is mostly due to sampling error, this is compounded in the subtraction process. In contrast, Method II averages over any sampling error before performing the subtraction. It could therefore be argued that this method provides a better approximation to the site mean.

The issue is further complicated by the fact that a separate average must be performed for each trace-feature when adopting Method II. In general, V_s calculated using pulse onsets tended to be slightly higher than that

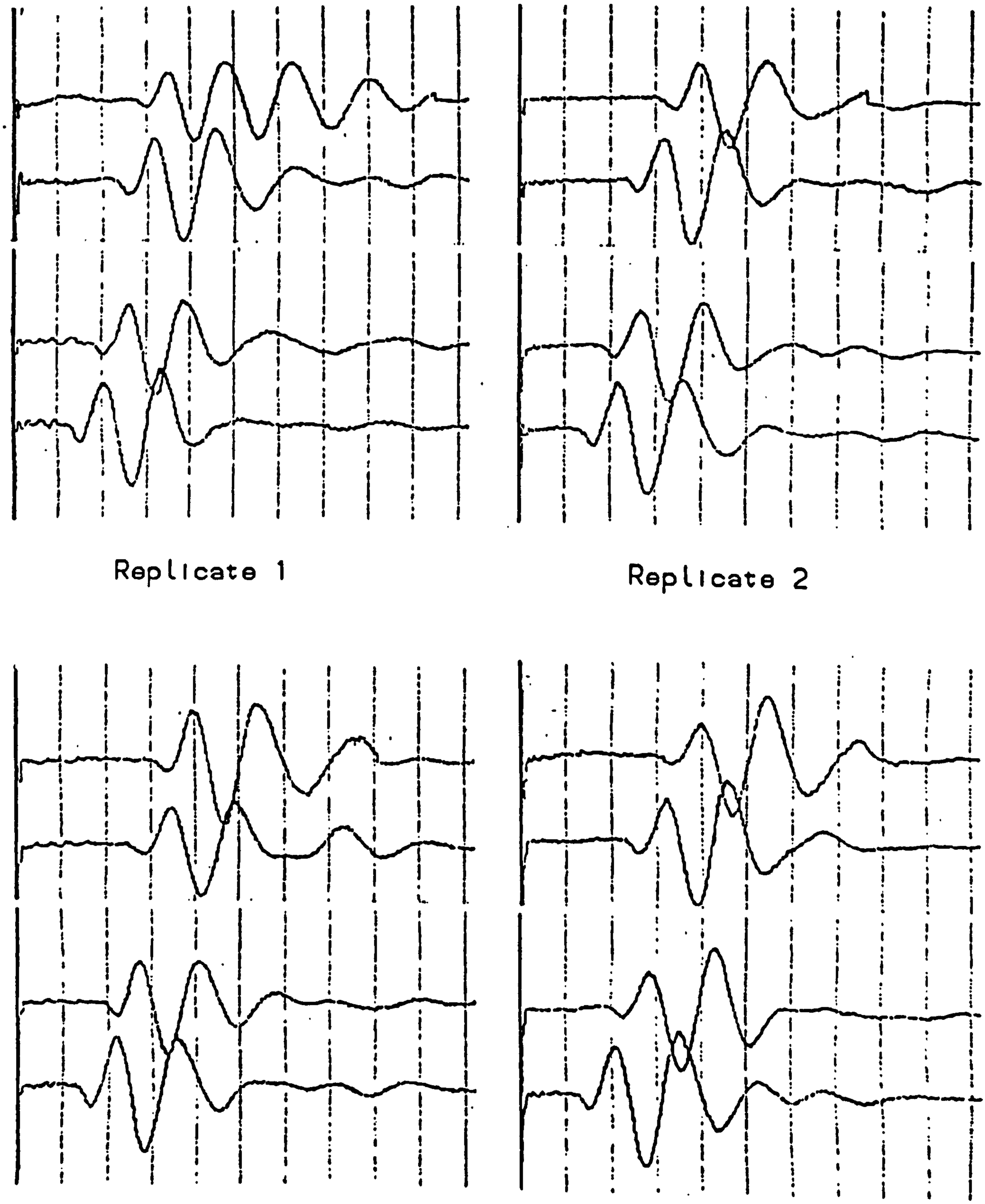

Fig. 5.1.5. Example within-site replicates. Cefni Estuary Site 1, Jan '87. 4 probe separations: 50, 75, 100, 125 mm.

using later trace features. Two factors affecting high separation signals may have contributed to this (Chapter 3): 'onset broadening' may result in overestimation for the onset calculation, and increased attenuation of higher frequency components may result in underestimation for that using later trace-features. Fortunately, a consistent and statistically significant difference was only measured at Traeth Llanddwyn, where the maximum probe separations were much higher. This influenced the decision to reduce the separation range for later experiments.

In contrast, because they are calculated before averaging for Method I, velocities from all trace features can be included. This can help to improve the accuracy of the calculated mean, provided that errors are random.

Fig. 5.1.6 illustrates data from Fig. 5.1.5, with site-mean regression velocities. Table 5.1.4 lists other site-mean velocities. All possible separation combinations have been included for illustrative purposes: bulk V_s corresponds to V^k_{14}; surface V_s corresponds to V^0_{01}. It is clear from this table that a very wide range can be obtained by the subtraction technique of velocity calculation (V^k_{ij}), especially for receiver positions only 25mm apart. A smaller range is obtained for V^0_{0i}, because only one separation is involved, thus halving the random error contribution. However, uncertainty in the 'true' separation adds additional systematic error in this case. Note that the intercepts of the regression calculation lie within the range 10±5mm used for calculation of surface V_s.

As expected, and despite the larger data-set involved, the Method I average yields generally higher variation. In fact, velocities calculated from previously averaged arrival times (Method II) exhibited the lowest coefficients of variation in the vast majority of cases. This indicates that much of the variability in individual velocity calculations was due to sampling error. Note that in this particular case there is not much difference between the two methods for bulk V_s, since separation errors are less important for increasing receiver-pair separation.

It should be emphasised that despite the differences in coefficients of variation, the means calculated by both methods were nearly always statistically equivalent. This fortunately removed much of the

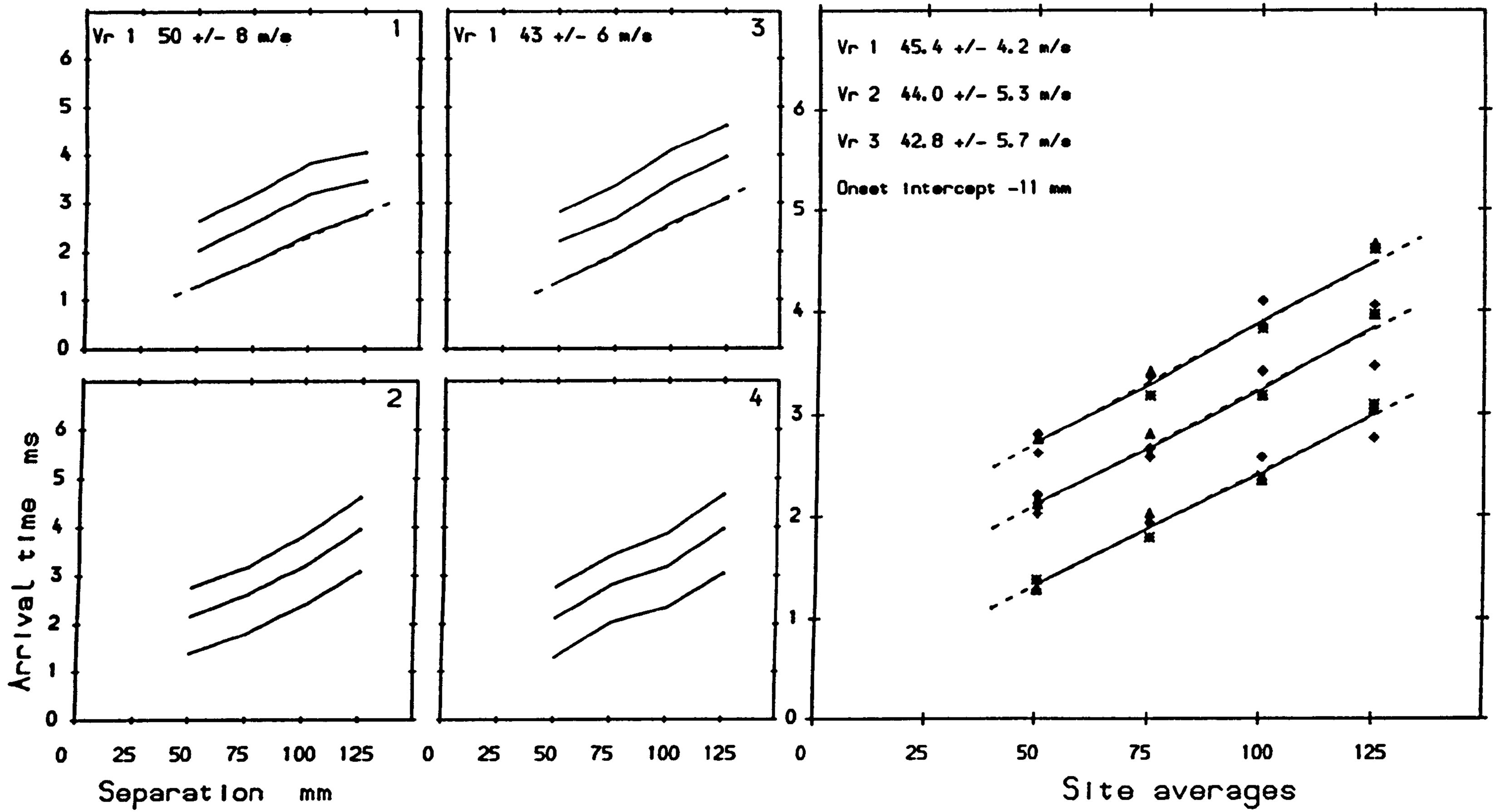

Fig. 5.1.6. Example time/probe-separation plots: individual and combined within-site replicates (from Fig. 5.1.5).

Table 5.1.4. Sample site-mean velocity calculations. Cefni Estuary, Site 1, January 1987.

SITE AVERAGES: (σ = standard deviation: ms^{-1})

V_{ij}^{k} $(i:j)$ (ms^{-1})

Method	(1:4)	σ	(1:2)	σ	(2:3)	σ	(3:4)	σ	(1:3)	σ	(2:4)	σ
I	44.5	5	47.3	9	46.5	14	50.2	25	45.0	3	44.4	8
II Onset	45.2	4	45.2	5	47.2	5	43.4	4	46.2	4	45.2	5
Max:1	44.0	4	46.2	3	44.3	3	41.7	4	45.2	3	43.0	3
Min:1	43.1	4	46.2	3	40.2	3	43.4	4	43.0	3	41.7	3
	0:1	σ	0:2	σ	0:3	σ	0:4	σ				
	44.9	2	45.0	2	45.5	3	45.1	2				

TABLE 5.1.5. Summary of error estimates.

PARAMETER	MEAN SAMPLING ERROR (actual)	(%)	RANGE IN SAMPLING ERROR (actual)	(%)
Porosity		2.0		0 - 8.1
Mode grain size	0.03		0.00 - 0.13	
Mean grain size	0.05		0.02 - 0.10	
Sorting	0.05		0.00 - 0.12	
Skewness	0.10		0.04 - 0.14	
%Fines	0.4	20	0.0 - 2.7	0 - 50
%Carbonate		5 - 14		4 - 14
%Organics	0.06	14		9 - 43
Macrofauna:				
Corophium		~50		10 - 60
Hydrobia		~20		10 - 40
Pygospio		~20		13 - 70
Surface V_s		7.4		1 - 22
Bulk V_s		7.7		1.6 - 20
FF:				
within-location		5.3		0.2 - 15
absolute		>10?		

apprehension about which averaging procedure to adopt for bulk V_s determination. In practice, decision was left until the results of each method could be compared. Provided that no significant differences were observed between different calculations, the method which resulted in the smallest coefficient of variation in any particular case was selected. This is reasonable, since genuine within-site spatial variability will form a constant 'core' of any standard deviation calculated, while additional variation must be due to sampling error.

5.1.3.6. Electrical Formation Factor

Processing of the electrical measurements was relatively straightforward. Sediment resistance, R_s, was converted into FF by dividing by the pore fluid resistance, R_w (eqn. 5.1.1.2), which was obtained either by direct measurement *in situ* using the beach probe, or by iteration of conductivity (σ_w) from measured pore fluid salinity and temperature using the empirical relationship described in 4.2.3. R_w was obtained from σ_w using the following relationship:

$$R_w = \frac{1}{2\pi a \sigma_w} \qquad (5.1.23)$$

Simple averaging was then performed to obtain site-means and coefficients of variation of FF for further analysis.

5.1.4. Errors : Sampling, processing and natural variance.

It would not be acceptable to quote a single value for a given site parameter without some indication of its within-site variability. Errors associated with instrumentation resolution, or operator and handling errors are inherent in every experimental technique. However, the variance associated with each site mean has two independent sources: sampling or processing error and natural within-site spatial heterogeneity.

It is possible in many cases to estimate experimental error (discounting operator error) from an understanding of the measurement technique. It is

also possible to measure overall within-site variability by performing a series of replicate measurements and calculating the coefficient of variation. In general, however, it is impossible to reliably separate genuine spatial heterogeneity from experimental error. Thus, wherever a within-site variability or 'error' is quoted, it should be remembered that this includes both sample processing error and natural spatial heterogeneity within the sampled site.

This section considers likely sources of experimental error for the variables measured during the study, provides estimates of magnitude where possible, and describes treatment of within-site variation of these properties. Measured properties fell into two categories: those whose estimated within-site variability was considered sufficiently large to warrant several replicate measurements at each site, and those where only a single measurement was made per site in general, but at least once during the study some replication was performed. Table 5.1.5 summarises estimated errors, obtained from measured within-site variability and from other published work, as discussed in the following sub-sections. Where only two replicates per site were processed, errors are expressed as a range (Δ), rather than as a standard deviation (σ).

The first category contains Vs, FF, sediment porosity and organics fraction, the number of replicates in each case being decided by balancing the need for accurate determination of the site mean against time constraints. In these cases, random sampling error can be estimated from coefficients of variation calculated from within-site replicates. This incorporates small-scale heterogeneity in addition to measurement error, and therefore represents an upper bound estimate. Systematic error has been considered separately. The second category contains the grain-size parameters, carbonate and fines content and macrofaunal counts.

5.1.4.1. Sediment porosity.

Porosity determination involves two predominant sources of error: that associated with obtaining an accurate core of sediment under field conditions, and uncertainty in mean granular density. The first represents random error and is therefore incorporated into measured within-site

variability. The second reflects uncertainty in precise composition of the sediment. The samples under consideration were split into quartz, carbonate and clay mineral constituents, which removed much of the potential error in grain density determination (eqn. 5.1.6).

5.1.4.2 Textural parameters.

Restrictions on sample processing effort inhibited replication of textural parameters, with the result that within-site textural heterogeneity could not generally be determined. At various times during the study, different textural parameters were replicated at sampling sites, but these results cannot necessarily be extrapolated to include all locations. Also, the decision to take small numbers of replicates, repeated at each site, was realised in retrospect to have been flawed. Were this study to be extended, sampling strategy would be modified to include intensive replication within one or two sampling sites at each location, to provide a more rigorous statistical estimate of within-site variability.

Grain size parameters.

The errors involved in grain-size analysis comprise sampling error (introduced in this case via within-site heterogeneity), preparation and splitting errors, systematic errors introduced by the analysis technique, and processing errors.

The degree of within-site variability should be sensitive to composition of the sediment, depositional environment and bioturbation. Within-site duplication was performed once during the study: the grain size distributions have been illustrated in Fig. 5.1.7. It is clear that between-site variation is significantly greater than within-site variation: mean grain size and sorting vary by 0.01 - 0.05phi at individual sites. A further indication of sampling error can be obtained by considering within-location variability, although this obviously may also include localised spatial heterogeneity. The minimum within-location variabilities obtained were: 0.02phi (mode grain size); 0.03phi (mean grain size); 0.02phi (sorting); 0.07phi (skewness).

Fig. 5.1.7. FREATHY SANDS. Duplicate grain size distributions: 5 sites.

Since they have been calculated from separately processed samples, the errors quoted above must incorporate all random experimental errors. A comparison of error contributions [Jago, 1974] found that sampling error was greater than splitting and processing errors, but smaller than variation between closely spaced sampling stations. Errors associated with the UCNW Fall-Tower have been investigated by several colleagues: Larcombe [1991] suggests 0.01-0.08 phi for mean, 0.02-0.09 phi for sorting, 0.08-1.05 for skewness. The sieving technique has been widely investigated: assuming the same operator and apparatus, processing errors of 0.05phi for both Folk mean and sorting are generally quoted [e.g. Griffiths, 1953]. An additional check performed during this study was on consistency between different batches, since comparisons had to be made between parameters characterised at different times during a three year period. Separate sub-splits of the same sample were sieved during three separate batches, yielding a range in mean grain size of 0.03phi, in sorting of 0.02phi.

Systematic error may also be introduced by any particular analysis technique. A gratifying confirmation of the reliability of dry-sieving procedure was obtained when results for two sampling locations in the Taf estuary in 1985 were compared with samples collected from the same locations and processed at Imperial College in 1969 [Jago, 1980]. Location means for grain-size mode were found to be 2.90 (1969), 2.88 (1985) at location T/8 and 3.01 (1969), 3.04 (1985) at T/11.

A comparison between sieve and fall-tower techniques was also performed, on separate sub-splits of the same sample. Very well-sorted fine sands, with around 13% carbonate content, were analysed. Since the Fall-tower is calibrated using median sieve diameter, the techniques should correspond closely for well-rounded particles. Fig. 5.1.8 compares grain-size mode and the Folk parameters obtained using the two methods.

It is clear that, while no consistent difference was found for mode, sieving results in a significantly (but not greatly) coarser, poorer sorted grain-size distribution. The coarse fraction probably contains more angular grains such as shell fragments, which may be hydraulically compatible with finer but more rounded grains, but which become trapped on coarser sieves because of their complex geometry. Thus the Fall-tower

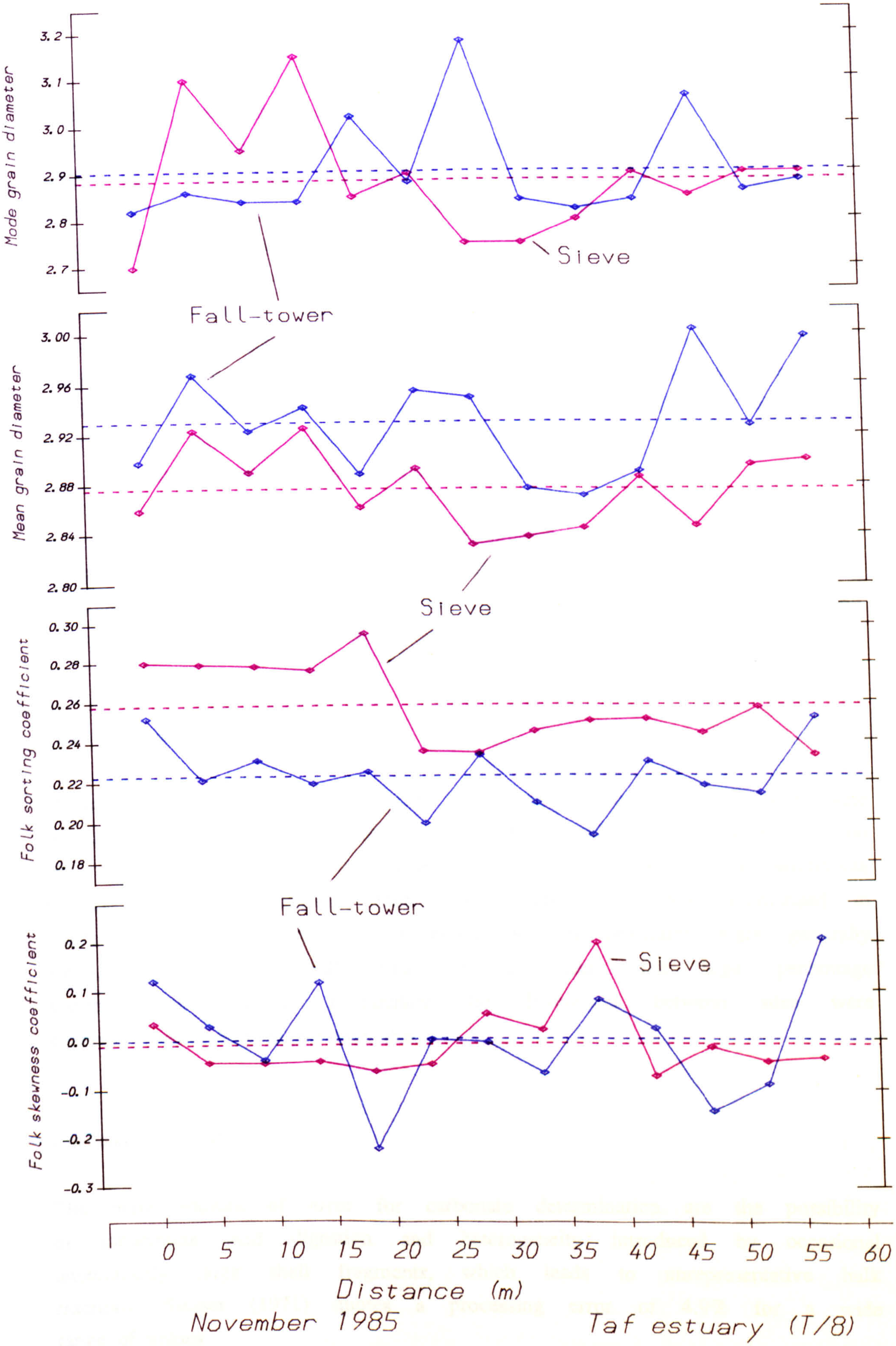

Fig. 5.1.8. Comparison between Sieve and Fall-tower techniques.

mimics a hydrodynamic sorting process, whereas sieving separates out different grain geometries. The sieved results were thought to be more useful for interpreting packing characteristics. Skewness was not significantly different, but this may reflect the higher sensitivity of this parameter to processing errors.

A final consideration was errors introduced via the method of data analysis. The Folk graphical method has been used throughout this study. Significant differences can be obtained using moments analysis, especially for incompletely determined distributions. The moments method is also more sensitive to fine-scale differences between samples, especially in the tails, which may be real or experimentally induced.

In conclusion, errors in grain-size determination are small enough to be negligible for comparison of bulk grain-size parameters between sampling locations. However, differences between sites at some locations were found to be approaching the limits of reliable resolution.

Fines Content.

Processing errors for fines content are mainly associated with incomplete wet-sieving. Site-duplicate fines content determination was performed on two occasions, in order to assess the combined effect of within-site heterogeneity and processing error. The results have been summarised in Table 5.1.5. While absolute differences between replicates were generally small, the equally small mean values meant that high percentage variability is obtained. Fortunately the differences between sites were generally considerably higher than this.

Carbonate content.

The main sources of error for carbonate determination are the possibility of incomplete acid digestion and heterogeneity introduced by occasional anomalously large shell fragments, which leads to unrepresentative bulk fractions. Siesser (1971) quotes a processing error of 4.9% for a wide range of values.

Within-site heterogeneity was thought to be potentially significant for carbonate content, especially at sites where large fragments or whole shells were present (vertical heterogeneity, for example the presence of thin shell laminae within the core samples, was not investigated). Carbonate content determination was performed on duplicates from each site at six locations (Table 5.1.5). Three exhibited an average within-site range comparable to the processing error quoted by Siesser. However, three showed much higher within-site variation, over a range of carbonate content, indicating significant small-scale spatial heterogeneity.

Organics content.

Two methods of organics determination were employed during the study. No standards were processed, nor were samples replicated in different batches. Thus both systematic and random processing error may have been introduced. Wet-oxidation by H_2O_2 was performed on site-duplicate samples. The main sources of error were probably weighing error, and difficulty in gauging when the reaction had stopped. In contrast, loss-on-ignition was performed on four replicate subsplits from one sample per site. In this case, the main sources of error were probably associated with powdering and splitting.

Table 5.1.5 combines results from both methods. As for fines content, errors represent high percentages of the (small) organic fraction.

5.1.4.3 Biological parameters.

The errors involved in counting organisms are specific to each organism. Within-site spatial heterogeneity does not contribute error when an overall number density per site is counted (*Arenicola* and *Lanice*), although there is obviously small-scale patchiness of organisms within each site. This patchiness will affect densities calculated from disturbed or sieved sub-samples (*Corophium*, *Pygospio* and *Hydrobia*). A set of four replicate samples was taken during the seasonal study in the Cefni Estuary to assess this error: ranges from a survey by Raffaelli and Milne [1986] have also been summarised in Table 5.1.5. Measured percentage coefficients

of variation were: 50% (*Corophium*); 20% (*Hydrobia*); 13% (*Arenicola*).

It should be noted that the method employed for *Arenicola* counting provides a measure of organism activity rather than number density, since it ignores any dormant organisms. This may in fact be a more important parameter, since the surface layers would only be affected by an active organism. In contrast, the techniques for *Lanice*, *Hydrobia* and *Pygospio* monitor organism tubes or shells, whether or not a live organism is present within. In this case, it can be argued that the physical manifestations of the organism would be expected to affect sediment properties, even if it is not itself active.

It is clear that very large errors are associated with biological characteristics, due to natural spatial heterogeneity. In particular, the quantitative parameters obtained by multiplying counts from sub-samples must be regarded as of limited value.

5.1.4.4. S-wave velocity.

Errors in V_s can be split into those associated with arrival-time determination and those associated with probe-separation measurement. For all field measurements, time-resolution of the oscilloscope was ±0.01ms. Enlarged paper records enabled measurement by ruler to within 0.25mm, which represented a similar time-resolution. This value represents the minimum possible error associated with arrival-time measurement. A further error is associated with 'picking error', or that associated with recognition of a 'true' trace-feature arrival time. This varies according to the trace-feature, and the frequency (and hence velocity) of the received signals. In particular, signal onsets were subject to highest uncertainty, and in some cases could not be determined at all. The error is also a function of signal quality, and therefore is highest at high probe separation, in sediments exhibiting high attenuation, and where wind or wave-noise is present.

Probe tip separation could be measured to within 1mm. The receiver, once in place, could be gently vibrated in the plane of insertion until an 'exact' separation was obtained. An additional error must be incorporated

to allow for inadvertent rotation of the transducer in the plane of propagation. The maximum angle off the vertical was estimated at 3°, after adjustment by eye using the vertical probe handles. This introduces a further offset of ±1mm in the position of the mid-point of the transducer plate. Thus probe separation was accurate to within 2mm.

These errors are all random, so within-site replication enables an upper bound estimate of their magnitude. Table 5.1.5 summarises estimated errors and measured mean within-site variability. Note that calculation of surface V_s also involves an error in the offset used to calculate true probe separation (Chapter 3). The chief source of this error is uncertainty in its measurement in the laboratory, therefore it represents a systematic bias which probably remained constant throughout the study.

5.1.4.3. Formation Factor.

The primary sources of error in FF determination can be separated into those affecting electrical resistance measurements and those affecting determination of the pore-fluid resistance.

Sediment resistance errors:

In contrast to the V_s measurement procedure, the electrodes were rigidly mounted on a frame, thereby removing all random separation errors. Any error due to manufacturing tolerance of the electrode array was negligible compared to the other sources of error. Equally, the instrumentation resolution was less than 0.1% over the range of environments monitored.

The only source of random sampling error is the variation in depth of insertion of the electrode tips. Strictly they should be adjusted so that only the tips of the electrodes are in contact with the sediment, since the theory assumes point current-sources (Chapter 4). However, especially on uneven surfaces, this introduces variation into the relative separation of the electrodes. In practice an adjustment was made at each location to allow for broad differences in load-bearing capacity of the surrounding sediment, so that when supported by the frame the electrodes were just in

contact with the sediment surface. This setting was then retained throughout sampling at that location, which resulted in some problems in rippled or bioturbated deposits. The effect on measured sediment resistance of non-point electrodes at non-zero penetration depths and an irregular boundary was beyond simple modelling techniques, but could be assumed to be second-order, incorporated into within-site heterogeneity.

The reasoning behind this decision was twofold: first, it saved time and enabled a greater number of replicates to be made per site, and second any variability measured by the technique was then known to have been introduced by spatial heterogeneity rather than by the instrumentation. This spatial heterogeneity includes variation in both sediment packing and surface topography.

Pore fluid resistance errors:

Measurement of pore-fluid resistance proved problematic, as indicated by the succession of techniques employed. Instrumentation errors, in all cases, were probably less important than the uncertainty in whether what was being measured was a representative sample of the pore-fluid (for salinity and temperature measurements they contribute an estimated 1.5% error). Further errors could be introduced by surface water run-off, suspended fine material, or pore fluid/sediment boundary effects.

Fortunately, however, errors in pore-fluid resistance contribute largely systematic errors to the FF measurement. This has been shown by reasonable stability of measurements over space and time at different locations, and by the good reproducibility of the one set of replicates taken, as summarised in Table 5.1.6. Thus FF measurements made within locations, and perhaps especially within sites, characterise genuine structural heterogeneity rather than random experimental error.

Therefore errors in FF measurement are important only when comparing results from different locations. The magnitude of this error is not known, but may be significant.

Table 5.1.6. Errors in pore-fluid resistance (R_w) determination.

Site replicates. Malltraeth Site 3 July.				
	n	Mean R_w	σ	σ(%)
	3	1.209	0.02	2.0
Location Replicates.				
Location	*n*	Mean R_w	σ	σ(%)
Taf T/11	3	2.88	0.06	2.2
" T/8	2	2.19	0.01	1.0
LLigwy A	2	0.441	0.02	3.5
" B	4	0.413	0.004	1.0
Freathy	5	0.374	0.004	1.0

5.1.5 Statistical treatment of data.

The large number of variables involved in site characterisation necessitated some careful statistical handling. Preliminary data manipulation and averaging has been dealt with in Section 5.1.3. This was performed in order to obtain as good an estimate of the site-mean of each parameter as possible, incorporating both random and systematic experimental error and within-site spatial heterogeneity. In order to simplify the analysis as much as possible, most subsequent data handling was performed on these site-means, while bearing in mind the associated variability.

The particular combination of statistical analysis procedures applied at different stages of the study varied according to the variables measured and the nature of the experiment, and will be described in the relevant sub-sections in 5.2 and 5.3. In this section the techniques employed have been introduced and discussed, in a logical progression following the order in which they were generally applied. The major source of reference for this section was Sokal and Rohlf, 1981.

All quantitative data was placed on computer file, in matrix format, on the UCNW VAX cluster. Rows of the matrix represented individual sites,

columns represented the different parameters measured. The first two columns were reserved for site and sampling-date descriptors.

In this form, the data could be manipulated, transformed and processed using the statistical software package MINITAB [Ryan, 1981]. Analysis techniques have been defined and discussed below. The choice of technique was often dictated by whether a parametric test was valid in any particular case. A statistic is defined as 'parametric' where it represents an estimate for the population from which sampling was performed, and therefore involves assumptions about the distribution of that population. In contrast, a 'sample statistic' makes no assumptions about the parent population. The term 'parameter' should strictly apply only to population statistics, but has been applied rather more loosely to all quantified properties in this study.

5.1.5.1 Single variable statistics.

Site-means of each variable were first averaged to obtain the location mean, within-location variance also being obtained. No assumptions have yet been made about their distribution: these parameters are therefore sample statistics rather than population estimates. In order to compare the relative sensitivity of properties, this variance was converted into a coefficient of variation. The distribution of each variable around its location mean was then tested for normality using MINITAB.

5.1.5.2. Analysis of variance.

Analysis of variance identifies significant differences in the sample means of two or more populations. It was applied in a variety of instances throughout preliminary data exploration and subsequent analysis:

(1) To identify significant differences between textural, biological or geophysical properties at different locations, and hence to infer potential interactions between these properties.
(2) To compare temporally varying properties at different sites in the seasonal study (Section 5.3).

(3) To compare S-wave velocities calculated using different probe separations or different trace-features at any one location.
(4) To compare the within-site variability (expressed as coefficients of variation) of different properties.

Two different tests were used, depending on whether the assumptions underlying the parametric test were valid. These are that the variable is normally distributed and that the different populations are homoscedastic, (i.e their variances are the same). The latter assumption was tested by examining the ratio of highest and lowest variances according to a method proposed by Sokal and Rolf [1969]. Where these assumptions were valid to 1% significance, one-way parametric analysis of variance was performed. Where these assumptions did not hold, the non-parametric Kruskal-Wallis test was adopted.

5.1.5.3 Bivariate statistics: Correlation analysis.

Once significant variation of a sub-set of two or more properties has been established, the logical next step is to identify any covariation between the properties. Potential 'cause and effect' relationships or interactions between properties can then be investigated. The obvious technique to apply for randomly sampled, naturally varying properties is that of correlation.

Two different correlation techniques were employed, once again depending on whether the assumptions underlying the parametric test were valid. The generally used parametric test calculates a 'Product-Moments' correlation coefficient normally attributed to Pearson. This is applicable only where each of the variables is normally distributed. Most of the properties involved in this study fell into this category. However, a further draw-back to the product-moments coefficient is that it measures only the *linear* component of any co-variation.

A correlation coefficient which, first, makes no assumptions about the distribution of the variables, and, second, tests for a general degree of association, rather than a linear relationship, is the Spearman coefficient of ranked correlation. This involves assigning integer ranks

to each of the pairs, then performing correlation on these ranks. It was preferred to the similar Kendal coefficient because it assigns greater weight to widely-spaced pairs of ranks, hence is more appropriate when sampling error leads to uncertainty about the order of close ranks.

Since it was considered desirable to test for general relationships between variables, the Spearman coefficient was calculated for all non-trivial pairs. In addition, a product-moments coefficient was obtained for those variables which behaved normally as a specific test for a linear relationship.

For sample sizes (m) greater than ten, which applied to nearly all the cases under consideration, the two coefficients are referenced to the same table of critical values, and hence can be directly compared. Significance was tested at the 5% level: however, the critical correlation coefficient had to be fixed at a higher level than 5%. This is because where several variables have been measured there is additional possibility of randomly obtaining a high correlation coefficient between any pair. For example, if 100 correlations are calculated using completely independent random data, then 5 of these will have correlation coefficients greater than the 5% significance level. To allow for this the Bonferroni technique was applied: where nc correlation coefficients are being considered, they should be greater than the critical value at the $(5/nc)$% significance level to ensure significance at 5%.

For some of the observed correlations, an immediate causal inference can be made, linking change in one of the variables to independently controlled change in the other. Alternatively, the two variables may be seen to be related due to their dependence on a 'common cause', in the form of another variable, or on some additional uncharacterised environmental control.

However, especially when discussing correlations found for different pairs of textural and biological characteristics, it must be assumed that the causal links between the variables may be very complex. For example, where the number of organisms is correlated with a textural parameter this may be caused by substrate preference on the part of the organism, by the effect of its activity on the sediment fabric, or by a common dependence

of both variables on one or more additional controls (for example, the hydrodynamic environment).

Significant correlation coefficients have been tabulated, presented and referred to under the relevant discussion sections in 5.2, 5.3 and 5.4. Ranked correlation coefficients were selected where the parametric test was invalid, or where the ranked coefficient was very much higher than the Pearson value, indicating a significant but *non-linear* co-variation.

Where significant correlations were identified, scatterplots were produced to illustrate the form of covariation. It should be emphasised that, in most cases, a high degree of scatter was obtained. This was due to two factors: first, the probability that at least one of the variables was dependent on additional, independently varying parameters and second, the fact that measurement and sampling errors were relatively high when compared to the maximum range of many of the properties under investigation. It should also be stressed that while serving to indicate possible relationships the observed correlations have no quantitative predictive relevance. Thus where straight lines (based on the related technique of linear regression) have been superimposed on scatterplots in sections 5.2-5.4 it is purely to illustrate the significant trend. No suggestion that predictive equations can be generated is implied.

5.1.5.4 Multivariate statistics: Multiple regression analysis.

Where an intuitively reasonable causal link can be argued between a clearly defined *dependent* and *predictor* variable, the coefficient of determination (R^2) can be calculated by squaring the correlation coefficient. In some cases R^2 can be improved by adding in the effect of other, independently controlled variables using the technique of multiple linear regression, although the nature of the data-set demanded caution both in application of the technique and in interpretation of the results.

Multiple linear regression calculates the partial regression coefficients b_i for a set of n_p predictor variables P_i, such that the 'dependent' variable u is given by:

$$u = b_0 + \sum_{i=1}^{n_p} b_i P_i \qquad (5.1.28)$$

Note that for simple linear regression, $n_p = 1$. The partial regression coefficient is interpreted as the effect of variation of one predictor while all others are held constant. The standard errors of these coefficients can also be calculated (and hence an estimate of their statistical significance). R^2 then represents the total percentage of variation in u explained by variation in the n_p predictor variables.

There are several assumptions and limitations of this technique. First, the property u should be clearly identifiable as 'dependent' on the other parameters. In other words it should not itself affect any of the predictor variables. This important point immediately limits the number of variables which can be analysed to the geophysical properties, porosity, and under certain circumstances bulk textural parameters. The remaining textural and biological characteristics were generally found to be highly interrelated, within a complex framework of direct and indirect causal relationships.

The second assumption of the multiple linear regression technique is that the predictor variables should be independent. In other words, they should not be significantly correlated with each other. If two or more predictors are correlated, only the independent contribution of each can be calculated. For high degrees of correlation, this leads to high standard errors in the partial regression coefficients, rendering the results meaningless.

The third assumption is that predictor variables have been independently varied under experimental control, rather than randomly sampled from natural populations. The only cases where this could be said to hold were those where sites were chosen deliberately because they contained different densities of a particular organism, or where different locations were sampled because of their obviously different textural properties. This assumption is required because only the dependent variable is treated as statistically variable. Joliffe [1986] states that errors are permitted for the independent variables, so long as the variances are all the same.

This was certainly not generally the case for this study. A final limitation of the technique is that only the linear components of partial dependence are calculated.

The problem of treatment of cases not satisfying this requirement has been solved for linear regression of bivariate normal distributions, but not generally for multivariate normally distributed predictors. Strictly, generalised multiple regression techniques should be employed if the object is to produce statistically rigorous predictive equations for these cases. Since the application of such predictive equations would in any case be extremely limited, it was felt that such time-consuming and complicated techniques were unnecessary.

Incidentally, Sokal+Rohlf [1981] state that published cases abound of the incorrect application of multiple linear regression in the construction of predictive equations. They also emphasise, however, that provided that its limitations are borne in mind, and that 'extreme caution' is exercised in forming conclusions, especially in quoting or using such equations, there is nothing fundamentally wrong in applying the technique.

For the data under consideration in this study, these assumptions and limitations all give cause for concern. However, they all tend, at least generally, to *underestimate* the significance, and effect, of the predictor variables, with important consequences. Since all that was required was an indication of which variables significantly affected the dependent variable, whether the effect was direct or inverse, and an estimate of the coefficient of determination, this was not too serious a limitation. Provided that the extent of interdependence between two or more predictor variables is known, that interdependence, and its likely effect, can be taken into account when interpreting the results. As far as the problem of statistical variability of predictors is concerned, this will introduce bias into the magnitude of partial regression coefficients, but will not change their sign.

The possibility of non-linear relationships was not addressed, mainly to simplify analysis procedures. It was felt that since, in most cases, the range in variables was relatively small, and the scatter due to error fairly large, most of any significant dependence could be approximated as

linear. This was also justified considering that only the sign, rather than the magnitude or mathematical formula, of any significant partial relationship was of interest.

Multiple regression analysis was therefore performed routinely on porosity, FF and V_s, to test for direct dependence on potential predictors. It was also applied to investigate the carbonate content of the grain size subpopulations and the dependence of bulk grain size statistics on proportion of these subpopulations. Two routines from the MINITAB package were utilised. First, the optimum combination of predictors for a particular dependent variable was selected by calculating R^2 for different combinations of an increasing number of selected properties, and adjusting this coefficient according to the number of variables used. The optimum combination arises when this adjusted coefficient is a maximum. Second, multiple linear regression was performed on this optimum combination, or on several similarly promising combinations, to establish whether partial regression coefficients were statistically significant to the 5% level.

For all combinations which did yield significant partial regression coefficients, the overall coefficient of determination (R^2) and the signs of those partial coefficients were tabulated. This includes single predictors, where R^2 can also be obtained from the computed correlation coefficient (although strictly, correlation should not be applied to dependent variables since there is an *a priori* implied causal link). In a few cases, the ranked correlation coefficient yielded a much higher R^2 than was obtained by linear regression: this indicates a non-linear relationship, and has been noted where relevant.

5.2. LOCAL SPATIAL VARIABILITY AND ASSOCIATED TEXTURAL AND BIOLOGICAL CONTROLS.

5.2.0.1 Introduction.

As previously stated in Section 5.1.1, results from the study of geophysical properties of intertidal sedimentary deposits will be presented in three separate sections. The first two cover findings from individual experiments, while the third draws together results from these and expands the scope of the investigation.

Individual experiments, based on the investigation of localised spatial variation in sediment properties in a variety of intertidal environments, are dealt with first. These experiments were planned with two objectives: first to establish the degree of variability over medium length-scales and secondly to exploit any such variability in furthering the investigation of biological and textural controls on geophysical properties.

The hypothesis proposed to describe localised geophysical variability relies on the assumption that geophysical properties are related to structural properties of the sediment. These in turn are known to be affected by textural composition, depositional environment, and post-depositional processes such as bioturbation and consolidation, although precise and universal empirical or theoretical relationships remain elusive. Most *in situ* studies to date have concentrated on the large scale effect of wide ranges in bulk textural parameters on mean geophysical properties. This is extremely useful for establishing broad or FIRST ORDER relationships with bulk parameters such as mean grain size or porosity [e.g. Hamilton, 1976], but must include a large amount of scatter due to additional SECOND ORDER controls which cannot adequately be described using a single bulk sediment characteristic.

The difference in the experiments performed during this study is that first order textural variation has been deliberately minimised, in order to investigate more specific factors. As will be shown, textural

properties at the different locations could in almost all cases be characterised as a high proportion of essentially uniform sand comprising the bulk sediment framework population, with second order variation introduced via varying proportions (or composition) of coarse or fine sub-populations. It seems reasonable to assume that the structural, and hence geophysical, properties of the sediment would be primarily controlled by these bulk framework properties and general hydrodynamic environment, which were uniform within the locations monitored. In addition, but to a lesser extent, they should be sensitive to second order textural variation, to site specific hydrodynamic controls, and to the presence and activity of benthic organisms. Fig. 5.2.1 illustrates the proposed network of controls on sediment properties.

It should be emphasised that this hypothesis, which has been formulated and tested for clean sands and sands containing at most 10% fines, is not intended to apply to fine-grained cohesive sediments. Depositional environment and biological activity will play a much more important role in determining packing configuration of cohesive sediments, because the sediment fabric is less dependent on the packing, and hence physical properties, of individual grains.

Data gathered from each intertidal location during this study have been analysed and interpreted in terms of this hypothesis. Textural characteristics were first investigated, and relevant *first* and *second* order parameters identified. The objective was to identify and characterise a uniform framework component of the sediment, and as many additional components as were necessary to fully describe observed variation. The localised variability of all selected parameters was then examined. This can be defined parametrically for normal distributions as the location coefficient of variation (5.1.3): however, for less well behaved variables this represents only an approximate quantitative assessment. Finally, statistical analysis was performed to test for relationships between textural and biological characteristics and the geophysical properties as proposed in Fig. 5.2.1. The appropriate analysis techniques have been described in 5.1.5.

With the exception of some preliminary discussion of localised variability

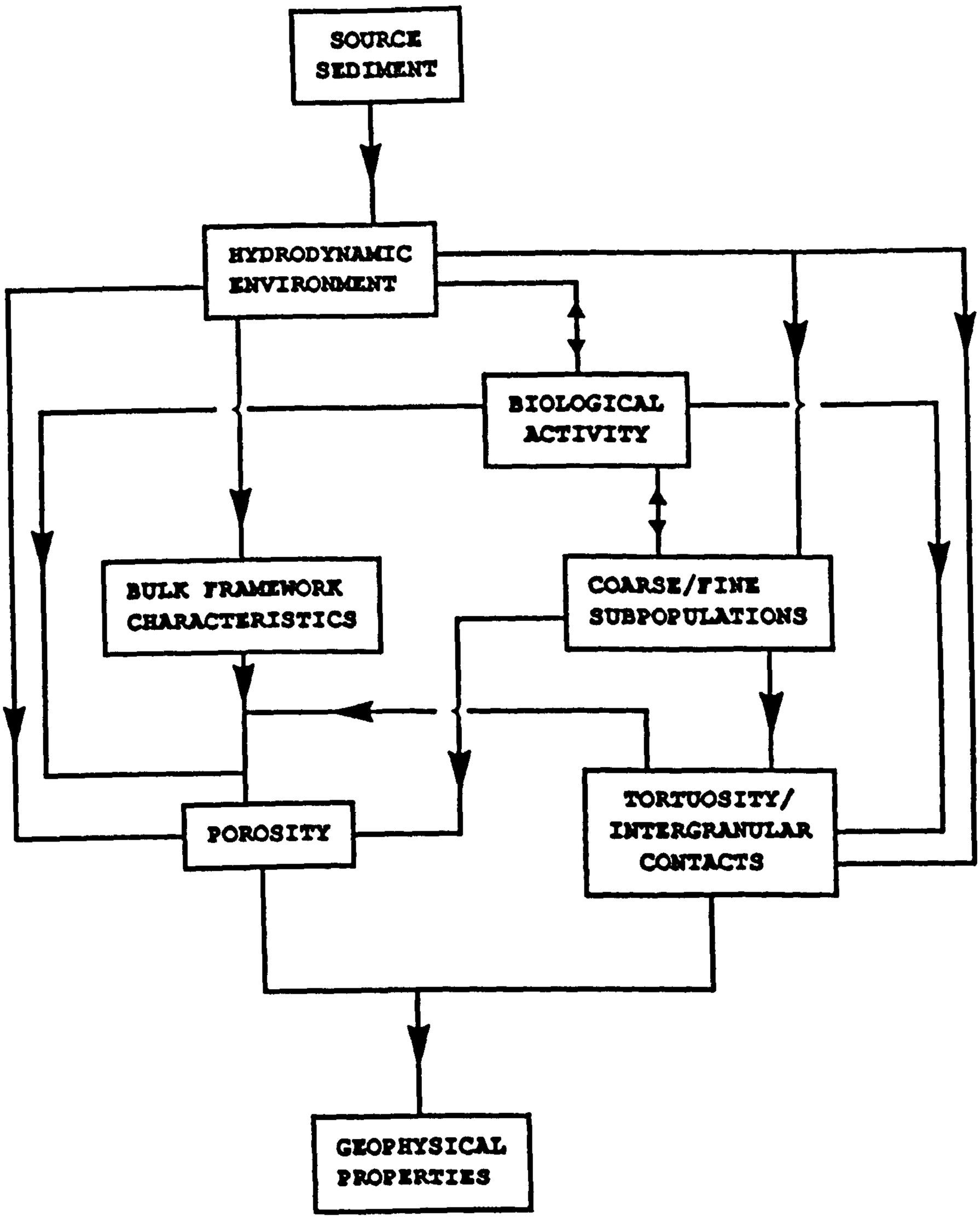

Fig. 5.2.1. Interacting network of controls on structural properties of sand.

in the following sub-section, the results from each experiment have been presented separately, in chronological order. The order of presentation and discussion reflects the aforementioned objectives, dealing with selection of important site characteristics, localised variability, and finally their interrelationships. Graphs designed to illustrate both the nature of the data and important interrelationships have been placed within the text, while additional graphs and tables intended for more detailed reference have been placed in Appendix B.

5.2.0.2. Relative variability of textural, biological and geophysical parameters.

The hypothesis proposed for interpretation of localised variability in sands can be tested by examining the relative variability of different measured properties. At each location, the grain size distribution was split into an invariant bulk framework population, and one or more secondary sub-populations. Thus the framework mode grain diameter should, by definition, be the least variable parameter. Mean grain diameter is controlled primarily by the bulk of the grain size distribution, so it should also be relatively uniform. It will, however, be affected to second order by localised variation in the coarse and fine sub-populations, so it should be more variable than the mode. Sorting is highly sensitive to the tails of the grain size distribution, and therefore should be considerably more variable. The variation in proportion or composition of the sub-populations should be by far the most variable textural parameters, since they have effectively been selected on that basis. Finally, since sites were usually selected specifically to include a wide range of organism density, the biological characteristics should be the most variable of all.

Sediment porosity is known to be sensitive to textural composition of sands (Chapter 1). Therefore this parameter should also be primarily influenced by the uniform framework properties, with second-order variability introduced via differences in the sub-populations. Note that it is variation in grain shape and size distribution, rather than actual size, which controls porosity. In addition, porosity should be sensitive

to variation in localised hydrodynamic environment (which may affect both deposition rate and post-depositional consolidation) and biological activity. For sands this represents an additional, but still probably secondary source of variation, so porosity should be more variable than mode grain size, but less variable than the sub-population properties and biological characteristics.

Geophysical properties can be accommodated by considering potential controls. For a given textural composition, FF is known to be directly related to porosity. Using similar arguments, it should also therefore be influenced primarily by the bulk framework characteristics, with second order variability introduced via textural and biological controls on porosity. In addition, variation could be introduced through textural and biological controls on the tortuosity of the pore-space, which may be considerably more important than their effect on porosity.

For V_s, the dominant control is the number and strength of intergranular contacts. Thus, once again, it should be primarily influenced by bulk framework properties of the sediment. For a given sediment, porosity is known to be a control, so that variability of V_s should be at least as great as that of porosity. Moreover, as for FF, additional sensitivity to textural and biological characteristics is hypothesised, in this case due to the effect on intergranular contact forces of variation in textural composition, burrowing and biological secretions.

Therefore both FF and V_s should be more variable than porosity, but less variable than the sub-population properties and biological parameters. Fig. 5.2.2 illustrates means and ranges of percentage coefficients of localised variation for parameters monitored at all eight sandy locations. These have been separately summarised in Table A1.2. Naturally some degree of error is involved in relating calculated coefficients of variation to variability, but several consistent patterns emerge.

The figure illustrates the expected trend in textural and biological parameters, with generally low variability in porosity and the geophysical parameters indicating that they are primarily influenced by properties of the uniform bulk of the sediment. Some further generalisations can also be

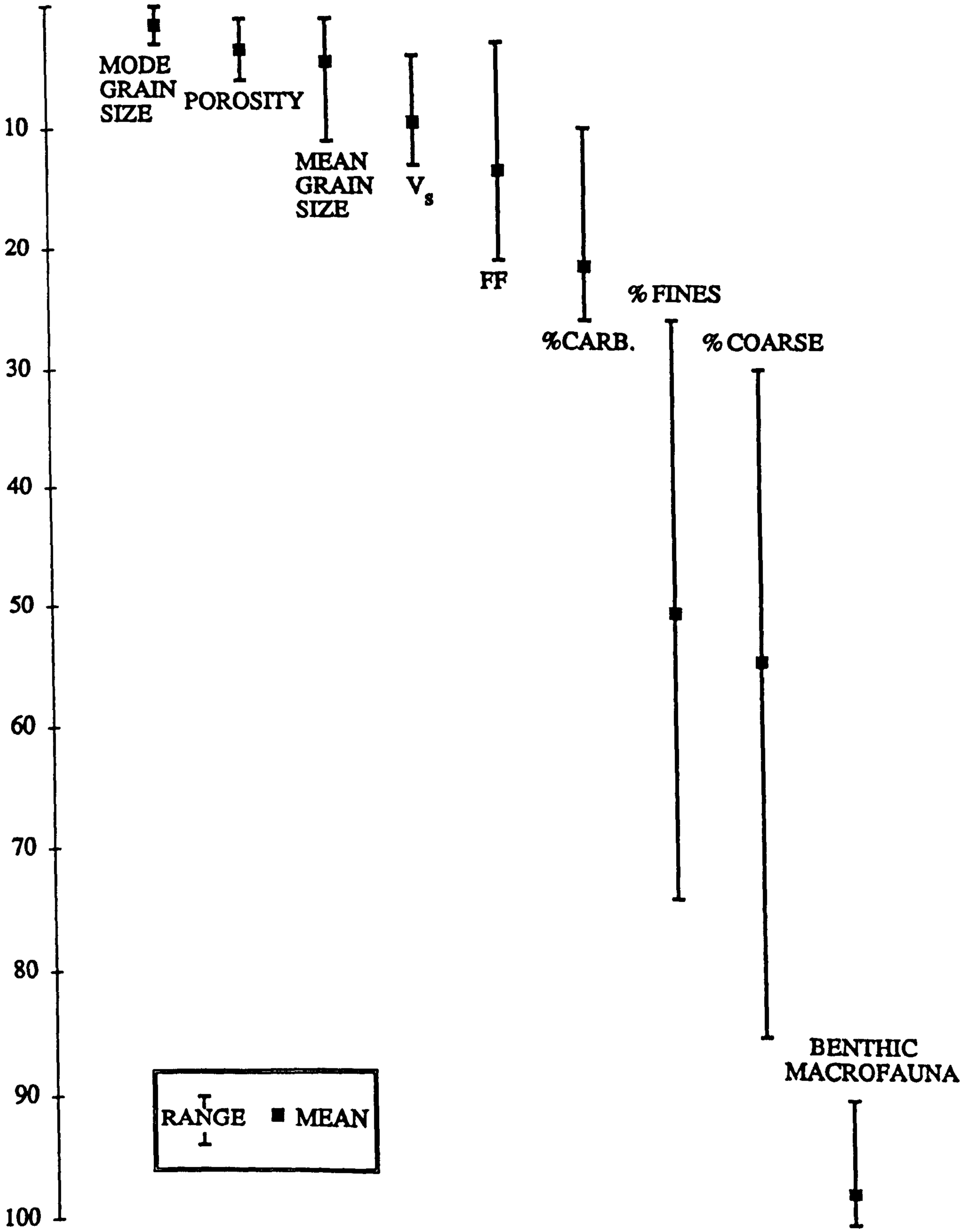

Fig. 5.2.2. Summary of relative localised variability of parameters.

stated based on relative variability at individual locations. Macrofaunal density was always the most variable parameter, followed by parameters characterising the coarse and fine subpopulations. As will be shown, carbonate content was generally partially associated with the variable coarse subpopulation, although a significant proportion could also be associated with the uniform framework population, which explains its intermediate variability. FF and V_s were always more variable than porosity. Variability in mean grain size was always less than all other textural parameters except mode, and was always either less than or similar to FF and V_s.

Further generalisation, regarding the relative variability of porosity and mean grain size, or of FF and V_s, was not possible since different results were obtained at each location. It should be noted that variability in porosity was always particularly low, indicating rather less sensitivity to strong localised variability in biological activity than expected. This will be discussed further during the following sections.

5.2.0.3. Selected benthic macrofauna: salient physiological and behavioural characteristics.

There were three criteria for selection of suitable benthic macrofaunal species: they should be common in intertidal deposits around the British Isles; they should be sensitive to localised environmental control so that a high degree of variability in number density can be monitored; and they should exhibit contrasting feeding and burrowing behaviour. Three species were selected using these criteria, to cover a range of possible effects on sediment structure. A brief description of each organism follows, along with a summary of these effects.

Arenicola marina.

Arenicola marina, the common lug-worm, is a large polychaete worm found in great abundance in the intertidal zone, both on beaches and on estuarine

sandflats. Fig. 5.2.3. illustrates the structure of a 'typical' U-shaped burrow, and summarises the important features of feeding activity [Wells, 1945]. *Arenicola* is categorised as a non-selective deposit feeder; that is, it indiscriminately ingests particles from the head-shaft, digests attached organic matter and excretes a characteristic coiled faecal cast at the top of the tail-shaft [Plate 2]. While the tide is in, oxygenated water is pumped in at the tail-shaft for respiration. This is then driven into the sediment in the head-shaft, causing liquefaction and settlement, which ensures that a fresh supply from the surface is maintained. This 'conveyor-belt' system allows the adult organism to remain in one place throughout its life, with continual replenishment of surficial organic material from microbiological regeneration and hydrodynamic processes.

Arenicola exhibits preference for sandy substrates with mean grain size between -0.2 and 3.65 phi [Wolff, 1973]. The size limits are imposed by mode of feeding and burrowing: coarse sands are too large for ingestion (and contain less organic material than an equivalent volume of finer sediment), while fine-grained sediments are unsuitable for maintaining burrow structure. It is tolerant to the wide range in salinity and temperature encountered in intertidal and estuarine environments, mainly because it resides at a depth of *c.* 150mm, and is therefore buffered from extremes of variation.

The effect of *Arenicola* activity on textural, structural and biological characteristics of the sediment is understandably significant. Several workers have studied the generation of biogenic graded bedding, or heterogeneous grain size distributions within the sediment, caused by rejection of coarse particles and shell fragments at the base of the head-shaft [Van Straaten, 1954; Cadee, 1976, 1979]. Although the organism is apparently incapable of 'sensing' the size of particle which it is about to swallow, it is nevertheless unable to either manipulate or ingest large particles, and fine grains are more likely to adhere firmly to the papillae of its proboscis [Baumfalk, 1979].

Arenicola secretes mucopolysaccharides, which line burrow walls and coat faecal casts, and which will affect intergranular adhesion and friction. It is also capable of altering bed roughness by generation of protruding

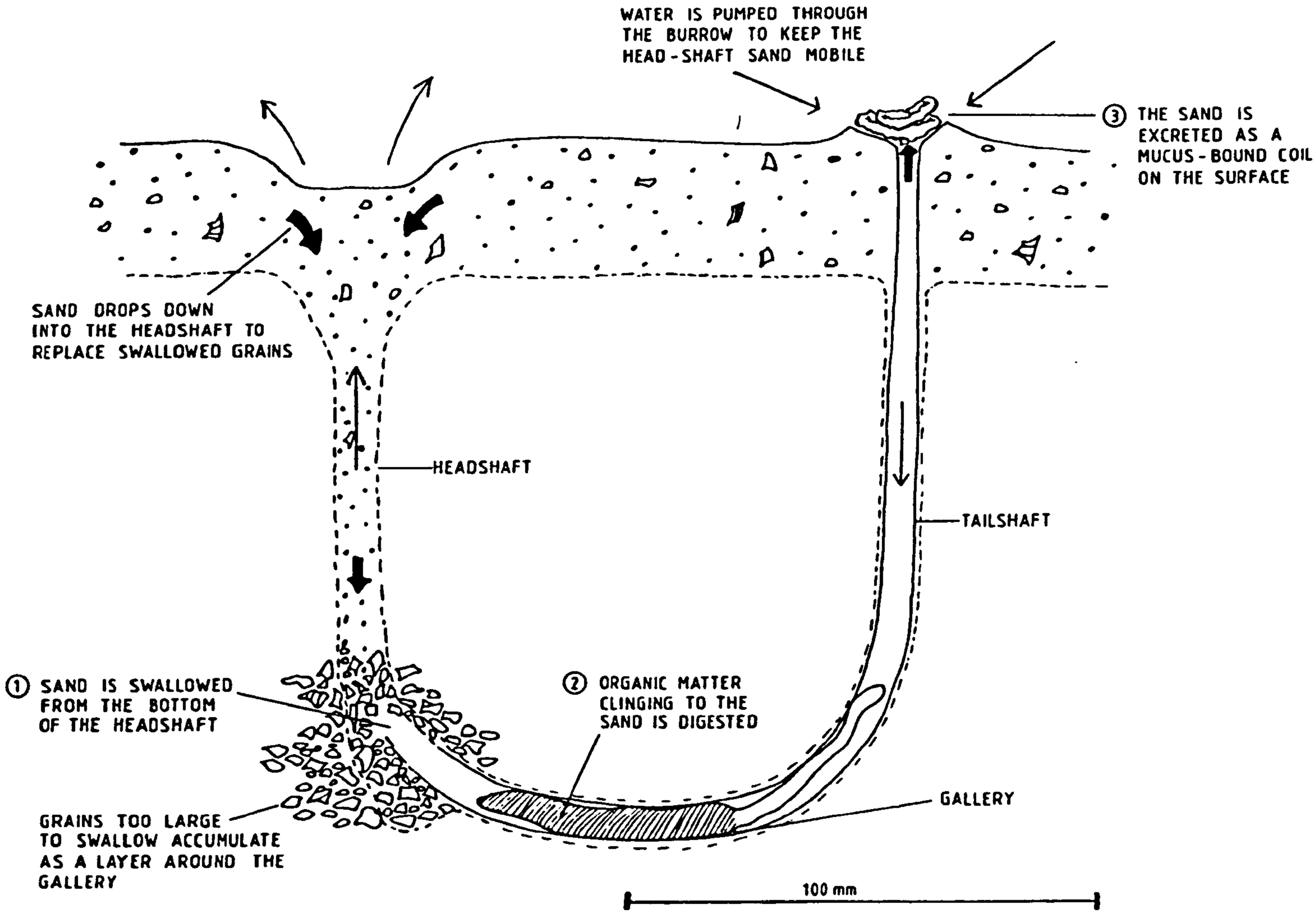

Fig. 5.2.3. Bioturbation by Arenicola Marina.

faecal casts containing finer sediment. This may enhance erosion, thus removing processed material from the vicinity of the head-shaft.

Finally, *Arenicola* affects microbiological processes within the sediment by irrigating its burrow with oxygenated water and sorting organic rich particles from the surface into the substrate. This has been shown to shift catabolic and anabolic microbial activity peaks down into the sediment, most conspicuously on the burrow walls [Reichardt, 1988].

Lanice conchilega.

Lanice conchilega, the sand-mason, is a polychaete Terebellid commonly found near low water mark on beaches and at estuary mouths. It is easily recognised by its protruding fringed tube, which is constructed by cementing carefully selected coarse sand and shell fragments with mucus [Plate 3]. The tube extends into the sediment, where it is lined with a strong, elastic, homogeneous mucous layer which binds the surrounding sediment, these particles being randomly, rather than selectively attached. Fig. 5.2.4. illustrates the structure of the burrow and summarises the mode of feeding [Schäfer, 1972]. Plate 4 shows a box core recovered from a *Lanice* community in the Menai Straits, North Wales: shell coated, oxidised tubes are present at very high densities.

Lanice tolerates salinity levels down to 13-14^{0}/oo, and prefers coarse to medium-fine sands [Wolff, 1973]. It is a suspension feeder, preferring areas of strong tidal currents. When the tide is in, its head is situated at the top of the protruding tube: the fringed crown acts as a net which entraps suspended plankton, these being harvested by long tentacles [Buhr and Winter, 1977]. When the tide is out, it climbs down the tube to escape from predators.

The effect of *Lanice* on textural and structural properties of the sediment is, once again, significant. The rigid, self-supporting tubes should affect both intergranular contacts and pore-space configuration. Bed roughness is also affected: individual tubes produce vortex patterns which may increase resuspension of sediment particles [Carey, 1983], while dense

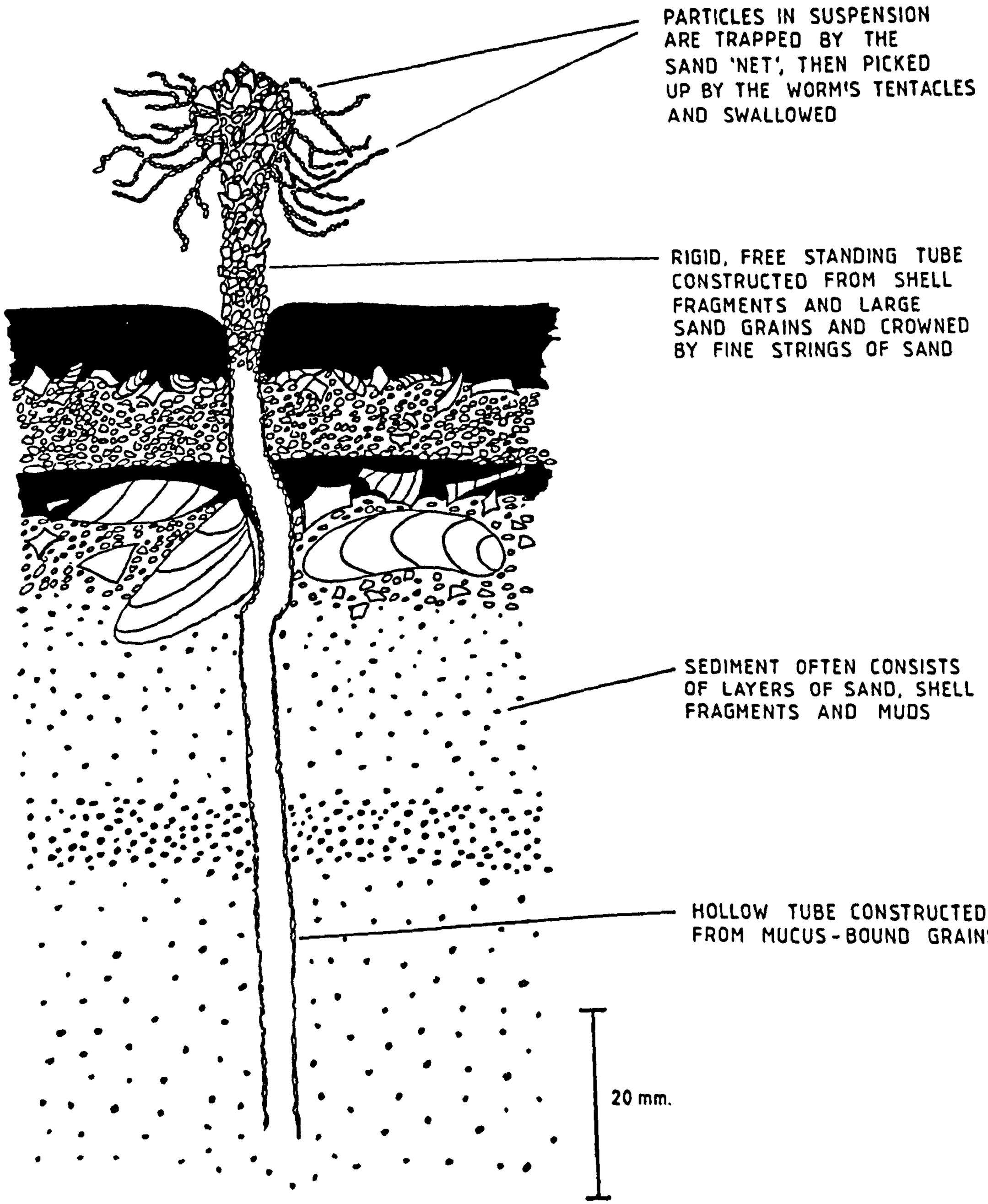

Fig. 5.2.4. Bioturbation by Lanice Conchilega.

'lawns' of tubes may have a stabilising effect by increasing the thickness of the viscous sublayer [Eckman, 1981].

Corophium.

Corophium is an amphipod genus with many species, the most common being *Corophium volutator* and *Corophium arenarium* [Meadows and Reid, 1966]. The most important difference between the two is in substrate preference, at least under laboratory conditions, with *C. volutator* selecting muds and *C. arenarium* selecting sands. They also differ in salinity tolerance, *C. volutator* being able to survive in freshwater for long periods, while *C. arenarium* dies after 1 hour. Gamble [1970] found both species coexisting at Red Wharf Bay, and it is likely that this was also the case for the locations sampled during this study. Since the two species cannot be distinguished without dissection, and since both exhibit similar burrowing and feeding behaviour, strict classification was not pursued.

Corophium is a selective suspension feeder, and builds a mucous-lined U-shaped burrow which is kept open at both ends. Plate 5 shows high densities of these burrows in muddy sand at Portmadoc, North Wales. Fig. 5.2.5. illustrates the burrow structure and mode of feeding for *Corophium volutator*. A slow water current is maintained, drawing in fine suspended sediment for ingestion. It is also capable of crawling (at slack water or when the tide is out) and swimming, leaving its burrow to be carried shoreward on the incoming tide [Wolff, 1973]. This behaviour, which has no direct relevance for the localised experiments described in this section, has been described more fully in Section 5.3.

Corophium will clearly affect the structural properties of the surface layers of the sediment, by constructing and maintaining open, oxygenated burrows lined with mucus. Although much smaller than *Arenicola*, it can reach densities of up to 20000 per m^2. Its activity would therefore be expected to increase sediment porosity and permeability and reduce tortuosity. It also affects the microbiological food chain within the sediment, by reworking and oxygenating the substrate and by feeding on diatoms and other microorganisms.

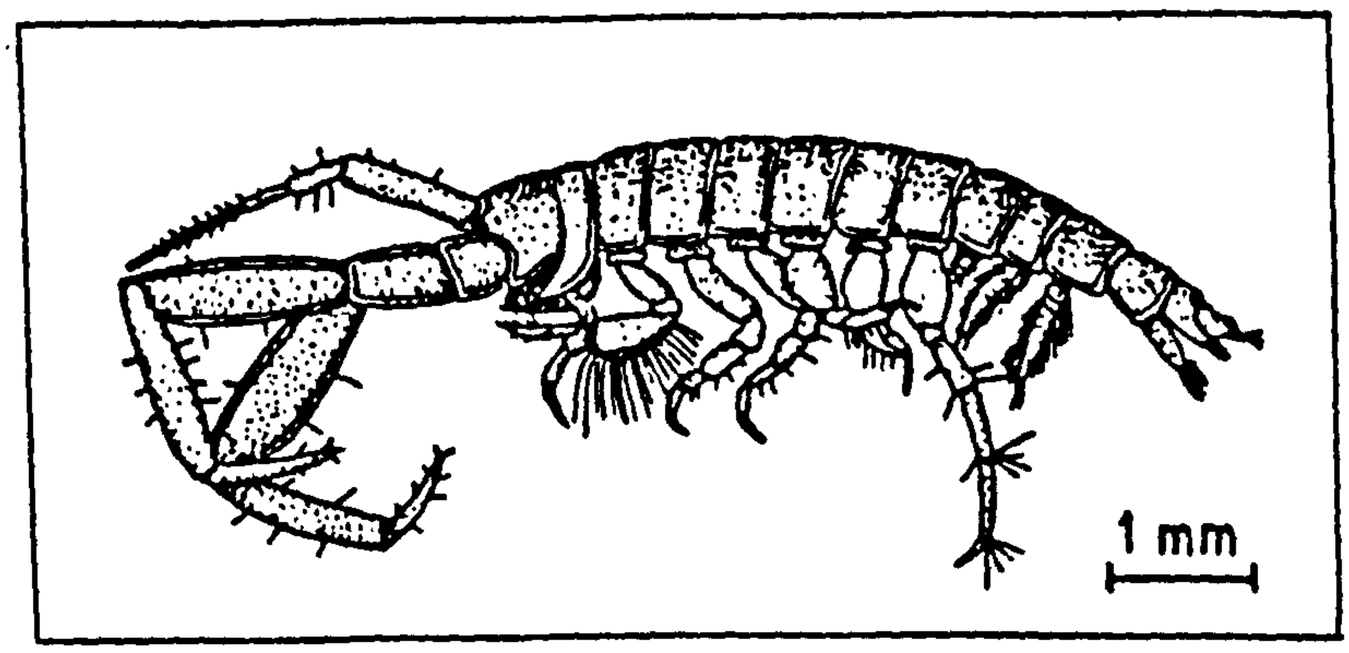

1. PARTICLES ARE SELECTED FROM THE SEDIMENT SURFACE .

2. ORGANIC MATTER CLINGING TO THE PARTICLES IS 'GRAZED' AND DIGESTED .

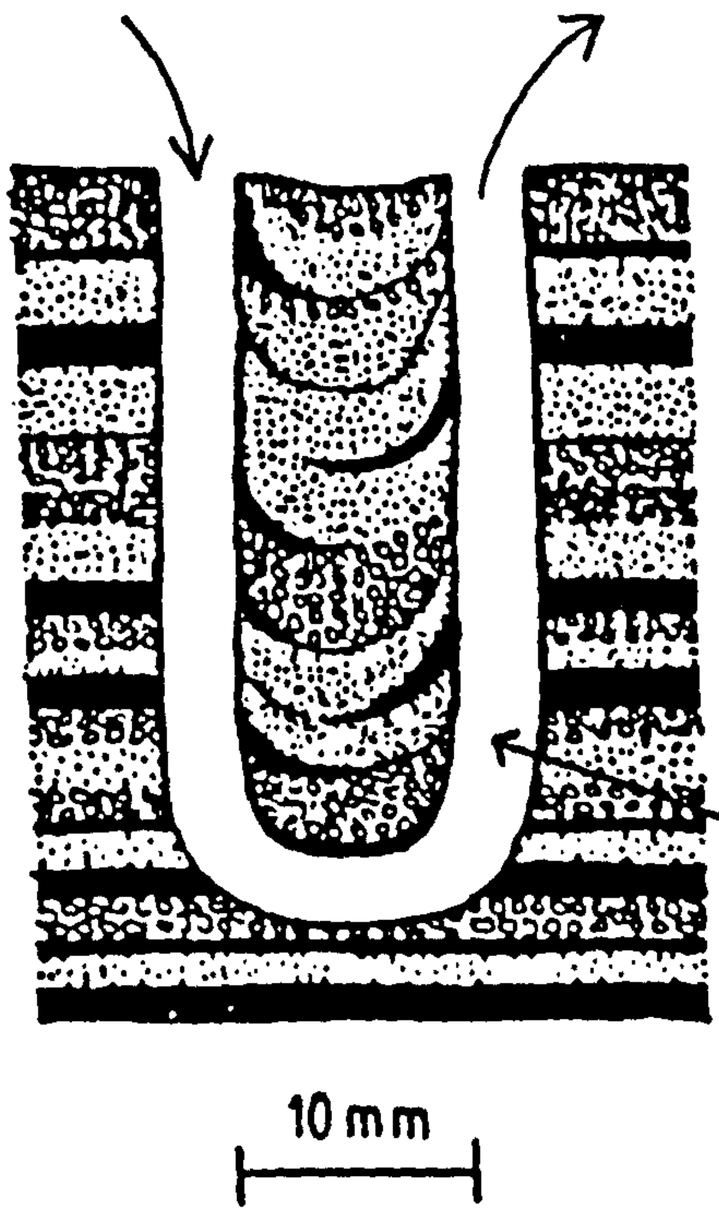

Fig. 5.2.5. Bioturbation by Corophium Volutator.

Therefore location selection was biased towards those which featured locally heterogeneous, and preferably monospecific, populations of these three organisms.

5.2.1 Traeth Llanddwyn : Preliminary measurements on a bioturbated foreshore.

Initial field trials of the geophysical probes were performed at Traeth Llanddwyn during four days over the two-month period June-July 1985. Care was taken to return to the same place using land-marks in the dunes: data from different sampling days were combined for analysis. Sampling was effected as the ebb-tide receded down the beach, on freshly exposed (but still saturated) sediment. The area sampled was approximately 100m x 40m.

The intertidal region at Llanddwyn consists of fine quartz sand with admixed shells and shell-fragments, deposited and reworked into a range of sedimentary structures from cavity sands through plane beds to wave- and current-rippled zones. It is also characterised by two separate macrofaunal benthic communities, *Arenicola marina* and *Lanice conchilega*, the abundance of each depending on position relative to low-water mark.

Selection of appropriate biological, textural and geophysical parameters will be justified, along with a general discussion of the results, in the following sub-sections.

5.2.1.1 Site characterisation.

Biological characteristics.

As already indicated, two benthic macrofaunal species dominated the study area. At around mid-tide level, *Arenicola marina* was observed at high population densities, with this density decreasing both seawards and landwards. *Lanice conchilega* was observed in gradually increasing abundance from near the limit of *Arenicola* activity to low-water mark

(and, it was assumed, beyond). The two species were observed to coexist over only a short stretch of the beach (where numbers of *Lanice* remained relatively low). This may indicate competitive inhibition, or a difference in tolerance of sub-aerial exposure between the two organisms.

Sites were selected to cover the full range of population densities observed. *Arenicola* was found in densities up to $11m^{-2}$, while *Lanice* reached $300m^{-2}$. In order to simplify interpretation, only one site containing both organisms was sampled. Since, for this experiment, the number of organisms was used as the criterion for site selection (given the primary constraint of saturation of the sediment) the biological parameters essentially represent controlled, rather than randomly sampled, variables. The counts cannot therefore be regarded as rigorous statistical estimates of population density for the area. In addition, they serve as exact indicators of number density at each site (allowing some uncertainty in relating surface indicators to individuals) since the total number was counted in each case. The concept of a site mean with within-site variability is therefore not valid for these parameters.

Textural characteristics.

Selection and interpretation of appropriate grain-size parameters were aided by examining the grain-size distributions at each site. Fig.5.2.6 illustrates a selection of (typical) weight-percentage frequency curves from different sampling days. The dominant feature is clearly the modal framework population, which remains essentially unchanged. Note that the frequency has been plotted on a log-scale to exaggerate other features of the curves. A second, coarser sub-population is present in several of the samples, with a rather broad and variable mode. The exact form of this mode is likely to be less consistent than that of the framework population because of the much lower numbers of particles involved.

Exploratory log-normal population splitting (described in Section 5.1.1.2) indicated a negligible fine sub-population, with a significant and highly variable coarse sub-population. It was noted that an effective 'cut-off' exists between this population and the framework at 2.0 phi, albeit with

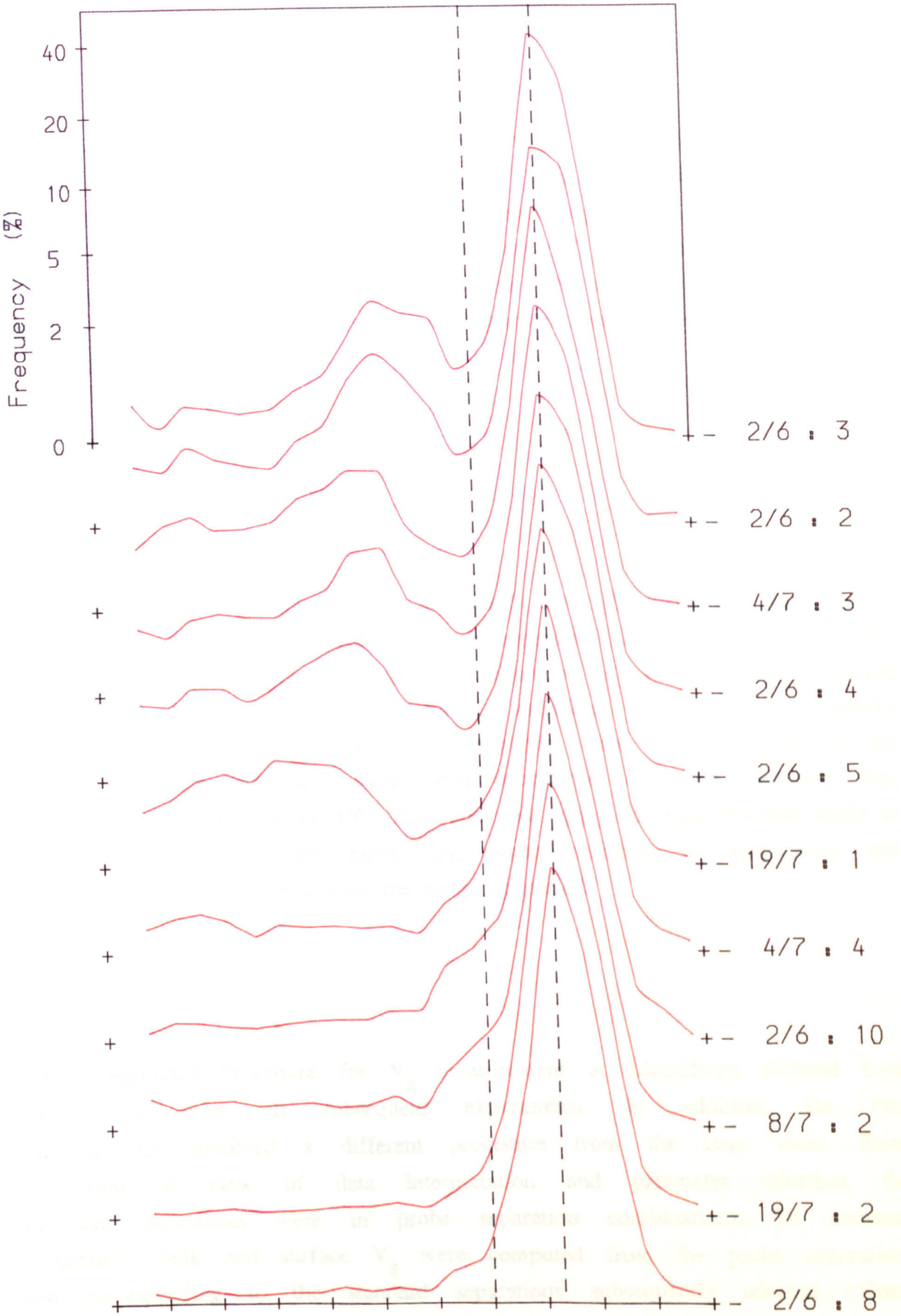

Fig. 5.2.6. TRAETH LLANDDWYN. Grain size distributions of selected samples. (Key: Date, Site No.)

some overlap. Therefore the cumulative percentage coarser than 2.0 phi was selected as an appropriate textural variable. This represents at most 25% of the grain size distribution, with the remaining 75% virtually identical for all samples. The total range (1-25%) provided a means of investigating the effect of admixing varying proportions of coarse particles into an otherwise uniform grain size matrix. Carbonate content was also retained as an important textural variable.

Geophysical parameters.

Formation Factor.

Site-mean sediment resistances were converted into FF using a single value of sea-water resistance measured on each sampling day (Table B1.1). They show reasonable consistency: what is uncertain is whether the observed variation was due to real temperature variation (assuming that salinity changes can be discounted) or to experimental error. If the latter is the case a systematic bias will have been introduced on each sampling day, amounting to a maximum of 8%. This does not apply to measurements made at the same site, or on the same day, when variation in temperature and salinity was assumed minimal over the sampling period.

S-wave velocity.

The experimental procedure for V_s measurement at Llanddwyn differed from that adopted for all subsequent experiments. In addition, the first sampling day involved a different procedure from the later visits. From the point of view of data interpretation and parameter selection, the important differences were in probe separation combinations. To maintain consistency, bulk and surface V_s were computed from the probe separations best corresponding to the standard separations subsequently adopted (50mm and 125mm). Thus velocity was computed from separations of 80mm and 150mm on the first sampling day, 50mm and 150mm on the remainder (thereby ignoring the data collected at 200mm separation).

There was no consistent significant difference between surface and bulk V_s (Fig. B1.1): basically the same controls were identified for each parameter. Therefore only bulk V_s has been discussed here.

5.2.1.2. Localised variability.

Location means, coefficients of variation and mean within-site variability (for parameters where site replicates were taken) have been listed in Table B1.2. In order to aid interpretation, the data-set was also split into two regimes or zones, based on the spatial distribution of *Lanice* and *Arenicola* between low and high water marks. Means for the two separate zones have also been listed in the table. Asterisks signify parameters which exhibit significant differences between zones. Marked textural differences were identified, there being much higher proportions of the coarse subpopulation in the *Arenicola* zone, apparently associated with high carbonate content. FF is also apparently sensitive to the contrasting biological and textural signatures of the two zones.

Variability in textural, biological and geophysical parameters was consistent with the model of localised perturbation of a uniform sediment framework proposed in 5.2.0.

5.2.1.3 Relationships between textural, biological and geophysical parameters.

The nature of the data collected from Traeth Llanddwyn dictated a threefold approach to the investigation of relationships between parameters. The data-set was first considered in its entirety, then split into the two 'zones' defined in the previous section. This served to separate out the effects of *Arenicola* and *Lanice*, and also ensured that much of the textural variation was removed, with the result that biological characteristics could be considered as predominant.

Table B1.3 lists significant correlation coefficients obtained for biological and textural parameters. While investigation of causal links

between textural and biological parameters was considered peripheral to the study, it was essential to appreciate any interactions before attempting to interpret relationships with geophysical properties.

Textural interrelationships.

The most important correlation between textural parameters was that identified between carbonate content and the fraction coarser than 2 phi (Fig.5.2.7). Linear regression has been performed to investigate the nature of the shell component. The intercept suggests that around 5% by weight is associated with the bulk framework population. The remainder increases with increasing coarse fraction, which indicates that shell fragments constitute a higher proportion of the coarse sub-population. The gradient of the regression line suggests that this proportion is around 20% (R^2: 0.88).

The coarse fraction is therefore distinct from the framework population by virtue not only of its grain size, but also its composition. The correlation was also found for the separate zones, despite reduced ranges in textural parameters.

Biological-textural interrelationships.

Since, for the full data set, two biological/textural regimes have been identified, correlations between characteristics based on the broad differences between zones were inevitable. These observed correlations could be coincidental, caused by separate position-dependent responses of biological and textural characteristics. A localised zone containing a shelly coarse deposit is common on sandy foreshores, possibly produced by wave-action in the breaker zone [Jago and Hardisty, 1984]. Species zonation is most probably controlled by ability to withstand sub-aerial exposure. However, it is also possible that more direct causal relationships contribute to the observed correlations. It is unlikely that a selection mechanism by organisms based on textural properties was in force, since both organisms are found in a wide variety of sediments

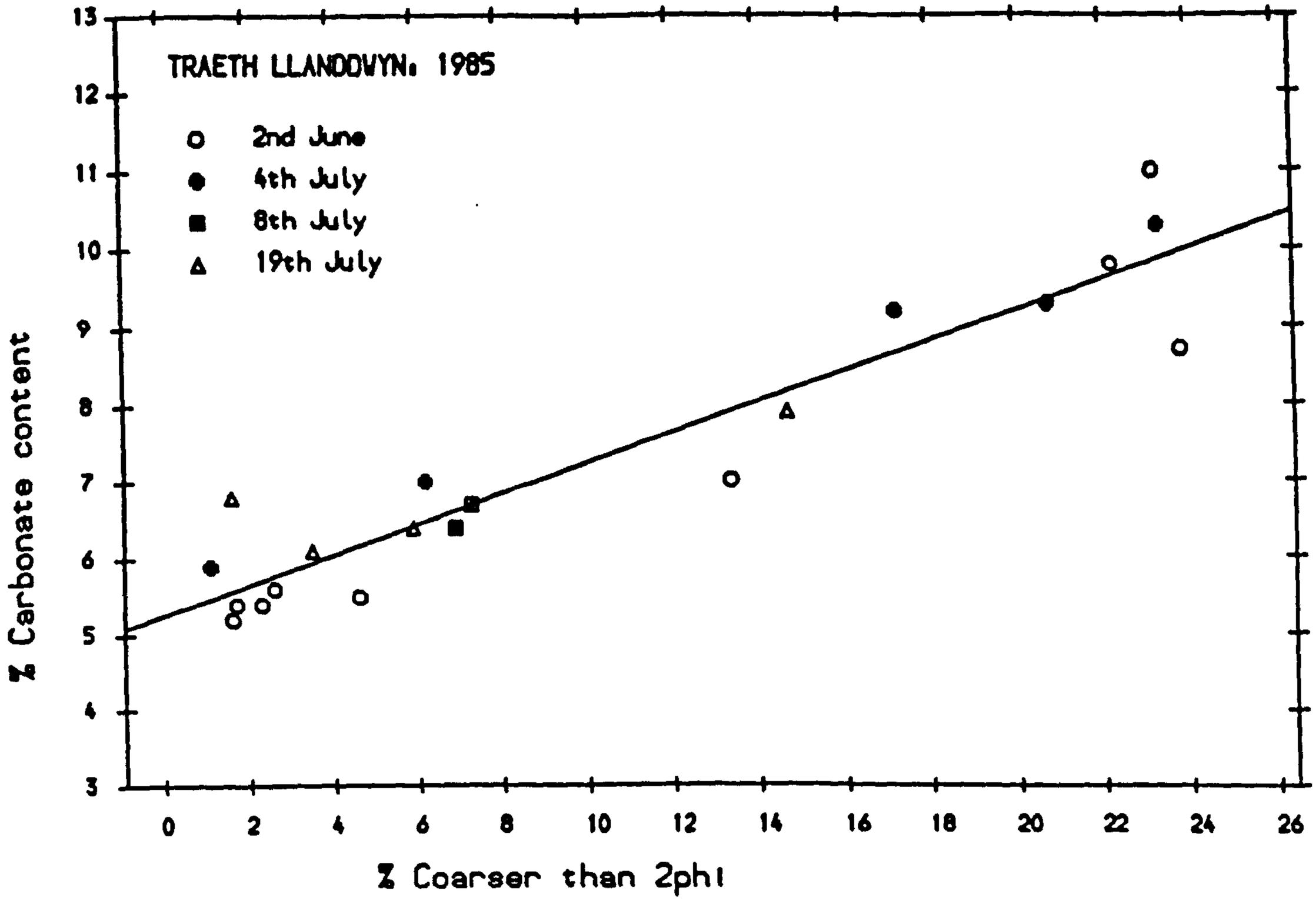

Fig. 5.2.7.

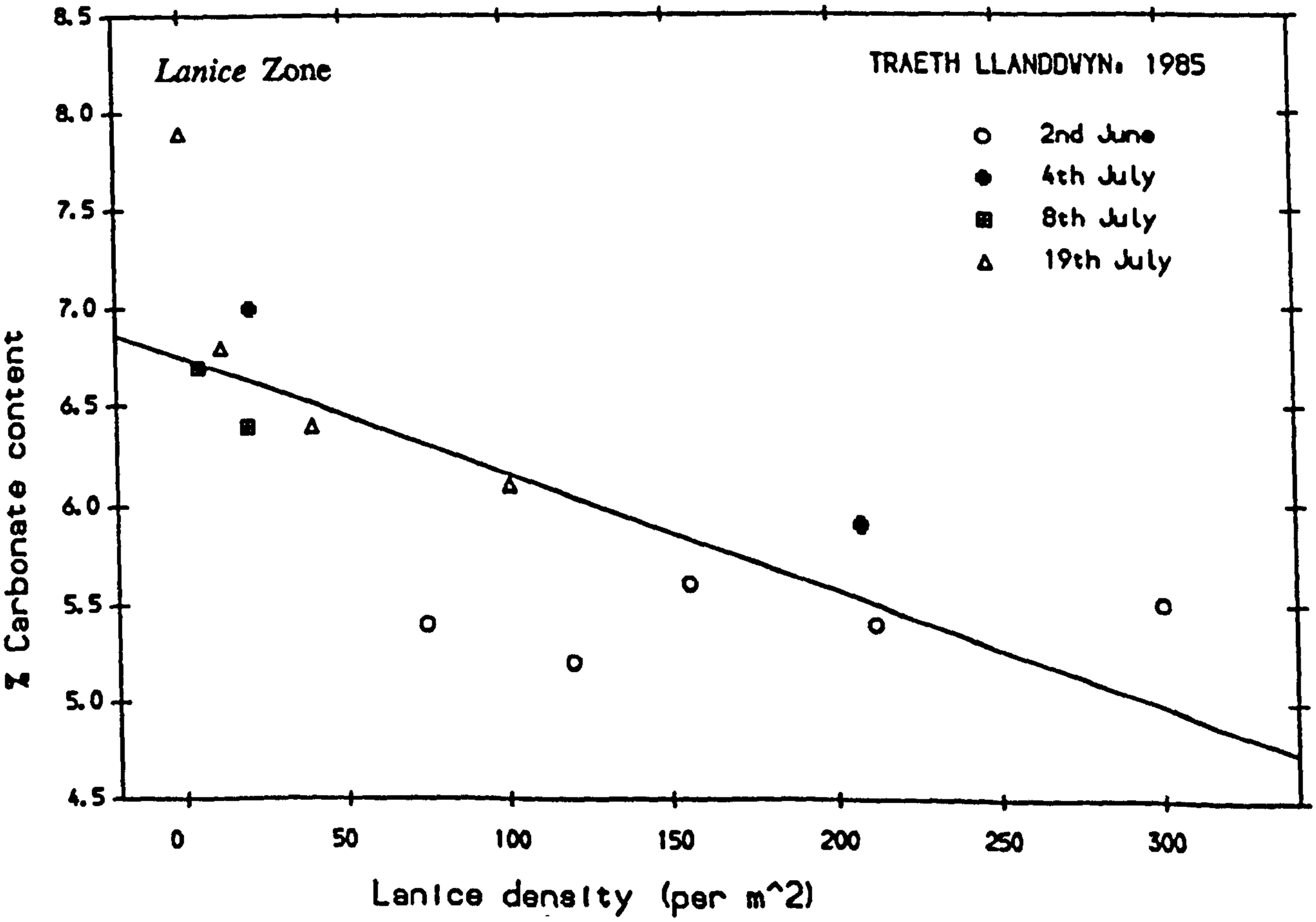

Fig. 5.2.8.

[Eltringham, 1971]. It is more likely that any direct causal link would be through biological activity affecting the textural properties. The strongest evidence supports a direct link between *Lanice* and carbonate content, with a significant negative correlation even within the *Lanice* zone (Fig.5.2.8). A possible mechanism is that *Lanice* selects coarse shell fragments for constructing the protruding section of its tube, thus removing them from the bulk sediment and reducing their likelihood of being sampled.

Relationships between geophysical properties and other parameters.

Investigation of geophysical properties involved a different approach to that employed for identification of textural and biological interrelationships. The geophysical properties can be considered as dependent parameters, with the other properties as potential controls. Table B1.4 summarises the significant results from linear regression of the geophysical parameters, following the procedure outlined in 5.1.5. As previously stated, the actual partial regression coefficients were not considered to be important or reliable, the sign of the relationship being sufficient for the purposes of this study.

Formation Factor.

FF would be expected to be influenced by variations in packing configuration which change either sediment porosity or tortuosity, although the degree of variation has been shown to be small due to the uniformity of the bulk sediment framework.

Significant relationships were identified for both carbonate content and the coarse fraction. The strong interaction between the two posed a dilemma in deciding which of the two properties directly affected FF. Mixtures of two log-normal populations tend to pack at lower porosity than a single population, with the porosity decreasing with increasing admixed coarse sub-population. Therefore FF may have been responding directly to variation in porosity. On the other hand, platy shell fragments would be

expected to pack into a configuration with higher pore-space tortuosity, and FF may have been affected by this. Of course, both mechanisms may have been involved independently, but this cannot be tested for because the textural properties were too closely related. Had sediment porosity been independently measured, the problem could perhaps have been resolved.

Fig.5.2.9 illustrates the observed dependence on coarse fraction. A large degree of scatter is present, indicating either that FF was measured with a high degree of error, or that some additional control was operating. Both relationships were also observed in the *Lanice* zone (Fig.5.2.10), but neither were significant in the *Arenicola* zone.

In addition, inverse relationships were observed between FF and *Lanice* in the *Lanice* zone (and overall) and between FF and *Arenicola* in the *Arenicola* zone. The implication is that both organisms act to reduce FF, although the *Lanice* relationship may be indirect through its interaction with carbonate content. It is intuitively reasonable that both organisms should directly affect FF. At the high densities observed, hollow *Lanice* tubes should contribute to an increase in bulk sediment porosity, whereas *Arenicola*, even at the relatively low densities observed, could increase porosity locally by sediment liquefaction and excretion. If *Lanice* is removing shell fragments from the sediment framework an additional, indirect effect on FF may be involved. Appropriate scatterplots have been presented in Figs.5.2.11 and 5.2.12.

The coarse fraction generally yielded higher R^2 values than carbonate content in multiple regression analysis, although either could be substituted to give significant results. This illustrates the problem of strong correlation between two potential predictor variables.

For the full data-set, variation in FF is best explained by a combination of the coarse fraction and *Arenicola* density. Adding in *Lanice* further increases R^2: however, since *Lanice* and the coarse fraction are related some degree of interaction must be assumed in this case.

In the *Arenicola* zone results for the full data-set are supported, with 82.6% of the observed variation explained by the coarse fraction and

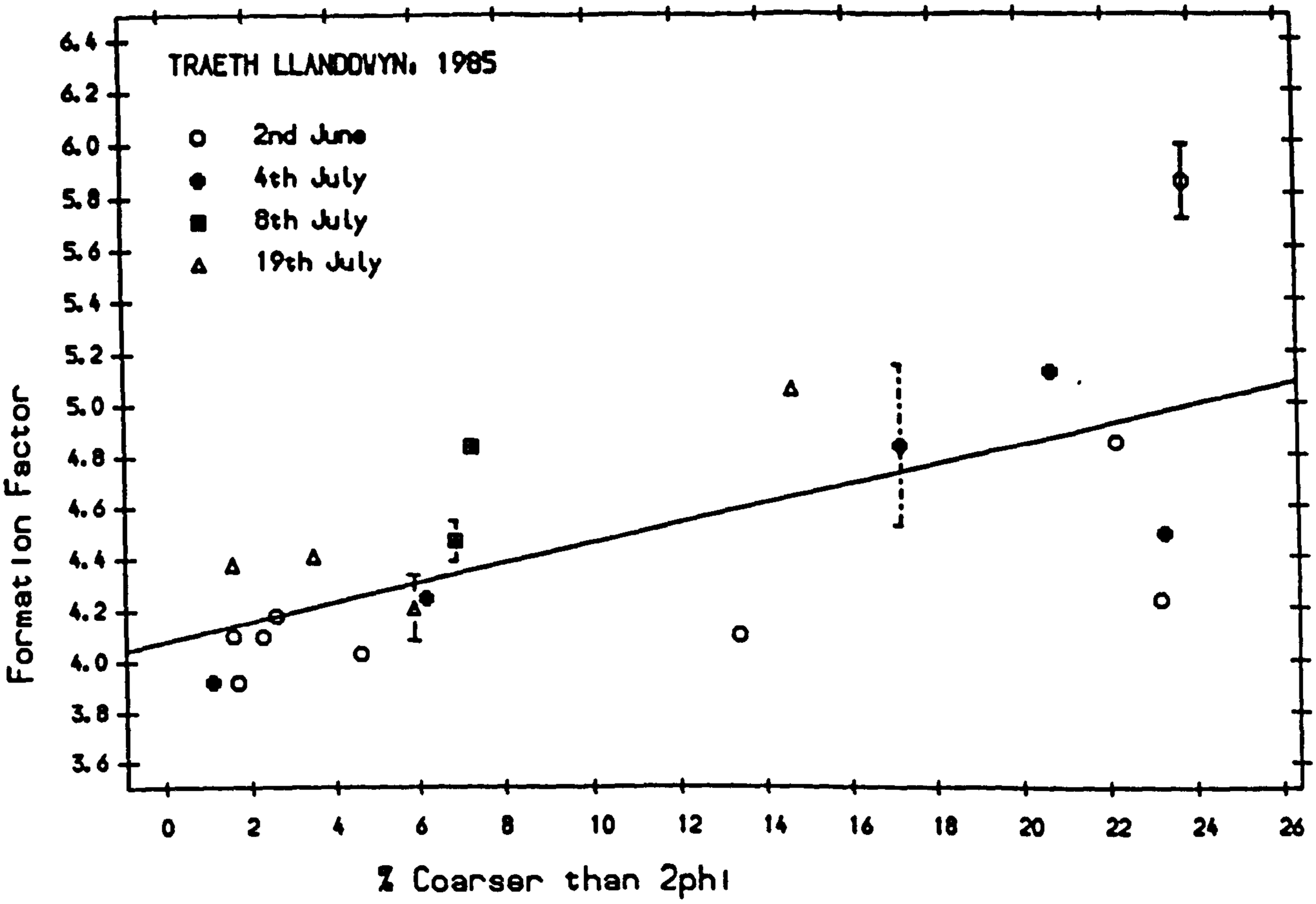

Fig. 5.2.9.

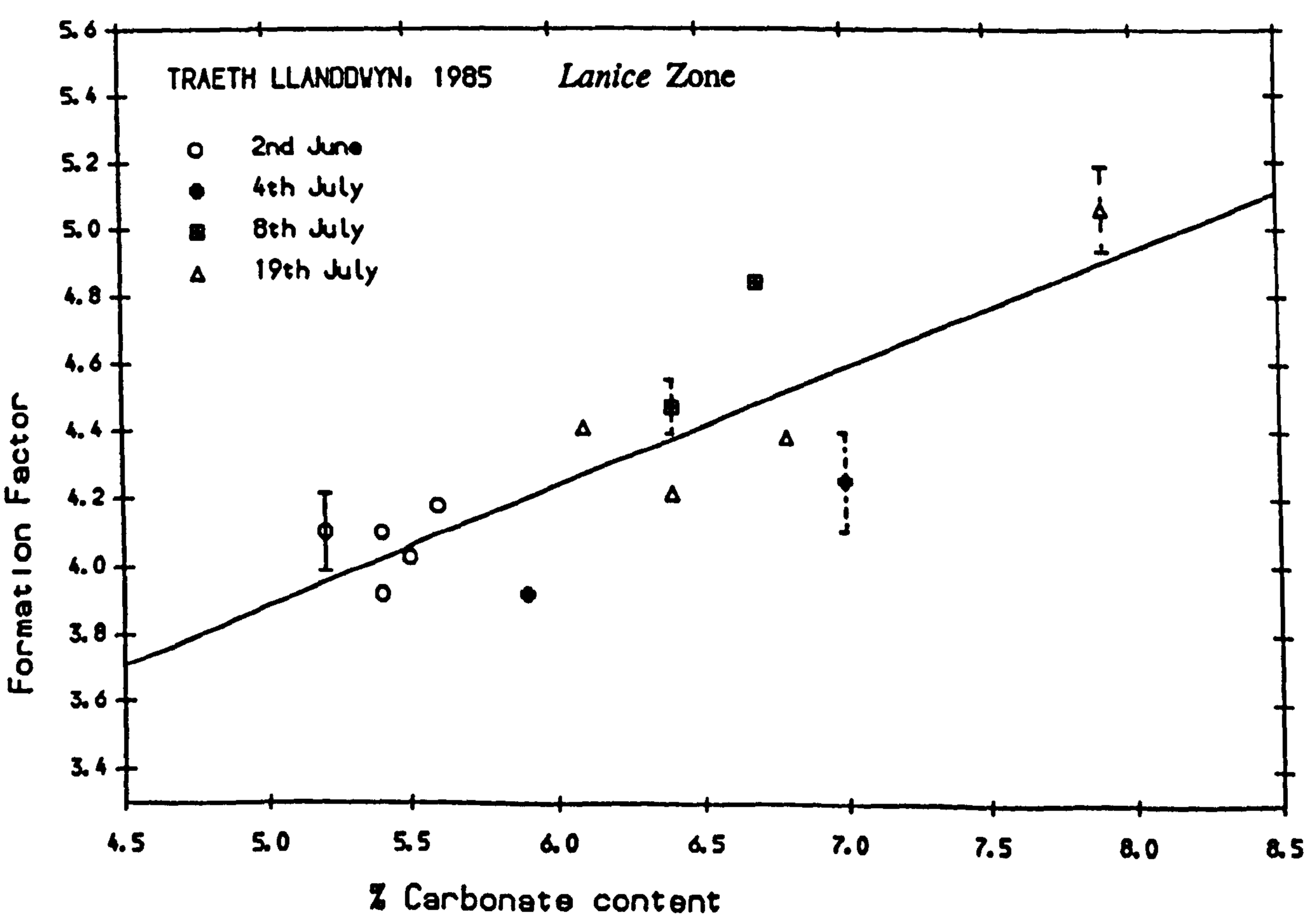

Fig. 5.2.10.

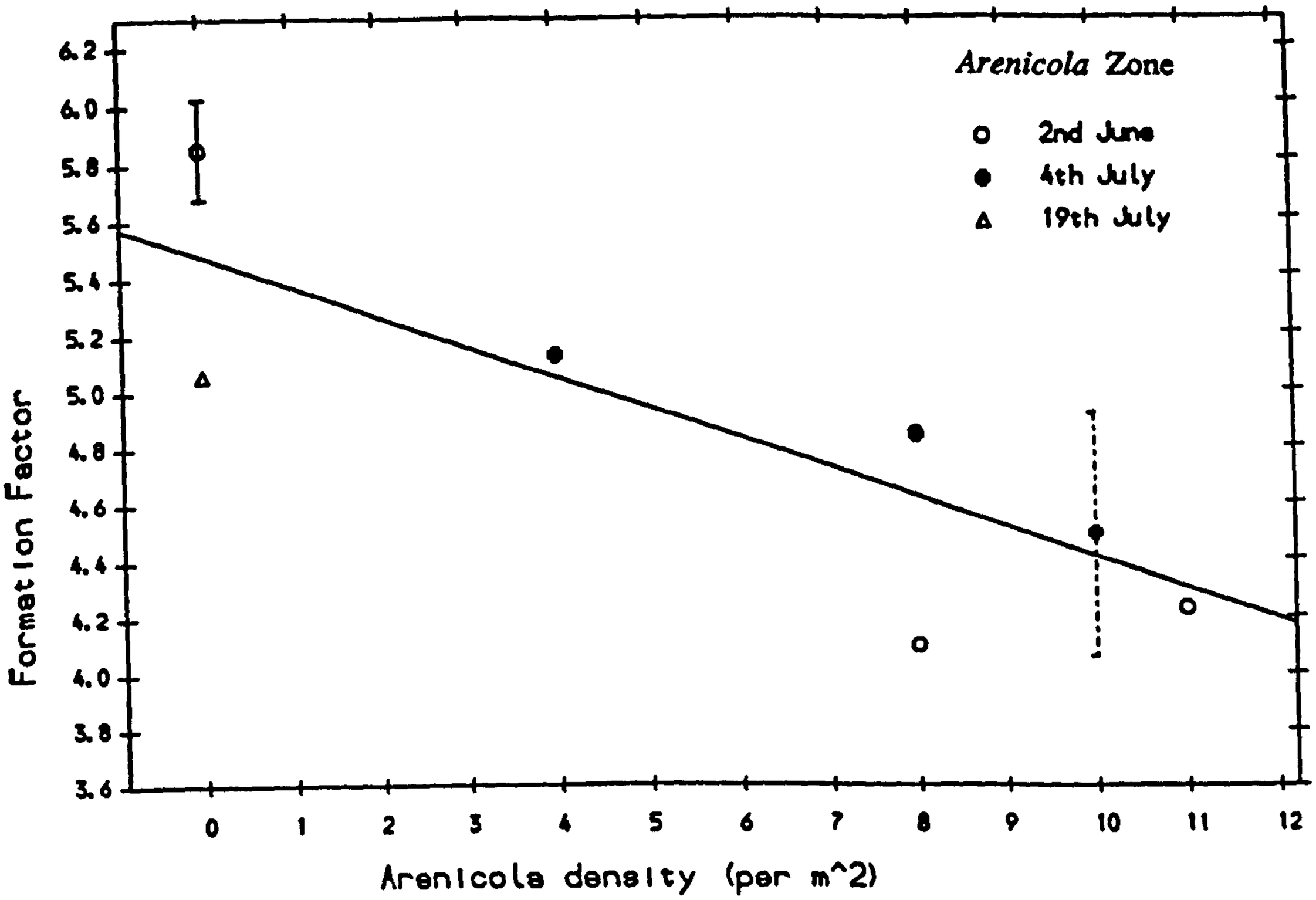

Fig. 5.2.11.

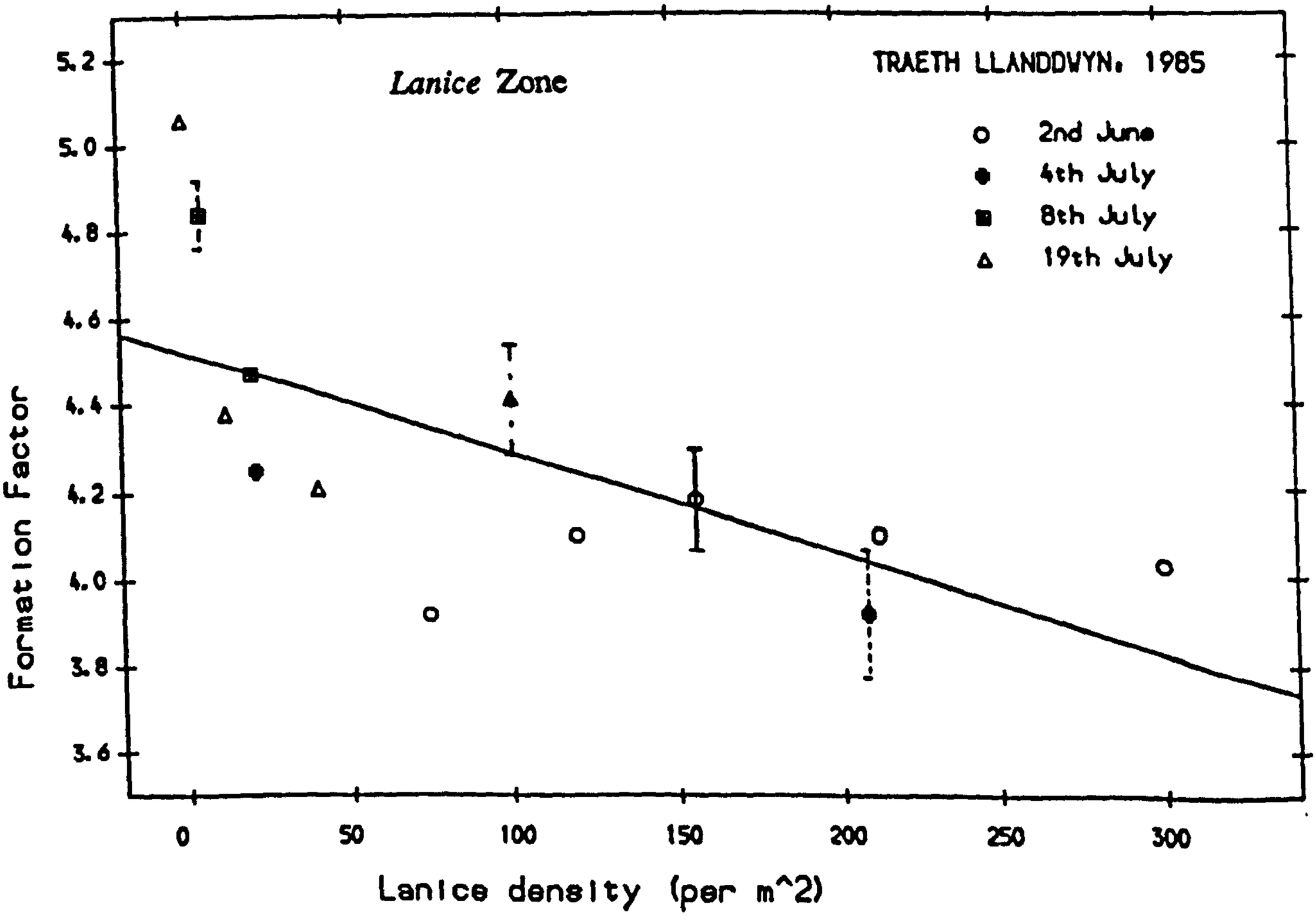

Fig. 5.2.12.

Arenicola density. No significant partial predictors were identified in the *Lanice* zone, possibly because of the high degree of interaction observed between textural and biological parameters.

Thus the scatter observed in Figs. 5.2.9 - 12 is due, at least in part, to variation in other site characteristics. The model suggested is that sediment porosity is reduced and tortuosity increased by increased proportions of the coarse shelly sub-population, resulting in an increase in FF. In addition, porosity is increased by *Arenicola* activity, and by *Lanice* tubes, resulting in a decrease in FF.

S-wave velocity.

V_s should be sensitive to variation in textural properties which affect FF, since both depend in complementary fashion on the sediment packing configuration. In fact, since each should be inversely related to porosity, they might reasonably be expected to show a positive, though not necessarily linear correlation. However, both will be additionally and independently sensitive to physical properties of the sediment matrix and pore-space. In this case, no relationship was found between the two.

The lack of significant difference in V_s between the two zones contrasts with marked differences in FF and textural properties. Clearly any effect on V_s induced by the porosity or tortuosity changes postulated in the previous section has been masked by other controlling factors which do not significantly affect FF. Although no single predictors were identified for the full data set, there are two (probably related) sets of partial predictors. V_s is apparently independently increased both by *Lanice* density and the coarse fraction, the coarse fraction being replaceable by carbonate content. The textural control is in direct agreement with that found for FF, indicating that V_s is increased by the proposed reduction in porosity (and increase in degree of interlocking) due to an increase in the highly angular, shelly coarse sub-population.

For the *Lanice* zone, the same positive dependence on *Lanice* was observed (Fig. 5.2.13). The observed negative dependence on carbonate content can

almost certainly be dismissed as indirect, due to its interaction with *Lanice* within this zone. This is supported by the fact that a direct relationship would be expected to apply across the full data set, since a much higher range in carbonate content is involved: in fact an opposite result was found in this case. No significant relationships were found for the *Arenicola* zone. This is disappointing given the postulated increase in porosity by *Arenicola* which the FF results indicate, and given the finding from laboratory work with hollow burrows.

The effect of *Lanice* on V_s is important. It should be noted that the observed relationship is opposite to that found for artificial tubes in the laboratory (Chapter 3). Clearly an additional mechanism is operating which counteracts any effect due to the presence of vertical cylindrical voids in the sediment matrix. *Lanice* builds its tube by incorporating coarse particles and shell fragments into an elastic mucous membrane, thus producing a vertical 'armoured' hollow rod, which should have greater rigidity than the surrounding sediment. An analogy with reinforced concrete suggests that an increase in rigidity (and hence V_s) may be associated with large numbers of these armoured tubes. More specifically, the tubes must act to resist horizontal shear of (and hence S_H propagation through) the sediment matrix.

If this hypothesis is correct, it must be assumed that localised distortions of packing structure around the tubes do not affect FF. That is, the effect on intergranular friction must be much more important than any effect on pore-space properties.

For measurements made on the first sampling day, the direct link between V_s and *Lanice* tubes was tested over much more localised spatial scales. On each emplacement of the receiver probe, the number of tubes between it and the transmitter was noted. Thus individual measurements of transmitter-receiver velocities were associated with tube numbers for direct comparison with the laboratory investigation of artificial hollow tubes. Since two probe separations were involved, the velocities measured from each were analysed separately. This was to avoid differences due more to separation-dependent pulse modification and measurement error than to any layering effect, which has been shown to be negligible in this case.

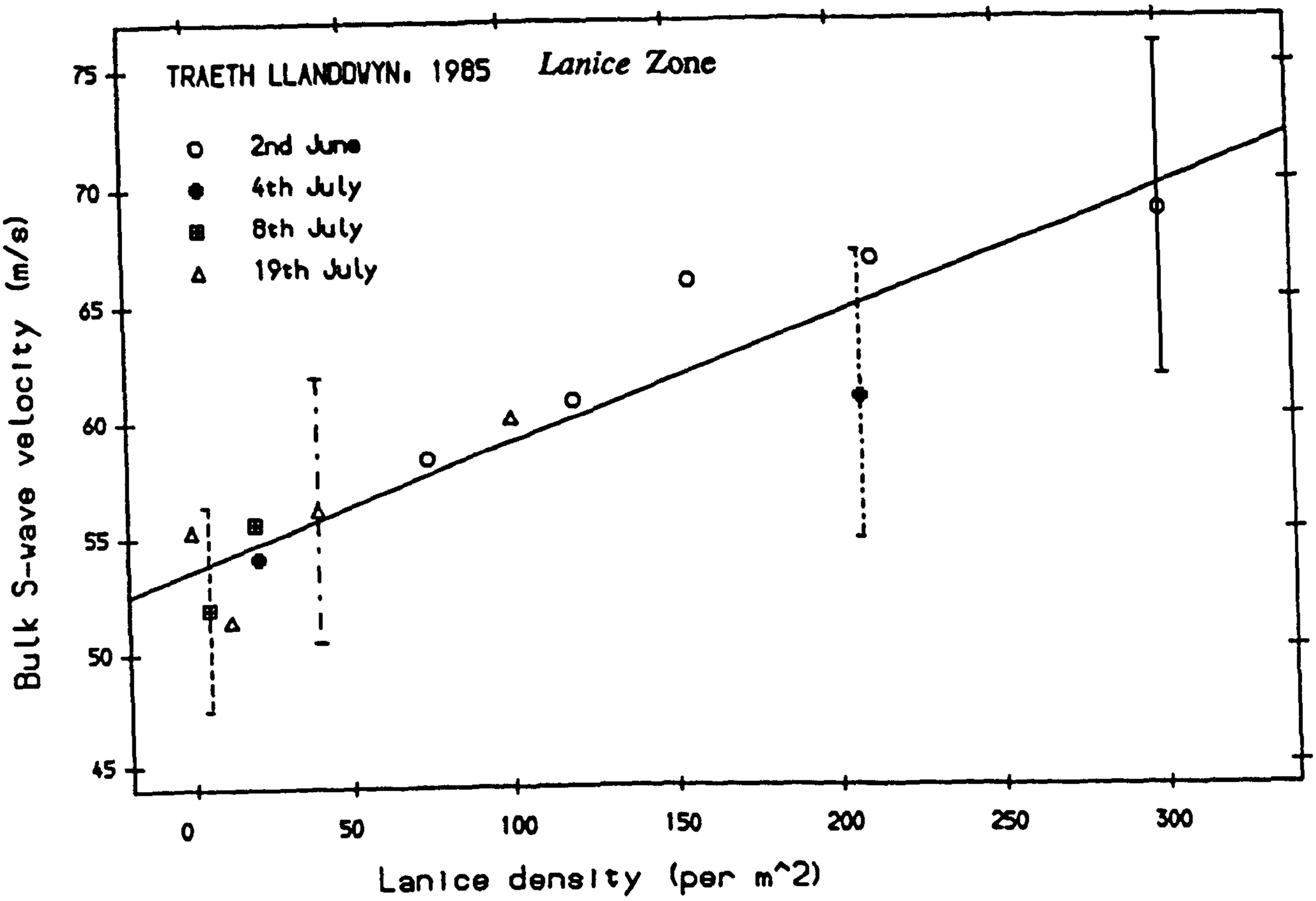

Fig. 5.2.13.

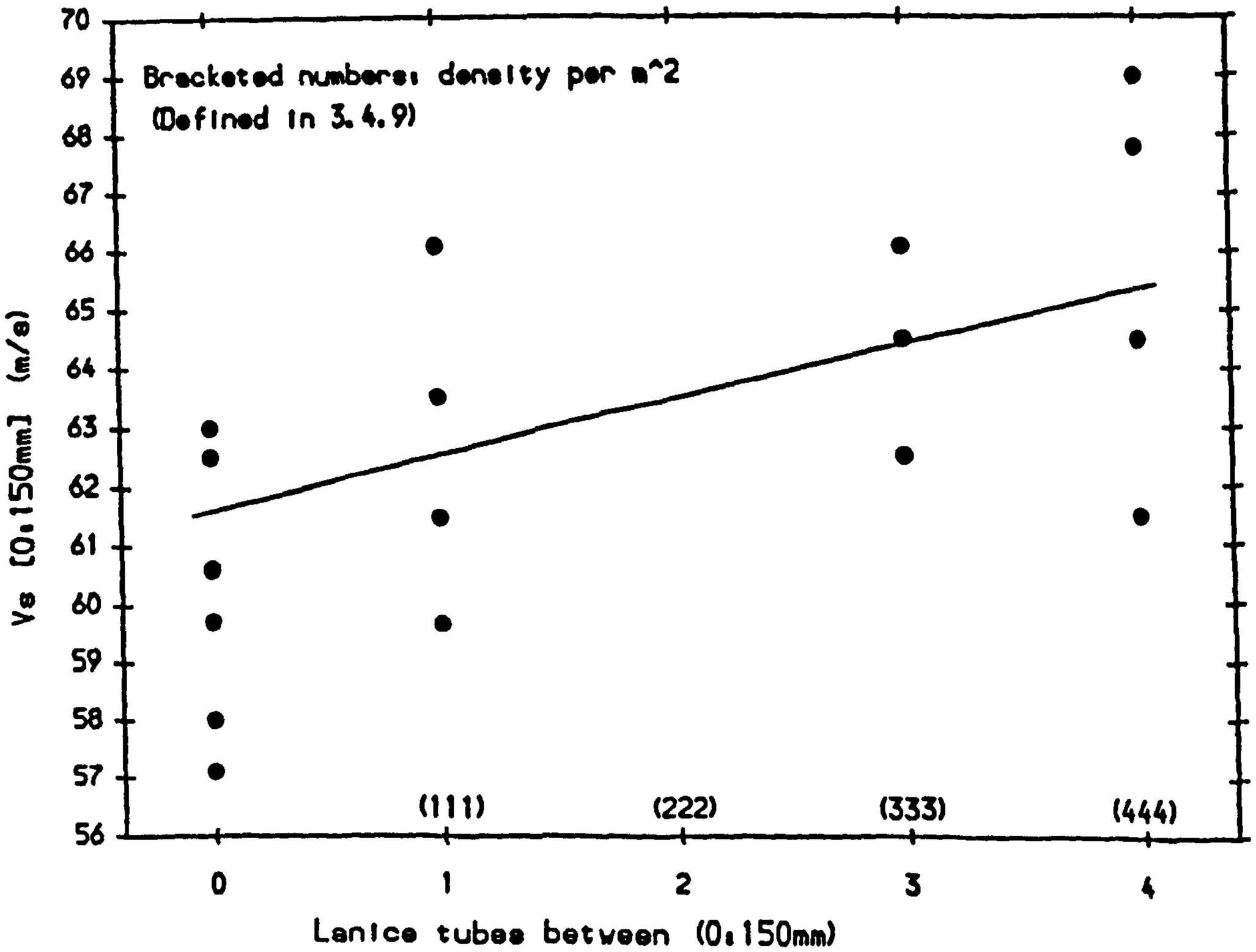

Fig. 5.2.14. (2nd. June only). V_s versus number of *Lanice* tubes between S-wave probes.

Naturally a high degree of scatter was obtained, caused by sampling error, textural variation and small-scale spatial heterogeneity. Significant correlations were found for V_s^0(0:150mm), as illustrated in Fig. 5.2.14, and for the combined data set, but not for V_s^0(0:80mm). The relationship was expected to be better for velocities measured over higher probe separations, since a larger range of tube numbers was possible combined with lower sensitivity to separation error and small-scale heterogeneity.

This result reinforces the argument that *Lanice* tubes directly affect the V_s, and represents a virtually independent confirmation since individual transmitter-receiver velocities were calculated rather than site-averaged values of bulk V_s.

5.2.1.4. Summary and interim conclusions.

In conclusion, the sedimentary deposits sampled at Traeth Llanddwyn consist largely of a uniform framework population with mode 2.7 phi, and shell-fraction around 5%. Textural variation is introduced via a coarse sub-population with mode approximately 1 phi and shell-fraction 20%, which comprises between 1 and 25% of the sediment matrix. FF and V_s measurements indicate that this coarse fraction acts to reduce sediment porosity in agreement with its predicted effect on packing configuration, although independent measurements of porosity were not made to test this. In addition, the shell component may increase intergranular friction and tortuosity of the pore-space.

Several biological/textural relationships were identified, most of which are probably indirect due to zonation of species and sediment texture between high and low water marks. There is an apparently direct reduction of carbonate content by *Lanice*, the proposed mechanism being selection and removal of shell fragments from the bulk grain size matrix and their concentration around protruding tube walls. This results in a textural sampling artefact, rather than a net removal of material.

The two macrofaunal communities significantly affect geophysical properties. *Arenicola marina* apparently reduces FF, indicating localised

increases in porosity by burrowing and feeding activity. However, V_s measurements do not support this assertion. *Lanice conchilega* also apparently reduces FF, although this may be an indirect relationship through its correlation with the shell fraction. In sharp contrast, V_s is increased by *Lanice,* indicating that shell-armoured vertical tubes cause an increase in sediment rigidity.

5.2.2 Taf Estuary : Measurements in clean sand and a muddy *Corophium* flat.

In order to extend the range of textural and biological characteristics monitored, two contrasting locations in the Taf estuary were sampled on successive days in November 1985. Both were situated on intertidal sandflats within 100m of low-water-mark. These two locations were fixed using marker posts from a long-term survey of the Taf estuary [Jago, 1980], and to maintain consistency they have been identified using the original system. They are characterised as:

TRANSECT T/8: Clean fine sand reworked by the ebb tide into small-scale two-dimensional current-ripples.

TRANSECT T/11: Muddy fine sand supporting an extensive community of *Corophium* some 1000m up-river from T/8.

At each location, spatial variability was monitored in a more quantitative sense than at Llanddwyn. The transect was identified using marker posts, and a section of this line which satisfied the requirements of full saturation during the sampling period was marked out with measuring tape. Sites were then sampled at fixed distances along this tape. Thus it was possible to investigate spatial trends in sediment characteristics.

Experience from the preliminary survey at Llanddwyn led to some modification of experimental procedure as discussed in Section 5.1. The two major differences were: first, an independent measurement of sediment porosity was made; and second, the probe separations employed for V_s assessment were fixed between 50 and 125mm.

Since procedure was identical at both locations, analysis could be performed either on data from each, or on a combined data-set from both. The justification for combining data from these widely spaced transects is relatively straightforward: it is known that sands in the estuary have a common provenance [Jago, 1980], and the framework populations from both locations are virtually identical. However, in any investigation of relationships between measured site characteristics, the possibility of additional unquantified location-dependent environmental controls must not be overlooked.

Data handling followed a similar pattern to that adopted for the Llanddwyn study, with two spatially separate 'sub-sets' contributing to overall variation in measured properties. An advantage of performing sampling along transects is that it provides a useful framework for graphical presentation of the data. Figs. B2.1-4 illustrate the spatial variation of selected properties along the two transects. The observed trends in several textural, biological and geophysical parameters provide a good indication of significant spatial variability in measured properties.

5.2.2.1 Site characterisation.

Structural characteristics.

The differences between the two sand flats monitored are clearly illustrated by box-cores taken at each location. Plate 6 shows a core recovered from T/8, with very fine sedimentary structures typical of intertidal sandflats in the estuary [Jago, 1980]. Small-scale cross-bedding, plane bedding, shelly deposits and cavity sand can be identified, indicating a highly mobile substrate responding to variable wave and current regimes over tidal, lunar and perhaps seasonal cycles. In complete contrast, Plate 7 shows an extensively bioturbated sedimentary deposit, with very few hydrodynamically-derived structures. The main features are relict *Corophium* burrows. Recent burrows were less well preserved in this core due to their inherent fragility, despite their observed abundance during sampling.

Textural characteristics.

A selection of grain-size distributions from each transect has been presented in Fig. 5.2.15. This illustrates first the marked uniformity of the sediment within each location, and second the slight but significant difference in modal population between the two locations. Log-normal population splitting was performed on all distributions. At T/8 at least 95% of the grain-size distribution comprised the log-normal modal population, with 1-5% as a slightly coarser truncated sub-population, and less than 1% in the fine tail. Comparison with the results from a fall-tower analysis of these samples (Fig.5.1.8) suggests that variation in the sieve-derived coarse tail, which affects grain sorting, is based on the trend in shell content across the transect (Fig. B2.1). At T/11, at least 90% comprised the log-normal framework, with 3-5% as a coarse fraction and an additional 2-6% fine sub-population which was directly related to fines content. The coarse fraction was consistent with that found for those T/8 samples with similar carbonate content. Therefore, at both locations, variation in the coarse tail of the grain size distribution could be attributed to variation in carbonate content, while variation in the fine tail could be related to fines content.

Biological characteristics.

There was no evidence of benthic macrofaunal activity in the highly mobile, clean sands at T/8. In sharp contrast, large numbers of *Corophium* were in evidence over the first part of T/11, tailing off in the 40m closest to the ebb-channel. Localised population density was estimated by fracturing the sediment surface-layer and counting exposed burrows. No quantitative estimate of within-site variability was made, although several fractures were generally examined before identifying a 'typical' density. This raises considerable doubt as to the quantitative reliability of the data. However the counts did serve as indicators of high and low density zones of the transect.

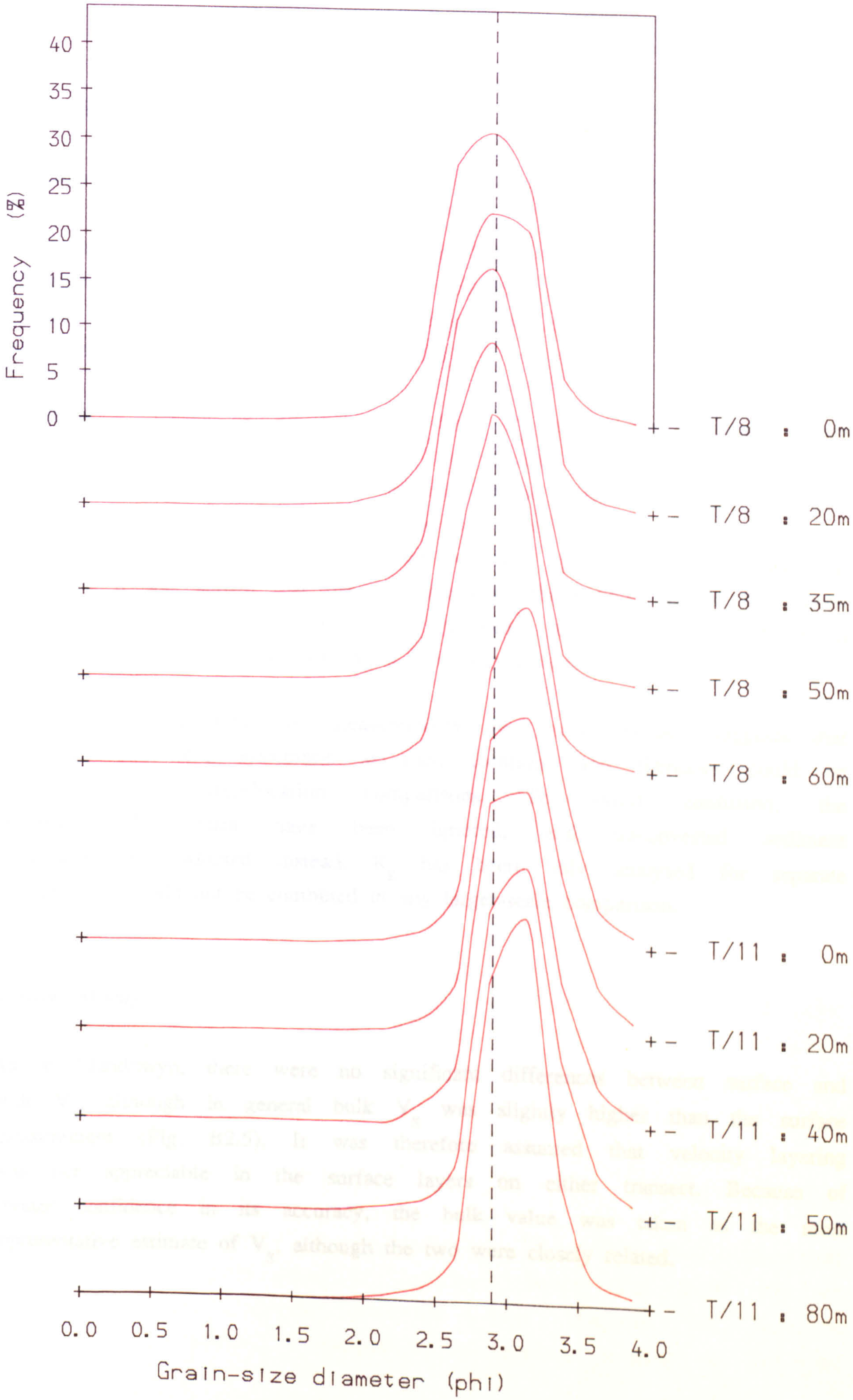

Fig. 5.2.15. TAF ESTUARY. Selected grain size distributions.

Geophysical characteristics.

Formation Factor

Site-mean sediment resistances have been listed in Table B2.2. Pore fluid resistance was obtained directly by digging several holes along the transect and monitoring the resulting pools: little variability was encountered along the transects (Table B2.1).

Unfortunately, values of FF calculated from R_s and these measured values of R_w are much lower than expected for natural sand deposits (Section 2). Therefore the R_w measurement was assumed to be erroneously high. The most probable explanation is that interference by the bottom and sides of the fluid-filled holes caused overestimation of the pore fluid resistance. In Chapter 4 it was shown that the dimensions of these holes should have been at least 400×200×250mm to avoid this problem: it is extremely difficult to create and maintain a hole of that depth in saturated sand.

However, the consistency of measurements over each transect suggests that errors in FF were systematic at each location, and therefore could be neglected for within-location comparisons. To avoid confusion, the erroneous FF values have been ignored, and unconverted sediment resistances (R_s) adopted instead. R_s has been fully analysed for separate transects, but could not be combined in any larger-scale comparison.

S-wave velocity

As at Llanddwyn, there were no significant differences between surface and bulk V_s, although in general bulk V_s was slightly higher than the surface measurement (Fig. B2.5). It was therefore assumed that velocity layering was not appreciable in the surface layers on either transect. Because of greater confidence in its accuracy, the bulk value was taken as the most representative estimate of V_s, although the two were closely related.

5.2.2.2. Localised variability.

Location means and coefficients of variation for properties measured along individual transects (and overall) have been summarised in Table B2.2. Relative variability of textural, biological and geophysical parameters was consistent with localised perturbation of a predominantly uniform sedimentary framework. There were significant between-transect differences in all properties except carbonate content and sorting (as indicated by asterisks in the table). These exceptions are consistent with the idea that the location-average population at T/11 is identical with that at T/8, except that it has been shifted finewards by about 0.2phi. It should be noted that the between-transect difference in R_s incorporates a significant (and unknown) difference in pore fluid resistance.

5.2.2.3. Relationships between variables.

Relationships between variables have been considered first at individual locations, then for the combined data-set, to include slightly larger scale spatial variation. Table B2.3 lists the significant correlation coefficients for textural and biological characteristics. Table B2.4 summarises the regression results found for FF, V_s and porosity.

Textural interrelationships.

As already indicated, textural parameters were highly uniform within each location. The absence of correlations indicates that fines and carbonate contents represent independent contributors to textural variability.

Biological/textural interrelationships.

No correlations were found for *Corophium* at T/11, which was unsurprising since the marked spatial trend in *Corophium* density (Fig. B2.4) was not observed for any textural parameter. This suggests that substrate selection by *Corophium* is controlled by position relative to low-water

mark, and therefore time of intertidal exposure, rather than by any sediment properties.

For the full data-set, differences between the two locations give rise to correlations with fines content. *Corophium* generally selects muddy sand for its habitat [Meadows & Reid, 1967]: however, its preference for T/11 may also reflect differences in hydrodynamic regimes.

Porosity.

At T/8, a direct relationship between porosity and carbonate content is observed (Fig. 5.2.16), suggesting that shell fragments serve to increase sediment porosity by 'bridging' across the framework grains, preventing close-packing of other sedimentary particles. In this case the effect of increasing the coarse subpopulation, which was thought to reduce porosity at Llanddwyn despite its higher carbonate content, must have been less important than the effect of increased angularity of grains.

At T/11 no signficant relationships were identified, despite significant variation in *Corophium* burrow density. Sampling error, complex biological/textural interactions and independent hydrodynamic control may all have influenced this result.

When the full data-set is considered, several relationships are obtained, largely reflecting the textural and biological differences between the two transects. Thus higher porosity is associated with *Corophium* burrowed, muddy sand at T/11, as expected. More significantly, there is positive partial dependence on both carbonate and fines contents, with no differences in carbonate content between transects. The fine particles must either have acted to force the framework apart (this mechanism being consistent with observed framework:fine size-ratio) or have been deposited more gently, resulting in a more open structure (Chapter 1). This may have been reinforced by bioturbation, despite the lack of a specific relationship with *Corophium* density at T/11.

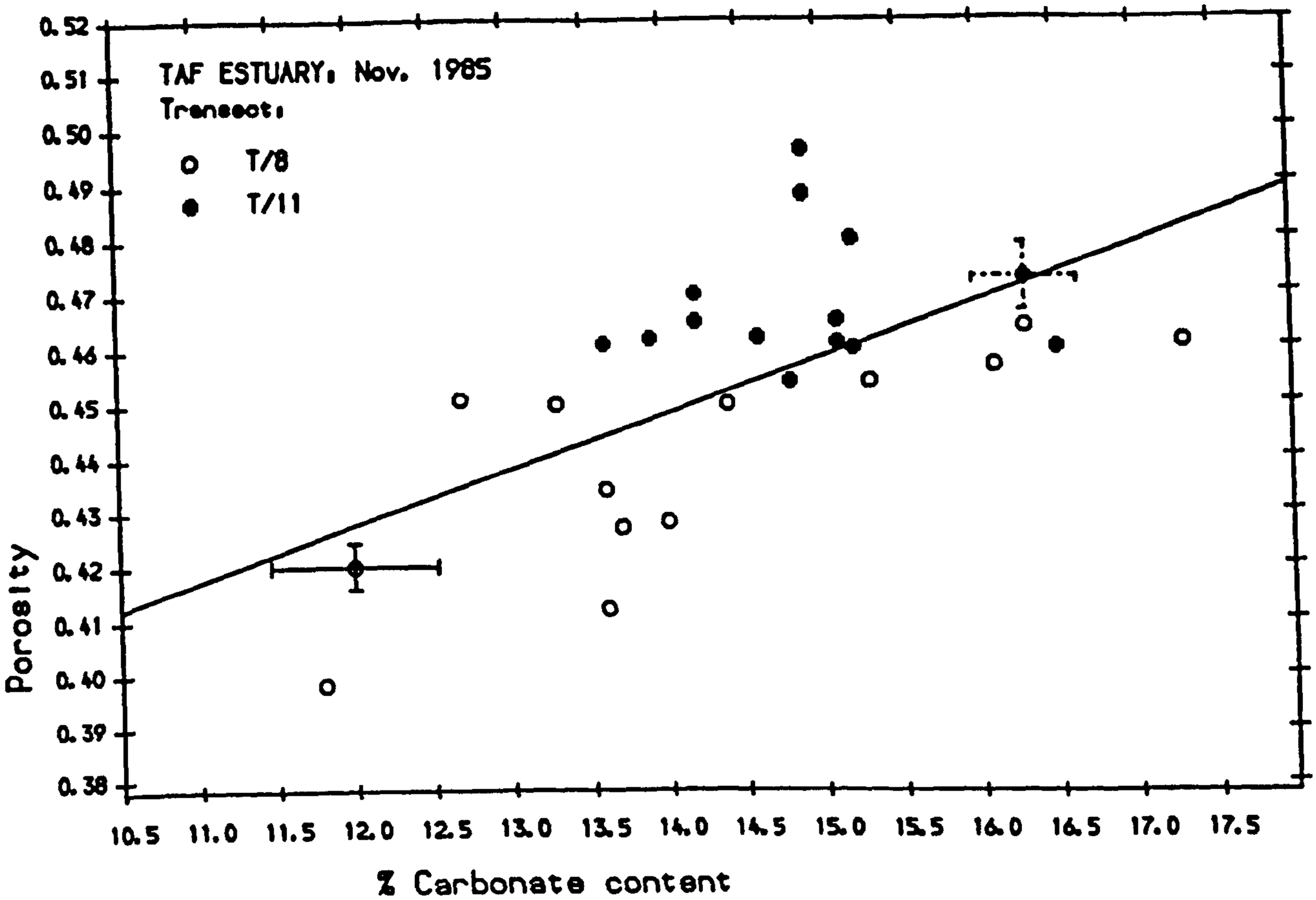

Fig. 5.2.16.

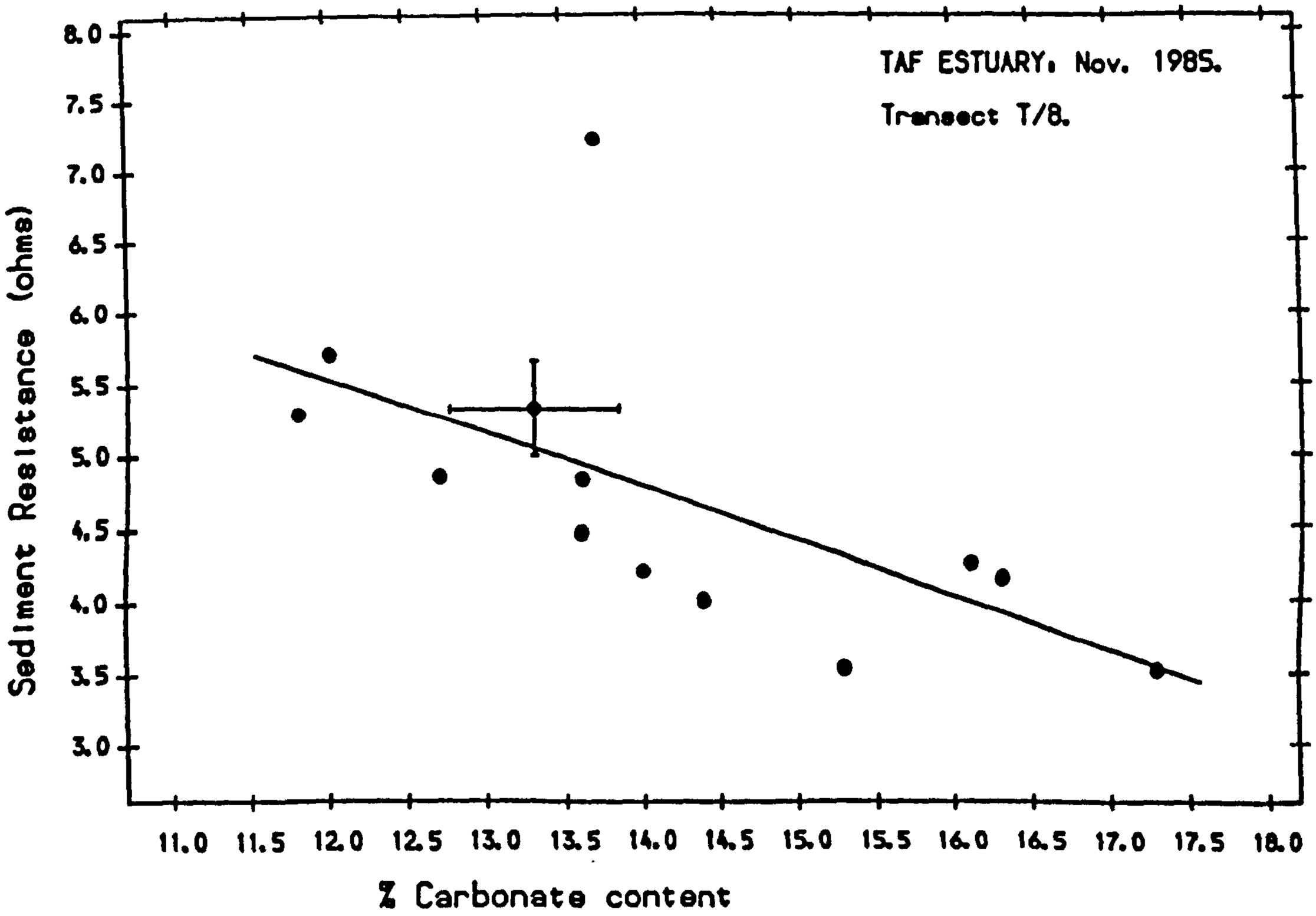

Fig. 5.2.17.

Formation Factor

As previously indicated the problems of pore fluid measurement prevented FF calculation, and therefore prevented statistical data-analysis for the full data-set.

At T/8 there is a negative relationship with carbonate content (Fig. 5.2.17), but rather surprisingly not with porosity, which is correlated with carbonate content and would be expected to affect FF directly. Sampling error or small-scale heterogeneity in R_s and porosity may have affected the results, since measurements were separately sampled within each site, and would be expected to be more variable than textural parameters. Note that the observed relationship with carbonate contradicts that found at Llanddwyn, where carbonate content is associated with a coarse subpopulation which was interpreted as reducing sediment porosity. A possible explanation is that a much larger range in carbonate was obtained at Llanddwyn, mostly associated with a sub-population having a much higher coarse:framework size-ratio, whereas the carbonate content in this case was at most only slightly coarser than the framework. Thus the 'bridging' mechanism postulated for the Taf samples may have been masked at Llanddwyn by the better packing efficiency of the binary mixture of distributions. This illustrates the problems associated with identifying universal controls on geophysical properties.

At T/11, R_s is inversely related to *Corophium* density (Fig.5.2.18), but not to porosity. Therefore a control based on the increase in sediment porosity by burrowing cannot be justified. It is possible that sampled porosity may not have been representative of the bulk sediment porosity influencing the geophysical probes. *Corophium* burrows are large scale structures compared to sediment grains, and may therefore only affect structural properties averaged over relatively large volumes. A further argument is that *Corophium* should also reduce tortuosity, thus affecting R_s more than porosity. There is significant negative partial dependence on both *Corophium* and fines content, with the fines dependence presumably related to the previously discussed effect of fines on sediment porosity. As at T/8, however, the direct dependence on porosity indicated by the textural predictor is conspicuous by its absence.

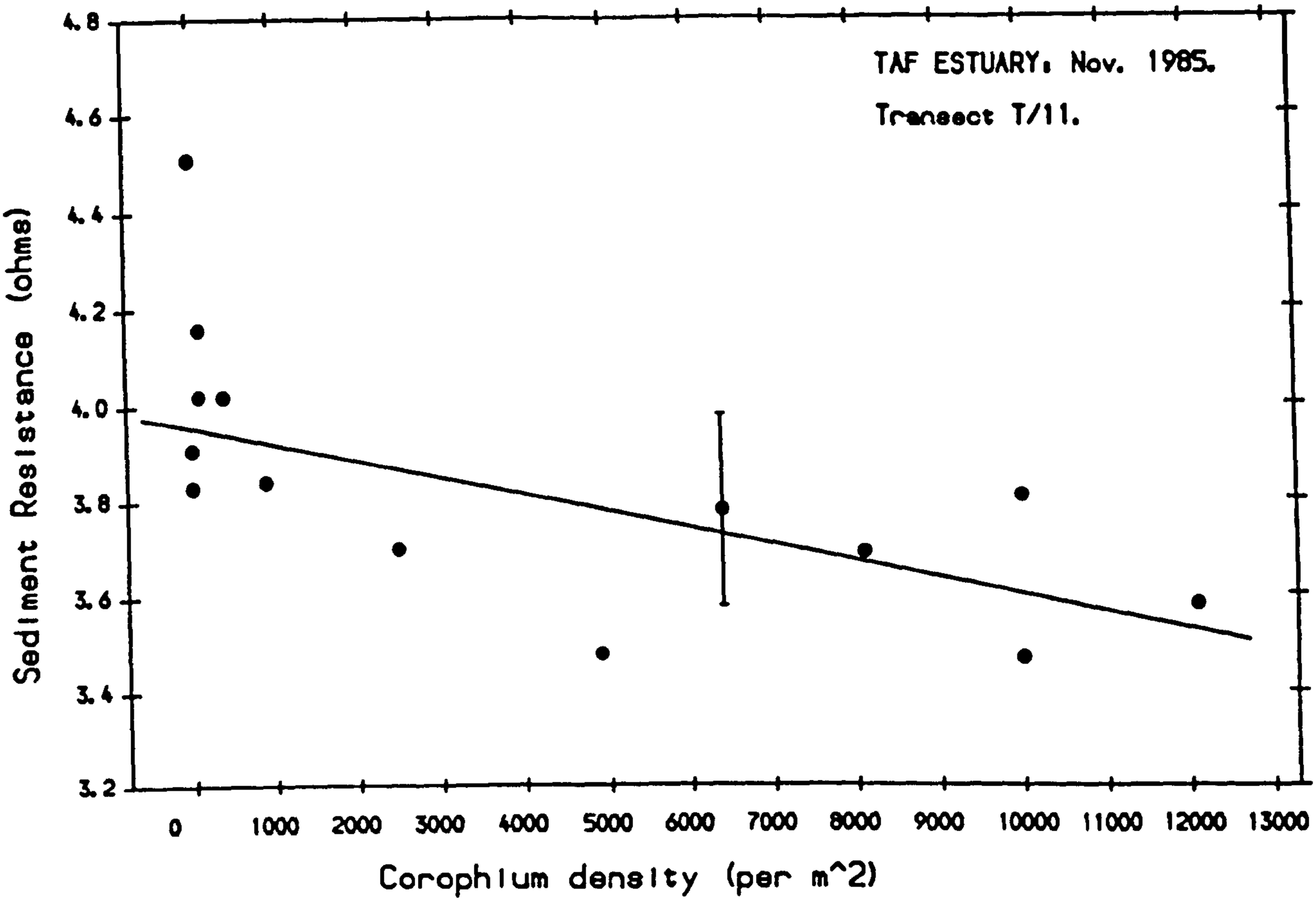

Fig. 5.2.18.

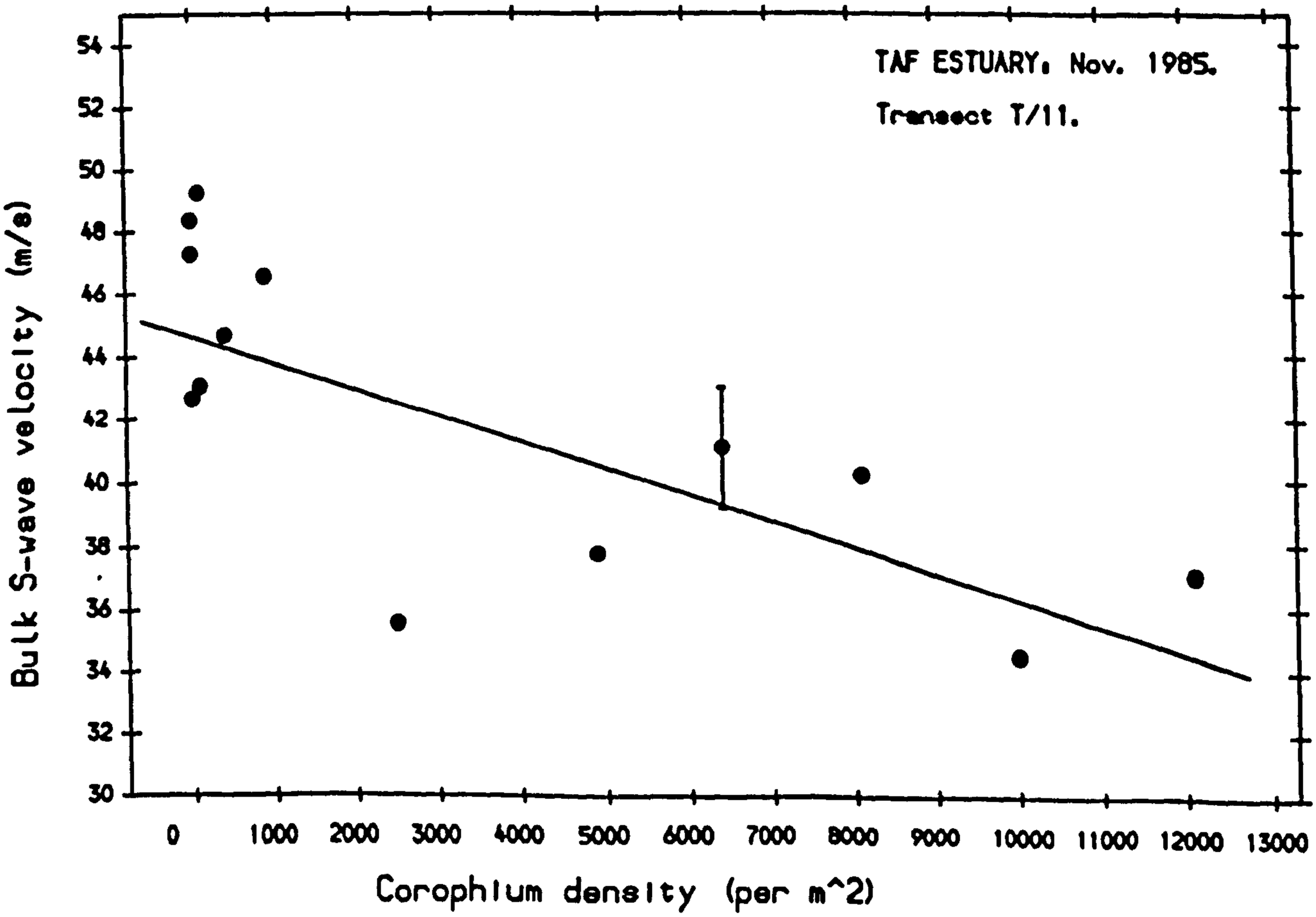

Fig. 5.2.19.

S-wave velocity.

For a given sediment, bulk V_s should be correlated with R_s, due to related (but fundamentally different) dependence on structural properties. Significant positive correlations have been obtained at both transects: correlation over the combined data-set could not performed.

At T/8 negative relationships are found between V_s and both carbonate content and porosity, these two also being directly interrelated. Thus V_s is assumed to be sensitive to porosity variation induced by changes in shell content.

At T/11, negative relationships were identified with carbonate content (as at T/8) and with *Corophium* (Fig.5.2.19). There is also significant negative partial dependence on both *Corophium* density and sediment porosity. This first confirms the laboratory findings that hollow tubes reduce V_s, and second suggests that the effect is independent of sediment porosity, at least as it has been measured here.

Since both transects show a negative dependence of V_s on porosity, this parameter would be expected to be significant for the combined data-set. A range of significant relationships is, in fact, obtained which reflects the significant differences between the two locations: V_s is negatively related to porosity (Fig. 5.2.20), fines content, and *Corophium* density. The best combination of partial predictors is porosity and *Corophium* density. However, this is not the only significant combination, with strong interaction between parameters causing difficulties in identifying direct causal links.

5.2.2.4. Comparison of *in situ* measurements with a laboratory simulation.

An additional 1500g sample was recovered from the start-point of T/8 and removed to the laboratory for geophysical assessment under more controlled conditions. A modified Jackson variable porosity cell [Jackson, 1975; and Schultheiss, 1983] was used to monitor V_s and FF for this sample over a range of artificially generated porosities. Experimental procedure has

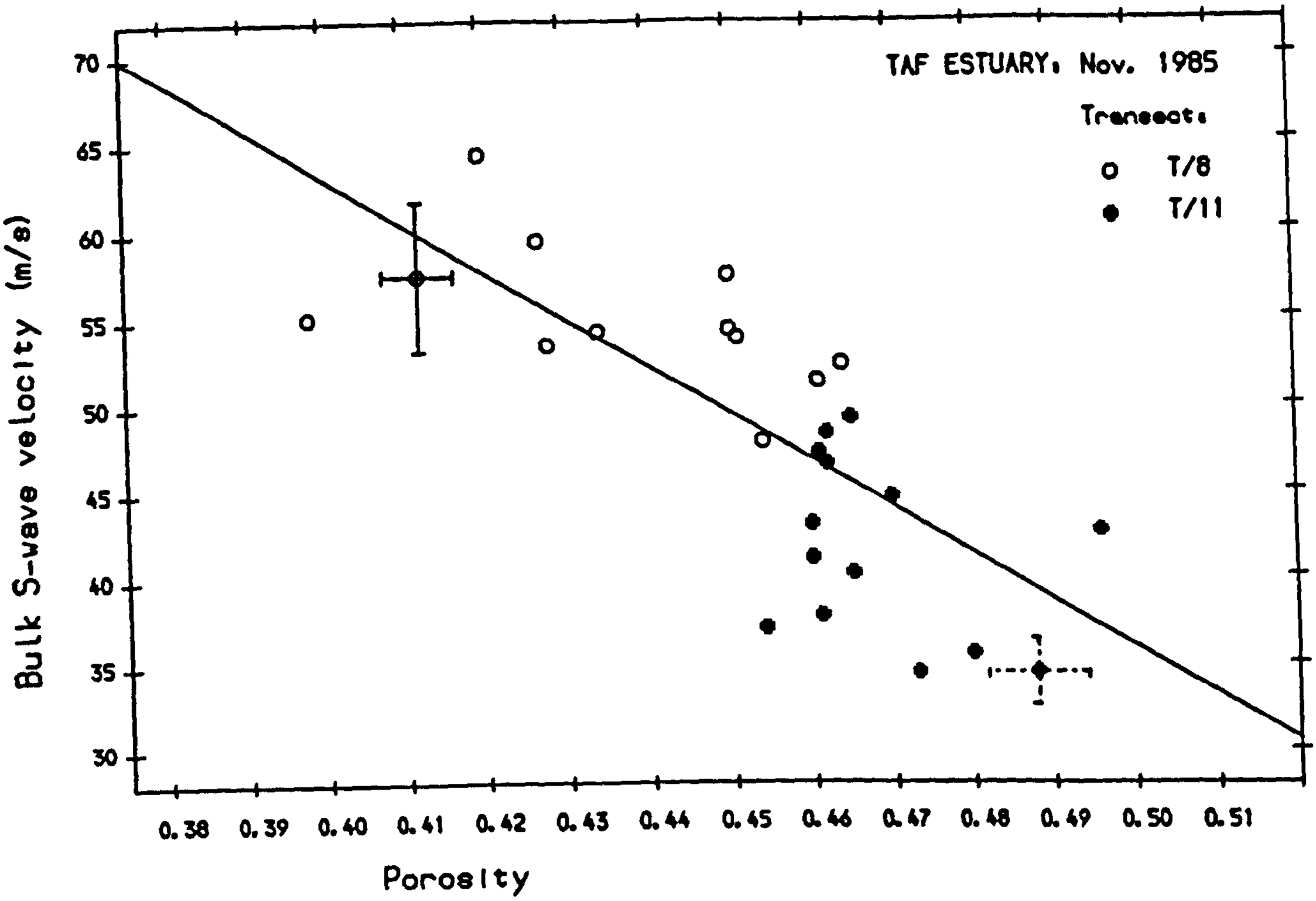

Fig. 5.2.20.

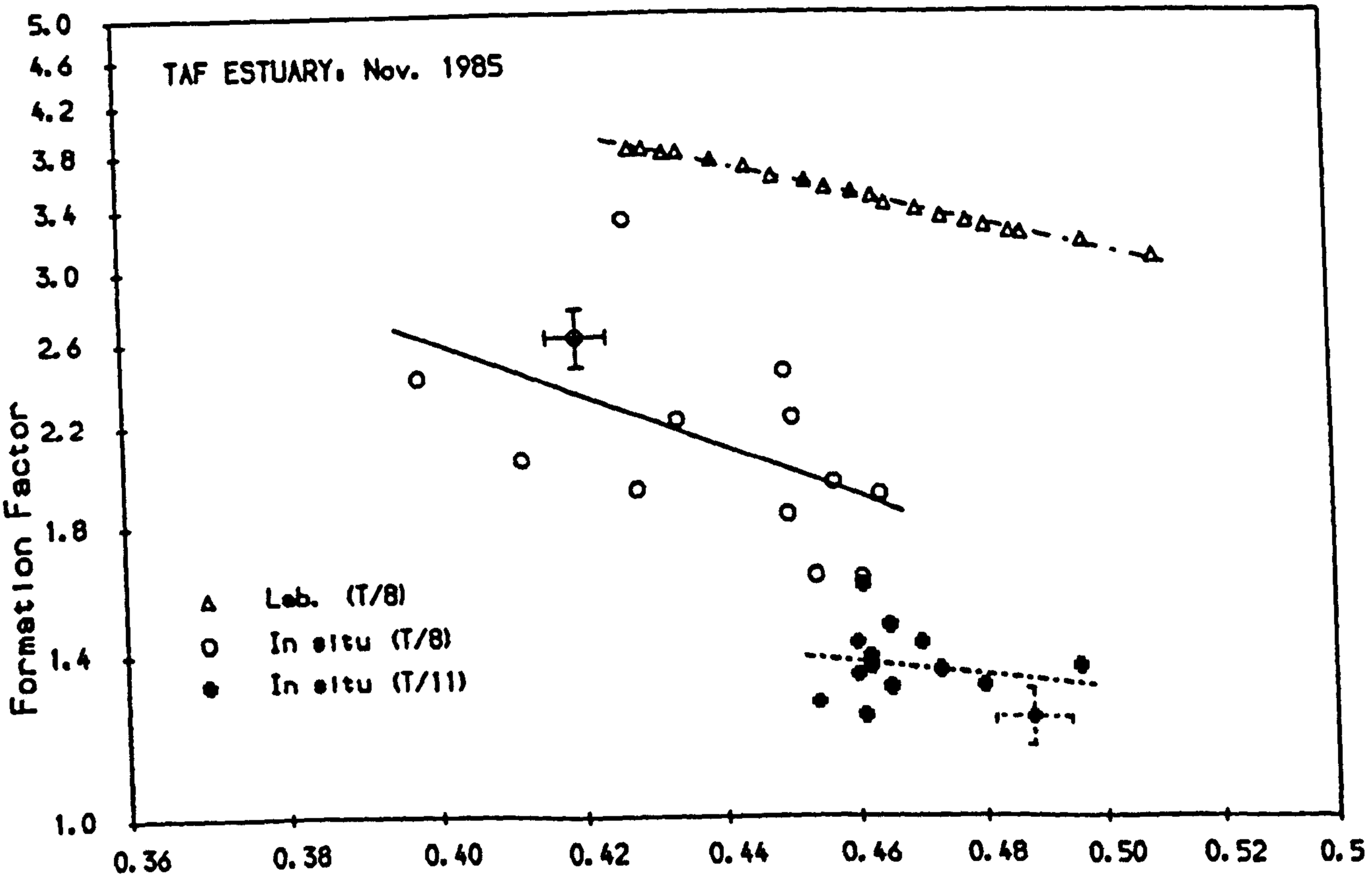

Fig. 5.2.21. FF:porosity relationships. Comparison between *in situ* and laboratory measurements.

been described in detail in the cited references: briefly, the washed, dried, weighed and re-saturated sample is gently added underwater to the graduated cell, achieving a maximum porosity depositional structure. FF and V_s are then determined over the range of porosities obtained by repeatedly tapping the cell, using probes fitted into the cell walls and calculating porosity from measured sample volume. Pore fluid resistance is measured before adding the sample, and corrected for any temperature variation during the experiment.

There are several points to consider before comparing *in situ* data with the laboratory measurements. The major difference between the two data-sets is that porosity variation is achieved in the laboratory by compaction of the same grain-size population, and in the field by spatial variation in textural characteristics combined with depositional environment and post-depositional reworking. If geophysical properties are primarily influenced, as expected, by the bulk framework characteristics, this should result in additional second order variation (and therefore considerably more scatter) for the *in situ* data.

Other important considerations are the difference in volumes and depths of sediment monitored in each case, the probable difference in depositional structures within the sediment, the use of different geophysical probes and the possibility of interference from the cell walls.

Figs. 5.2.21-22 illustrate the results for FF and bulk V_s respectively, with *in situ* data from both transects superimposed for comparison. It is interesting that the lowest porosities were achieved *in situ*: these correspond to samples with less carbonate content than the laboratory sample. *In situ* porosity for the site from which the laboratory sample was recovered was 0.464.

FF values were, as expected, much higher than those calculated from the erroneous *in situ* measurements of pore fluid resistance. The laboratory simulated FF:porosity relationship yields an Archie coefficient (m, Eqn. 2.38) of 1.37 and constant (a_F) 1.18, (R^2 = 0.99). If this relationship can be assumed to apply *in situ*, then pore fluid resistance (calculated from R_s and porosity at the appropriate site) should have been 1.58ohms.

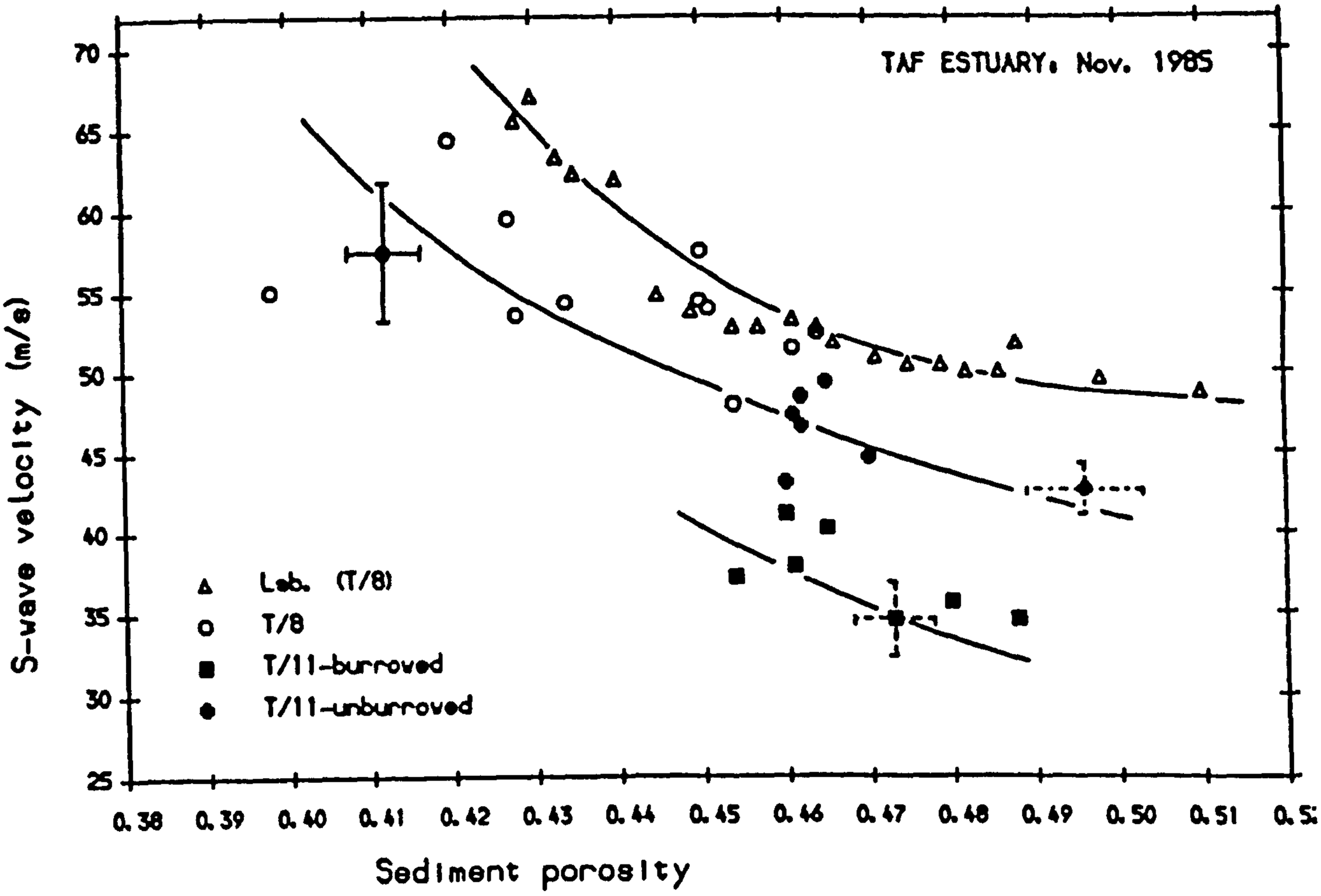

Fig. 5.2.22. V_s:porosity relationships. Comparison between *in situ* and laboratory measurements.

Regression lines superimposed on the *in situ* data do not represent significant linear relationships. However, they do illustrate that the data are not incompatible with a linear relationship, allowing for high scatter induced by textural variation (and hence tortuosity) and sampling error. Since log-scales have been used in the figure, the error in R_w translates to a simple linear 'offset'.

The V_s results show much better agreement in absolute terms. The fact that the S-wave probes are positioned at a depth of *c.* 15cm may partially explain the slightly higher velocities observed in the Jackson cell. Straight lines are clearly inappropriate for any of the data-sets: the hand-fitted curves in Fig. 5.2.22 are for illustrative purposes only. *In situ* and laboratory data show similar V_s:porosity relationships provided that data from the sites containing 'high densities' of *Corophium* (taken as the first 70m of the transect in Fig. B2.4) are ignored. This sub-set of data is offset below the general trend, indicating that an additional control which is independent of sediment porosity is in operation.

5.2.2.5. Summary and interim conclusions.

The sediments sampled along Transects T/8 and T/11 in the Taf Estuary consist of a uniform lognormal framework population of fine sand, comprising at least 90% of the grain size distribution, with variable proportions of a shelly coarse 'tail' and admixed fines comprising the remainder. Although there are significant between-transect differences in mode of this framework population, they are very small, and are assumed unimportant as controls on packing configuration. Increasing both coarse and fine subpopulations (as measured by carbonate and fines content respectively) causes an increase in porosity, this being shown directly from measurements of porosity and supported indirectly by R_s and V_s measurements. The proposed mechanisms are: 'bridging' by platy shell fragments; and less energetic deposition rate and distortion of the framework by fines. The ratio of framework grain size to that of both coarse and fine sub-populations is compatible with these mechanisms.

In addition to significant (if second order) textural variability along

and between the two transects, marked spatial heterogeneity in density of *Corophium* was measured along the muddier Transect T/11. The absence of *Corophium* at T/8, and along the portion of T/11 closest to the ebb-channel, is probably governed by hydrodynamic environment. Surprisingly, a direct inverse relationship between *Corophium* density and sampled porosity is not observed. However, inverse relationships with both R_s and V_s indicate that *Corophium* burrows do have a significant effect on sediment packing configuration, reducing both tortuosity and rigidity. It is suggested that porosity samples were less representative of bulk sediment properties than the geophysical measurements in this case.

5.2.3. Traeth Lligwy: further measurements on *Arenicola* flats.

Two locations at Traeth Lligwy were sampled on successive days in May 1986. The first (A) was concentrated in an area of depressed beach-level near a fresh-water outflow, the second (B) traversed a shallow ebb-channel some 150m seawards. Both featured variable number densities of *Arenicola*: regions of *Arenicola* abundance corresponded closely with those parts of the foreshore which remained saturated over most of the tidal cycle.

Location (A) was sampled, as at Llanddwyn (5.2.1), by selecting for organism abundance within a 20 × 5m area. Location (B) was sampled at 2m intervals along a measuring tape. Both sets of samples served to characterise shore-parallel, rather then shore-normal variation, since locally high water-table levels rendered it unnecessary to follow the ebbing tide level down the beach.

5.2.3.1 Site characterisation

Structural characteristics.

The most striking surficial features were *Arenicola* casts, with surface topography most pronounced at location (A). This observation, combined with the presence of algal blooms, suggested that the sediment was more

protected from tidal reworking at this location. This was also supported by the hydrodynamically derived bedforms: planed-off ripples (not necessarily recent) at (A), plane beds at (B).

One further observation is relevant: exploration of the sub-surface revealed a distinct shell/pebble layer at approximate depths of 7cm at (A), 10cm at (B). These were below the maximum depth penetrated by the sediment sampler, so could not have contributed to measured textural variability. However, their presence might have influenced some of the geophysical measurements, as will be discussed later.

Textural characteristics.

Fig. 5.2.23 illustrates a selection of typical grain-size distribution curves from both locations. Once again, remarkable uniformity of the framework population is indicated. Population splitting was performed for all samples, and identified a highly uniform log-normal framework with significant but small differences between the two locations: an average 0.1 phi finer and 0.01 phi better sorted at (A) than at (B).

The fine sub-population varies between 0.3 and 0.5%, and was therefore discarded as irrelevant. The coarse sub-population ranges between 8 and 24%, with higher percentages (and greater variability) at (B). These percentages correspond closely with the fraction coarser than 1.25 phi (r = 0.99), which was therefore selected as an appropriate cut-off. Further examination of the grain-size distributions (Fig. 5.2.23) reveals that the coarse sub-population can be further split into two: one component of mode c. 1.0 phi and a second component (which causes variation in the extreme coarse tail), selected as the fraction coarser than 0 phi. This coarsest fraction was, not unexpectedly, the major contributor to observed variation in sorting.

Therefore two parameters were selected as significant contributors to textural variability at Lligwy: the fraction coarser than 0 phi, and the fraction between 0 and 1.25phi, with each representing a sub-population of different sub-mode:framework size ratio. The small between-location

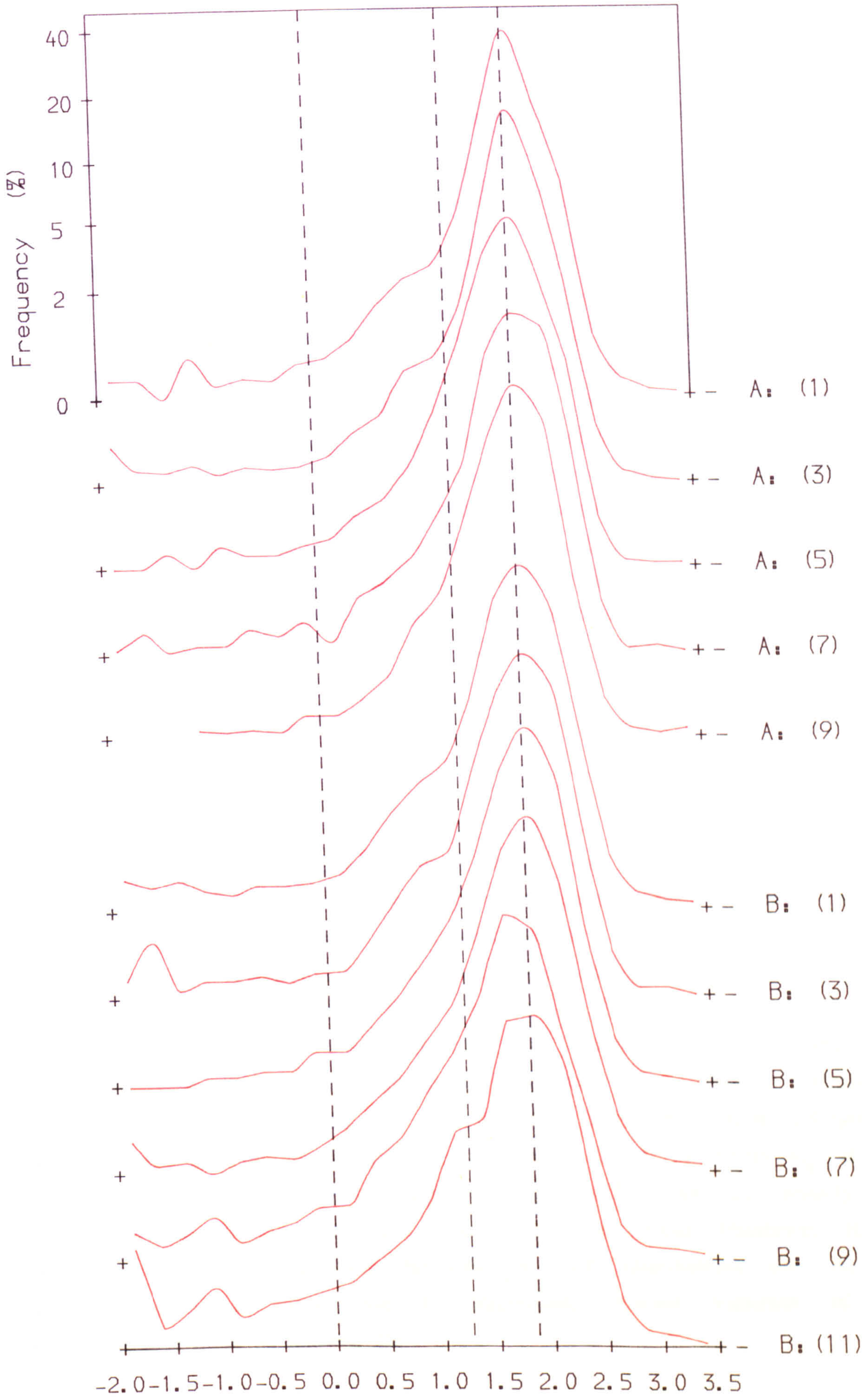

Fig. 5.2.23. TRAETH LLIGWY. Selected grain size distributions.
(Key: Location reference, Sample No.).

differences in size distribution of the modal population were not thought to be important.

Biological characteristics.

Arenicola was characterised, as at Llanddwyn, by counting casts. One of the casts at (B) was sampled to investigate the textural characteristics of excreted material. Its grain-size distribution was very similar to that of the surrounding material except that no material coarser than 1mm (0phi) was present. This was expected, since *Arenicola* is unable to manipulate or ingest coarse particles [Baumfalk, 1979]. Furthermore, carbonate content was 4%, which is more than 1% lower than the minimum fraction sampled at either location, and which indicates that shell fragments are even less likely to be ingested by *Arenicola*.

Geophysical characteristics.

Formation Factor.

Six replicate R_s measurements were made at each site, to improve estimation of small-scale heterogeneity. Site-means were converted to FF using pore fluid resistances calculated from salinity and temperature values measured at intervals throughout the sampling period. Table B3.1 details these measurements. The significant difference in pore fluid salinity between the two locations can be attributed to the fresh-water supply observed near (A). Temperature changes were probably related to diurnal warming and cooling of the exposed foreshore. Linear interpolation between measured pore fluid values was employed at A to obtain R_w at each site from the time of sampling. At (B) differences in salinity and temperature resulted in little net change in pore fluid resistance: it had to be assumed that this was the case at each intermediate site. At both locations, additional error due to imprecisely known variation in pore fluid resistance must be allowed for.

S-wave velocity.

At both locations the complication of velocity layering affected V_s selection. Surface V_s was significantly lower than bulk V_s, with the greatest difference at (B) (Fig. B3.1). Therefore V_s measurements were influenced at both locations by strong vertical heterogeneity, with that at (B) having a steeper gradient. This supports the observation of sub-surface layers of contrasting texture at both sites, although it is not suggested that these can be directly characterised by measured 'surface' and 'sub-layer' velocities.

At both locations, the parameter thought most likely to be related to sampled textural characteristics and porosity was surface V_s, since this corresponds to the upper 40mm of strongly heterogeneous deposits. Both surface and bulk parameters were retained throughout analysis, however, because bulk V_s was thought to be a more reliable measurement. Table B3.2 lists location means of selected parameters, along with coefficients of variation and mean within-site variability where appropriate.

5.2.3.2 Localised variability of measured properties.

At (A), spatial distribution of sites was dictated by organism density, while at (B) measurements were constrained along a shore-parallel line. Figs. B3.2-3 illustrate variation of parameters at (B). Variability in porosity is lower than in mean grain size at (B); higher than in mean grain size at (A). As will be shown, this may be explained by the fact that two opposing controls on porosity are directly correlated at (B).

With the exception of sediment porosity and *Arenicola* density, the observed spatial variability of any one parameter is significantly higher at (B) than at (A). Indeed, location variances at (A) are not much higher than sampling error estimates, especially for the geophysical properties, which caused problems in identifying significant relationships between parameters.

Significant (1%) between-location differences are obtained for the 0:1.25

phi fraction, the highest values being at (B). Surface V_s and FF yield higher location mean values at (A), albeit with a reduced level of significance (5%). There are no significant differences in bulk V_s, porosity or carbonate content.

5.2.3.3. Relationships between variables.

Relationships between measured properties have been considered first at individual locations, then for the combined data-set, in order to include investigation over larger spatial scales. Table B3.3 lists significant correlation coefficients for textural and biological parameters, while Table B3.4 summarises regression results obtained for porosity, FF and V_s.

Textural interrelationships.

The primary textural controls on mean grain diameter and sorting have already been identified as the two coarse fractions %>0phi and %0:1.25phi. The fact that correlations were not observed between these fractions suggests that they are effectively independently controlled contributors to textural variability.

At (A) textural variability is relatively small in all parameters except the 0phi fraction. At (B), higher ranges in textural parameters lead to positive correlations between carbonate content and the coarse fractions, especially the combined fraction coarser than 1.25phi (Fig. 5.2.24). This indicates that, as expected, the shell fraction is mostly associated with the coarse tail of the distribution. Linear regression indicates that *c.* 3% of the modal population, and 20% of the coarse fraction is carbonate. This also explains the lower shell fraction found in the *Arenicola* cast, which contained no grains coarser than 0phi. It is interesting that carbonate content is independent overall, which indicates differences in textural composition between the two locations. This is illustrated by the data from (A) in Fig. 5.2.24, with higher carbonate content than (B) for a given coarse fraction. Whether this is caused by more shell in the framework population (i.e. higher intercept) or in the coarse fraction

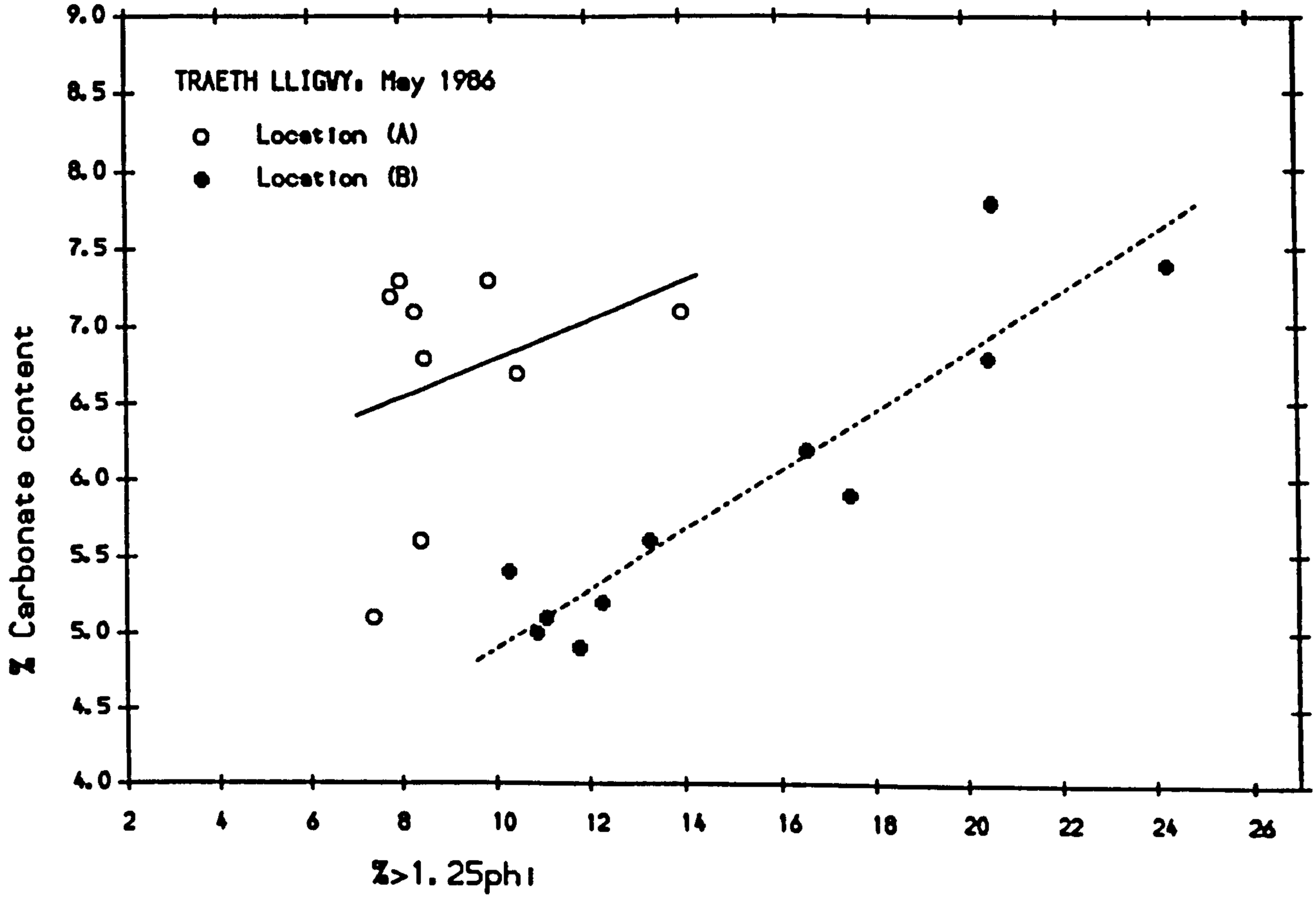

Fig. 5.2.24.

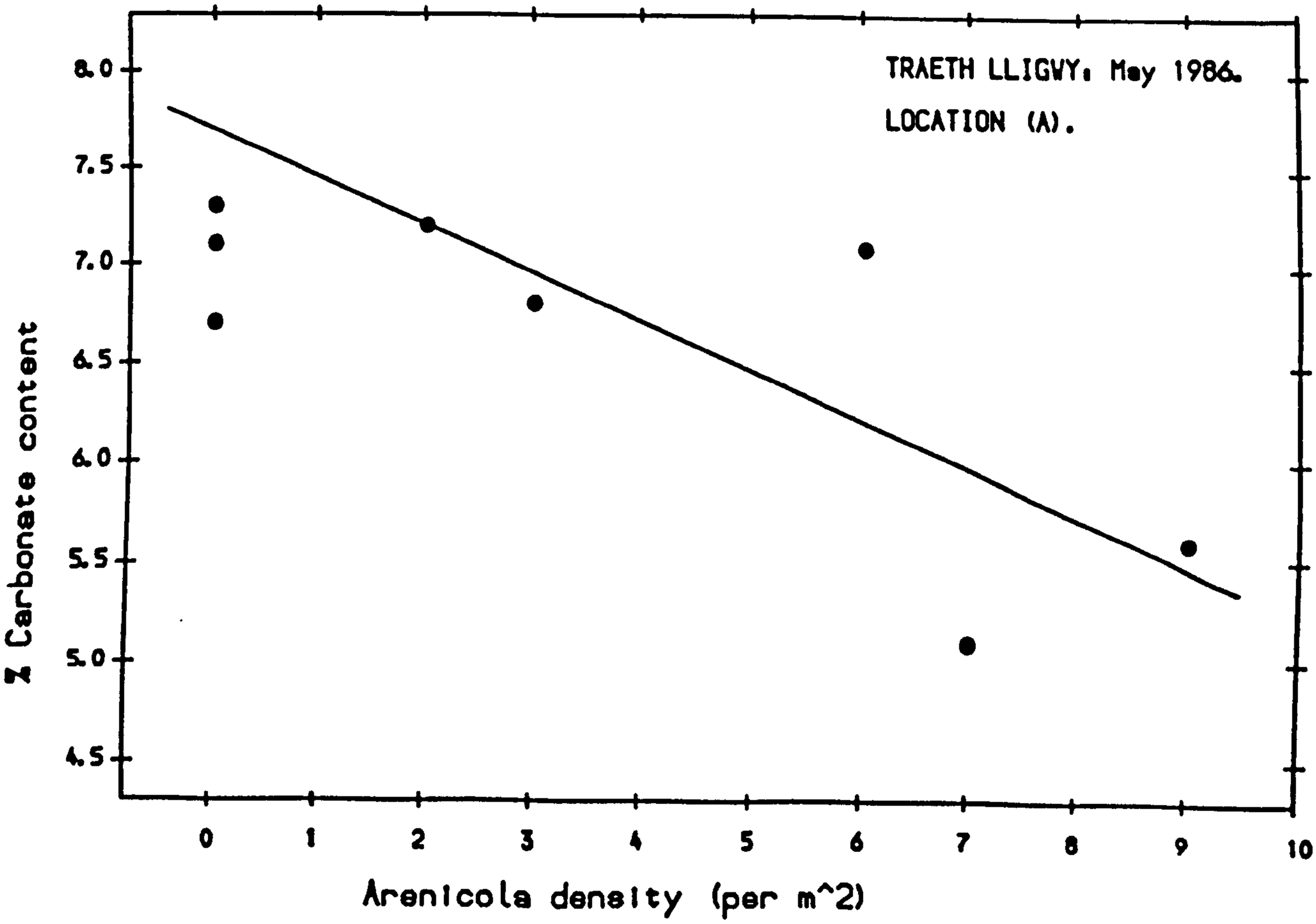

Fig. 5.2.25.

(higher slope) is uncertain due to scatter. It does suggest that caution should be exercised in combining data from the two locations, since these unexplained textural differences may affect other properties.

Textural/Biological interrelationships.

The fact that the *Arenicola* cast at (B) differed in textural composition from the surrounding sediment suggests that *Arenicola* activity can affect textural properties of a deposit. However, at (B) this biologically-mediated sorting was not verified by a correlation between *Arenicola* density and textural properties of the substrate. At this location casts are completely eroded and reworked on each tide, with the result that any change must have been relatively widely distributed, irrespective of within-site organism abundance.

In contrast, at (A) the sediment was apparently much more stable, as previously described. It is likely that reworking is only significant during storms or on spring tides, providing individual organisms with more time to affect local textural properties. Accordingly, negative correlations are observed between *Arenicola* density and the fraction coarser than 0phi, and independently with carbonate content (Fig. 5.2.25). Thus, as expected, *Arenicola* funnels sediment down the head shaft, rejects particles coarser than 0phi, and excretes the remainder at the surface.

This mechanism may also serve to explain the observed shell layer at 7cm. The same mechanism should also have been in force at (B), with progressive build up of coarse material in a layer around head-level of the organisms (as observed in this case at 10cm). The difference is that the effect should be much more concentrated around, and therefore related to, individual organisms at the less mobile (A).

Porosity.

No relationships were identified between porosity and textural or biological predictors at (A). Significant partial regression coefficients

are obtained at (B), indicating a positive relationship with carbonate content and negative one with the fraction coarser than 0phi. This result is interesting because the shell fraction and coarse fraction are themselves directly correlated, so that the significance of their opposing effects must represent an underestimate. Note that this is precisely the scenario proposed to explain the apparent lack of variability of porosity at location (B), with two controls effectively cancelling each other out.

The combination serves to tie in results at both Llanddwyn and the Taf. At Llanddwyn a coarse sub-population of high coarse:framework size-ratio, containing a large proportion of shell fragments, was thought to reduce sediment porosity, while in the Taf estuary the shell fraction, this time in a sub-population of much smaller coarse:framework size-ratio, was shown to increase it. At (B), the shell fraction is related to both coarse sub-populations, most significantly to the 0:1.25phi fraction. The regression results indicate that sub-populations with high coarse:framework size-ratio act to reduce sediment porosity by improving packing efficiency, while platy shell fragments rather closer in size to the framework population act to increase porosity by bridging across adjacent sediment grains on deposition, thus preventing close packing. Since similar textural interrelationships were not identified at (A), and since overall ranges were rather less, the absence of significant controls on porosity at this location does not contradict this argument. Overall, results support the relationships identified at (B).

It had been expected that *Arenicola* activity would affect bulk sediment porosity, this mechanism having been proposed to explain FF variation at Llanddwyn. However, as with the measurements on *Corophium* in the Taf estuary, the small sample size may have been unrepresentative of the bulk sediment influencing geophysical measurements, especially since porosity cores were generally taken in areas between casts.

Formation Factor.

The only significant relationship identified for FF is negative, with *Arenicola*, at (B) (Fig. 5.2.26). This corresponds well with the results

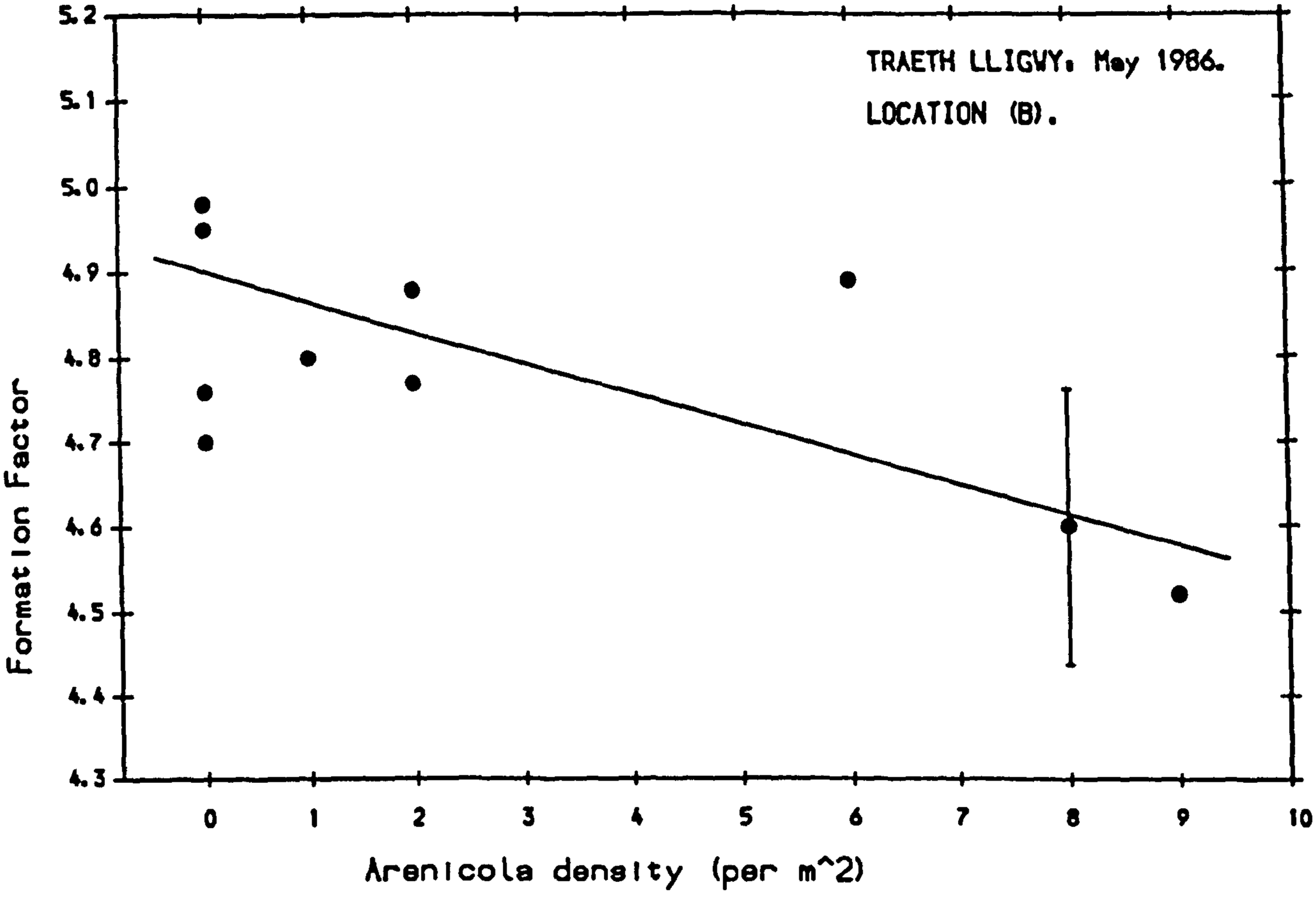

Fig. 5.2.26.

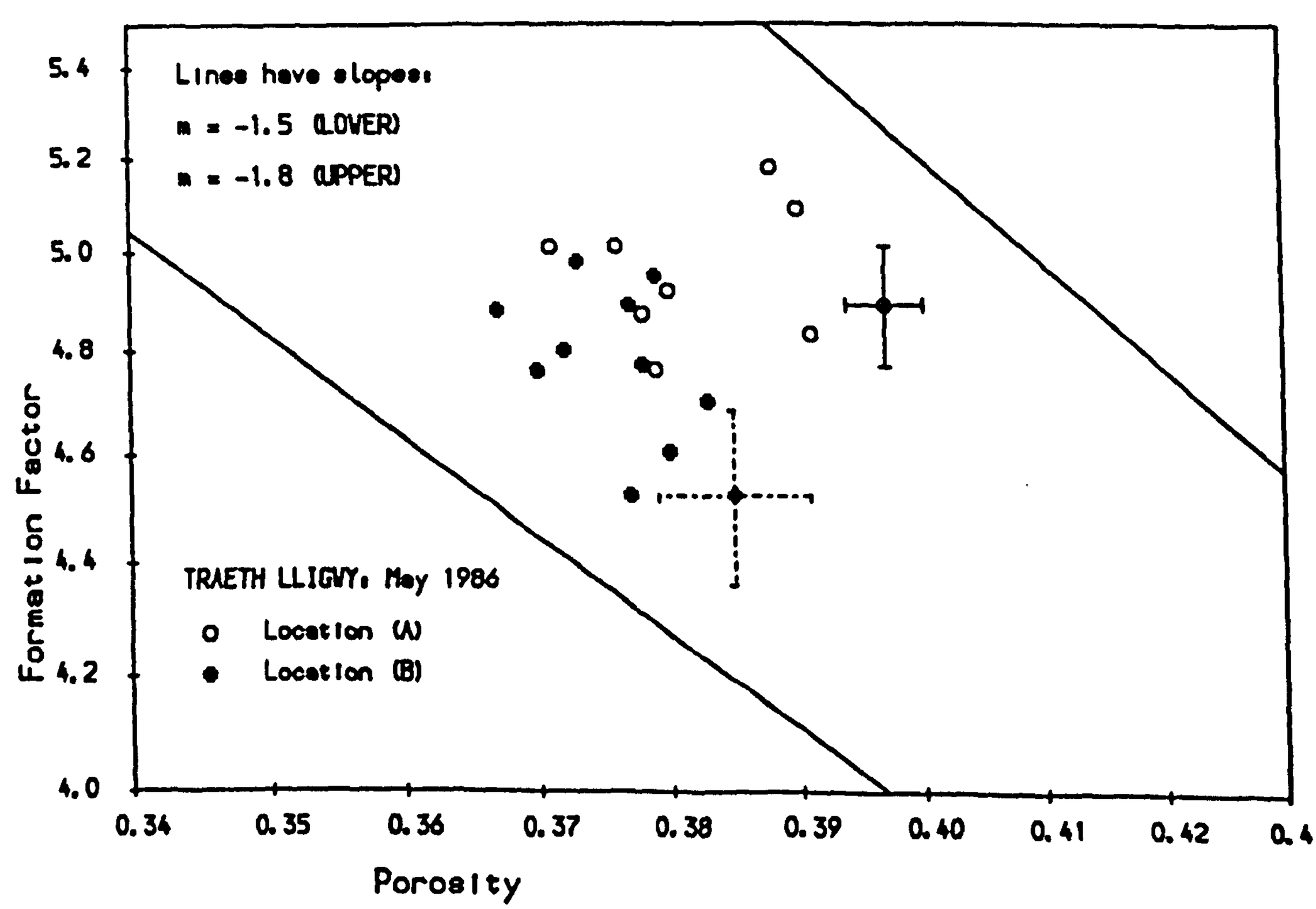

Fig. 5.2.27.

observed at Llanddwyn, but is unfortunately not observed at (A). There are no significant multiple regression results for either location, indicating poor correspondence with measured sediment properties. Fig. 5.2.27 illustrates both sets of data on an FF:porosity plot, with typical Archie relationships for sand superimposed. It is clear that the small ranges in both porosity and FF rendered the results susceptible to sampling error, although the absolute values do at least appear to be reasonable. Note that this figure indicates between-location differences in the measured FF:porosity relationship, represented by higher FF for given porosity at (A). If this were interpreted using Archie's relationship, the inference is that m is higher at (A), although no suggestion that the data supports an Archie relationship is implied, since observed scatter is of the order of sampled range at both locations. The difference may have been caused by the apparent differences in textural composition of the two locations, associated with the size distribution of the shell fraction. This might, for example, affect pore-space tortuosity.

Apart from sampling error, the lack of significant relationships between measured properties may reflect differences in sampled volumes. Hence, as already suggested, porosity was unrelated to *Arenicola* activity because much larger sediment samples would have been required to incorporate burrows. Perhaps most importantly, FF measurements could have been influenced by sub-layers to a depth of more than 15cm, with the result that they could have been affected by un-characterised sediment properties in addition to those of the surface layer.

S-wave velocity

As stated in 5.2.3.1, two S-wave velocities were required to characterise the vertically heterogeneous deposits at Traeth Lligwy. Bulk V_s therefore corresponds to an effective sub-layer below *c.* 40mm, and should not necessarily correlate with sampled textural characteristics. In fact the only significant relationship found is with *Arenicola* density at (B). This is consistent with the inverse relationship observed for FF, although the geophysical properties were not significantly correlated. Note that *Arenicola* should affect properties of the sublayer as well as the surface.

When surface V_s is considered, more relationships with measured properties are obtained at (B) (but not at (A)). Surface V_s is directly related to the 0phi fraction and inversely related to *Arenicola* density (Figs. 5.2.28-29). There are two significant combinations at (B), the best being a positive partial dependence on the percentage coarser than 0phi combined with a negative partial dependence on the 0:1.25phi fraction. *Arenicola* density could also be substituted for the latter. It is natural to interpret these relationships as indirect (as at Llanddwyn), through textural and biological controls of porosity, with admixed coarse particles reducing porosity and *Arenicola* activity increasing it. However, measured sediment porosity is not significantly related to V_s.

It is interesting that the coarse fractions should act in this way on V_s. The shell fragments associated with the 0:1.25phi fraction have been shown to increase sediment porosity at this location, while the 0phi fraction reduces it. As in the Taf estuary, underlying controls on sediment porosity appear to have the expected effect on measured geophysical properties without a specific dependence on porosity being identified. *Arenicola* may also have increased bulk porosity, as indicated by the FF results at Llanddwyn, but only over volumes not represented by the porosity sampler.

Overall, a negative dependence on *Arenicola* is obtained, but with considerable scatter. This suggests that *Arenicola* is the dominant control at these highly bioturbated locations, but that V_s is also sensitive to other controls. Significant partial regression coefficients have also been obtained for the two coarse fractions as at (B): however, the reduced R^2 values imply that the data at (A) tends to detract from, rather than support, this relationship, despite the higher textural ranges involved.

The difference observed between locations (A) and (B) for FF can also be identified for surface V_s. Fig. 5.2.30 illustrates V_s plotted against measured porosity: once again, values for the different locations are clustered, with (A) generally higher for a given porosity. This supports the assertion that there were textural or structural differences between the two locations which cannot be identified using the selected parameters. One possibility is the difference in size-distribution of the

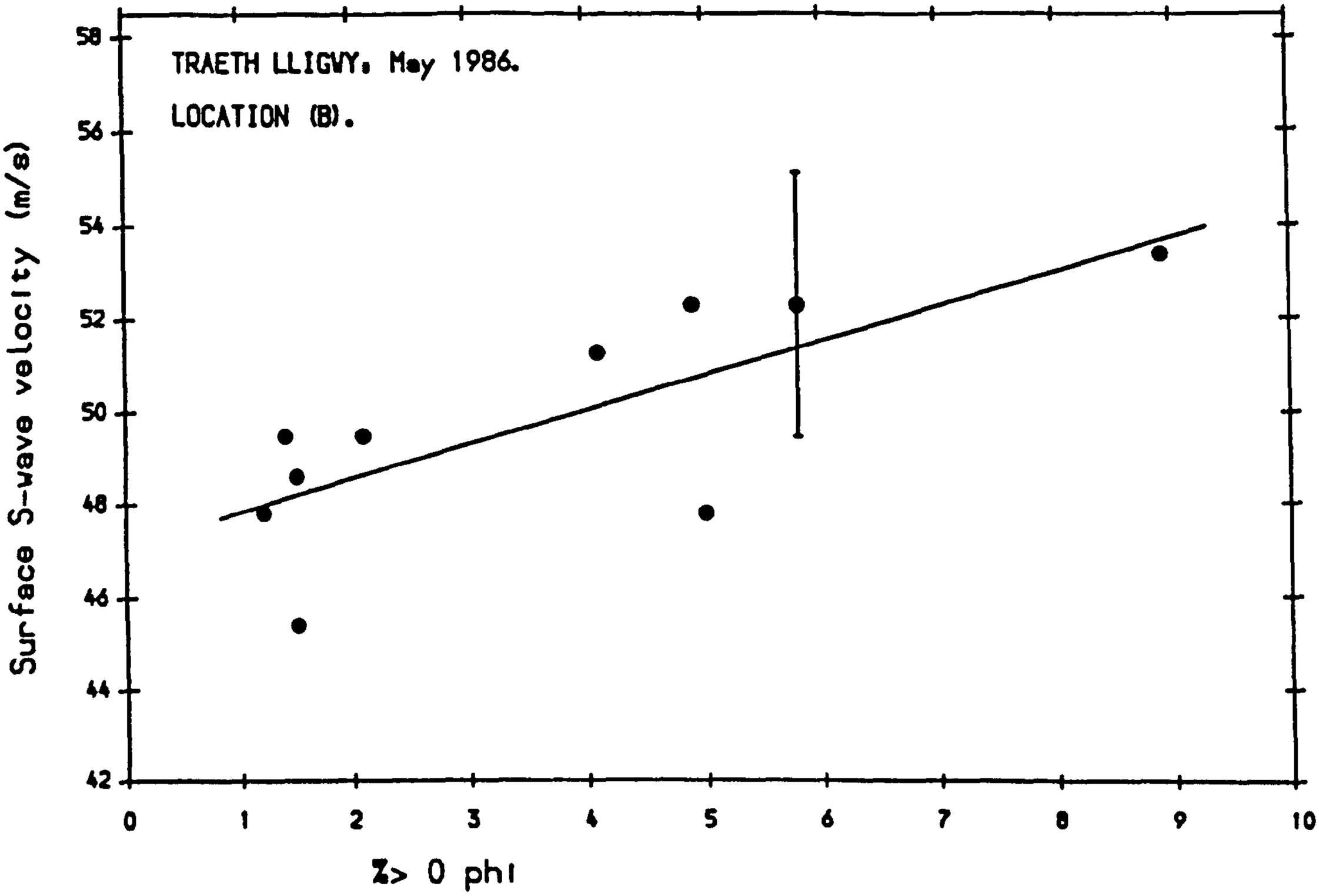

Fig. 5.2.28.

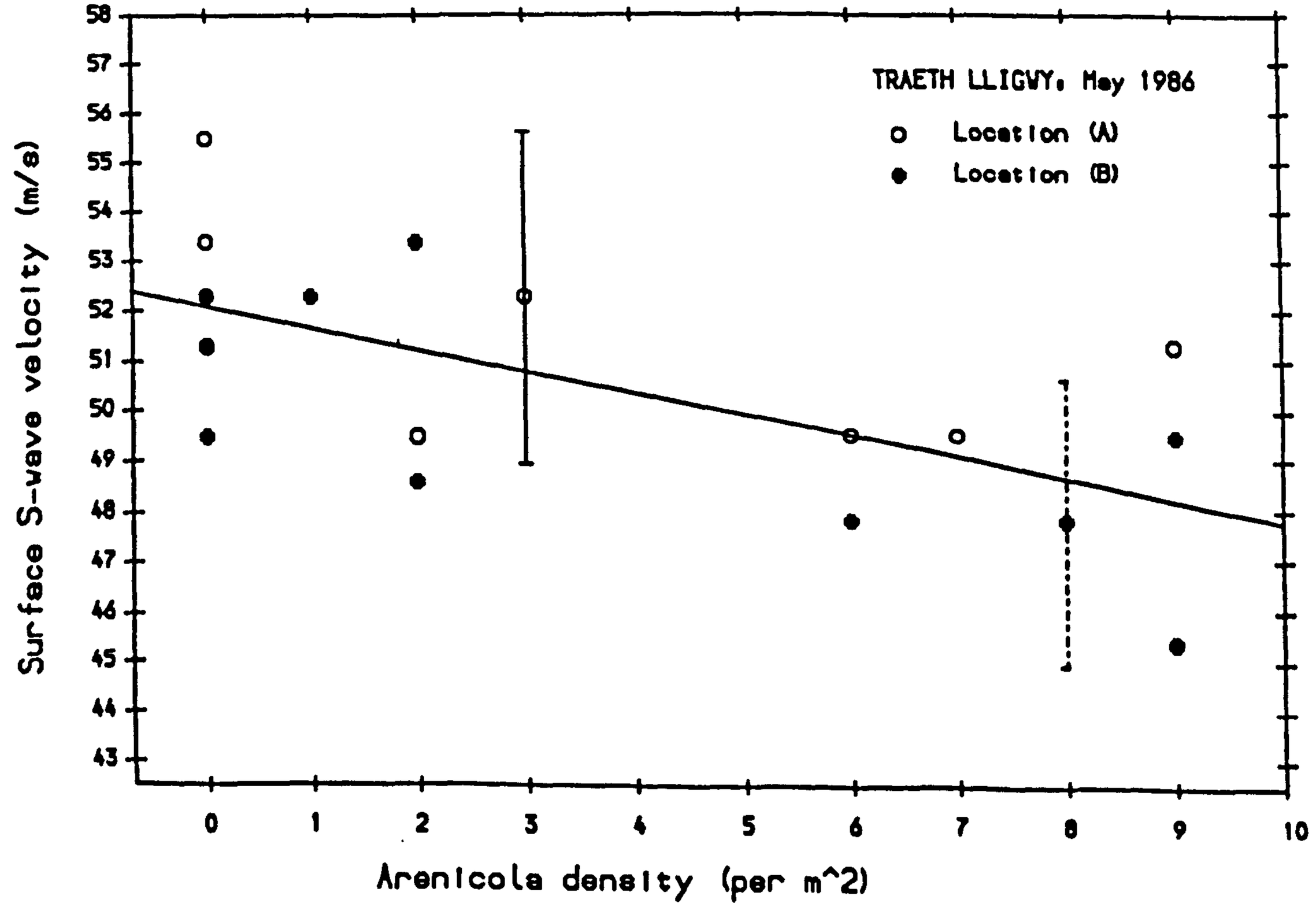

Fig. 5.2.29.

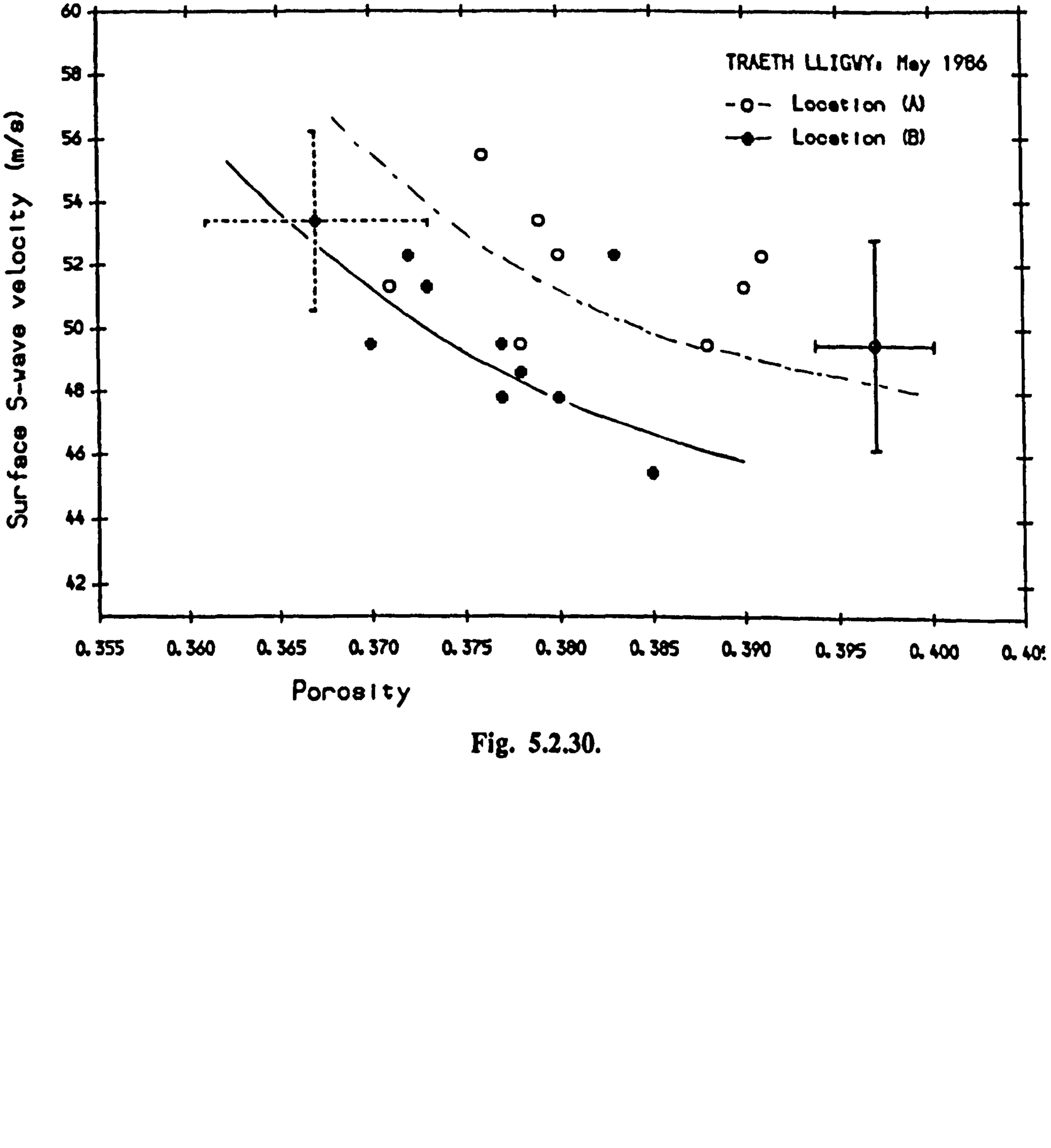
TRAETH LLIGWY: May 1986
-o- Location (A)
-●- Location (B)
Surface S-wave velocity (m/s)
60
58
56
54
52
50
48
46
44
42
0.355
0.360
0.365
0.370
0.375
0.380
0.385
0.390
0.395
0.400
Porosity

Fig. 5.2.30.

shell-fraction, or textural composition of the sub-populations, indicated by the carbonate:%>1.25phi scatterplot (Fig. 5.2.24). For example if, as the FF results indicate, tortuosity is increased, the number of intergranular contacts (and hence V_s) might also be expected to increase.

5.2.3.4. Summary and interim conclusions.

Sediments sampled at Locations (A) and (B) at Traeth Lligwy consist of a uniform lognormal framework population comprising a minimum of 75% of the grain size distribution. Textural variation is introduced via two independent shelly coarse fractions, parametrised as the percentage coarser than 0phi and that between 0 and 1.25phi, which between them comprise between 8 and 24% of the grain size distribution. There is apparently a difference in textural composition of the subpopulations at the two locations: sediment at (A) contains higher carbonate content for a given proportion of coarse particles.

At (A), there are no relationships between measures of packing configuration and textural parameters. It is possible that within-location variability observed at this location is too low to allow analysis of controls, given the high degree of within-site heterogeneity. At (B), porosity is increased by carbonate content and reduced by %>0 phi. The proposed mechanisms for this relationship are supported by observations in the Taf Estuary and at Traeth Llanddwyn. Shell fragments associated with the less coarse of the two subpopulations act to increase porosity by 'bridging', whereas the coarsest particles reduce porosity by allowing a closer packing configuration.

Although FF is unrelated to any textural parameter, between location differences in tortuosity are indicated by comparison of FF:porosity scatterplots. This supports the proposed differences in textural composition, with higher tortuosity at (A); and is further supported by similar differences in V_s:porosity plots, indicating increased inter-granular friction at (A).

Both locations featured variable population densities of *Arenicola marina*.

At (A) an inverse correlation with both % > 0 phi and carbonate content confirmed the proposed sorting of coarse particles into the substrate by *Arenicola* feeding activity, with cast material containing no coarse fraction and reduced carbonate content. *Arenicola* does not directly affect sampled porosity, in apparent contradiction to its proposed effect at Traeth Llanddwyn. However, FF is reduced by *Arenicola* at (B), in direct support of the Llanddwyn findings, and V_s is also reduced by *Arenicola* in agreement with the laboratory experiment (3.4.9). As in the Taf Estuary, it is thought that geophysical measurements, rather than sampled porosity, may have been the more representative of bulk sediment properties in these spatially heterogeneous bioturbated deposits. This does not, however, explain the absence of any effect on either FF or V_s at (A). A failure of the field measurement strategy is indicated at (A), either because the wrong parameters were selected, or because within-location variability was less than the resolution of adopted measurement techniques.

5.2.4. Red Wharf Bay: further measurements in *Lanice* flats.

Further investigation of the effect of *Lanice conchilega* on sediment properties was required in order to support and extend the scope of the Llanddwyn findings (5.2.1). A suitably accessible location was found near the ebb channel on the western flank of Red Wharf Bay.

Sampling was concentrated at 2m intervals along two separate parallel lines: one following the edge of the shallow ebb channel and one on a shelly sandbank in mid-channel, covering in total an area of 20×30m. Considerable variability in sedimentary structure and textural composition was apparent, even over this relatively small area. *Lanice* was present at a range of densities, from zero in the most mobile, sandy parts to very high-density 'patches' which were apparently associated with erosion-resistant deposits, since they formed slightly raised platforms with evidence of erosion around their edges.

5.2.4.1. Site characterisation.

Textural characteristics.

Fig. 5.2.31 illustrates the grain-size distributions of the samples from each of the eleven sampled sites. Samples from the channel edge have been separated for comparison with those from the sandbank. It is clear that the mode of the dominant or framework population remains virtually constant over the sampling area, but that its distribution is much broader for the samples from the sandbank. Population-splitting indicated a framework mode of 2.2 +/- 0.1, with framework sorting increasing from 0.19 +/- 0.01 on the channel edge to 0.29 +/- 0.02 on the sandflat. This represents significant variation in framework population characteristics, with the result that the framework population cannot, as in the preceding experiments, be ignored.

In addition to framework variability, there is significant variation in the coarse tail of the distribution, with between 14 and 35% of the total forming a truncated coarse sub-population. Fine sub-populations comprise less than 0.4% of the total, and have therefore been ignored. The coarse sub-populations could not in this case be related to a coarse cut-off, because differences in framework sorting would additionally affect the fraction coarser than any appropriate size.

From these considerations the textural parameters selected as important were the sorting of the framework population and the coarse sub-population fraction, both these parameters being estimated from population splitting. The grain-size distributions did not indicate the need for a secondary coarse sub-population as at Lligwy, since the shape of the coarse tail was similar for all samples.

Biological characteristics.

Lanice density was estimated by counting exposed tubes within 0.5×0.5m sites, and multiplying up to obtain a density per square metre for comparison with the Llanddwyn data. A similar range of organism density

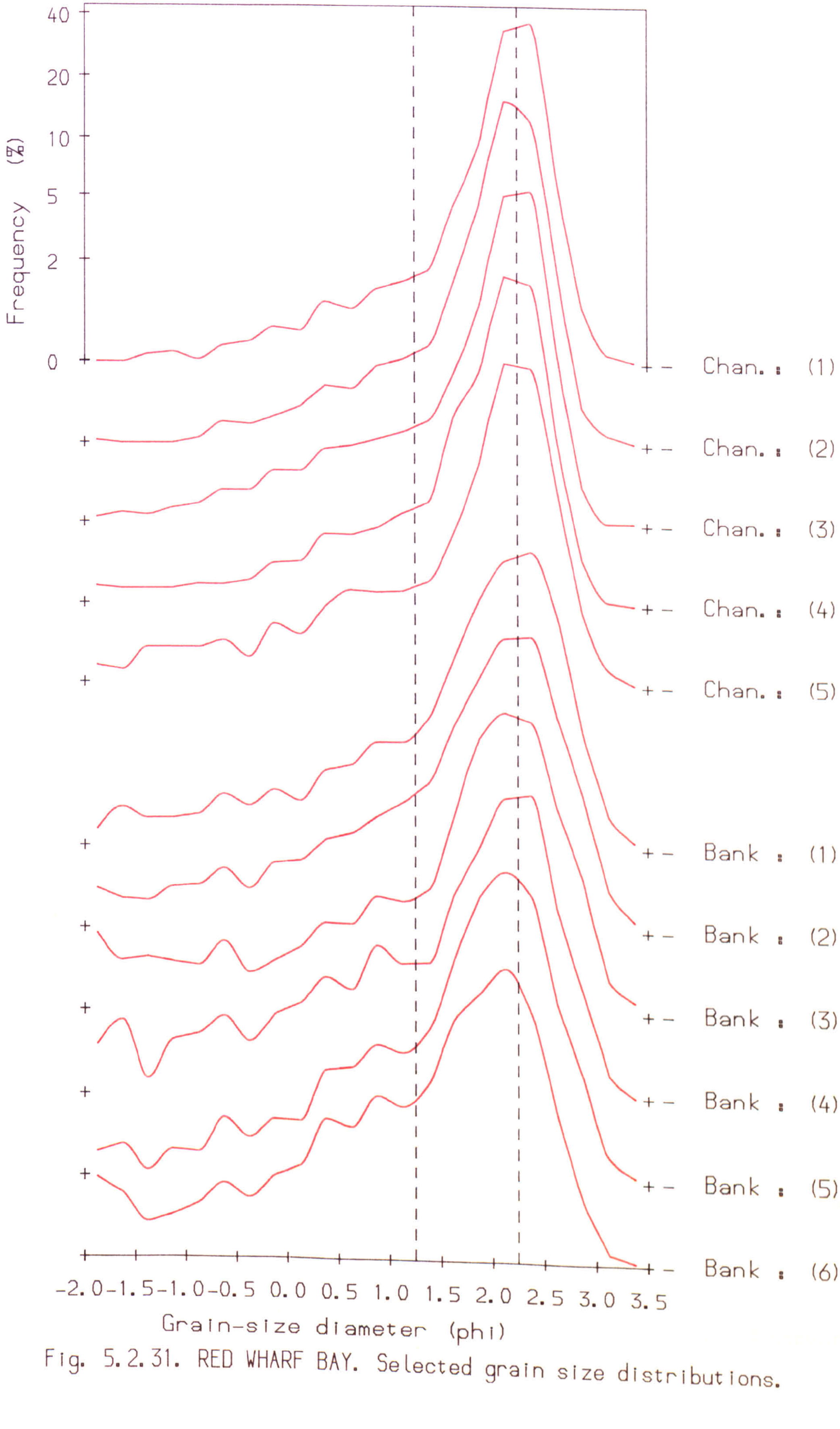

Fig. 5.2.31. RED WHARF BAY. Selected grain size distributions.

was obtained. Some tubes were gently separated from the substrate, washed, dried and examined: they were found to be constructed almost entirely of shell fragments, adhering to the tube-walls in overlapping layers.

Formation Factor.

Six replicate R_s measurements per site were averaged and converted to FF using the *in situ* measurements of pore fluid salinity and temperature listed in Table B4.1. No significant variation in pore fluid salinity or temperature was identified over the sampling period.

S-wave velocity.

Significant overall differences between bulk and surface V_s were not obtained (Fig. B4.1). However, since a distinct coarse shell layer was observed at 40mm depth at two of the channel edge sites, the surface calculation was retained in the analysis for completeness, and was checked for significant differences in behaviour.

5.2.4.2. Localised variability of measured properties.

Means and coefficients of variation for the full data set, and for channel edge and sandbank 'zones', have been listed in Table B4.2. Figs. B4.2-3 illustrate the spatial distribution of selected parameters, and indicate significant variation in textural characteristics, especially between the two areas separated by the channel. Ideally, samples from these two sub-locations should have been independently analysed: however, sample sizes would have been too small to be statistically representative, given the high degree of sampling error and small ranges. The fact that significant differences between the two lines were not apparent for the geophysical properties is important, and will be discussed in more detail in 5.2.4.3.

Since, for the full data-set, significant variation in framework

properties was observed, the hypothesis concerning perturbation of a uniform framework population is no longer strictly valid. However, mode grain size diameter remained relatively uniform, allowing some scope for interpretation of selected textural and biological parameters in terms of their independent effect on packing configuration. As at Lligwy (B), porosity was surprisingly uniform, despite considerable variability in textural and biological parameters.

5.2.4.3. Relationships between measured properties.

Table B4.3 lists significant correlation coefficients among textural and biological characteristics at Red Wharf Bay. Table B4.4 summarises regression results for porosity and the geophysical properties.

Textural interrelationships.

Carbonate content correlates positively with the coarse fraction, as has been found at both Llanddwyn and Lligwy (B) (Fig. 5.2.32). However, it is also strongly correlated with framework sorting (Fig. 5.2.33), indicating that the broader framework distribution observed for the sand-bank samples is related to an increased proportion of shell fragments in the modal population. Multiple regression indicates that 85% of the observed variation in carbonate content can be explained by a combination of these two parameters. The partial regression coefficient indicates that approximately 36% of the coarse fraction is shell, from which the proportion of shell fragments in the framework population is calculated as varying between 14 and 37%.

Biological/textural interrelationships.

There were no significant relationships between *Lanice* density and textural parameters, which suggests that there are no simple direct biological/textural interactions at this location. This contrasts with the inverse relationship between *Lanice* and carbonate content observed at

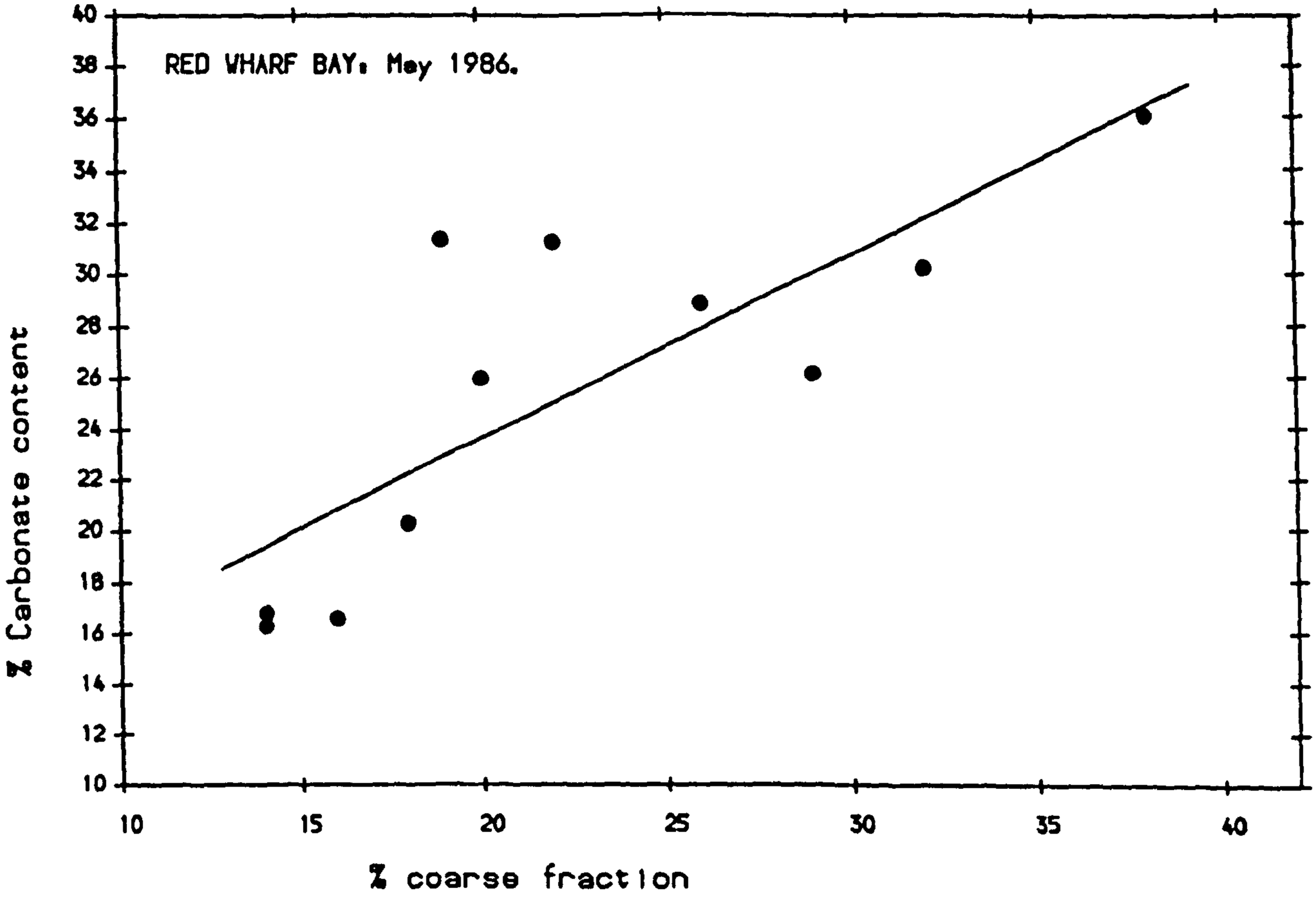

Fig. 5.2.32.

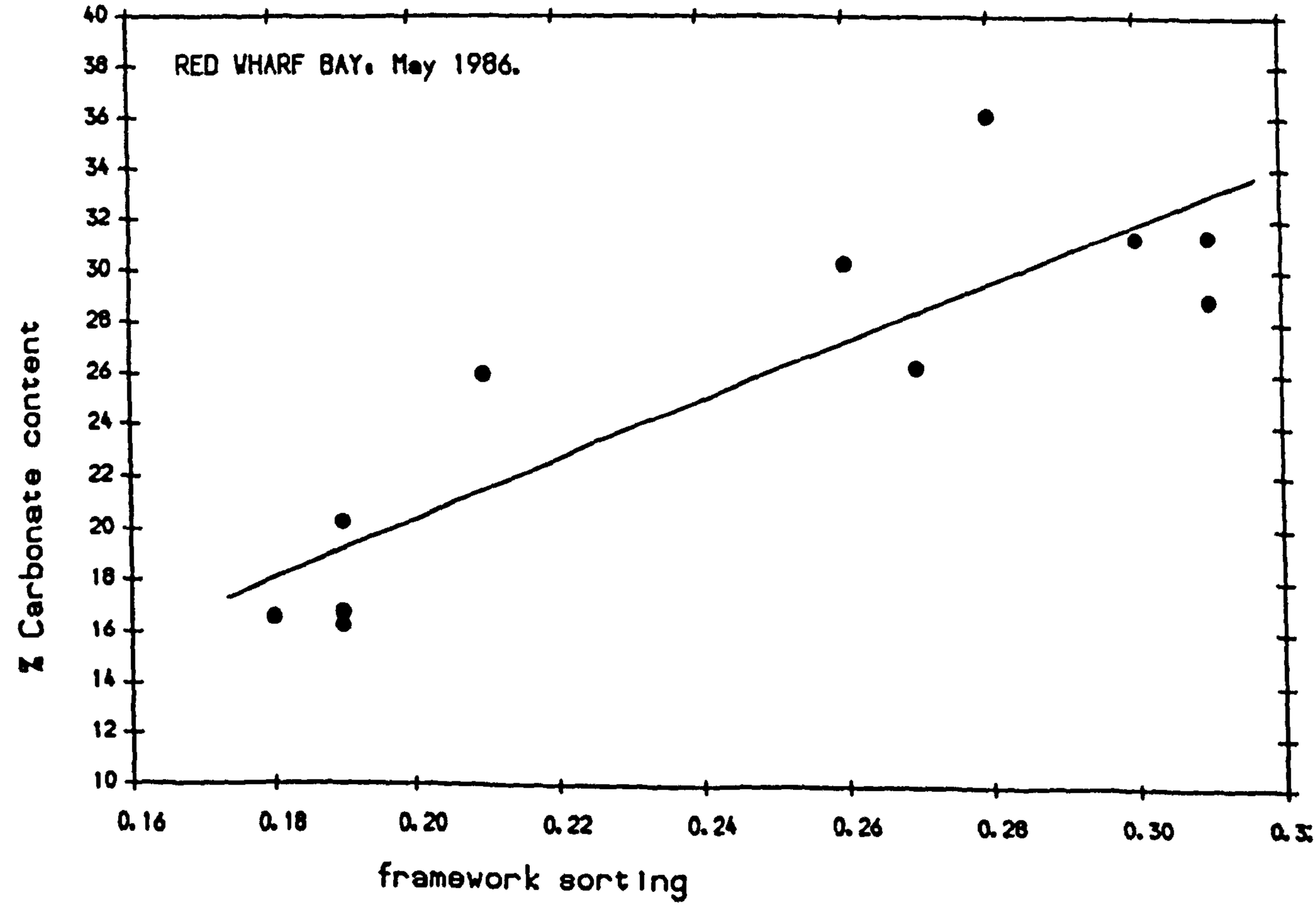

Fig. 5.2.33.

Llanddwyn, which was thought to be a sampling artefact.

Porosity

While porosity shows a relatively low degree of variability, that variability is nevertheless significant and is, moreover, directly related to textural and biological characteristics of the sediment. It is related to carbonate content, the coarse fraction and framework sorting, although the last two could be indirect through their interaction with carbonate content. The relationship with the shell fraction is the most significant, illustrated in Fig. 5.2.34, and is in agreement with findings from the Taf and Lligwy (B). The proposed mechanism is of 'bridging' by platy shell fragments, which clearly counteracts any potential improvement in packing efficiency due to the associated wider range of sizes.

The best combination of predictors is the coarse fraction (which is, in turn, related to the coarser component of the shell population) and *Lanice* density, with both acting to independently increase measured porosity. The observed effect of the coarse fraction is opposite to that found for binary mixtures of well-rounded grains, and illustrates the importance of grain shape in porosity determination. The relationship with *Lanice* provides a possible mechanism to explain the inverse dependence of FF on *Lanice* observed at Llanddwyn.

Geophysical relationships.

Formation Factor.

No significant relationships are observed for FF. Fig. B4.3 indicates anomalously high values at -2m and -4m which cannot be related to other measured properties. It is thought that the shell layer observed at these sites may have influenced measured sediment resistance values. If the surface layer is assumed to have the same resistivity as, say, Site 3 (ρ_{s1} = 132 Ωcm) then eqn. 4.33 can be iterated to calculate the resistivity of the sub-layer (from ρ_{s2}, eqns. 4.33, 4.20). For a depth of 40mm, measured

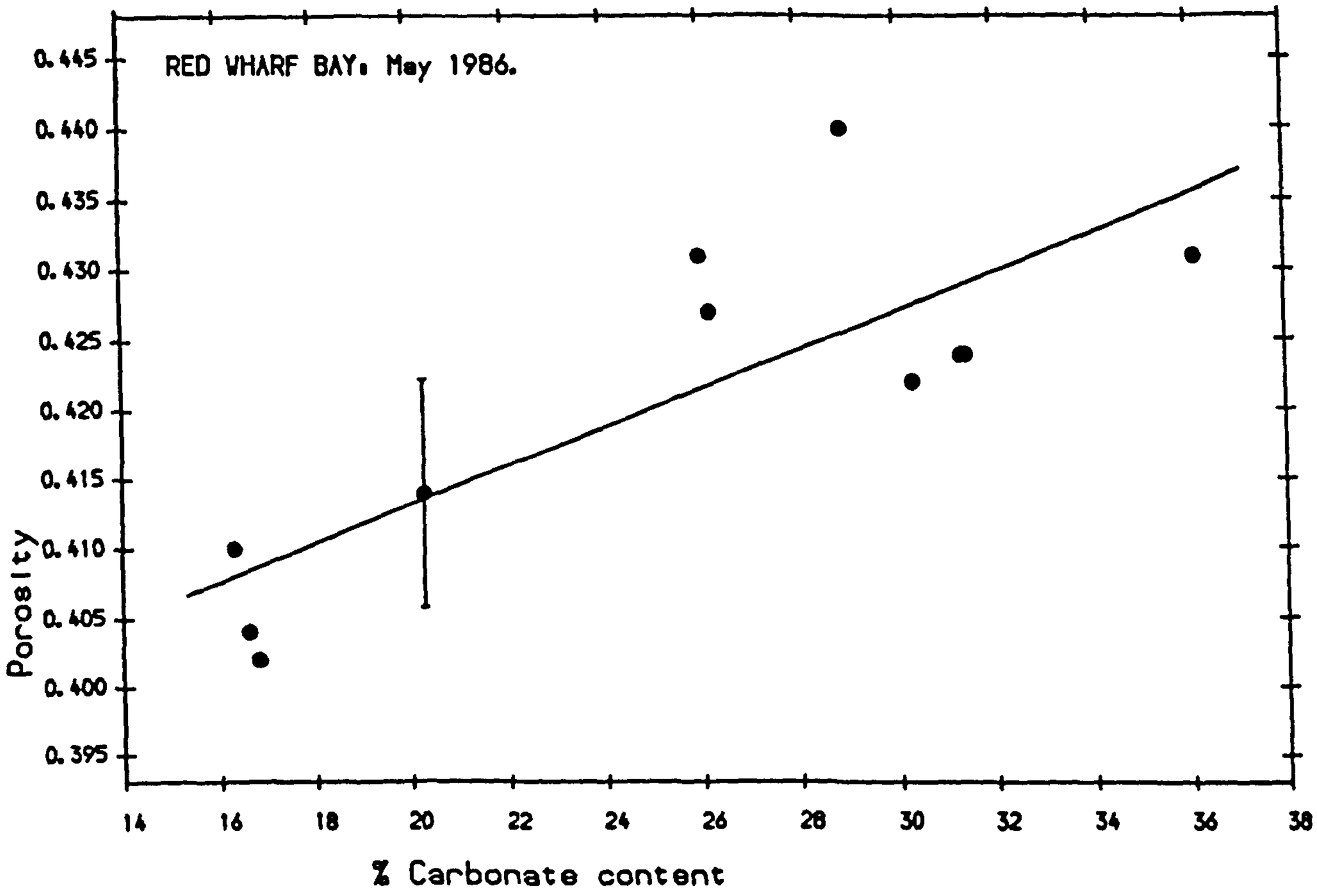

Fig. 5.2.34.

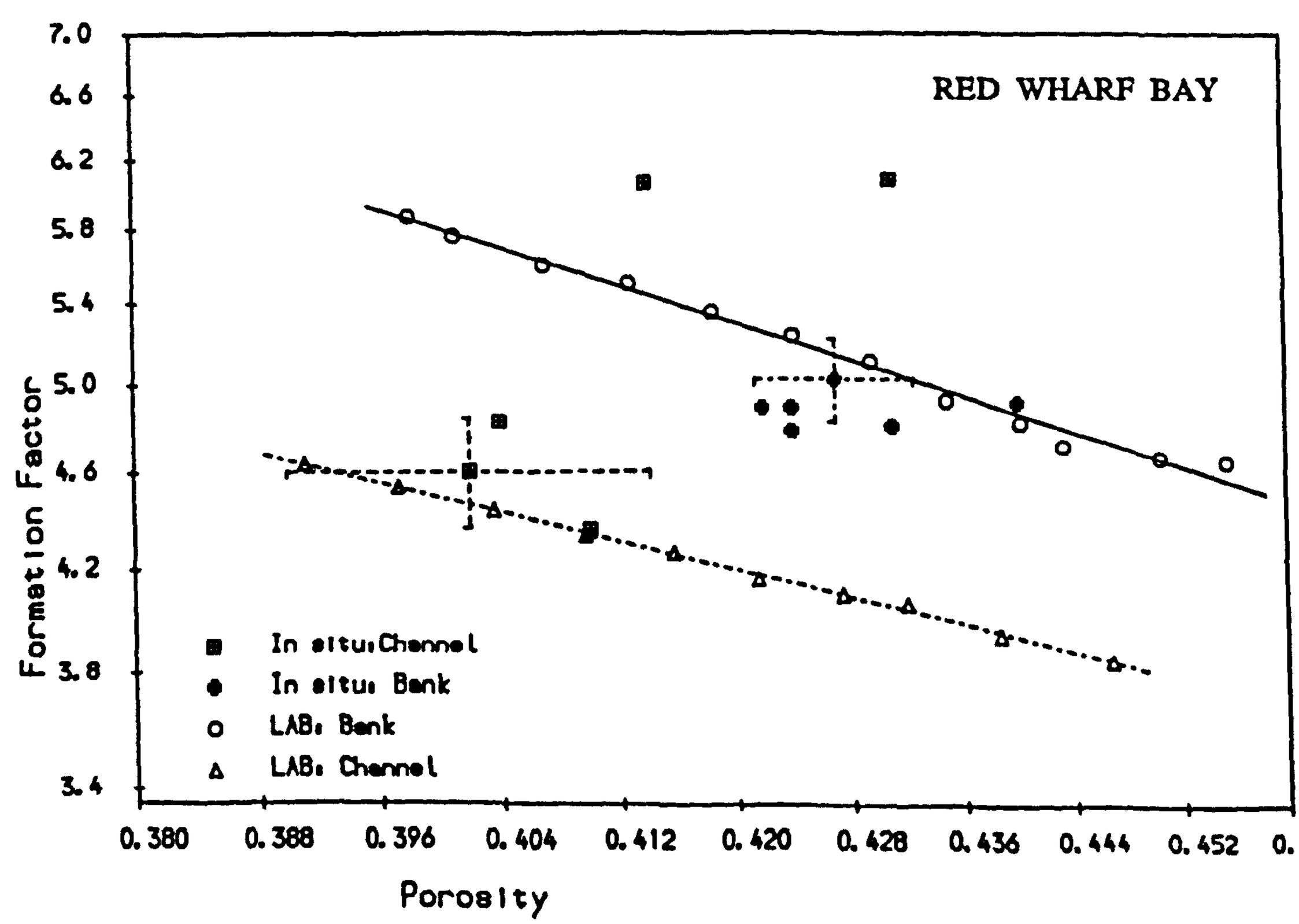

Fig. 5.2.35. FF:porosity relationships. Laboratory and *in situ* data.

sediment resistance indicates a sub-layer value of 201 Ωcm (FF = 7.2Ω). This is just within measured ranges for unconsolidated sediments and might be reasonable for large horizontally aligned shell fragments, which should act as an insulating layer. It is unfortunate that the V_s results do not support this finding, either by exhibiting similarly anomalous values or by indicating strong velocity layering. However, FF measurements can be influenced by considerably deeper layers than V_s, so that the effect of the observed sub-layer may have been much more significant.

The electrical properties of these sediments were further explored using the Jackson Cell (Section 5.2.2.4). Two 1500g samples were recovered from the channel edge and the sand-bank respectively, in each case in areas with zero or very low *Lanice* density (-10m [Site 1] and +12m [Site 11], Fig. B4.3). FF was determined in artificial deposits of these two samples over a range of sediment porosities.

Fig. 5.2.35 illustrates the results obtained, with *in situ* data superimposed for comparison. The regression results for the laboratory simulations indicate values of a_F and m of 1.25, 1.40 for the lower carbonate, better sorted Site 1, and 1.05, 1.86 at Site 11. The increased m-value for sediment containing a high proportion of shell fragments is in agreement with other studies involving the Jackson Cell [e.g. Jackson *et al*, 1978], interpreted as caused by higher tortuosity for a given porosity.

Comparison with *in situ* data indicates first reasonable agreement between measured porosity and the range obtained in the Jackson cell, and second a good correspondence between FF values from the relevant sample lines. Neglecting the two anomalously high readings, FF clusters around the two FF:porosity relationships identified in the laboratory. Thus both field and laboratory data indicate higher FF for given porosity in the shellier, poorer sorted sandbank sites. The overall effect is to reduce FF variability, since *in situ* porosity is higher on the sandbank. It is interesting that, while significant differences in porosity are obtained *in situ*, the laboratory simulation indicates only slightly higher minimum and maximum values for porosity for the sandbank sample. Thus *in situ* porosity, which is close to its artificially obtained minimum value at

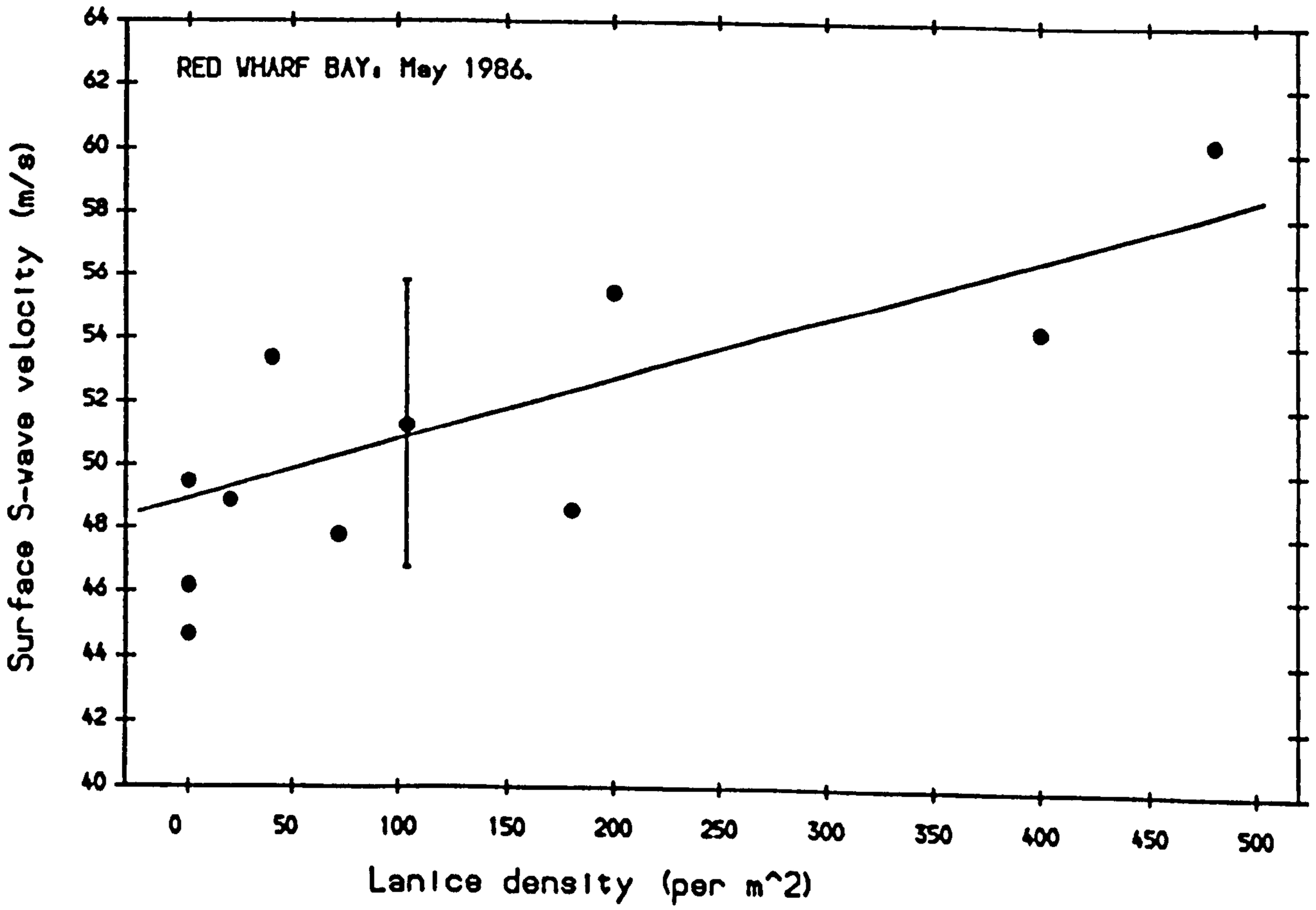
RED WHARF BAY: May 1986.
Surface S-wave velocity (m/s)
64
62
60
58
56
54
52
50
48
46
44
42
40
0
50
100
150
200
250
300
350
400
450
500
Lanice density (per m^2)

Fig. 5.2.36.

Site 1, is nearer its median at Site 11.

S-wave velocity.

Bulk V_s is increased by *Lanice* density as at Llanddwyn, but in this case the issue is complicated by an additional negative dependence on porosity. Porosity can also be replaced as a predictor by the coarse fraction, which has already been shown to be related to porosity, and therefore can be assumed to be an indirect control (Had V_s been measured during the Jackson Cell runs, this could have been investigated further). Surface V_s measurements are also related to *Lanice* density, in direct agreement with the results at Llanddwyn (Fig. 5.2.36).

5.2.4.4. Summary and interim conclusions.

In contrast to the preceding sections, sediments sampled from Red Wharf Bay could not be split into a predominantly uniform lognormal framework population. The framework is of uniform mode, but exhibits variable sorting and carbonate content, in response to spatial variability in hydrodynamic environment. In addition a variable, coarse, shelly subpopulation is present, comprising between 14 and 35% of the grain size distribution.

Porosity is increased by increasing carbonate content, in agreement with findings from the Taf Estuary and Lligwy (B). The shell fragments associated with this increase comprise both framework and coarse subpopulation, and must be generating 'bridging' structures within the sediment. FF is also sensitive to carbonate content, with laboratory and *in situ* results indicating higher tortuosity at shellier sites, although the associated higher porosity masks any direct relationship. This latter point may also explain the lack of relationship between V_s and carbonate content.

Lanice represents an additional, independent, spatially variable control on packing configuration, and significantly increases V_s, in direct

support of the findings at Traeth Llanddwyn. Thus two independent studies have identified an increase in sediment V_s associated with *Lanice* tubes.

5.2.5. Freathy Sands: *in-situ* measurement of the effect of drainage.

A series of measurements was performed on the sandy foreshore of Freathy Sands, just West of Plymouth in Whitesands Bay. The five sites monitored showed no evidence of macrofaunal activity, and were selected by following the limit of saturation by the ebbing tide, down a line 60m in length. At each of four sites the geophysical measurements were repeated after the surface layers of the sediment had drained, so that a comparison of *in situ* data with the laboratory study of the effect of sediment drainage could be made. The fifth site was monitored in a state of 'partial drainage', where the water table was only just beneath the surface. At the same time, sediment samples were taken at all sites for porosity and textural analysis. Table B4.4 lists location means for all measurements.

The number of individual sites sampled was too small to allow statistical analysis of measured properties as in the preceding sections, although the saturated measurements were included in the combined study discussed in Section 5.4. Discussion at this stage has therefore concentrated on temporally, rather than spatially, derived variation due to drainage of the surface layers. A Jackson cell simulation was also performed on a sample from the top 50mm of Site 1 to check the FF measurements.

Textural characteristics.

Site-replicate bulk textural characteristics determined at Freathy were used to estimate textural sampling errors, as discussed in Section 5.1.4.2. The location was chosen for its textural uniformity (and absence of benthic macrofauna), since it was not intended to investigate relationships between measured parameters. Therefore further discussion of textural characteristics was considered unnecessary.

S-wave velocity.

Bulk V_s was significantly higher than surface V_s (Fig. B5.1), indicating marked velocity layering under both saturated and drained conditions. Figs. 5.2.37-38 illustrate the effect of full or partial drainage at each site. As expected, both surface and bulk V_s were significantly increased under fully drained conditions, but remained uniform at site 5. This last measurement effectively represents an experimental 'control'. Bulk V_s was the most strongly affected, with drainage causing on average a 25% increase compared with 14% for surface V_s. Negative effective pore pressures may build up more readily in the subsurface layers, where the overlying sediment prevents rapid diffusion of air into capillary-sealed voids. This also implies that velocity gradients increase on drainage.

The *in situ* values of V_s under saturated and 'fully drained' conditions have been compared with laboratory simulations (3.4.6) in Fig. 5.2.39. It is clear that both sets of *in situ* velocity measurements show a less marked effect on drainage than do the laboratory data. The laboratory measurements, which were all surface V_s calculations (over a range of probe separations), indicate an increase of *c.* 60% on full drainage. This difference is thought to relate to two factors: first, the sediment was drained in the laboratory down to a depth of 200mm, which may not have been the case in the field, and second the laboratory test tank may have introduced effects due to its finite volume, with impermeable rigid sides.

The effect of drainage, while not apparently as significant as predicted from laboratory work, remains nevertheless considerably more important than much of the localised variability due to textural and biological control discussed in the preceding sections. This confirms the importance of measuring the geotechnical properties of intertidal deposits only under highly controlled conditions, if any useful conclusions are to be drawn.

Formation Factor.

Since pore fluid salinity could be safely assumed to be uniform at this location, R_w was estimated by monitoring sediment temperature throughout

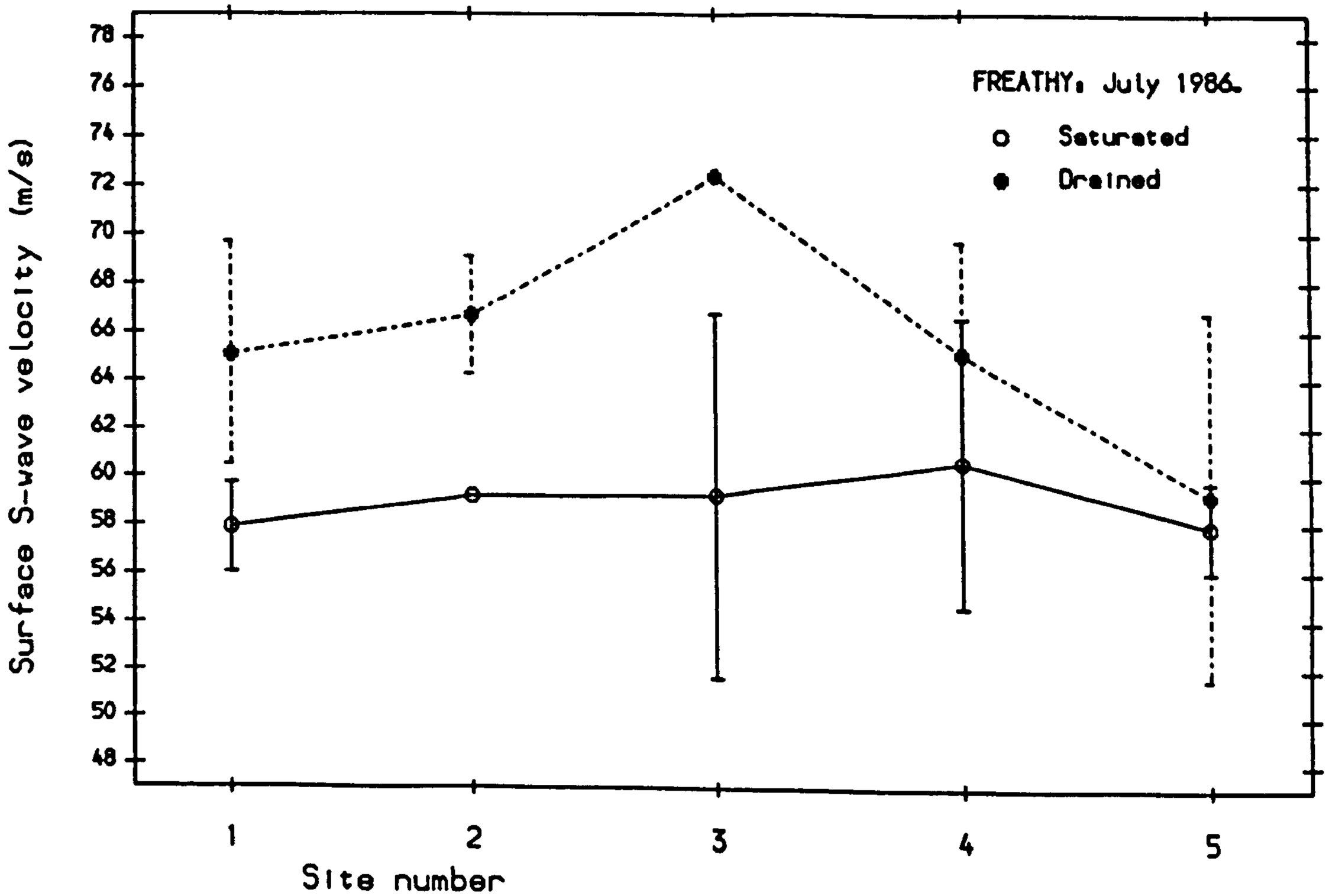

Fig. 5.2.37.

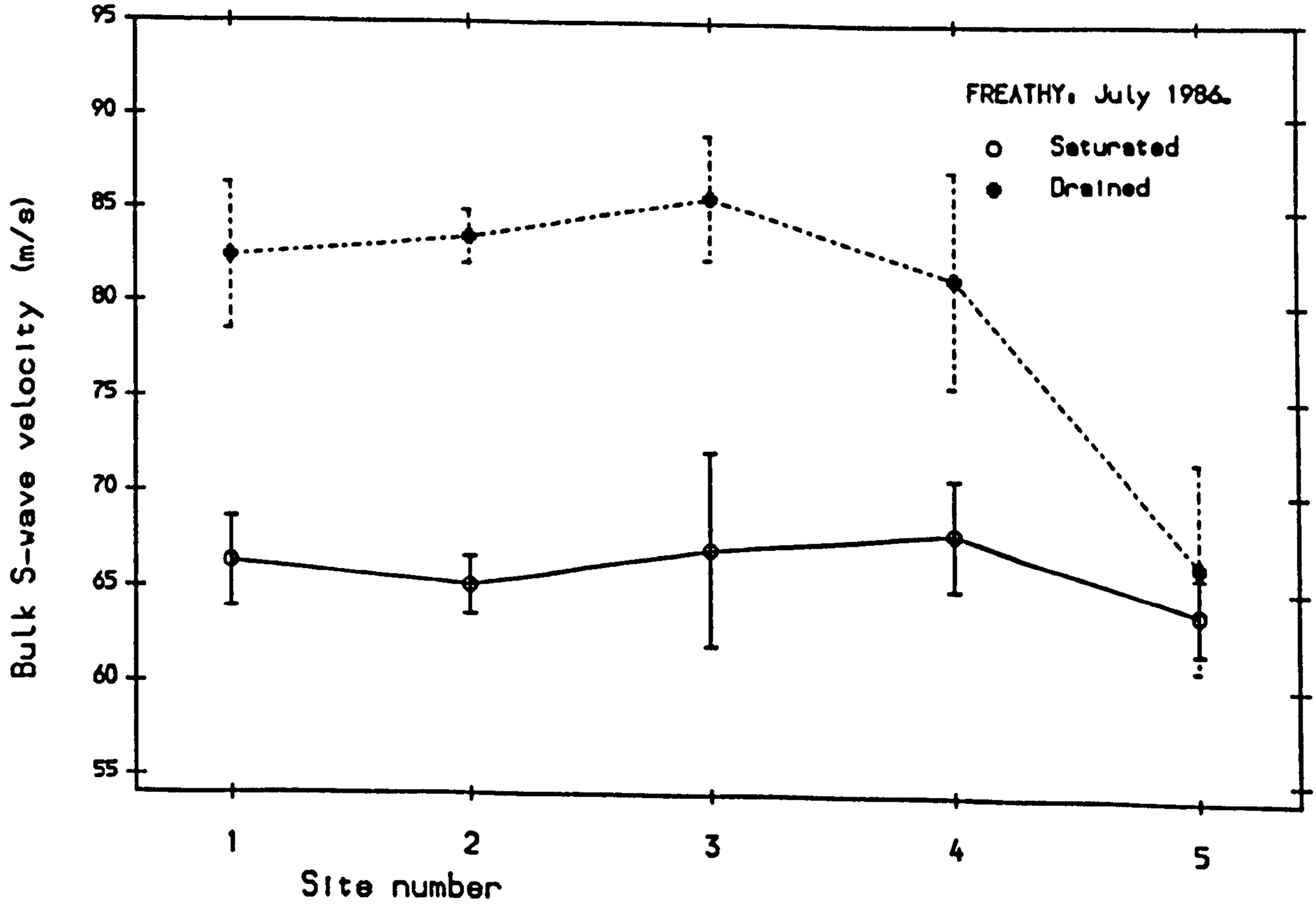

Fig. 5.2.38.

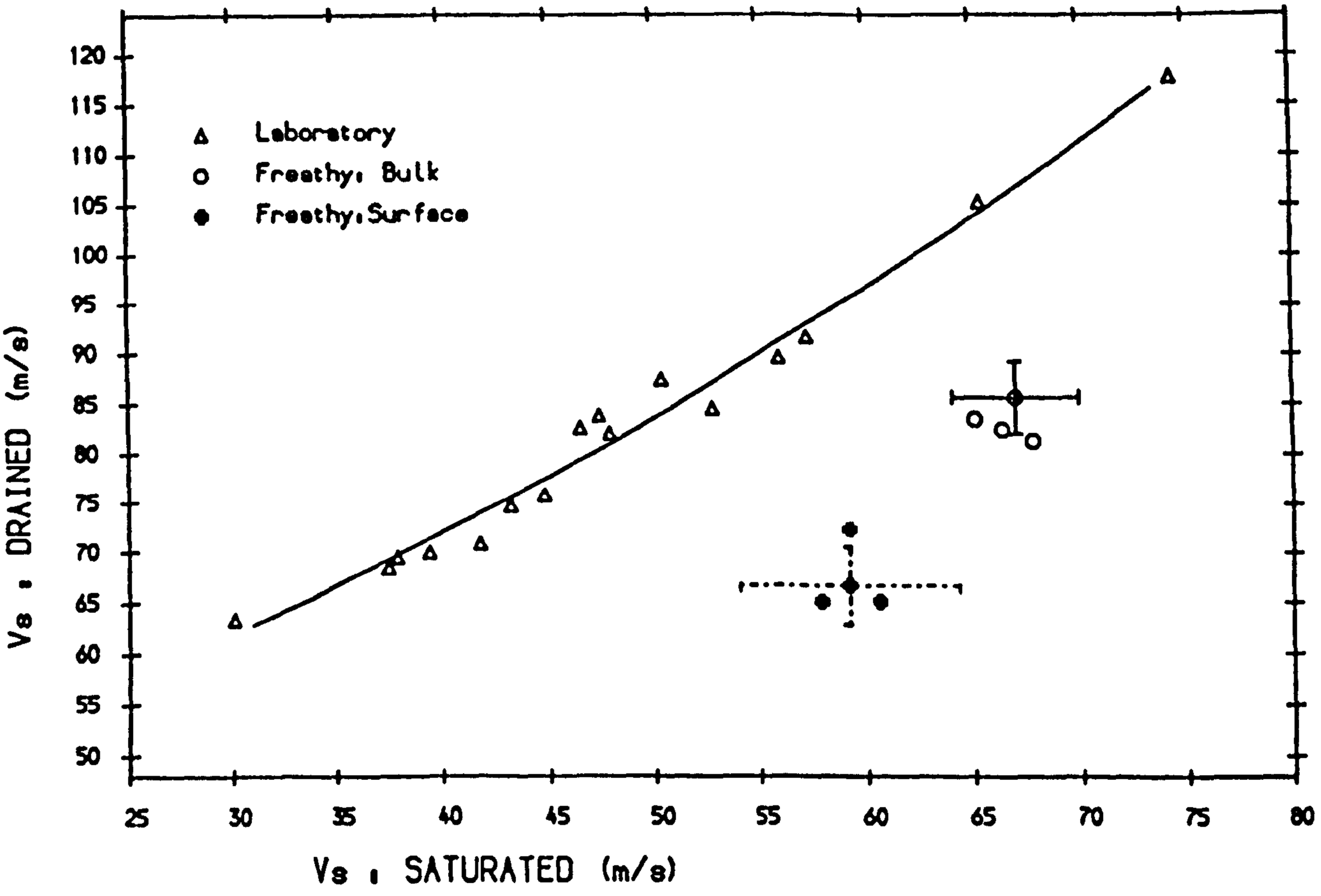

Fig. 5.2.39. Comparison between laboratory and *in situ* effect of drainage.

sampling, and combining this with salinity of the sea-water measured at the start of the experiment. Table B5.1 lists relevant measurements. The surface temperature changed quite dramatically on drainage, presumably due to warming in the August sunshine. Sub-surface temperatures were not monitored, which may have introduced errors for drained conditions.

Fig. 5.2.40 illustrates FF for each site under drained and saturated conditions. In contrast to the V_s results, no consistent differences can be identified. This represents an interesting contradiction, which can be explained by two arguments. First, the electrical measurements monitor larger volumes than V_s, and so may still have been largely influenced by fully saturated sub-layers. Second, the voids contributing negative pore pressures may have initially represented a relatively small proportion of the pore-space, and therefore would have had little effect on Formation Factor (FF is unaffected by effective stress). This is supported by the observation that, in contrast to the acoustic properties, small quantities of entrapped air do not significantly affect electrical properties in the Jackson Cell [Schultheiss, 1983]. These measurements provide *in situ* confirmation of the laboratory simulation described in Chapter 4.

Fig. 5.2.41 illustrates the FF:porosity relationship obtained in the Jackson cell, with *in situ* data superimposed for comparison. Two features require comment: first, the *in situ* porosities are at, and in one case below, the artificially obtained extreme minimum; and second, *in situ* FF is significantly higher than in the laboratory, even allowing for sampling error. The low values of porosity might be expected for sediment on beaches exposed to post-depositional compaction by wave-action, although it is interesting that wave action is apparently more efficient than the artificial compaction employed for the Jackson Cell experiment.

The high values of FF raise important questions about the validity of either the laboratory or *in situ* procedures. Neglecting between-site differences, the mean *in situ* FF was 12% higher than that obtained in the Jackson Cell at a porosity corresponding to the *in situ* mean. This is not a wild discrepancy, given the uncertainties associated with field measurements. The cause may be a systematic error in pore fluid resistance, perhaps due to negative temperature gradients in the surface

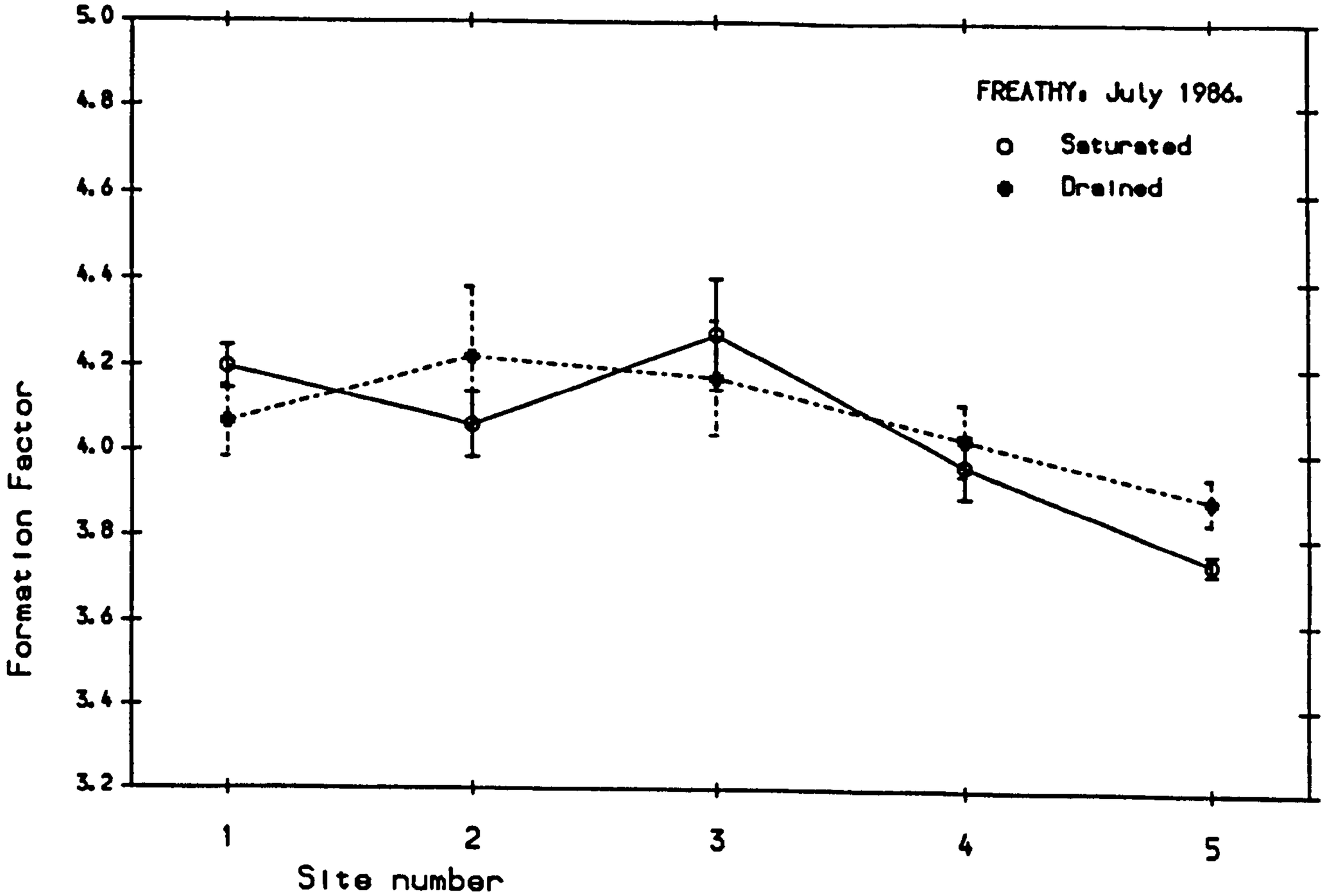

Fig. 5.2.40.

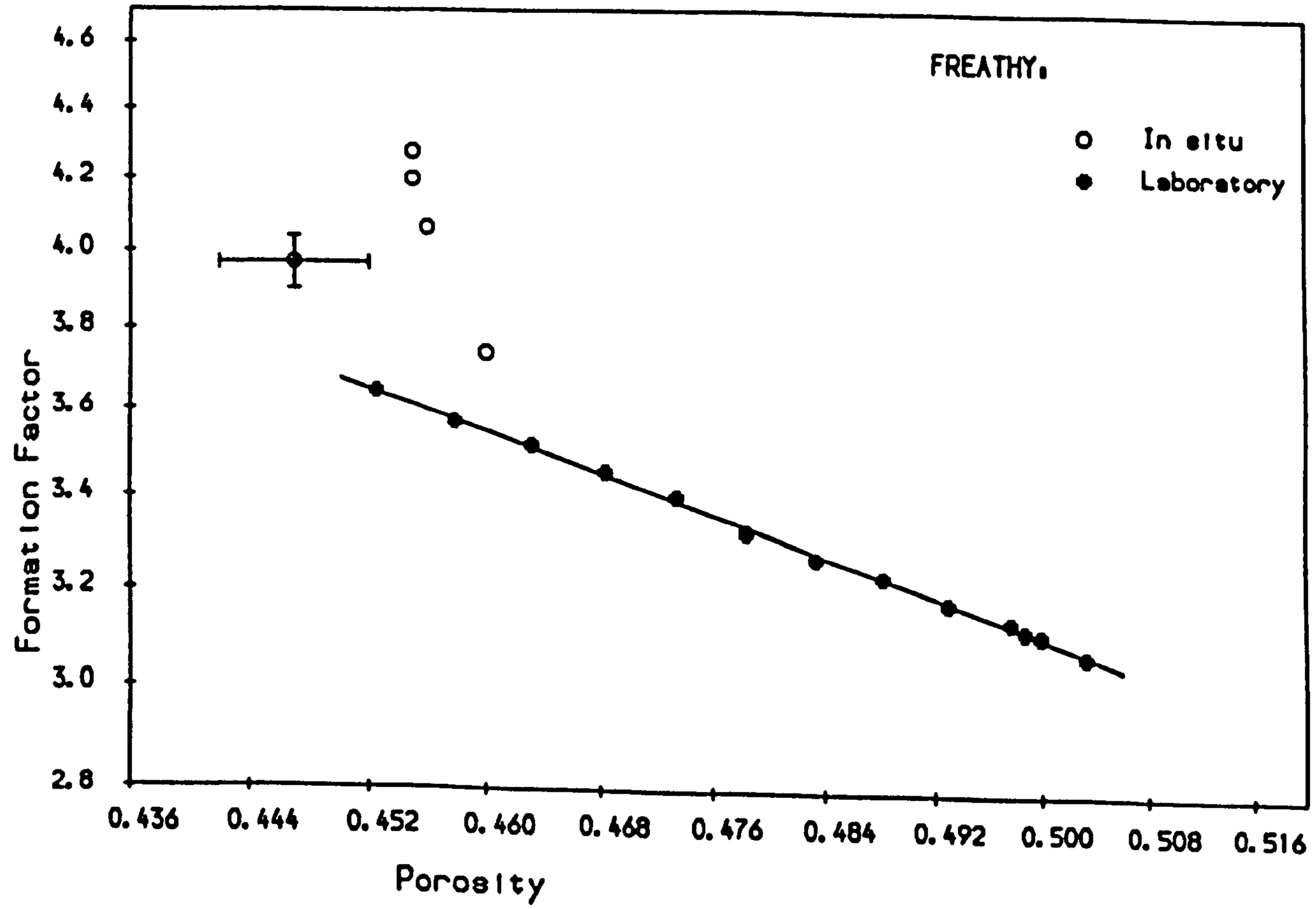

Fig. 5.2.41.

layers even for the saturated samples. This would lead to underestimates of pore fluid resistance and hence overestimates of FF. However, an equally likely cause would be the influence on FF by sub-surface layers which were not sampled by the porosity cores. Sub-surface layering is indicated by the V_s measurements, and high values in FF due to shell layers have already been identified at Red Wharf Bay. The implication is that the substrate is composed of contrasting textural properties, since surface porosity is already apparently at its minimum.

5.2.6. Tamar estuary: measurements on mud-flats.

During a separate experiment in the Tamar estuary, the opportunity arose to perform measurements of spatial variability on three exposed intertidal mudflats, henceforth referred to as Cotehele (C.H), Salters Mill (S.M) and Tamar Bridge (T.B). National Grid References for these locations are SX 425 685; SX 432 637; SX 432 585. C.H is the furthest upriver; T.B is the furthest downriver.

The mudflats imposed considerable strain on the experimental strategy adopted for *in situ* measurements in sands, not least because of equipment transportation problems in the deep, soft deposits typical of intertidal mudflats. Sites were selected along lines perpendicular to low water mark as the tide receded, although the water-retention ability of muds meant that sites remained saturated for considerable periods after exposure. Fewer measurements were possible in any sampling period because of time constraints. For this reason, statistical analysis of relationships between properties has been restricted to the combined data-set from all three areas, covering in total 12 sites.

5.2.6.1. Site characteristics.

Table B6.1 lists location means of measured properties. Although benthic macrofaunal communities were observed and identified at all three locations, no quantitative analysis was performed. This study represented

a pilot assessment of the feasibility of *in situ* geophysical monitoring of cohesive sediments, rather than a detailed investigation.

Textural characteristics.

Because of the cohesive nature of muds, their grain-size characteristics require more cautious interpretation than those of sands. The size distribution is experimentally determined using a fully dispersed sample, which will bear little resemblance to the *in situ* properties of the deposit. In addition, the physical and geophysical properties of the deposit are more likely to be controlled by the extent of flocculation on deposition, and on post-depositional consolidation processes, than on the sizes of individual constituent mineral grains.

The fact that separate analysis procedures are required for the mud and sand fractions leads to other problems in interpretation of grain-size distributions. Between 2 and 25% sand was present in the Tamar samples, with Fall-tower analysis being performed for sand fractions greater than 5%. Figs. 5.2.42-43 illustrate the size distributions obtained at all sites, separated into the three locations. They appear to be consistent in form within each location, with variable proportion and distribution of sand. At T.B, the sand fraction forms part of the dominant modal population. The double peak at 4phi may reflect mismatches in the two analyses rather than genuine bimodality. At S.M, the sand fraction exhibits a much coarser mode at about 0.25phi at all sites except the most seaward.

The mud fraction at all sites shows evidence of modes at 4.25, 5.75, 8 and 10phi, which may have been artefacts of the pipette analysis. However, between-location differences are apparent in the relative importance of these modes, which could indicate genuine textural variability. Given the complex and probably irrelevant size distribution of the mud fraction, population splitting was not considered appropriate. The most important textural parameter has been selected as the proportion of sand, since sand and mud exhibit contrasting physical properties. The percentage coarser than 1.0 phi was also selected as a parameter capable of distinguishing

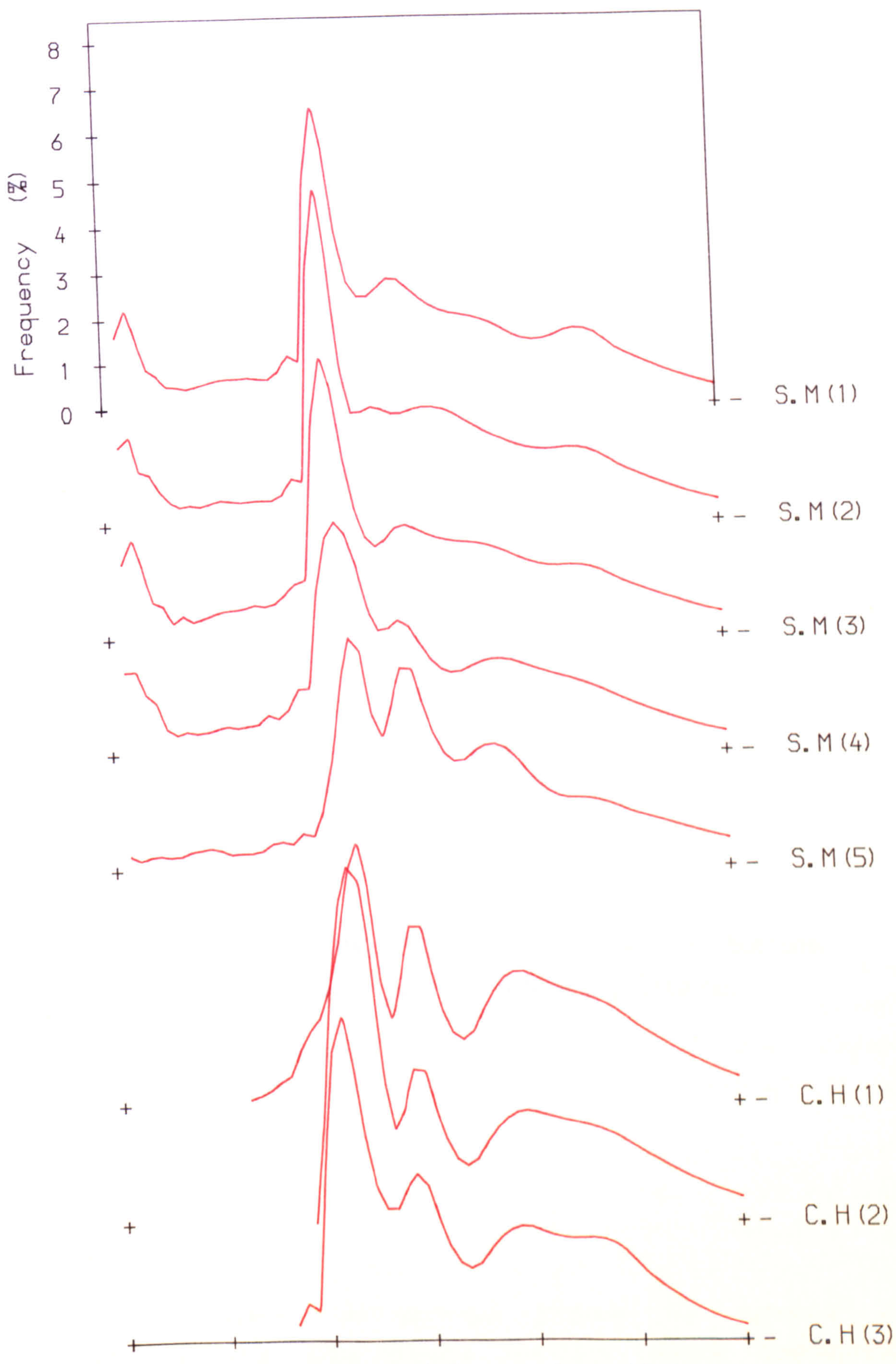

Fig. 5.2.42. TAMAR ESTUARY. Grain size distributions.
Key: Location reference, Site No.

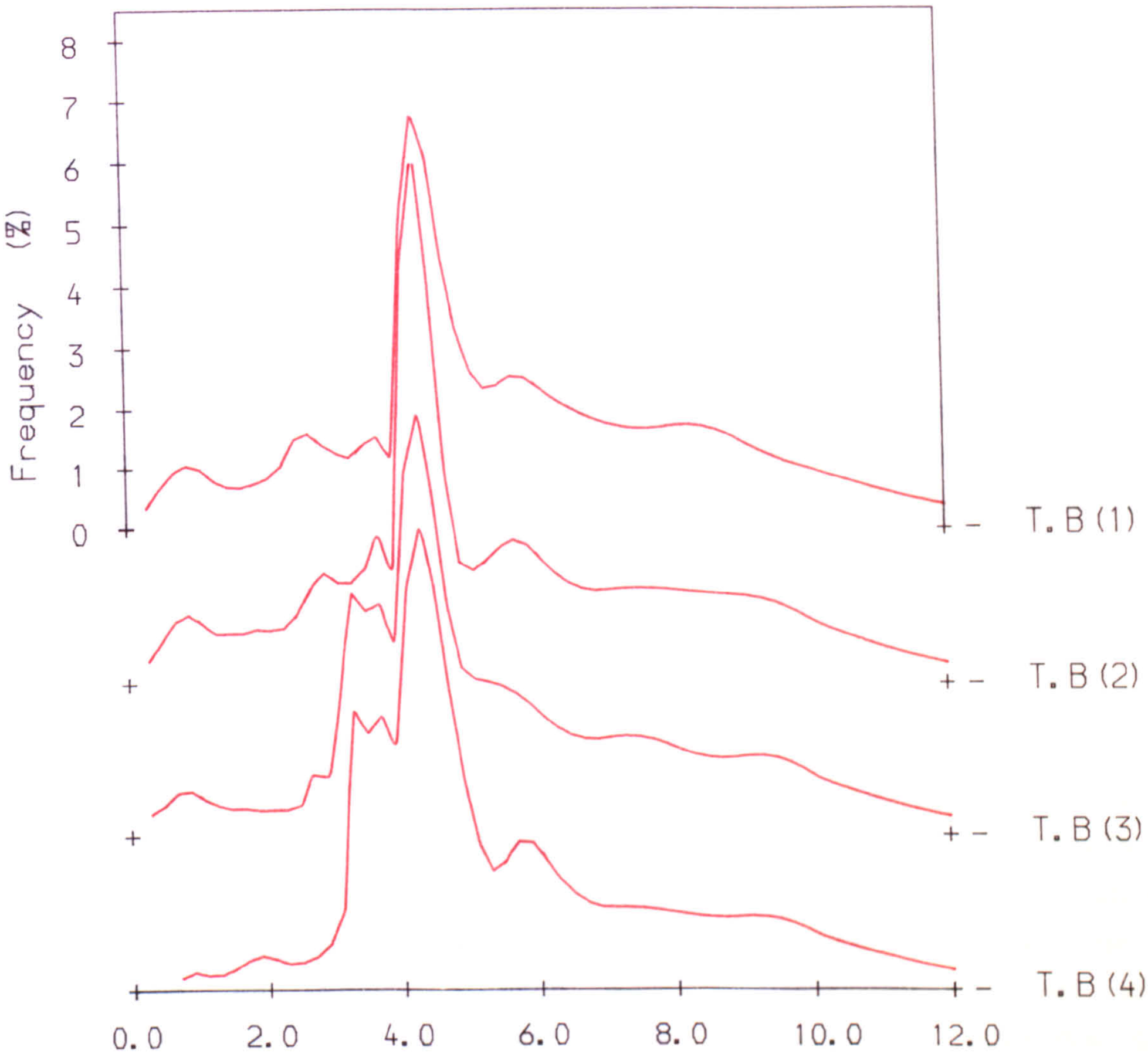

Fig. 5.2.43. TAMAR ESTUARY. Grain size distributions.
Key: Location reference, Site no.

differences in size distribution, and hence packing configuration, of the sand fraction.

The remaining important textural parameter is the organics fraction, which was determined from H_2O_2 oxidation as described in 5.1.3.2. Carbonate content was not determined, because the coarser fractions of the Tamar sediments were seen to be primarily terrigenous and lithic (composed of shale fragments). This does mean that any biogenic contribution to the inorganic constituents was ignored.

Formation Factor.

As discussed in Chapter 2, the electrical properties of muds are complicated because electrochemical properties of clay minerals can contribute to electrical conduction. Furthermore, these are sensitive to salinity and temperature which introduces additional factors into data interpretation. FF remains a valid parameter, dependent at least in part on porosity, but it is no longer purely a function of properties of the pore-space. The limited data-set obtained during this study was not expected to yield much new information about the complex electrical properties of muds.

Table B6.2 lists pore fluid salinities, measured once at each location, and temperatures, which were monitored more regularly throughout the sampling period. No attempt was made to monitor sub-surface gradients in salinity or temperature, which may have introduced systematic or random error into FF determination.

S-wave velocity.

The S-wave probes were developed primarily for assessment of the properties of sands. Their physical size and resonant characteristics had only been tested in sands, and therefore deployment in muds was not expected to be quite as successful. Data quality was indeed found to be significantly impaired, with low signal-noise ratio and high attenuation

of the transmitted pulse. Very few onset times could be confidently determined, so surface V_s could not be reliably measured. More success was achieved, however, for bulk V_s values calculated from signal maxima and minima. The location means listed in Table B6.1 indicate exceptionally low velocities, in agreement with other measurements in surficial muds [Schultheiss, 1983, McDermott, *pers. comm.*].

Because surface V_s could not be reliably measured, the standard investigation of velocity layering employed for measurements on sands was not possible. In addition to bulk V_s calculation, some exploration of received frequencies from these measurements was performed in order to compare them with the laboratory investigation in sands. (*In situ* measurements of received frequency in sand were not systematically investigated, but all those checked confirmed the laboratory finding of a received 'resonant' wavelength corresponding to twice the transducer width, as described in 3.4.7.1).

Fig 5.2.44 illustrates received frequency plotted against measured bulk V_s. The pulse frequency was estimated from the first complete signal period on enlarged paper records and averaged over all separations and site replicates. Error bars correspond to a standard deviation. The superimposed straight line has been extrapolated from the relationship obtained between received pulse frequency and V_s in sands [3.4.7.1]. It is clear that received frequencies were substantially higher than predicted. This indicates that the model of frequency-dependent transducer/sediment response breaks down in media of substantially lower rigidity than saturated sands.

This can be explained by the fact that the response modelled in Chapter 3 is only valid where the transducer is properly coupled with the sediment. This was illustrated by good correspondence between unloaded transducer resonance and that obtained in saturated sands. In the Tamar muds, the theoretical resonance corresponds to a very low amplitude region of the unloaded response. The result of this is that the transducer decouples from the sediment, since maximum energy will be transmitted at a frequency nearer its unloaded resonance, which is faster than the response time of the surrounding material. The mechanism can then be modelled as a plate

vibrating in a highly viscous fluid, which damps the vibration. This is competely different from the closely coupled transducer/sediment resonance postulated for saturated sands.

5.2.6.2. Variability of measured properties.

The hypothesis used to explain variability in preceding sections is not necessarily relevant for these measurements. This is because fine-grained cohesive deposits cannot be viewed as a framework of individual grains, supported via friction between the grain contacts, with perturbation of the packing configuration by addition of coarse and fine particles. Fines content is much less variable than at other locations, because it comprises the bulk of the grain size distribution.

Significant differences between one or more location means were obtained for mean grain size, sorting, % fines, % organics, porosity, %>1phi, and FF, but not for mode grain size and bulk V_s. The inference is that the spatial variability in most sediment properties is more significant over larger scales, due to differences in extent of tidal and fluvial influence along the estuary, than over more localised scales due to variation in time of exposure on an intertidal flat. The fact that this does not appear to be the case for the V_s measurements will be discussed in 5.2.6.3. The lack of variation in mode may reflect uniformity of material when dispersed in the laboratory, rather than when *in situ*.

5.2.6.3. Relationships between measured properties.

Since only small numbers of sites were sampled at each location, the investigation of relationships between variables has been restricted to the combined data-set from all three locations. Moreover, since significant differences between location means of textural and physical properties were found, it was expected that significant correlations based on these differences might be obtained. These correlations will be more tenable than those obtained for measurements from only two locations, where significant between-location differences in properties will always

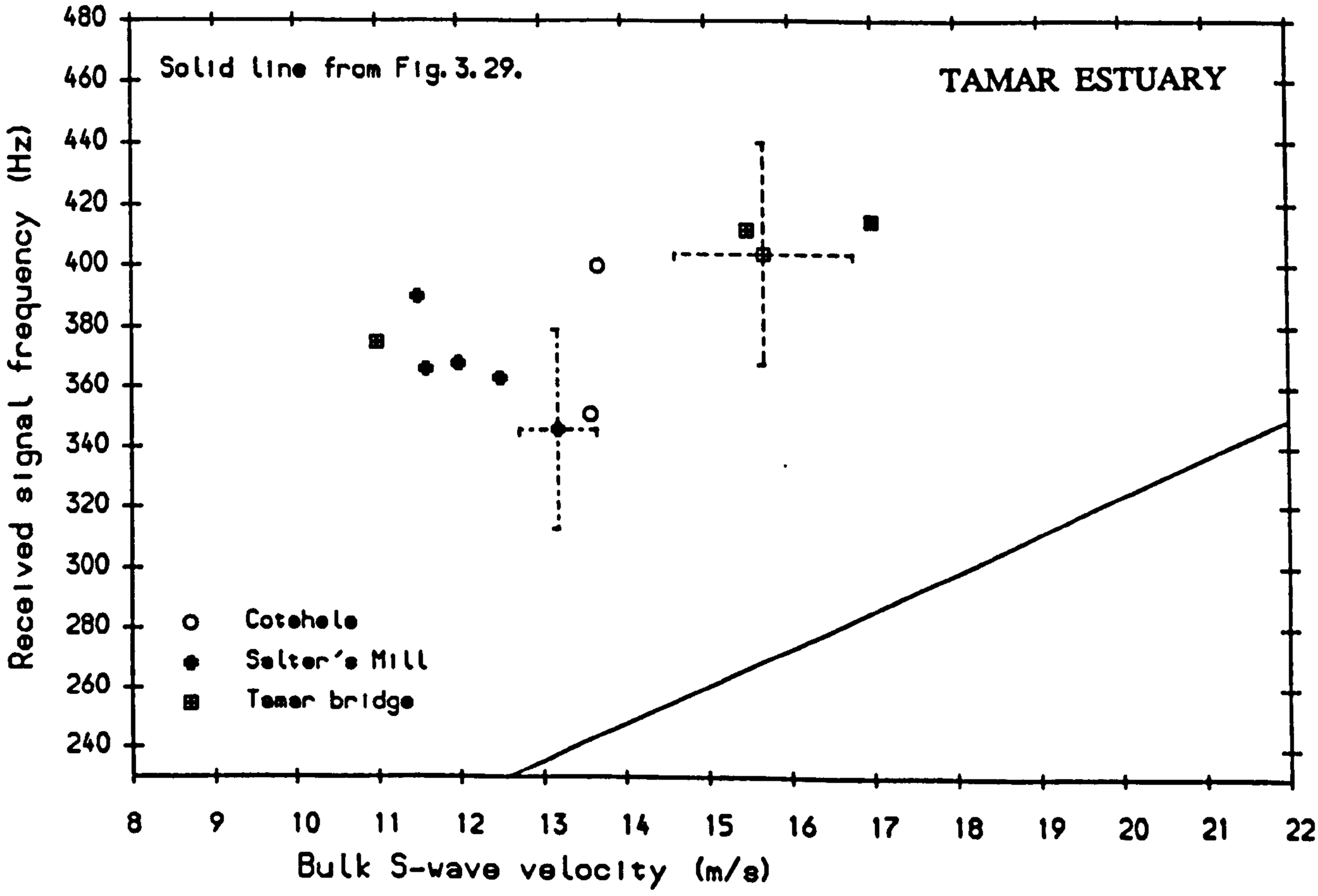

Fig. 5.2.44. Resonant frequency: V_s relationship for muds.

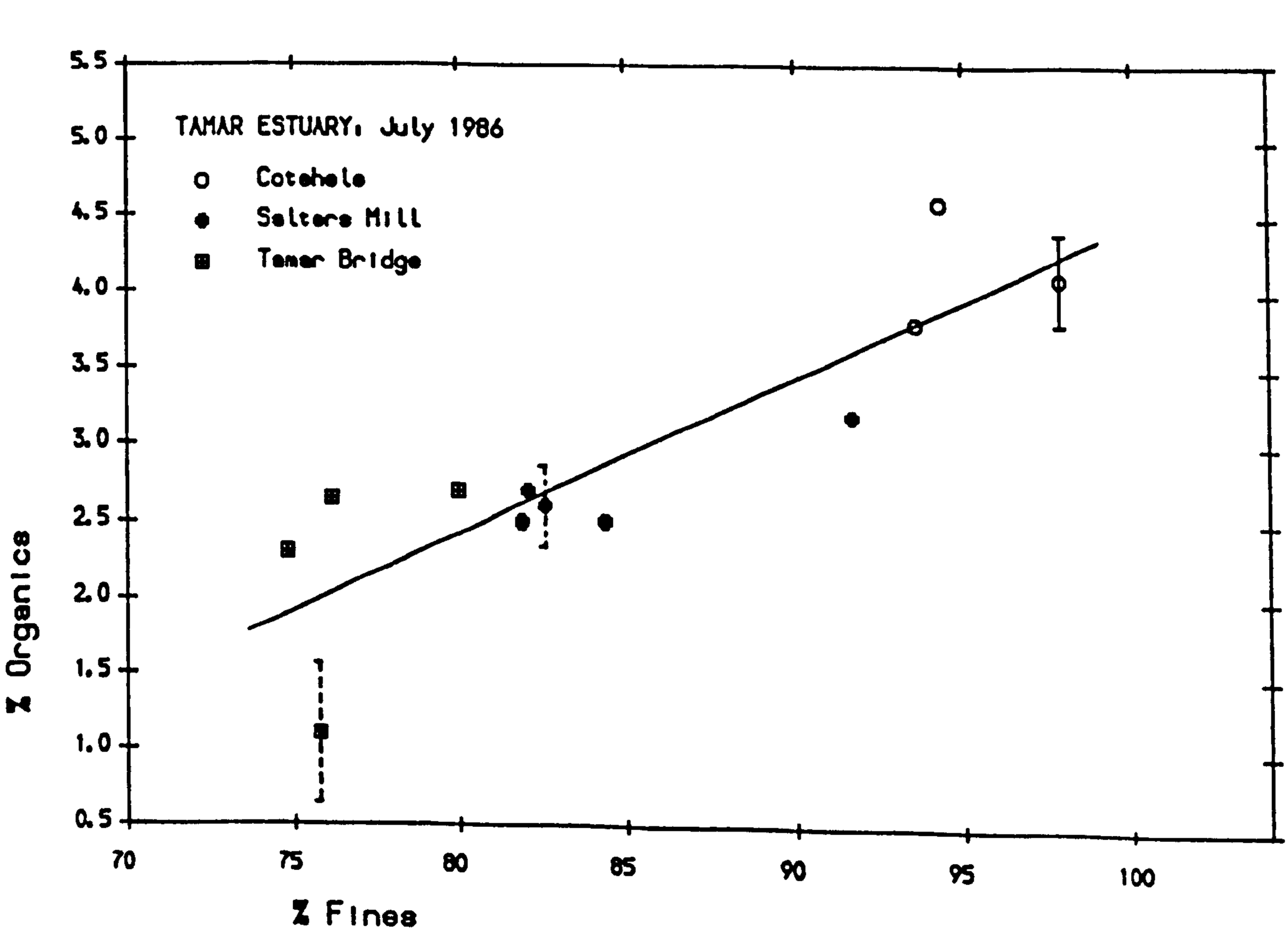

Fig. 5.2.45.

produce spurious correlations, whether or not direct causal links are present. Significant correlation coefficients have been tabulated in Table B6.3: regression results are summarised in Table B6.4.

Textural interrelationships.

Significant correlations have been identified between mean grain diameter and fines content, and sorting and the fraction coarser than 1phi, with strong positive relationships indicating that these two size fractions are the important textural parameters.

Significant correlations are also identified between organics content and fines (Fig. 5.2.45). Estuarine organic matter is composed of detritus and microorganisms. Two factors tend to associate organic material with the presence of inorganic fine particles: first, many organic detrital particles have settling velocities comparable to mud flocs (or act as fine sediment traps as they sink); and second, the surface area of fine particles is much higher than for equivalent volumes of sands, which allows enhanced microbial colonisation and mucous adhesion.

Porosity.

There is a strong positive dependence of porosity on fines content (Fig. 5.2.46), in agreement with the Taf study (5.2.2) and other work (Chapter 1). The relationship with organics is probably a direct consequence of this. The best combination of predictors involves fines content and a positive partial dependence on the fraction coarser than 1phi. Therefore the coarse sub-population acts independently to increase sediment porosity. This may be explained by the fact that the coarse fraction was lithic in origin, and consisted primarily of platy shale fragments. However, a model based on 'bridging' across voids in a cohesionless framework is not applicable in these sediments, where coarse particles are probably suspended in a fine-grained cohesive matrix.

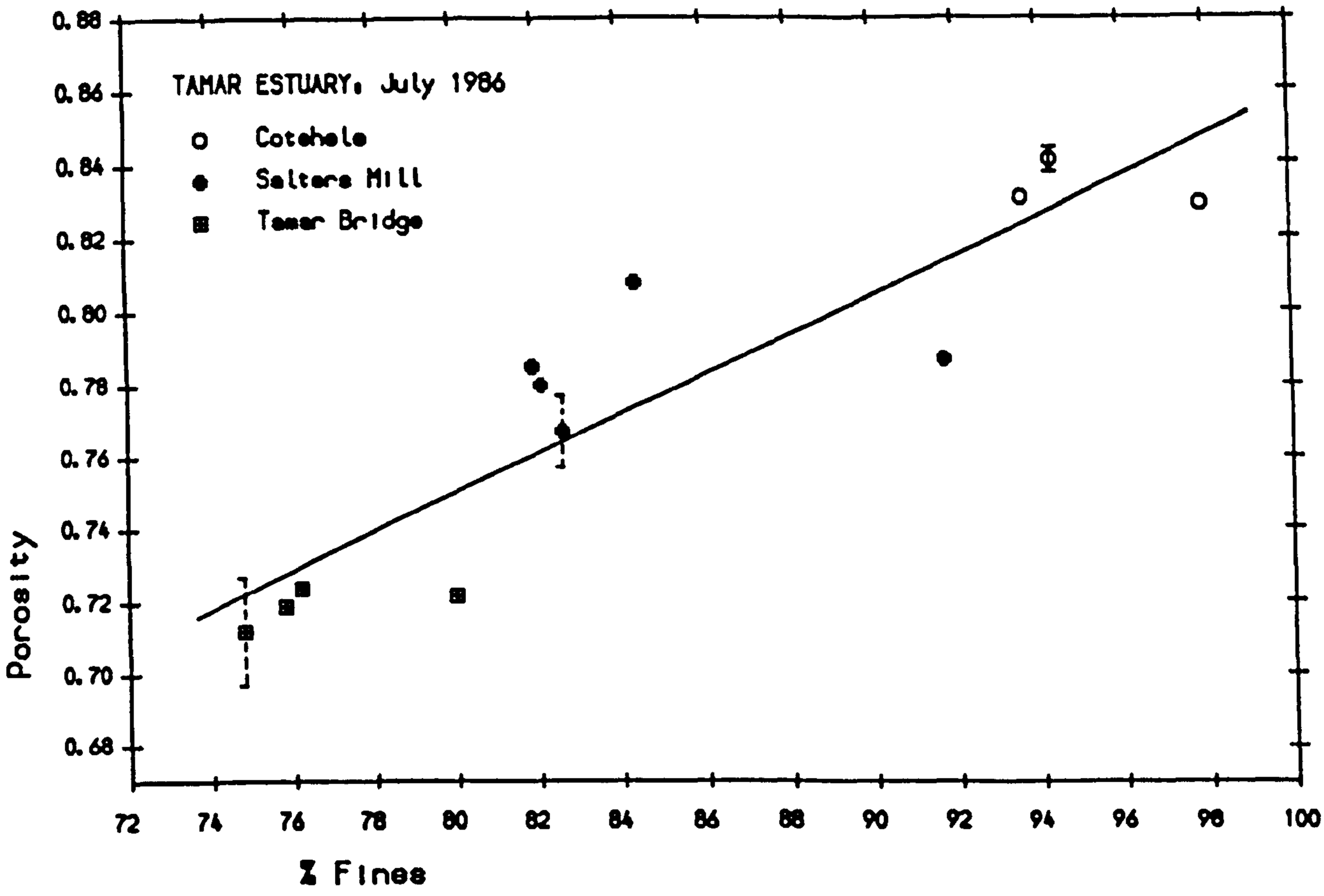

Fig. 5.2.46.

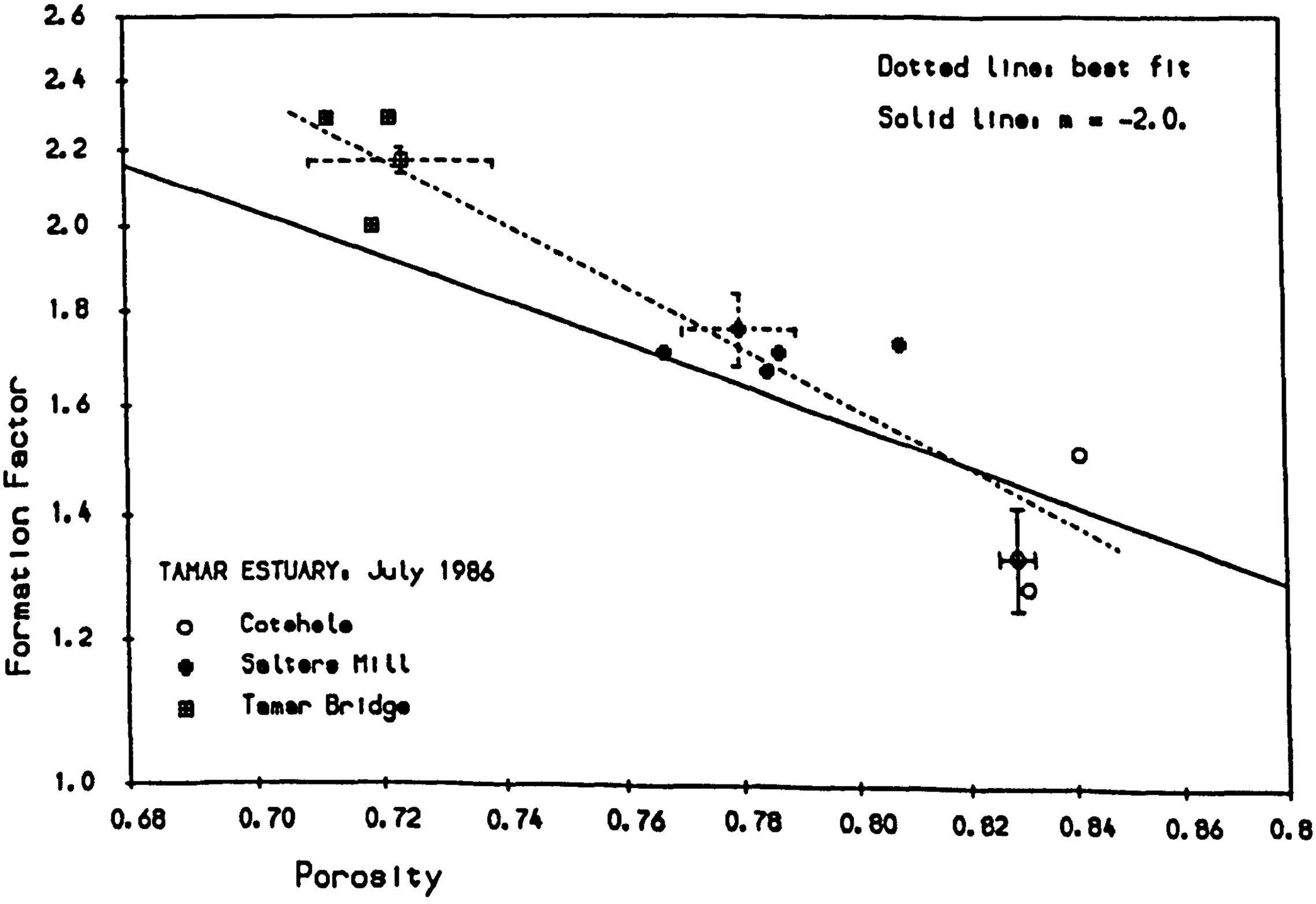

Fig. 5.2.47.

Formation Factor

Two, probably related, relationships were identified for FF. The strongest relationship is obtained with porosity; that with % fines is probably indirect through its control on porosity. Fig. 5.2.47 illustrates FF plotted against porosity, on log scales for consistency with established practice. A line corresponding to the empirically derived Archie relationship for muds [Taylor Smith, 1971] has also been superimposed, indicating reasonable but not absolute agreement.

S-wave velocity.

Since a strong dependence on porosity has been obtained for FF, a similar relationship would be expected for V_s. However, this is not found to be the case. No significant correlations are obtained, which suggests that the expected effect of between-location differences in sediment porosity is masked by some additional locally varying control. An obvious candidate is biological activity, either on macrofaunal or microbiological scales.

5.2.6.4. Summary and interim conclusions

Because of small sample sizes and poor data quality, a rather limited analysis was possible for the three locations sampled in the Tamar Estuary. Fine-grained, cohesive sediments cannot be treated as assemblages of individual particles as in the preceding sections. However, marked between-location differences were identified in textural parameters, including form of the grain size distribution. Porosity was strongly correlated with fines content, in agreement with accepted relationships. Further, FF was inversely correlated with porosity, in broad agreement with empirical relationships obtained in the laboratory. However, no such relationship was identified for V_s.

This preliminary foray into muds has proved the viability of techniques developed primarily for intertidal sands. It has also, however, indicated that some improvements are required before full-scale investigation of

fine-grained cohesive deposits is performed. In particular, the transducers should be re-designed so that their response is better suited to the extremely low rigidities encountered, and to enable measurements capable of resolving gradients in the near-surface layers. This implies that smaller probe separations should be employed for both V_s and FF characterisation.

5.2.7. Overall summary and conclusions.

Localised spatial variability of textural and structural properties has been assessed in a variety of fully-saturated intertidal sediments, from estuarine mudflats to exposed sandy foreshores. This has enabled investigation of localised *in situ* controls on porosity, and most importantly on the geophysical properties FF and V_s. Two V_s parameters were measured at each location, effectively characterising the upper 80mm of sediment. At Llanddwyn and in the Taf Estuary, where bulk and surface V_s were not significantly different, bulk V_s was adopted as a single representative parameter. However, at Lligwy, Freathy Sands and Red Wharf Bay, strong vertical heterogeneity in textural or structural characteristics was observed. Both surface and bulk V_s were therefore required to characterise the upper 40mm and 40-80mm of sediment respectively.

The effect of drainage of the surface layers was monitored *in situ* at Freathy Sands, and a sharp increase in V_s was obtained, albeit slightly less marked than that observed in the laboratory (Chapter 3). Bulk V_s increased more than surface V_s, indicating an additional increase in vertical heterogeneity. In contrast, no significant change in FF was observed, which again supports the laboratory findings (Chapter 4), but remains unexplained.

At each of the other locations, textural parameters have been selected in order to fully characterise observed textural variability, and at the same time to aid interpretation of the effect of this variability on sediment structure. At all locations except the Tamar mudflats, this was achieved

by splitting the grain size distribution into a lognormal modal population, and one or more coarse or fine sub-fractions. Definition of these fractions is specific to each location, depending on the form of the grain size distribution. They were not constrained to be lognormal, and were parametrised approximately by the selection of coarse and fine 'cut-off' sizes, selected to delineate differences in form of the grain size distribution.

The lognormal population comprises between 75 and 95% of the total sediment. Furthermore, at five out of the six sandy locations monitored, this population was found to be uniform in both size distribution and composition. Thus at these locations textural variability is controlled only by variation in proportion of the sub-populations. This allows interpretation of the sedimentary deposits at each location as a uniform framework having given structural characteristics controlled by the textural characteristics of the lognormal population, with secondary distortion or 'perturbation' of this framework caused by addition of coarser or finer particles.

Size is not the only important textural characteristic. At all locations except Lligwy (A), carbonate content is directly linked to variation in coarse fraction, indicating that the coarse subpopulations have higher shell content, and therefore exhibit marked differences in grain angularity and sphericity. Also, at the only location requiring definition of a fine subpopulation (Taf: T/11), this was directly related to fines content, which has very different sedimentary behaviour from sand.

At Red Wharf Bay, the lognormal population exhibits strong variability in both size distribution and carbonate content, these two being probably related. However, mode grain size remains uniform throughout, which allows some interpretation of sediment packing in terms of both proportion of coarse subpopulation and sorting of the framework population.

There has therefore been ample opportunity to verify the proposed hypothesis concerning variability of properties of predominantly uniform sands. Properties describing the uniform framework population, such as mode grain size, are the least variable. Variability in other bulk

sediment properties, namely mean grain size, porosity and geophysical properties, are lower than those textural parameters which define *second order* textural variability (proportion or composition of the fine and coarse sub-populations) and biological activity, because they are governed primarily by the uniform bulk sediment framework. Further, the proposed hierarchy of variability among the structural parameters is confirmed. Thus porosity is more variable than mode grain size because it is additionally sensitive to (*second order*) variation in grain shape and size distribution, to biological activity and to deposition rate. FF and V_s are even more variable because they are sensitive to factors such as tortuosity and intergranular contact forces, in addition to porosity.

Interpretation of localised structural variability in terms of perturbation of a uniform sedimentary framework by the admixture of coarse and fine sub-fractions and by macrofaunal activity has proved successful at most sandy locations. The limited data-set collected from mudflats in the Tamar Estuary should be interpreted differently: further measurements are clearly required in a wide range of silts and muds. The proposed textural and biological controls on packing configuration are by necessity specific to each location, and have been summarised at the end of each subsection. A summary of significant controls on porosity, FF and V_s has been presented in Table 5.2.1. This includes all possible significant partial predictors, and combines results for both surface and bulk V_s. Despite the high degree of scatter, small sample sizes, and interaction between parameters, which detract from the significance of individual relationships, it is possible to draw some general conclusions from the more consistent results.

The effect of second order textural variation on packing configuration depends on size, shape and composition of the admixed subpopulations. Shell fragments increase porosity for a given size distribution by forming 'bridged' structures within the sediment on deposition, preventing close packing. However, since the coarse fraction often contains higher carbonate content, the opposing effect of increasing the overall size distribution, and hence allowing more efficient packing, cannot be overlooked. Results suggest that where the shell fraction is reasonably close in size to the framework population (as in the Taf Estuary, at Red

Table 5.2.1. Summary of significant controls on Porosity, FF, V_g.

PARAMETER	PREDICTOR	EFFECT	LOCATIONS	Total
POROSITY	% Carbonate	[+]	TAF(ALL) TAF(8) LLIG(ALL) LLIG(B) RWB	5
		NONE	TAF(11) LLIG(A)	2
	% Fines	[+]	TAF(ALL) TAMAR	2
		NONE	TAF(11)	1
	Coarse sub-fraction	[+]	{TAF(ALL) TAF(8)}↑ RWB TAMAR	4
		[-]	LLIG(B) LLIG(ALL)	2
		NONE	LLIG(A) {TAF(11)}↑	2
	Arenicola	NONE	LLIG(A) LLIG(B) LLIG(ALL)	3
	Lanice	[+]	RWB	1
	Corophium	[+]	TAF(ALL)	1
		NONE	TAF(11)	1
FF	Porosity	[-]	TAMAR	1
		NONE	TAF(11) TAF(8) LLIG(A) LLIG(B) LLIG(ALL) RWB	6
	% Carbonate	[+]	LLA(ALL) LLA(*Lan*)	2
		[-]	TAF(8)	1
		NONE	LLA(*Aren*) TAF(11) LLIG(A) LLIG(B) LLIG(ALL) RWB	6
	% Fines	[-]	TAF(11) TAMAR	2
	Coarse sub-fraction	[+]	LLA(ALL) LLA(*Lan*) LLA(*Aren*)	3
		[-]	TAF(8)	1
		NONE	TAF(11) LLIG(A) LLIG(B) LLIG(ALL) RWB TAMAR	6
	Arenicola	[-]	LLIG(B) LLA(*Aren*) LLA(ALL)	3
		NONE	LLIG(A) LLIG(ALL)	2
	Lanice	[-]	LLA(ALL) LLA(*Lan*)	2
		NONE	RWB	1
	Corophium	[-]	TAF(11)	1

/contd.....

PARAMETER	PREDICTOR	EFFECT	LOCATIONS	Total
V_s [Bulk and Surface]	Porosity	[-]	TAF(8) TAF(ALL) TAF(11) RWB	4
		NONE	LLIG(A) LLIG(B) LLIG(ALL) TAMAR	4
% Carbonate		[+]	LLA(ALL)	1
		[-]	LLA(*Lan*) TAF(8) TAF(11) TAF(ALL)	4
		NONE	LLA(*Aren*) LLIG(A) LLIG(B) LLIG(ALL) RWB	5
% Fines		[-]	TAF(ALL)	1
		NONE	TAF(11) TAMAR	2
Coarse sub-fraction		[+]	LLA(ALL)$^{+}$ LLIG(B)$^{+}$ LLIG(ALL)	3
		[-]	{TAF(8) TAF(11) TAF(ALL)}$^{\uparrow}$ RWB LLIG(B)* LLIG(ALL)*	6
		NONE	LLA(*Aren*) LLA(*Lan*) LLIG(A) TAMAR	4
	Arenicola	[-]	LLIG(B) LLIG(ALL)	2
		NONE	LLA(*Aren*) LLA(ALL) LLIG(A)	3
	Lanice	[+]	LLA(ALL) LLA(*Lan*) RWB	3
	Corophium	[-]	TAF(11) TAF(ALL)	2

Abbreviations: LLIG: Traeth Lligwy, RWB: Red Wharf Bay
LLA: Traeth Llanddwyn, *Lan*: *Lanice* zone
Aren: *Arenicola* Zone.

Symbols/footnotes:

{ }$^{\uparrow}$: Carbonate content related to coarse fraction (TAF)

+ : % > Ophi (TRAETH LLIGWY)
*** : % 0:1.25phi (")**

Wharf Bay and in the 0:1.25phi fraction at Lligwy(B)), porosity is increased, but where it forms part of a much coarser subpopulation (as at Llanddwyn and in the %>0phi fraction at Lligwy(B)), porosity may be reduced.

The effect of increasing fines content must also be interpreted in terms of size relative to the framework population. If they are small enough they may sit within the interstices of the framework, and hence reduce porosity. However, additional factors are their ability to form high-arched, cohesive structures and their low deposition energy. Results suggest that the latter effects are predominant in the Taf estuary, and also on the Tamar mudflats (where the fine component constitutes the framework).

Porosity was found to be rather less sensitive to variation in biological activity than expected. A possible explanation is that the porosity samples were too small to adequately characterise the effects of macrofaunal burrows and tubes: a further rather speculative possibility is that hydrodynamic, biological and textural factors tend to cancel each other out in natural deposits, resulting in a narrower range of stable (and hence preserved) structures. This was borne out by the low porosity variability observed at Lligwy (B), due to the opposing effects of two correlated textural controls.

Several consistent controls on the geophysical properties were also identified. Both FF and V_s should be inversely related to sediment porosity for a given sediment, and all significant relationships identified were indeed inverse. However, there is an unexpectedly poor correspondence between measured FF and porosity, which can perhaps be explained partially by the difference in sample volumes involved. In the Taf Estuary, FF is reduced by factors which do, in fact, increase porosity, notably fines and carbonate contents, although a direct relationship is absent. At Lligwy and Red Wharf Bay, simple FF:porosity relationships are complicated by additional dependence on tortuosity, due to variation in textural composition. Thus higher carbonate content tends to increase porosity but also increases tortuosity, thereby counteracting any effect of porosity variation on FF. It also increases intergranular

friction, and hence V_s, at Llanddwyn, although elsewhere the associated increase in porosity has the most significant effect. Fines content reduces V_s in the Taf, either indirectly through its effect on porosity or directly through a reduction in intergranular friction.

Perhaps most importantly, while porosity is not apparently directly affected, the geophysical parameters are consistently related to biological activity at all locations except Lligwy (A). This may have been due to the relatively small sample volumes involved in porosity determination, or alternatively to the fact that geophysical parameters are additionally sensitive to factors such as tortuosity and intergranular rigidity.

Where identified as significant, biological activity reduced FF. This includes *Arenicola* at Llanddwyn and at Lligwy (B), *Corophium* in the Taf, and *Lanice* at Red Wharf Bay. It is therefore suggested that both tubes and burrows increase bulk porosity and reduce tortuosity at these locations. In marked contrast, opposing effects are identified for V_s. Thus burrowing organisms, such as *Corophium* in the Taf and *Arenicola* at Lligwy (B), tend to reduce V_s by creating fluid filled voids within the sediment fabric. However, *Lanice* tubes increase V_s at both Red Wharf and Llanddwyn, indicating that these rigid-walled structures act to increase sediment rigidity.

5.3. TEMPORAL AND SPATIAL VARIABILITY: SEASONAL CONTROLS.

5.3.1. Introduction.

The previous section describes a series of experiments designed to measure variability of a sedimentary deposit over medium spatial scales, by sampling several sites within a location at a given time. This work was complemented by a further study during which a localised set of sites was monitored at regular time intervals. The fact that there is marked temporal variability in many biological and hydrodynamic processes suggests that sediment physical properties should also vary with time: clearly this has important implications for interpretation of point geophysical measurements.

A seasonal temporal scale was selected, which involved sampling at monthly intervals over a 13 month period. The effects of shorter term variation such as spring-neap and tidal cycles were removed by sampling always at the same stage of the tide (sediment surface just saturated, towards low-water on or near neaps).

Several constraints influenced the selection of sampling sites. Limitations on data processing time and the need to sample during one ebb tide restricted the number of sites to 5 within a single location, which had to be easily accessible from the laboratory. Further, to maintain as wide a scope as possible, these 5 sites were characterised by a range of biological or textural properties. With these requirements in mind, an area of the Cefni estuary was chosen (Fig. 5.3.1). The five sites were marked out one week prior to sampling in January, 1987.

Sampling and data-processing procedure remained essentially the same as that for earlier work in intertidal sediments, and has been described in general in section 5.1, and summarised in Table A1.1. The number of site-replicates of Formation Factor, V_s and porosity was increased to improve estimates of within-site variability and site means.

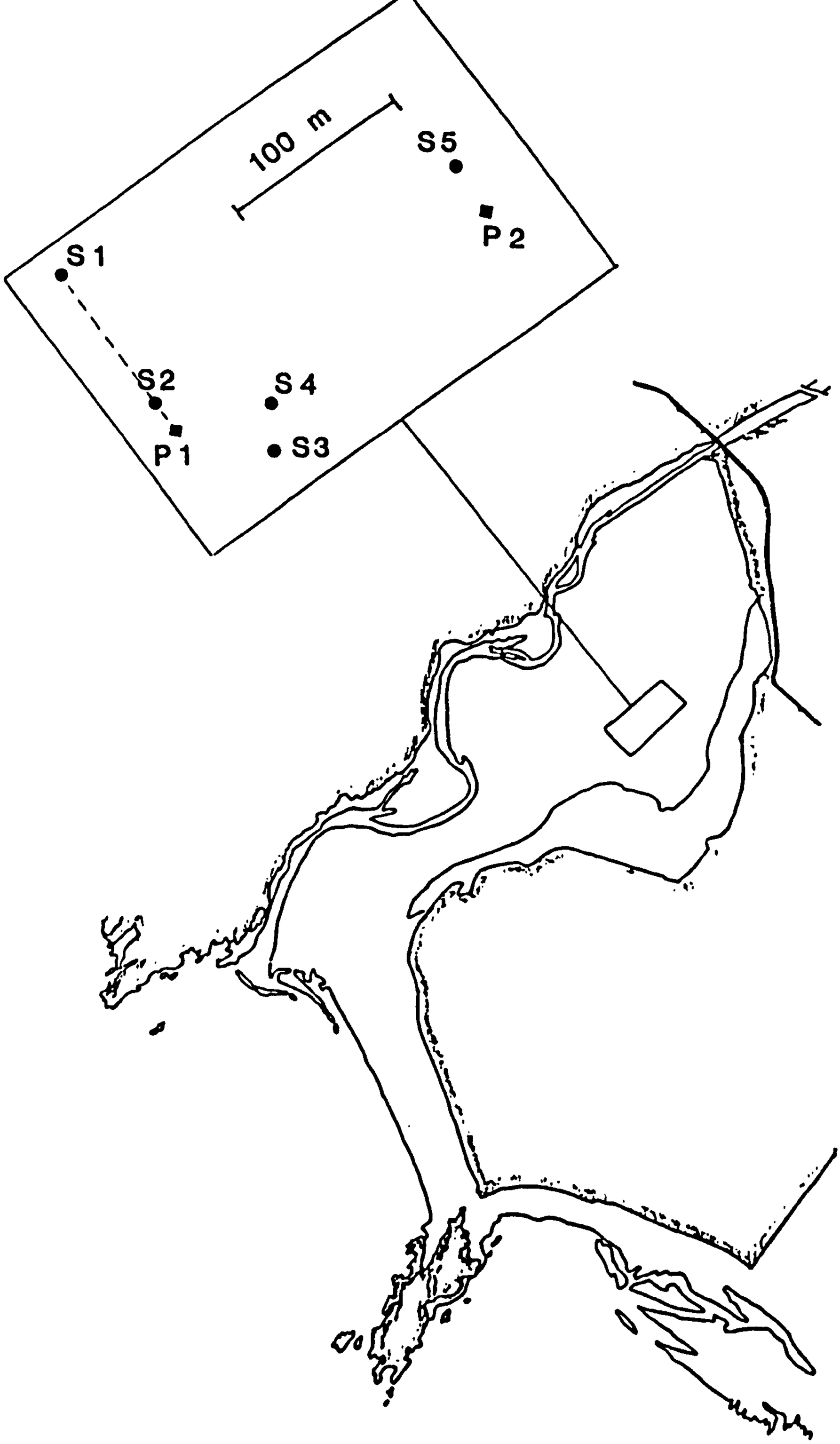

Fig. 5.3.1. Sites sampled in the Cefni Estuary.

Sampling, analysis and data processing yielded a set of quantitative variables associated with each site for each sampling date over the study period, with additional qualitative data such as meteorological conditions and box-cores. Section 5.3.2 summarises the qualitative descriptors obtained and justifies selection of appropriate quantitative parameters. In 5.3.3, relevant environmental factors and qualitative observations have been briefly summarised. Finally, in 5.3.4, the extent and nature of observed temporal variation has been described and discussed. In 5.3.5, relationships between measured properties were investigated, with the aim of identifying biological or textural controls on observed geophysical variation. This includes consideration of specific time-varying controls at individual sites, and combined spatial and temporal variation of measured parameters for the full data set.

5.3.2. Site characterisation.

Site location and description.

The positions of the five sites were all fixed relative to a concreted post, marked P1 in Fig.5.3.1. Permanent landmarks such as buildings or a second fixed post (P2) were lined up with P1 to provide bearings for locating the sites: distances along these bearings from P1 were measured using a 100m tape. Sites could therefore be relocated, to within $10m^2$, on subsequent sampling days. Most sampling was effected within $1m^2$ at each site, the exceptions being the more destructive pore-fluid samples and box-cores. These were taken within 2-3m of each site.

The original intention was to return to the same five sites each month over a 13 month period, with Site 1 providing the 'control', selected because it contained no evidence of macrofaunal activity. However, problems with falling water table and a widespread encroachment of organisms around the original site during the summer led to some modification of this intention. The primary requirement of sediment saturation, followed by the secondary criterion of minimal biological activity, resulted in control-site sampling being performed at a variety of distances along the P1-S1 line (Fig. 5.3.1). There were also problems

at Site 5 in August and September, when measurements had to be taken at the limit of sediment saturation along P1-S5.

Originally it was assumed that monthly measurement of the height of the fixed post P1 would be sufficient indication of any subsequent erosion or accretion. Unfortunately this plan was thwarted by a February storm during which this post fell over. The procedure then had to be modified because it was observed that different changes in level were occurring at each site. From June onwards the sites were levelled in using the remaining upright post P2 as temporary bench-mark.

In July a box-core was recovered from each site for investigation of sedimentary structure. It would have been helpful to have obtained a complete set of cores for each sampling date, so that seasonal changes could have been qualitatively assessed. However, this would have involved both an unacceptable degree of local sediment disturbance and an excessive increase in processing effort, and was not considered feasible.

Textural characteristics.

Parameterisation of measured grain-size distributions followed the pattern established in Section 5.2. Exploratory population-splitting was performed on time-averaged grain-size distributions for each of the five sites, which have been presented in Fig. 5.3.2. This can be justified since, as will be shown, there were far greater differences in distribution between the five sites than were observed during the sampling period at any one site. These distributions were then split into a uniform log-normal modal population and separate coarse and fine tail populations, following the procedure outlined in 5.1. The fine sub-population corresponded to the fraction finer than 4.0 phi. The coarse sub-population overlapped with the modal population and have been plotted on an expanded scale in Fig.5.3.3.

75% of the log-normal modal population, and a further 10% from the modal region of the coarse sub-population, were present at all sites, and at all times during the study. The variation in textural parameters was therefore limited to the remaining 15%.

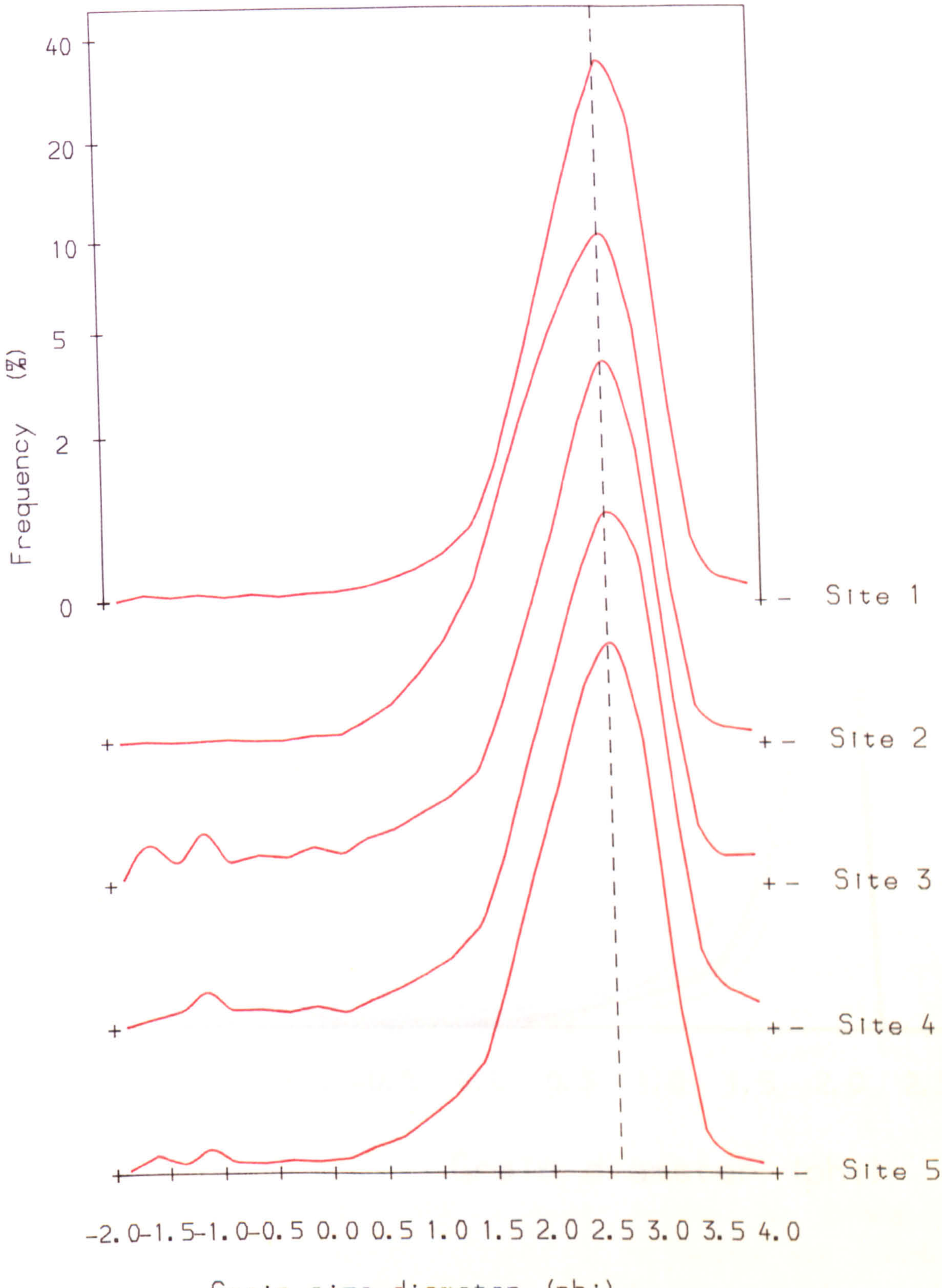

Fig. 5.3.2. Time averaged grain size distributions in the Cefni Estuary.

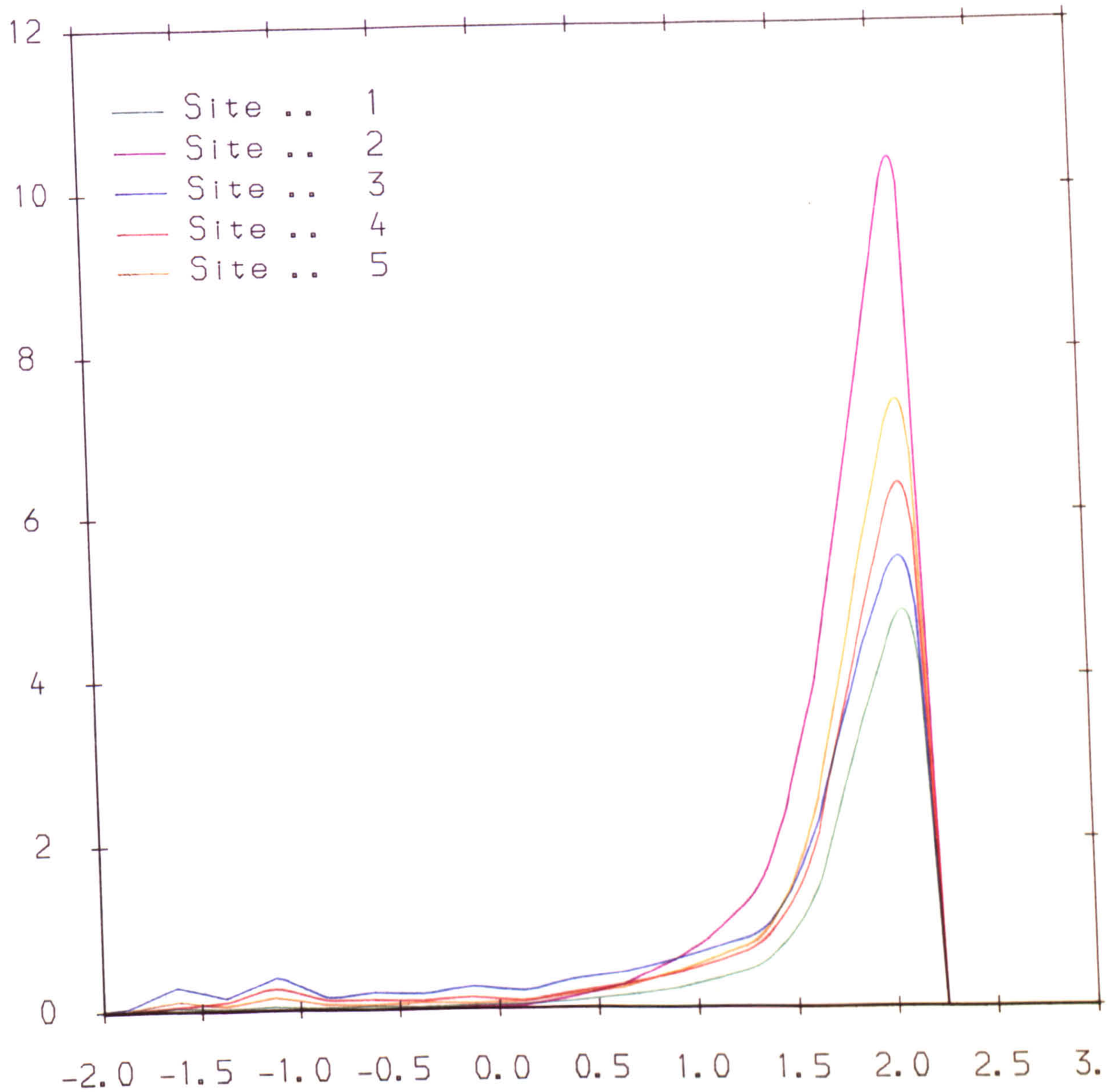

Fig. 5.3.3. Coarse subpopulations obtained from time-averaged grain-size distributions. Cefni Estuary.

Examination of Fig.5.3.3 reveals that the coarse sub-population itself can be further split into a uniformly shaped modal region and a much coarser fraction present at Sites 3, 4 and 5. For this reason, two coarse sub-population parameters were selected in addition to the fine population to fully characterise textural variation in this location. Once again, rather than perform laborious population-splitting, a series of 'cut-off' sizes was employed to parameterise individual cumulative percentage curves. The fine sub-population was estimated simply as the fines content, and the coarse sub-population was split into a fraction between 1 and 2phi, to describe the dominant coarse mode, and a fraction coarser than 1phi, to describe the extreme coarse tail.

Biological characteristics

In contrast to the previous studies, (and excepting the case of *Arenicola)* macrofaunal characterisation involved sieving sediment samples and counting the organisms themselves. *Pygospio, Hydrobia* and *Corophium* were all counted in this manner. On the first sampling date, this was attempted on site but had to be abandoned due to poor light. Subsequently samples were removed to the laboratory before sieving. Three mesh-sizes were used (5.1), because it was thought that organism size, as well as number, should affect the extent of bioturbation. In practice, however, the small sample sizes and absence of replicates, coupled with sampling errors in other parameters, rendered such complicating factors unnecessary. Analysis was found to be insensitive as to whether total density, or density weighted according to size, was considered. Therefore only total organism counts have been discussed in Section 5.3.5.

The different size classes were, however, retained for investigation of temporal variation, because an indication of reproduction and growth could be inferred. *Corophium* was observed on all three sieves, the smallest corresponding to juvenile forms. *Hydrobia* was found only on the larger two sieves, presumably because smaller forms remain in the plankton. *Pygospio* tubes were only counted on the largest sieve: fragments which passed through were ignored.

Geophysical properties.

Formation Factor.

The twelve site-replicate measurements of sediment resistance were converted to FF after calculating effective pore-fluid resistance from measured values of pore-fluid salinity and sediment temperature.

The increased number of replicates meant that a quantitative estimate of within-site heterogeneity could be obtained. Sediment resistance was thought to be the best means of obtaining such an estimate, because the technique is non-disruptive, fast, and subject only to small random errors. Therefore the measured variability of this property must relate to genuine small-scale heterogeneity in structural characteristics of the sediment, such as tortuosity, porosity, and permeability, which all affect electrical properties of the pore-fluid matrix and hence sediment resistance.

The coefficient of variation of FF, expressed as a percentage and henceforward referred to as cv(FF), was therefore treated as a separate parameter, and investigated for potential textural and biological controls.

S-wave velocity.

S-wave arrival-time/probe separation measurements were processed and averaged as described in 5.1, with an increased number of replicates to improve data quality. Surface and bulk V_s have been compared in Fig. 5.3.4. Surface V_s was significantly less than bulk V_s in many cases (44 out of 66 yielded differences outside sampling error), indicating significant velocity layering at some stage at all sites.

Because layering was apparently time-dependent, it was impossible to select a single velocity to describe the sediment properties in this study. Therefore both V_s parameters have been retained throughout analysis. Furthermore, the extent of layering was independently

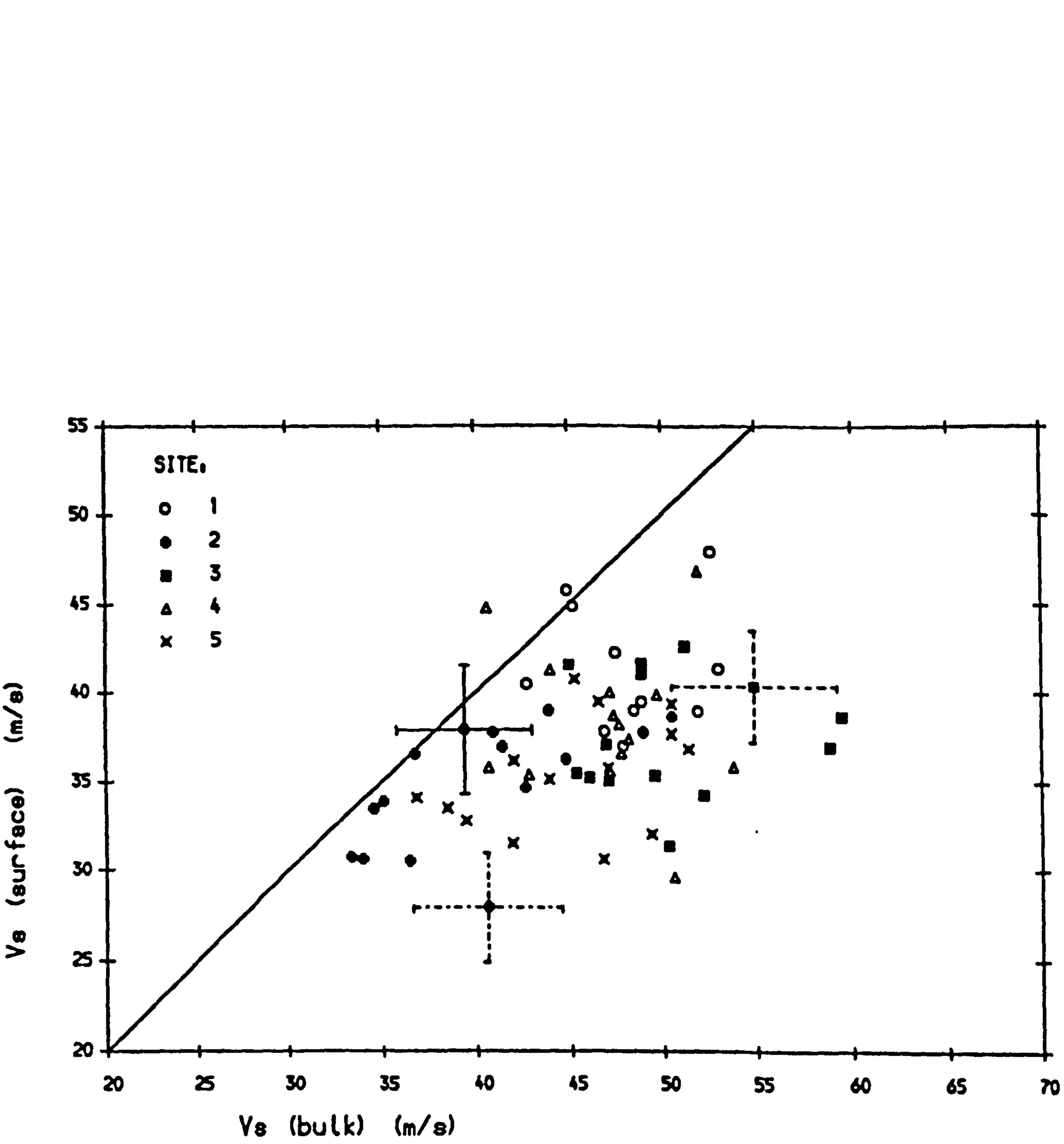

Fig. 5.3.4. Cefni Estuary. Relationship between bulk and surface V_s.

investigated, since it may have been temporally and spatially controlled by measured textural and biological characteristics. It was conveniently quantified as the ratio between surface and bulk V_s:

$$V_s^R = \frac{V_s(\text{surface})}{V_s(\text{bulk})} \qquad (5.3.1)$$

Note that this measure of vertical heterogeneity complements the coefficient of variation of FF, which measures lateral spatial heterogeneity. However, because of the high degree of sampling error compounded from the individual velocities (perhaps especially for surface V_s), it was not considered to be as reliable.

5.3.3. Temporal and spatial variation of environmental factors.

5.3.3.1. Background climatological factors

Before examining time-series of individual site variables, overall climatological variation was considered. Sediment temperature was measured at each site during sampling, and weather conditions were noted. To provide a background for this data, daily estimates of wind-speed and direction, taken from the *Daily Weather Summary* [publ. by the London Weather Centre, Meteorological Office], based on 4 point values at six-hourly intervals at Valley, Anglesey, have been presented in Fig.5.3.5. The directions have been roughly sorted into four subdivisions and colour-coded, prevailing storms being South-Westerly and therefore blowing straight up the Cefni estuary.

The differences between monthly mean air temperatures and their 30-year averages have also been compiled (from the same source) and presented in Fig.5.3.6 to illustrate some of the atypical conditions which prevailed over the sampling period. The number of nights of frost has also been included for completeness. Comparing months one year apart, it can be seen that December 1986 was much stormier than December 1987, while January 1987 was very much colder than January 1988. This lack of consistency in

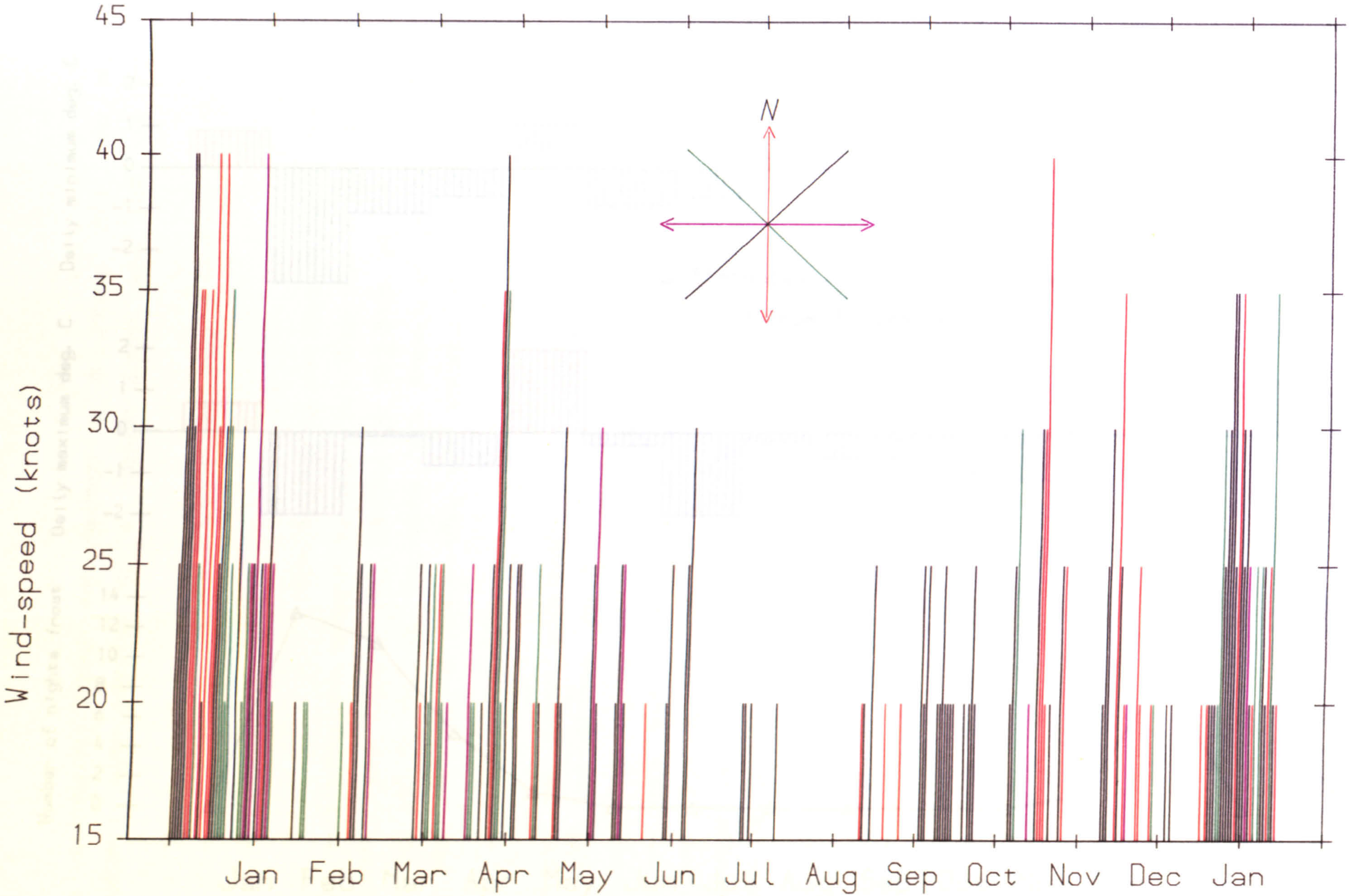

Fig. 5.3.5. Wind speeds at R.A.F. Valley Meteorological Station, Dec. 1987-Jan. 1988.

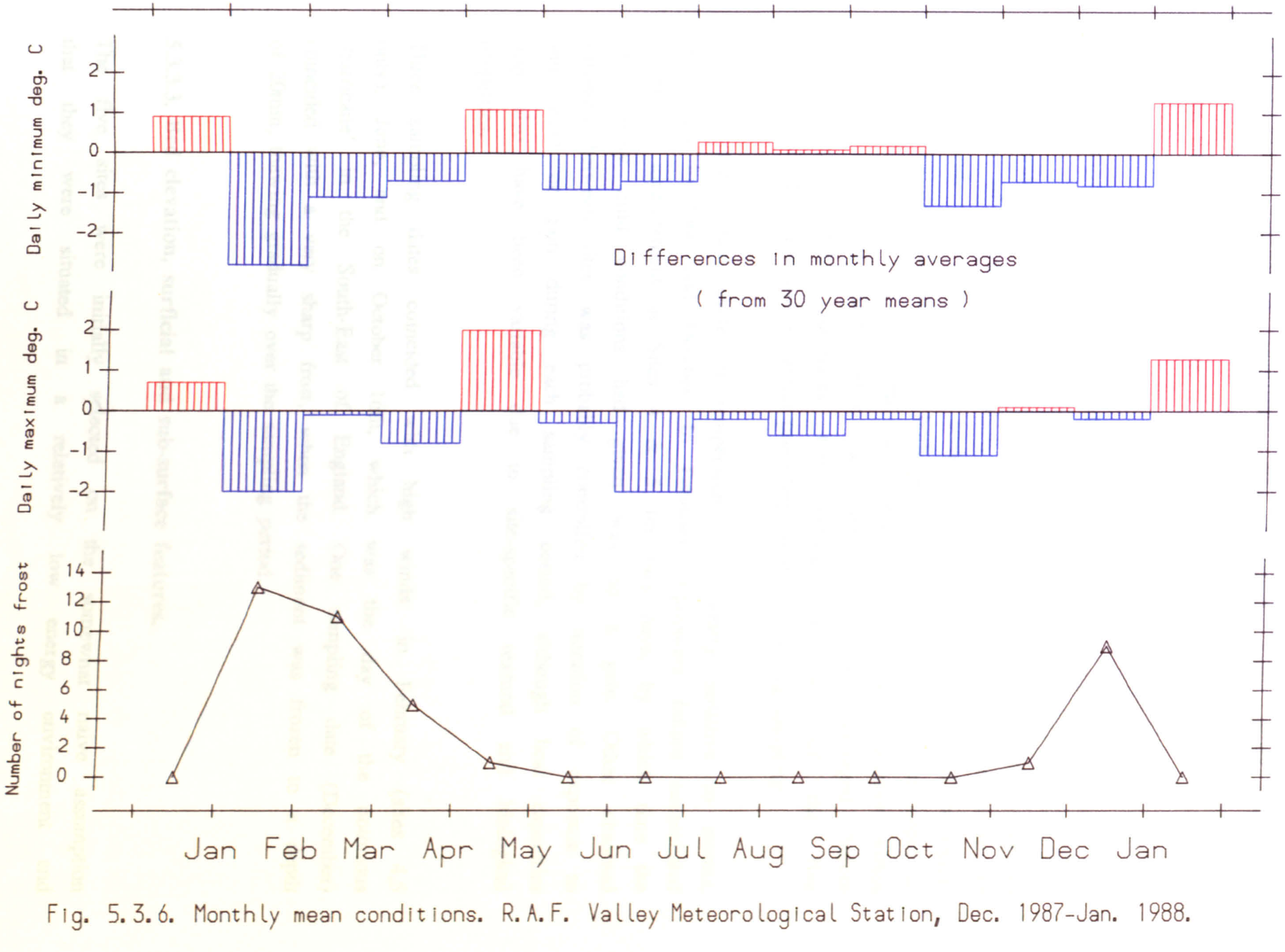

Fig. 5.3.6. Monthly mean conditions. R.A.F. Valley Meteorological Station, Dec. 1987-Jan. 1988.

conditions complicated the experimental aim of identifying seasonal periodicity in measured properties. The seasonal cycle itself was less well marked than usual, with a cold winter, followed by a cool, wet summer, then a very mild winter.

5.3.3.2. Sampling conditions and sediment temperature.

The temperature of the surface layer of intertidal sediments will vary as a function of sea-water temperature, air-temperature, time of exposure to sun or wind, and on a smaller scale to geochemical factors and biological activity. Measurements were taken both at the surface and at 50mm depth to check for gradients. In fact, the two were found to be invariably within less than 1°C of each other, so they have been averaged before presentation. Fig.5.3.7 illustrates this average at each of the five sites, combined with comments about prevailing conditions during sampling.

The expected annual cycle in temperature was clearly sensitive to storms, with dips in June and October. In February, equipment failure necessitated postponing measurement at Sites 4 & 5 for two days, by which time the exceptionally mild conditions had given way to a gale. Other observed variation between sites was probably controlled by duration of exposure to sun, wind or rain during each sampling period, although heat capacities may also have been variable due to site-specific textural and biological properties.

Three sampling dates coincided with high winds: in February (sites 4,5 only), June, and on October 16th, which was the day of the notorious 'hurricane' in the South-East of England. One sampling date (December) coincided with a very sharp frost, when the sediment was frozen to a depth of 20mm, thawing gradually over the sampling period.

5.3.3.3. Bed elevation, surficial and sub-surface features.

The five sites were initially selected on the somewhat naive assumption that they were situated in a relatively low energy environment and

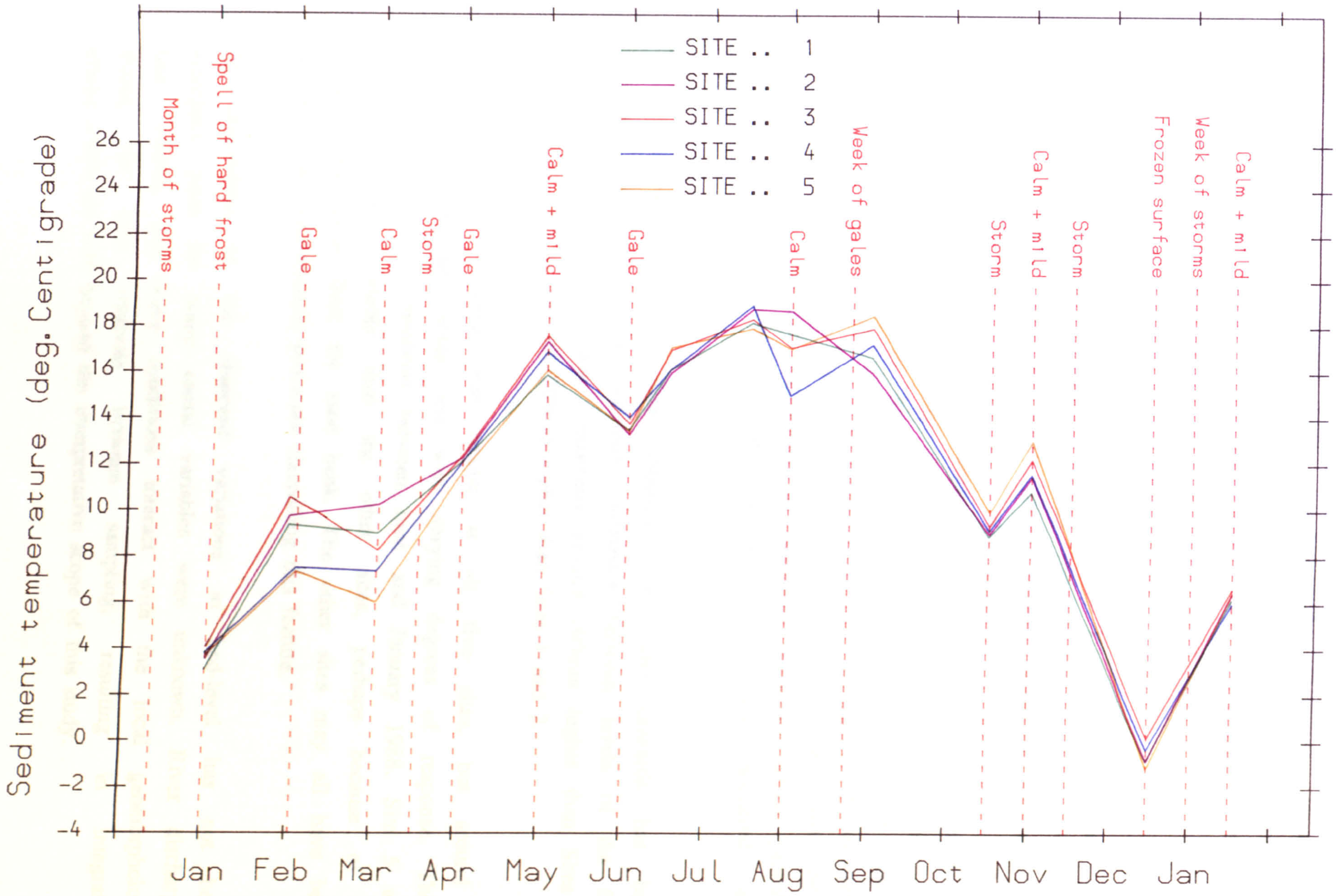

Fig. 5.3.7. Sediment temperature and sampling conditions, Cefni Estuary, 1987-1988.

therefore would not be subject to significant relative changes in bed level induced by seasonal local morphological adjustment. However it became apparent that the sites were changing relative to each other, so monthly levelling-in of individual sites was introduced in June. Unfortunately, the change over the first five months which led to this decision has no quantitative data to support it.

The major morphological change occurred at Sites 1 and 2. In January 1987 P1 and Site 2 lay in a shallow trough which remained water-covered for much of the tidal cycle. A broad, gently sloping sand-bank separated this area from the main ebb-channel. Site 1 was situated between Site 2 and the crest of this sand bank, at the limit of saturation of the sediment. By May, this feature had virtually disappeared, and 10-15cm accretion was recorded in the vicinity of Site 2. This was accompanied by a gradual encroachment of *Arenicola* towards S1. By June, no appreciable difference in elevation between the two sites could be measured. The most logical explanation is a seasonal adjustment of deposited material, which probably involved general accretion, most significantly in the sheltered area around Site 2.

The quantitative bed-level data obtained from June onwards has been presented in Fig.5.3.8. The maximum difference between levels of the five sites was 300mm. Site 4 was consistently around 100mm higher than Sites 3 and 5, which were in turn 100-200mm higher than Sites 1 and 2.

The pattern of variation was similar at all five sites, but around a different time-averaged mean and with varying degrees of response. There is a net increase in bed-level between June and January 1988. Site 5 was considerably less variable than the other sites, perhaps because of its situation well away from the sand bank. The other sites may all have been influenced by hydrodynamic processes controlling this feature.

An explanation of the observed variations in bed-level has not been attempted, since too many causal variables were unknown. River discharge, tidal currents, and wave conditions interact with the local geomorphology during the time intervals between sampling, resulting in integrated effects which are well beyond the interpretative scope of this study.

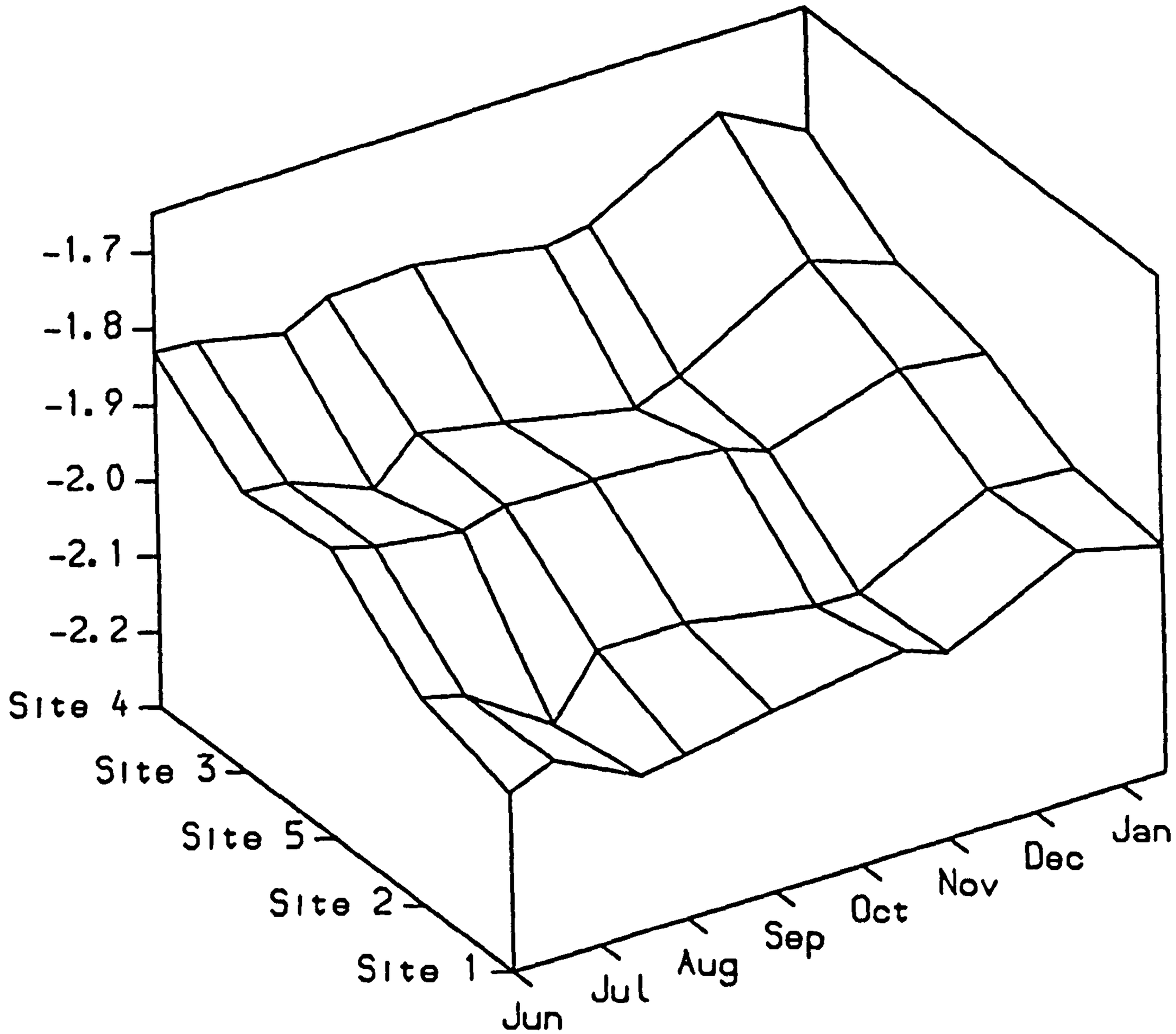

Fig. 5.3.8. Temporal variation in bed-level (m) relative to arbitrary datum. Cefni Estuary, 1987-1988.

One of the experimental objectives was to identify the response of physical properties to hydrodynamic 'events', such as erosion or accretion of the deposit. There are obvious problems involved, the most important being that because measurements were performed at monthly intervals the difference between two consecutive measurements represents an integration of reponses over time. For example, an erosional step of 150mm followed by deposition of 90mm during one month would be recorded as erosion of 60mm, but sediment sampling would be in freshly deposited material. For this reason, a high degree of consistency of response was not anticipated. At each site, step changes in bed-level have been defined as significant if they represent more than +/-20mm, as summarised in Table C1.1.

The descriptive comments made during sampling could also be used to aid interpretation of variation in quantitative sediment properties. Striking differences between sites were observed during the sampling period, as summarised below.

Site 1.

The exact location of Site 1 varied along the P1:S1 line (Fig.5.3.1), in response to encroachment of *Arenicola* and the requirement of full saturation of the sediment on sampling. The data have been grouped into three zones. In Zone 1 (80-110m from P1), rippled sand with crests perpendicular to the line P1-S1 was found throughout the year, except in October when the entire area was reworked into a plane bed.

A box core recovered from this zone in July indicates a 10cm surface layer which was apparently more permeable than the sub-layers, because the resin penetrated further [Plate 8]. The burrow was probably *Nereis*: otherwise little structure was observed, although the surface was rippled. There is more structure beneath this layer, with laminae disturbed by bioturbation, relict conical head-shafts and *Pygospio* tubes.

Zones 2 (40-60m) and 3 (30-40m) were colonised by *Arenicola* during the study. In January and February, the surface consisted of rippled sand identical to that described in Zone 1. During March and April, and continuing through until September, surface features similar to those found at Site 2 were obtained, with hydrodynamic structures destroyed by

Arenicola casts and feed pits. In December a smooth, flat surface, covered by an ice layer was found at all sites, but by January ripple marks had returned with small, anoxic *Arenicola* casts.

Site 2.

Between January and March, Site 2 was characterised by a dark, strongly cohesive algal 'mat' which retained the imprints of birds' feet, and by remanent anoxic *Arenicola* casts. Few active casts were present. This mat was observed to be breaking down in March, and by April had been replaced by a very soft surface layer with high-relief *Arenicola* casts, which characterised the site for the remaining spring, summer and autumn months. The only exceptions were observed during high winds, when a rippled surface with planed-off (but active) casts was formed. The algal mat reappeared in December, but by January 1988 it had broken down again, perhaps due to re-activation of *Arenicola* under anomalously mild conditions.

The July box core [Plate 9] is characterised by an uneven surface, due to feed pits and casts. An *Arenicola* burrow with oxidised walls lies beneath a conical head-shaft structure, and a single *C. edule* is visible at 10mm. All visible structures were biogenic, including many *Pygospio* tubes. The large protruding feature at around 25cm may have been part of a hollow U-tube, curving out of the plane of the core.

Site 3

Site 3 was generally characterised by a smooth, muddy surface. *C. edule* was observed on the surface in February, stranded by recent storms. In June, the surface was covered by a soft 10mm layer of the dinoflagellate *Phaeocystis*, with many *Hydrobia* tracks on the surface. Long strands of the green algae *Enteromorpha* covered the surface in July. In August a small opportunistic community of *Arenicola* appeared, but this had disappeared again by September, as had all the algae. By December and January the smooth muddy surface first described had returned.

The July box core [Plate 10] indicates marked vertical heterogeneity, with a fine, darker coloured surface layer of 50-80mm depth, containing many small (30mm) *Corophium* burrows and *Pygospio* tubes. Some *Hydrobia* are

preserved at the surface. Beneath the surface layer a further 100mm of coarser, laminated sediment is apparent, containing aligned shell fragments and two large vertical tubes which may have been relict *Arenicola* burrows.

Site 4

Site 4 was similar in appearance to Site 3 until May, when it changed in character, with small *Arenicola* casts encroaching on the site, and many active *Hydrobia*. All *Arenicola* had disappeared by July. The October storm caused significant erosion, but the site soon recovered its soft, tracked surface. As at Site 3, the sediment surface returned to its original state in December and January, apparently as an accreted layer.

The July box core [Plate 11] indicates a fine surface layer extending 50mm, with one well preserved *Corophium* in its burrow. The oxidised layer was only 5mm: many *Hydrobia* have been preserved on the surface. Other features are mainly *Pygospio* tubes.

Site 5.

The main variation of surface characteristics at Site 5 was the degree of erosion of *Arenicola* casts. Where calm spells had prevailed, as in January 1987, March, April and early June, these features built into large mounds and craters, producing surface relief of up to 100mm. During high winds, these were reworked, planed off, and formed into ripple marks and, in extreme cases, plane beds. In December and January conditions appeared to be similar to those at Site 2, with less active *Arenicola* producing anoxic casts. However, no winter algal mat was observed at Site 5. The other difference, which may be related, is that much larger numbers of active *Hydrobia* were observed at Site 5.

The Site 5 box-core was unfortunately damaged before it could be photographed: it was in fact very similar to that at Site 2, with oxidised *Arenicola* burrows, *Pygospio* tubes, and high surface relief.

The bed levels and structural features just described, together with weather conditions, provide a qualitative environmental background, against which the quantitative observations can be set. It is clear that

significant temporal variation in bed level, surficial characteristics and temperature occurred during sampling, with the result that significant variation in sediment properties should also have been obtained. In the following sections the observed variation of these parameters is quantitatively described and discussed.

5.3.4. Temporal and spatial variation of sediment properties.

Full presentation of the time-variation of relevant sediment properties at each of the five sites involves a cumbersome set of time-series of site means, or point values where appropriate, which have been presented for reference in Appendix C2.

The nature of temporal variation can be summarised by limiting discussion to four basic 'types': Annual or seasonal cycles (systematic variation with a period of twelve months), temporal trends (gradual increase or decrease over the study period), response to accretion, erosion and high winds, and spatial coherence (covariation at different sites).

The first two have been dealt with together. Trends were identified in parameters which showed significant correlations with the time in months relative to December 1987 (t_m). Seasonal behaviour was tested at each site (and overall) by performing correlation with a cosine-wave calculated from the time:

$$a(t_m) = a_0 \cos in\left(\frac{2\pi}{12}(t_m + \Delta)\right) \qquad (5.3.2)$$

A series of calculations was performed, increasing the phase offset (Δ) by one month each time, and significant correlation coefficients (and their phase) were noted. As an obvious illustration, sediment temperature yielded significant seasonal periodicity with phase offset 7 months, i.e a maximum in July, minimum in January, ($r = 0.889$). Of course, proper investigation of seasonal periodicity would require several years of data.

Response to erosion or accretion involves examination of step-change

significance and direction for each parameter at the time (and site) when a net bed-level change was observed (Table C1.1). A step was judged significant if it lay outside the associated error bars. The number of positive and negative significant step-changes, and the number of insignificant steps, were counted. The procedure is obviously fraught with uncertainty, not least in identifying genuine eroded or accreted deposits. A particular response of a property was considered to be consistent if at least half the measurements indicated that response, while less than a quarter indicated the opposite change. This requirement was initially tested for statistical significance by comparison with computer-generated random distributions. A similar test was applied to the measurements made during high winds, to identify consistent responses to storm events.

A parameter was defined as spatially coherent if a significant correlation was obtained between synchronous measurements at two or more sites during the study period. It is interesting that very few correlations of this kind were found: that is, temporally induced variation, in nearly all cases, was site-specific and independent.

Discussion of the site-specific time-variation of measured properties, grouped into textural, biological and geophysical characteristics, has been combined with analysis of variance for each property, to test for significant differences between sites. Time-averaged site means and associated coefficients of temporal variation have been listed in Table C1.2. The differences between sites have been illustrated in Fig.5.3.9, in which the bars correspond to calculated 95% confidence limits for the time-averaged mean of each site. For parametric variables, the difference between a pair of time-averaged means is significant if these bars do not overlap. Strictly, standard errors cannot be defined for non-parametric variables (which were tested using the Kruskal-Wallis method): however, the graphs still serve to indicate relative differences. Each graph has been scaled from zero to the maximum mean value of that parameter.

Observed between-site differences have been discussed in the following sub-sections. It is clear that in many cases temporal variation, while significant, was considerably less important than the spatial separation of the sites, so that site characteristics were less variable over

Time-averages

SITE: 1 2 3 4 5

Grain size mean

% Carbonate

Porosity

% Fines

Formation Factor

% Organics

Vs (Bulk)

Arenicola

Vs (Surface)

Pygospio

Vs ratio

Hydrobia

% 1-2 phi

Corophium

% > 1 phi

FF (coeff var)

0 Max 0 Max

Fig. 5.3.9. Cefni Estuary. Site means +/- 95% confidence limits.

seasonal time-scales than over medium spatial scales at any one time. Since the sites were initially selected for their different biological and textural signatures, this was not particularly surprising.

Because the grain size distribution was predominantly uniform throughout the study, the relative variability of parameters provided a further test of the hypothesis outlined in 5.2.0. In this case, two components of variability could be investigated, namely temporal variation at individual sites, and overall temporal and spatial variability of the full data-set. (Spatial variability could not be reliably separated because only five sites were sampled each month).

Figure 5.3.10 illustrates, for each parameter, percentage coefficients of variation of site-specific time-averages, expressed as percentages of the overall mean and scaled from 1-100%. The observed progression in temporal variability from mean grain size to porosity, then the geophysical parameters, and finally to second order textural parameters and biological characteristics, supports the hypothesis that the uniform sedimentary framework determines bulk sediment properties, with varying degrees of second order variation introduced via the tails of the grain size distribution and biological activity. The fact that carbonate content exhibits fairly low variability indicates that a significant proportion is associated with the uniform framework population. The figure also illustrates the extent of combined spatial and temporal variability (as the overall percentage coefficient of variation). Although this is higher than temporal variability alone for some textural parameters, it is not markedly higher for the geophysical properties. This indicates that localised spatial variability is still essentially second order, despite significant between-site differences.

5.3.4.1. Textural characteristics.

Temporal variability and spatial controls.

Time series of the textural parameters have been presented in Figs. C2.1-10. Bulk statistical parameters (mean grain size and sorting) have

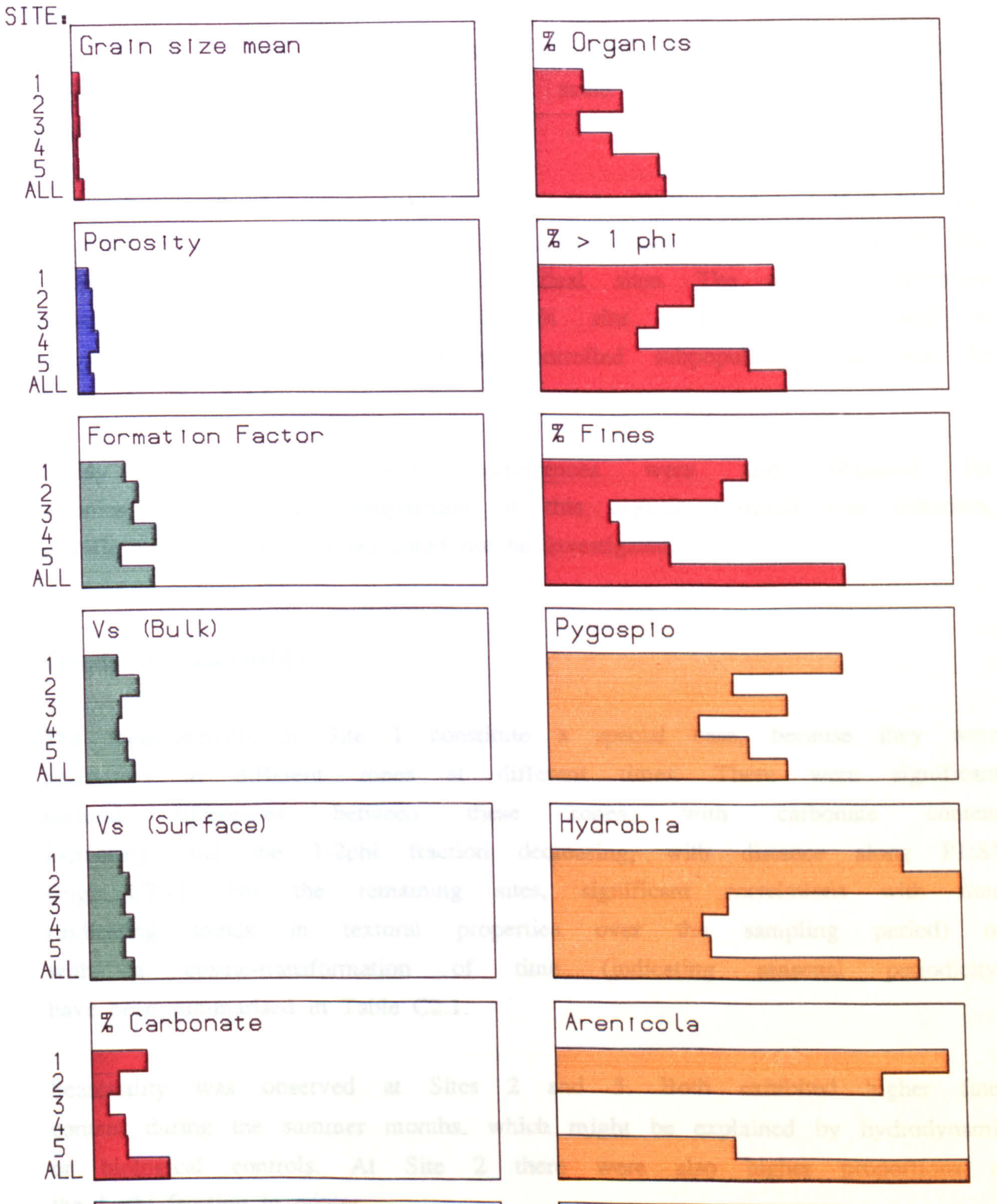

Fig. 5.3.10. Cefni Estuary. Relative temporal variability.

been included for completeness: their variability is directly related to that of the coarse and fine tail fractions. These fractions exhibited significant temporal variability, at the same time maintaining consistent strong differences between sites.

The carbonate fraction was composed of whole shells such as *Hydrobia* and *C. edule* in addition to fragments from local and offshore sources. It was relatively invariant over time at individual sites. The marked differences between sites reflect differences in *in situ* biogenic sources and in composition of the hydrodynamically controlled subpopulations, as will be discussed in 5.3.5.

Highly significant between-site differences were also obtained for organics content. Since composition of this organic material was unknown, specific microbiological factors could not be investigated.

Trends and seasonality.

The measurements at Site 1 constitute a special case, because they were performed in different zones at different times. There were significant textural differences between these zones, with carbonate content increasing, and the 1-2phi fraction decreasing, with distance along P1:S1 (Fig. C2.1). For the remaining sites, significant correlations with time (indicating trends in textural properties over the sampling period) or with a cosine-transformation of time (indicating seasonal periodicity) have been summarised in Table C2.1.

Seasonality was observed at Sites 2 and 5. Both exhibited higher fines content during the summer months, which might be explained by hydrodynamic or biological controls. At Site 2 there were also higher proportions of the 1 phi fraction in winter.

Significant trends in textural properties were identified at Sites 2, 3 and 4. At Sites 2 and 3 opposite trends in the 1-2phi fraction were observed (reducing at Site 2, increasing at Site 3). Sites 3 and 4 also showed an upward fines trend. No textural trends were observed at Site 5.

Response to accretion and erosion.

Identification of hydrodynamic controls on textural properties cannot even be attempted, since no flow data was available. However, the effect of specific 'events' could be investigated. Consistent responses to changes in bed-level and high winds have been illustrated in Fig. 5.3.11. Step-changes of each parameter, expressed as fractions of the maximum range found for that parameter at any one site, have been plotted on a scale from -1 to +1 so that magnitudes of step changes relative to overall temporal variability can be compared.

The only consistent response to erosion was obtained for fines content, which generally increased, while after deposition steps the 1-2 phi and 1 phi fractions were generally reduced. It seems reasonable to assume that material deposited in major events should be hydrodynamically well-sorted and probably log-normal, which explains the associated reduction in coarse fractions. The increase in fines with erosion is harder to explain. More general erosional events elsewhere within the estuary may have caused a higher suspended fines load, which was stranded on the surface as the tide receded. Fines content also generally increased during high winds, presumably for the same reason.

Spatial coherence.

The only significant textural between-site correlation was *negative*, obtained for the 1-2 phi fraction at Sites 2 and 3. This was, in fact, caused by the opposing trends observed at these two sites: this is not an example of spatial coherence. It is clear that textural parameters exhibited site-specific, independent temporal variation.

5.3.4.2. Benthic macrofaunal characteristics.

Temporal variation in the numbers and activity of benthic macrofauna, algae and microfauna was expected in response to seasonal factors such as

CEFNI ESTUARY.

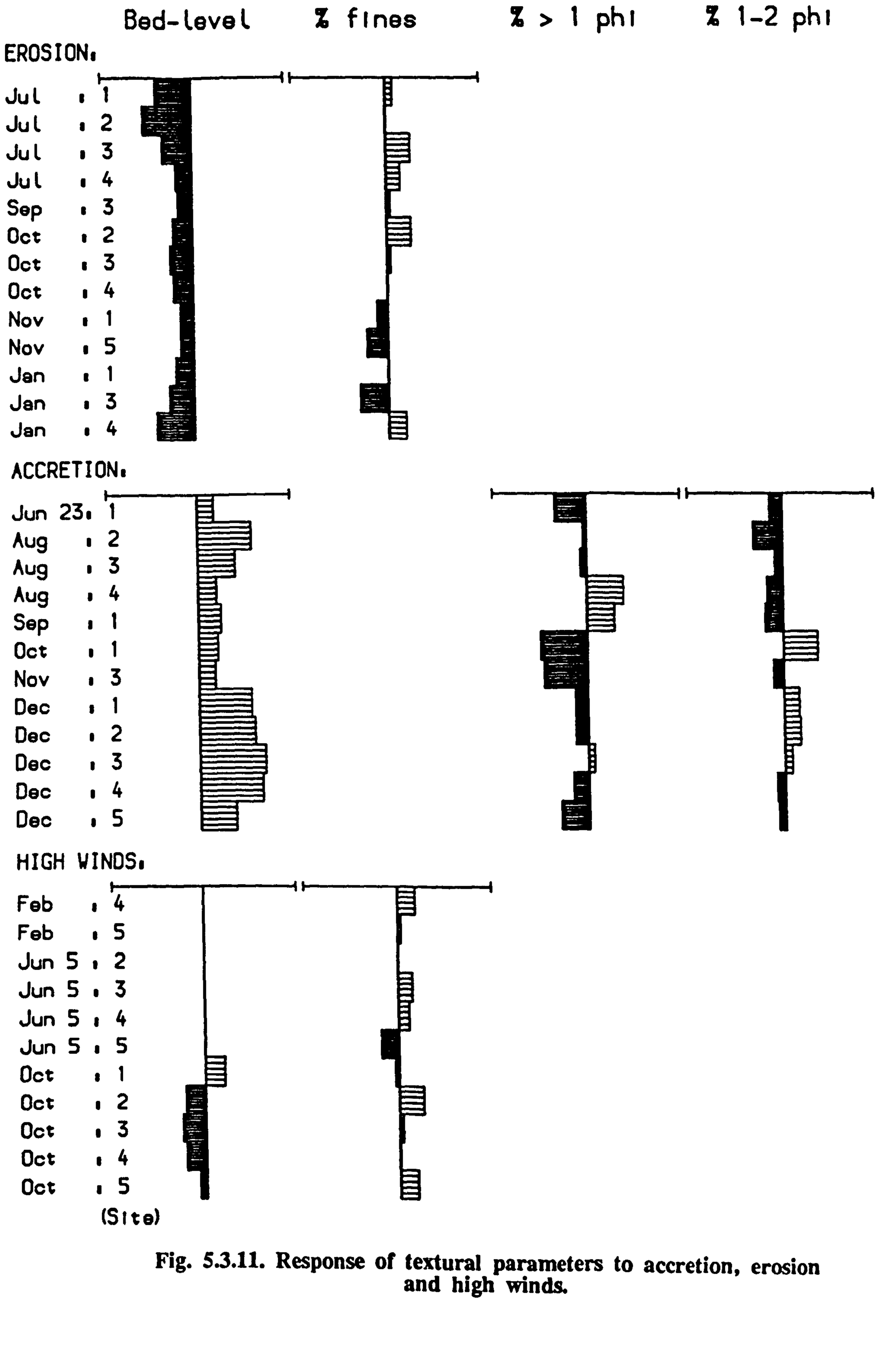

Fig. 5.3.11. Response of textural parameters to accretion, erosion and high winds.

temperature, hours of daylight and hydrodynamic environment. In Figs. C2.11-15, time series of *Corophium*, *Hydrobia*, *Pygospio* and *Arenicola* densities have been presented. It should be borne in mind that errors may represent as much as 50% of measured values, therefore only broad trends can be discussed with any confidence. Low counts from sieved subsamples may have been particularily prone to error due to within-site patchiness.

Temporal variability of macrofaunal densities was expected to be high, and ranged in some cases from 0 to 20,000 per m^2 at one site over the year. None of the distributions behaved normally or homoscedastically, but significant differences between sites, using the Kruskal-Wallis test, were found for all organisms except *Pygospio* (Fig. 5.3.9). All sites exhibited variation from very low to very high densities of *Pygospio*.

Some simple explanations of the observed temporal variation in macrofaunal characteristics have been proposed, but the overall picture is far from complete. Considering the abnormal conditions of 1987-1988, with a cool, wet summer followed by an extremely mild winter, it is hardly surprising that the organisms behaved, in several cases, contrary to expectations. In particular there was no general reduction in numbers over the winter of 1987-88. It is assumed that the mild conditions in late December and early January contributed to this, with the extremely cold January of the previous year causing low densities at the start of the study period. Another possible explanation is that the morphological change observed around Sites 1 and 2 served to create more favourable conditions for benthic communities in the area, not forgetting that the organisms themselves may have contributed to the change.

Corophium.

Corophium has already been briefly described, as has its U-shaped burrow: however, a further brief discussion of its migratory and reproductive habits, and response to environmental variation, is pertinent. While the tide is out it remains inactive in its burrow [Gamble, 1970]. Once the flood tide has returned it will emerge and is carried shorewards, to return on the ebb, eventually landing back more or less where it started.

This tidal swimming, coupled with active substrate selection, is the primary mechanism of dispersal, since eggs are carried in a brood pouch by the female and the young tunnel into the walls of the parent burrow on hatching. Two peaks of breeding activity have been observed during the year [Wolff, 1973], with large specimens beginning in February. The young develop into adult forms by late March or April, and start breeding in July. However, breeding can be spread throughout the year.

Corophium was found in varying quantities at all sites, its time variation indicating two peaks in breeding activity. However, it is unlikely that *Corophium* was breeding at Sites 1, 2 and 5, since *Arenicola* would disturb the developing young. The small numbers found at these sites were probably 'overshoots' from adult tidal swimming among the main populations at Sites 3 and 4. At these sites much higher variation in organism density was observed, with maximum counts occurring at Site 3. The larger organisms disappeared almost completely between June and November, with medium and juvenile sizes finally falling off in September. Depletion occurred about a month earlier at Site 4 than at Site 3.

The most likely cause of this depletion in numbers is variation in either oxygen levels or in anaerobic resistance of *Corophium*. Gamble [1970] found that its anoxic tolerance was considerably lower than more sedentary species, and was further reduced by high temperatures. Anaerobosis occurs in intertidal deposits containing sufficient organic matter to use up all available oxygen (supplied dissolved in the water column during tidal inundation). Site 4 was exposed for at least 8 hours per tide, and the reduction in adult forms, probably due to migration, was first observed at this site in May, when a sharp rise in sediment temperature was recorded. Similarly their return coincided with the fall in temperature in October. The generally depleted summer oxygen levels in the water column, and the summer *Phaeocystis* bloom which further restricts oxygen exchange between water and sediment, would have exacerbated the anoxic conditions.

At Site 3, adult depletion did not begin until June, the juvenile population remaining high until September (except for a drop associated with an erosion step in July), and counts were generally significantly higher than at Site 4. The most likely explanation for the difference is

the lower position of Site 3, which was not observed to drain at all on neap tides. Hence the increase in temperature was less important than the arrival of of the *Phaeocystis* bloom in June followed by *Enteromorpha* in July. Hull [1987] reports that *Corophium* counts are considerably reduced by *Enteromorpha*, and postulated oxygen-exchange reduction as the main cause, combined with tangling of adult forms. A similar seasonal pattern was observed at his test-sites, with larger sizes depleted relative to the smaller ones.

Hydrobia.

Hydrobia is a small gastropod mollusc, commonly known as the mudsnail. Several species are known, including *H.ulvae* and *H.ventosa*, but they are ecologically and morphologically very similar, and often occur together, so further classification was not attempted.

At low tide, the organism crawls about on the sediment surface, leaving erratic mucous tracks, grazing on microbial films attached to sediment particles [Eltringham, 1971]. As the surface drains it burrows into the sediment. It is capable of surviving more extreme and prolonged exposure than *Corophium* by sealing itself into its shell. When the flood tide arrives *Hydrobia* emerges and floats on the water surface by means of a mucous 'raft' which also serves as a food net, assuming that conditions are suitable. This floating ability is controllable: by withdrawing the raft and sealing itself the organism settles to the bottom. It returns on the ebb-tide, to be stranded close to its starting point.

Hydrobia selects fine-grade sediments, this factor being more important than organic content [Newell, 1965]. This is due to the fact that microbial films form only a small fraction of the organic matter in sediments, and are related to grain surface area (and hence particle size). The breeding season varies, spawning occurring over several months [Wolff, 1973]. Around 20 eggs are produced which are encased in capsules and suspended in a mucilaginous base attached to its shell. It is not certain whether or not a planktonic form is hatched - if so it spends only a few hours in the plankton before settling. Again, as for *Corophium*, the

main dispersal mechanism is by migration on tidal currents.

Hydrobia shells were found in densities of up to 30,000 per m^2, both on the surface of and within the sediment. It is not known what proportion of these shells contained living organisms. Reduction in numbers could have been caused by migration, predation by birds (e.g. shellduck) and fish (e.g flounders), erosion during storms, and sorting into the subsurface by *Arenicola*. Surface numbers were sharply reduced after high winds and during severe frosts. The highest densities were found at Sites 3, 4 and 5. More *Hydrobia* were present at Site 2 during the 1987-88 winter, which might have been related to other trends observed at this site, in particular to fining mean grain size. At Site 3 an overall upward trend was also observed, with a sharp step in counts of the small size in late June, followed one month later by the larger size. At Sites 4 and 5 a broad seasonal pattern was observed, with higher counts during late summer. Generally more small, and fewer large organisms were observed at Site 4.

Arenicola.

The burrow and method of feeding of *Arenicola marina* have already been described in 5.2.1. Breeding usually occurs in the Autumn [Wolff, 1973]. On spawning the eggs are transported shoreward. After 4-5 days they hatch and the larvae immediately bury themselves, remaining beneath the surface until final metamorphosis, usually during the following spring. The young adults migrate during the next winter from the high shore level to lower intertidal areas, normally establishing themselves in suitable permanent substrates. However migration at all stages of development is possible if conditions become unfavourable. *Arenicola* can tolerate wide ranges of salinity for short periods, especially since at 150-300mm they are buffered from the rapidly changing water column. It is more susceptible to cold, although again buffered from the worst effects.

Arenicola was found in high densities at Sites 2 and 5, virtually all year. The extent of colonisation around Site 2 increased sharply during March, with the area covered by casts extending up to 100m from P1,

including zones 2 and 3 of Site 1. Shoreward encroachment was also observed, towards Site 4. It is proposed that the observed spring appearance of small casts over a wide area shoreward of site 2 was caused by maturation of larval forms from spawning the previous autumn. These disappeared from Sites 3 and 4 quite rapidly, probably through migration, but remained elsewhere on the shoreward side. Similarly, it is proposed that the earlier encroachment around Site 1 was due to migration of year old young from other shoreward areas. This separate rearing of juveniles is sensible considering the indiscriminate feeding habits of adult organisms.

The absence of *Arenicola* at Sites 3 and 4 can be explained by a variety of factors: too much competition for reduced levels of oxygen and low pore-fluid salinity levels being the most reasonable (tolerance levels are around 70% sea-water [Wolff, 1973]). *Arenicola* has been observed in sediments of up to 3.5phi, so a textural control was unlikely.

At Sites 2 and 5 a seasonal pattern was observed, although peak activity occurred three months earlier at Site 5, and overall variability was less. The reduction observed in October was probably related to erosion of cast material (and possible suppression of activity during high winds). The seasonal pattern probably reflects cyclicity in activity, controlled mainly by temperature, with breeding affecting the extent of colonisation rather than localised densities.

Pygospio

Pygospio elegans is a small polychaete which constructs and resides in tubes of translucent chitinous material coated with shell fragments and sand-grains. Large numbers of these tubes, each about 90mm long and barely 1mm in diameter, form dense 'lawns' [Wolff, 1973]. Long filaments protruding from the top of the tube reach out across the sediment surface and pull in particles for ingestion. Like *Hydrobia*, it is a selective deposit feeder, gathering in mainly small green algae and diatoms: however it is also capable of sessile suspension feeding.

Sexual reproduction occurs between February and September, eggs being deposited in the tube of the female. These develop and hatch into a planktonic phase which can last for up to two months, before settlement and metamorphosis. Migration after the initial pelagic phase has not been reported. Asexual reproduction can also occur [Godmunsson, 1985]. The adult form, being sedentary, must be well adapted to harsh estuarine conditions. It can tolerate a wide range of salinities, down to 1.2% for short periods, and has a high temperature tolerance (up to 30°C). It is susceptible to erosion, although its tube may increase bed stability.

With the exception of Site 3, the temporal variation of *Pygospio* was erratic and inconsistent. Site 3 showed a continuous upward trend in numbers, which ties in with other trends observed at this site. In contrast to the other organisms, no significant differences in time-averaged density between sites were identified. *Pygospio* was clearly able to thrive equally well in the range of textural and biological environments encountered.

Trends and seasonality.

The significant temporal trends and seasonal patterns identified have been summarised in Table C2.2. Two points of interest should be noted: first, the two sites which exhibited time trends in textural properties also indicate trends in at least one organism count, (*Hydrobia* at Site 2; *Hydrobia, Pygospio* at Site 3) indicating some degree of interaction between biological and textural characteristics, and second, rather more seasonal behaviour was observed for the remaining organism counts than for the textural properties, indicating stronger seasonal controls on biological activity. Note that both trends and seasonality are identified for *Hydrobia* counts at Sites 2 and 3, and for *Pygospio* at Site 3, which illustrates a fundamental problem of distinguishing cyclicity from trend over limited time periods. This was exacerbated for the macrofaunal sieve-counts because no data was available for January 1987.

CEFNI ESTUARY, 1987-1988.

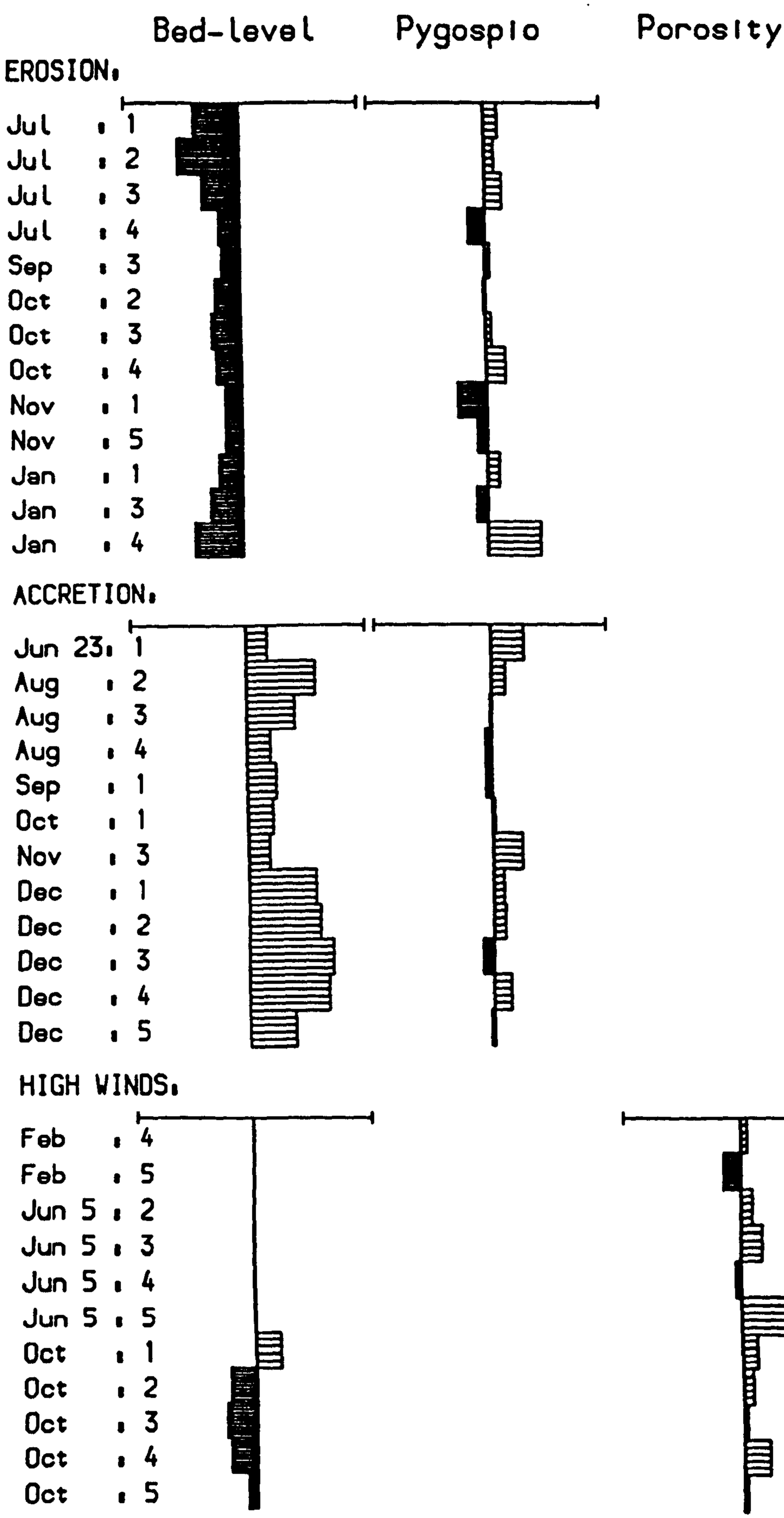

Fig. 5.3.12. Response to accretion, erosion and high winds. *Pygospio* and porosity.

Response to erosion and accretion

The only consistent response of organism density to erosion or accretion was found for *Pygospio* (Fig.5.3.12). The lack of response was not wholly unexpected, considering the relatively mobile nature of *Hydrobia* and *Corophium*, and the fact that *Pygospio* and *Arenicola*, while generally sessile, extended well below the erosion steps recorded. The fact that *Pygospio* numbers were generally increased by erosion, accretion and high winds is extremely difficult to explain in terms of removal or addition of substrate. It is possible that any substrate disturbance causes more fragile tubes, resulting in fragmentation and hence an apparent increase.

Spatial coherence

Two sites exhibited partial coherence of *Corophium* density (Table C2.3). Juvenile *Corophium* covaried at Sites 1 and 5: large specimens covaried at Sites 3 and 4. Generally, patterns of *Corophium* density were similar at all sites, with the requirement of linear correlation being perhaps too rigorous considering the errors involved. However it may be significant that more spatially coherent biological counts were not obtained, since this suggests that seasonally controlled behaviour can be modified by spatially distinct textural, hydrodynamic and biological factors.

5.3.4.3. Porosity and the geophysical properties.

Time series of site mean geophysical parameters, combined with porosity, have been presented in Figs. C2.16-20.

Temporal variability and spatial controls.

Porosity.

Examination of the temporal variability of porosity (Table C1.2) reveals a significant component compared to within-site variability, but not a high

degree of variation, especially at Sites 1 and 5. The most striking result is the fact that no significant differences between site-specific time averages were found. In other words, whatever the controls were on the textural and biological parameters which maintained differences at different sites, these were ineffective for porosity, either because they were not causally linked, or because their effects were swamped by additional, more important causes.

This lack of spatial variability, combined with an overall low degree of temporal variation in spite of high variation in macrofaunal populations and densities, suggests that porosity is unresponsive to all but the bulk framework of sediment, at least within the accuracy of the measurements. However, as was found at Lligwy in the previous section, the possibility of opposing effects 'cancelling out' must also be considered.

Geophysical properties.

In contrast to porosity, significant between-site differences in time-averaged means were found for both FF and V_s. FF was highest at Sites 3 and 4, followed by Sites 1 & 5, then Site 2. Site 3 exhibited a higher bulk V_s, but a lower surface V_s, than Site 1, while Sites 2 and 5 exhibited the lowest values of both bulk and surface V_s. Vertical heterogeneity (V_s^R) was strongest at Site 3 and weakest at Sites 1 & 2. Lateral heterogeneity (cv(FF)) was strongest at Site 4, weakest at Site 1.

These differences suggest that the geophysical properties were more sensitive than sediment porosity to between-site differences in textural and biological signature. They also, incidentally, serve to vindicate experimental procedure. Had a random scatter of data been obtained it would have been harder to assert that measured variation was genuine.

Trends and seasonality.

Significant time trends and seasonal patterns have been summarised in Table C2.4. It is clear that once again the two sites which were

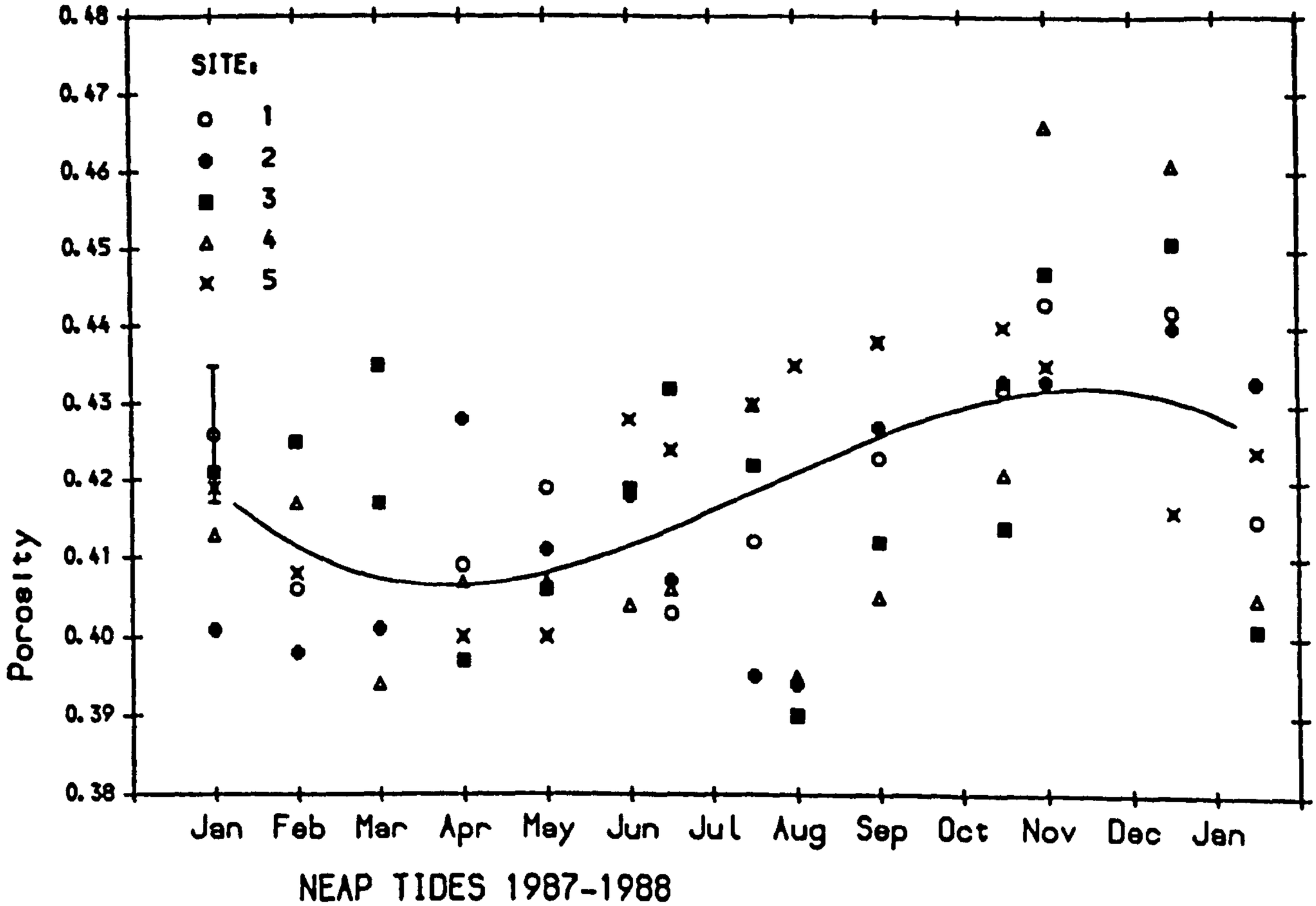

Fig. 5.3.13. Cefni Estuary. Overall seasonal variation of porosity.

characterised by overall trends in biological and textural properties also exhibited trends in some geophysical properties (and in porosity for Site 2). This implies textural and biological controls on sediment physical properties, which have been further investigated in 5.3.5. The seasonal patterns found also suggest that temporal variation in textural and biological characteristics could be as important as the localised spatial variation identified in Section 5.2. Some interesting differences between sites emerge: bulk and (most significantly) surface V_s showed significant seasonality at Site 2, with highest values in March, while at Site 4 bulk V_s was highest in October.

Porosity was the only parameter (other than sediment temperature) to exhibit significant seasonality for the combined data set from all sites. Despite a high degree of scatter (Fig.5.3.13), a minimum occurs in spring, maximum in November. This indicates the importance of seasonally varying, large scale external controls on porosity, probably related to weather patterns in combination with seasonal biological activity.

Response to erosion and accretion.

The consistent responses to erosional and depositional step-changes have been illustrated in Fig.5.3.14. In contrast to the textural and biological parameters, several parameters exhibited complementary responses to erosion and accretion. Both heterogeneity parameters (cv(FF) and V_s^R), and surface V_s were consistently affected, while the bulk parameters (FF and bulk V_s) were not. This is reasonable considering that both these parameters should be primarily affected by the protected bulk of the sediment.

The most consistent response was for cv(FF), which was reduced after erosion and increased after accretion. This parameter was assumed to represent small-scale spatial variability, so that erosion apparently reduced heterogeneity within the surface layers. The response of surface V_s, while not strictly significant because few 'steps' were outside the associated error bars, is nevertheless highly consistent. In nearly all cases, erosion steps caused a reduction in site-mean surface V_s, while

CEFNI ESTUARY 1987-1988.

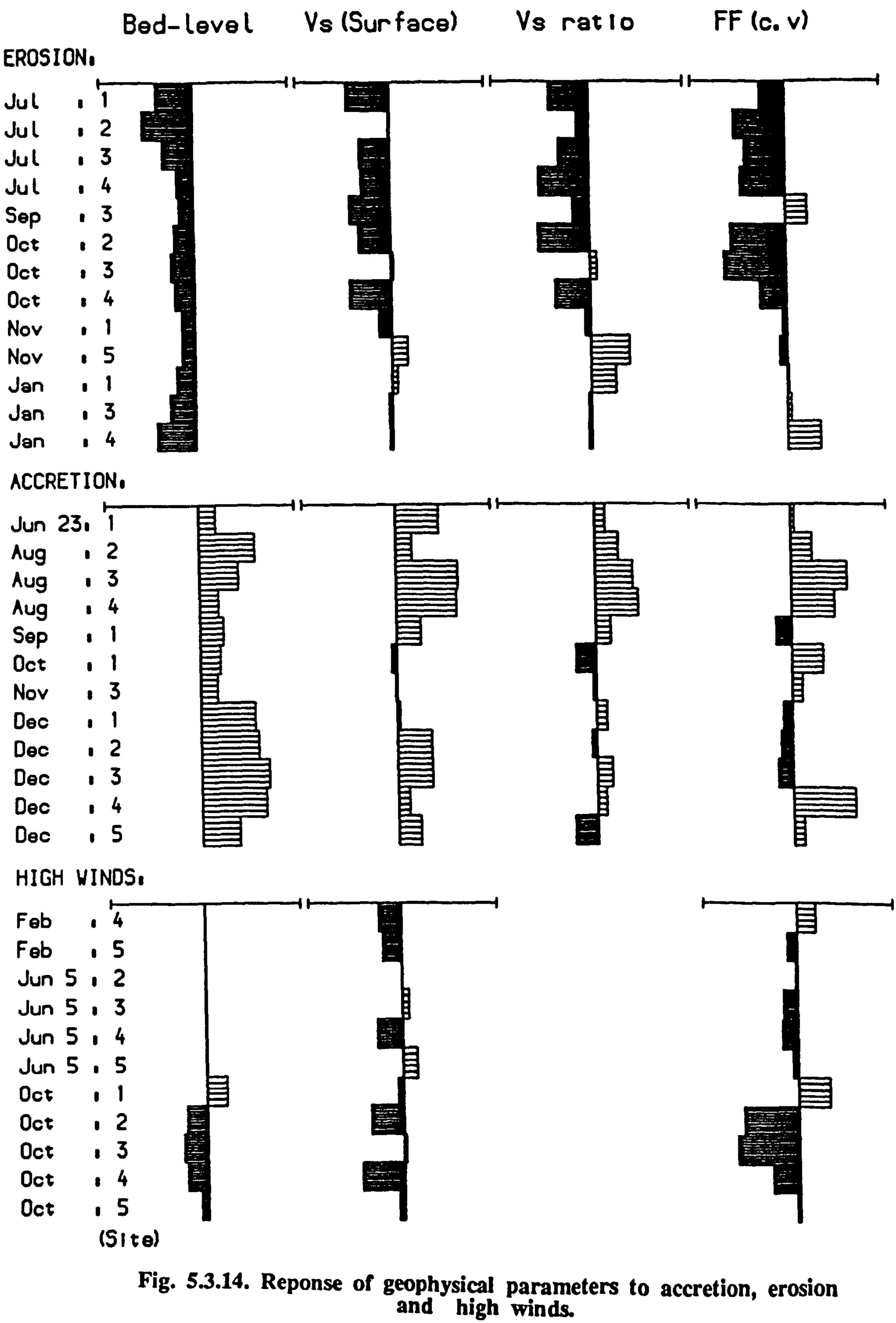

Fig. 5.3.14. Reponse of geophysical parameters to accretion, erosion and high winds.

deposition steps caused an increase. Therefore the surface layers are reworked during erosion events into less rigid, more structurally uniform deposits, with less surface relief and less biological 'patchiness', while net deposition results in increased rigidity and heterogeneity.

During high winds, both surface V_s and cv(FF) were also consistently reduced. This suggests that relatively loosely-packed, homogeneous mobile deposits are obtained after wave-enhanced bed-load transport. To support this a consistent increase in porosity was also measured (Fig.5.3.12).

Finally, contrary to the observed response of small scale lateral heterogeneity (from cv(FF)), vertical heterogeneity (V_s^R) is *increased* by erosion and *reduced* by accretion (although consistent changes were not observed during high winds).

Spatial coherence.

In contrast to the low degree of spatial coherence of both textural and biological parameters, several positive correlations of geophysical properties between pairs of sites were identified. They have been listed in Table C2.5. Both surface V_s and porosity covaried at Sites 3 and 4, while porosity also covaried at Sites 1 and 4. Bulk V_s covaried at Sites 2 and 5, despite the apparent absence of a trend at Site 5. No coherent variation was identified for FF.

This geophysical covariation may have been in reponse to relatively large scale temporal control. As one example, the spatially coherent response to high winds has already been discussed. The contemporary algal blooms associated with both Sites 3 and 4 may also have caused a coherent reponse in sediment properties, while porosity (which should affect the geophysical parameters), has already been shown to respond coherently to seasonal variation.

Having identified, quantified, compared and discussed the temporal and spatial variability in sediment properties observed during the study, it remains to investigate general relationships between those variables, and

specifically to identify the primary sources and controls of variation in geophysical properties.

5.3.5. Relationships between sediment properties.

Now that the existence of significant variation of textural, biological and geophysical characteristics on both temporal and spatial scales has been established, the task of identifying relationships between the various quantitative parameters can be addressed. The methods of data analysis employed were the same as those described in Section 5.1.3. This investigation includes separate analysis of data from individual sites, as well as of combined data from all sites. This is because the different sites may have been subject to additional unquantified highly localised controls, for example the depositional environment, sediment exposure time, or predator activity. Also, there may have been site-specific parameter interactions.

The primary aim of this part of the analysis was to establish which, if any, of the measured textural and biological characteristics affected the geophysical parameters. However, before discussing the geophysical parameters the relationships between textural and biological characteristics have been considered. This was undertaken in order to establish which groups of properties varied together, to aid causal interpretation of identified geophysical relationships, rather than to investigate biological/textural interactions.

5.3.5.1. Interaction between biological and textural characteristics.

As indicated in 5.3.3, variation in textural properties can be almost completely described by three 'size' parameters (fines content, the 1 phi fraction and the 1-2phi fraction), and two 'composition' parameters (carbonate and organics content). When the macrofaunal counts (*Pygospio*, *Arenicola*, *Corophium* and *Hydrobia*) are included a set of nine variables is obtained, each being a potential predictor of the geophysical parameters.

Significant correlation coefficients obtained for the combined variable set have been listed in matrix form in Table C3.1. The large number of significant interrelationships identified led to considerable interpretation problems. Postulation of plausible causal relationships, combined with inspection of the set of significant correlation coefficients, has yielded a conceptual framework for the variation of these parameters which has been illustrated in Fig. 5.3.15. Single arrows represent simple one-way cause and effect relationships, whilst double arrows represent those where feedback is possible, or where the two variables may have been correlated due to an additional, unquantified common cause.

The network illustrated has not been rigorously statistically tested. The proposed chains, based loosely on the technique of 'path analysis' [Sokal & Rohlf, 1986], are in broad agreement with both plausible causal arguments and the calculated correlation coefficients. The model applies to the complete data-set, thereby incorporating the widest possible ranges in textural and biological characteristics. Some additional external controls had to be postulated in order to explain observed correlations which could not be reasonably causally related. For example, zonation in pore-fluid salinity may have independently influenced macrofaunal substrate selection and deposition of flocculated suspended fine material.

Discussion of the overall conceptual framework has been sub-divided into textural, biological-textural, and biological interrelationships, and includes the few significant correlation coefficients obtained at individual sites (Table C3.2).

Textural interrelationships.

Table C3.1 indicates a considerable number of interrelationships between textural parameters. In contrast, far fewer correlations were observed at individual sites (Table C3.2), although those that were significant were generally consistent with the overall relationship. This paucity of site-specific relationships was probably caused by increased sensitivity

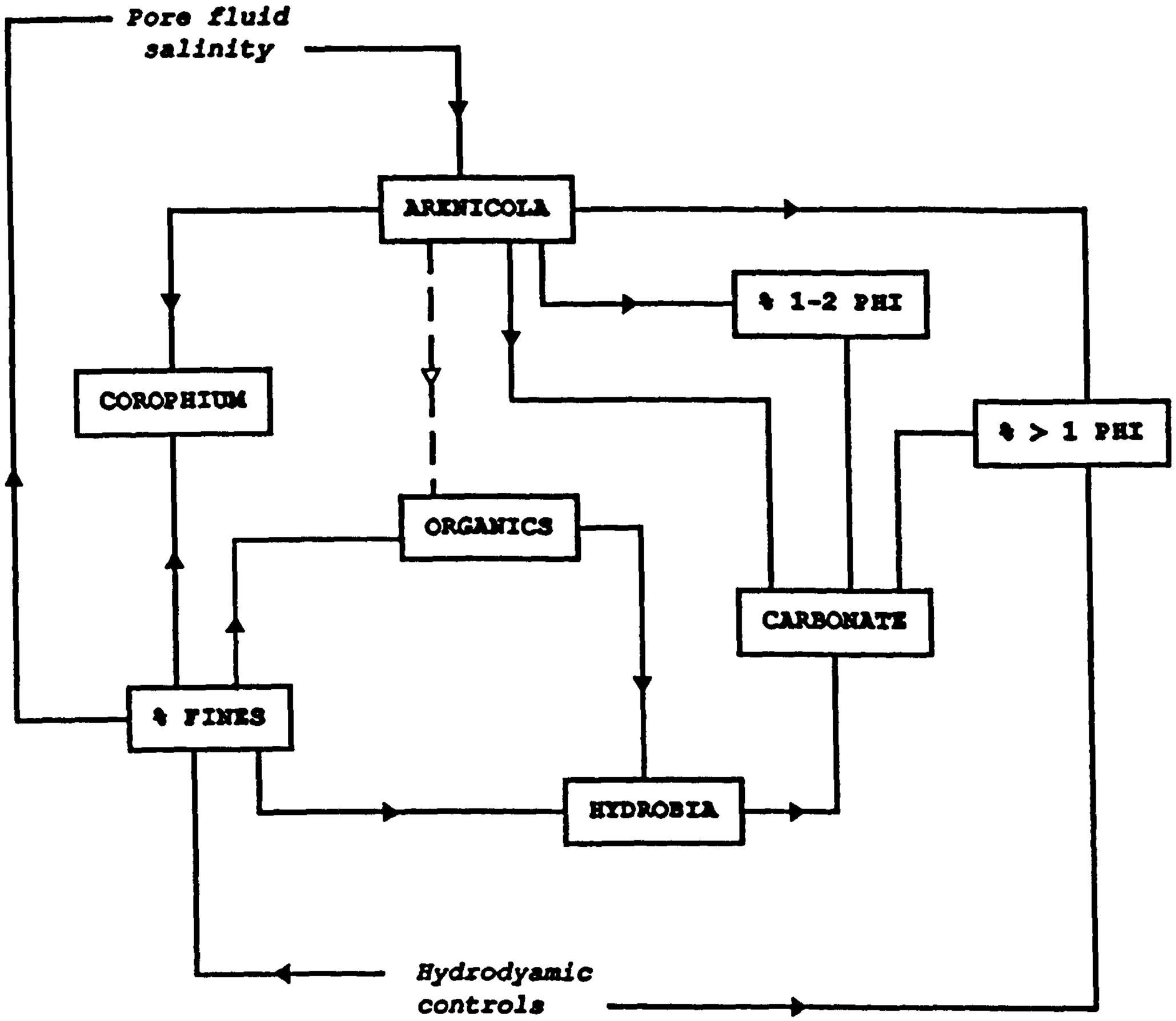

Fig. 5.3.15. Interaction between textural and biological characteristics. Cefni Estuary.

to sampling error over the lower ranges and fewer samples at individual sites.

As in the previous section on localised spatial variability, the most important textural interrelationships comprise the dependence of composition parameters on the relative proportions of sub-populations. From these a picture of the composition of individual populations can be constructed which aids interpretation of their effect on packing structure and the geophysical properties.

As previously stated, the fine sub-population corresponded directly to the fines content, indicating separate control of fine-grained deposition processes. It is interesting that the two coarse fractions were uncorrelated, overall and at all sites. Clearly two separate and independent coarse subpopulations were present, presumably derived from a different combination of processes.

From the previous sections, carbonate content was expected to be concentrated in the coarser parts of the grain size distribution, this being supported by a positive correlation with the 1 phi fraction. However, a significant negative correlation with the 1-2phi fraction, identified overall and at Site 1, indicates a rather more complex population structure than had been found earlier (Fig. 5.3.16). Multiple regression of combined data yields highly significant partial dependence on both these size-fractions (R^2 = 73.1), suggesting that the 1 phi fraction contains most shell fragments, followed by the framework population, with the 1-2phi sub-population containing the highest proportion of lithic material. Therefore the four subpopulations identified are distinct by virtue not only of their size, but also of their composition.

Another significant relationship between composition and size parameters is the expected strong dependence of organics on the fines fraction, in agreement with the relationship observed in the Tamar Estuary (5.2.6). The remaining textural interrelationships were considered to be indirect, through common causes or interconnecting paths on Fig. 5.3.15. The most marked of these was between fines and % > 1 phi, with a strong positive

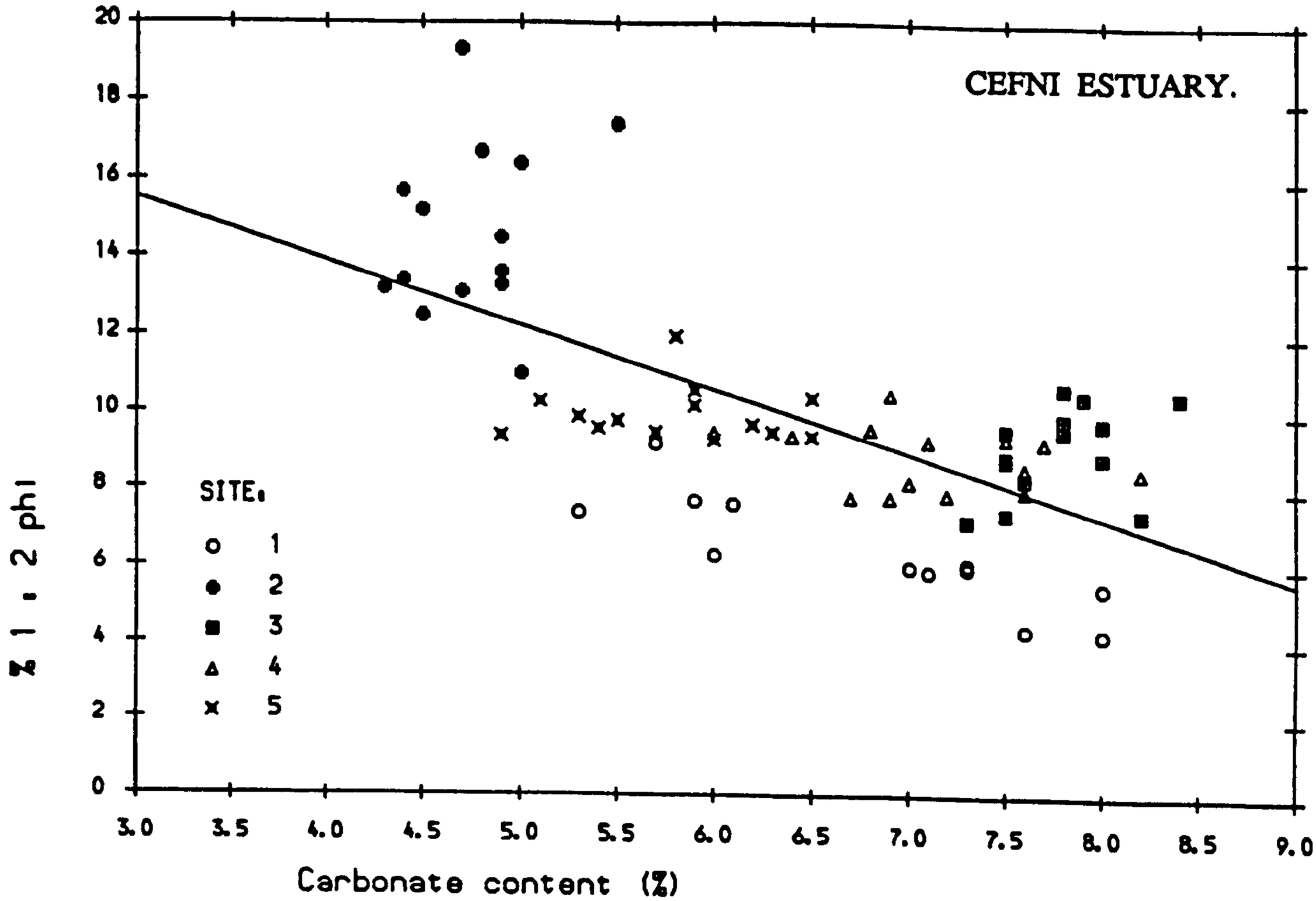

Fig. 5.3.16.

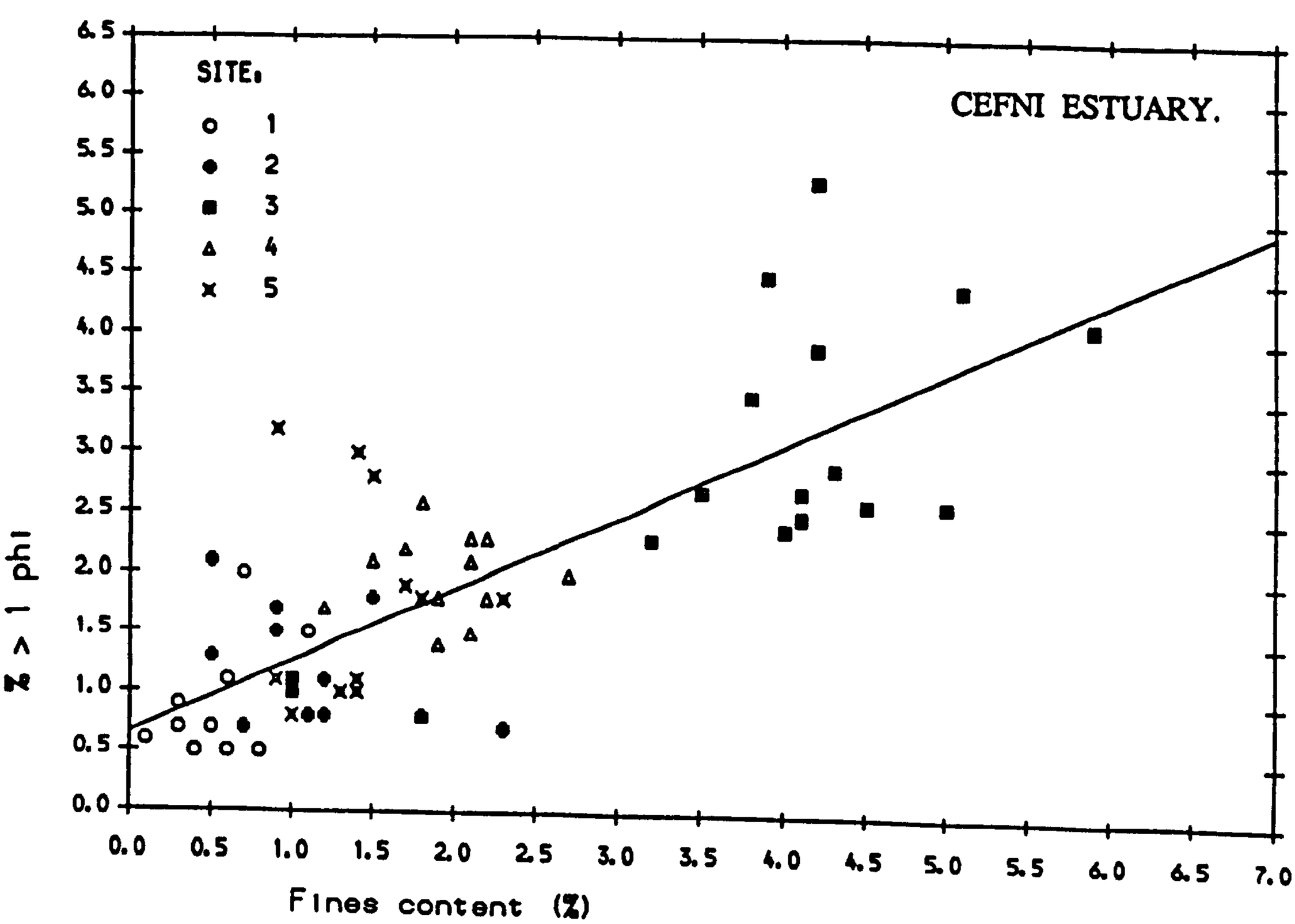

Fig. 5.3.17.

correlation dominated by the high proportions of these fractions at Site 3, and to a lesser extent Site 4 (Fig. 5.3.17). It is difficult to justify a direct causal relationship linking these two extremes of the grain-size distribution. The link via *Hydrobia* density shown in Fig. 5.3.15, which will be discussed in the following section, is not strong enough to explain the correlation coefficient obtained. For this reason, an additional external control has been postulated, indicating a site-specific combination of processes which affects both mud deposition and the coarse sub-population at the shoreward sites.

Biological-textural relationships.

Biological-textural interrelationships can take two forms: the effect of sediment texture on settlement and successful establishment of a particular species, and the subsequent effect of macrofaunal activity on the textural properties of the selected substrate. Identification and interpretation of biological-textural interactions are complicated by additional, independent temporal responses of organism counts, most notably due to reproduction and natural mortality. There are several significant correlations between macrofaunal counts and textural parameters, caused by broad differences in texture and population between sites, rather than temporal interaction at any one site. This is because textural controls on benthic community structure involve substrate selection on settlement, resulting in spatial zonation according to time-averaged sediment properties, rather than rapid small-scale adjustment of population density to highly localised temporal variation. Further, biological controls on sediment texture must involve a considerable time-lag between establishment of the population and manifestation of its effect.

Arenicola

The primary controls on *Arenicola* settlement, over these low ranges of grain size parameters, are exposure time, pore-fluid salinity and oxygen availability. Most of the significant overall correlations identified

relate to the confinement of *Arenicola* to Sites 2, 5 and to a lesser extent 1, with virtually no organisms recorded at the lower salinity, muddier, more anoxic Sites 3 and 4.

Arenicola has been shown to ingest only particles finer than 1 phi, hence there is a negative correlation with the 1phi fraction. The much stronger correlation with carbonate content indicates an additional preference for rounder lithic particles, perhaps especially within the 1-2phi fraction. Note that the *Arenicola*:carbonate scatterplot (Fig.5.3.18) is 'wedge-shaped', indicating that while an increase in *Arenicola* activity is always associated with lower carbonate content, a reduction does not cause immediate recovery. This is typical of scatterplots found for biological-textural relationships.

The positive correlation with the 1-2phi fraction may be due simply to independently controlled high values of both parameters at Site 2, but may also have been caused by surficial depletion of finer material through exposure of cast material to erosion. Thus *Arenicola* may sort coarse and shelly material into the subsurface, and encourage erosion of framework material and fines, leaving a carbonate-reduced, coarser-skewed deposit.

The observed correlations with fines and organics were probably indirect, due to low pore-fluid salinity and increased competition for oxygen at the muddier sites. *Arenicola* has been shown to cause depletion of organic material by reworking into the subsurface and digestion, but cast material soon recovers its organic component [Reichardt, 1988].

No significant correlations are observed at individual sites. This probably reflects the buffering of the established organism from small-scale changes in the surface layers, and the time-lag involved in any effect on sediment texture of a change in counts or activity.

Pygospio.

No significant correlations were found overall for *Pygospio.* Since it was found at comparable, if extremely variable densities at all sites, there

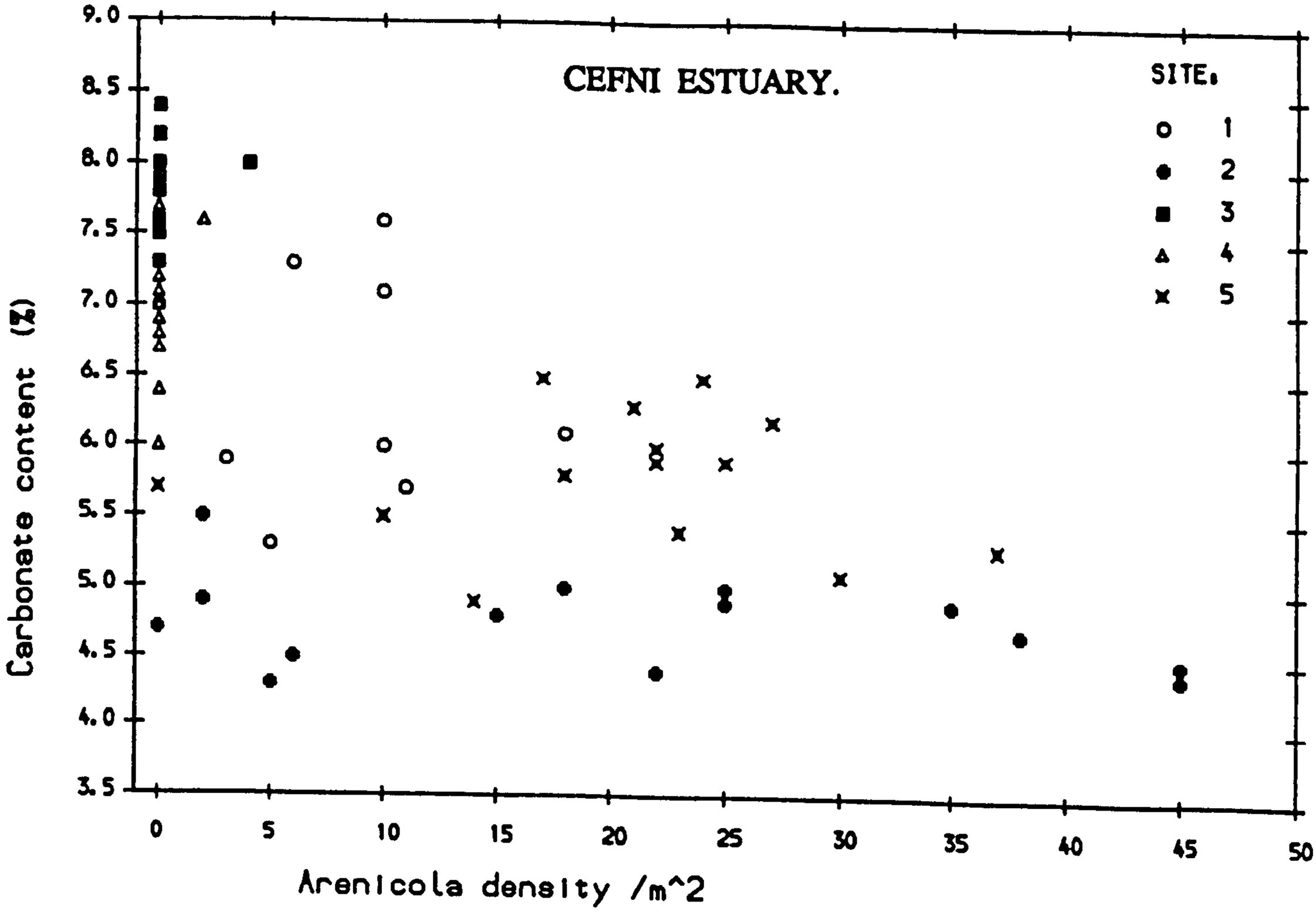

Fig. 5.3.18.

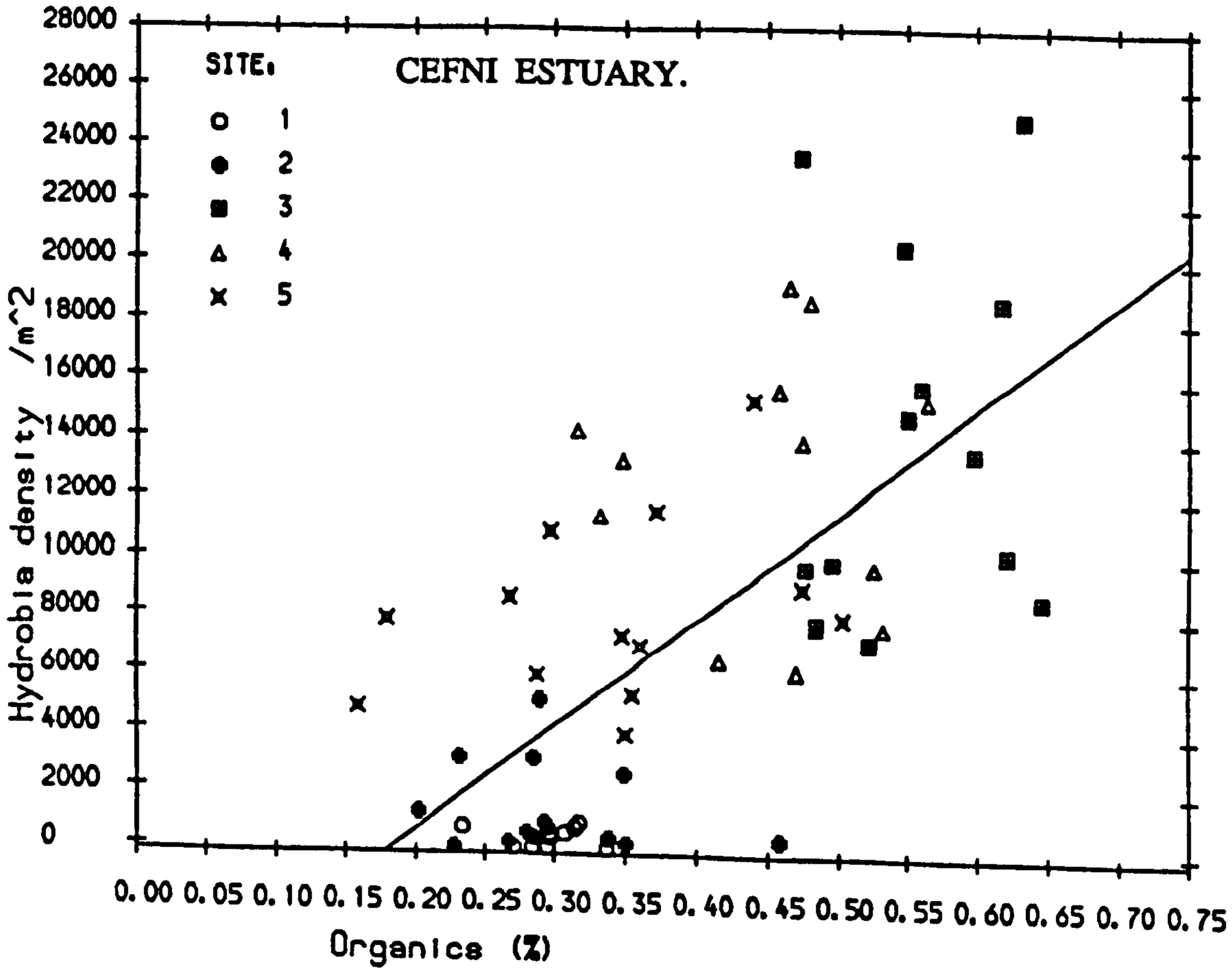

Fig. 5.3.19.

was no evidence of substrate selection within the textural and environmental ranges monitored. Also, since tubes were constructed from available sand, bulk composition properties should not have been affected (note that their much smaller size reduces the textural 'patchiness' postulated in the Llanddwyn *Lanice* samples).

The single significant correlation observed was positive, with fines content, at Site 3, where both *Pygospio* counts and fines content increased over the study period. A possible, but speculative, reason for this might be that the increasing numbers of *Pygospio* tubes served to stabilise the muddy deposit at site 3, so that deposited fines were allowed to build up. This is supported by the observed increase in bed-level over the year.

Hydrobia

Hydrobia should be relatively responsive to textural variation outside its preferred limits, since it is highly mobile. Its mode of feeding should dictate a preference for substrate with a ready supply of organic-coated fine particles. This implies causal links with both organics and fines content. A further link with these parameters may be a hydrodynamic common cause: both fines and *Hydrobia* will tend to be stranded in the same place. Strong positive correlations with both fines and organics content were identified overall, but not at individual sites (Fig. 5.3.19)

Because of its size and mobility, *Hydrobia* is less likely to affect textural properties than large sessile organisms such as *Arenicola*. An obvious exception is the direct effect of the physical presence of *Hydrobia* shells in the 1phi fraction, which results in positive overall correlations with both the coarse fraction and carbonate content.

Corophium

Corophium is similar to *Hydrobia* in its ability to migrate rapidly to a more favourable environment and in its preference for finer, organic-coated particles. It differs by its burrowing activity, which may

result in more discriminative substrate selection, and in the absence of a protective shell, which may result in reduced tolerance to exposure time and extreme salinities.

Positive overall correlations were identified for both fines and organics content, although with considerable scatter. This was thought to be due to the extreme variability of *Corophium* at all sites in response to reproduction, migration due to oxygen depletion and algal blooms, none of which could be quantified. Weak positive overall correlations were also identified for the 1 phi fraction and carbonate content, but this was probably caused by common between-site differences in time-averages.

Biological interrelationships.

Most of the overall correlations between biological parameters relate to the marked zonation of the different species. Thus *Pygospio* was not found to correlate with any other organism overall, while correlations were identified between *Arenicola* and both *Corophium* and *Hydrobia*. These relationships could be indirect, caused by differences in substrate preference, or by direct inhibition or predation. Thus *Arenicola* and *Corophium* were virtually completely exclusive (Fig.5.3.20), probably because disturbance by *Arenicola* and reduced microbial grazing potential rendered Sites 1, 2 and 5 extremely unattractive to *Corophium*, whereas at Sites 3 and 4 competition for oxygen and low salinity levels inhibited colonisation by *Arenicola*.

Hydrobia was also inversely correlated with *Arenicola*, both overall and at Sites 1 and 5. Fig. 5.3.21 provides evidence for direct interaction in addition to a substrate preference mechanism. *Arenicola* may also provide a mechanism for removal of dead *Hydrobia* from the surface layers.

Perhaps the most important conclusion concerning textural and biological interrelationships is that between-site differences form the major control. This implies that localised hydrodynamic conditions interact with equally localised benthic communities to produce relatively invariate textural and biological signatures within the surface layers.

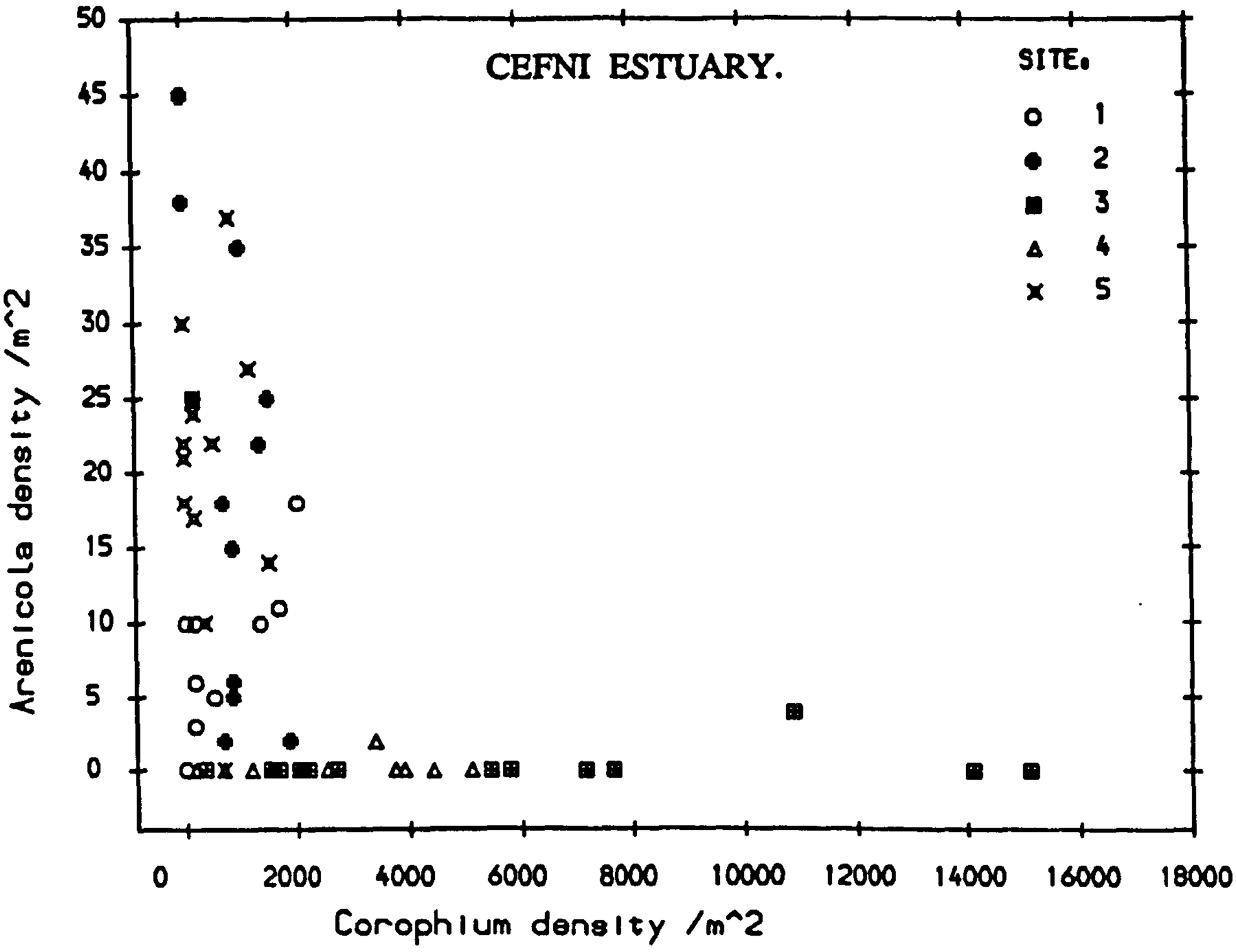

Fig. 5.3.20.

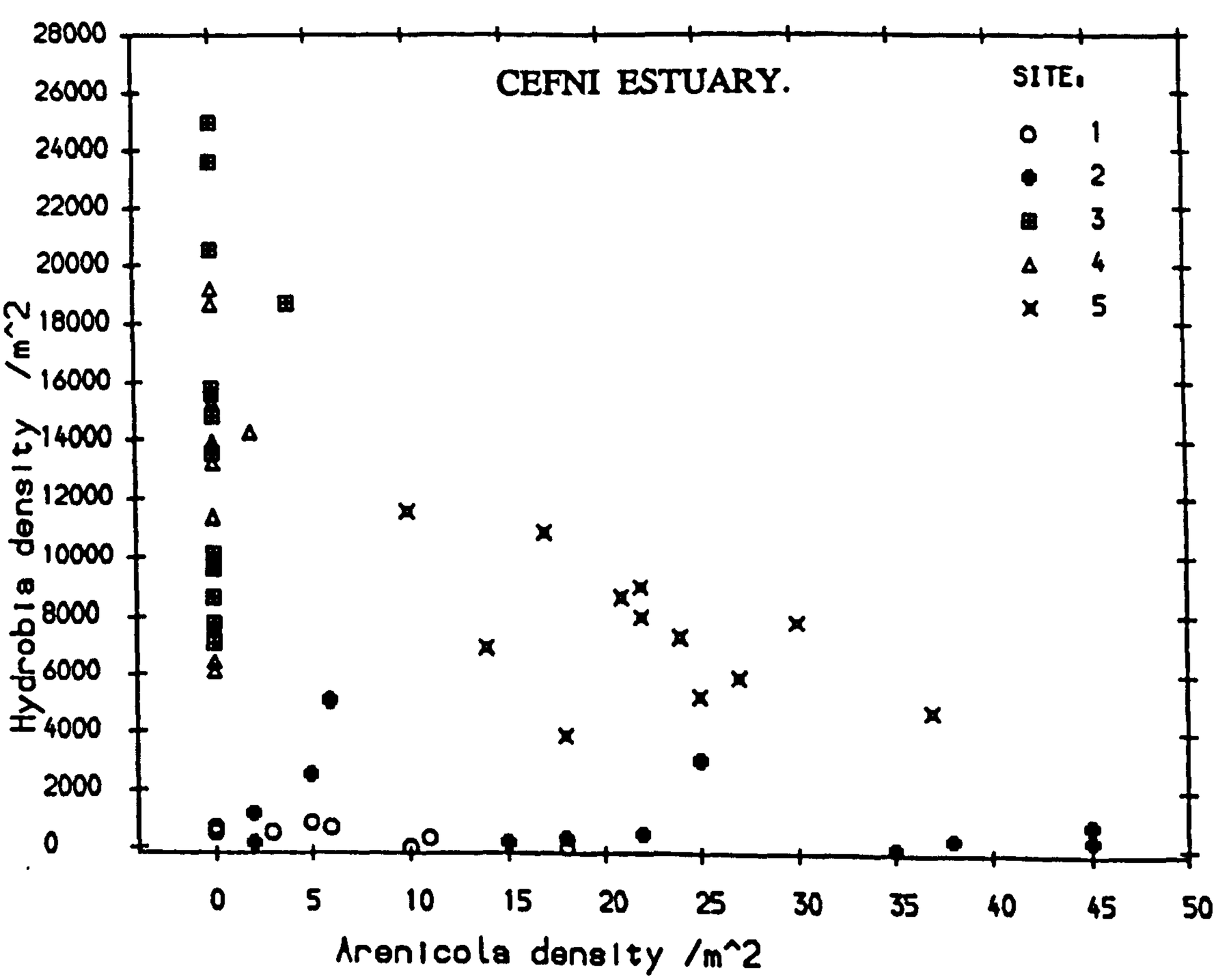

Fig. 5.3.21.

5.3.5.2. Controls on structural and geophysical properties.

Now that the textural and biological parameters have been placed within a conceptual causal framework, the correlations observed for the geophysical parameters can be discussed. The textural and biological data set can be split into dependent (or interrelated) and independent parameters. Correlations between geophysical properties and the interrelated parameters may be first order, due to a direct causal link, or higher order, via indirect linkage to the true causal parameter. For the combined data set the only completely independent parameters were *Pygospio* density and sediment temperature. At individual sites, of course, rather larger subsets of independent parameters were identified.

Following the pattern of discussion introduced in Section 5.2, the controls on porosity have been discussed first, followed by those on FF and V_s. Significant correlations have been identified for the combined data-set and at individual sites, and multiple regression analysis has been applied to establish more complex interactions between biological and textural predictors. As in Section 5.2, the controls identified represent 'second-order' effects on properties which have been shown to be primarily controlled by the high proportion of uniform sediment in the study area.

Porosity.

Porosity is a 'structural' parameter which should be dependent on textural and biological characteristics and the hydrodynamic sedimentary and post-depositional environment, and should also be an important predictor of the geophysical properties. The rather surprising absence of significant differences in time-averaged site means, despite significant (if second-order) differences in textural and biological parameters, is reflected in a complete lack of significant overall correlations between porosity and any of the expected predictor variables.

Several explanations are possible. First, the effect on porosity may have been less then the resolution of measurement. However, observed ranges in potential controls such as fines and carbonate content are comparable with

previous experiments where significant correlations have been obtained. Second, complex site-specific combinations of time-averaged textural and biological controls may have acted to cancel each other out (multiple regression analysis failed to identify any simple universal opposing effects). Finally, the fact that significant time variation in porosity was observed, over generally smaller ranges in textural and biological characteristics than were found overall, suggests that an important additional control was in operation. One such could be hydrodynamic processes which independently affect packing configuration, this being supported by the observed covariation of porosity at some sites and by its overall seasonal cyclicity.

Even at individual sites, the few significant partial relationships identified (Table C3.3) generally fail to support postulated controls based on simple packing arguments. Thus, while a positive correlation between porosity and carbonate has been found in the Taf, at Lligwy and at Red Wharf Bay, the only relationship identified in the Cefni is negative, at Site 1. Porosity should also be reduced by addition of coarse particles, perhaps especially by the low carbonate %1-2 phi fraction. This is indeed observed at Site 2, which exhibited the greatest individual range in this parameter, but is not observed overall. Addition of fine sediment may have two effects, depending on its mean size relative to that of the framework population. For a size ratio greater than about 3:1, small quantities of fines tend to fall into the interstices between the coarser grains, thus reducing porosity. This will occur for particles finer than *c.* 4.2 phi for the Cefni samples, which should include most of the fine fraction. However, this mechanism ignores the lower energy of deposition and intergranular cohesion associated with fine-grained sediment, both of which should increase porosity. In fact, no relationships are observed.

Both *Corophium* and *Arenicola* should increase bulk sediment porosity, although direct relationships have been conspicuously absent throughout this investigation. In the Cefni, the only significant relationships are negative. The observed relationships with *Corophium* are almost certainly indirect: *Corophium* was found at Sites 1 and 5 only during the winter months, when porosity was also lower.

Two important conclusions can be drawn. First, the observed significant temporal variation in porosity at individual sites cannot be simply or consistently related to measured changes in textural or biological characteristics. The most reasonable explanation for this is that it is responsive to external environmental controls which have not been monitored. Therefore it represents an important additional sediment parameter which should in turn affect geophysical properties. The second point is that marked differences in packing configuration, caused by a different temporally persistent textural and biological signature at each site, can result in indistinguishable bulk mean porosities. This suggests that porosity is not a particularly sensitive structural parameter, and therefore may be a poor predictor of important geotechnical properties of the sediment. These points lead naturally to discussion of the measured geophysical properties.

Formation Factor.

The significant relationships identified for FF have been listed in Table C3.4. FF has been plotted against sediment porosity in Fig.5.3.22. The high degree of scatter is partially explained by the fact that the porosity range was very small. Much more important, however, is the variation in textural and biological parameters which, for a given porosity, would be expected to affect sediment tortuosity and hence FF. These are shown to be considerably more important than porosity by two arguments: first, stronger relationships were identified between FF and a number of textural and biological parameters, and second, while differences in porosity between any of the five sites were not found despite marked differences in textural and biological characteristics, significant differences in FF between sites were identified.

Interpretation of the significant relationships identified is complicated by interdependence of the predictors. Thus several of the observed relationships are probably indirect, through their strong correlation with more direct controls.

Of the significant single predictors, carbonate content (Fig. 5.3.23) and

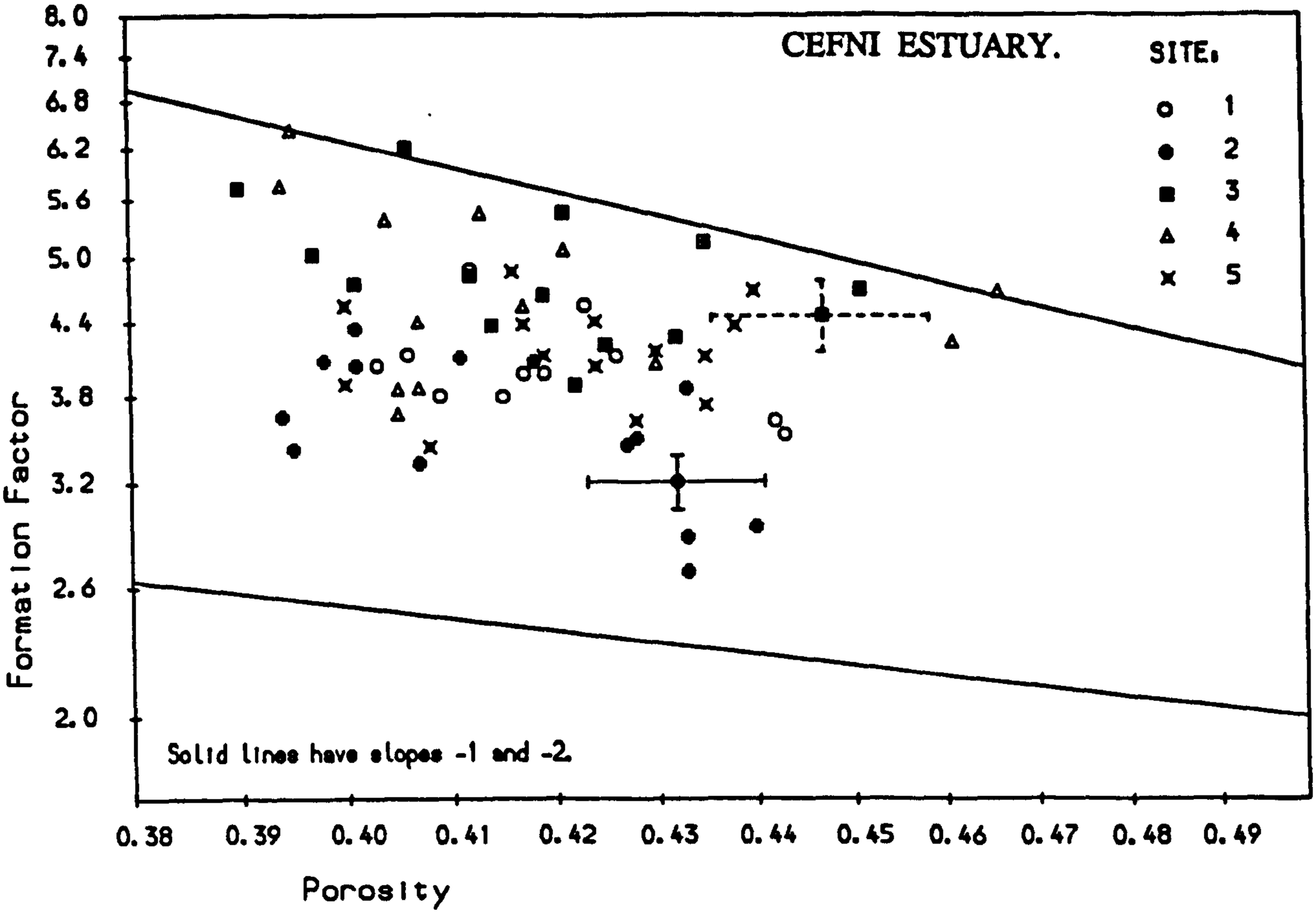

Fig. 5.3.22.

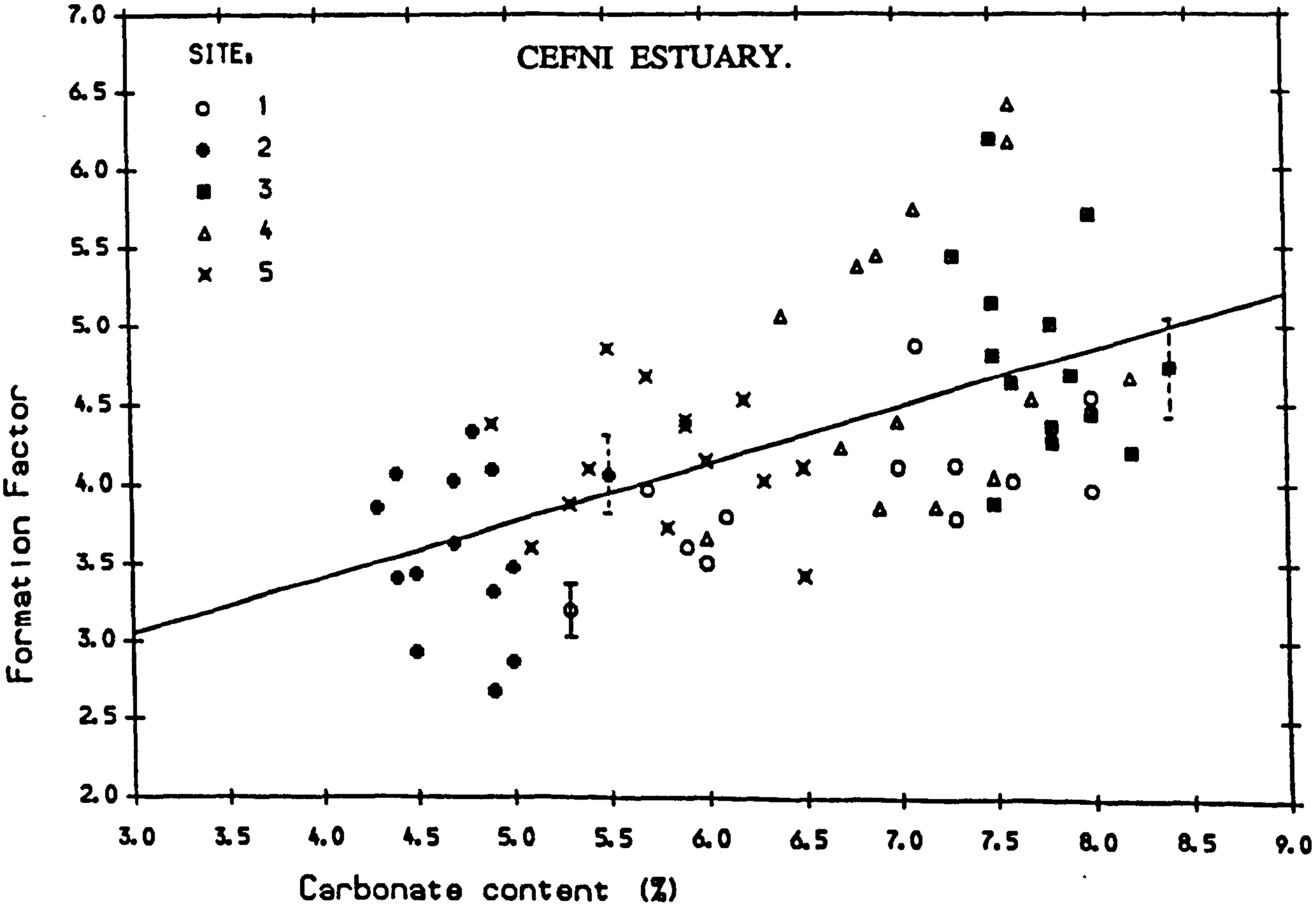

Fig. 5.3.23.

the 1 phi fraction would be expected to be direct, by increasing pore-space tortuosity. Note that FF was apparently unaffected by the 1-2phi fraction. This may have been because this fraction was lower in carbonate than either the 1phi fraction or the framework population, so that any reduction in porosity due to this coarse subpopulation was counteracted by a reduction in tortuosity. A similar argument has been applied to the observed controls on V_s, as will be seen.

It has been argued that the fine fraction (and presumably organics) may be largely interstitial, therefore will serve to clog up the pore space, thus increasing tortuosity. The relationship with *Hydrobia* is probably indirect. Finally, *Arenicola* should reduce FF by its liquefaction and excretion activities, as has been observed in Section 5.2.

A variety of potential partial predictors was indicated, with uncertainty as to which parameters represent the dominant controls because of the high degree of interdependence. Porosity is a significant (negative) partial predictor in all cases, indicating that it represents an important independent sediment parameter. Significant partial regression coefficients are obtained for porosity when combined with carbonate, fines, organics or *Arenicola*. If three predictors are considered, the best combination is carbonate, *Hydrobia* and porosity, although *Arenicola*, fines and porosity or carbonate, organics and porosity yield only slightly lower R^2 values.

It is difficult to select independent partial controls because many of the predictors are interrelated. Thus *Hydrobia* is thought to represent a strong partial predictor through its dependence on organics and fines content rather than through any direct control. The strongest relationships are probably obtained for parameters which incorporate the effects of several controls; in particular, *Arenicola* is associated with reduction in both carbonate and fines content, and may also directly reduce FF by its burrowing activity.

Analysis at individual sites should have removed the problems of independence of predictors and enabled site-specific combinations of parameters to be investigated. However, significant controls on FF were

only identified at Sites 1 and 2. The paucity of significant relationships at individual sites reflects the reduced sample sizes and ranges as well as the possibility that additional unquantified controls may have been in operation. In particular, vertical heterogeneity may have complicated the results at Sites 3 and 4 so that FF was influenced by uncharacterised subsurface layers.

At Site 1, multiple regression yielded significant partial dependence on porosity and the 1 phi fraction, implying that the coarse fraction increases tortuosity. At Site 2 two probably related combinations of predictors have been identified. The best R^2 value is obtained by a combination of *Hydrobia* and *Arenicola*, but the combination of porosity and *Arenicola* was thought to be the most direct and reasonable.

At this stage it is worth examining the question of why FF should have been more sensitive to between-site differences in packing configuration than porosity. It was argued in the previous section that effects on mean porosity due to site-specific textural and biological signatures may have counteracted each other. If this is the case, then the effect on FF must be incomplete, so that significant between-site differences remain. The obvious conclusion is that whereas for porosity the different effects are linear, additive and of similar magnitude, for FF they are not. Multiple regression results indicate that the data in Fig. 5.3.22 can be interpreted as a set of Archie curves of different exponent or tortuosity factor. While the total volume of pore space remains more or less uniform, both number and shape of individual pores are clearly affected by differences in textural and biological characteristics. Thus the muddy, organic rich Sites 3 and 4 exhibited highest tortuosity (and hence highest FF for a given porosity), while the low carbonate, *Arenicola*-burrowed Site 2 exhibited the lowest.

S-wave velocity

The significant relationships identified for both surface and bulk V_s have been listed in Table C3.5. They have been retained as separate parameters since differences between the two were identified at some sites, and since

statistical analysis revealed some interesting differences in textural and biological controls. Before further discussion, it is worth considering what these two measurements represent. For samples where there is no difference between surface and bulk V_s, vertical heterogeneity can be assumed to be negligible and the two should be similarly related to measured site characteristics. However, where surface V_s is significantly less than the bulk estimate, vertical heterogeneity is indicated. In this case the bulk V_s corresponds to a 'sub-layer' velocity, which may or may not be a physical reality within the sediment. It is then possible that the textural and biological characteristics sampled only apply to the surface layer, so that bulk V_s is controlled by uncharacterised deposits. The exception to this is the effect of *Arenicola*, which should extend throughout the zone of influence of all geophysical measurements (as was observed at Traeth Lligwy).

As for FF, significant relationships for the complete data-set were dominated by between-site differences in textural and biological signatures. This was reinforced by the fact that significant between-site differences in both velocities were obtained. Once again, interdependence between parameters caused difficulties in proving direct controls in a number of cases.

Arenicola is as expected associated with reduced V_s in both surface and sub-surface layers (Fig. 5.3.24), presumably due to its liquefaction and ingestion activities, while carbonate content increases V_s due to increased intergranular friction (Fig. 5.3.25). Both these parameters were also identified as controls on FF.

The best predictor of bulk V_s is *Arenicola* density. The only significant combination involves both coarse fractions: the 1-2phi fraction reducing V_s, while the 1 phi fraction increases it. The 1-2phi fraction has been shown to contain proportionally less carbonate in it than either the 1 phi fraction or the framework, suggesting that the grains are rounder. Thus, this sub-population should cause fewer, smoother intergranular contacts, which tends to reduce V_s. Note that *Arenicola* is associated with high proportions of the 1-2 phi fraction, so that both textural and biological controls might be contributory.

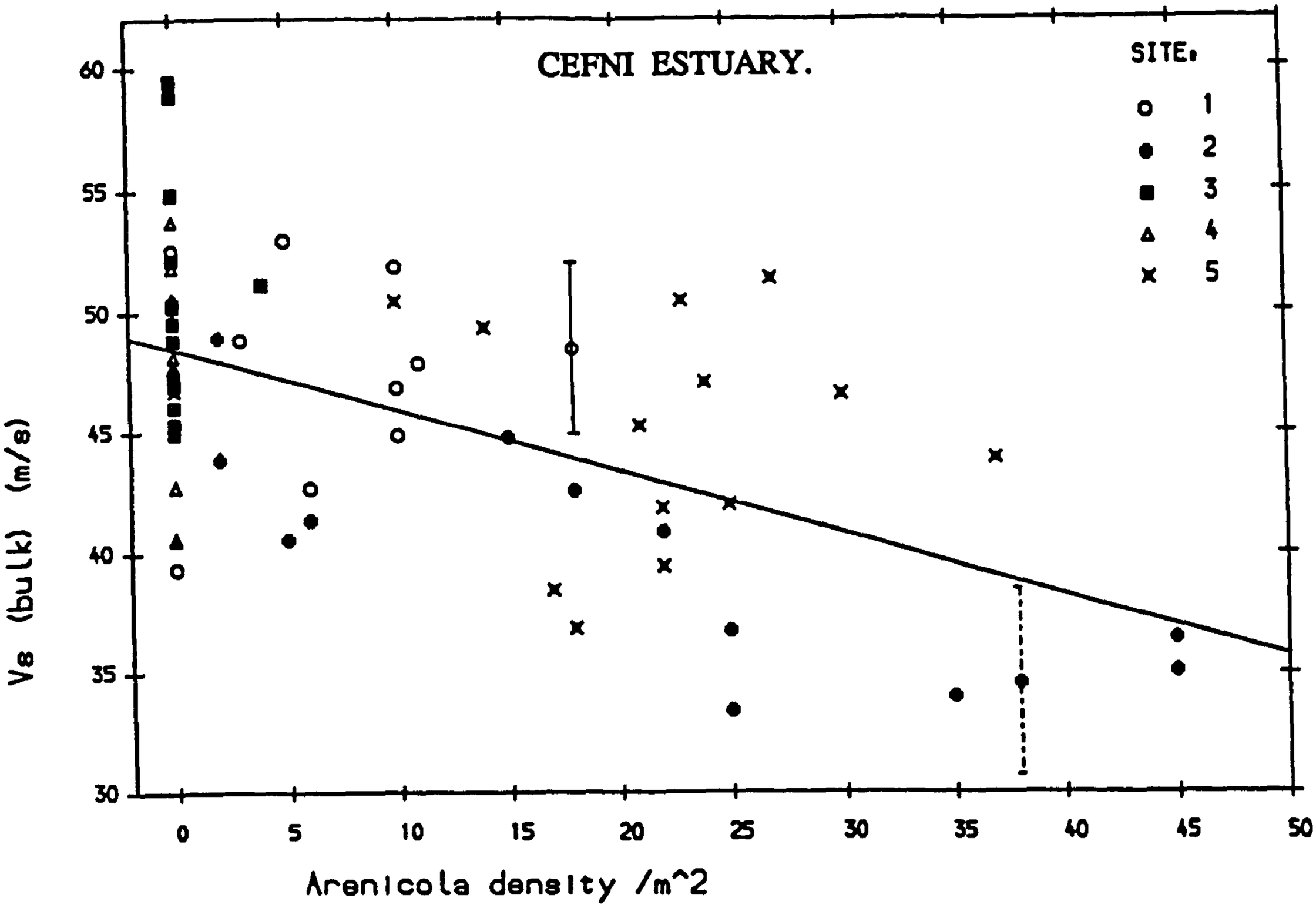

Fig. 5.3.24.

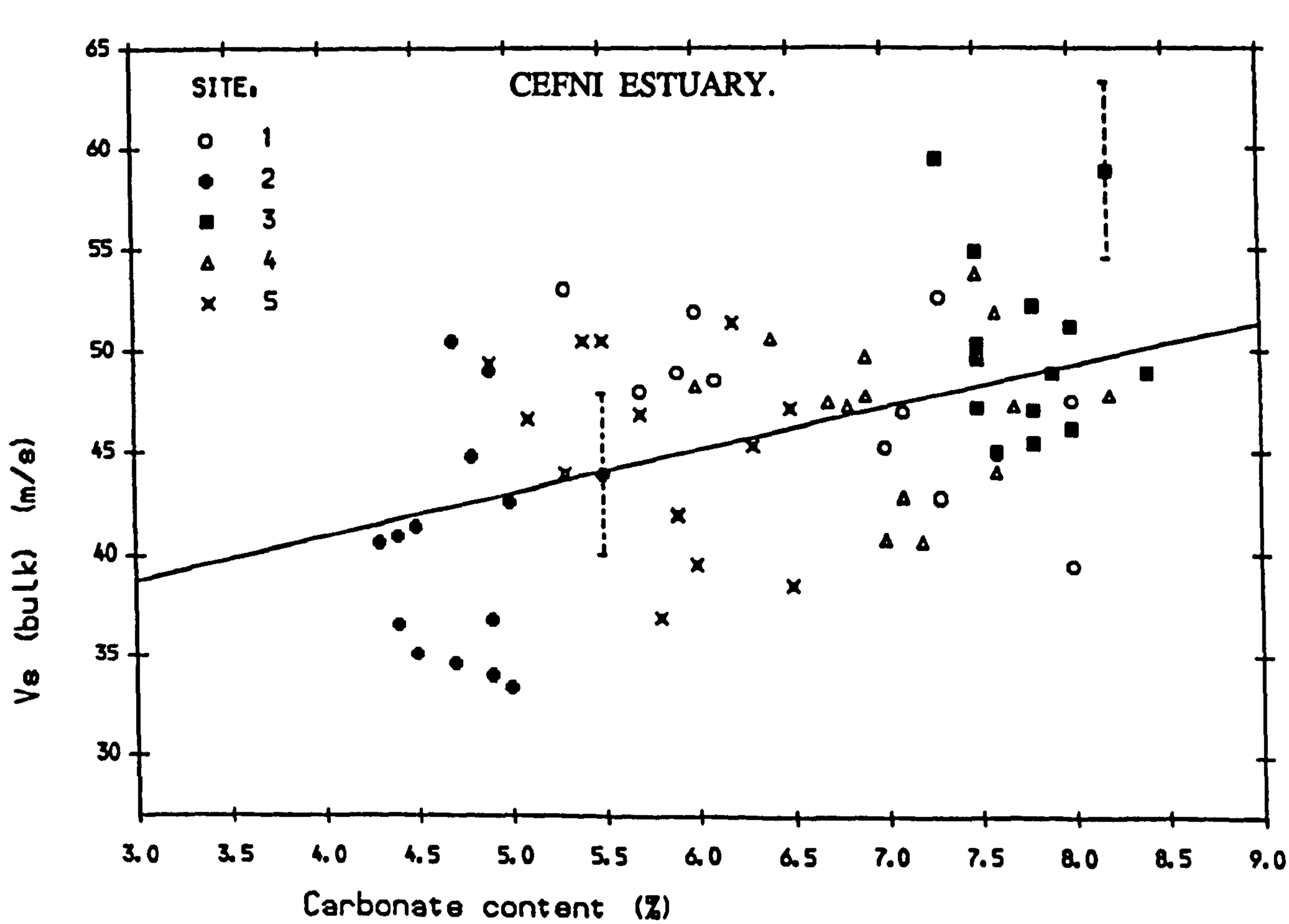

Fig. 5.3.25.

Surface V_s is best described by a combination of carbonate and fines content, these controls corresponding well with previous findings. Fig. 5.3.26 illustrates the dependence on fines, indicating a strong inverse relationship for the sandy Sites 1, 2 and 5 (Sites 3 and 4 being offset above this trend). Small quantities of fine particles must have acted to reduce intergranular friction, either as 'lubricants' between sand grains, or as low-rigidity layers providing slippage planes within the sediment. There is also inverse dependence of surface V_s on *Arenicola*, porosity and the 1-2 phi fraction, although the R^2 value was slightly lower. The fact that porosity is identified as a partial predictor for surface V_s only suggests that sampled porosity was less representative of some of the bulk V_s measurements, presumably due to strong vertical heterogeneity.

These results immediately suggest a different hierarchy of controls of V_s than was obtained for FF, due to fundamental differences between the two. Thus, while controls on FF were interpreted in terms of porosity and tortuosity, the additional factor of intergranular rigidity must be incorporated before interpreting those on V_s. The two main differences are the negative dependence on the 1-2phi fraction (compared with no relationship for FF) and on fines content (compared with the positive dependence of FF). The effect of rounded, coarser particles must affect intergranular friction (and number of intergranular contacts) but not tortuosity of the pore space. On the other hand, fine particles within the grain interstices act as 'lubricants' within the grain matrix, but also increase tortuosity, and therefore have opposing effects on V_s and FF.

Similar problems to those identified for FF affected results at individual sites, although significant relationships were identified at all sites except Site 3. The better resolution of vertical heterogeneity enabled by investigating two V_s parameters may have contributed to this improvement. Site 3 exhibited the most complicated variation in surficial characteristics and vertical heterogeneity during the study period, and consistently remained the most resistant to statistical analysis.

At Site 1 the best combination of two predictors involves *Pygospio* and porosity. The positive dependence on *Pygospio* supports the findings for *Lanice* at Llanddwyn and Red Wharf, suggesting that tube-building

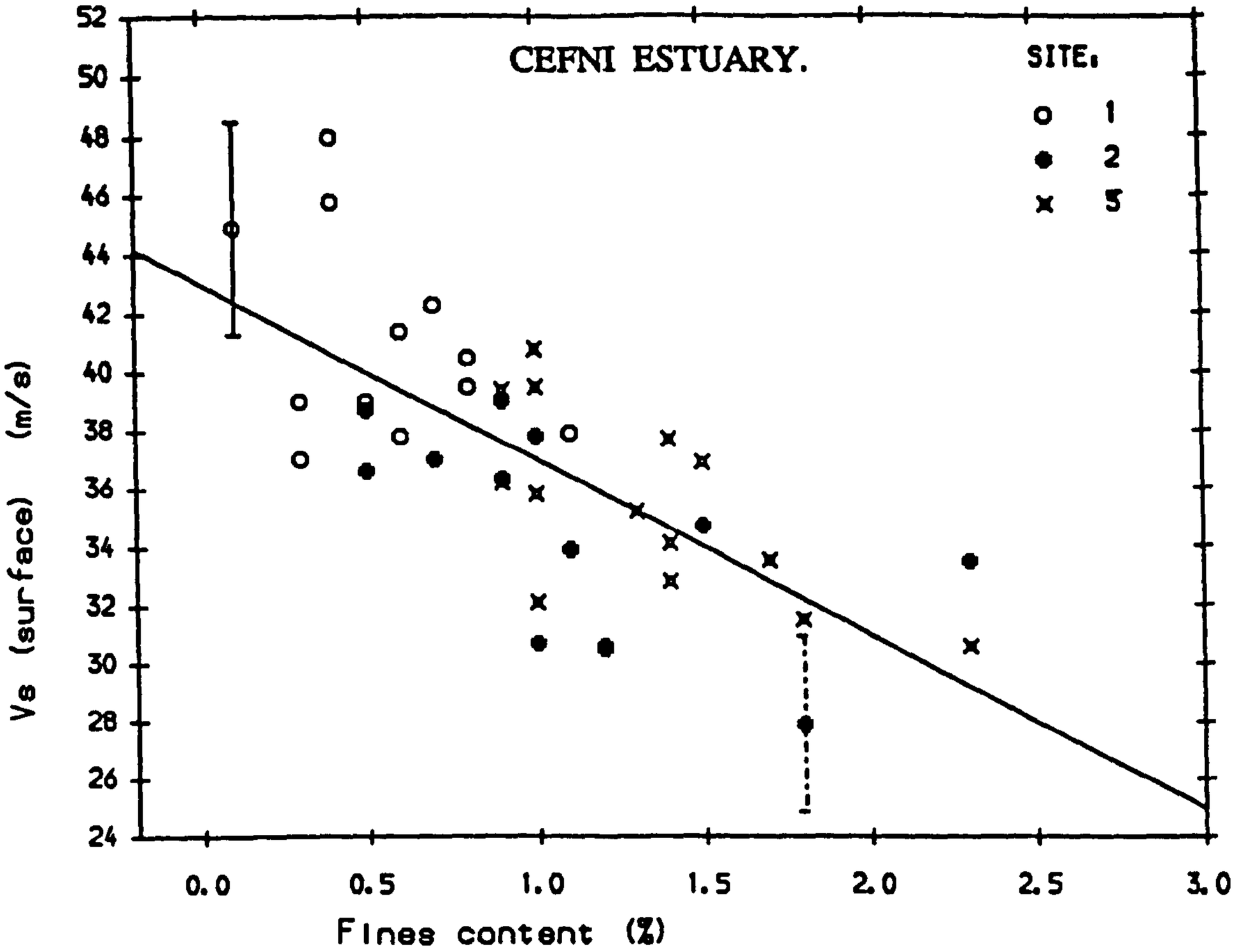

Fig. 5.3.26.

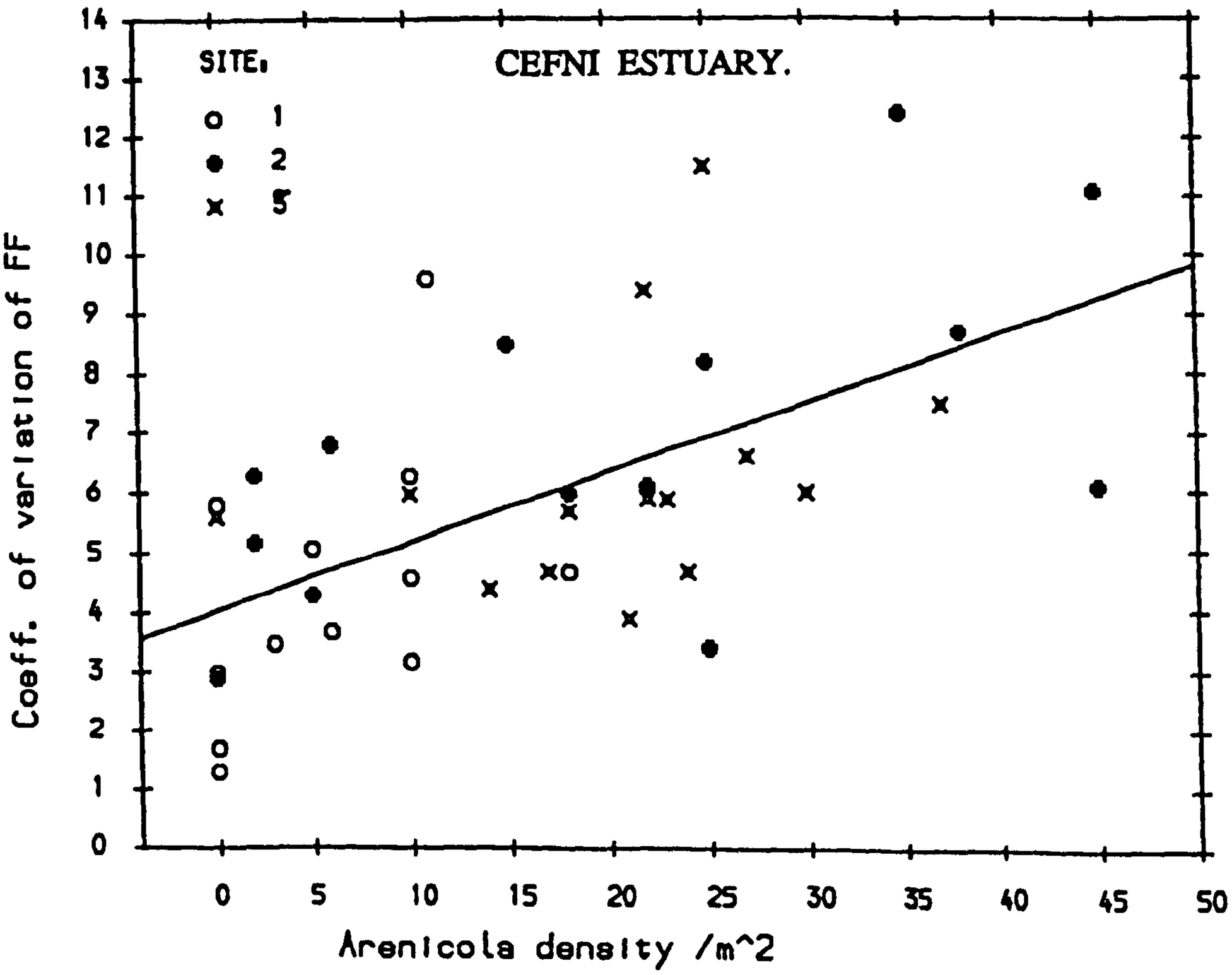

Fig. 5.3.27.

polychaetes act to increase V_s. The positive dependence on porosity was doubly surprising considering its inverse dependence on carbonate at this site. This is illustrated by a negative dependence on carbonate in an alternative significant combination, which also introduces a negative dependence on organics. Site 1 was complicated by spatial zonation, so that differences in depositional environment and post-depositional hydrodynamic reworking may have affected the results. Surface V_s is also positively dependent on *Pygospio*, in combination with the expected inverse dependence on the 1-2 phi fraction.

At Site 2, a strong negative relationship with *Arenicola* dominates variation of bulk V_s. Adding in the inverse effect of sediment porosity yields an R^2 of 73.3%. This was thought to be the most significant combination of predictors, porosity being inversely related to the 1-2 phi fraction at this site. In this case the effect on porosity must have outweighed that due to reduced angularity of this fraction. Surface V_s is inversely related to fines.

Despite the absence of any relationships at Site 3, significant combinations of predictors were identified at the similar Site 4. Bulk V_s is increased by *Pygospio* and reduced by *Corophium*, in agreement with the expected effects of tube-building and burrowing organisms. Surface V_s, however, is more sensitive to textural parameters, with negative dependence on the 1-2 phi fraction and fines content. It is interesting that *Corophium* affects only bulk V_s, despite its apparent concentration in the surface layers.

Finally, at Site 5, bulk V_s is related to porosity and *Arenicola* as at Site 2 (or, presumably indirectly, to porosity and *Hydrobia*). Surface V_s is once again inversely dependent on fines content, while a combination of porosity and *Corophium* (both negative) also yielded a significant R^2.

Geophysical interrelationships.

While being fundamentally different geophysical properties, FF and V_s are expected to respond in similar ways to variation in certain bulk sediment

properties such as porosity, and properties which act independently to increase both intergranular rigidity and tortuosity such as carbonate content. Therefore the observed significant positive correlation between FF and bulk V_s was not unexpected (r = 0.473). However, this relationship does provide an important means of comparison of two completely independent measures of sediment packing configuration. The fact that surface V_s was not correlated with FF supports the assertion that these FF measurements were predominantly influenced by bulk sediment properties.

5.3.5.2. Parameters describing small-scale heterogeneity.

The two remaining geophysical parameters have been included because they represent potential means of quantifying important *in situ* properties of sedimentary deposits, namely small-scale heterogeneity (including both structural and textural components) over length-scales of centimetres. This should be sensitive to lateral and vertical variation in textural and biological characteristics, since marked heterogeneity is associated with macrofaunal activity and depositional structure.

cv(FF): Small-scale lateral heterogeneity.

It has previously been proposed that the relatively high numbers of replicates involved, non-invasive procedure and intrinsic repeatability of the technique suggest that cv(FF) should be the best available estimate of genuine *in situ* heterogeneity. The contributory causes of this heterogeneity include surface relief and any temperature and salinity 'patchiness' as well as variation in structural characteristics of the pore-fluid matrix.

Statistical analysis results have been summarised in Table C3.6. Despite significant between-site differences (5.3.4), no significant relationships could be identified for the full data set. This suggests that different controls on heterogeneity were present at different sites, which is perhaps hardly surprising. However, significant relationships were also conspicuously absent at individual sites. This lack of results can be

explained by several arguments. Additional environmental controls, or more complicated relationships may have contributed: for example, *Corophium* might be expected to increase heterogeneity at low densities, but reduce it as burrow distribution becomes more uniform at higher densities.

The one significant relationship listed was identified for the sandy sites 1, 2 and 5 only. Fig. 5.3.27 illustrates a significant increase in spatial heterogeneity due to *Arenicola* activity. This was expected considering the patchiness of individual burrows, and the surface relief caused by casts and feed-pits.

V_s^R : *vertical heterogeneity.*

The V_s ratio defined in 5.3.2 was selected as a means of quantifying vertical heterogeneity, albeit on a rather coarse scale of resolution. The significant relationships identified have been summarised in Table C3.7. Overall, weak relationships with fines content and the (related) 1phi fraction indicate that the muddier sites tend to exhibit stronger velocity gradients, reflecting the significant between-site differences obtained.

The significant relationships obtained at individual sites reflect highly site-specific combinations of controls on heterogeneity. At Site 1, positive dependence on carbonate content probably reflects the spatial zonation already discussed for this site. At Site 2 a positive dependence on *Arenicola* was obtained, indicating that *Arenicola* tends to reduce vertical heterogeneity. This represents an interesting contrast with its proposed increase of lateral heterogeneity, and suggests that its activity causes homogenisation of sedimentary structures within the surface layers. This implies that any vertical textural grading, thought to be caused by *Arenicola*, does not have a measurable effect on V_s.

At Site 3, *Pygospio* and *Corophium* were both identified as significant partial predictors of vertical heterogeneity. *Pygospio* tubes extend throughout the top 10-15cm of the deposit, therefore would be expected to 'bind together' any lower velocity surface layers, thus increasing the velocity ratio. *Corophium*, however, resides only in the top 5cm, and

therefore its observed positive control is difficult to explain. It is possible that burrowing serves to mix in deposited fines, but the relationship could also have been indirect. At Site 4, both fines and the 1-2phi fraction were identified as significant negative partial predictors. This implies that muddy, poorly sorted deposits exhibit sharper velocity gradients. At Site 5, a significant negative dependence on *Corophium* was indicated, which could also be combined with a negative partial dependence on *Hydrobia*. Both organisms may have reduced the velocity of the surface layer: on the other hand they may only have settled at this site when such a layer was present.

In conclusion, the two heterogeneity parameters were clearly complex and not simply and consistently dependent on measured site characteristics, although the results do suggest that benthic macrofaunal activity, in particular, can introduce sampling variability into *in situ* measurements.

5.3.6. Summary and conclusions.

Sampling of textural, biological and geophysical properties of five sites in the Cefni estuary was performed on neap tides, generally at monthly intervals between January 1987 and January 1988. The five sampling sites exhibit very similar bulk (or first-order) textural properties, but distinct biological and second-order textural signatures which resulted in persistent differences between sites despite considerable temporal variability in most parameters. The textural properties are characterised by four sub-populations: the log normal framework, comprising 75-85% of the total, a fine sub-population corresponding to an organic-rich mud population (0-5%), a coarse sub-population comprising less carbonate than the framework (10-22%), and an even coarser, shelly coarse 'tail' (0-4%). The four macrofaunal species monitored were observed at some stage at each site during the study period: however, variation in hydrodynamic environment, pore fluid salinity, textural properties and biological interaction has caused the establishment of distinct site-specific benthic communities.

The geophysical properties monitored included both bulk and surface V_s in addition to FF, because significant differences between the two were obtained. This indicates vertical heterogeneity within the sediment, and an attempt was made at characterising this by defining the surface/bulk velocity ratio (V_s^R). To complement this, small scale spatial heterogeneity in the horizontal plane was characterised by the coefficient of variation of FF [cv(FF)] obtained from 12 replicate FF samples at each site. FF and bulk V_s were correlated overall, proving that the two independent but related measures are reliably monitoring packing configuration.

The geophysical parameters FF and V_s are shown, from consideration of their variability both over time and overall, to be primarily dependent on the uniform bulk properties of the sediment. They are, however, more variable than sediment porosity and yet more variable than mean grain size, indicating additional sensitivity to biological and second-order textural variation, and also possibly to additional, temporally variable environmental control. Significant differences were identified between at least two sites for all geophysical parameters, indicating a geophysical response to the observed differences in biological/textural signature.

No significant between-site differences in sediment porosity were identified, which was surprising considering the textural and biological differences, and the observed geophysical response. Two possible explanations have been proposed: first the effects of site-specific combinations of second-order textural and biological characteristics are simply additive in the case of porosity and tend to cancel each other out; and second, additional environmental factors are more important in determining the packing configuration of a given deposit, so that time-averaged between-site differences are swamped by additional controls operating at all sites. The observed significant temporal variation at individual sites cannot have been a direct response to textural variability, since significant differences due to increased textural ranges must then have been obtained between sites. Either temporal variation in biological activity or, perhaps most probably, variation in hydrodynamic environment, must be the dominant control. This was supported by the observed coherence of temporal variation of porosity at different sites, indicating a spatially uniform external control.

The temporal variability of properties at individual sites can be characterised either as random variation, as a persistent trend or as seasonal variation. Sites 2 & 3 were both subject to trends in some textural, biological and geophysical characteristics during the study. This indicates long term temporal adjustment at these sites, and also implies interaction between textural, biological and geophysical parameters. Thus at Site 2 the sediment became finer and better sorted; increased in porosity; and therefore became more attractive to *Hydrobia*, whilst both bulk V_s and FF were reduced. Meanwhile at Site 3 the sediment became coarser, poorer sorted, muddier; *Pygospio* and *Hydrobia* increased; and bulk V_s decreased. The only seasonal behaviour observed for textural parameters was in fines content, which was significantly higher in summer at Sites 2 and 5 (and which may have been hydrodynamically or biologically controlled) and in the >1phi fraction, which was at a maximum during the Winter at Site 2. As expected, biological characteristics exhibited more seasonality, in response to temperature-driven life cycle patterns. Seasonal variation in porosity was also observed, both overall and at Sites 1 & 2, with a maximum in November. This provides further evidence of a spatially coherent seasonal control of bulk packing configuration which dominates any second order textural controls. Seasonal variability was also observed in surface V_s at Site 2, and in bulk V_s at Site 4.

The response to specific 'events' during the study was also monitored in an attempt to identify external controls on the temporal variability of sediment properties. Few consistent textural responses were identified, although fines content tended to be increased after erosion and during high winds, and the coarse fractions were generally reduced after deposition. Consistent responses of macrofaunal density were not found, presumably because only extreme changes in bed level would disturb the species monitored. The most important responses identified were in surface V_s and cv(FF). Their apparent reduction during erosion events and high winds indicates that bed load transport results in a homogeneous, lower rigidity surface layer (further supported by a consistent increase in porosity during high winds). Their corresponding increase after deposition is less easy to explain, but may be caused by depositional sedimentary structures. Bulk geophysical parameters are unaffected, but vertical heterogeneity (V_s^R) increased on erosion and reduced on deposition.

Investigation of textural and biological controls on geophysical properties was hampered by extensive interaction between potential predictor variables (Fig. 5.3.15). Most overall variability is related to site-specific textural and biological signatures: correlations based on mutual between-site differences do not necessarily imply a direct causal link. Even the causal relationships identified are generally based on time-averaged between-site differences, rather than on rapid interactive temporal response at individual sites. Organics is strongly correlated with fines content, probably due to the increased surface area available for microbial colonisation. *Arenicola* is associated with carbonate-reduced, coarser skewed deposits, perhaps because the shelly coarse fraction has been sorted into the sub-surface, while fines and the framework population are exposed to erosion on excretion. *Arenicola* activity is also observed to inhibit *Corophium* and, to a lesser extent, *Hydrobia*. *Hydrobia* exhibits strong preference for organic-rich substrate, and directly contributes to the carbonate fraction.

Porosity has been identified as an important additional sediment property, since in this study it is not consistently related to any simple combination of textural or biological parameters. This indicates the necessity of measuring porosity independently. Since it was also reasonably consistently identified as a control of the geophysical properties, it is clearly a fundamental property of the deposit.

In addition to porosity, several significant textural and biological controls of the geophysical properties were identified. Significant correlators and partial predictors have been summarised in Table 5.3.1. Given the high degree of natural structural heterogeneity and sampling error involved, and the interaction between predictors, individual results (especially from multiple linear regression) must be considered to be of limited value. However, when viewed together, the more consistent relationships identified can be more confidently considered as general controls. Thus porosity, where significant, consistently reduces V_s and FF as expected, and the 1-2phi fraction consistently reduces V_s, perhaps because of the increased grain roundness of this low-carbonate fraction. Fines consistently reduces surface V_s but increases FF, indicating that it reduces intergranular friction but increases pore-space tortuosity.

Table 5.3.1. Summary of significant controls on FF, V_s.

Predictor		SITE:	ALL	1	2	3	4	5
Porosity	V_s (Bulk)			[+]	[-]			[-]
	V_s (Surface)		[-]					[-]
	FF		[-]	[-]	[-]			
% Carbonate	V_s (Bulk)		[+]	[-]				
	V_s (Surface)		[+]					
	FF		[+]	[+]				
% 1-2 phi	V_s (Bulk)		[-]	[-]	[+]			
	V_s (Surface)		[-]	[-]			[-]	
	FF							
% >1 phi	V_s (Bulk)		[+]	[-]				
	V_s (Surface)			[-]				
	FF		[+]	[+]				
% Fines	V_s (Bulk)							
	V_s (Surface)		[-]		[-]		[-]	[-]
	FF		[+]					
Arenicola	V_s (Bulk)		[-]		[-]			[-]
	V_s (Surface)		[-]					
	FF		[-]		[-]			
Pygospio	V_s (Bulk)			[+]			[+]	
	V_s (Surface)			[+]				
	FF							
Corophium	V_s (Bulk)		[+]				[-]	
	V_s (Surface)							[-]
	FF		[+]					
Hydrobia	V_s (Bulk)							[+]
	V_s (Surface)							
	FF		[+]		[-]			
% Organics	V_s (Bulk)		[+]	[-]				
	V_s (Surface)							
	FF		[+]					

Carbonate increases both V_s and FF overall, due to increased intergranular friction and tortuosity.

Significant biological controls were identified, although to a lesser extent than was expected considering the wide range in densities observed. High sampling error and the effects of additional microbiological and hydrodynamic controls are thought to have complicated the analysis. *Arenicola* is found consistently to reduce both V_s and FF, overall and at the most abundant sites, to support the findings at Lligwy (5.2.3). The tube-building *Pygospio* was associated with localised increases of V_s at two of the five sites (but not overall), partially supporting the findings for *Lanice* (5.2.1, 5.2.4). *Corophium* was associated with reduced V_s at two sites, in support of the marked reduction observed in the Taf estuary (5.2.2). However, no relationship was identified overall, nor at Site 3, which exhibited the maximum range in *Corophium* density.

Small scale spatial variability, characterised by cv(FF), is increased by *Arenicola* at the most abundant sites, but other simple overall controls were not identified. V_s^R is highest at Sites 3 and 4, and is locally increased by fines content at Site 4, indicating that vertical gradients are strongest in muddy deposits. *Arenicola* reduces vertical layering at Site 2, while increasing horizontal spatial heterogeneity.

In conclusion, significant but second order temporal variability of geophysical properties has been measured which can partially be related to variation in textural parameters, biological activity and the depositional environment (which affects sediment porosity). In this study, medium-scale spatial controls are more important than temporal variability, preserving local differences in textural, biological and hence geophysical properties over the study period.

5.4. LARGER SCALE VARIABILITY: GENERALISED CONTROLS.

5.4.1. Introduction.

In the previous sections, data analysis and interpretation has centred around highly localised spatial or temporal variability in bulk textural and geophysical properties. This variability has been shown to be largely second order, due to the predominantly uniform nature of the source material and processes affecting depositional texture and structure within the locations studied.

It is also possible to investigate larger scale variability by comparing and combining data from different locations. This provides a much wider range in bulk textural properties, depositional environments and benthic community structure, all of which might be expected to contribute to first order variability of geophysical properties. Furthermore, general textural and biological controls can be investigated and compared with those identified at specific locations, thus extending the study beyond the localised, *second order* effects which have been discussed so far.

Data from each location were therefore combined, generating a total of 157 sets of site parameters. Analysis followed the same pattern as that described in 5.3.1, extended to include between-location (as well as within-location and within-site) variability.

5.4.2. Parameter selection.

Parameter selection at individual locations was dictated by benthic community and textural characteristics, in particular the form of the grain-size distribution. Textural parameters could be restricted to second-order descriptors of coarse and fine tail populations, ignoring the uniform bulk of the sediment framework. In order to combine data from different locations, however, the use of location-specific cut-off fractions is clearly unsuitable, since parameters which effectively describe bulk framework properties are required. This was achieved by

reverting to use of the standard bulk textural parameters grain size mode, mean, sorting and skewness, in addition to carbonate and fines content. Thus it was hoped that the effect of variation in overall grain size distribution and shape might be investigated.

Biological parameters were restricted to counts of those organisms which were observed at more than one location, namely *Lanice*, *Arenicola* and *Corophium*. This allowed more general effects of these organisms to be investigated, although care had to be exercised because the overall distributions were clearly non-parametric.

The geophysical parameters, since they had been measured more or less consistently at all locations, could be simply combined in general. The distinction between surface and bulk V_s was maintained, so that measurement procedure for each variable was consistent. FF could not be calculated for the Taf data set (due to erroneous pore-fluid resistivity measurements): therefore analysis of large-scale variability of FF involved a reduced sample set. Similarly, porosity was not measured at Llanddwyn.

Within-site variability of all three geophysical parameters, expressed as percentage coefficients of variation, were also included as measures of small-scale spatial heterogeneity. Finally the velocity ratio V_{SR}, defined in Section 5.3, provided information on vertical heterogeneity for the full data set.

5.4.3. Overall variability: Comparison with laboratory data.

The ideal data set for a study of large scale variability would have encompassed the widest possible range of sediment types, hydrodynamic environments and biological activity. Unfortunately, limitations on project time and emphasis on identification of simple macrofaunal controls severely limited the range so far investigated. It is naturally hoped that this range will be extended in the near future, thus providing an improved data set for analysis of controls.

Fig. 5.4.1. illustrates the nature and spread of Bulk V_s data so far

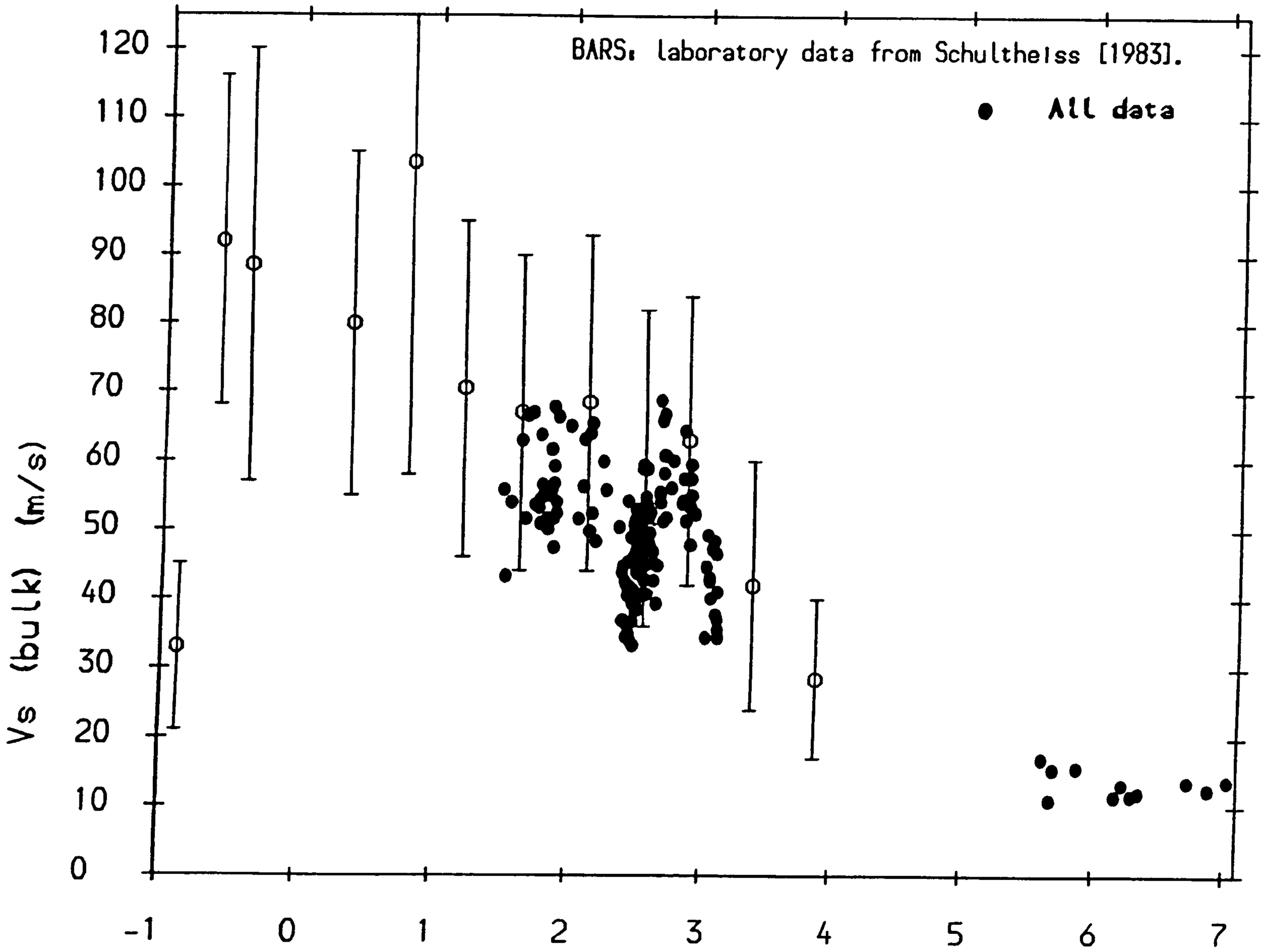

Fig. 5.4.1. Bulk Vs versus grain size mean: ALL DATA.

collected, as a function of mean grain size. A selection of direct measurements of V_s made in the laboratory under atmospheric confining pressures has also been included [Schultheiss, 1983]. This has been compiled from experiments in the variable porosity cell described in 5.2, with bars indicating the range in V_s between minimum and maximum porosity for that sediment. The *in situ* data are clearly in reasonable agreement with comparable laboratory measurements, with a broad trend upwards with coarsening mean grain size. Note that at the extreme coarse size V_s reduces again, due to increased porosity (the sample indicated consisted purely of shell fragments). Unfortunately *in situ* data has not yet been collected to test this further. This effect has also been obtained and discussed by Hamilton [1976], although his absolute values are significantly higher. This is probably because Hamilton used V_s measurements which generally involved much greater depth averages than can be obtained *in situ* or in the variable porosity cell.

Fig. 5.4.2 illustrates a similar comparison for FF, this time plotted as a function of sediment porosity (and therefore as a reduced data set). Comparison with the error envelope suggested by Jackson *et al* [1978], after a series of variable porosity cell runs with different natural sediments, indicates reasonable agreement between *in situ* and laboratory data, but with rather more scatter above the laboratory prediction for the *in situ* measurements. This indicates increased tortuosity for naturally (rather than artificially) deposited and compacted sediments, which could be caused by shell fragments and fines in the *in situ* deposits, or by hydrodynamically-derived sedimentary structures. FF has also been plotted against mean grain size in Fig. 5.4.3, thereby enabling inclusion of the results from Traeth Llanddwyn. *In situ* subtidal data from Tremadoc Bay [Jackson, 1976] have been included for comparison and show broad agreement, although Jackson's data are less highly scattered.

For both geophysical parameters, the range in *in situ* measurements is dominated by the sharp difference between the majority of measurements in sands and muddy sands, and the few measurements made in muds. Statistical investigation of this full data set has not been attempted because the distribution of measurements is not evenly spread across the range, and because all relationships would be based primarily on the difference between muds and sands.

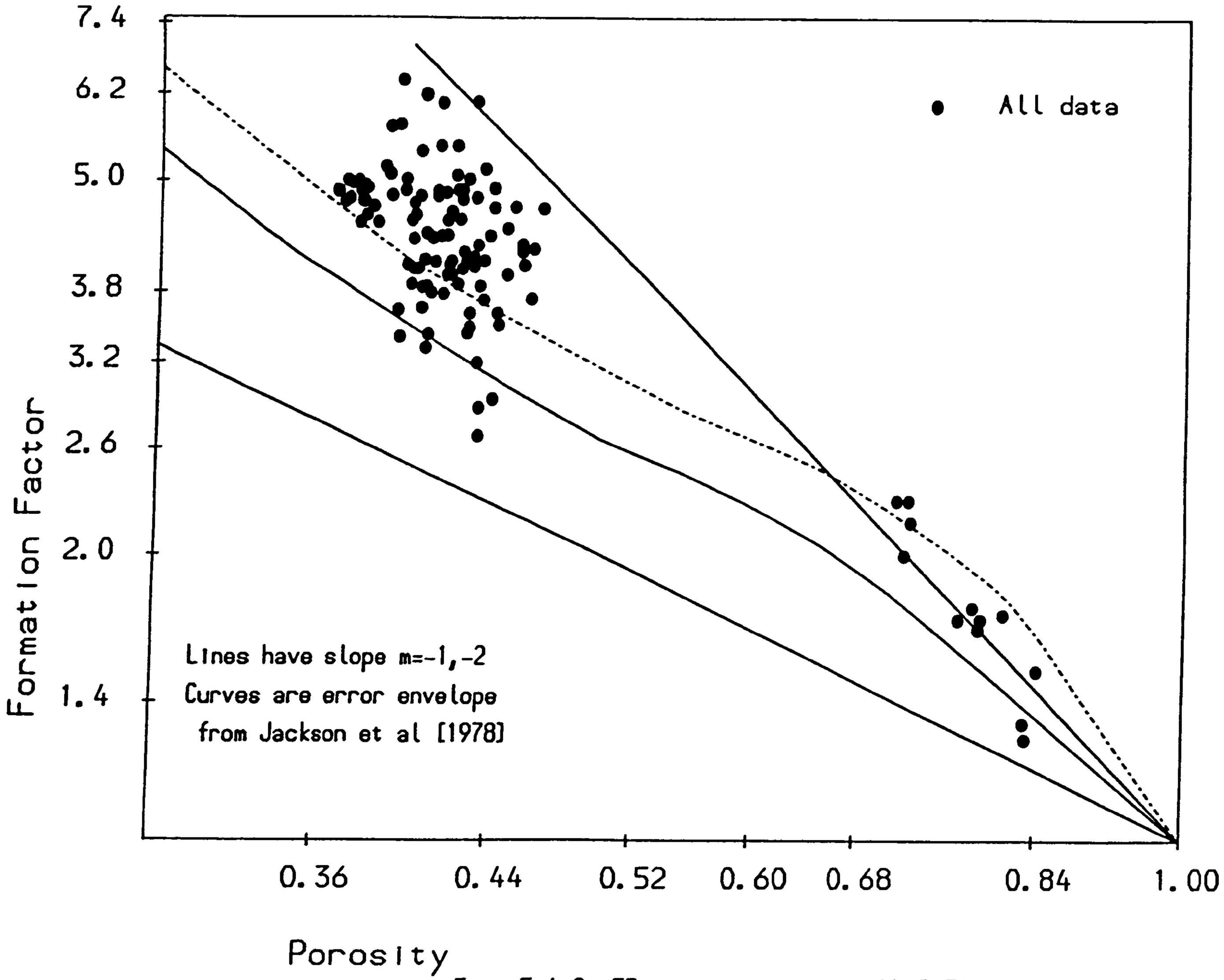

Fig. 5.4.2. FF versus porosity: ALL DATA.

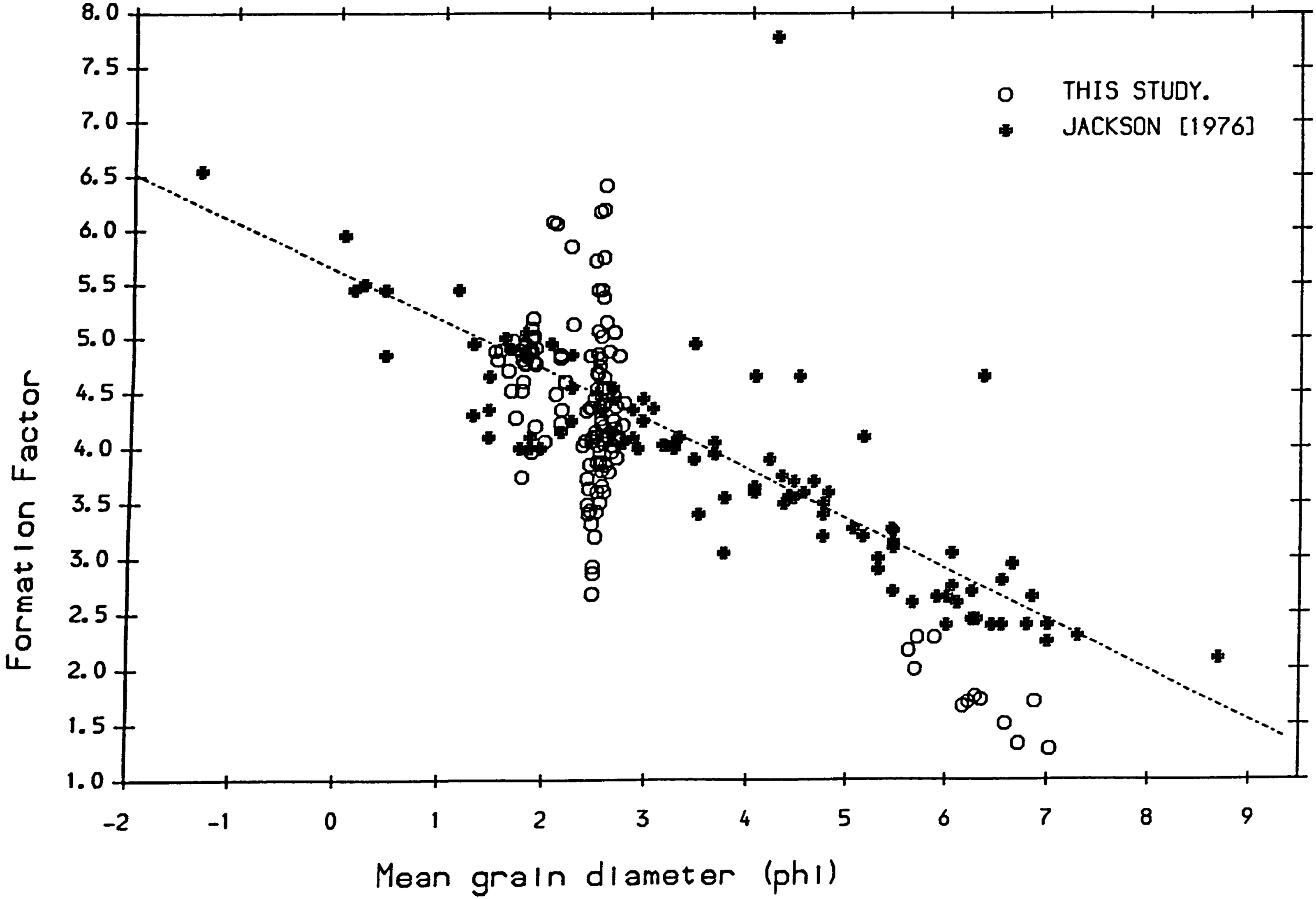

Fig. 5.4.3. FF versus mean grain size: comparison with other in situ data.

It is clear from both figures that a considerable amount of scatter is involved, so that predictions of geophysical parameters based on simple relationships with bulk textural parameters are of extremely limited use. This scatter includes both medium-scale spatial heterogeneity and seasonal variability in response to variation in second order textural characteristics, biological activity and hydrodynamic environment, as well as larger scale differences in bulk textural properties such as spread of sizes and grain shape. The nature of this scatter, the relative contributions of spatial and temporal variability, and its textural and biological controls, are discussed in the following section. For these purposes measurements from the Tamar mud banks have been ignored until a much larger data set encompassing sandy muds to fine clays has been collected.

5.4.4. Variability in intertidal sands.

5.4.4.1. Relative scales of spatial and temporal variability.

The scales of variability measured can be defined and obtained as follows:

(1) Small-scale spatial variability (< 1m): from within-site replicates of geophysical parameters.
(2) Medium scale spatial variability (< 200m): from individual site means within a sampling location.
(3) Large scale spatial variability (> 500m): from differences between sampling locations.
(4) Seasonal variability: from a time series of measurements at a given site.

Note that the definition of large scale variability has been restricted to variability among intertidal sands (containing up to 5% mud). From Figs. 5.4.1, 2 & 3 it is clear that this would be increased considerably by incorporating the full range of intertidal sediments from gravels to muds. Thus genuine large scale variability has yet to be fully investigated.

One obvious means of examining large scale spatial variability is to look for significant between-location differences in bulk textural, and hence

geophysical, parameters. In other words, if significant differences can be identified between geophysical parameters at locations exhibiting different bulk textural properties, then a first-order dependence on the bulk sediment framework which exceeds second-order within-location variability would be indicated.

For the purpose of this analysis, data was grouped according to the above definition of large-scale variability. Thus individual sites in the Cefni Estuary were spaced closer than 500m, therefore were combined as a single location (significant between-site differences have already been discussed in 5.3), whereas the more widely spaced paired data sets in the Taf and Lligwy were maintained as separate locations. Analysis of variance was performed according to the procedure outlined in 5.3.

The results have been illustrated for selected parameters in Figs. 5.4.4-6. Error bars correspond to the range measured at each location: blocks represent 95% confidence limits for sample means. Thus where a pair of blocks does not overlap, a significant difference between that pair of locations is indicated. Fines content and the biological parameters have not been included because they were not normally distributed: they obviously exhibited marked between-location differences, controlled by the depositional environment and benthic community structure.

It is clear from these figures that, in addition to differences in species composition and fines content, there is considerable between-location variation in bulk textural parameters (mode, mean, sorting, carbonate content). This was expected, and reflects gross differences in sediment source, transport processes and depositional environment, ranging from exposed beaches to muddy estuarine sandflats. Furthermore, there are significant between-location differences in all three geophysical properties and porosity, indicating large scale differences in packing configuration, as a result of variation in bulk textural properties and post-depositional reworking.

There are some interesting contrasts: for example, porosity is relatively high at Freathy Sands, and FF is correspondingly low. V_s, however, is relatively high. Similar values of FF and V_s are also found at Traeth Llanddwyn, although porosity was not measured. This indicates that

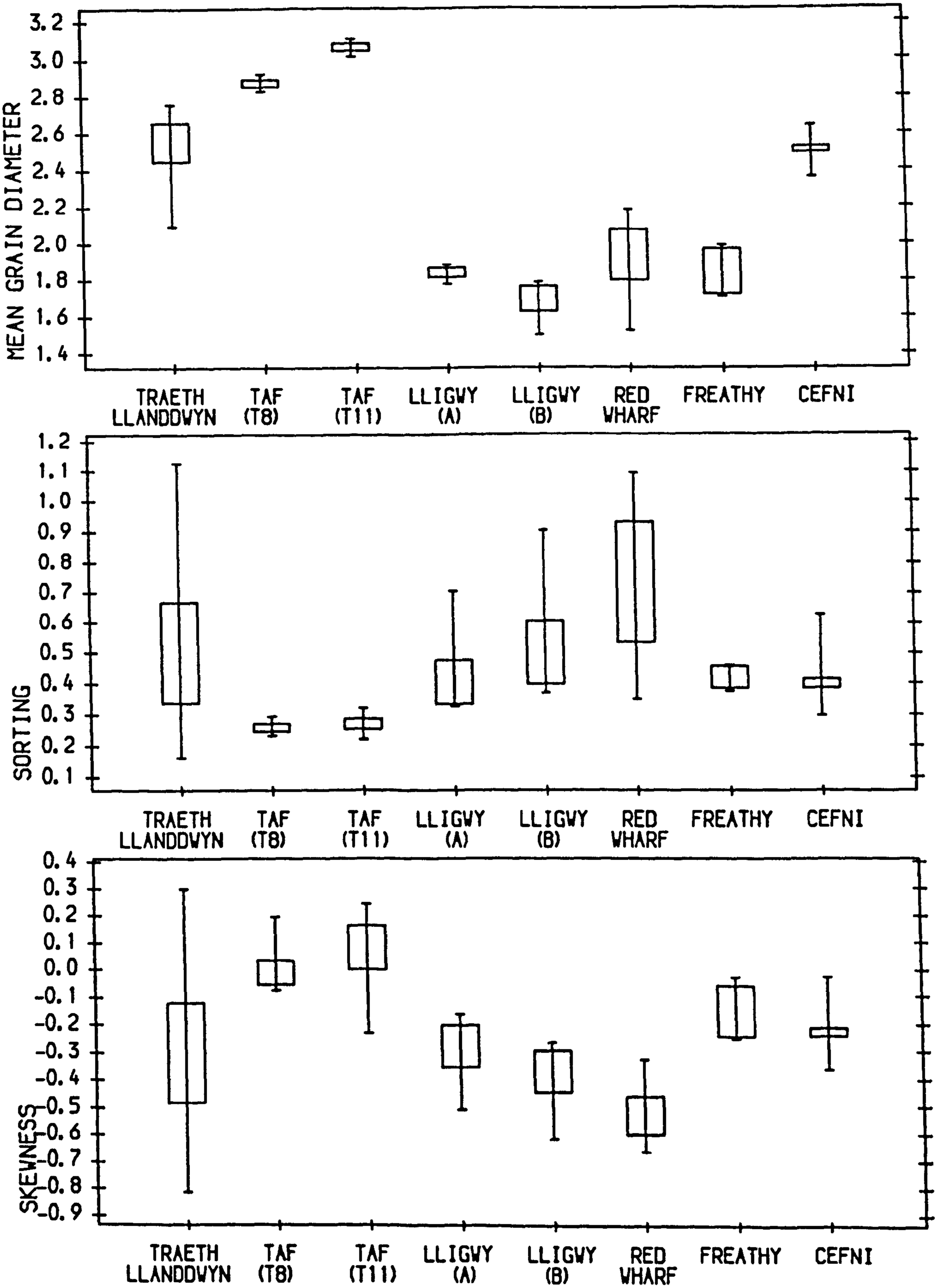

Fig. 5.4.4. Location means for intertidal sands (1).

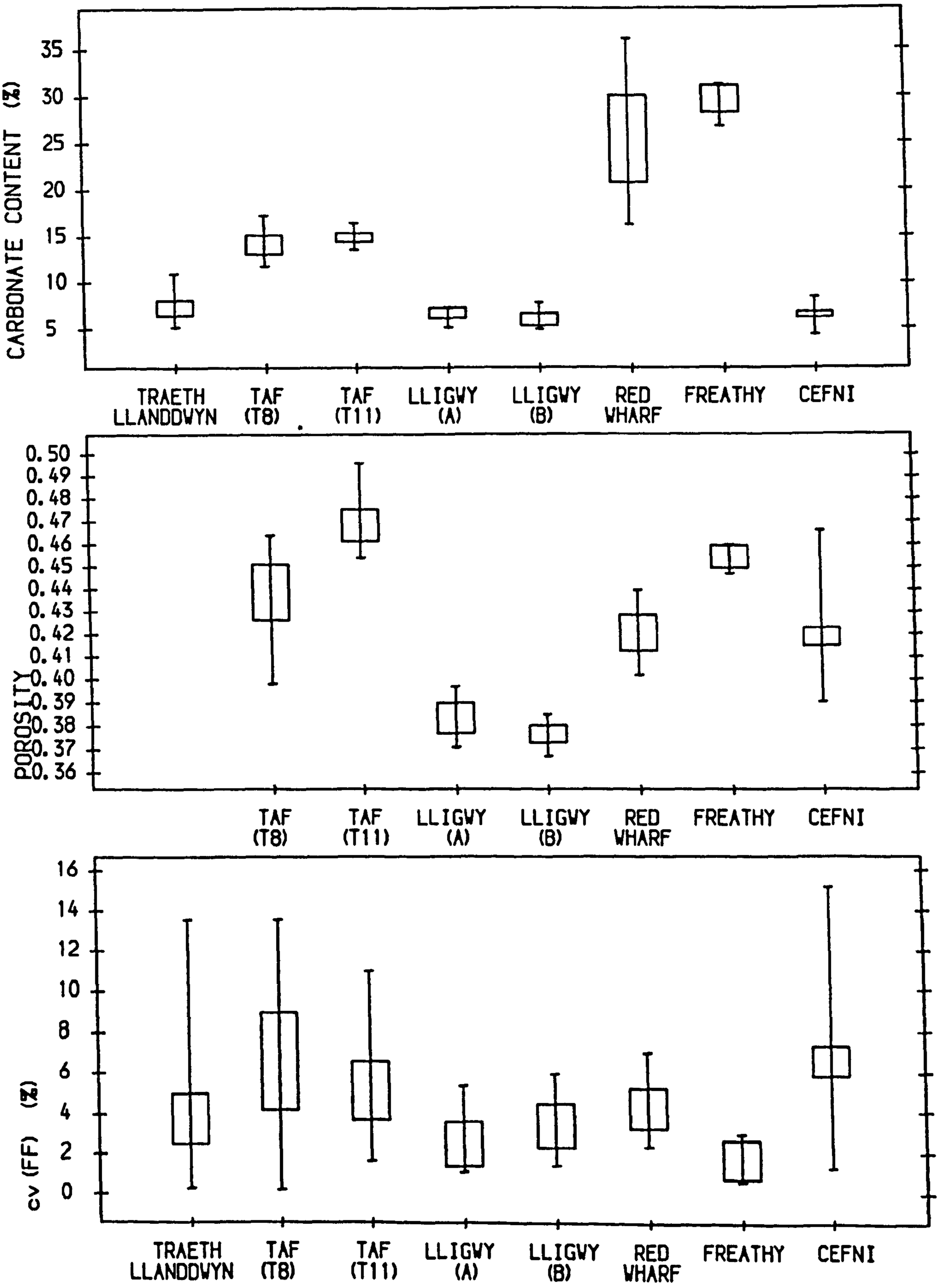

Fig. 5.4.5. Location means of intertidal sands (2).

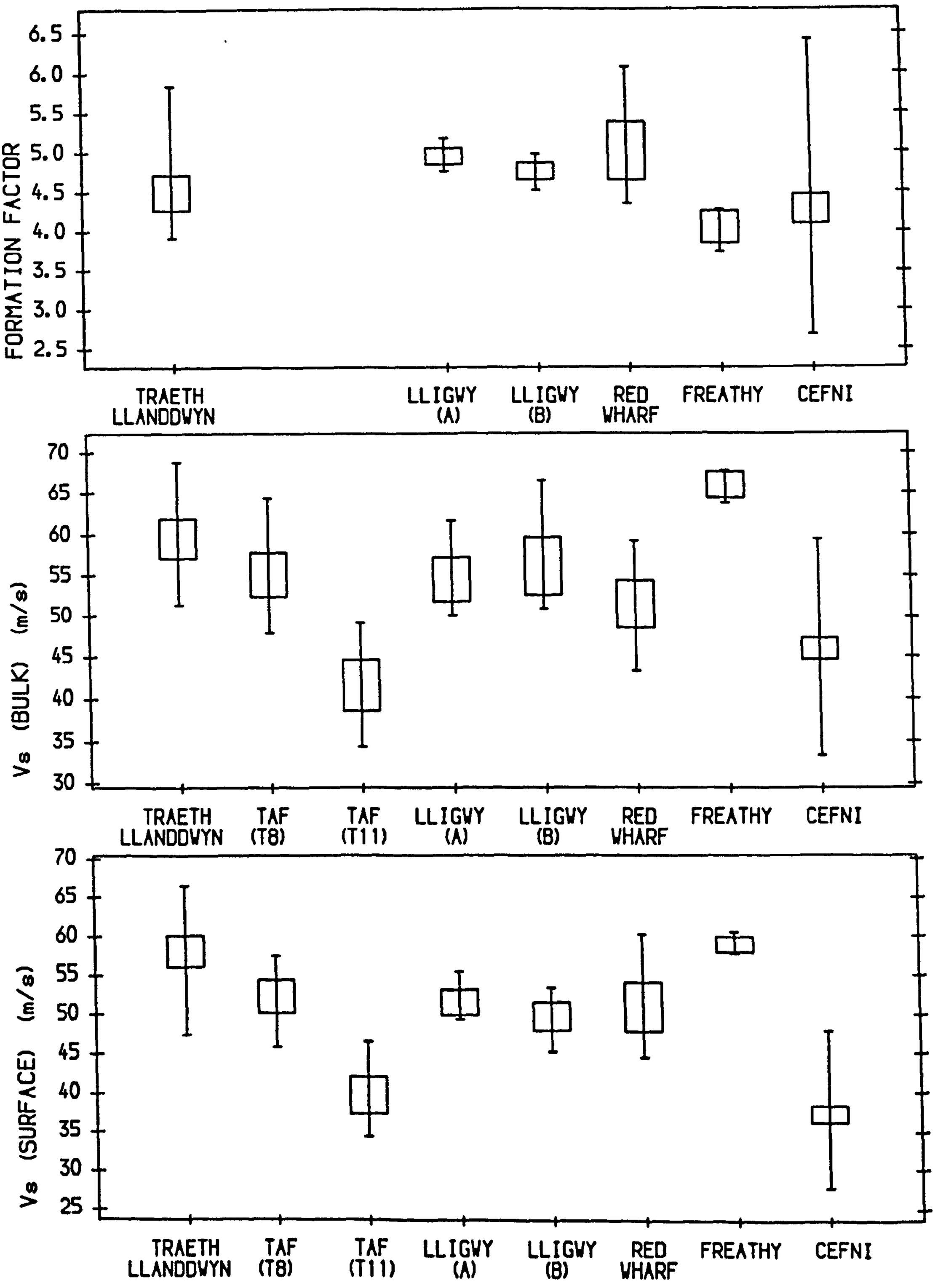

Fig. 5.4.6. Location means of intertidal sands (3).

sedimentary structures on exposed foreshores have high rigidity despite their relatively high porosity. Meanwhile, both muddy locations (Taf T/11 and the Cefni) exhibit significantly reduced V_s, although fines content never exceeds 5%. This represents strong sensitivity to a second order textural parameter, probably due to its effect on intergranular contact forces rather than on packing configuration.

A direct comparison between different contributions to variability is best illustrated by a set of bar charts. Fig. 5.4.7 illustrates a series of percentage coefficients of variation calculated for selected textural and geophysical parameters (The biological parameters were not suitable for this analysis because their distributions are not normally behaved: it is clear from Sections 5.2 & 3 that they exhibit strong spatial and temporal variability, as well as marked zonation over larger scales). Where possible, small-scale heterogeneity was calculated from the coefficient of variation of within-site replicates. Medium-scale spatial variability was obtained for each parameter from a pooled standard deviation calculated during analysis of variance between locations: this allowed for differences in sample size. Note that for the Cefni data set, seasonal variability at each site within the sampling location was unavoidably incorporated into this. Large-scale spatial variability was obtained from the coefficient of variation of the full data-set, and therefore implicitly includes medium-scale and temporal variability. Finally temporal variability was calculated by pooling the coefficients of time variation from the five sites in the Cefni estuary. Table A1.3. summarises these values.

Several points arise out of the comparative exercise illustrated in Fig. 5.4.7. The bulk textural parameters mode and mean grain size indicate marked differences between variability within locations, where much of the sediment population has been shown to be uniform, and that between locations, where differences in source material and depositional environment leads to gross textural variation. Seasonal variability of these parameters is even lower than medium-scale spatial variability, especially for mean grain size, indicating dependence of bulk textural properties on time-averaged processes, rather than on rapid temporal response.

The remaining textural parameters show the same relative importance of spatial and temporal variability, indicating temporally persistent, locally variable and generally highly variable distribution and composition. The difference between medium and large scale spatial variability in sorting and skewness is rather less than that for mode and mean grain size. This suggests that the deposits measured were mature, having been subjected to considerable hydrodynamic sorting and reworking along their transport paths, which might be expected from intertidal sediments.

Porosity also shows a marked increase between medium and large scale spatial variability, presumably in response to variability in bulk textural properties and depositional environment. It is interesting that the increase is not as great as that measured for grain-size mode and mean: this may reflect the fact that porosity is independent of grain size for a given shape, and is more dependent on parameters affecting packing configuration such as sorting, skewness and depositional environment. Thus a significant contribution to textural variability, namely the mean grain size, has no effect on porosity. A further contrast is that seasonal variability is of the same order as medium-scale spatial variability, indicating that porosity is more responsive to changes in biological activity or the hydrodynamic environment than in bulk textural parameters.

Variability in the geophysical parameters can be investigated on a wider range of scales. Small-scale variability of FF is less than that of V_s, which was expected since sampling errors were thought to be less for FF. V_s showed a progression from medium-scale to large scale variability which supports the hypothesis that first order variation in bulk textural properties leads to increased variability in geophysical properties. The difference between the two is slightly more than that for porosity. The results for FF are less convincing: its medium-scale (and seasonal) variability is considerably higher than that of V_s and is not much less than the large scale value. One possible explanation is that FF is particularly sensitive to second order textural variation, such as admixture of small quantities of fines, which was obtained over both medium and large spatial scales, and over time. Finally, seasonal variability was of the same order as medium-scale spatial variability, in agreement with the finding for sediment porosity.

PERCENTAGE COEFFICIENTS OF VARIATION

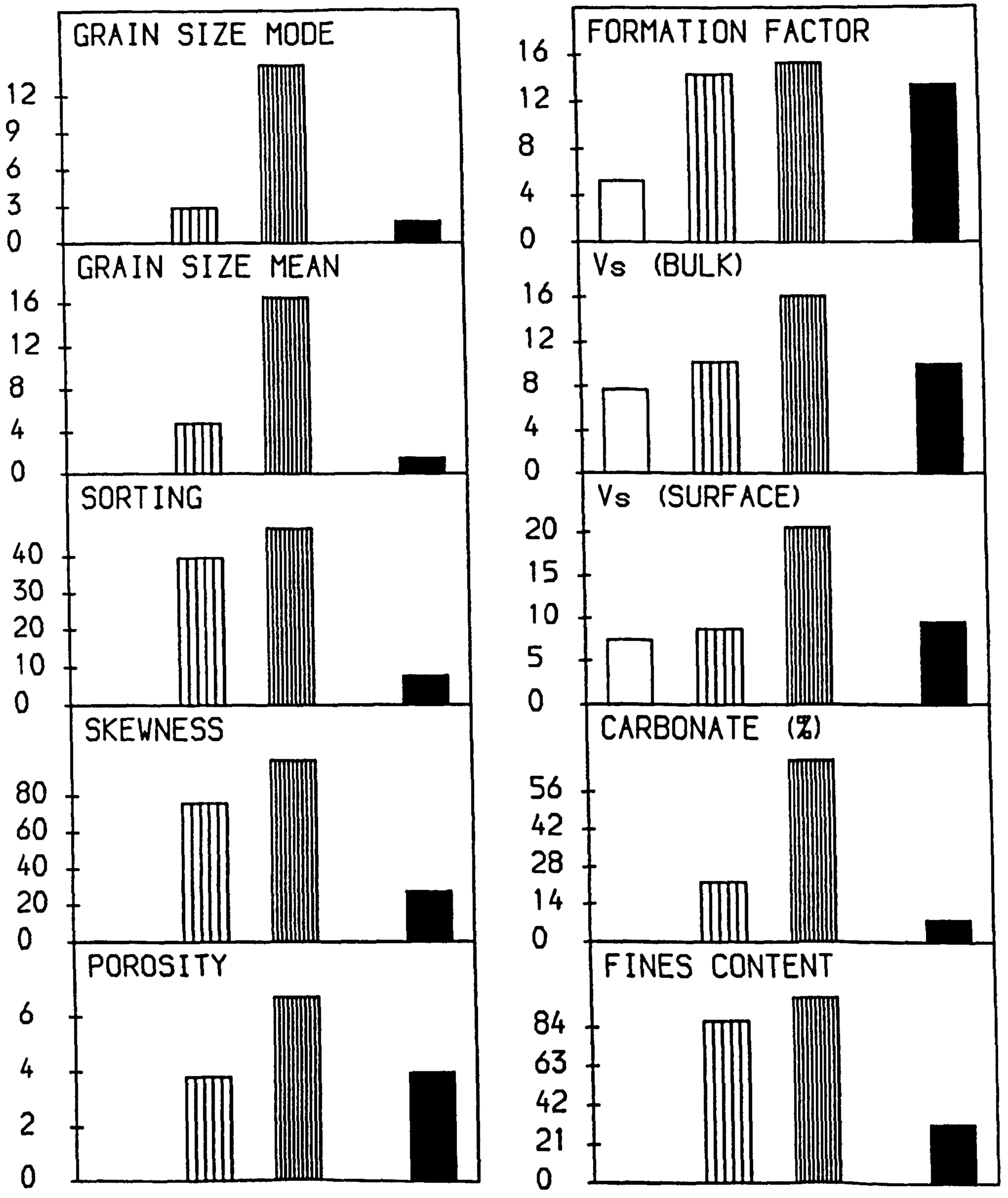

Fig. 5.4.7. All intertidal sands: relative scales of spatial and temporal variability.

5.4.4.2. Relative variability of textural, biological and geophysical parameters.

In Sections 5.2 and 5.3 it was shown that, over medium spatial and seasonal scales, there was a general progression in variability from first-order textural parameters through sediment porosity, the geophysical properties and finally second order textural and biological parameters. It is clear from from Table A1.3 that sediment porosity represents the least variable parameter, followed by grain size mode and mean, FF and Bulk V_s, then Surface V_s. Sorting follows, then carbonate content and finally fines content. Biological parameters are obviously the most variable, since there was large scale variation in benthic community structure and density.

The observed lack of variability in porosity can be explained by a number of arguments. As already stated, porosity is independent of grain size, and depends on grain shape, size distribution, and the manner in which the sediment grains are packed. Although it is possible to obtain significant variation in porosity of a given sediment in the laboratory there may be a much lower range of equilibrium (and therefore preserved) packing states after deposition under tidal and/or wave action. This implies that porosity is sensitive to first order textural variation, but not highly so, and is more sensitive to hydrodynamic environment. In a variety of subtidal surficial sediments, Richardson [1985] also found a generally lower degree of variability in porosity when compared to mean grain size.

The geophysical parameters exhibit rather higher variability, indicating increased sensitivity to bulk textural variation in addition to their expected dependence on porosity. Thus factors affecting bulk tortuosity and intergranular rigidity should cause increased variation in FF and V_s.

Carbonate content represents a measure of grain shape, and will be controlled by sediment source and depositional environment. Among the environments measured a range from 4% to 36% was encountered, mostly as shell fragments. This indicates significant variability in textural composition. Fines content varied from 0% to 5%, representing a small and highly variable fraction of the total sediment population.

The large scale variability of the geophysical properties, in relation to medium-scale spatial and seasonal variability as well as to that of other parameters, broadly supports the assertion that geophysical properties are primarily affected by properties of the bulk sediment framework, with additional variability due to localised and seasonal perturbation of this framework. Further work, over rather larger ranges in textural properties, should help to clarify these preliminary conclusions.

5.4.4.3. Generalised controls on porosity and the geophysical parameters.

Now that significant large-scale variation in sediment properties has been identified and discussed, controls on these properties can be investigated. Procedure was identical to that described in 5.1 for the results described in 5.2 & 3. All non-trivial pairs of textural and biological parameters were first tested for significant correlation. This enabled identification of interaction between potential controls on sediment structural properties. Linear regression analysis was then performed to identify controls on porosity and the geophysical properties..

The results have been discussed and presented according to the format adopted in 5.2 and 5.3. For reference, significant correlation coefficients have been listed in Table A1.4: regression analysis has been summarised in Table A1.5.

Textural interrelationships.

Since the locations sampled were generally both widely spaced and randomly selected, there is little point in performing detailed analysis of large-scale textural interrelationships. The few significant correlations identified have been listed, more to indicate interaction between potential predictor variables than to make any statements about textural characteristics of natural deposits. For these generally well-sorted intertidal sediments, mean grain size is strongly correlated with mode, and finer sands tend to be better sorted. Nearly all sediments are coarse skewed, with the bulk of the contribution to sorting arising from coarse

tail populations. There are no relationships with carbonate content, indicating that this parameter is independent, controlled predominantly by the nature of the sediment source.

Textural-biological interrelationships.

Analysis of overall biological variability was complicated because organisms were only present at some of the locations studied. This leads to problems in identifying genuine causal links between textural and biological parameters, since relationships may be obtained via unconnected differences between locations. Thus the correlations obtained do not constitute the basis for a proper study of organism/sediment interaction. *Corophium* is strongly correlated with fines content, indicating its preference for muddy sediment, while *Arenicola* is significantly inversely correlated with carbonate content. This may indicate either site-preference or a biogenic control, with unmanageable coarse shell fragments being sorted into the subsurface layers.

Controls on sediment porosity.

Several significant relationships have been identified between porosity and textural parameters. The most significant is with mean grain size, which apparently contradicts the earlier assertion that porosity should be independent of grain size. Fortunately, this can be explained by the fact that finer sands tend to be more angular, and deposited more gently, than coarser sands, resulting in a more highly arched packing configuration. This is supported by other work in natural sediments [e.g. Muskat, 1946].

Porosity is also increased by increasing carbonate content, due to the high angularity of shell fragments, and by increasing fines, probably for the reasons proposed for the relationship with mean grain size. The relationships with sorting and skewness are in agreement with other work [e.g. Sohn & Morland, 1968]. No biological controls were identified, which supports similar findings at individual locations. Thus porosity is strongly dependent on bulk textural parameters which relate to grain shape and depositional environment.

Controls on Formation Factor.

As expected, FF is significantly inversely related to porosity (for those locations where both FF and porosity were measured). Inverse relationships are also obtained with sorting and skewness, although these may be indirect due to their control on porosity.

The best significant combination of partial predictors includes positive dependence on carbonate and fines content and negative dependence on porosity and *Arenicola*. If porosity is left out of the analysis (to allow incorporation of results from Traeth Llanddwyn) no significant relationships are obtained. Clearly porosity represents an important independent predictor of FF, in addition to the expected effect on tortuosity of fines and shell fragments. *Arenicola* activity may also affect tortuosity, by liquefaction of the sediment and by the burrows themselves. All of these partial controls have also been identified at least once at individual locations.

Controls on V_s.

As expected, surface and bulk V_s are strongly correlated ($r = 0.765$), although they apparently differ in their sensitivity to some textural and biological controls. Surface V_s has already been shown to be more variable over large scales than bulk V_s, presumably because of its increased exposure to the effects of hydrodynamic processes and biological activity. Both parameters are inversely related to fines content and *Arenicola*, with surface V_s being most strongly influenced by fines. Both are also rather weakly related to *Lanice* and *Corophium*, in agreement with relationships identified at individual locations. Surface V_s is also directly related to carbonate content. As in the case of FF, all relationships identified support findings at one or more individual locations.

Variation in bulk V_s is best explained by a combination of grain size mode, *Arenicola* density and fines content. This indicates dependence on a bulk textural parameter, as well as the expected reduction due to burrowing activity and fines. Surface V_s is also related to *Arenicola* and fines, this time in combination with *Lanice*. An alternative combination

incorporates carbonate content and porosity instead of *Lanice*.

The higher R^2 values and increased overall variability suggest that surface V_s is the more representative parameter of the deposits sampled overall. This is reasonable, since for sediments exhibiting strong vertical heterogeneity, bulk V_s would have been representative of layers below the sampling zone. As in the Cefni Estuary, bulk V_s is significantly correlated with FF ($r = 0.336$), but surface V_s is not.

It is interesting that all the geophysical properties have been shown to be significantly partially controlled by biological activity, in agreement with findings from individual locations. Thus biological factors are clearly highly significant in determining variability of intertidal sediments.

The small-scale spatial heterogeneity parameters cv(FF) and V_{SR} exhibit some significant but rather weak relationships, but no significant combinations of partial predictors were identified. The velocity ratio V_{SR} is inversely dependent on fines, indicating enhanced vertical heterogeneity in muddy sediments. It is also directly correlated with carbonate, which indicates that the shelly deposits sampled were more homogeneous over depth scales of a few cm, although the reasons for this are unclear. The relationships observed for cv(FF) indicate that fine-grained, muddy deposits exhibit higher small-scale lateral heterogeneity.

CHAPTER 6.

CONCLUSIONS.

The primary objective of this study was to further the investigation of *in situ* variability in the physical properties of surficial sediments over a range of spatial and temporal scales. These physical properties govern rates of fluid and particulate exchanges between the sea floor and the water column, and are therefore extremely important for understanding sedimentation, contaminant trapping and release, benthic ecological succession and biogeochemical cycling in the marine environment.

Geophysical techniques are potentially powerful tools for *in situ* monitoring of the physical properties of a sedimentary deposit. The two geophysical properties selected for the purposes of this study were electrical Formation Factor (FF) and acoustic shear-wave velocity (V_s). They were chosen because of their empirically and theoretically proven relationships with important structural properties of the sediment. FF is controlled primarily by the structure of the fluid-filled pore space: V_s is controlled primarily by the composition and structure of the sedimentary framework, and by the number and strength of the intergranular contact forces.

Geophysical techniques for assessment of surficial sediment properties.

The techniques used for *in situ* monitoring of these geophysical properties over length and depth scales of a few centimetres were adapted from existing techniques under development at UCNW at the time of the study. Electrical measurements were performed via a simple Wenner array of current and potential electrodes in point contact with the sediment surface. Acoustic shear-wave generation and reception was performed by piezoelectric bender transducers.

A preliminary laboratory investigation provided information on transducer behaviour and validated the proposed technique for measuring V_s in

saturated intertidal sands. V_s is only slightly frequency dependent over the resonant frequency range encountered in saturated sands, and can be assumed constant within estimated sampling error. For 'spike' excitation of the transmitter, received frequency corresponds to the resonant frequency of the transducer/sediment system. This is inversely related to separation between source and receiver probes, due to increased attenuation of higher frequency components of the transmitted pulse, but can be regarded as approximately constant for the separation ranges employed. Results suggest that, provided that transducer compliance is well matched to the surrounding sediment, this resonant frequency is linearly related to V_s via a constant disturbance wavelength of approximately twice the width of the bender plate. The transducers used are well-matched in saturated sands: however, in drained sand and in saturated intertidal mud, the transducers decouple from the sediment and revert to frequencies nearer their unloaded resonance. In drained sand this causes breakdown of the received signal into a lower than predicted frequency; in muds the frequency is higher. Since optimal signal quality is achieved when the transducer-sediment system is perfectly coupled, these results suggest that the width of the bender element should be an important design criterion when designing transducers for future experiments.

V_s is measured *in situ* from received signal arrival times at two fixed probe separations. This allows calculation of two velocities defined as: *bulk* V_s, obtained from the difference between signal arrival times at the two receiver positions; and *surface* V_s, obtained from the arrival time at the shortest receiver separation. Marked velocity gradients are observed in the upper few centimetres of laboratory deposits. FF measurements also apparently increase with depth, suggesting a gradient in degree of compaction. However, the effect is less marked, suggesting that the chief source of the increase in V_s is rapidly increasing effective stress at the intergranular contacts due to increasing overburden. Provided that the probes are inserted to a fixed depth of 40mm these gradients do not cause significant curvature in time-separation relationships over a probe separation range of 50-150mm in homogeneous sands. Therefore, surface and bulk V_s are not significantly different and a single effective velocity can be defined. However, at several *in situ* locations marked surficial vertical heterogeneity is indicated by significant differences between the two velocities. Strongest heterogeneity is observed in fine-grained, muddy

deposits and at locations where texturally contrasting subsurface layers were present.

Because natural deposits exhibit lateral and vertical heterogeneity, both V_s and FF measurements are significantly affected by the volume of sediment monitored. They provide an 'apparent' value for an effectively homogeneous volume within which resolution of finer scale variability is impossible. The limits to this volume can be defined as the limits outside which marked structural or textural heterogeneity will not affect the measured value. It is clearly dependent on the length scales of the measurement technique: in this case the transducer or electrode separation of the proposed *in situ* probes. Computer simulation indicates that heterogeneity within an area of of 400 × 200mm, and a maximum depth of 250mm may significantly affect *in situ* FF measurements. V_s is influenced by a rather smaller volume: an area of 60 × 50mm, and a depth of 40mm for surface V_s, an area of 60 × 125mm and a depth of 80mm for bulk V_s. It was realised too late that a smaller electrode separation may have provided better representation of near surface electrical properties in strongly heterogeneous deposits: future developments will benefit from this realisation.

Drainage of the sediment on tidal exposure causes a marked increase in V_s both *in situ* and during a laboratory simulation. The cause is probably increased effective stress at the intergranular contacts, caused by negative pore-pressures in the capillary-sealed voids left within the sediment. The increase is more marked in the laboratory (*c.* 60%) than *in situ* (14-25%), perhaps because drainage is more effective in the laboratory test tank. In contrast, very little difference in FF is observed on drainage, both *in situ* and in the laboratory. This was unexpected, considering the associated effective reduction in porosity and increase in tortuosity of the remaining pore fluid matrix, and remains unexplained.

Measurements of V_s in the intertidal zone (or in box-cores from subtidal deposits) can therefore only be usefully compared if they are performed under conditions of full saturation. In addition, FF measurement is highly sensitive to overlying water, which imposes the additional requirement of sampling only where the water table is situated just at the sediment surface.

Variability in properties of surficial intertidal sediments.

Variability in the textural, biological and geophysical properties of saturated intertidal sediments has been assessed *in situ* over a range of spatial scales, and over a seasonal cycle. As expected, the highest variability in all parameters is encountered over large spatial scales, encompassing gross or *first order* differences in textural characteristics and packing configuration due to the nature of the sediment source, the local depositional environment, and activity by the benthic infaunal community.

Significant localised variability is obtained over scales of tens to hundreds of metres. In particular, marked trends or contrasting zones have been observed across exposed intertidal sandflats and in sandy foreshores, presumably controlled by variation in duration of tidal exposure and the tide-averaged hydrodynamic environment. Temporal variability over a year is also significant, as annual trends and apparently random variability in addition to seasonal cycles. Chief controls in this case are temperature (which affects biological activity) and seasonal or other temporal variation in the localised hydrodynamic environment.

Over medium spatial scales, bulk textural variability is drastically reduced. In general, for sandy sediments, this allows interpretation of the deposit as predominantly comprising an invariant modal grain size distribution, with localised (or seasonal) *second order* variation introduced via the admixture of variable proportions of coarser or finer particles. These coarse and fine fractions must be defined separately for each location. The fine sub-fraction corresponds to the fines content at all locations: in addition, between one and two coarse sub-fractions, generally containing higher carbonate content, were required to adequately characterise textural variation. Seasonal variability is even lower than medium-scale spatial variability, suggesting that the textural signature of a deposit reflects a highly localised, time-averaged response to hydrodynamic environment and benthic community.

Porosity, V_s, and FF are also less variable over localised spatial scales than over larger scales, although the difference is not as great as for the bulk textural parameters. These structural parameters exhibit comparable

seasonal variability to medium-scale spatial variability, which provides an interesting contrast to the textural parameters. This indicates that packing configuration is more sensitive than textural composition to seasonal variation in hydrodynamic environment and biological activity. This is borne out by the observed seasonal cycle in sediment porosity, and by direct relationships between temporal variation in geophysical and biological parameters. It is further supported by the evidence of a rapid response of packing configuration to specific 'events': low rigidity, structurally homogeneous surface layers are generated after erosion or during high winds, while higher rigidity, heterogeneous deposits are generated after deposition.

Small-scale spatial heterogeneity, which has only been measured for the geophysical parameters, is less than medium scale spatial variability. Further, small-scale variability is lower for FF than for V_s. This is probably because sampling error is less, because less sediment disturbance is associated with measurement, and because many more replicates are feasible for FF. Replication of FF measurements provides an excellent method for characterising surficial structural heterogeneity.

The variability of the different textural, biological and structural parameters has also been usefully compared. On local and seasonal scales, it is proposed that the packing configuration of sandy deposits is primarily controlled by the properties of the uniform sediment framework, with secondary distortion or 'perturbation' of this framework introduced via variation in the second order textural parameters, via the depositional environment and via post-depositional reworking by hydrodynamic processes or biological activity. Thus variability in porosity and the geophysical parameters should be less than that in the second order textural parameters or biological characteristics.

Further inference is possible concerning the bulk textural and structural parameters. While mean grain size is affected only by the proportion of second order textural parameters, porosity should be additionally sensitive to variation in grain shape, the hydrodynamic environment and biological activity. FF and V_s should be affected by porosity, but will in turn be additionally sensitive to variation in factors controlling tortuosity or the number and nature of intergranular contacts.

This hypothesis is supported in general by a hierarchy in localised or seasonal variability, from the most uniform grain size mode, through grain size mean and porosity, then FF and V_s, then the second order textural characteristics and finally the biological parameters.

Over larger spatial scales, encompassing variation in composition of the sediment framework (but not including data from the sharply contrasting mudflats), porosity is the least variable parameter. This relatively low degree of *in situ* variability in the porosity of natural sands is interesting. Porosity should be independent of absolute grain size, so there is no reason to expect comparable variability to the mode or mean. Significant between-location differences are identified, indicating some sensitivity to large scale variation in grain shape, spread of sizes, the hydrodynamic environment and the benthic community. While a relatively wide range of porosities can be obtained artificially for a given sediment, there may be a rather lower range of stable (and hence preserved) packing configurations in sandy intertidal environments. FF and bulk V_s are much more variable than porosity, and slightly more variable than mode and mean grain size. This indicates their additional sensitivity to tortuosity and to the number and nature of intergranular contacts, which should all be related to absolute grain size, size distribution and shape. Surface V_s is even more variable, indicating increased sensitivity of the extreme near-surface to biological and hydrodynamic controls.

Controls on the geophysical properties of surficial intertidal sediments.

Statistical analysis of measured parameters allows investigation of controls on porosity and geophysical properties. While high scatter and interaction between parameters may cast some doubt on the relevance of individual relationships (especially those obtained from multiple linear regression), the more consistently identified controls inspire rather greater confidence in their importance.

Interpretation of localised and temporal controls is based on the assumption that structural properties of sands are primarily controlled by the uniform bulk sediment framework, with additional but lesser sensitivity to variation in proportion of the second order textural parameters and in

biological activity. This technique has identified some simple controls at several locations, although none of these relationships are universally applicable. This is understandable, given the clearly complex and interactive nature of textural and structural variation, the small sample sizes and ranges in parameters, and the fact that important additional controls may not have been measured.

Overall controls are obtained over much larger sample sizes, and incorporate greater ranges in parameters due to bulk textural variation. However, in contrast to the localised data sets, there is a more complex range of contributors to textural and hence structural properties of the sediment, which can only be characterised partially by use of standard statistical grain size parameters.

Porosity

Porosity should be independent of absolute grain size. However, since finer particles have a lower energy of deposition and tend to be more angular, overall broad increases with fining mean grain size are obtained..

For a given size distribution, shell fragments increase porosity by forming 'bridges' over gaps between grains during deposition. Therefore porosity should be increased by increasing carbonate content. This is found to be the case over the full range of sandy sediments monitored. However, since the coarse sub-fraction often contains a higher proportion of shell fragments, the counteracting effect of increasing overall size distribution associated with increasing carbonate content, and hence improving packing efficiency, must also be considered. With the exception of the Cefni estuary, where no relationships with porosity were identified, results suggest that where the shell fraction is reasonably close in size to the framework population (as in the Taf, at Red Wharf Bay and at LLigwy), porosity is increased, but where it forms part of a much coarser subpopulation (as at LLanddwyn), porosity may be reduced.

The effect of addition of fines can also be interpreted in terms of size relative to the framework population. The dominant control is thought to be the tendency of fine-grained cohesive sediments to form high-arched

structures on deposition, thus increasing porosity. This explains the strong positive correlation between fines content and porosity for the full data set (incorporating measurements from the Tamar mudflats). However, if the fines are small enough relative to the framework population they can fall between the framework grains and cause reduced porosity. In the Taf the framework population is too fine to allow silt and clay particles to form an interstitial population, so porosity is increased by fines. In the Cefni, some of the fine sub-fraction may be interstitial, and no direct relationship is identified.

Porosity is rather surprisingly not shown to be affected directly by variation in biological activity. It is thought that the sample volumes used for porosity measurement were too small to allow proper representation of the effect of spatially heterogeneous arrays of burrows and tubes. However, it is also possible that the organisms monitored do not significantly affect overall porosity, because their burrowing activity causes compaction of the adjacent sediment or liquefaction and homogenisation of sediment into a closer packing configuration.

During the seasonal study in the Cefni estuary, no textural or biological controls on porosity could be identified. This may have been caused by interaction between opposing textural or biological controls, which explains the absence of significant differences between time-averaged porosity at individual sites despite differences in textural and biological signature. Porosity is also much more sensitive to temporal hydrodynamic environment than the textural parameters, exhibiting a spatially coherent response to seasonal and shorter term variation. This implies that porosity is an important additional parameter which cannot be completely described by consideration of textural or biological characteristics.

Formation Factor.

FF should be controlled by sediment porosity and by factors affecting the tortuosity of the pore fluid matrix. Overall, significant inverse dependence on porosity has been identified, both over the full data set and in sands. A high degree of scatter is involved, reflecting differences in tortuosity for a given porosity. At individual locations, FF correlates

with porosity in the Tamar and Cefni estuaries, but not elsewhere.

Due to the increased angularity of shell fragments, carbonate content should increase tortuosity for a given porosity, although because it does also tend to increase porosity some relationships may have been obscured. Positive relationships are found between FF and carbonate content in the Cefni, at LLanddwyn, and for the data set comprising all sandy locations. Laboratory measurements on samples from Red Wharf Bay and LLigwy suggest that simple FF:porosity relationships are complicated by the fact that higher carbonate, higher porosity sediments also exhibit higher tortuosities, leading to low localised variability in FF.

Fines content should also affect tortuosity, since fine particles are platelike in shape, and they may fall between sand grains and clog up the pore space. Fines are also capable of electrical conduction along their surfaces, which will additionally affect FF, although this is only significant for the Tamar samples. FF is reduced by fines in the Taf and in the Tamar, due to the associated increases in porosity. However, overall and in the Cefni, FF is increased by fines for a given porosity, indicating that tortuosity is increased.

In contrast to the case for porosity, there are reasonably consistent significant biological controls on FF. *Arenicola* reduces FF overall, in the Cefni estuary, at LLanddwyn and at LLigwy (B). This suggests a significant effect on packing configuration of the sediment which was not measured by the porosity samples. If bulk porosity is not significantly increased, then tortuosity must be reduced, although sampled porosity may not have been representative of bulk porosity in these sediments. In the Cefni Estuary, small scale spatial heterogeneity measured from within-site variability of FF is increased by *Arenicola* activity, suggesting that averaging over larger areas may be required in order to effectively characterise bulk surficial sediment properties.

Corophium activity reduces FF in the Taf, but not in the Cefni, where equally high ranges in burrow densities are encountered. The Taf data was much simpler to interpret because only one species was present, and because the complicating factor of sensitivity to temporal variation in hydrodynamic environment was avoided. *Lanice* reduces FF at LLanddwyn, but

not at Red Wharf.

Where they have been found, the biological controls all act to reduce FF. This suggests that fluid-filled burrows and tubes contribute significantly to electrical conduction within the pore fluid matrix. This also suggests that permeability will be enhanced in these deposits, despite the apparent lack of effect on porosity, which is of considerable importance for studies of pore fluid exchange across the sediment water interface.

S-wave velocity.

V_s should be inversely related to porosity for a given sediment, but will also be strongly affected by the number and strength of intergranular contact forces within the sediment frame. Overall, only a weak inverse relationship is found with porosity, while at individual locations inverse relationships are identified in the Taf, at Red Wharf Bay, and in the Cefni. This suggests that where bulk textural properties are varying, V_s is more sensitive to factors affecting intergranular rigidity than to bulk porosity, but where there is only second order textural variation, porosity is rather more important. It is interesting that this is opposite to the pattern of controls identified for FF, porosity being the strongest overall control in this case.

For a given porosity, addition of shell fragments should increase the number of intergranular contacts per grain, causing increased intergranular friction. Since carbonate content also tends to increase porosity, however, opposing effects have been identified. Thus increasing carbonate content increases V_s overall, in the Cefni, and at LLanddwyn, but reduces V_s in the Taf.

Addition of small amounts of fines significantly reduces V_s in sands, especially in the case of surface V_s. This is observed in the Taf and Cefni estuaries, and for the full data set, and is independent of porosity. Fine particles may serve to lubricate the rough sand grains of the framework, causing reduced intergranular friction, in addition to their proposed increase in tortuosity. This inverse relationship was not observed on the Tamar mudflats, where no simple controls on V_s have been identified.

As in the case of FF, there are significant biological controls on V_s. The nature of these controls, however, are different. *Arenicola* reduces V_s overall, in the Cefni, and at LLigwy. *Corophium* reduces V_s in the Taf and at two sites in the Cefni, although not at the most abundant site. A similar reduction in V_s has also been simulated using artificial burrows in drained sand in the laboratory. In complete contrast, *Lanice* increases V_s, both at LLanddwyn and at Red Wharf Bay, and overall. *Pygospio* also increases V_s at two sites in the Cefni.

Thus, where significant controls are identified, burrowing organisms reduce V_s, while tube-building organisms increase it. This is important, because it suggests that structural properties of the sediment framework can be significantly altered by biological activity, and further that opposing effects can be generated depending on organism behaviour. It can be inferred that stability of the bed, and response to hydrodynamic forcing, are modified by the organisms that live within it.

REFERENCES

Allen, J.R.L., 1974. Packing and resistance to compaction of shells. *Sedimentology* 21:71-86.

Allen, J.R.L., 1982. *Sedimentary structures.* Vols I,II. Amsterdam: Elsevier.

Allen, J.R.L., 1985. *Principles of Physical Sedimentology.* George Allen & Unwin, London.

Allen, P.L. and Moore, J.J., 1987 Invertebrate macrofauna as potential indicators of sandy beach instability. *Est. Coast. Shelf Sci.* 24:109-125.

Aller, R.C. and Yingst, J.Y., 1978. Biogeochemistry of tube dwellings: A study of the sedentary polychaete *Amphitrite ornata* (Leidy). *J. Mar. Res.* 36:201-254.

Aller, R.C. and Yingst, J.Y., 1980. Relationships between microbial distributions and the anaerobic decomposition of organic matter in surface sediments of Long Island Sound, U.S.A. *Mar. Biol.* 56:29-42.

Amos, C.L., Wagoner, N.A. and Daborn, G.R., 1988. The influence of sub-aerial exposure on the bulk properties of fine-grained intertidal sediment from Minas Basin, Bay of Fundy. *Est. Coast. Shelf Sci.* 27(1):1-13.

Aspiras, R.B., Allen, O.N., Harris, R.F. and Chesters, G., 1971. The role of microorganisms in the stabilisation of soil aggregates. *Soil Biol. Biochem.* 3:347-353.

Archie, G.E., 1942. The electrical resistivity log as an aid in determining some reservoir characteristics. *Am. Inst. Min. Metall. Pet. Eng. tech. Rept.* 1422.

Atkins, E.R. and Smith, G.H., 1961. The significance of particle shape in Formation Factor-porosity relationships. *J. Petrol. Tech.* 13:285-291.

Attenborough, K., 1982. Acoustical characteristics of porous materials. *Physics Reports* (Review section of *Physics Letters*) 82(3):179-227.

Bader, R.G. 1953. *Local variability in marine sediments.* Univ. Washington, Dept. Oceanography, Tech. Rep. 16:17pp.

Bagnold, R. and Barndorff-Nielsen, O., 1980. The pattern of natural size distributions. *Sedimentology* 27:199-207.

Barndorff-Nielsen, 0., 1977. Exponentially decreasing distributions for the logarithm of particle size. *Proc. Roy. Soc. London Ser.A* 353:401-419.

Barnes, B.B., Corwin, R.F., Beyer, J.H. and Hildenbrand, T.G., 1972. *Geologic prediction: developing tools and techniques for the*

geophysical identification and classification of sea floor sediments U.S Dept. Commerce Publicatiom, NOAA Tech.rep. ERL224-MMT-C2, 163pp.

Baumfalk, Y.A., 1979. Heterogeneous grain-size distributions in tidal-flat sediment caused by bioturbation activity of *Arenicola marina* (polychaeta). *Neth.J.Sea.Res.* 13:428-440.

Bedford, A., Costley, R.D. and Stren, M., 1984. On the drag and virtual mass coefficients in Biot's equations. *J. Acoust. Soc. Am.* 76(6):1804-1809.

Bell, D.W, 1979. *Shear wave propagation in unconsolidated fluid-saturated porous media.* Technical report No. ARL-TR-79-31. Applied Research Laboratories, University of Texas at Austin.

Bell, D.W. and Shirley, D.J., 1980. Temperature variation of the acoustical properties of laboratory sediments. *J. Acoust. Soc. Am.* 68(1): 227-231.

Bennell, J.D., Jackson, P.D., Schultheiss, P.J., 1982. Further developments of sea floor geophysical probing. *Proceedings of Oceanology International Conference*, Brighton (Society for Underwater Technology):0I82 4:8.

Bennell, J.D., Davis A.M. and Taylor-Smith, D. 1984. Resonant column testing of marine sediments. *Oceanology International*, Brighton. 1984, OI 1.9:1-11.

Bennett R.H., Keller, G.H. and Busby, R.F., 1970. Mass property variability in three closely spaced deep-sea sediment cores. *J. Sedim. Petrol.* 40(3):1038-1043.

Bennett, R.H., Bryant, W.R. and Keller, G.H., 1981. Clay fabric of selected submarine sediments: Fundamental properties and models. *J. Sedim. Petrol.* 51:217-232.

Berryman, J.G., 1980a. Long wavelength propagation in composite elastic media. Parts I and II. *J. Acoust. Soc. Am.*, 68:1809-1823.

Berryman, J.G., 1980b. Confirmation of Biot's theory. *Applied Physics Letters.* 37:382-384.

Berryman, J.G., 1981. Elastic wave propagation in fluid-saturated porous media. *J. Acoust. Soc. Am.* 69:416-424.

Bikerman, 1970. *Physical Surfaces.* Academic, New York.pp 370-431.

Biot M.A., 1956a. Theory of propagation of elastic waves in a fluid-saturated porous solid. I. Low frequency range. *J. Acoust. Soc. Am.* 28:168-178.

Biot M.A., 1956b. Theory of propagation of elastic waves in a fluid-saturated porous solid. II. Higher frequency range. *J. Acoust. Soc. Am.* 28:179-191.

Biot, M.A., 1962a. Mechanics of deformation and acoustic propagation in porous dissipative media. *J. Appl. Phys.* 33:1482-1498.

Biot, M.A. 1962b. Generalised theory of acoustic propagation in porous dissipative media. *J. Acoust. Soc. Am.* 34:1254-1264.

Biot, M.A. and Willis, D.G., 1957. The elastic coefficients of th theory of consolidation. *J.Appl. Mech.* 24:594-601.

Black, C.A., 1965 (ed.). *Methods of soil analysis.* American Society of Agronomy, Pt 2, 1572pp.

Boer, P.L. De, 1981. Mechanical effects of microorganisms on intertidal bedform migration. *Sedimentology* 28:129-132.

Bogoslovsky, V.A., and Ogilvy, A.A., 1974. Detailed electrometric and thermometric observations in offshore areas. *Geophysical Prospecting* 22: 381-392.

Booth, J.S., Dahl, A.G., 1987. A note on the relationship between organic matter and some geotechnical properties of marine sediment. *Marine Geotechnology* 6(3):281-298.

Bouma, A.H., Sweet, W.E.M., Chemlik, F.B. and Heubner, G.L., 1971. Shipboard and *in situ* electrical resistivity logging of unconsolidated marine sediments. *Third Offshore Technology Conference Preprints*, 1:253-268.

Boyce, R.E., 1968. Electrical resistivity of modern marine sediments from the Bering sea. *J. Geophys. Res.* 73:4759-4766.

Bradshaw, A.L. and Schlacher, K.E. 1980. Electrical conductivity of seawater. I.E.E.E J. Oceanic Engineering 5(1) 50-62. Special Issue: The Practical Salinity Scale.

Briggs, K.B., Richardson, M.D. and Young, D.K., 1985. Variability in geoacoustic and related properties of surface sediments from the Venezuela Basin, Caribbean Sea. *Marine Geology* 68:73-106.

Brown, R.J.S., 1980. Connection between formation factor for electrical resistivity and fluid-solid coupling factor in Biot's equations for acoustic waves in fluid-filled porous media. *Geophysics* 45(8):1269-1275.

Buhr, K.J. and Winter, J.E., 1977. Distribution and maintenance of a *Lanice conchilega* association in the Weser estuary (FRG), with special reference to the suspension feeding behaviour of *Lanice conchilega.* In: *Biology of benthic organisms* (Keegan, B.F., O'Ceidigh, P.O. and Boaden, P.J.S. eds.). Pergamon Press. pp101-113.

Cadée, G.C., 1976. Sediment reworking by *Arenicola marina* on tidal flats in the Dutch Wadden Sea. *Neth. J. Sea Res.* 10(4):440-460.

Cadée, G.C., 1979. Sediment reworking by the polychaete *Heteromastus filiformis* on a tidal flat in the Dutch Wadden Sea. *Neth. J. SEa Res.* 13(3/4):441-456.

Carey, D.A., 1983. Particle resuspension in the benthic boundary layer induced by flow around polychaete tubes. *Can. J. Fish. Aquat. Sci.* 40(S1):301-308.

Carman, P.C., 1956. *Flow of gases through porous media.* Academic Press, N.Y.

Carney, R.S., 1981. Bioturbation and biodeposition. In: *Principles of Benthic Marine Paleoecology* (A.J. Boucot, ed.) pp 357-400, Academic Press, New York.

Carver, R.E., 1971. *Procedures in Sedimentary Petrology.* Wiley Interscience, New York.

Celikkol, B. and Vogel, P.M. 1973. A new shear wave velocity measurement technique in ocean bottom soil samples. *Proc. 6th Offshore Technology Conference*, Houston, Texas, OTC 1794.

Cullen, D.J., 1973. Bioturbation of superficial marine sediments by interstitial meiobenthos. *Nature* 242:323-324.

Dapples, E.C., 1942. The effect of macroorganisms on near-shore sediments. *J. Sedim. Petrol.* 12:118-126.

Davis, A.M. and Schultheiss, P.J. 1980. Seismic signal processing in engineering site investigation - a case history. *Ground Engng*, 13, No 4: 44-48.

Davis, A.M. and Bennell, J.D, 1985. Dynamical properties of marine sediments. In: *Ocean Seismo-acoustics* (T. Akal, and J. Berkson, eds.), Plenum, New York.

Davis, A.M., Bennell, J.D., Huws, D.G. and Thomas, D., 1989. Development of a seafloor geophysical sledge. *Marine Geotechnology* 8:99-109.

Dexter, A.R. and Tanner, D.W., 1971. Packing density of ternary mixtures of spheres. *Nature* 230:177-179.

Domenico, S.N., 1977. Elastic properties of unconsolidated porous sand reservoirs. *Geophysics* 42(7):1339-1368. (Discussion, *Geophysics* 44(4):830, 1979).

Dyer, K.R., 1986. *Coastal and Estuarine sediment dynamics.* Wiley Interscience, New York.

Dyvik, R. and Madshus, C., 1985. Laboratory measurements of $G_{(max)}$ using bender elements. In: *Advances in the art of testing soils under cyclic conditions*, Vijay Khosla, ed. New York: American Society for Civil Engineering, pp 186-196.

Eckman, J.E., Nowell, A.R.M. and Jumars, P.A., 1981. Sediment destabilisation by animal tubes. *J. Mar. Res.* 39:361-374.

Eltringham, S.K., 1971. *Life in mud and sand.* English Universities Press.

Erchul, R.A. and Nacci, V.A., 1972. Electrical resistivity measuring system for porosity determination of marine sediments. *Marine Tech. Soc. J.* 6(4):47-53.

Faas, R.W., 1973. Mass property variability of some estuarine sediments. *Sediment. Geol.* 10:205-213.

Fazio, S.A., Uhlinger D.J., Parker, J.H. and White, D.C., 1982. Estimations of uronic acids as quantitative measures of extracellular polysaccharide and cell wall polymers from environmental samples. *Applied and Environmnetal Microbiology* 43:1151-1159.

Featherstone, R.P. and Risk, M.J., (1977). Effect of tube building polychaetes on intertidal sediments of the Minas Basin, Bay of Fundy. *J Sedim. Petrol.* 47:446-450.

Folk, R.L., 1955. Student operator error in determination of roundness, sphericity and grain size. *J. Sed. Petrol.* 25:297-301.

Frankel, L. Mead, D.J., 1973. Mucilaginous matrix of some estuarine sands in Connecticut. *J. Sedim. Petrol.* 43:1090-1095.

Frey, R.W., 1973. Concepts in the study of biogenic sedimentary structures. *J. Sedim. Petrol.* 43:16-19.

Frostick, L.E. and McCave, I.N., 1979. Seasonal shifts of sediment within an estuary mediated by algal growth. *Est. Coast. Mar. Sci.* 9:569:576.

Gamble, J.C., 1970. Anaerobic survival of the crustaceans *Corophium volutator, Corophium arenarium* and *Tanais chevreuxi. J. M. Biol. Ass.* 50:657-671.

Gassmann, F., 1951. Elastic waves through a packing of spheres. *Geophysics* 16(4):673, errata *Geophysics* 18(1):269, 1953.

Geertsma, T. and Smit, D.C., 1961. Some aspects of elastic wave propagation in fluid-saturated porous solids. *Geophysics* 26:169-181.

Gehrmann, T., Gimpel, P. and Theilen F. 1985. Marine shear-wave profiling. *Geophysics*, 50:336.

Ginsberg, R.N. and Lowenstam, H.A., 1958. The influence of marine bottom communities on the depositional environment of sediments. *J. Geol.* 66: 310-318.

Godmunsson, H., 1985. Life history patterns of polychaete species of the family spionidae. *J. M. Biol. Ass.* (U.K.) 65:93:101.

Grant, J., 1983. The relative magnitude of biological and physical sediment reworking in an intertidal community. *J. Mar. Res.* 41:673-689.

Grant, W.D., Boyer, L.F. Sanford, L.P., 1982. The effects of bioturbation on the initiation of motion of intertidal sands. *J. Mar. Res.* 40(3):659-677.

Griffiths, J.C., 1953. Estimation of error in grain-size analysis. *J. Sed. Petrol.* 23:75-84.

Hamilton, E.L., 1971. Elastic properties of marine sediments. *J. Geophys. Res.* 76:579-604.

Hamilton, E.L., 1976a. Attenuation of shear waves in marine sediments. *J. Acoust. Soc. Am.* 60:334-338.

Hamilton, E.L., 1976b. Shear wave velocity versus depth in marine sediments: A review. *Geophysics* 41(5):985-996.

Hamilton, E.L., 1980. Geoacoustic modelling of the sea floor. *J. Acoust. Soc. Am.* 68:1313-1340.

Hamilton, E.L. and Bachman, R.T., 1982. Sound velocity and related properties of marine sediments. *J. Acoust. Soc. Am.* 72(6):1891-1904.

Hardin, B.O. and Richart, Jr., F.E., 1963. Elastic wave velocities in granular soils. *J. Soil Mech. Found. Div.* ASCE 89(SM1):33-65.

Hardin, B.O. and Drnevich, V.P., 1972. Shear modulus and damping in soils: design equations and curves. *J. Soil Mech. Found. Div. ASCE* 98: 667-693.

Hargrave, B.T., 1980. Factors affecting the flux of organic matter to sediments in a marine bay, in: *Marine benthic dynamics* (K.R. Tenore and B.C Coull, eds.), University of South Carolina Press, pp243-264.

Haughey, D.P. and Beveridge, G.S.G, 1969. Structural properties of packed beds: a review. *Can. J. Chem. Eng.* 47:130.

Hepton, P. 1988. Shear wave velocity measurements during penetration testing. In: *Penetration testing in the U.K.* Thomas Telford, London.

Hepton, P. 1989. *Shear wave velocity measurements during penetration testing.* PhD Thesis, University College of North Wales, Bangor.

Herdan, G. 1960. *Small particle statistics.* Butterworth and Co Ltd,London.

Higginbottom I.E 1976. The use of geophysical methods in engineering geology. *Ground Engng* 9:(2):34-38.

Hill, H.J. and Milburn, J.D., 1956. Effect of clay and water salinity on electrochemical behaviour of reservoir rocks. *Trans AIME* 207:65-72.

Holland, A.F., Zingmark, R.G and Dean, J.M., 1974. Quantitative evidence concerning the stabilisation of sediments by marine benthic diatoms. *Mar. Biol.* 27:191-196.

Honjo, S., 1976. Coccoliths: Production, transportation and sedimentation. *Mar. Micropaleontol.* 1:65-79.

Hovem, J.M. and Ingram, G.D., 1979. Viscous attenuation of sound in saturated sand. *J. Acoust. Soc. Am.* 66:1807-1812.

Hoyer, W.A., and Rumble, R.C., 1976. Dielectric constant of rocks as a petrophysical parameter. Society of Petroleum and Well Logging Analysts. *17th Annual logging Symposium, June 9-12,* 1-27.

Hryciw, R.D. and Dowding, C.H., 1987. Cone penetration of partially saturated sands. *Geotechnical Testing Journal, GTJODJ* 10(3):135-141.

Hull, S.C. (1987). Microalgal mats and species abnundance: a field experiment. *Est. Coast. Shelf Sci.* 25:519-532.

Hurley, M. T. 1989. The application of Biot's theory to sea-bed sediments. PhD thesis, University College of North Wales, Bangor.

Inman, D.L., 1949. Sorting of sediment in light of fluid mechanics. *J.Sed. Petrol.* 19:51-70.

Iwasaki, T., Tatsuoka, F. and Takagi, Y., 1977. Shear modulus of sands under cyclic torsional shear loading. *J. Japan Soc. Soil Mech Found Engng* 17(3):19-35.

Jackson, J.D., 1975. *Classical Electrodynamics.* 2nd. Ed., John Wiley and Sons, New York.

Jackson, P.D., 1975. An electrical resistivity method for evaluating the *in-situ* porosity of clean marine sands. *Marine Geotechnology* 1(2):91-115.

Jackson, P.D. 1976. *Geotechnical mapping of the sea bed.* NERC Contract No. F60/4/22 Final Report, Part II.

Jackson, P.D., Taylor Smith, D., Stanford, P.N., 1978. Resistivity-porosity-particle-shape relationships for marine sands. *Geophysics* 43(6):1250-1268.

Jackson, P.D., Baria, R.,McCann, D.M., 1980. Geotechnical assessment of superficial marine sediments using *in-situ* geophysical probes. *Oceanology International 80*, pp33-46.

Jackson, M.L., 1958. *Soil chemical analysis*, Prentice-Hall, p222-225.

Jago, C.F., 1974. *The sedimentology of estuarine and coastal plain deposits between Pendine and Wharley point, Carmarthen Bay.* PhD. Thesis, Imperial College of Science and Technology, London.

Jago C.F., 1980. Contemporary accumulation of marine sand in a macrotidal estuary, Southwest Wales. *Sed. Geol.* 26:21-49.

James, A.E., Williams, D.J.A. and Williams, P.R., 1987. Direct measurement of static yield properties of cohesive suspensions. *Rheol. Act.* 26(5):437-446.

Johnson, D.L. and Plona, T.J., 1984. Recent developments in the acoustic properties of porous media. In: *Proc. of Enrico-Fermi Summer School "Frontiers of Physical Acoustics", Varenna, Italy..*

Johnson, D.L. and Sen, P.N., 1981. Multiple scattering of acoustic waves with applcation to index of refraction of 4th sound. *Phys. Rev. B* 24:2486-2496.

Johnson, R.G., 1971. Animal-sediment relations in shallow water benthic communities. *Mar. Geol.* 11:93-104.

Johnson, R.G., 1972. Conceptual models of marine benthic communities. In: J.M. Schopf, (ed.), *Models in Paleobiology*, pp149-159, Freeman and Cooper, San Francisco.

Johnson, R.G., 1977. Vertical variation in particulate matter in the upper twenty centimetres of marine sediments. *J. Mar. Res.* 35:273-282.

Joliffe, F.R. 1986. *Survey design and analysis*. Ellis Horwood Ltd.

Jumars, P.A. and Nowell, A.R.M. 1984. Effects of benthos on sediment transport: difficulties with functional grouping. *Cont. Shelf Res.* 3(2):115-130.

Keller, G.H. 1974. Marine geotechnical properties: interrelationships and relationships to depth of burial. In: A.L.Inderbitzen (Ed.), *Deep Sea Sediments, Physical and Mechanical Properties*. Plenum Press, New York pp77-100.

Keller, G.V. and Frischknecht, F.C., 1966. *Electrical methods in geophysical prospecting*. London, Pergamon Press 519pp.

Kelly, J.C. and McManus, D.A., 1970 Hierarchical analysis of variance of shelf sediment texture. *J. Sed. Petrol.* 40:1335-1338.

Kermabon, A., Gehin, C. and Blavier, P., 1969. A deep-sea electrical resistivity probe for measuring porosity and density of unconsolidated sediments. *Geophysics* 34:554-571.

Kolbuszewski, J., 1950. Notes on deposition of sands. *Research* 3:478-83.

Krantzberg, G., 1985. The influence of bioturbation on physical, chemical and biological parameters in aquatic environments: A review. *Environ. Pollut. (A.Ecol.Biol.)* 39(2):99-122.

Krumbein, W.C., 1934. The probable error of sampling sediments for mechanical analysis. *Amer. J. Sci.* 27:204-214.

Kullenberg, B., 1952. On the salinity of water contained in marine sediments. *Meddelanded Oceanografiska Instit. i Goteborg*, No. 21, 37pp.

Kunetz, G., 1966. *Principles of direct current resistivity prospecting*. Geoexploration monographs, Series 1, No. 1, Berlin, Gerbruder Borntaeger, 103pp.

Lambert, D.N.,Valent, P.J., Richardson, M.D. and Merrill, G.F., 1985. Spatial variability in selected geotechnical property measurements from three sedimentary provinces in the Venezuela basin. *Mar. Geol.* 68:107-123.

Landau, L.D. and Lifshitz, E., 1960. *Electrodynamics of continuous media*. Pergamon Press, New York.

Laughton, A.S., 1957. Sound propagation in compacted ocean sediments. *Geophysics* 22:233-260.

Larcombe, P., 1990. *The post-glacial evolution and present-day processes of the Mawddach Estuary*. PhD thesis, University College of North Wales, Bangor.

Lee II, H. and Swartz, R.C., 1980. Biological processes affecting the distribution of pollutants in marine sediments. In: *Contaminants and Sediments* (Baker, R.A., ed) Vol II. Science Publishers Ann Arbor, MI 555-605.

Leroy, S.D., 1981. Grain-size and moment measures: a new look at Karl Pearson's ideas on distributions. *J. Sed. Petrol.* 51(2):625-630.

Lovell, M.A and Ogden, P., 1983. Remote assessment of permeability/thermal diffusivity of consolidated clay sediments. Report to the European Atomic Energy Community. Brussels:EUR-Series, Report No. EN 9206.

Lovell, M.A., 1984. Thermal conductivity and permeability assessment by electrical resistivity measurements in marine sediments. *Marine Geotechnology* 6(2):205-240.

Mayer, L.M., Rahain, P.T., Guernin, W., Macko, S.A., Watling, L. and Anderson, F.E., 1985. Biological and granulometric controls on sedimentary organic matter of an intertidal mudflat. *Est. Coast. Shelf. Sci.* 20(4):491-503.

McCann C. and McCann, D.M. 1969. The attenuation of compressional waves in marine sediments. *Geophysics*, 24:882-892.

McCann C. and McCann, D.M. 1985. A theory of compressional wave attenuation in noncohesive sediments. *Geophysics* 50(8):1311-1317.

McCarter, W.J., 1984. Electrical resistivity characteristics of compacted clays. *Geotechnique* 34(2):263-267.

McDermott, I. (1991). A laboratory method to investigate shear waves in a soft soil consolidating under self weight. In: Hovem, J.M., Richardson, M.D. and Stoll, R.D., (eds), *Shear waves in marine sediments*, Kluwer Academic Publishers (in press).

Meadows, P.S. and Reid, A., 1966. The behaviour of *Corophium volutator*. *J. Zool. Soc. Lond.* 150:387-399.

Mendelsohn, K.S. and Cohen, M.H., 1982. The effect of grain anisotropy on the electrical properties of seidmentary rocks. *Geophysics* 47:257-263.

Moss, A.J., 1962. The physical nature of common sandy and shelly deposits, Part 1. *Am. Jou. Sci.* 260:337-373.

Moss, A.J., 1972. Bed load sediments. *Sedimentology* 18:159-219.

Myers, A.C., 1977. Sediment processing in a marine subtidal sandy bottom community. I. Physical aspects. *J. Mar. Res.* 35:609-632.

Nacci, V.A., Wang, M.C. and Gallagher, J., 1974. Influence of anisotropy and soil structure on elastic properties of sediments. In: *Physics of sound in Marine sediments,* (ed. L. Hampton), Plenum, New York, pp63-87.

Newell, R.C., 1965. The role of detritus in the nutrition of two marine deposit feeders, the prosobranch *Hydrobia ulvae* and the bivalve

Macoma balthica. *Proc. Zool. Soc. Lond.* 144:25-45.

Nolle A.W., Hoyer, W.A., Mifsud, J.F., Runyan, W.R. and Ward, M.A., 1963. Acoustic properties of water-filled sands. *J. Acoust. Soc. Am.* 35(9):1394-1408.

Nowell, A.R.M., Jumars, P.A. and Eckman, J.E., 1981. Effects of biological activity on the entrainment of marine sediments. *Marine Geology*, 42:133-153.

Officer, C.B. and Lynch, D.R., 1989. Bioturbation, sedimentation and sediment water exchanges. *Est. Coast. Shelf Sci.* 28(1-12).

Ogushwitz, P.R., 1984(a,b,c). Applicability of the Biot theory. Pts. I,II,III. *J.Acoust. Soc. Am.* 77(2):429-464.

Parasnis, D.S., 1972. *Principles of applied geophysics.* London, Chapman Hall, 214pp.

Partheniades, E., 1965. Erosion and deposition of cohesive soils. *J Hydraul. Div.* ASCE 91(HY1):105-139.

Paterson, D.M., (1989). Short term changes in the erodibility of intertidal cohesive sediments related to the migratory behaviour of epicyclic diatoms. *Limnol. Oceanogr.* 34(1):223-234.

Patnode, H.W. and Wyllie, M.R.J., 1950. The presence of conductive solids in reservoir rocks as a factor in electric log interpretation. *J. Pet. Technol.* 189:47-52.

Pettijohn, F.J. and Potter, P.E., 1964. *Atlas and glossary of primary sedimentary structures.* Berlin-Gottingen-Heidelberg-New-York: Springer. 370pp.

Pfannkuch, H.O., 1969. On the correlation of electrical conductivity properties of porous systems with viscous flow transport coefficients. Paper presented at the 1st International Symposium on the Fundamentals of transport phenomena in porous media. *Int. Assoc. Hydraul. Res.*, Haifa.

Pilbeam, C.C. and Vaisnys, J.R., 1973. Acoustic velocities and energy losses in granular aggregates. *J. Geophys. Res.* 78(5):810-824.

Prior, W.A.J., 1985. GHOST-80 User manual, Release 7, UKAEA: CLM R241, HM Stationery Office.

Raffaelli, D. and Milne, H., 1987. An experimental investigation of the effects of shorebird and flatfish predation on estuarine invertebrates. *Est.Coast.Shelf.Sci.* 24:1-13.

Reichardt, W., 1988. Impact of bioturbation by *Arenicola marina* on microbiological parameters in intertidal sediments. *Mar. Ecol. Prog. ser.* 44:149-158.

Reineck, H.E., 1961. Sediment bewengungen an kleinrippelin im watt. *Senckenbergiana Bd.*,42(1/2):51-67.

Reineck, H.E. and Singh, I.B., 1975. *Depositional Sedimentary Environments*. Springer-Verlag, New York.

Rhoads, D.C., 1967. Biogenic reworking of intertidal and subtidal sediments in Barnstable Harbor and Buzzards Bay, Massachusetts. *J. Geology* 75:461-476.

Rhoads, D.C., 1974. Organism-sediment relations on the muddy sea floor. *Oceanogr. Mar. Biol. Ann. Rev.* 12:263-300.

Rhoads, D.C. and Boyer, L.F., 1982. Effects of Marine Benthos on physical properties of sediments. A successional perspective. In: *Animal Sediment relations* (P.L. McCall and M.J.S. Tevesz, eds.) Plenum Publishing Corporation.

Rhoads, D.C. and Stanley, D.J., 1963. Biogenic graded bedding. *J. Sedim. Petrol.* 35:956-963.

Rhoads, D.C. and Young, D.K., 1970. The influence of deposit feeding organisms on sediment stability and community trophic structure. *J. Mar. Res.* 28(2):150-177.

Rhoads, D.C., Yingst, J.Y. and Ullman, W. 1978. Seafloor stability in Central Long Island Sound. Part I. Temporal changes in erodibility of fine-grained sediment. In: *Estuarine Interactions*, (M.L. Wiley, ed.), Academic Press, New York, pp221-244.

Rice, A.L. and Chapman, C.J., 1971. Observations on the burrows and burrowing behaviour of two mud-dwelling decapod crustaceans, *Nephrops norvegicus* and *Goneplax rhomboides*. *Mar. Biol.* 10:330-342.

Richards, A.F., 1962. Investigations of deep-sea sediment cores II. Mass physical properties. U.S. Navy Hydrographic Office Tech. Rep. 106.

Richards, A.F., 1964. Local sediment shear strength and water content variability on the continental slope off new England. *In: Mar. Geol.* Shepard Commemoration Volume, (ed. R.L. Miller) pp474-487, McMillan Co., N.Y.

Richards, A.F. and Parks, J.M., 1976. Marine geotechnology: average sediment properties, selected literature and review of consolidation, stability and bioturbation-geotechnical interactions in the benthic boundary layer. In: *The Benthic Boundary Layer*, (I N McCave, ed). Plenum Press, New York.

Richardson, M.D., 1983. The effects of bioturbation on sediment elastic properties. *Bull. Soc. Geol. Fr.* 25:505-513.

Richardson, M.D., 1985. Spatial variability of surficial shallow water sediment acoustic properties. In: *Ocean Seismo-Acoustics* (T.Akal and J. Berkson eds.), Plenum, New York.

Richardson, M.D., Briggs, K.B. and Young, D.K., 1985. Effects of biological activity by abyssal benthic macroinvertebrates on a sedimentary structure in the Venezuela Basin. *Marine Geol.* 68:243-267.

Richardson, M.D. and Young D.K., 1981. Geoacoustic models and bioturbation. *Mar. Geol.* 38:205-218.

Richardson, M.D., Young, D.K. and Briggs, K.B., 1983. Effects of hydrodynamic and biological processes on sediment geoacoustic properties in Long Island Sound, USA. *Marine Geol.* 52:210-226.

Rogers, J.J.W., 1959. Detection of lognormal size distributions in clastic sediments. *J. Sed. Petrol.* 29:402-407.

Rogers, J.J.W., 1965. Reproducibility and significance of measurements of of sediment distributions. *J. Sed. Petrol.* 45:722-732.

Rogers, J.J.W. and Head, W.B., 1961. Relationship between porosity, median size and sorting coefficients of a synthetic sand. *J. Sed. Petrol.* 13: 79-81.

Rowe, G.T., 1974. The effects of the benthic fauna on the physical properties of deep-sea sediments. In: *Deep sea sediments: Physical and Mechanical Properties* (A.L. Inderbitzen, ed.) pp381-400. Plenum Press, NY.

Ryan, T.A. Jr., 1981. MINITAB Reference manual.

Sachs, S.B. and Spiegler, K.W., 1964. Radiofrequency measurements of porous conductive plugs. *J. of Phys. Chem.* 68:1214-1222.

Schäfer, W., 1972. *Ecology and Paleoecology of Marine Environments* (I. Oertel and G.Y Craig, translators), University of Chicago Press, Chicago, Illinois.

Schlumberger, C., Schlumberger, M. and Leonardon, E.G., 1934. Electrical exploration of water-covered areas. *Transactions of the American Institute of Mining and Metallurgical Engineers*, Vol 110:122-134.

Schultheiss, P.J. 1981. Simultaneous measurements of P and S wave velocities during conventional laboratory soil testing procedures. *Marine Geotechnology* 4(4): 343-367.

Schultheiss, P.J., 1983. The influence of packing structure on seismic wave velocities in sediments. *UCNW Marine Geology Report* No. 83/1.

Scoffin, T.P., 1970. The trapping and binding of subtidal carbonate sediments by marine vegetation in Bimini Lagoon, Bahamas. *J Sedim. Petrol.* 40:249-273.

Scott, G.D., 1960. Packing of equal spheres. *Nature* 188:908-909.

Seilacher, A., 1953. Studien zur palichnologie, I. Uber die methoden der palichnologie. *Nues Jahrbuch der Geol Palaontol.*, 96:421-451.

Seed, H.B. and Idriss, I.M., 1970. *Soil moduli and damping factors for dynamic response analyses.* Report No. EEERC70-10, Earthquake Engineering Research Center, University of califomia, Berkely, C.A.

Sen, P.N., 1984. Grain shape effects on dielectric and electrical properties of rocks. *Geophysics* 49:586.

Sen, P.N., Scala, C. and Cohen, M.H., 1981. A self-similar model for sedimentary rocks with application to the dielectric constant of fused glass beads. *Geophysics* 46(5):781-795.

Shirley, D.J., 1978. An improved shear wave transducer. *J. Acoust. Soc. Am.* 63(5): 1643-1645.

Shirley, D.J., 1981. *Acoustical properties of sediments.* Annual Report (ARL-TR-81-20). Applied Research Laboratories, The University of Texas at Austin, Texas.

Shirley, D.J., and Anderson, A.L., 1975. Acoustic and engineering properties of sediments. *Technical Report* (ARL-TR-75-58), Acoustics Research Laboratory, University at Austin, Texas.

Shirley, D.J. and Bell, D.W., 1978. Acoustics of in-situ and laboratory sediments. *Technical Report* (ARL-TR-78-36), Acoustics Research Laboratory, University at Austin, Texas.

Shirley, D.J., and Hampton, L.D., 1978. Shear wave measurements in laboratory sediments. *J.Acoust. Soc. Am.* 63, 607-613.

Shirley, D.J., Bell, D.W. and Hovem, J.M., 1979. Laboratory and field studies of sediment acoustics. *Annual report* (ARL-TR-79-26), Acoustics Research Laboratory, University at Austin, Texas.

Siesser, W.G. and Roberts, J. 1971. An investigation of the suitability of four methods used in routine carbonate analyses of marine sediments. *Deep Sea Res.* 18:135-139.

Siever, R., Beck, K.C, and Berner R.A., 1965. Composition of interstitial waters of modern sediments. *Journal of Geology* 73:39-73.

Sills, G.C. and Thomas, R.C., 1984. Settlement and consolidation in the laboratory of steadily deposited sediment. *in: Seabed Mechanics* (ed. Bruce Denness), Graham and Trotman.

Silva, A.J. 1974. Marine Geomechanics: Overview and Projections. In: A.L.Inderbitzen (ed.), *Deep-Sea sediments: Physical and mechanical properties*. Plenum Press, N.Y. pp45-62.

Singer, J., 1982 Role of benthic organisms in sediment erosion and entrainment. *Antarctica J. U.S.* 17(5):118-119.

Sohn, H.Y. and Moreland, C., 1968. The effect of particle size distribution on packing density. *Can. J. Chem. Eng.* 46:162-167.

Sokal, R.R. and Rohlf, F.J., 1981. *Biometry*, 2nd edition. W.H Freeman & Co., San Fransisco.

Sokal, R.R. and Rohlf, F.J., 1969. *An introduction to biostatistics.* W.H. Freeman & Co., San Fransisco.

Stanley, D.J. and Swift, D.J.P. (eds.), 1976. *Marine Sediment Transport and Environmental Management.* John Wiley and Sons, New-York.

Statham, I., 1974. The relationship between porosity and angle of repose to mixture proportions in assemblages of different sized materials. *Sedimentology* 21:149-162.

Stephenson R.W. 1978. Ultrasonic testing for determining dynamic soil moduli. In : *Dynamic geotechnical testing*. ASTM STP 654, 179-195.

Stoll, R.D., 1974. Acoustic waves in saturated sediment. In: L. Hampton (ed.), *Physics of sound in marine sediments*, Plenum, New York, pp19-39.

Stoll, R.D., 1977. Acoustic waves in ocean sediments. *Geophysics* 42:715-725.

Stoll, R.D., 1980. Theoretical aspects of sound transmission in sediments. *J. Acoust. Soc. Am.* 68(5):1341-1350.

Stoll, R.D. and Bryan, G.M., 1970. Wave attenuation in saturated sediments. *J. Acoust. Soc. Am.* 47:1440-1447.

Straaten, L.M.J.U. Van, 1952. Biogene textures and the formation of shell beds in the Dutch Wadden Sea. *Proc. K. ned. Akad. Wet.* (B):500-516.

Swinbanks, D.D., 1981. Sediment reworking and the biogenic formation of clay laminae by *abarenicola pacifica*. *J. Sedim. Petrol.* 51:1137-1145.

Taghon, G.L., Nowell, A.R.M. and Jumars, P.A., 1984. Transport and breakdown of fecal pellets: biological and seidmentological consequences. *Limnol. Oceanog.* 29(1):64-72.

Tamaki, A., 1987. Comparison of resistivity to transport by wave action in several polychaete species on an intertidal sand flat. *Marine Environmental Progress Series* 37:181-189.

Taylor Smith, D., 1971. Acoustic and electric techniques for sea-floor sediment identification: In: *Proc. Int. Symp. on Engineering properties of Sea-Floor soils and their Geophysical Identification*, Seattle Washington, pp253-267.

Taylor Smith, D. 1975. Geophysical assessment of sea-floor sediment properties: In: *Oceanology Int. '75 Conference Papers*, Brighton, England, p.320-328.

Taylor Smith, D., 1985. Geotechnical characteristics of the sea bed related to seismo-acoustics. In: *Ocean Seismo-acoustics* (T. Akal and J. Berkson, eds), Plenum, New York.

Telford, W.M., Sheriff, R.E, Geldart, L.P. and Keys, D.A., 1976. *Applied Geophysics*. Cambridge Universities Press.

Thayer, C.W., 1979. Biological bulldozers and the evolution of marine benthic communities. *Science*, 203(2):458-461.

Trueman, E.R., 1968. The burrowing activities of bivalves. *Symp. Zool. Soc. Lond.* 22:167-186.

Twenhofel, W.H., 1932. *Treatise on Sedimentation*. 2nd. ed. Williams and Wilkins, U.S.

Urish, D.W., 1981. Electrical resistivity-hydraulic conductivity relationships in glacial outwash aquifers. *Water Resources Research*. 17(5):1401-1408.

Valent, P.J., 1974. Deep sea foundation and anchor engineering. In: A.L.Inderbitzen (ed.), *Deep-Sea sediments: physical and mechanical properties*. Plenum Press, N.Y. pp245-269.

Visher, G.S., 1969. Grain-size distributions and depositional processes. *J. Sed. Petrol*. 39:1074-1106.

Viskne, A. 1976. Evaluation of in-situ shear-wave velocity measurement techniques. *Engineering and Research Centre Report*, REC-ERC-76-6, Bureau of Reclamation, Denver, Colorado, 40pp.

Wakeman, R.J., 1975. Packing density of particles with log-normal size distributions. *Powder Technol*. 11:297-299.

Webb, J.E. and Theodor, J. 1968. Irrigation of submerged marine sands through wave action. *Nature. Lond*. 220:682.

Webb, J.E. 1969. Biologically significant properties of submerged marine sands. *Proc. Roy. Soc. Lond. B*. 174:355-402.

Webb, J.E., Djorges, D.J., Gray, J.S., Hessler, R.R, van Andel, Tj. H., Werner, F., Wolff, T., Zijlstra, J.J. and Rhoads, D.C 1976. Organism-sediment relationships (Working Group Reports-Group E) In: *The Benthic Boundary Layer* (I.N McCave, ed.) pp.273-295. Plenum Press, New York.

Wells, G.P., 1945. The mode of life of *Arenicola marina*. *J. Mar. Biol. Ass. U.K*. 26:170-207.

Wells, G.P., 1969. Mechanisms of movement in worms. *Proc. Challenger Soc.* 4:36-50.

Whitlatch, R.B., 1981. Animal-sediment relationships in intertidal marine benthic habitats: some determinants of deposit feeding species diversity. *J. Exp. Mar. Biol. Ecol*. 53:31-45.

Wheeler, S.J., 1986. *The Stress-strain behaviour of Soils containing gas bubbles*. D Phil thesis, Oxford University.

Whitmarsh, R.B and Lilwall, R.C., 1982. A new method for determination of *in-situ* shear wave velocity in deep-sea sediments, *Oceanology International* '82, 4.2:21.

Williams, C.E., 1970. In-situ Formation Factor measurements at the water-sediment interface. *In*: Interocean 1970, vol. 2, Dusseldorf, VDI Verlag, 87-88.

Windle, D. and Wroth, C.P., 1975. Electrical resistivity method for determining volume changes that occur during a pressuremeter test: *Proc. Specialty conf. on In-situ Measurement of Soil Properies, Am.*

Soc. Civil Engnrs., Raleigh N.C., June 1-4, p.497-510.

Winsauer, W.O., Shearin, H.M., Masson, P.H. and Williams, M., 1952. Resistivity of brine saturated sands in relation to pore geometry. *Bull. Am. Assoc. Pet. Geol.* 6:213-228.

Winston, J.E. and Anderson, F.E., 1971. Bioturbation of sediments in a Northern temperate estuary. *Mar. Geol.* 10:39-49.

Wolff, W.J., 1973. *The estuary as a habitat. An analysis of data on the soft-bottom macrofauna of the estuarine area of the rivers Rhine, Meuse and Scheldt.* Comm. No. 106 of the Delta Institute for Hydrobiological Research, Leiden.

Wood, A.B., 1930. *A textbook of sound.* 3rd. ed. McGraw-Hill.

Wright, L.D., 1987. Spatial variability of bottom types in the inner lower Chesapeake Bay and adjoining estuaries and inner shelf. *Est. Coast. Shelf Sci.* 24(6):765-784.

Wu, S., Gray, D.H. and Richart, F.E., 1984. Capillary effects on dynamic modulus of sands and silts. *J. Geotech. Eng.* ASCE, 110(9):1188-1203.

Wyllie, M.R.J. and Gregory, G.R., 1953. Formation Factors of unconsolidated porous media: Influence of particle shape and effects of cementation. *Petrol. Trans. AIME* 198:103-110.

Yerazumis, S., Bartlett, J.W. and Nissan, A.H., 1962. Packing of binary mixtures of spheres and irregular particles. *Nature,* 195: 33-35.

Yingst, J.Y. and Rhoads, D.C., 1978. Sea floor stability in central Long Island Sound. Part II. Biological interactions and their potential importance for seafloor erodibility. In: *Estuarine Interactions,* (M.L. Wiley, ed.), Academic Press, New York, pp245-260.

Yingst J.Y. and Rhoads, D.C., 1980. The role of bioturbation in the enhancement of bacterial growth rates in marine sediments. In: *Marine Benthic Dynamics* (B.C. Coull, eds.), University od South Carolina Press, pp407-421

Young, D.K., 1971. Effects of infauna on the sediment and seston of a subtidal environment. *Vie et Milieu (Suppl.)* 22:557-571.

Young, R.A. and Southard, J.B., 1978. Erosion of fine-grained marin sediments: Sea-floor and laboratory experiments. *Geol. Soc. Am. Bull.* 89:663-672.

APPENDIX A.

ALL *IN SITU* INTERTIDAL SAMPLING: PROCEDURAL SUMMARY AND GENERAL REFERENCE TABLES.

This appendix contains a summary of experimental procedures adopted during intertidal sampling, which have been described in detail in Section 5.1.1.

Tables intended for supplementary reference to Section 5.4.4 have also been resented. This includes tables of the degree of observed medium-scale spatial and temporal variability at individual locations, contrasted with overall and mean small-scale spatial variability.

Finally, the results of statistical analysis for the full data set obtained by combining all locations except the Tamar mud-flats have been presented according to the format described in Appendix B.

Table A1.1. Summary of procedures adopted for *in situ* intertidal sampling, as detailed in Section 5.1.2. Numbers in brackets denote within-site replicates.

LOCATION:	LLANDD-WYN	TAF	LLIGWY	RED WHARF	FREATHY	TAMAR	CEFNI
Sampling dates	1985 2/6 4/7-19/7	1985 15/11 16/11	1986 1/5 2/5	1986 6/5	1986 11/7	1986 July 7,8,10	Jan 87-Jan 88.
Site selection	Organism density	Transect [5m] [10m]	Org. Den. T [5m]	Transect [5m]	Ebb-tide level	Ebb-tide level	5 Sites sampled monthly
Site area	1 m^2	0.25 m^2	0.25 m^2	0.25 m^2	0.25 m^2	0.25 m^2	1 m^2
Porosity	-	(2)	(2)	(2)	(2)	(2)	(3)
Grain-size technique	(1): Sieve	(1): Sieve	(1): Sieve	(1): Sieve	(2): Sieve	(1):Fall Tower/ pipette	(1): Sieve
Fines	(-)	(-)	(-) (2)	(-)	(-)	(1)	(1)
Carbonate	(1)	(2)	(2)	(2)	(2)	(-)	(1)
Organics	(1): H_2O_2	(-)	(-)	(-)	(-)	(1): H_2O_2	(4): ignition loss
V_s: Range (mm)	80-150 50-200	50-125	50-125	50-125	50-125	50-125	50-125
Interval (mm)	70 50	25	25	25	25	25	25
	(6) (6)	(2)	(2)	(2)	(2)	(2)	(4)
R_s	(4)	(6)	(6)	(6)	(6)	(6)	(12)
R_w	Seawater R_s probe *in situ*	R_s probe *in situ*	S-T bridge *in situ*	S-T bridge *in situ*	Seawater R_s probe *in situ*	*in situ* thermo-meter/ S-T bridge in lab	*in situ* thermo-meter/ S-T bridge in lab.

Table A1.2. Summary of observed medium-scale spatial variability in sands. (Percentage coefficients of within-location variation).

Parameter	LLAN-DDWYN	TAF		LLIGWY		RED WHARF	FREATHY	COMBINED AVERAGE
		T/8	T/11	(A)	(B)			
Mode grain size	3.3	2.8	1.5	2.0	3.9	2.1	2.2	2.5
Mean grain size	9.1	1.2	1.1	1.9	6.0	11	5.7	5
Porosity	-	4.7	2.6	2.2	1.5	2.8	1.0	4
FF	11	21	7.3	2.7	3.4	11	5.2	14
Bulk V_s	9	10	13	6.5	9.1	8.4	2.5	9
Surface V_s				3.9	5.0	9.0	1.9	10
Carbonate content	25	12	5	12	17	27	6	22
Fines content	-	-	28	-	-	-	-	51
Coarse fraction	85	-	-	86	67	35	-	55
Biological parameters	100	-	100	100	100	100	-	100

Table A1.3. Coefficients of variation over varying spatial and temporal scales.

PARAMETER	SPATIAL			TEMPORAL
	SMALL SCALE	MEDIUM SCALE	LARGE SCALE	SEASONAL
Mode grain size	-	2.5	14.5	1.8
Mean grain size	-	4.8	16.5	1.5
Sorting	-	39.5	47.6	7.6
Skewness	-	76.0	99.5	27.5
% Carbonate	-	22.2	68.0	8.2
% Fines	-	51.0	100.0	31.8
Porosity	-	3.8	6.7	4.0
FF	5.3	14.3	15.3	13.4
Surface V_s	7.4	8.7	20.6	9.6
Bulk V_s	7.7	10.2	16.1	10.0

Table A1.4. Significant correlation coefficients for all *in situ* sandy sediments. [r_{crit} = 0.264]

PARAMETERS		Correlation coefficient: Product Moments	Ranked
TEXTURAL INTERRELATIONSHIPS			
Grain size mean:	Grain size mode	0.941	0.889
	Fines content	0.429	0.338
Sorting:	Grain size mean	-0.556	-0.705
Skewness:	Sorting	-0.804	-0.732
	Fines	0.337	0.301
TEXTURAL-BIOLOGICAL INTERRELATIONSHIPS			
Corophium:	Fines	0.639	0.814
Arenicola:	Carbonate	-0.340	-0.593

Table A1.5. Significant controls of porosity and the geophysical properties.

	Mean	Sort.	Skewn.	% Carb.	% Fines	*Arenicola*	*Lanice*	$\%R^2$
POROSITY	[+]	[-]	[+]	[+]	[+]			38 15 R 31 20 11
	[+]			[+]				67
	Porosity							
FF	[-]	[+]	[-]	[+]		[-]		11 9 11 16 R 22
	[-]					[-]		37
	[-]			[+]	[+]			32
	[-]			[+]	[+]	[-]		43
		Coroph	Mode					
BULK V_s		[-]	[-]		[-]	[-]	[+]	21 8 10 17 24
					[-]	[-]		39
			[-]		[-]	[-]		43
Surface V_s		[-]		[+]				12
					[-]	[-]	[+]	13 15
					[-]			40
					[-]	[-]		58
	[-]			[+] [+]	[-] [-]	[-] [-]	[+]	61 67
					[-]	[-]		70
CV (FF)					[+]			7
V_s^R				[+]	[-]			10 14

APPENDIX B.

LOCAL SPATIAL VARIABILITY AND CONTROLS OF GEOPHYSICAL PROPERTIES: REFERENCE TABLES AND FIGURES.

This appendix is intended as supplementary reference for the experiments described in Section 5.2. Tables of location mean values (with associated percentage coefficients of variation) for selected textural, biological and geophysical parameters have been compiled. The following key applies for all these tables:

Symbols:

n = number of sites sampled, CV = coefficient of variation.

var. = within-site percentage coefficient of variation.

* = significant difference between zones

Units:

Textural parameters in phi units,

Size fractions as weight percentages.

Velocities in m/s.

Organism densities in numbers per square metre.

Where data was collected along transects, graphical representation of spatial distribution has also been included, in order to illustrate trends or other systematic spatial variation. Site means, with error bars corresponding to the within-site standard deviation (where replicates were taken) have been plotted as a function of distance along the transect.

For each location, significant correlations among textural and biological parameters have been listed. The critical correlation coefficient corresponds to that at $(5/(1/2n(n-1))\%$, where n is the number of variables. This ensures 95% confidence that correlations are significant (Section 5.1.5). Where distributions were not normal, or where the ranked

correlation coefficient was much more significant than the product moments coefficient, the ranked value has been tabulated, denoted by the suffix R.

Porosity and the geophysical properties were also tested for correlation with textural and biological parameters. However, since these properties were expected to be dependent on textural and biological predictors, it is more rigorously correct to perform regression analysis (although the mathematical procedures involved are identical). Significant apparent dependence on single predictors, obtained from linear regression or from ranked correlation, has been tabulated with the multiple linear regression results, which involve a linear combination of predictors. Results have been summarised using the percentage coefficient of determination (R^2), obtained from linear regression or from the square of the correlation coefficient, and the sign of the implied relationship, i.e [-] indicating inverse control, [+] indicating direct control. In some cases, several possible combinations yielded significant results, interpretation being hampered by interaction between variables.

CONTENTS.

B1. Traeth Llanddwyn (Section 5.2.1)
B2. Taf Estuary (Section 5.2.2)
B3. Traeth Lligwy (Section 5.2.3)
B4. Red Wharf Bay (Section 5.2.4)
B5. Freathy Sands (Section 5.2.5)
B6. Tamar Estuary (Section 5.2.6)

TRAETH LLANDDWYN (SECTION 5.2.1)

Table B1.1. Pore fluid resistances (seawater).

SAMPLING DAY (1986)	R_w (*in situ*) (Ω)	Estimated Temp. (^{0}C) for Sal. = 32.5^0/00
June 2	0.390	14
July 4	0.372	16
July 8	0.376	15
July 19	0.356	18

Table B1.2. Location means of measured parameters.
(Data from different sampling days have been combined)

	OVERALL		*Arenicola* Zone			*Lanice* Zone		
PARAMETER	MEAN	CV(%)	n	MEAN	CV(%)	n	MEAN	CV(%)
Mode grain size	2.670	3.3	8	2.694	3.2	12	2.654	3.4
Mean grain size*	2.549	9.1	8	2.330	10.0	12	2.695	1.2
Folk sorting *	0.497	75	8	0.894	28	12	0.232	31
% Carbonate *	7.3	25	8	9.2	14	12	6.0	10
% > 2phi *	10.2	85	8	19.8	21	12	3.8	60
Arenicola *	3	100	8	6	72	12	0	-
Lanice *	64	100	8	0	-	12	106	90
FF *	4.5	11	8	4.8	12	12	4.2	6.2
(var.FF)	3.8	-	8	5.4	-	12	2.8	-
Bulk V_s	59.8	8.9	8	60.5	8.0	12	59.2	9.7
(var.V_s)	9.5	-	8	9.5	-	12	9.3	-

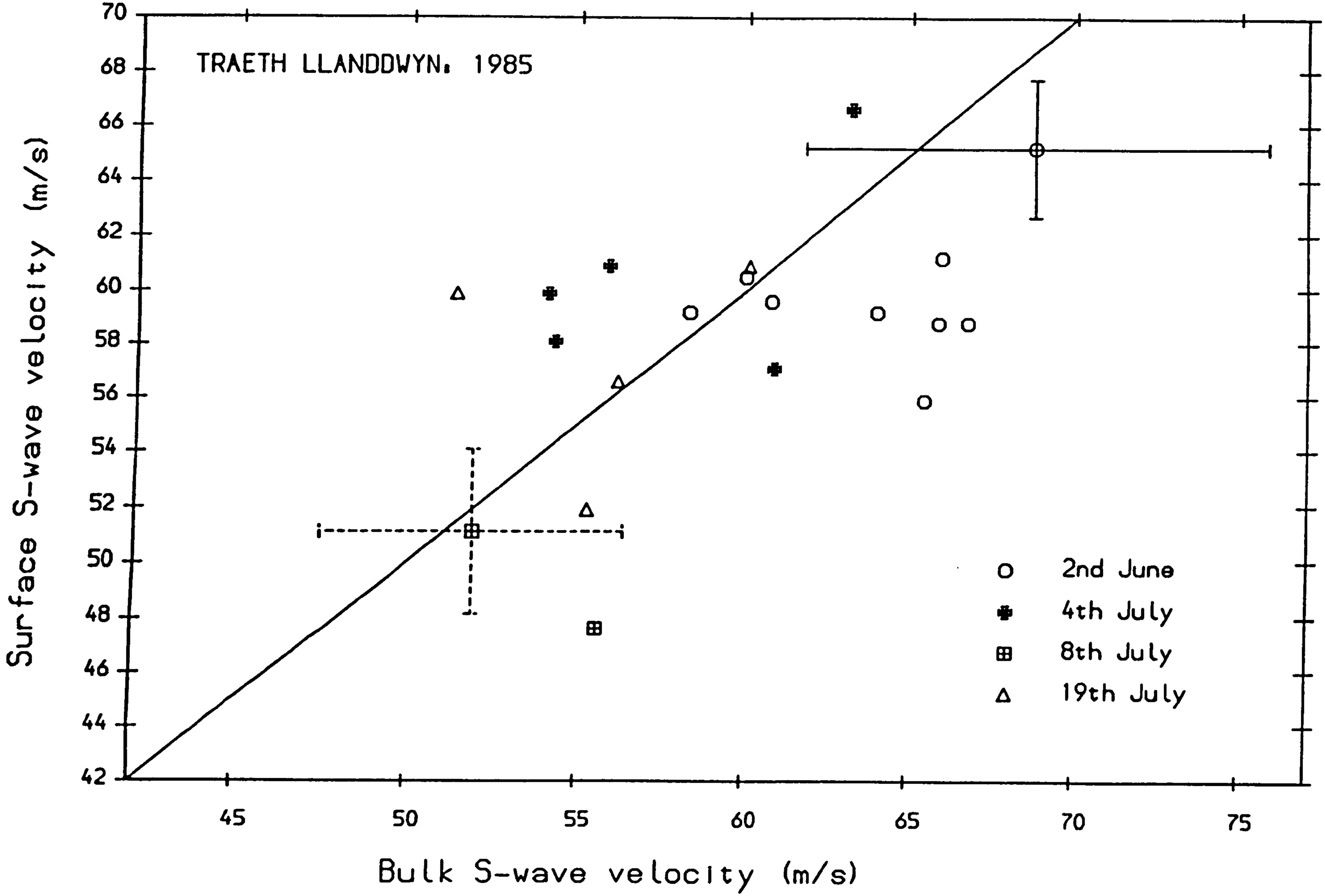

Fig. B1.1. Comparison of bulk and surface V_S. Straight line has slope 1.

TRAETH LLANDDWYN (SECTION 5.2.1)

Table B1.3. Correlations among textural and biological characteristics.

Parameters	All data [r^c = 0.561]	*Lanice* Zone [r^c = 0.684]	*Arenicola* Zone [r^c = 0.798]
TEXTURAL INTERRELATIONSHIPS.			
% Carb. : % > 2 phi	0.941	0.799	0.810
BIOLOGICAL / TEXTURAL INTERRELATIONSHIPS.			
Lanice : *Arenicola*	-0.687^R	-	-
: % Carb.	-0.662^R	-0.722	-
: % > 2phi	-0.623^R	-	-
Arenicola : % Carb.	0.794^R	-	-
: % > 2phi	0.684^R	-	-

Table B1.4. Apparent controls of geophysical properties.

MULTIPLE LINEAR REGRESSIONS.					
FORMATION FACTOR					
	% > 2 phi	% Carb.	*Lanice*	*Arenicola*	$\%R^2$
ALL DATA	[+]				42
		[+]			26
			[-]		28
	[+]			[-]	69
	[+]		[-]	[-]	74
Lanice Zone	[+]				66
		[+]			66
			[-]		67
Arenicola Zone	[+]			[-]	63
				[-]	83
Bulk V_s					
	% > 2 phi	% Carb.	*Lanice*	*Arenicola*	$\%R^2$
ALL DATA	[+]		[+]		56
		[+]	[+]		45
Lanice Zone			[+]		84
		[-]			49
Arenicola Zone					

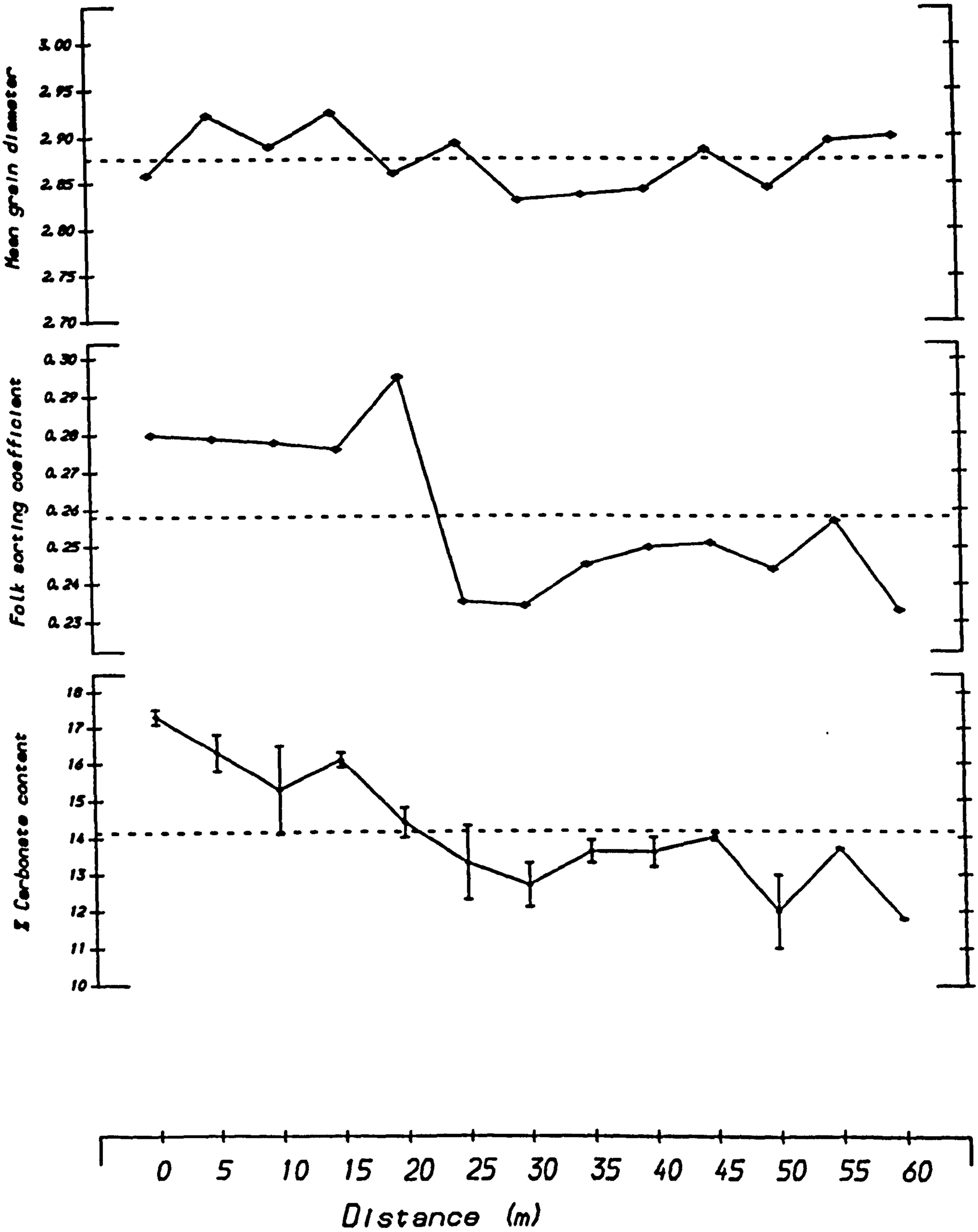

Fig. B2.1. Taf Estuary, Transect T/8.
Spatial variation of textural parameters.

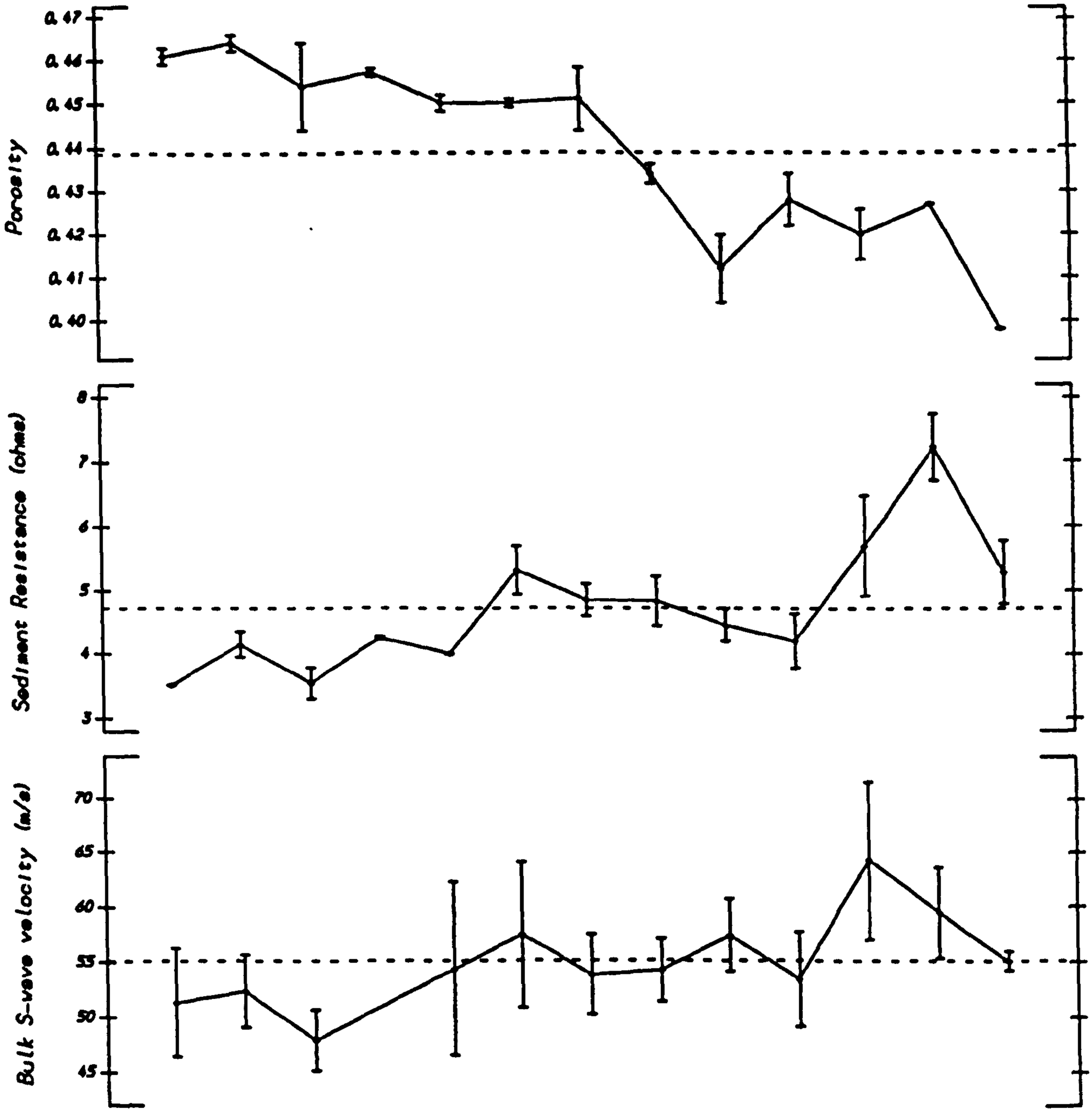

Fig. B2.2. Taf Estuary, Transect T/8.
Spatial variation of geophysical parameters.

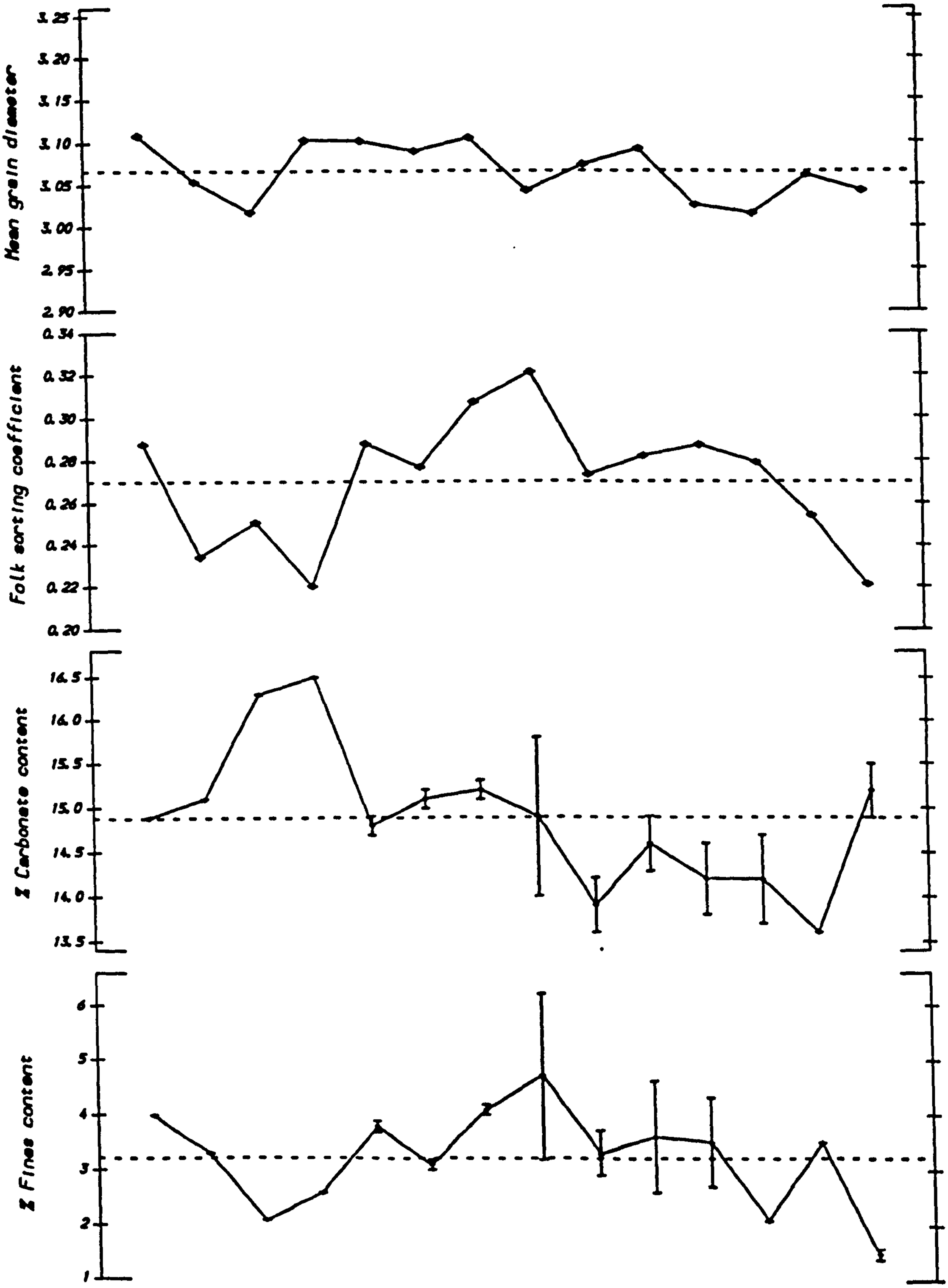

Fig. B2.3. Taf Estuary, Transect T/11.
Spatial variation of textural parameters.

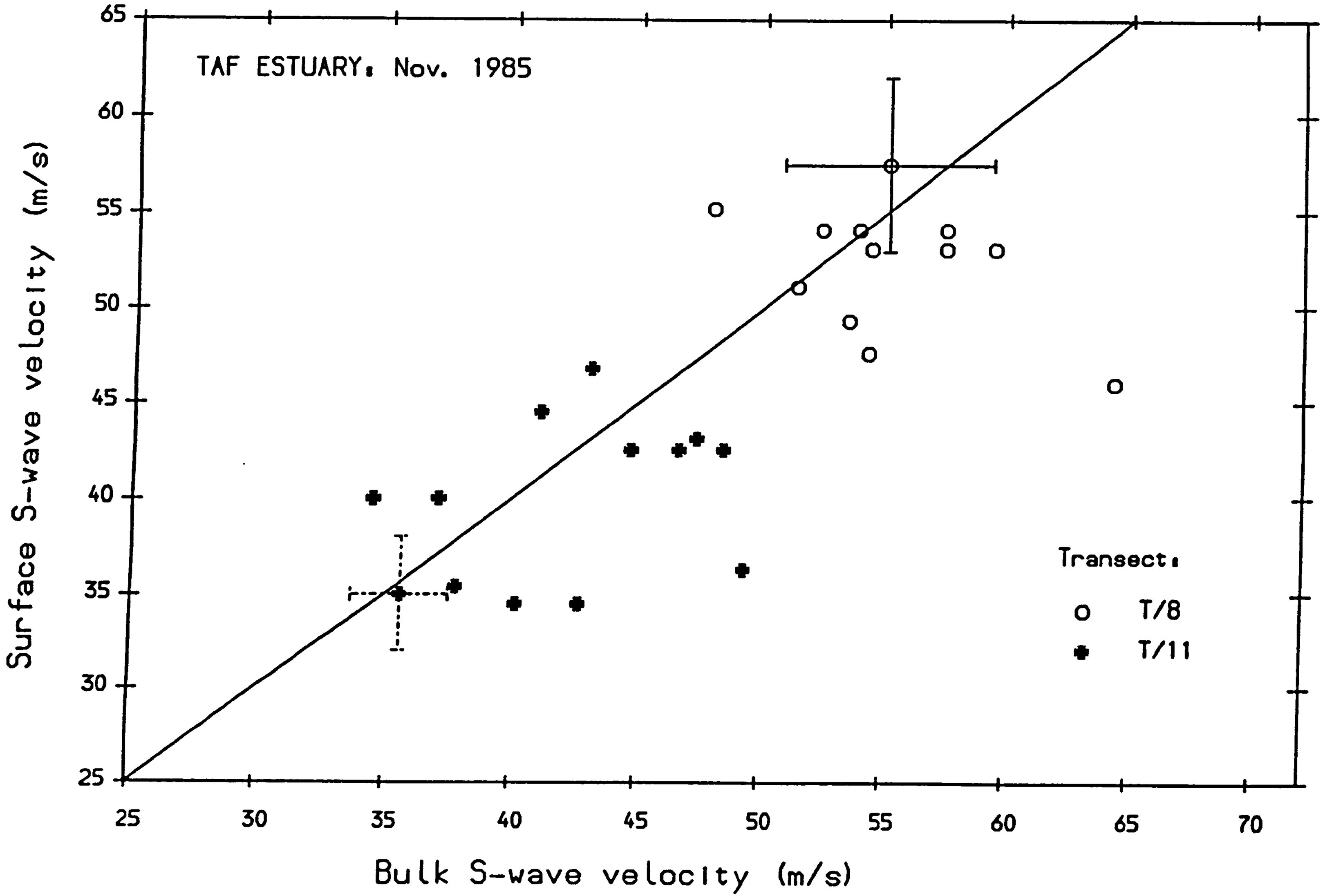

Fig. B2.5. Comparison of bulk and surface V_s. Straight line has slope 1.

TAF ESTUARY (SECTION 5.2.2)

Table B2.1. Pore fluid resistances.

LOCATION	SAMPLING POSITION	R_w (*in situ*) (Ω)
TRANSECT T/8	0m	2.18
	35m	2.20
TRANSECT T/11	0m	2.83
	60m	2.85
	130m	2.99

Table B2.2. Location means of measured parameters.

		OVERALL		TRANSECT T/8			TRANSECT T/11		
PARAMETER		MEAN	CV(%)	n	MEAN	CV(%)	n	MEAN	CV(%)
Mode grain size*		2.965	4.0	13	2.885	2.8	14	3.039	1.5
Mean grain size*		2.975	3.4	13	2.876	1.2	14	3.067	1.1
Folk sorting		0.264	10	13	0.258	8	14	0.270	11
% Carbonate		14.5	9	13	14.2	12	14	14.9	5.4
% Fines	*	1.7	100	13	0	-	14	3.2	28
Corophium	*	2056	100	13	0	-	14	3964	100
Porosity	*	0.454	4.9	13	0.439	4.7	14	0.468	2.6
R_s	*	-	-	13	4.7	21	14	3.8	7.3
R_s (var.R_s)		5.8	-	13	6.6	-	14	5.2	-
Bulk V_s	*	47.9	17	13	55.2	9.5	14	41.6	13
($var.V_s$)		6.1	-	13	7.5	-	14	4.7	-

Table B2.3. Correlations among site characteristics.

Parameters	All data [r^c = 0.479]	Transect T/8 [r^c = 0.684]	Transect T/11 [r^c = 0.661]
(NO TEXTURAL INTERRELATIONSHIPS)			
BIOLOGICAL / TEXTURAL INTERRELATIONSHIPS			
Corophium : % Fines	-0.668^R	-	-
GEOPHYSICAL INTERRELATIONSHIPS			
Bulk V_s : Sed. Res.	N/A	0.844^R	0.744

TAF ESTUARY (SECTION 5.2.2)

Table B2.4. Apparent controls of porosity and geophysical properties.

MULTIPLE LINEAR REGRESSIONS.

POROSITY

	% Carb.		% Fines	*Corophium*	$\%R^2$
TRANSECT T/8	[+]				54
TRANSECT T/11					
ALL DATA	[+] [+]		 [+] [+]	[+]	35 29^R 48 69

SEDIMENT RESISTANCE

	% Carb.	Porosity	% Fines	*Corophium*	$\%R^2$
TRANSECT T/8	[-]				33
TRANSECT T/11			 [-]	[-] [-]	40 63

BULK V_s

	% Carb.	Porosity	% Fines	*Corophium*	$\%R^2$
TRANSECT T/8	[-]	 [-]			35 27^R
TRANSECT T/11	 [-]	 [-]		[-] [-]	59 39 70
ALL DATA	[-] [-] [-]	[-] [-] [-]	 [-] [-] [-]	 [-] [-] [-]	33 53 59 53 75 79 83 82

TRAETH LLIGWY (SECTION 5.2.3)

Table B3.1. Pore-fluid salinity, temperature and Electrical Resistance.

LLIGWY (A)				
TIME	SITE	TEMPERATURE (^{0}C)	SALINITY (^{0}/00)	R_w (Ω)
18:00	-	14.1	29.9	0.436
21:00	-	12.2	29.8	0.458
LLIGWY (B)				
TIME	SITE	TEMPERATURE (^{0}C)	SALINITY (^{0}/00)	R_w (Ω)
9:00	0m	11.0	34.4	0.414
10:00	4m	11.1	34.7	0.412
11:00	20m	13.1	32.2	0.418
11:30	22m	13.6	32.5	0.416

Table B3.2. Location means of measured parameters.

	OVERALL		LLIGWY (A)			LLIGWY (B)		
PARAMETER	MEAN	CV(%)	n	MEAN	CV(%)	n	MEAN	CV(%)
Mode grain size*	1.845	3.7	9	1.889	2.0	11	1.809	3.9
Mean grain size*	1.762	6.1	9	1.842	1.9	11	1.696	6.0
Folk sorting *	0.459	32	9	0.406	29	11	0.503	31
% Carbonate	6.3	15	9	6.7	12	11	5.9	17
% 0:1.25phi *	9.7	34	9	7.1	8	11	11.8	26
% > 0 phi	2.9	76	9	2.1	86	11	3.6	67
Arenicola	3	100	9	3	100	11	3	100
Porosity	0.380	2.0	9	0.383	2.2	11	0.376	1.5
FF *	4.846	3.6	9	5.0	2.7	11	4.8	3.4
(var.)	3.0	-	9	2.5	-	11	3.4	-
Bulk V_s	55.4	7.7	9	54.6	6.5	11	56.6	9
(var.)	4.7	-	9	4.5	-	11	4.8	-
Surface V_s *	50.7	5	9	51.6	3.9	11	49.2	5.0
(var.)	4.6	-	9	5.1	-	11	4.1	-

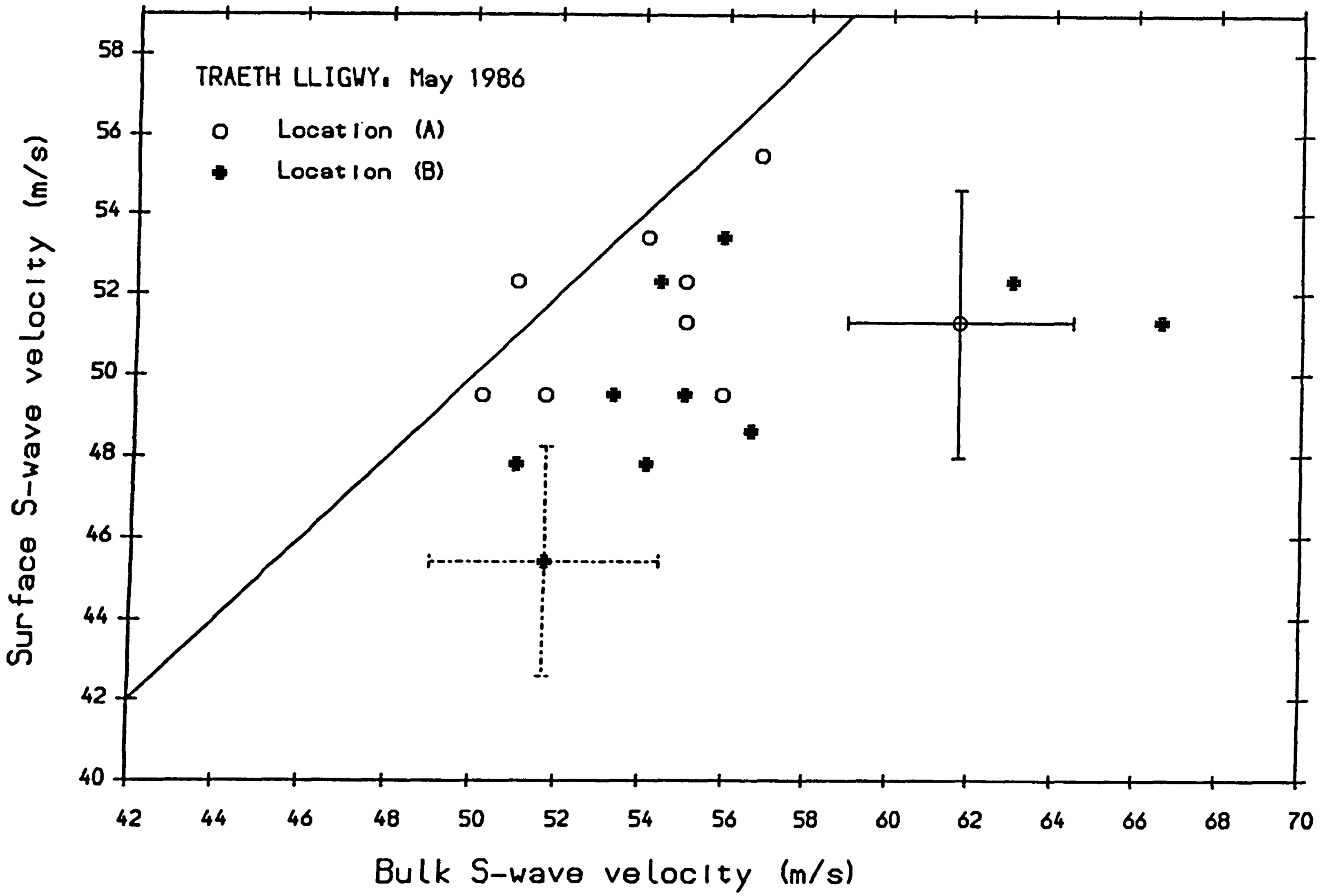

Fig. B3.1. Comparison of bulk and surface V_s. Straight line has slope 1.

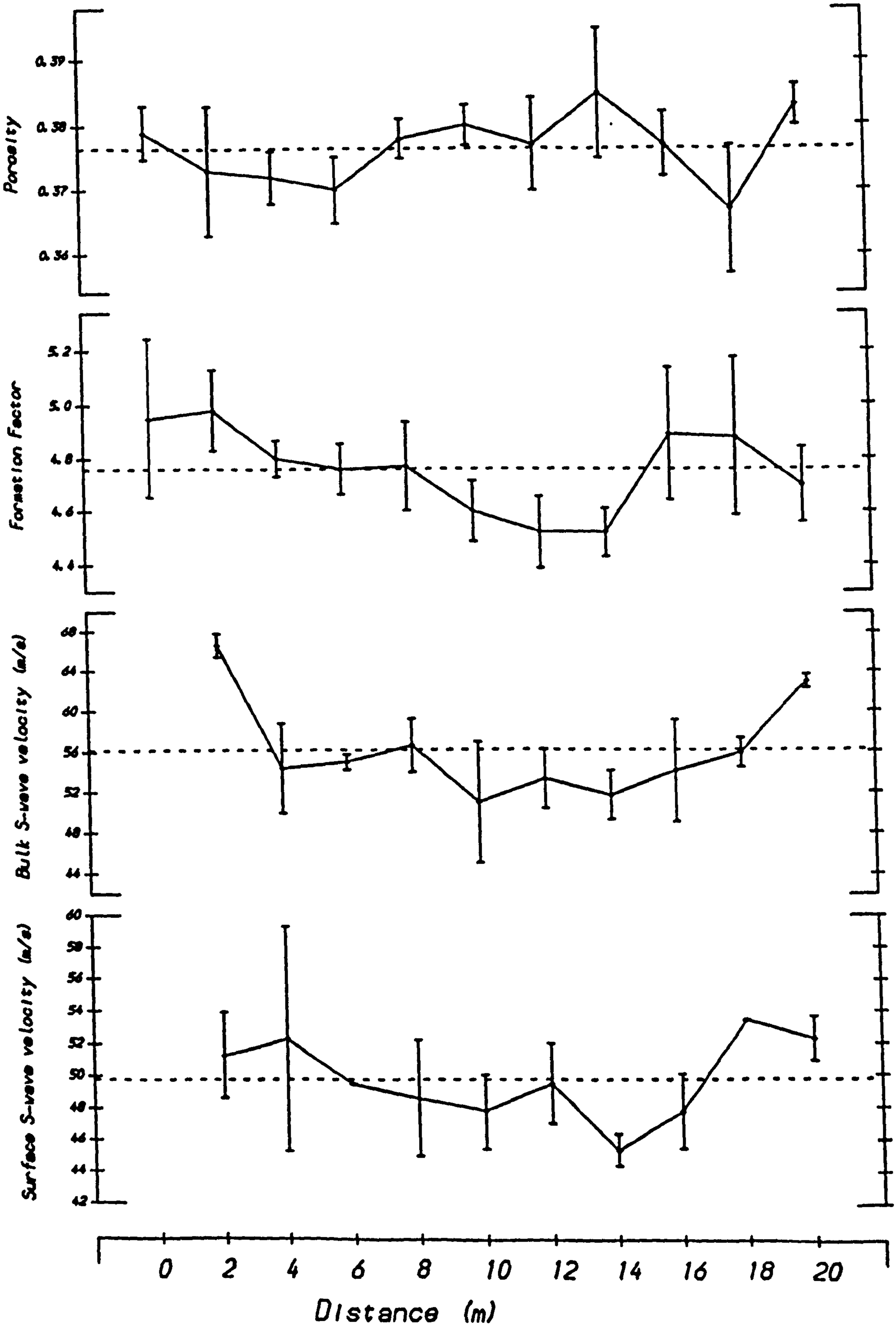

Fig. B3.2. Traeth Lligwy, Location (B).
Spatial variation of geophysical parameters.

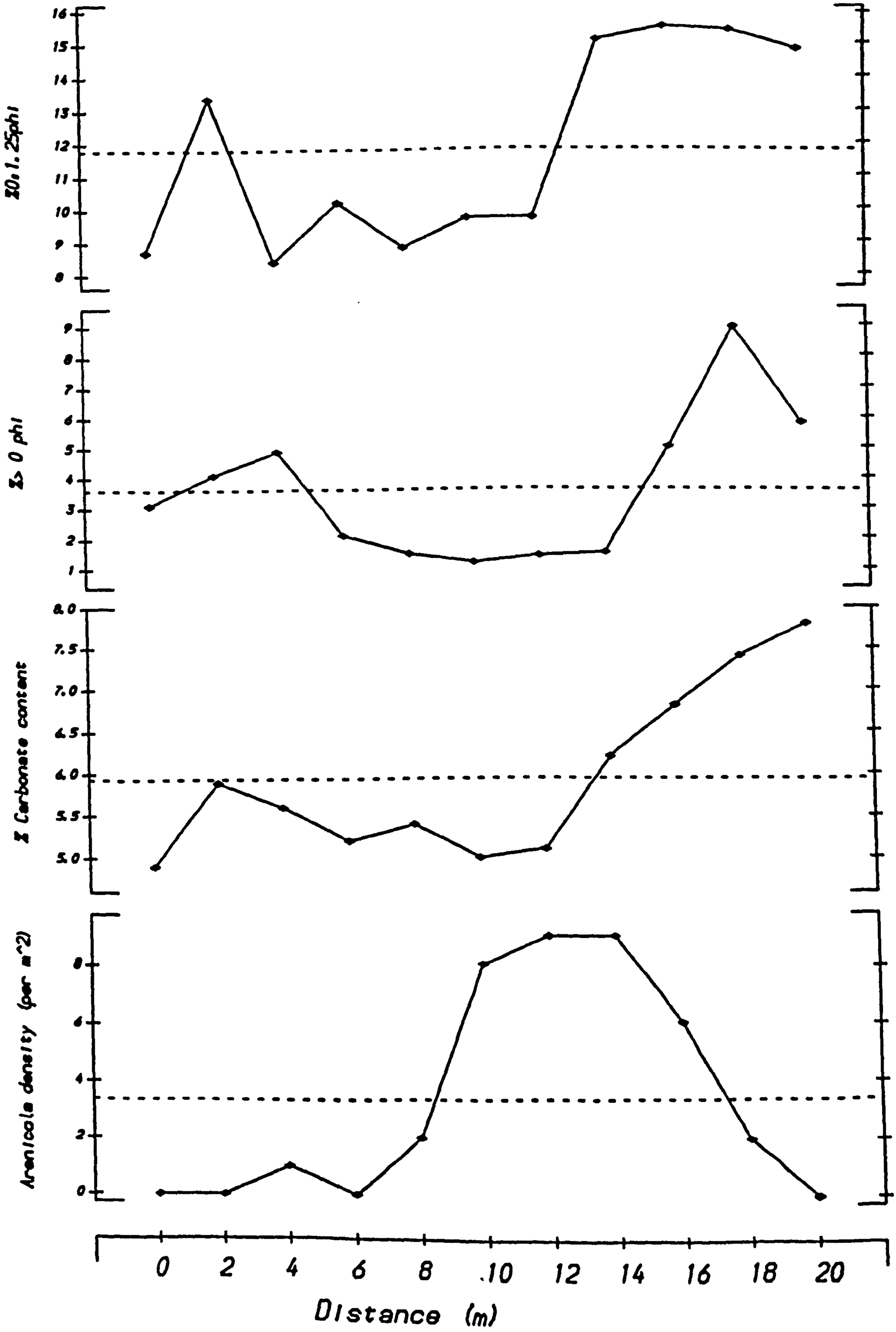

Fig. B3.3. Traeth Lligwy, Location (B).
Spatial variation of textural and biological parameters.

TRAETH LLIGWY (SECTION 5.2.3)

Table B3.3. Correlations among textural and biological characteristics.

Parameters	ALL DATA [r^c = 0.537]	LLIGWY (A) [r^c = 0.735]	LLIGWY(B) [r^c = 0.684]
TEXTURAL INTERRELATIONSHIPS.			
% Carb. : % > 0 phi	-	-	0.789
% 0:1.25phi	-	-	0.854
% > 1.25phi	-	-	0.930
BIOLOGICAL / TEXTURAL INTERRELATIONSHIPS			
Arenicola : % Carb.	-	-0.767	-
: % > 0 phi	-	-0.743^R	-

Table B3.4. Apparent controls of porosity and geophysical properties.

MULTIPLE LINEAR REGRESSIONS.

POROSITY

	%0:1.25phi	% > 0 phi	% Carb.	*Arenicola*	$\%R^2$
LLIGWY (B)		[-]	[+]		52
ALL DATA		[-]	[+]		42

FORMATION FACTOR

	%0:1.25phi	% > 0 phi	% Carb.	*Arenicola*	$\%R^2$
LLIGWY (B)				[-]	49

BULK V_s

	%0:1.25phi	% > 0 phi	% Carb.	*Arenicola*	$\%R^2$
LLIGWY (B)				[-]	43

SURFACE V_s

	%0:1.25phi	% > 0 phi	% Carb.	*Arenicola*	$\%R^2$
LLIGWY (B)		[+]			52
				[-]	46
	[-]	[+]			76
		[+]		[-]	65
ALL DATA				[-]	38
	[-]	[+]			43

RED WHARF BAY (SECTION 5.2.4)

Table B4.1. Pore-fluid salinity, temperature and Electrical Resistance.

RED WHARF BAY				
TIME	SITE	TEMPERATURE (^{0}C)	SALINITY (^{0}/oo)	R_w (Ω)
17:45	20m	10.1	32.6	0.444
19:55	20m	9.8	32.5	0.449

Table B4.2. Location means of measured parameters.

	OVERALL		SANDBANK			CHANNEL EDGE		
PARAMETER	MEAN	CV(%)	n	MEAN	CV(%)	n	MEAN	CV(%)
Mode grain size	2.205	2.1	6	2.200	3.0	5	2.210	1.8
Mean grain size*	1.939	11	6	1.785	7.9	5	2.124	2.4
Folk sorting *	0.733	40	6	0.971	12	5	0.447	25
% Carbonate *	25.5	27	6	30.7	49	5	19.2	22
% Coarse *	22.6	35	6	27.7	97	5	16.4	16
Frame Sorting *	0.24	22	6	0.29	7.4	5	0.19	5.8
Lanice	136	100	6	199	100	5	61	100
Porosity *	0.421	2.8	6	0.428	2.8	5	0.412	1.6
FF	5.0	11	6	4.9	1.7	5	5.2	16
(var.)	4.3	-	6	4.0	-	5	4.5	-
Bulk V_s	51.5	8.4	6	51.3	11	5	51.8	6
(var.)	8.7	-	6	11.5	-	5	5.2	-
Surface V_s	51.0	9	6	52.2	9	5	49.4	9
(var.)	8.0	-	6	10.4	-	5	5.0	-

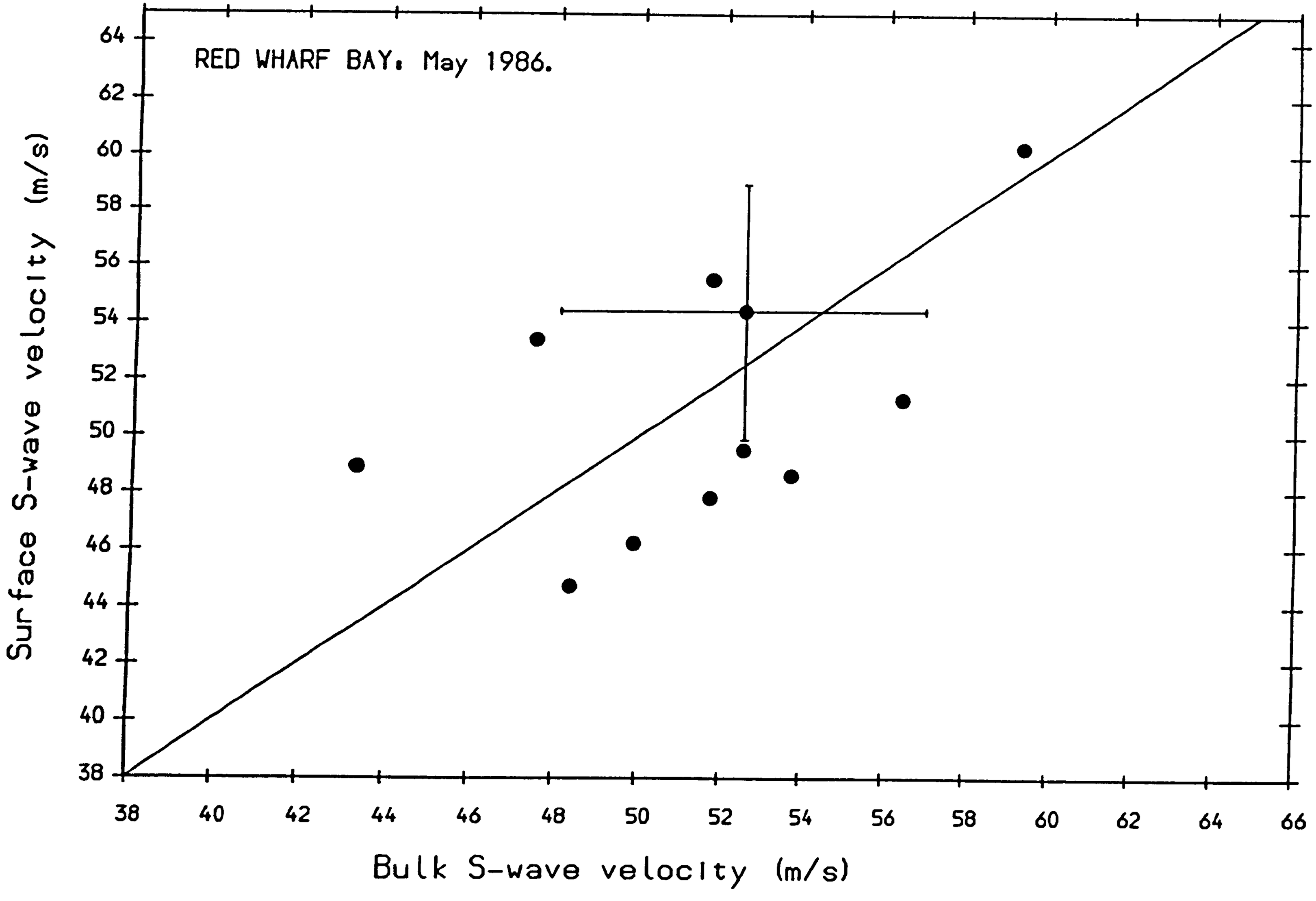

Fig. B4.1. Comparison of bulk and surface V_s. Straight line has slope 1.

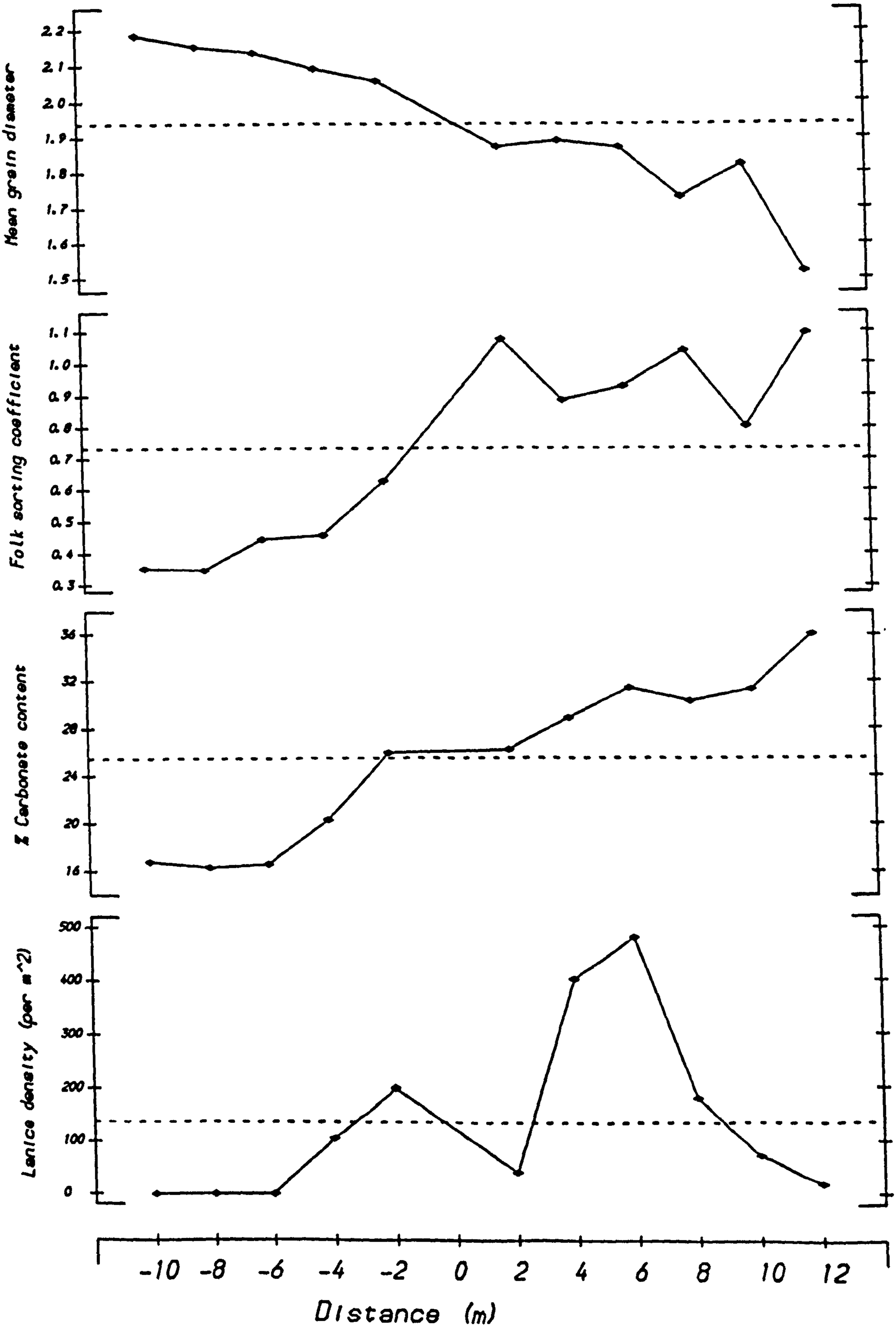

Fig. B4.2. Red Wharf Bay. Spatial distribution of textural and biological parameters. (*Distance < 0: Channel Edge; distance > 0: Sand bank*).

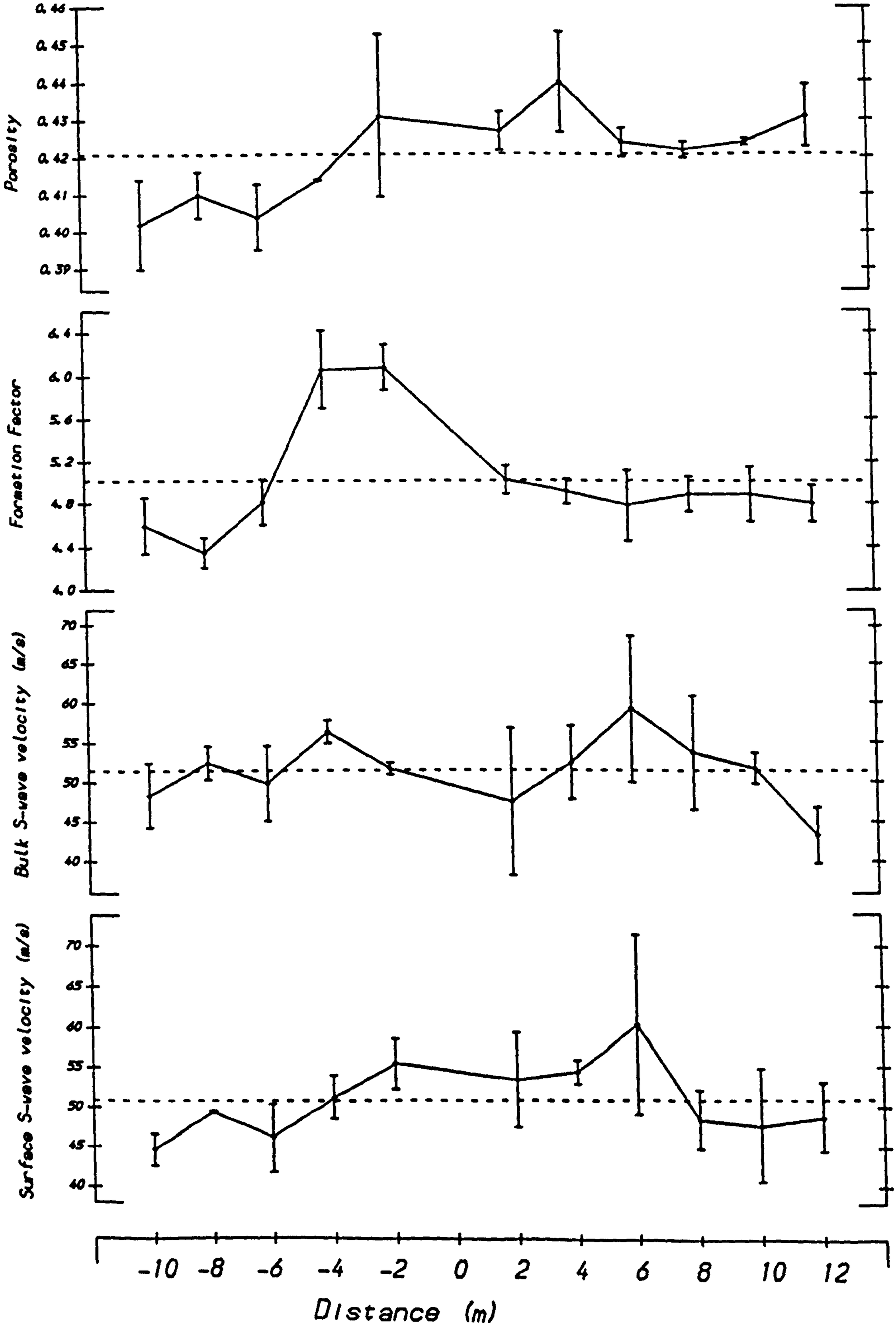

Fig. B4.3. Red Wharf Bay. Spatial distribution of geophysical parameters.
(Distance < 0: Channel Edge; distance > 0: Sand bank).

RED WHARF BAY (SECTION 5.2.4)

Table B4.3. Correlations among textural and biological characteristics.

Parameters	ALL DATA [r^c = 0.684]
TEXTURAL INTERRELATIONSHIPS.	
% Carb.: % Coarse	0.800
: Framework sorting	0.885
(NO BIOLOGICAL/TEXTURAL INTERRELATIONSHIPS)	

Table B4.4. Apparent controls of porosity and geophysical properties.

MULTIPLE LINEAR REGRESSIONS.					
POROSITY					
	% Carb.	% Coarse		*Lanice*	$\%R^2$
ALL DATA	[+]				62
		[+]			39
		[+]		[+]	66
FORMATION FACTOR	(NONE)				
BULK V_s					
		% Coarse	Porosity	*Lanice*	$\%R^2$
ALL DATA				[+]	37
			[-]	[+]	60
		[-]		[+]	59
SURFACE V_s					
		% Coarse	Porosity	*Lanice*	$\%R^2$
ALL DATA				[+]	62

FREATHY SANDS (SECTION 5.2.5)

Table B5.1. Location means of measured parameters.

	(SATURATED ONLY)		
PARAMETER	n	MEAN	CV(%)
Mode grain size	5	1.790	2.2
Mean grain size	5	1.846	5.7
Folk sorting	5	0.419	7.6
% Carbonate	5	29.7	5.6
Porosity	5	0.455	1.0
FF	5	4.0	5.2
(var.)	5	1.7	-
Bulk V_s	5	66.0	2.5
(var.)	5	4.2	-
Surface V_s	5	58.9	1.9
(var.)	5	5.8	-

Table B5.2. Pore-fluid salinity, temperature and Electrical Resistance.

FREATHY				
TIME	SITE	TEMPERATURE (^{0}C)	SALINITY (^{0}/00)	R_w (Ω)
09:40	1 (sat)	15.8	32.5	0.388
10:15	2 (sat)	16.1		0.388
10:50	3 (sat)	16.0		0.388
11:15	2 (dr.)	17.5		0.379
11:40	4 (sat)	16.0		0.388
12:20	3 (dr.)	17.5		0.379
12:45	5 (sat)	16.3		0.388
13:10	4 (dr.)	19.5		0.359
13:30	1 (dr.)	21.5		0.344
14:05	5 (sat)	21.5		0.359

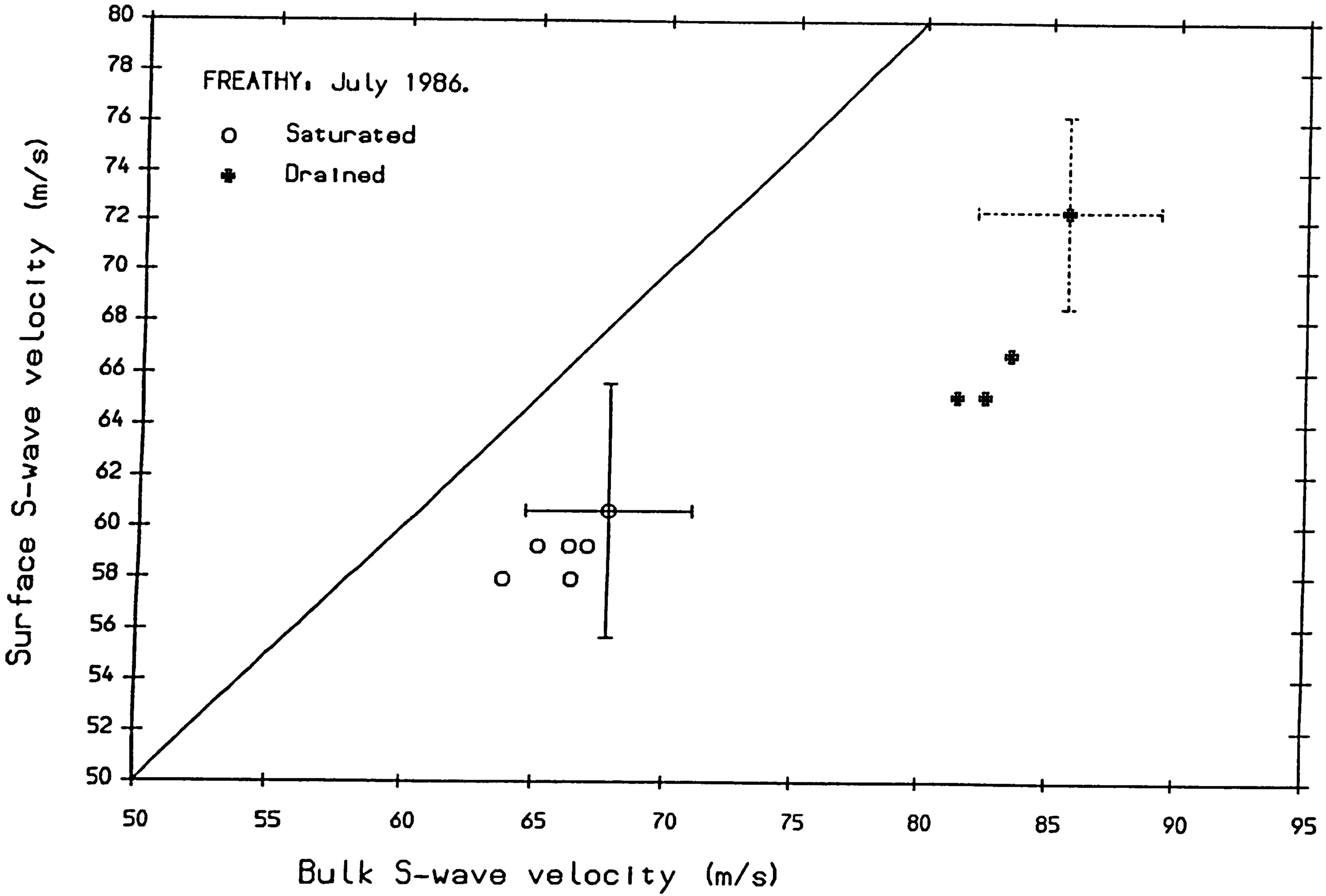

Fig. B5.1. Comparison of bulk and surface V_S. Straight line has slope 1.

TAMAR ESTUARY (SECTION 5.2.6)

Table B6.1. Location means of measured parameters.

	COTEHELE			SALTER'S MILL			TAMAR BRIDGE		
PARAMETER	n	MEAN	CV(%)	n	MEAN	CV(%)	n	MEAN	CV(%)
Mode grain size	3	4.33	7.1	5	4.38	4.1	4	4.30	0
Mean grain size*	6	6.78	3.3	6	6.38	4.5	5	5.72	1.9
Folk sorting *	6	2.34	20	6	2.84	67	5	2.66	69
% Fines *	6	95.	2	6	85	5	5	77	3
% Organics *	6	4.2	9.7	6	2.7	11	5	2.2	34
% > 1phi *	6	0	-	6	6.3	43	5	2.6	49
Porosity *	6	0.83	0.8	6	0.79	2	5	0.72	0.7
FF *	6	1.37	9	6	1.72	1.9	5	2.19	6
(var.)	6	6.0	-	6	4.6	-	5	1.5	-
Bulk V_s	6	13.7	?	6	12.2	5.8	5	14.8	18
($var._s$)	6	9.	-	6	3.	-	5	7.	-

Table B6.2. Pore-fluid salinity, temperature and Electrical Resistance.

TAMAR ESTUARY				
LOCATION	SITE	TEMPERATURE (^{o}C)	SALINITY (^{o}/00)	R_w (Ω)
Cotehele	1	17.0	2.5	4.032
	2	18.5		3.905
	3	19.5		3.819
Salter's Mill	1	16.0	22.0	0.551
	2	17.0		0.539
	3	18.1		0.527
	4	19.2		0.516
	5	20.3		0.505
Tamar Bridge	1	16.5	27.0	0.453
	2	18.2		0.436
	3	18.2		0.436
	4	17.5		0.433

TAMAR ESTUARY (SECTION 5.2.6)

Table B6.3. Correlations among textural characteristics.

TEXTURAL INTERRELATIONSHIPS.	
Parameters	ALL DATA [r^c = 0.661]
% Organics : % Fines	0.869

Table B6.4. Apparent controls of porosity and geophysical properties.

MULTIPLE LINEAR REGRESSIONS.					
POROSITY					
	% Fines	% Organics		% > 1 phi	$\%R^2$
ALL DATA	[+] [+]	[+]		[+]	80 59 87
FORMATION FACTOR					
	% Fines	% Organics	Porosity	% > 1 phi	$\%R^2$
ALL DATA	[-]		[-]		87 73
BULK V_s (NONE)					

APPENDIX C.

SEASONAL VARIABILITY AND CONTROLS OF GEOPHYSICAL PROPERTIES: REFERENCE TABLES AND FIGURES.

This appendix is intended as supplementary reference for the seasonal and spatial study in the Cefni Estuary described in Section 5.3. It has been divided into three sections:

C1. Reference tables.
C2. Time series and temporal variation analysis.
C3. Relationships among measured parameters.

APPENDIX C1

Reference Tables.

Time averages at individual sites, and overall averages have been summarised, along with associated coefficients of variation. The format corresponds to that used for location means in Appendix B.

Table C1.1. Significant (>20mm) changes in bed-level, ΔL.

EROSION			DEPOSITION		
Date	Site	ΔL (mm)	Date	Site	ΔL (mm)
July	1	-55	June 23	1	+25
	2	-75			
	3	-45	August	2	+82
	4	-25		3	+57
				4	+28
September	3	-22			
			September	1	+35
October	2	-30			
	3	-35	October	1	+30
	4	-30			
			November	3	+25
November	1	-20			
	5	-20	December	1	+80
				2	+85
January	1	-28		3	+100
	3	-38		4	+95
	4	-58		5	+55

Table C1.2. Summary of selected site parameters.

Parameter	Site	*n*	Mean	σ	%cv
Grain size mode	1	12	2.638	0.053	2.0
	2	14	2.571	0.032	1.2
	3	14	2.596	0.041	1.6
	4	14	2.646	0.075	2.8
	5	14	2.571	0.038	1.5
	ALL	68	2.604	0.058	2.2
Grain size mean	1	12	2.578	0.049	1.9
	2	14	2.431	0.034	1.4
	3	14	2.523	0.043	1.7
	4	14	2.541	0.027	1.1
	5	14	2.487	0.030	1.2
	ALL	68	2.510	0.062	2.4
Sorting	1	12	0.327	0.018	6
	2	14	0.409	0.026	6
	3	14	0.484	0.077	16
	4	14	0.394	0.019	5
	5	14	0.371	0.019	5
	ALL	68	0.399	0.064	16
% Carbonate	1	12	6.8	0.9	13
	2	14	4.8	0.3	6
	3	14	7.8	0.3	4
	4	14	7.1	0.6	8
	5	14	5.8	0.5	9
	ALL	68	6.4	1.2	19
% Fines	1	12	0.6	0.3	50
	2	14	1.1	0.5	45
	3	14	4.3	0.7	16
	4	14	2.0	0.4	20
	5	14	1.3	0.4	31
	ALL	68	1.9	1.4	74
% > 1 phi	1	12	0.83	0.5	60
	2	14	1.18	0.4	34
	3	14	3.31	1.0	30
	4	14	1.91	0.5	26
	5	14	1.62	0.8	49
	ALL	68	1.80	1.0	55
% 1-2 phi	1	12	6.4	1.4	22
	2	14	14.7	2.2	15
	3	14	9.1	1.2	13
	4	14	8.8	0.8	9
	5	14	10.0	0.7	7
	ALL	68	9.9	3.0	30

(contd.....

Table C1.2 (.....contd.)

	Site	*n*	Mean	σ	%cv
% Organics	1	12	0.30	0.04	13
	2	14	0.30	0.06	20
	3	14	0.56	0.06	11
	4	14	0.46	0.09	20
	5	14	0.35	0.11	31
	ALL	68	0.40	0.13	33
Corophium	1	11	4	4	100
	2	13	4	4	100
	3	13	35	29	83
	4	13	14	10	71
	5	13	3	3	100
	ALL	63	12	18	100
Pygospio	1	11	43	31	72
	2	13	26	12	46
	3	13	30	18	60
	4	13	47	17	36
	5	13	28	14	50
	ALL	63	34	13	38
Hydrobia	1	11	2	2	100
	2	13	8	9	100
	3	13	84	36	43
	4	13	72	26	36
	5	13	48	18	38
	ALL	63	44	39	89
Arenicola	1	12	6	6	100
	2	14	20	16	80
	3	14	0	0	-
	4	14	0	0	-
	5	14	21	9	43
	ALL	63	10	10	100
Pore-fluid Salinity	1	12	25.0	6.7	27
	2	14	21.3	7.3	34
	3	14	11.0	1.8	16
	4	14	14.8	3.5	24
	5	14	25.3	4.4	17
	ALL		19.3	7.5	39

(contd....

Table C1.2 (.....contd.)

Parameter	Site	*n*	Mean	σ	%cv
Porosity	1	12	0.421	0.013	3
	2	14	0.416	0.016	4
	3	14	0.419	0.018	4
	4	14	0.417	0.022	5
	5	14	0.422	0.013	3
	ALL	68	0.419	0.020	5
FF	1	12	3.96	0.5	13
	2	14	3.59	0.5	14
	3	14	4.83	0.6	12
	4	14	4.82	0.9	19
	5	14	4.16	0.4	10
	ALL	68	4.28	0.8	19
Vs (Bulk)	1	12	47.5	4.0	8
	2	14	40.3	5.5	14
	3	14	50.4	4.6	9
	4	14	47.1	3.9	8
	5	14	45.0	4.7	10
	ALL	68	46.0	5.6	12
Vs (Surface)	1	12	41.1	3.5	9
	2	14	34.6	3.6	10
	3	14	37.7	3.4	9
	4	14	38.3	4.3	11
	5	14	35.4	3.2	9
	ALL	68	37.3	4.3	12
cv(FF)	1	12	4.4	2.2	50
	2	14	6.9	2.7	39
	3	14	6.4	2.8	44
	4	14	8.8	3.3	38
	5	14	6.3	2.0	32
	ALL	68	6.6	2.9	44
Vs ratio	1	12	0.87	0.10	11
	2	14	0.87	0.09	10
	3	14	0.75	0.09	12
	4	14	0.82	0.12	15
	5	14	0.80	0.09	11
	ALL	68	0.82	0.10	12

APPENDIX C2

Time Series and temporal variation analysis.

A set of time series of selected site means has been presented for each site, with error bars corresponding to within-site standard deviation where within-site replication was performed, an estimated standard error (Table 5.1.6) otherwise. At Site 1 the three zones defined in Section 5.3.2 have been separated for textural and geophysical parameters as follows:

Zone 1: Blue
Zone 2: Red
Zone 3: Black

At Site 5, the two sets of samples obtained at different distances along P1:S5 (Fig. 5.3.1) have also been separated. The biological counts were combined together at both sites, because they were too complex to allow alternative presentation.

Also listed are tables of significant correlation coefficients indicating the nature of temporal variation. Thus correlations with time, with a cosine-transformation of time and among pairs of sites indicate trends, seasonal periodicity and spatial coherence, as described in Section 5.3.4. Critical correlation coefficients have been calculated as described in Appendix B.

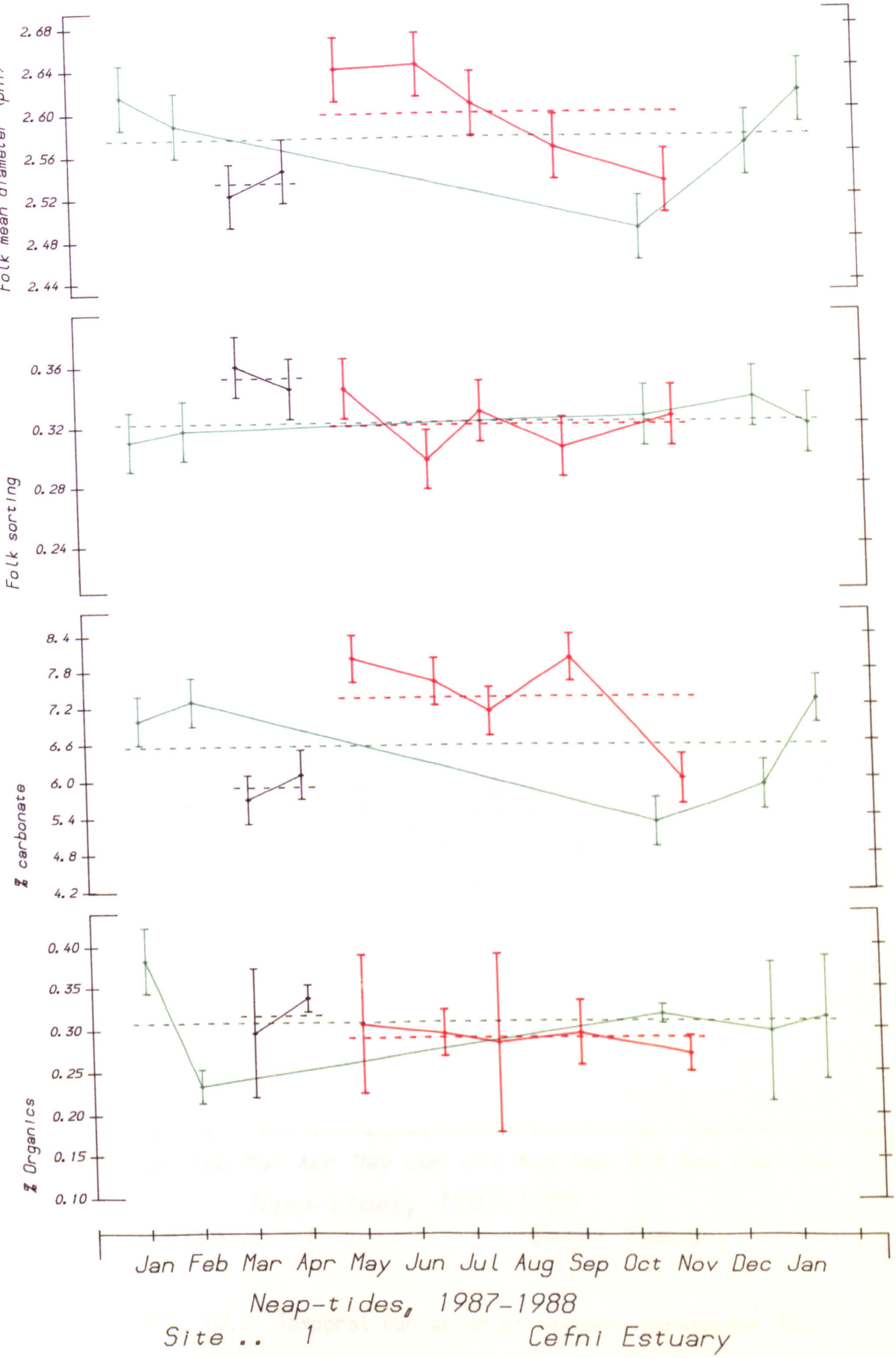

Fig. C2.1 Cefni Estuary. Time series of textural parameters (1).

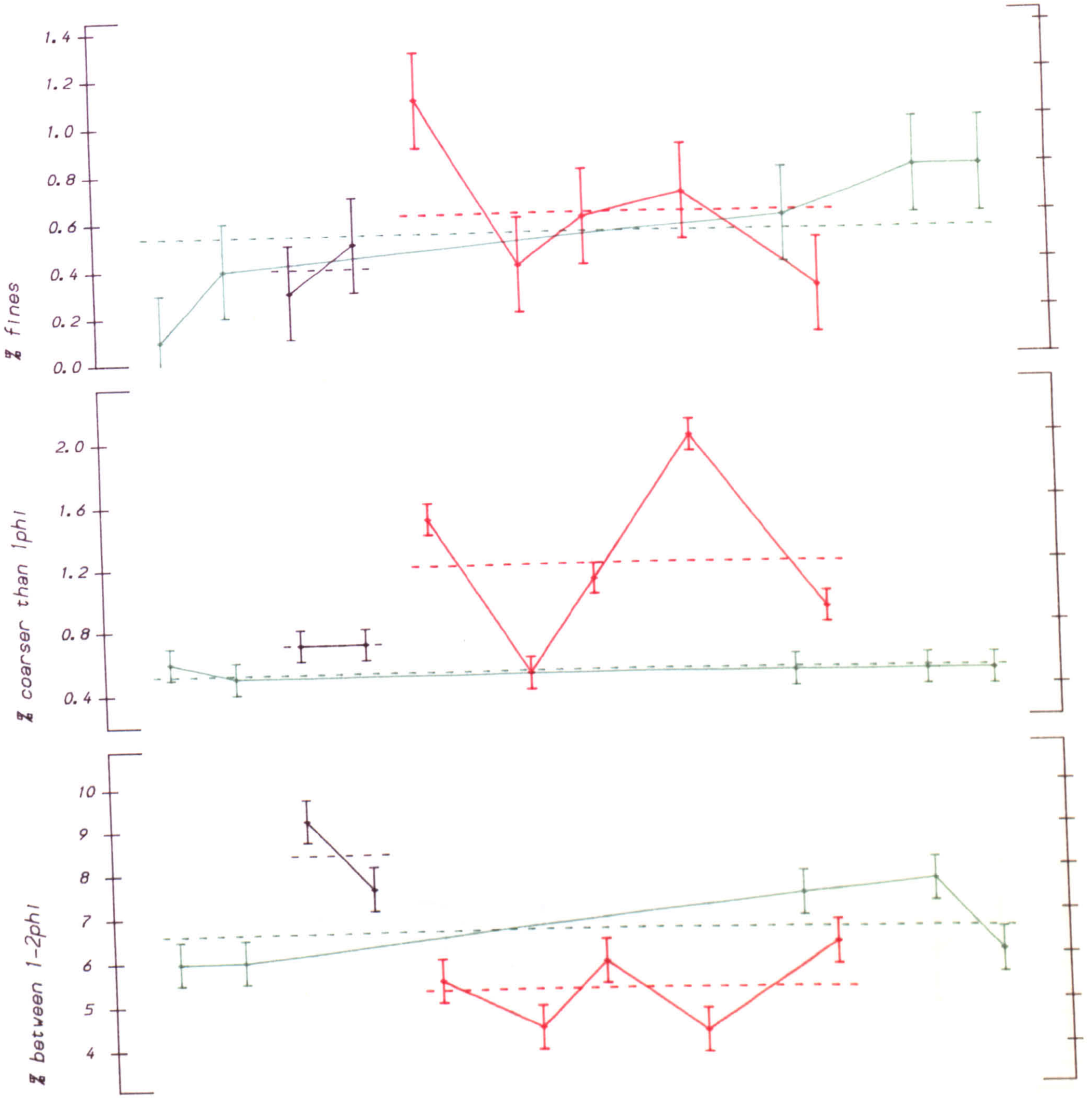

Fig. C2.2. Temporal variation of textural parameters (2).

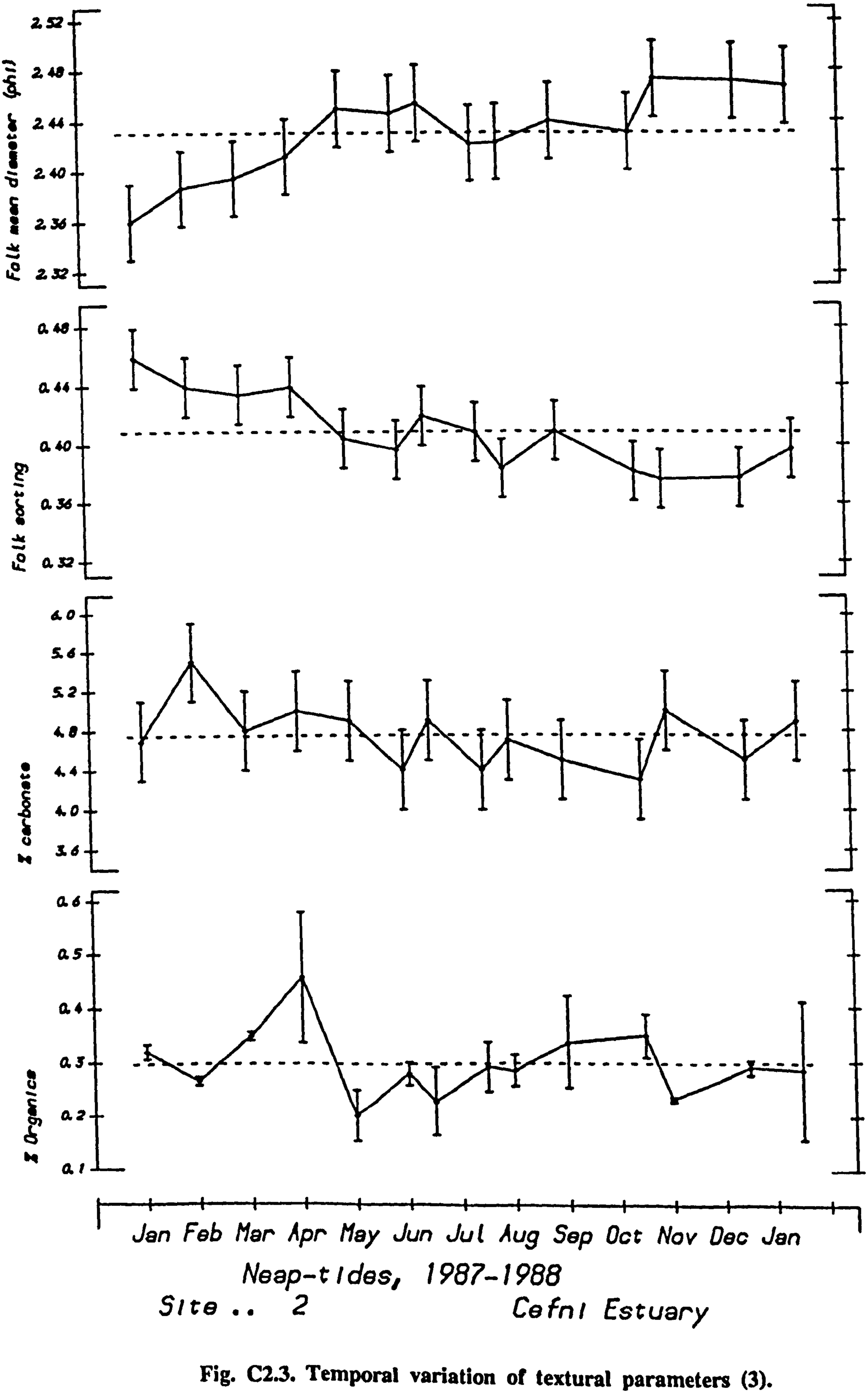

Fig. C2.3. Temporal variation of textural parameters (3).

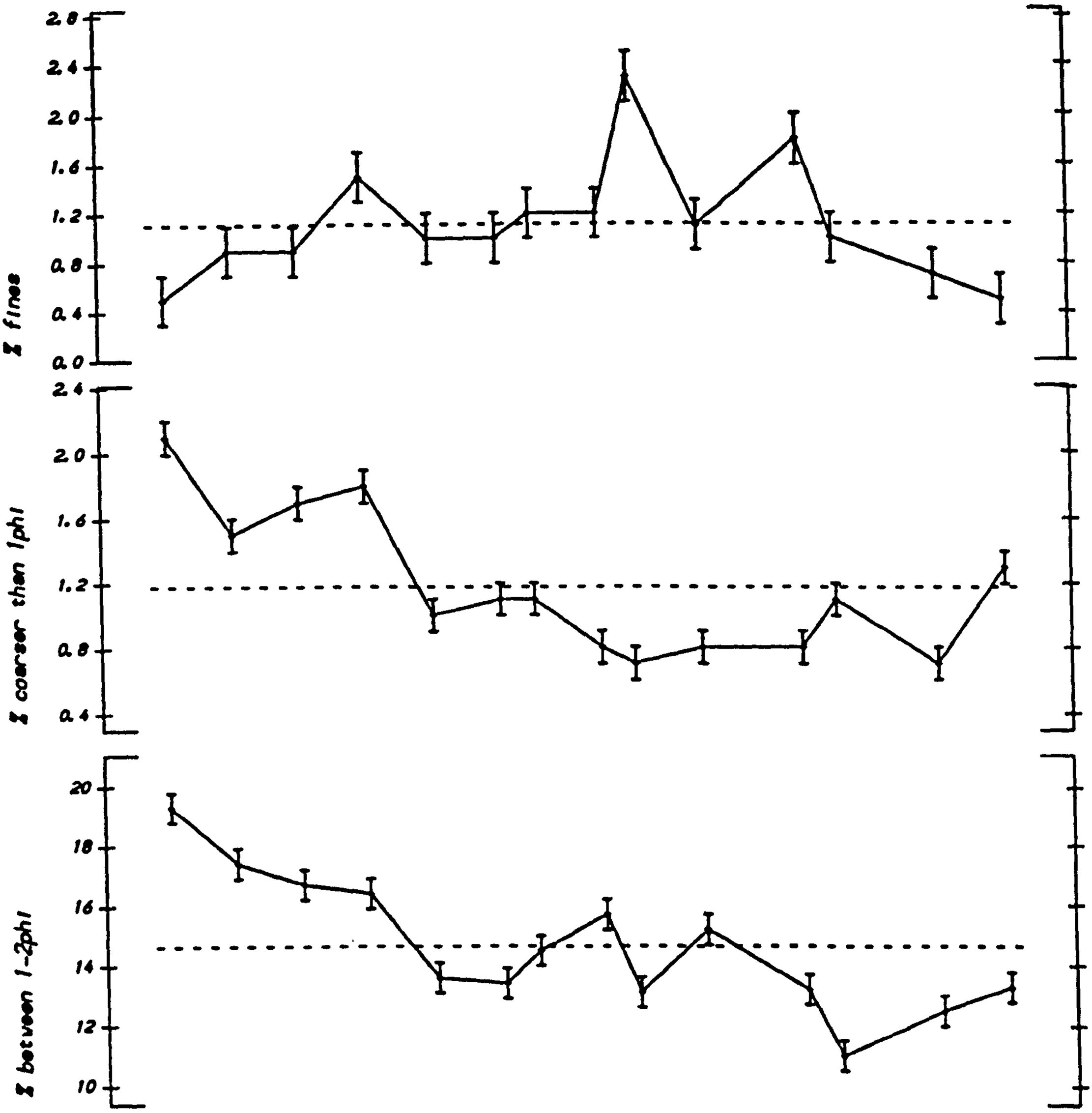

Fig. C2.4. Temporal variation of textural parameters (4).

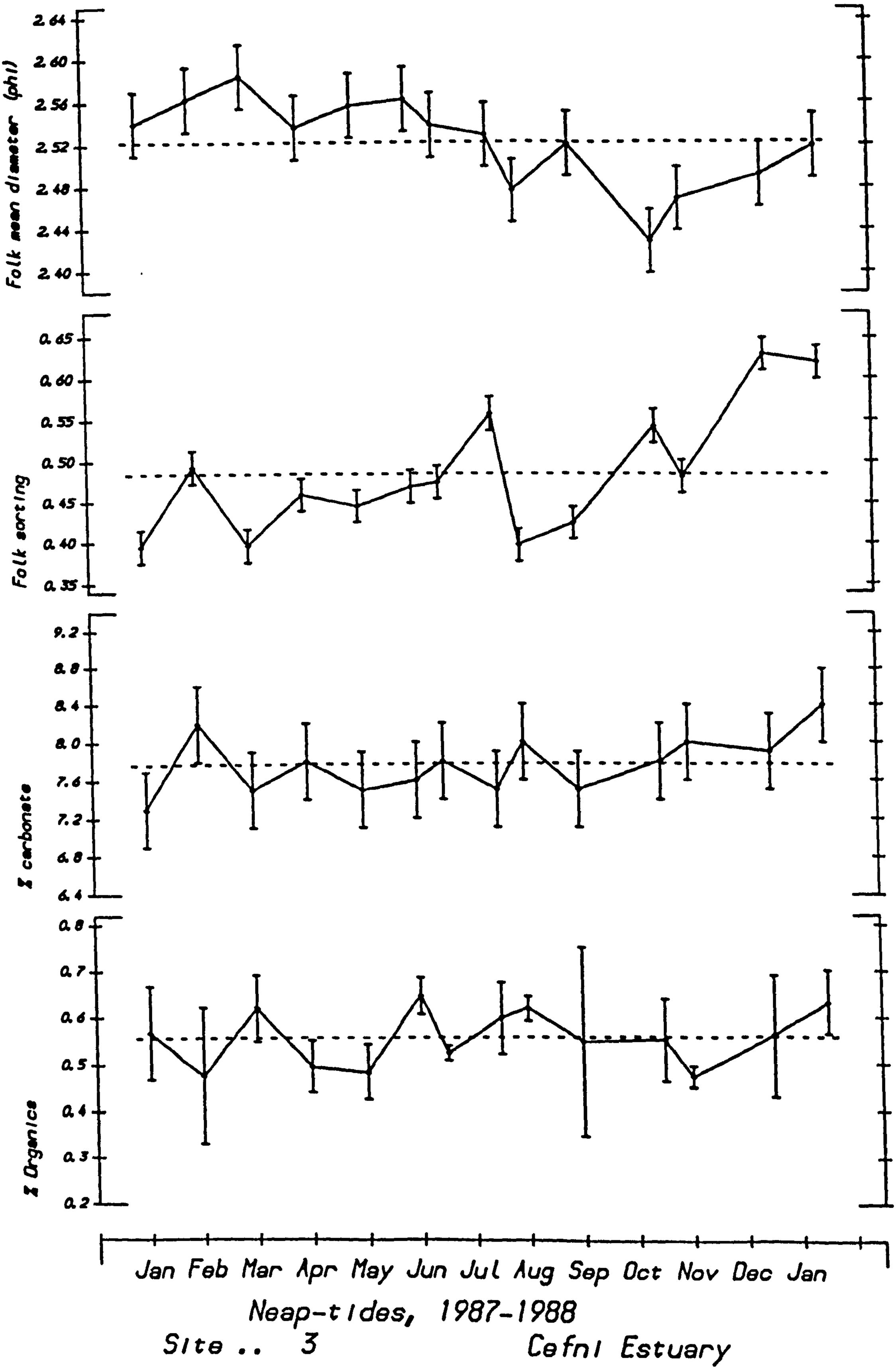

Fig. C2.5. Temporal variation of textural parameters (5).

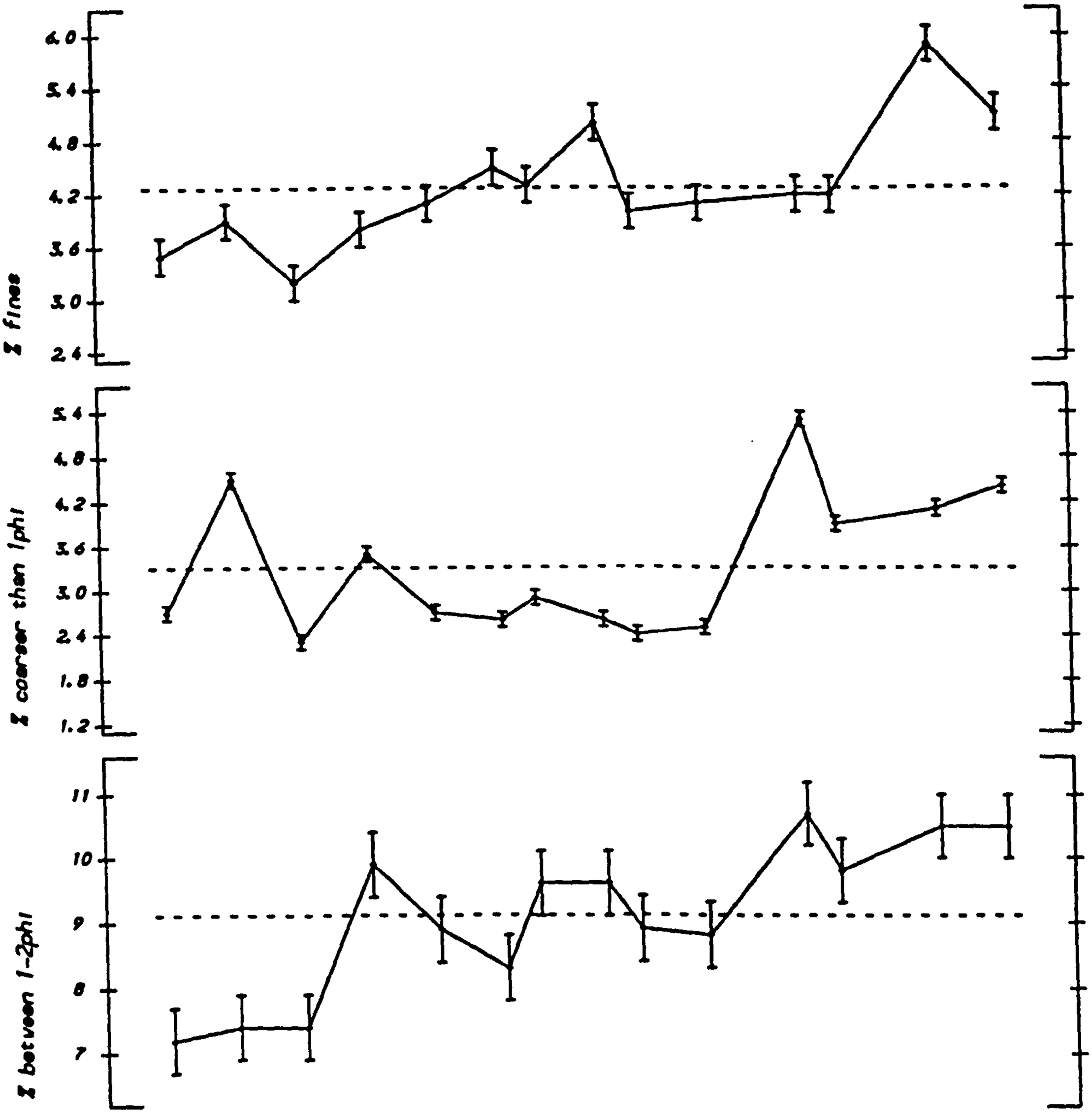

Fig. C2.6. Temporal variation of textural parameters (6).

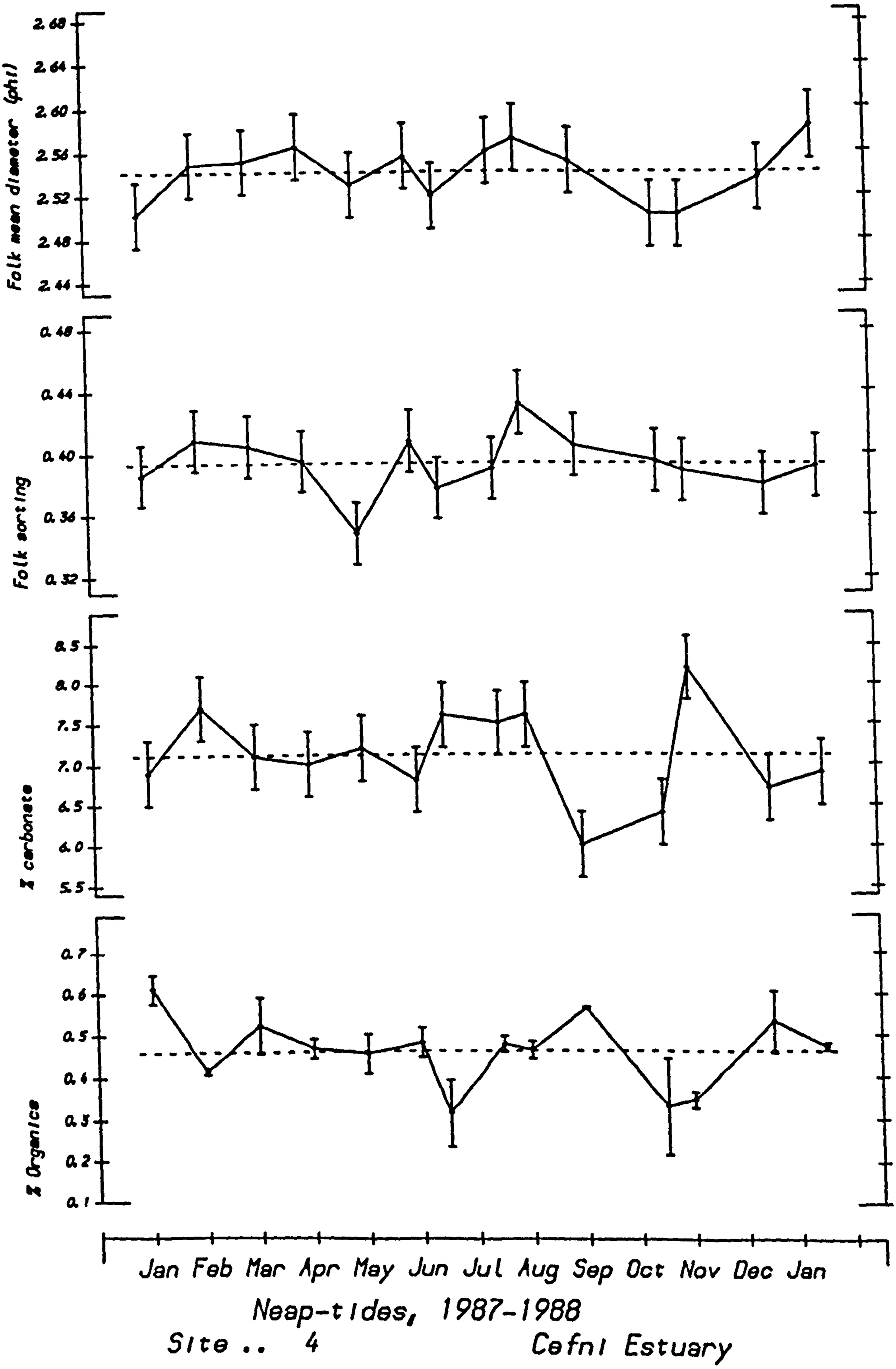

Fig. C2.7. Temporal variation of textural parameters (7).

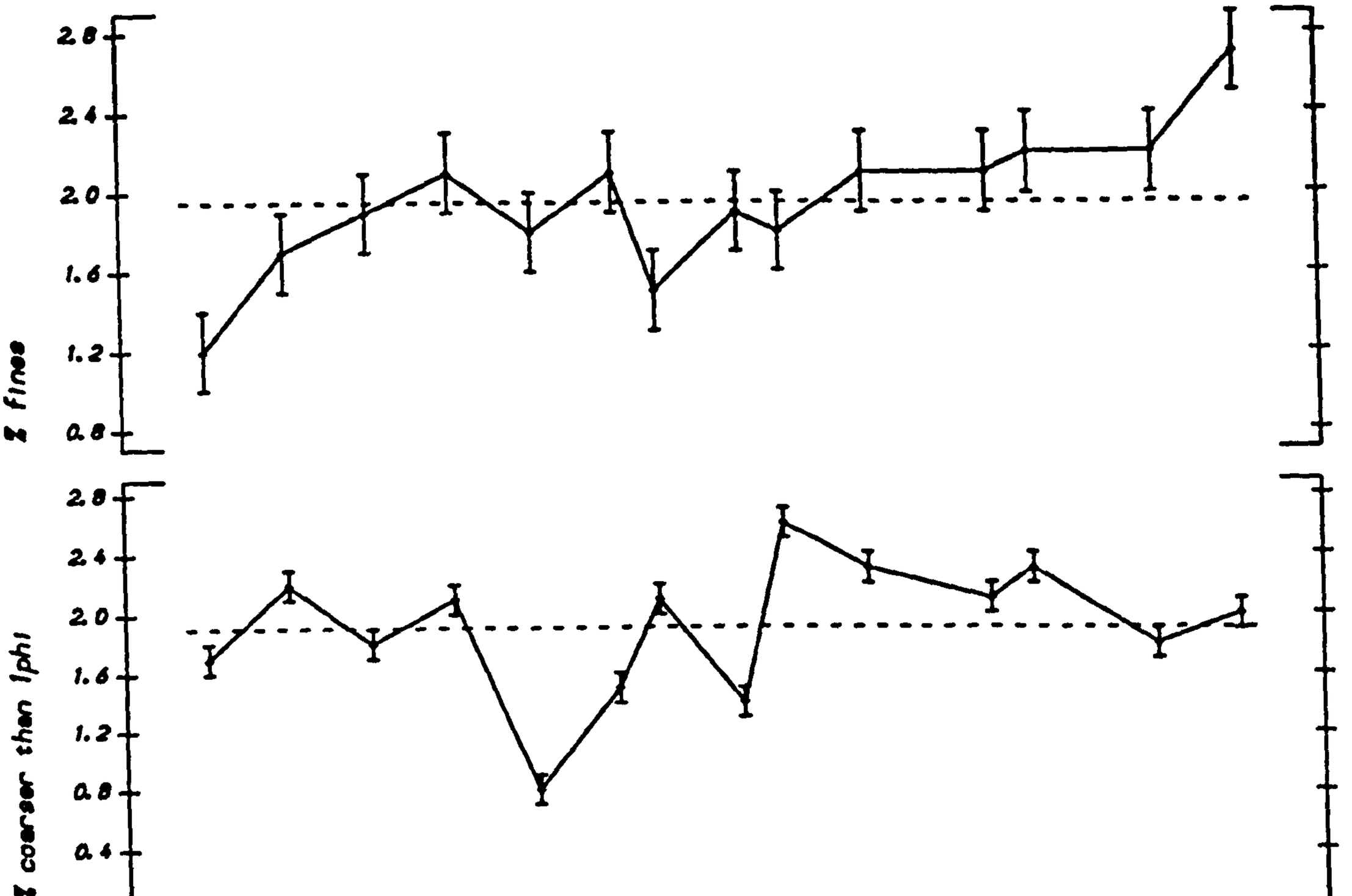

Fig. C2.8. Temporal variation of textural parameters (8).

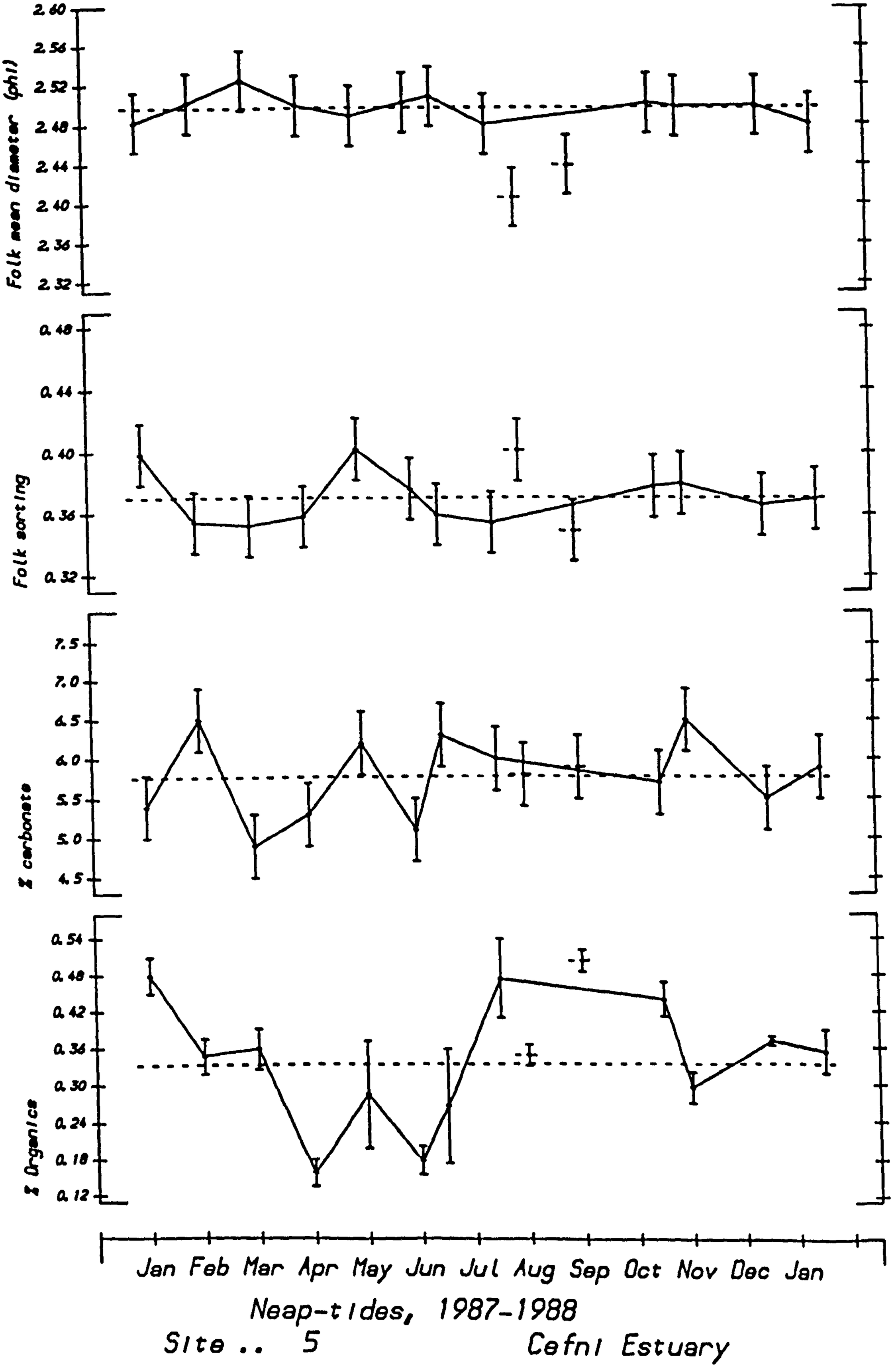

Fig. C2.9. Temporal variation of textural parameters (9).

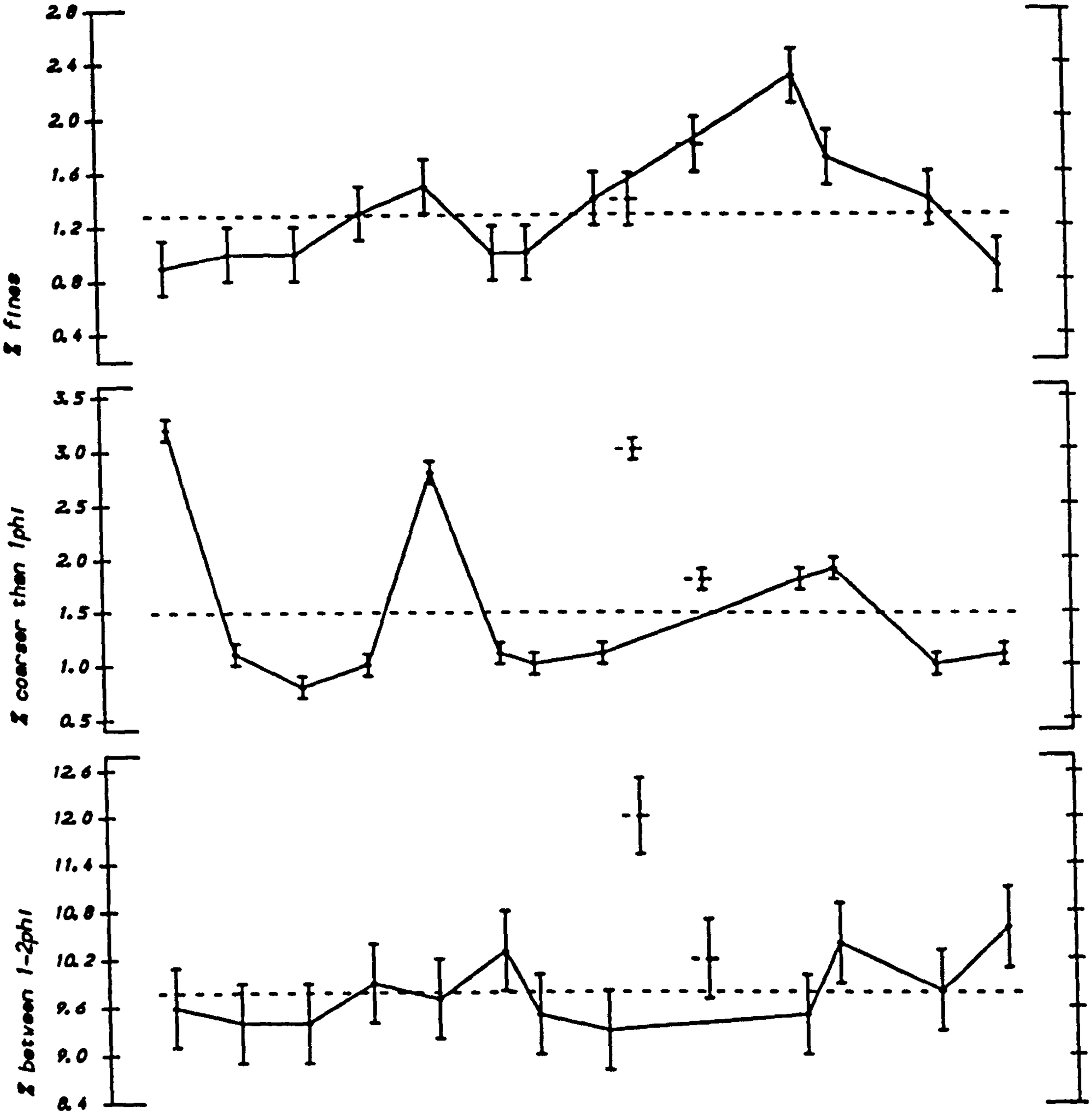

Fig. C2.10. Temporal variation of textural parameters (10).

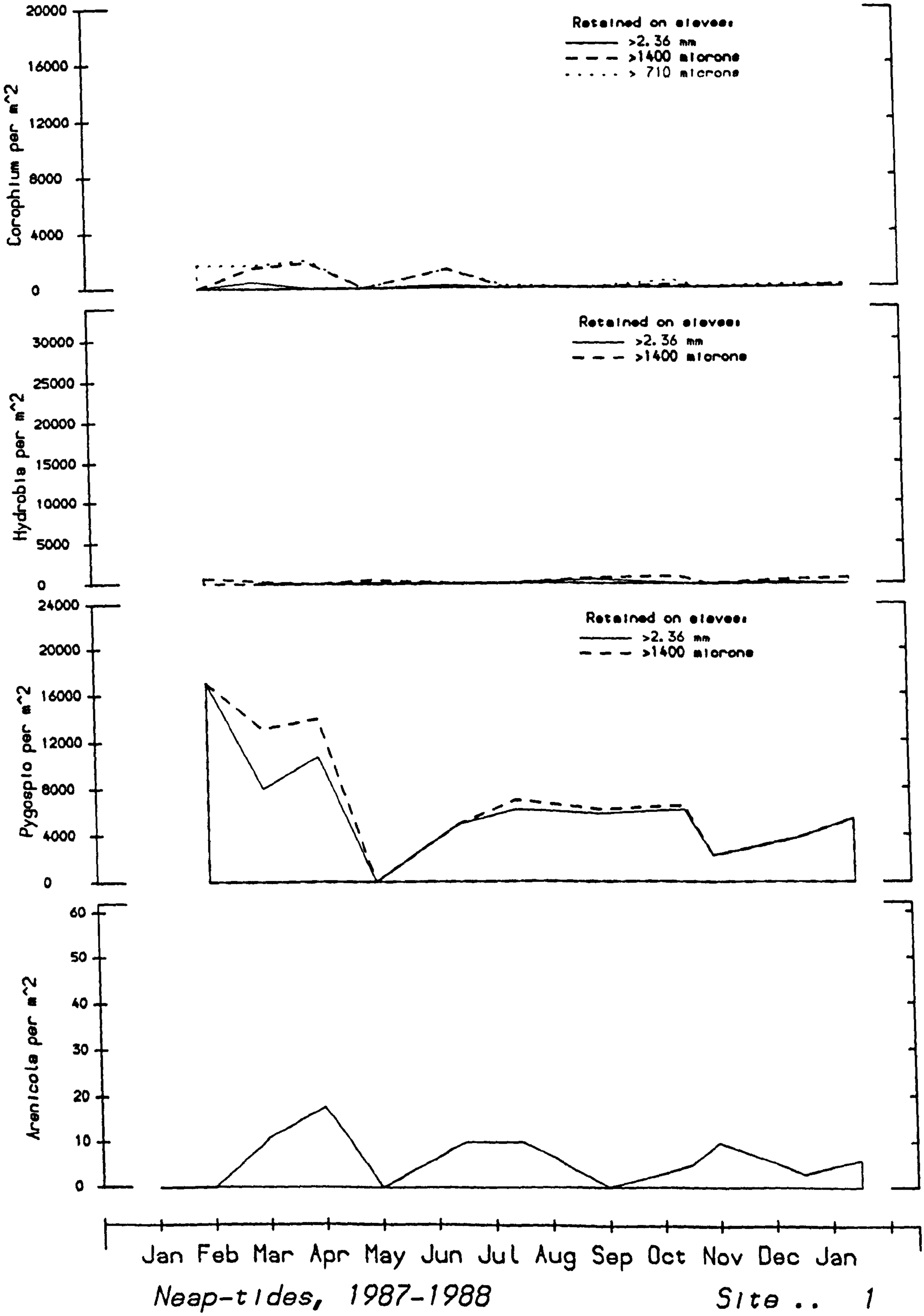

Fig. C2.11. Temporal variation of biological parameters (1).

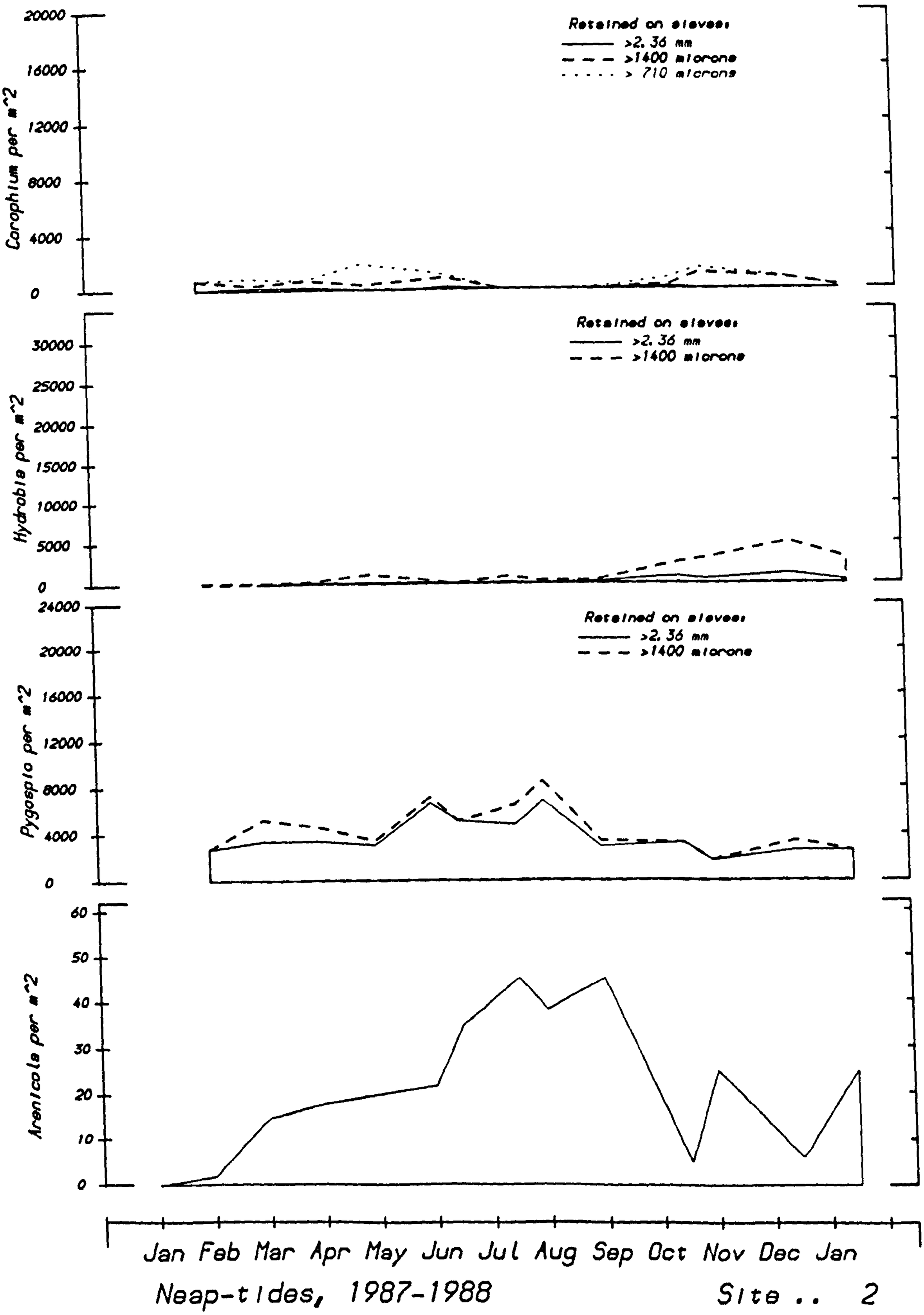

Fig. C2.12. Temporal variation of biological parameters (2).

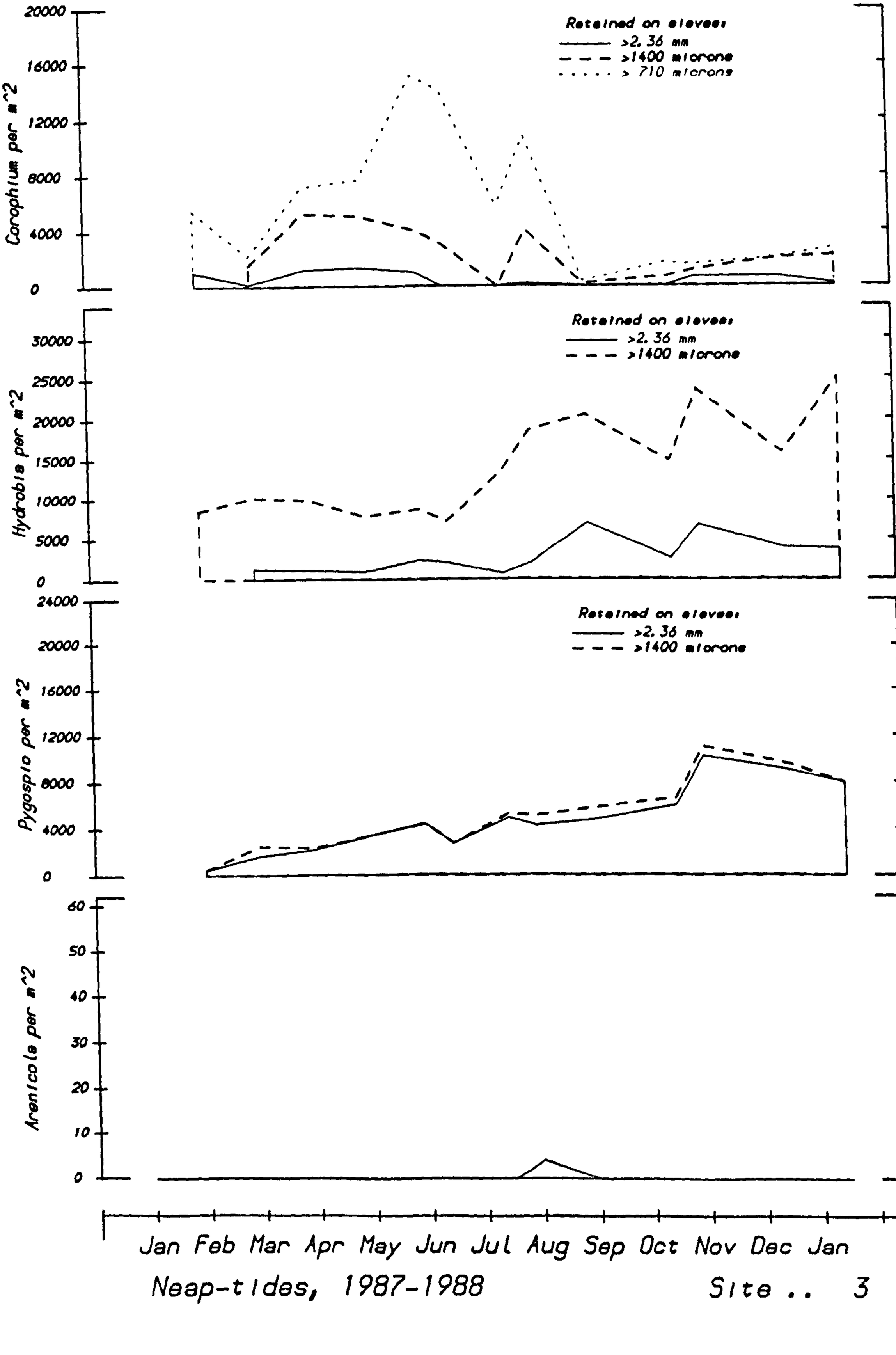

Fig. C2.13. Temporal variation of biological parameters (3).

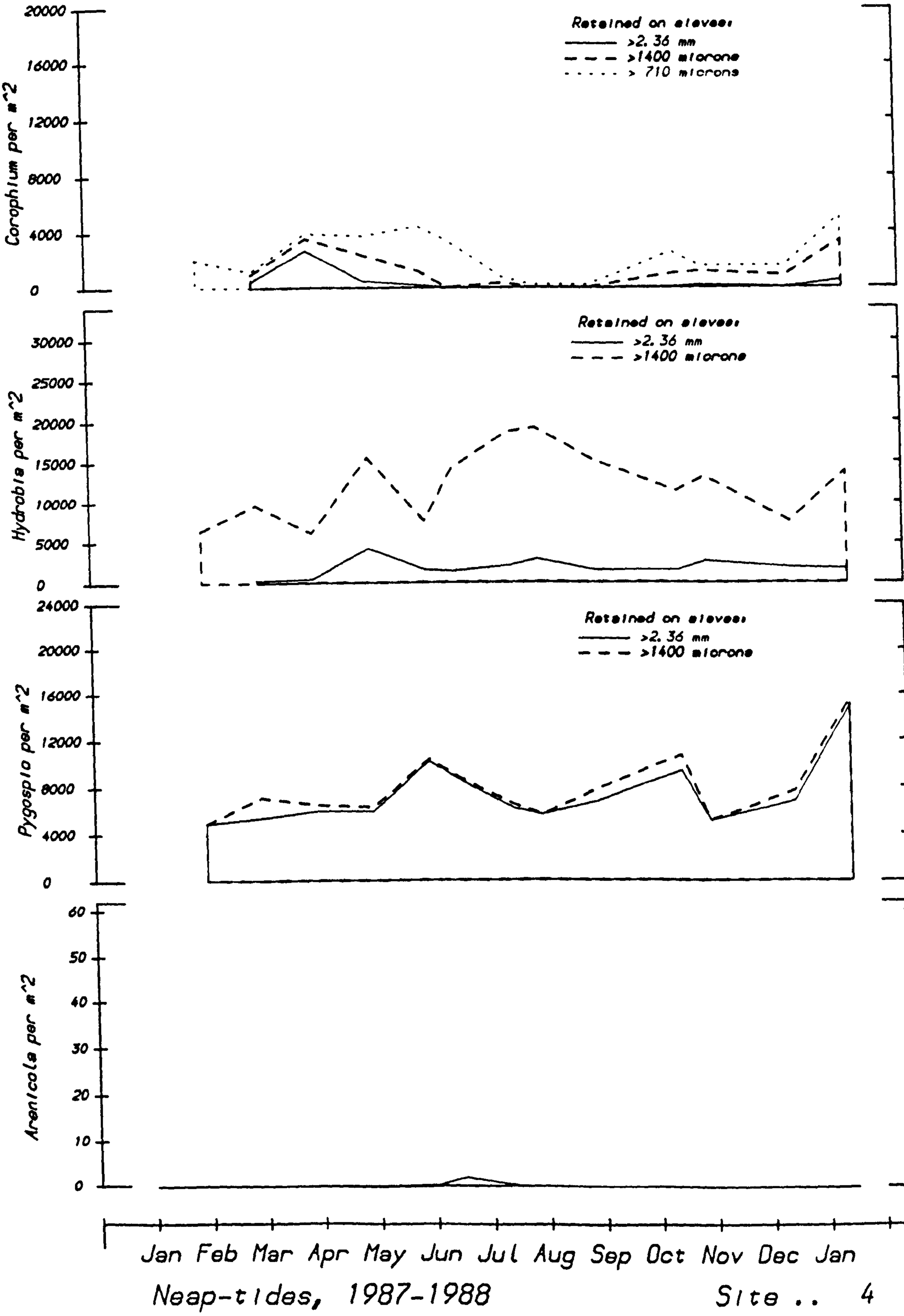

Fig. C2.14. Temporal variation of biological parameters (4).

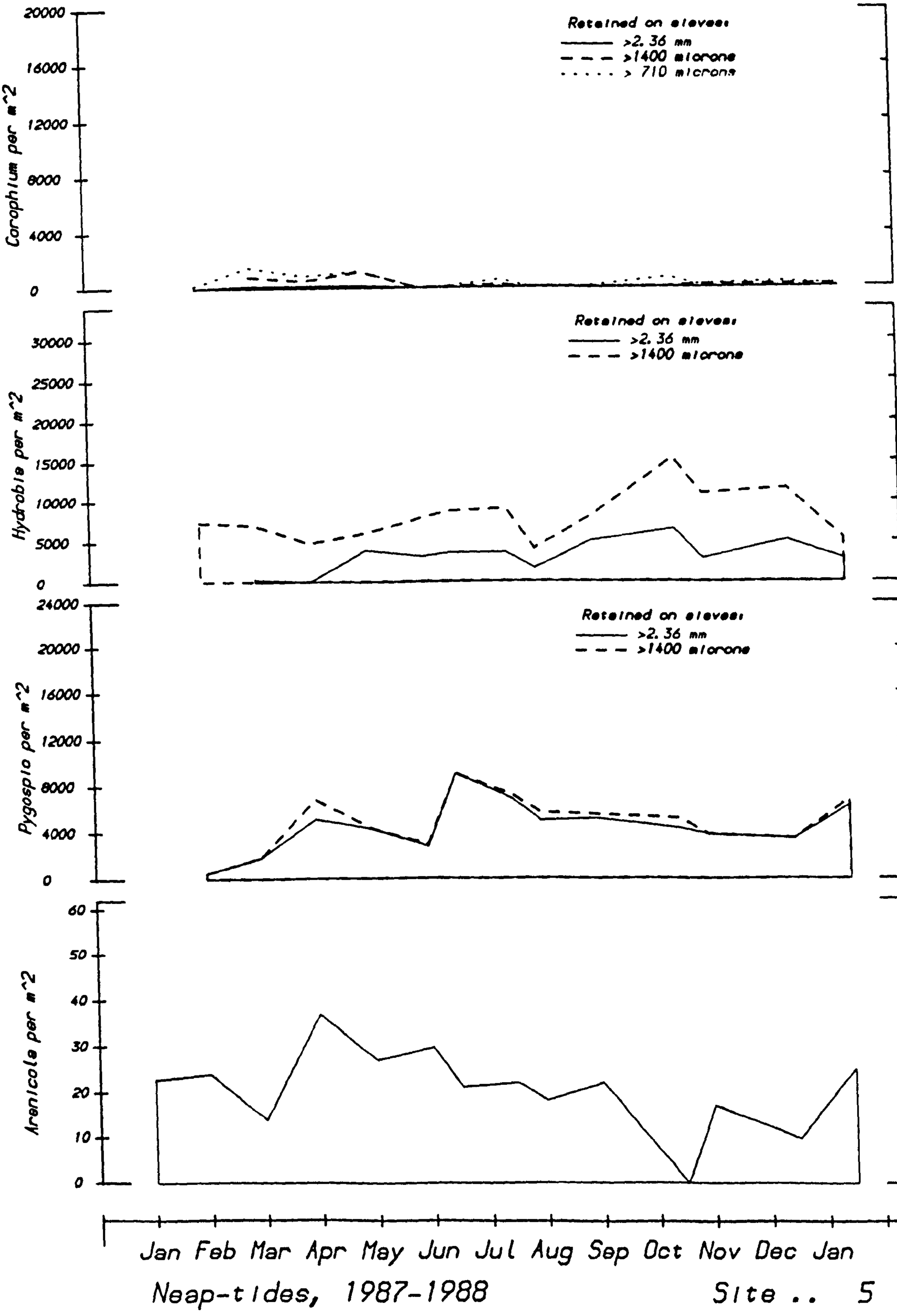

Fig. C2.15. Temporal variation of biological parameters (5).

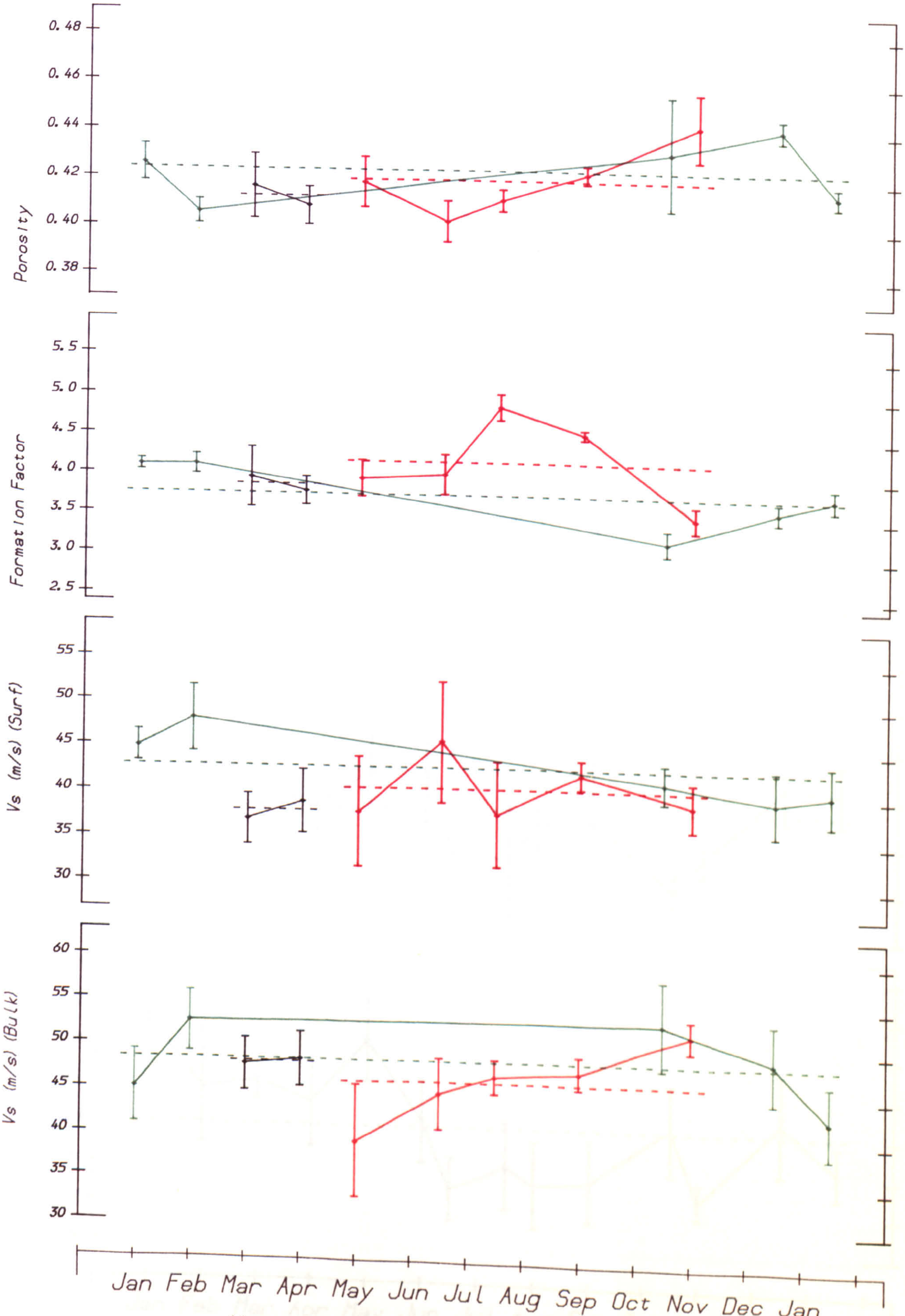

Fig. C2.16. Temporal variation in geophysical parameters (1).

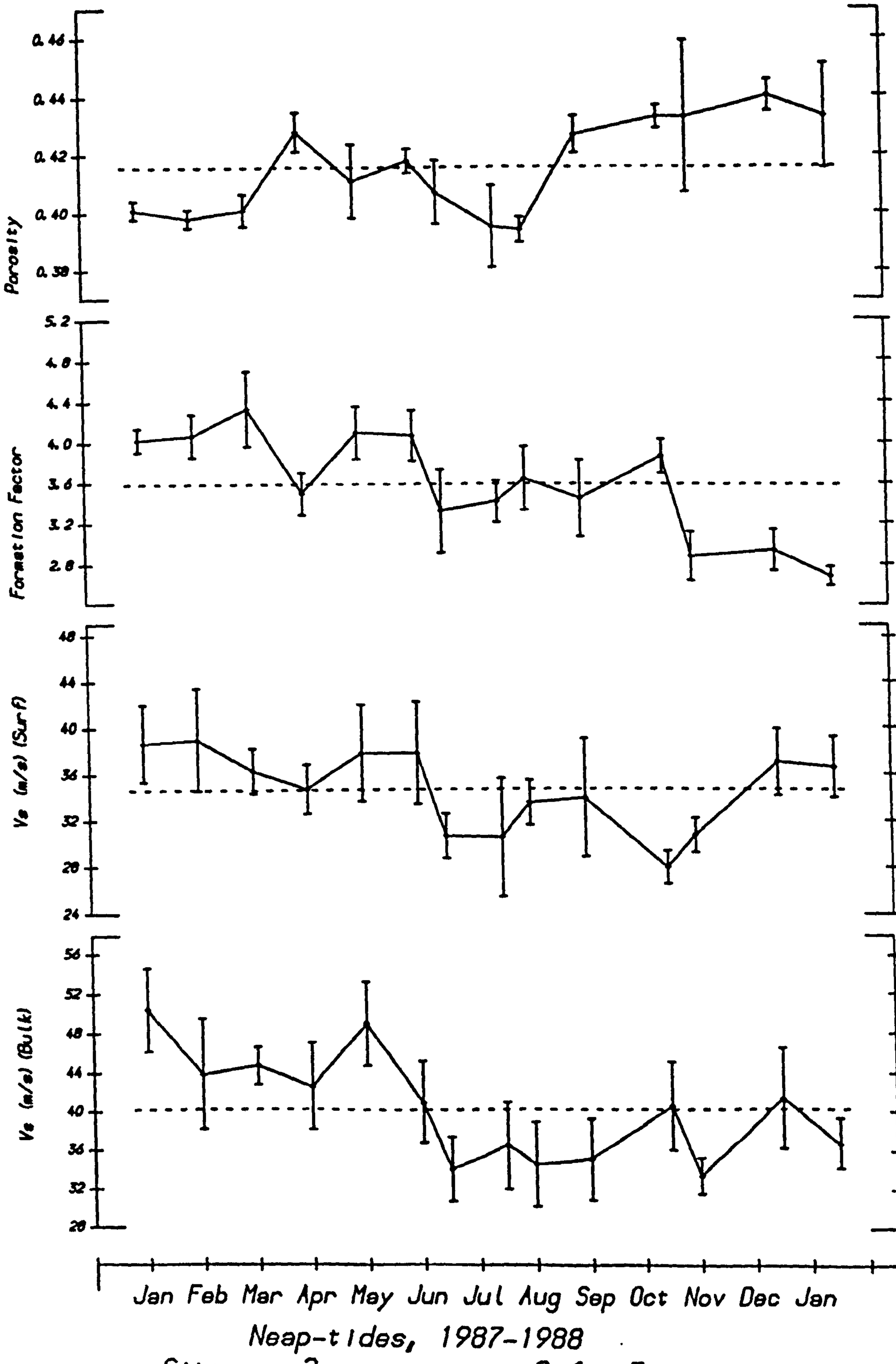

Fig. C2.17. Temporal variation of geophysical parameters (2).

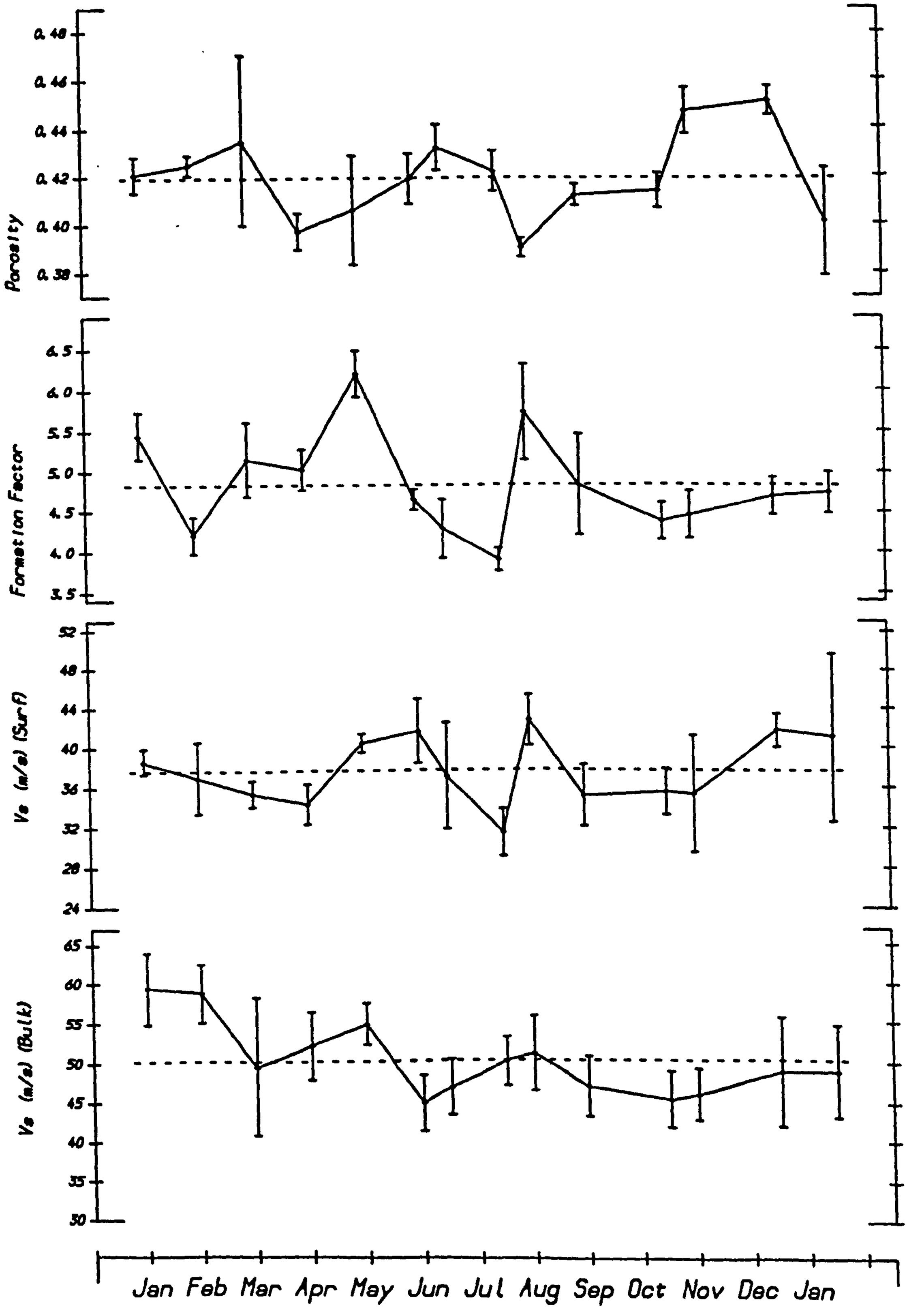

Fig. C2.18. Temporal variation of geophysical parameters (3).

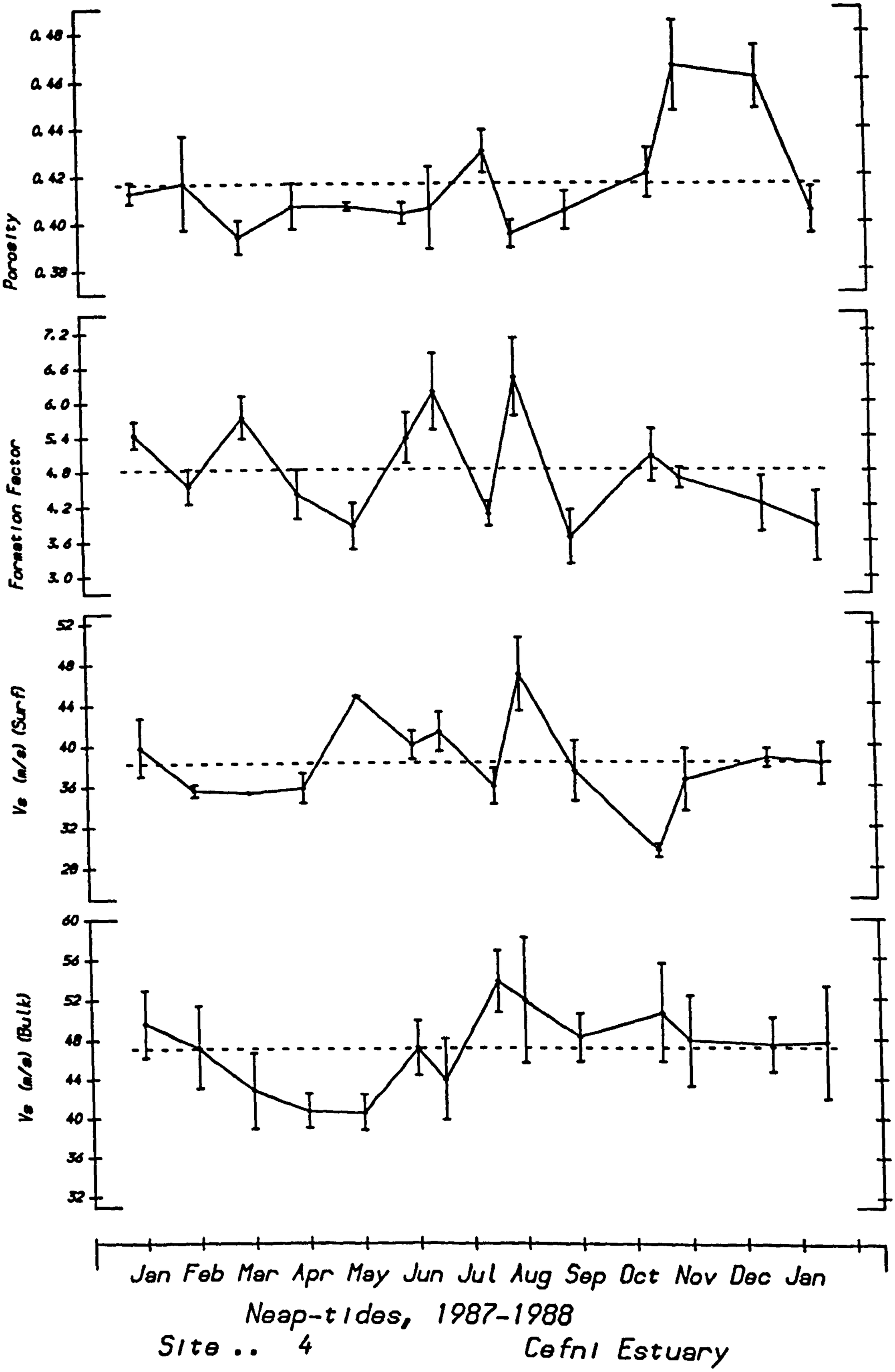

Fig. C2.19. Temporal variation of geophysical parameters (4).

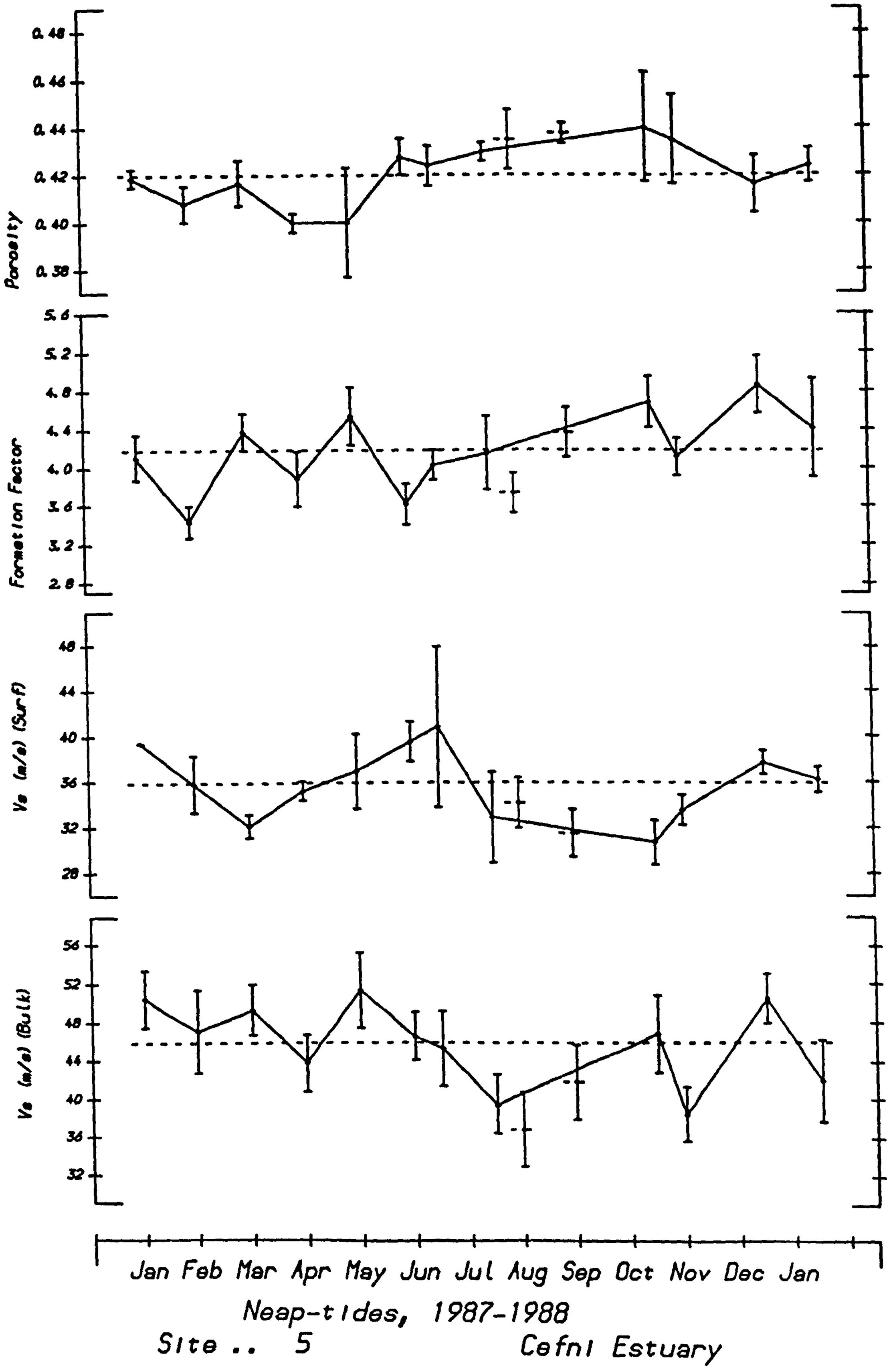

Fig. C2.20. Temporal variation of geophysical parameters (5).

Table C2.1. Significant temporal patterns in textural parameters. r^c=0.703 (Sites 2-5), 0.750 (Site 1).

TRENDS WITH TIME			SEASONALITY			
Parameter	Site	r	Parameter	Site	r	Max.
% Fines	3	0.741	% Fines	2	0.773^R	Aug.
	4	0.763		5	0.703^R	Sep.
%1 - 2 phi	2	-0.813	% > 1 phi	2	0.744	Mar.
	3	0.831				

Table C2.2. Significant temporal patterns in biological parameters. r^c=0.703 (Sites 2-5), 0.750 (Site 1).

TRENDS WITH TIME			SEASONALITY			
Parameter	Site	r	Parameter	Site	r	Max.
Pygospio (Tot)	3	0.911	*Pygospio*	2	0.766	Jul.
				3	0.703	Nov.
Hydrobia (Tot)	2	0.800	*Hydrobia* (T)	2	0.729	Dec.
	3	0.789		3	0.758	Nov.
				4	0.674	Aug.
			Corophium (T)	3	0.796	Jun.
			Arenicola	2	0.733	Aug

Table C2.3. Spatial coherence of biological parameters. (r^c=0.703).

Parameter	Sites	r
Corophium (S)	1,5	0.855(R)
Corophium (L)	3,4	0.734(R)

Table C2.4. Significant temporal patterns in porosity and the geophysical parameters. [r^c=0.703 (Sites 2-5), 0.750 (Site 1), 0.352 ALL.]

TRENDS WITH TIME			SEASONALITY			
Parameter	Site	r	Parameter	Site	r	Max.
FF	2	-0.800	V_s (Bulk)	2	0.705(R)	Mar.
				4	0.738	Oct.
V_s (Bulk)	3	-0.704(R)				
			V_s (Surf)	2	0.715	Mar.
Porosity	2	0.710(R)	Porosity	1	0.771	Nov.
				5	0.848	Oct.
				ALL	0.508	Nov.

Table C2.5. Spatial coherence of geophysical properties. [r^c = 0.703].

Parameter	Sites	r
Porosity	1,4	0.734
	3,4	0.695
V_s (Bulk)	2,5	0.833
V_s (Surface)	3,4	0.718(R)

APPENDIX C3

Relationships among measured parameters.

Reference tables of significant correlation coefficients and multiple regression combinations from Section 5.3.5 have been presented according to the format described in Appendix B.

Table C3.1. Significant correlations among textural and biological characteristics. [r^c = 0.408, n = 63-68.]

Parameter								
% > 1phi	1							
% 1-2 phi		1						
% Fines	0.732^R		1					
% Carb.	0.555^R	-0.659	0.506^R	1				
%Organics	0.626		0.715^R	0.558	1			
Arenicola	-0.478^R	0.428	-0.493^R	-0.692^R	-0.597^R	1		
Corophium	0.416^R		0.502^R	0.440^R	0.471^R	-0.545^R	1	
Hydrobia	0.630^R		0.745^R	0.525^R	0.671^R	-0.553^R		1
Salinity	-0.537^R		-0.663^R	-0.424^R	-0.604	0.536	-0.584^R	-0.508^R
	%>1 phi	%1-2phi	%Fines	%Carb.	%Org.	*Arenic.*	*Coroph.*	*Hydrob.*

Table C3.2. Correlations of textural and biological characteristics at individual sites. [r^c = 0.795 (Site 1), 0.745 (Sites 2-5)].

TEXTURAL INTERRELATIONSHIPS.					
Parameters	Site 1	Site 2	Site 3	Site 4	Site 5
% Carb. : % 1-2 phi	-0.877	-	-	-	-
BIOLOGICAL / TEXTURAL INTERRELATIONSHIPS.					
Parameters	Site 1	Site 2	Site 3	Site 4	Site 5
% Fines : *Pygospio*	-	-	0.745^R	-	-
BIOLOGICAL INTERRELATIONSHIPS.					
Parameters	Site 1	Site 2	Site 3	Site 4	Site 5
Arenicola : *Hydrobia*	-0.765	-		-	-0.756

Table C3.3. Apparent controls of sediment porosity.

	%Carb.	*Pygos.*	*Coro.*	*Arenic*	%1-2phi	%Org.	Fines	$\%R^2$
ALL SITES								
Site 1	[-]	[-]						60
	[-]		[-]					77
Site 2					[-]	[+]		45
Site 5			[-]	[-]				51

Table C3.4. Apparent controls of FF.

	Poros.	% Carb.	*Hydro.*	*Arenic*	%>1 phi	%Org.	Fines	$\%R^2$
ALL SITES		[+]						31
							[+]	17
						[+]		23
					[+]			16
				[-]				23
			[+]					23
	[-]	[+]						38
	[-]	[+]				[+]		41
	[-]	[+]	[+]					42
	[-]			[-]			[+]	37
Site 1	[-]				[+]			47
Site 2	[-]			[-]				50
			[-]	[-]				70

Table. C3.5(b). Apparent controls of bulk V_s.

	Poros.	% Carb.	*Hydro.*	*Arenic*	%>1 phi	%1-2phi	Fines	$\%R^2$
ALL SITES		[+]						19
						[-]		14
				[-]				32
					[+]	[-]		25
		% Carb.	*Pygos.*	*Arenic*	%>1 phi	%1-2phi	% Org.	
Site 1	[+]		[+]					60
		[-]					[-]	54
			[+]		[-]	[-]		68
Site 2	[-]			[-]				73
				[-]		[+]		80
		Coroph.						
Site 4		[-]	[+]					39
			Hydr.					
Site 5	[-]		[+]					53
	[-]			[-]				46

Table. C3.5(b). Apparent controls of surface V_s.

	Poros.	% Carb.	*Pygos.*	*Arenic*	%>1 phi	%1-2phi	Fines	$\%R^2$
ALL SITES		[+]						17
						[-]		18
	[-]			[-]		[-]		27
		[+]					[-]	31
Site 1			[+]					45
					[-]	[-]		48
Site 2				[-]				35R
							[-]	27
Site 4						[-]	[-]	36
			Coroph.					
Site 5	[-]		[-]					44
							[-]	41

Table C3.6. Controls of small-scale spatial heterogeneity [cv(FF)].

PREDICTOR	R^2
Arenicola (Sites 1,2,5 only)	35.2

Table C3.7. Controls of vertical heterogeneity [V_s^R].

	%Carb.	*Pygos.*	*Coro.*	*Hydro.*	%1-2phi	%>1 phi	Fines	$\%R^2$
ALL SITES						[-]	[-]	10 11
Site 1	[+] [+]					[-]		57 79
						Arenic.		
Site 2						[-]		30
Site 3		[+]	[+]					46
Site 4					[-]		[-]	44
Site 5			[-] [-]	[-]				46 61

APPENDIX D

PLATES

Plate 1.

Laboratory test tank.

The laboratory testing facility used for most of the experiments described in Chapter 3. The OYO SONIC VIEWER (to the left of the picture) is being used to monitor V_s in drained sand containing vertical cylindrical voids.

Plate 2.

Characteristic coiled faecal cast of *Arenicola marina*.
Traeth Llanddwyn, Anglesey, North Wales (Fig. 5.1.1).

Plate 3.

High density U-shaped burrows of *Corophium volutator*.
Taf Estuary, South Wales (Fig. 5.1.1)

Plate 4.

Protruding fringed tubes of *Lanice conchilega*.
Traeth Llanddwyn, Anglesey, North Wales (Fig. 5.1.1).

Plate 5.

Resin-impregnated box-core showing high densities of tubes of *Lanice conchilega*.
Traeth Llanddwyn, Anglesey, North Wales (Fig. 5.1.1).


5cm

Plate 6.

Laquered box-core recovered from Transect T/8 in the Taf Estuary (Section 5.2.2). Note ripplemarks, cross and plane bedding.


5cm

Plate 7.

Laquered box-core recovered from Transect T/11 in the Taf Estuary (Section 5.2.2). Note *Corophium* burrows and mud laminae.

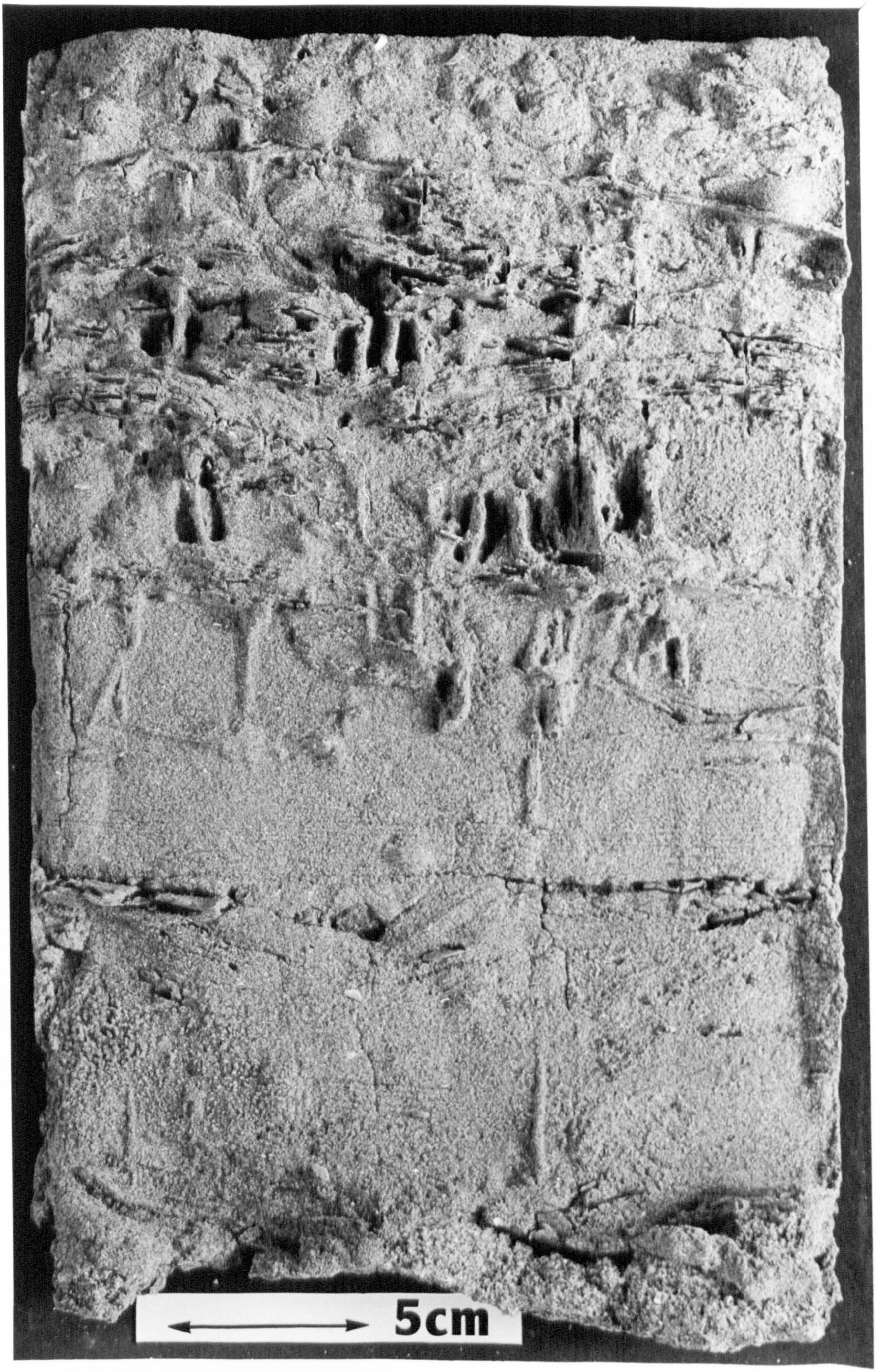
5cm

Plate 8.

Resin impregnated box core.
Cefni Estuary, Site 1, July 1987.
Note *Nereis* burrow at 3cm, lighter coloured surficial layer and bioturbation structures.


5cm

Plate 9.

Resin impregnated box core.
Cefni Estuary, Site 2, July 1987.
Note large protruding *Arenicola* burrow and other bioturbation structures.


5cm

Plate 10.

Resin impregnated box core.
Cefni Estuary, Site 3, July 1987.
Note high densities of *corophium* burrows,
contrasting 5cm surface layer and
hydrodynamic structures at depth.


5cm

Plate 11.

Resin impregnated box core.
Cefni Estuary, Site 4, July 1987.
Note single well-preserved *Corophium* burrow,
5mm oxidised layer and many surface *Hydrobia*.


5cm